

THE JOURNAL OF PHYSICAL CHEMISTRY

VOLUME 67, NUMBER 8 AUGUST, 1963

Edward S. Woolner, Jr., and Douglas G. Hill: Activity Coefficient of Silver Sulfate in Molten Sulfates and Comparison with the Quasi-Lattice Theory.....	1571	Kiser: Singly- and Doubly-Charged Ions from Methyl and Ethyl Isothiocyanates by Electron Impact.....	1684
A. R. Alvarez-Funes and D. G. Hill: Electromotive Force Measurements in the System Silver Nitrate-Potassium Nitrate-Potassium Chromate and their Comparison with the Quasi-Lattice Theory.....	1573	Graham S. Pearson: The Photooxidation of Acetone....	1686
F. R. Jones and R. H. Wood: The Enthalpy and Entropy of Dilution of Lithium Perchlorate.....	1576	Herman F. Cordes: The Thermal Decomposition of Nitryl Perchlorate.....	1693
K. C. Hou and Robbin C. Anderson: Comparative Studies of Pyrolysis of Acetylene, Vinylacetylene, and Diacetylene.....	1579	J. A. Barry and George D. Halsey, Jr.: The Interaction and Noninteraction of Ions with a Natural Polysaccharide.....	1698
M. S. B. Munson and Robbin C. Anderson: Effects of Oxygen and Chlorine on Thermal Reactions of Acetylene.....	1582	Lars Lindqvist: The Triplet State of Fluorescein in Sulfuric Acid.....	1701
Oscar H. Krikorian: The Vapor Pressure of Scandium Metal.....	1586	Alessandro D'Aprano and Raymond M. Fuoss: Electrolyte-Solvent Interaction. XI. Conductance in Isodielectric Mixtures.....	1704
D. E. Woessner and J. R. Zimmerman: Nuclear Transfer and Anisotropic Motional Spin Phenomena: Relaxation Time Temperature Dependence Studies of Water Adsorbed on Silica Gel. IV.....	1590	Jean-Claude Justice and Raymond M. Fuoss: Conductance of the Alkali Halides. VII. Cesium Chloride in Dioxane-Water Mixtures at 25°.....	1707
Andrew Teh-An Cheng, Reed A. Howald, and David L. Miller: Ion Pairs. III. Glass Electrode Potentiometry in Glacial Acetic Acid.....	1601	Andrée J. Lorquet and William H. Hamill: The Energy Dependence for Reaction Cross Sections of Ion-Molecule Reactions of Some Pentyl and Cyclopentyl Halides.....	1709
Shlomo Nehari and Joseph Rabani: The Reaction of H Atoms with OH ⁻ in the Radiation Chemistry of Aqueous Solutions.....	1609	E. W. Anacker and H. M. Ghose: Counterions and Micelle Size. I. Light Scattering by Solutions of Dodecyltrimethylammonium Salts.....	1713
S. Ainsworth: Spectrophotometric Analysis of Reaction Mixtures. II.....	1613	Lawrence B. Friedman and James C. Nichol: Electrophoresis of Glutamate-Tartrate Mixtures in Acetate Buffers.....	1716
C. E. Klots and R. H. Johnsen: Energy Partition in the Radiolysis of Aromatic Mixtures.....	1615	NOTES	
J. B. Kirwin, F. D. Peat, P. J. Proll, and L. H. Sutcliffe: A Kinetic and Spectrophotometric Examination of Silver (II) in Perchlorate Media.....	1617	E. P. Marram, E. J. McNiff, and J. L. Ragle: Pure Quadrupole Resonance of Chlorine (Cl ³⁵) in Potassium Tetrachloroplatinate.....	1719
L. Bertsch and H. W. Habgood: An Infrared Spectroscopic Study of the Adsorption of Water and Carbon Dioxide by Linde Molecular Sieve X.....	1621	Robert W. Kunze, Raymond M. Fuoss, and Benton B. Owen: Limiting Conductance of the Rubidium Ion..	1719
Chava Lifshitz and S. H. Bauer: Mass Spectra of Valence Tautomers.....	1629	Y. Tomimatsu and K. J. Palmer: Reflection Corrections for Light-Scattering Measurements for Various Cells with the Brice-Type Photometer.....	1720
Lawrence Dresner: Electrokinetic Phenomena in Charged Microcapillaries.....	1635	Alessandro D'Aprano and Raymond M. Fuoss: Electrolyte-Solvent Interaction. X. Dipole Solvation....	1722
Charles P. Nash, Earl L. Pye, and Don B. Cook: Solutions of N-Substituted Amino Acids. I. The Solubility of N,N-Diethyl- β -aminopropionic Acid in Benzene.....	1642	R. A. Robinson and Adam Peiperl: The Ionization Constants of <i>o</i> -Nitrophenol and 4-Nitro- <i>m</i> -cresol from 5 to 60°.....	1723
E. T. Turkdogan, P. Grievesson, and L. S. Darken: Enhancement of Diffusion-Limited Rates of Vaporization of Metals.....	1647	Jehudah Eliassaf, Raymond M. Fuoss, and John E. Lind, Jr.: Conductance in Dimethylsulfolane.....	1724
George S. Hammond and Robert C. Neuman, Jr.: Amidinium Ions. I. Hindered Internal Rotation....	1655	A. J. Kidnay and M. J. Hiza: The Adsorption of Methane and Nitrogen on Silica Gel, Synthetic Zeolite, and Charcoal.....	1725
Robert C. Neuman, Jr., and George S. Hammond: Amidinium Ions. II. Mechanisms of Exchange of Protons Bound to Nitrogen.....	1659	A. H. Ewald: The Effect of Pressure on the Quenching of Fluorescence.....	1727
P. D. Cratin and J. K. Gladden: Excess Thermodynamic Properties of the Binary Liquid System Ethylene Glycol-Methanol.....	1665	A. Loewenstein: Activation Energies of Proton Transfer Reactions: Di- and Trimethylammonium Solutions..	1728
Rapier Dawson, Elizabeth B. Brackett, and Thomas E. Brackett: A High Temperature Calorimeter; the Enthalpies of α -Aluminum Oxide and Sodium Chloride.....	1669	Elmer J. Huber, Jr., Earl L. Head, and Charles E. Holley, Jr.: The Heat of Formation of Uranium Dicarbide..	1730
Priscilla Chang Kaufman: Radiolysis of <i>n</i> -Butenes.....	1671	Elmer J. Huber, Jr., George C. Fitzgibbon, Earl L. Head, and Charles E. Holley, Jr.: The Heat of Formation of Scandium Oxide.....	1731
Paul R. Geissler and John E. Willard: Chemical Effects of (ν, γ)-Activation of Halogen Atoms in Alkyl Halide-Pentane Solutions; Auger Electron Reaction Hypothesis.....	1675	O. K. Rice: Further Remarks on the "Rate-Quotient Law".....	1733
W. H. Melhuish: Effect of Solvent Viscosity on Excitation Energy Transfer between Unlike Molecules.....	1681	G. Stöcklin, H. Stangl, D. R. Christman, J. B. Cumming, and A. P. Wolf: The Reactions of Energetic Carbon Atoms in Methane; Oxygen and Phase Dependence; Radiation Damage Effects.....	1735
Brice G. Hobrock, Roger C. Shenkel, and Robert W.		Wallace S. Brey, Jr., and John W. Legg: Dielectric Properties of the Hydrate of Trichlorofluoromethane..	1737
		Herbert S. Harned: The Thermodynamic Properties of the System: Hydrochloric Acid, Lithium Chloride, and Water from 15 to 35°.....	1739

Sture Forsén: Long-Range Spin Couplings Involving Methoxy Groups in Aromatic Compounds..... 1740

COMMUNICATIONS TO THE EDITOR

Thomas P. Onak, Robert E. Williams, and Ronald Swidler: Structural Rigidity and Internal B-N

Coordination Influences on the Hydrolysis Resistance of Borate Esters..... 1741
 George H. Lee, II, Walter H. Bauer, and Stephen E. Wiberley: Formation and Infrared Characterization of Boroxine..... 1742

AUTHOR INDEX

- | | | | | |
|-----------------------------|--------------------------------------------|--------------------------------|--------------------------------|---------------------------|
| Ainsworth, S., 1613 | Dresner, L., 1635 | Hobrock, B. G., 1684 | Loewenstein, A., 1728 | Rabani, J., 1609 |
| Alvarez-Funes, A. R., 1573 | Eliassaf, J., 1724 | Holley, C. E., Jr., 1730, 1731 | Lorquet, A. J., 1709 | Ragle, J. L., 1719 |
| Anacker, E. W., 1713 | Ewald, A. H., 1727 | Hou, K. C., 1579 | Marram, E. P., 1719 | Rice, O. K., 1733 |
| Anderson, R. C., 1579, 1582 | Fitzgibbon, G. C., 1731 | Howald, R. A., 1601 | McNiff, E. J., 1719 | Robinson, R. A., 1723 |
| Barry, J. A., 1698 | Forsén, S., 1740 | Huber, E. J., Jr., 1730, 1731 | Melhuish, W. H., 1681 | Shenkel, R. C., 1684 |
| Bauer, S. H., 1629 | Friedman, L. B., 1716 | Johnsen, R. H., 1615 | Miller, D. L., 1601 | Stangl, H., 1735 |
| Bauer, W. H., 1742 | Fuoss, R. M., 1704, 1707, 1719, 1722, 1724 | Jones, F. R., 1576 | Munson, M. S. B., 1582 | Stöcklin, G., 1735 |
| Bertsch, L., 1621 | Geissler, P. R., 1675 | Justice, J.-C., 1707 | Nash, C. P., 1642 | Sutcliffe, L. H., 1617 |
| Brackett, E. B., 1669 | Ghose, H. M., 1713 | Kaufman, P. C., 1671 | Nehari, S., 1609 | Swidler, R., 1741 |
| Brackett, T. E., 1669 | Gladden, J. K., 1665 | Kidnay, A. J., 1725 | Neuman, R. C., Jr., 1655, 1659 | Tomimatsu, Y., 1720 |
| Brey, W. S., Jr., 1737 | Grieverson, P., 1647 | Kirwin, J. B., 1617 | Nichol, J. C., 1716 | Turkdogan, E. T., 1647 |
| Cheng, A. T., 1601 | Habgood, H. W., 1621 | Kiser, R. W., 1684 | Onak, T. P., 1741 | Wiberley, S. E., 1742 |
| Christman, D. R., 1735 | Halsey, G. D., Jr., 1698 | Klots, C. E., 1615 | Owen, B. B., 1719 | Willard, J. E., 1675 |
| Cook, D. B., 1642 | Hamill, W. H., 1709 | Krikorian, O. H., 1586 | Palmer, K. J., 1720 | Williams, R. E., 1741 |
| Cordes, H. F., 1693 | Hammond, G. S., 1655, 1659 | Kunze, R. W., 1719 | Pearson, G. S., 1686 | Woessner, D. E., 1590 |
| Cratin, P. D., 1665 | Harned, H. S., 1739 | Lee, G. H., II, 1742 | Peat, F. D., 1617 | Wolf, A. P., 1735 |
| Cumming, J. B., 1735 | Head, E. L., 1730, 1731 | Legg, J. W., 1737 | Peiperl, A., 1723 | Wood, R. H., 1576 |
| D'Aprano, A., 1704, 1722 | Hill, D. G., 1571, 1573 | Lifshitz, C., 1629 | Proll, P. J., 1617 | Woolner, E. S., Jr., 1571 |
| Darken, L. S., 1647 | Hiza, M. J., 1725 | Lind, J. E., Jr., 1724 | Pye, E. L., 1642 | Zimmerman, J. R., 1590 |
| Dawson, R., 1669 | | Lindqvist, L., 1701 | | |

THE JOURNAL OF PHYSICAL CHEMISTRY

(Registered in U. S. Patent Office) (© Copyright, 1963, by the American Chemical Society)

VOLUME 67, NUMBER 8

AUGUST 15, 1963

ACTIVITY COEFFICIENT OF SILVER SULFATE IN MOLTEN SULFATES AND COMPARISON WITH THE QUASI-LATTICE THEORY

BY EDWARD S. WOOLNER, JR.,¹ AND DOUGLAS G. HILL

Department of Chemistry, Duke University, Durham, N. C.

Received September 10, 1962

The activity coefficient of Ag_2SO_4 has been studied by e.m.f. measurements in a concentration cell using Ag electrodes and solutions of Ag_2SO_4 in a eutectic of molten lithium and potassium sulfates to which KCl is added. The cell is well behaved, and the results may be fitted to the quasi-lattice theory. The excess association energy for formation of AgCl in a sulfate melt at 700° is -3.9 kcal.

The quasi-lattice theory developed by Blander² and co-workers has been thoroughly tested by e.m.f. experiments using AgNO_3 as solute in a concentration cell of fused KNO_3 and several other nitrates. Its application to a different solvent has been limited.³

Such a solvent is the eutectic mixture of K_2SO_4 and Li_2SO_4 , 71.5 mole % Li_2SO_4 . This melt may be used from below 600° up to at least 700° with simple techniques. The solute was Ag_2SO_4 , and as a first study, KCl was added to change the activity of Ag^+ ion.

The higher temperature makes the work only slightly more difficult, and the formalism of the theory appears to apply as well as in the nitrate systems.

Experimental

Ag_2SO_4 was prepared by precipitation with dilute H_2SO_4 from AgNO_3 solution, washed until the washings were neutral, and dried in the dark, first in air, finally in a desiccator over P_2O_5 . After drying the salt was stable at 110° , which was not the case when wet.

Li_2SO_4 was prepared from monohydrate heated for two days at 85° in a slow stream of dry air. It was then finally dried at 130° .

KCl and K_2SO_4 were dried at 110° or higher. Possible hydrolysis of the sulfate mixture, either during the drying or in use, producing LiOH or Li_2O would have been a source of trouble causing both attack on the Vycor equipment, and reaction with silver salts. Experiment showed that both reactions occurred with eutectic as prepared, but that both ceased if the melt was treated either with $\text{K}_2\text{S}_2\text{O}_7$ or H_2SO_4 , about 5 g. for 800 g. eutectic. In either case the excess of SO_3 (and water) was removed by holding the melt at 600° for at least 24 hr., preferably with a mechanical stirrer and a stream of dry gas, He or N_2 passing through it slowly. These melts did not appear to pick up water from the atmosphere if the gas stream was shut off or to hydrolyze at the temperature of melting. A gas stream was kept flowing during most of the runs.

Complete removal of the excess acid was necessary, since if sufficient time was not allowed, the first additions of KCl did not cause the expected change in the e.m.f. Presumably KCl reacted with acid and was slowly removed as HCl. It was found best to

maintain the melt at temperature for three days before proceeding, and one case in which a week elapsed behaved very well. Corrosion of Vycor is very slight in the acid melts, while if even a little base is present, corrosion is serious. Pyrex is attacked too rapidly for use, even in the acidified melts.

The apparatus was similar to that described by others⁴ for the nitrate systems. The melt was contained in an open 800-ml. Vycor beaker, and Vycor stirrer and inlet tubes were used. The reference electrode was a 12-mm. Vycor tube containing the eutectic and a different concentration of Ag_2SO_4 , and communicating through an asbestos fiber at the bottom. It is not possible to seal asbestos into Vycor, but equally good results are obtained by packing a small drawn out tip with asbestos. Considerable practice was needed to get the packing correct so that it did not leak, but did not offer too high resistance. Both requirements may be checked experimentally, the latter merely by observing whether the potentiometer works correctly, which will not be the case if the resistance is too high. If the reference electrode is placed in the bath with its liquid level 1 cm. lower than the level in the beaker, observation over 24 hr. shows whether there is a leak.

The electrodes were silver wire, No. 24 gage, coiled loosely so that at least 15 cm. of wire was immersed in the melt. Short electrodes tended to give unstable potentials.

Temperature was measured by a chromel-alumel thermocouple enclosed in a Vycor tube and immersed in the beaker. It was calibrated at 100° and at the melting point of Zn, 419.5° . Temperature control was not too precise, but by constant adjustment of a Variac supplying the Hoskins (5 in.) pot furnace, a constancy of $\pm 2^\circ$ was maintained.

Potentials were measured on a Leeds and Northrup Type K potentiometer.

Procedure.—The measurements were conducted in the same manner as the series which have been made in nitrates, described by Blander, Newton, and Blankenship.⁴ After a concentration cell had come to equilibrium, as shown by constancy of potential, usually overnight, additions of weighed amounts of KCl were made to the beaker and the resulting potential measured. Equilibrium was apparently attained quickly after each addition, usually in less than one hour, and a series of addition were possible in one day. As mentioned above, on occasions in which insufficient time had been allowed for the original equilibrium to be reached, in respect to fuming off all excess H_2SO_4 , the fact was evident. The e.m.f. vs. R_{KCl} (mole ratio $(\text{Cl}^-)/(\text{Ag}^+)$) curve showed an abrupt change in slope after all excess acid was removed. This is attributed to loss of the added chloride as HCl (see ref. 5).

(1) The data in this paper are taken from a thesis submitted by E. S. Woolner, Jr. to the Graduate School of Duke University in partial fulfillment of the requirements for the degree of M.A.

(2) M. Blander, *J. Phys. Chem.*, **63**, 1262 (1959).

(3) H. Kühnl, *Z. anorg. allgem. Chem.*, **313**, 48 (1961).

(4) M. Blander, F. F. Blankenship, and R. F. Newton, *J. Phys. Chem.*, **63**, 1259 (1959).

TABLE I
 ACTIVITY COEFFICIENTS OF Ag_2SO_4 IN $\text{Li}_2\text{SO}_4\text{-K}_2\text{SO}_4$; KCl ADDED

$R_{\text{KCl}} \times 10^3$	$-\Delta e.m.f. (mv.)$ $T = 600^\circ$	$-\log \gamma_{\text{Ag}_2\text{SO}_4}$	$R_{\text{KCl}} \times 10^3$	$-\Delta e.m.f. (mv.)$ $T = 650^\circ$	$-\log \gamma_{\text{Ag}_2\text{SO}_4}$
	$R_{\text{Ag}_2\text{SO}_4} = 0.0020$			$R_{\text{Ag}_2\text{SO}_4} = 0.0006$	
0.5	1.26	0.015	0.25	1.14	0.013
1.0	2.20	.024	0.50	1.14	.013
1.5	3.43	.039	0.75	1.79	.019
2.0	4.56	.051	1.0	2.34	.025
2.5	5.60	.063	2.0	4.61	.050
3.0	6.57	.073	3.0	6.85	.074
	$R_{\text{Ag}_2\text{SO}_4} = 0.0018$		4.0	9.20	.100
1.0	1.3	0.014	5.0	10.59	.114
2.0	5.1	.057	7.0	14.55	.156
3.0	6.8	.075		$T = 700^\circ$	
4.0	9.8	.110		$R_{\text{Ag}_2\text{SO}_4} = 0.002$	
4.5	10.8	.121	0.5	1.11	0.012
5.0	12.0	.134	1.0	1.99	.020
5.5	13.1	.146	1.5	2.83	.028
6.0	14.3	.160	2.0	3.82	.039
6.5	15.4	.172	2.5	4.74	.047
7.0	16.4	.183	3.0	5.04	.049
	$T = 650^\circ$			$R_{\text{Ag}_2\text{SO}_4} = 0.0018$	
	$R_{\text{Ag}_2\text{SO}_4} = 0.002$		1.5	3.01	0.030
0.5	1.11	0.012	2.5	5.54	.055
1.0	2.15	.023	3.5	7.46	.074
1.5	3.23	.035	4.5	9.26	.092
2.0	3.71	.039	5.8	11.68	.115
2.5	5.12	.055	6.8	13.42	.133
3.0	6.05	.065		$R_{\text{Ag}_2\text{SO}_4} = 0.0006$	
	$R_{\text{Ag}_2\text{SO}_4} = 0.0018$		0.25	0.72	0.007
0.5	1.97	0.022	0.50	1.60	.017
1.0	4.04	.044	0.75	2.23	.022
2.0	6.47	.070	1.00	2.80	.028
3.0	8.82	.096	2.00	6.03	.060
4.0	11.02	.120			
5.0	13.17	.143			
7.0	17.27	.187			

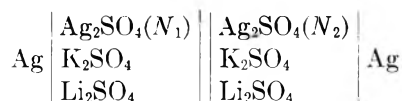
After one or more additions under these conditions, further additions gave a change in e.m.f. agreeing in slope with that obtained in runs in which the initial incorrect slope was not observed. These slopes were therefore used, even though the extrapolation to zero KCl gave a different value from that found before the first addition.

The additions required were fairly large, and a correction for the actual concentration change upon adding KCl was made. Allowing for this change, the activity coefficient was calculated from the equation

$$\log \gamma_{\text{Ag}_2\text{SO}_4} = + \frac{2N_{\text{Cl}^-}}{2.303} + \frac{F\Delta E}{2.303RT}$$

where N_{Cl^-} is ion fraction of $\text{Cl}^- = m_{\text{Cl}^-}/(m_{\text{Cl}^-} + m_{\text{SO}_4^{2-}})$. The derivation is similar to that given by Watt and Blander.⁶ The reference state, with activity coefficient equal to unity is the infinitely dilute ideal solution.

The arguments relative to the validity of activity coefficients determined by e.m.f. studies in concentration cells in fused salt solvents have been given.² Such a cell should obey the Nernst law for a pure concentration cell, in which only the concentration of Ag_2SO_4 in one compartment is varied, the cell then being



The potential of this cell should be given by

$$e.m.f. = \frac{RT}{nF} \ln \frac{N_1}{N_2}$$

where N is ion fraction of $\text{Ag}^+ = \frac{m_{\text{Ag}^+}}{m_{\text{Ag}^+} + m_{\text{K}^+} + m_{\text{Li}^+}}$.

Agreement with this equation was found at the higher concentrations of Ag_2SO_4 , but unfortunately it was not extended to the lowest concentrations used in this work. However, the cell does obey the Nernst law at concentrations of Ag_2SO_4 down to 2×10^{-3} mole fraction, giving an observed slope for $\log N_2$ against e.m.f. of 0.172 (theoretical 0.173) at 600° . Liu⁷ has shown similar agreement in a similar melt down to approximately the same concentration at 625° .

The experiments were carried out at 600 , 650 , and 700° , and at three concentrations at the higher temperatures. It would have been desirable to extend the dilute measurements to 600° and to examine still more dilute solutions, but as is well known from the work in other solvents, more dilute solutions are more difficult to control, and only the data presented here were obtained. In Table I are listed the values of the calculated activity coefficient of Ag_2SO_4 for each addition of KCl.

The values of $\log \gamma$ were plotted against R_{KCl} , and a line was drawn through the points. The lines are straight

(5) The loss of very small quantities of HCl formed by reaction of KCl with H_2SO_4 is apparently fairly slow. No bubbles were observed. However, after excess H_2SO_4 is exhausted, further increments of KCl will have the effect on the activity of Ag_2SO_4 to be expected in a melt in which the slight loss of excess H_2SO_4 had not occurred.

(6) W. J. Watt and M. Blander, *J. Phys. Chem.*, **64**, 729 (1960).

(7) C. H. Liu, *ibid.*, **66**, 164 (1962).

at the lower concentrations and may curve at higher additions. However, curvatures were not surely within experimental error, so no use was made of them. The slopes of the straight lines were read from the graph.

According to well known thermodynamic reasoning and to the quasi-lattice theory,⁸ the limiting slope at infinite dilution and temperature T may be used to calculate both the association constant for Ag-Cl in this solution and the extra coulombic association energy

$$-\frac{1}{2} \frac{d \ln \gamma}{dN_{\text{Cl}^-}} = Z(\beta - 1) = K_1 = \frac{[\text{Ag-Cl}]}{[\text{Ag}^+][\text{Cl}^-]}$$

where Z is the coordination number and $\beta = e^{-\Delta A/RT}$, $-\Delta A$ being the association energy. The reagents in this study are far from those for which the quasi-lattice theory was derived—monovalent ions, all of the same

TABLE II
ASSOCIATION CONSTANTS AND ENERGIES

Temperature	$\frac{2.3}{2}$ slope = $K_1 = Z(\beta - 1)$	$-\Delta A$ (kcal.)
	$R_{\text{Ag}_2\text{SO}_4} = 0.0006$	
650°	28.0	3.81
700°	27.2	3.97
	$R_{\text{Ag}_2\text{SO}_4} = 0.002$	
600°	31.9	3.81
650°	24.8	3.62
700°	17.4	3.24

(8) J. Braunstein, M. Blander, and R. M. Lindgren, *J. Am. Chem. Soc.*, **84**, 1529 (1962).

size—so that it is interesting that the curves are of the same type as those found for cases where the assumptions of the theory are followed. Applying the equations of the theory will then give corresponding numbers, which may or may not have theoretical significance. Such an application does, however, give constancy in the calculated association energy, which was one of the tests for the theory. The calculated association constants and energies are given in Table II.

A coordination number of 4 has been assumed in the calculation of association constants and energies. The coordination in the liquid is unknown, but in the solid alkali sulfates there are four sulfates about each metal ion, and assuming the same or less for the liquid is not unreasonable.

The data show the importance of the more dilute solutions, which give a more constant association energy, agreeing better with the predictions of theory. As was shown by Braunstein, Blander, and Lindgren,⁸ more concentrations should be studied and an extrapolation to infinite dilution performed. In this first study in sulfate melts a less complete treatment seemed worthwhile. More complete data would also permit evaluation of higher association constants, which would be of much interest.

We recognize that fitting our data into the framework of the quasi-lattice theory is not proof of the structure of sulfate melts. However, the fact that agreement is obtained is consistent with the hypothesis of a simple structure for melts with large, nearly spherical anions and small cations arranged more or less as in the solid alkali sulfates.

ELECTROMOTIVE FORCE MEASUREMENTS IN THE SYSTEM SILVER NITRATE-POTASSIUM NITRATE-POTASSIUM CHROMATE¹ AND THEIR COMPARISON WITH THE QUASI-LATTICE THEORY

BY A. R. ALVAREZ-FUNES² AND D. G. HILL

Department of Chemistry, Duke University, Durham, N. C.

Received September 10, 1962

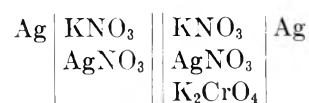
The e.m.f. developed in a concentration cell of AgNO_3 in molten KNO_3 is changed by the addition of K_2CrO_4 in a manner interpretable by the quasi-lattice theory. The association constants and energies are larger than those for the similar system involving sulfate rather than chromate. Only 1-1 type association may be calculated from the measurements in either system, and the energies are smaller than those found for the monovalent halide ions.

The quasi-lattice description of molten salt solutions as developed by Blander³ and co-workers has been shown to hold for silver ion with several anions, giving a constant "specific bond energy" and an association constant for ion pair formation. The postulate of spherical ions of the same diameter and charge was adopted for simplicity, and most of the confirmation has come from studies in which only the size equality restriction has been violated. However, Watt and Blander⁴ showed that the formalism of the theory could be applied to a

study of sulfate-silver ion association with some success. The present work examines the association of chromate and silver ions. The formalism of the theory applies as well to this case as to the sulfate case and seems to demand next-nearest-neighbor interaction for explanation.

Experimental

In the experiments, the quantity measured was the e.m.f. of a concentration cell represented by



The solution to which K_2CrO_4 was to be added was maintained in an open Pyrex beaker at the chosen temperature and a reference electrode inserted in the beaker, making contact through an

(1) Some of the experimental data were rechecked by D. G. Hill using the facilities of Oak Ridge National Laboratory, Reactor Chemistry Division, for which kindness we are grateful.

(2) University of Tucuman, Tucuman, Argentina. Fellow of the Consejo Nacional de Investigaciones Cientificas y Tecnicas of Argentina.

(3) M. Blander, *J. Phys. Chem.*, **63**, 1262 (1959).

(4) W. J. Watt and M. Blander, *ibid.*, **64**, 729 (1960).

asbestos fiber bridge as described previously.⁵ All salts were reagent grade compounds, used without further purification. The melt in the beaker was stirred with a mechanical stirrer and sparged with either He or N_2 with no apparent difference. Potentials were measured on a Type K Leeds and Northrup potentiometer, and temperatures were measured with a thermocouple calibrated at 100° and at the melting point of Zn.

After preparing a cell, it was allowed to come to equilibrium as shown by constancy of its measured potential, a matter of a few hours. Then weighed quantities of K_2CrO_4 were added to the right hand compartment (the beaker) and the resulting potential measured in each case.

In most of the e.m.f. studies made in this series the change in potential measures the activity coefficient directly. However, as shown by Watt,⁴ in cases where comparatively large amounts of salt are added, a correction should be made for the concentration change introduced by the addition. In the present case the activity coefficient of AgNO_3 is given by

$$\log \gamma_{\text{AgNO}_3} = \frac{F\Delta E}{2.303RT} + \frac{3N_{\text{CrO}_4^{-2}}}{2.303}$$

Here ΔE is the change (actually a decrease) in potential of the cell brought about by $N_{\text{CrO}_4^{-2}}$ ion fraction of chromate. The activity coefficient, γ_{AgNO_3} , is defined in terms of an infinitely dilute solution of AgNO_3 in molten KNO_3 .

The data obtained at 410° are plotted in Fig. 1, showing log of the calculated activity coefficient as a function of added chromate. R is the molar ratio of chromate to silver ion, nearly equal to the mole fraction. Although the quasi-lattice theory predicts a dependence of the activity coefficient on the original AgNO_3 concentration as well as upon that of the added salt, such dependence was not observable in our experiments. As shown, a ten-fold change in AgNO_3 concentration causes a negligible change in slope, within experimental error. A similar result was found in the sulfate study referred to above. Therefore the best straight line was drawn through the several points and the AgNO_3 concentration effect neglected. The data obtained at a series of temperatures are given in Table I. The temperature range was from 357 to 490° , above which the decomposition of nitrate to nitrite became troublesome. Previous work, still unpublished, has established that small amounts (1%) of nitrite when added to an AgNO_3 concentration cell in KNO_3 do not change the potential, though the effect of large changes has not been established. The decomposition was much less than 1%.

In terms of well known thermodynamics and of the quasi-lattice theory

$$-\frac{d \ln \gamma}{dN_{\text{CrO}_4^{-2}}} = Z(\beta - 1) = K_1 = \frac{[\text{Ag-CrO}_4^-]}{[\text{Ag}^+][\text{CrO}_4^{-2}]}$$

Since, up to the point at which precipitation of Ag_2CrO_4 occurred, no curvature was apparent in the log plots, the slope of the best straight line drawn through the points was used to determine the association constant K_1 and β (which is equal to $e^{-\Delta A/RT}$). These values are listed in Table II. The term ΔA represents the excess energy of the $\text{Ag}^+\text{-CrO}_4^{-2}$ association.

TABLE II
ASSOCIATION CONSTANTS AND ENERGIES

Temp., °C.	(2.3) Slope = $Z(\beta - 1) =$		$-\Delta A$ (kcal.)	
	K_1	$Z = 6$	$Z = 4$	
357	48.6	2.8	3.2	
377	41.5	2.7	3.1	
410	37.6	2.7	3.2	
450	34.6	2.8	3.3	
490	32.0	2.8	3.3	

The association energy is constant, within experimental error, over the temperature range studied. In the calculation of ΔA , values of 4 and 6 have been arbitrarily assumed for the coordination number, Z . There is no justification for assuming any particular number, although in solid K_2SO_4 , and thus presumably in K_2CrO_4 and Ag_2CrO_4 , the coordination (SO_4^{-2} ion) about each alkali ion is 4, while in solid nitrates the coordination is 6. If 5 were chosen instead, the constancy of the ΔA values would not

(5) M. Blander, F. F. Blankenship, and R. F. Newton, *J. Phys. Chem.*, **63**, 1257 (1959).

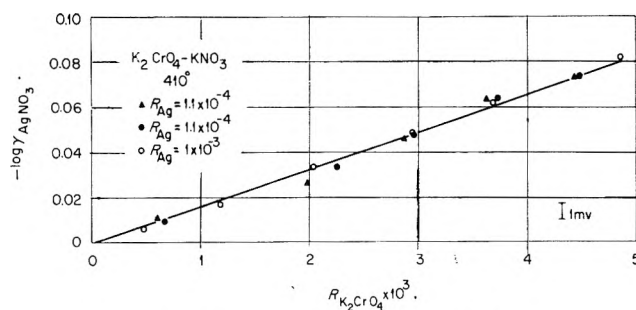


Fig. 1.—E.m.f. in $\text{AgNO}_3\text{-KNO}_3\text{-K}_2\text{CrO}_4$.

be appreciably affected, though their absolute magnitude would be different.

The experimental data seem to be approximately as precise as those obtained by Watt, but within our experimental error, the variation in ΔA with temperature observed by Watt was not found. However, the association constants found for chromate with Ag ion are several-fold larger than those for sulfate, and the association energies are correspondingly larger. Watt found association constants of the order of 11 and energies of about 1.3 kcal. This is in the direction to be expected from ionic diameters, the Cr-O distance in chromates being 1.60 Å, while the S-O distance in sulfates is 1.68 Å. Since the coordination is almost certainly through the O atoms, the next nearest neighbor, Cr in the case of chromate is nearer to Ag than is S in sulfate. However, the difference in distance is small, and would lead one to look for other forces than those with a simple inverse distance dependence. The same effect has been observed in additions of halides to dilute AgNO_3 solution. The binding energy and association constants for Ag-I, Ag-Br, and Ag-Cl change in the same sense as the distance, rather than inversely.

It is unfortunate that the data in both this case and in that of the sulfates cannot be extended to high enough concentrations to permit the determination of higher association constants by the method of Braunstein, Blander, and Lindgren.⁶ Unfortunately, precipitation of the silver salt occurs at quite low concentrations, both with sulfate and chromate. Generally, however, K_2 and K_{12} in Braunstein's terminology are expected to be smaller than K_1 , and that in itself is quite small.

The calculation of excess association energy, $-\Delta A$, from the limiting slope of the equation for the activity coefficient, valid in the limit of infinite dilution

$$-\frac{d \ln \gamma_{A^+}}{dN_C} = Z(\beta - 1) \text{ with } \beta = \exp\left(\frac{-\Delta A}{RT}\right)$$

has been compared with the equation for the same quantities proposed by Flood, Fjørland, and Grjotheim,⁷ who obtain

$$\frac{d \ln \gamma_{A^+}}{dN_C} = \frac{Z(-\Delta A)}{RT}$$

by a derivation differing in the entropy calculated for the system. Mathematically the two equations become identical at small values for $\Delta A/RT$, and it is interesting to look for cases in which this might be observed experimentally.

TABLE III

Solute	Reactant	Solvent	Interaction energy (kcal.)	
			Flood	Blander
AgNO_3	K_2CrO_4	KNO_3	7.7	2.8
Ag_2SO_4^a	KCl	$\text{K}_2\text{SO}_4\text{-Li}_2\text{SO}_4$	11	3.9
AgNO_3^d	K_2SO_4	KNO_3	2.9	1.6
AgNO_3^b	NaCl	NaNO_3	43.0	4.6

^a E. S. Woolner and D. G. Hill, *J. Phys. Chem.*, **67**, 1571 (1963). ^b D. G. Hill, J. Braunstein, and M. Blander, *ibid.*, **64**, 1038 (1960).

Small values of the exponent result either from small association energies, ΔA , or high temperatures. Table III lists several systems which have been investigated by the same methods as in

(6) J. Braunstein, M. Blander, and R. M. Lindgren, *J. Am. Chem. Soc.*, **84**, 1529 (1962).

(7) H. Flood, T. Fjørland, and K. Grjotheim, *Z. anorg. allgem. Chem.*, **276**, 289 (1954).

the present paper, with the calculated values for ΔA by each method.

Only in the case of the association energy for Ag-SO_4 is the energy small enough that the two approaches give approximately

the same value. The study in molten sulfates was at a much higher temperature, 700° , but this is not enough. Temperatures much above these, as used by Flood in his applications to slags, make the simpler theory applicable.

THE ENTHALPY AND ENTROPY OF DILUTION OF LITHIUM PERCHLORATE

BY F. R. JONES¹ AND R. H. WOOD

Department of Chemistry, University of Delaware, Newark, Delaware

Received November 3, 1962

The heat of dilution of lithium perchlorate in the concentration range of 4.0 to 0.01 molal has been measured with a new twin calorimeter. The results have been calculated using a new method for correcting for heat leaks in the twin calorimeter. The relative apparent molal heat contents have been determined by a least squares extrapolation of the heats of dilution. The excess relative partial molal enthalpy and entropy of lithium perchlorate have been calculated from the relative apparent molal heat content and the activity coefficient. The excess relative partial molal entropy of lithium perchlorate fits the correlation of Wood at all concentrations using the value $P = 0.455$ for the perchlorate ion.

Introduction

The deviations of activity coefficients of electrolyte solutions from the Debye-Hückel limiting law have received considerable attention in the last forty years.² However, deviations in the entropy (excess relative partial molal entropy) from the predictions of the Debye-Hückel law have received much less attention.¹ Frank and Robinson^{3a} and Friedman^{3b} have discussed the factors influencing the general trend of the entropy and, in particular, Frank and Robinson have shown that the structure of the water around an ion has a great influence on the entropy of concentrated solutions. Pitzer and Brewer⁴ have shown that there is a rough correlation between the heats and free energies (and thus between entropies and free energies) of the 1-1 electrolytes. The existence of this correlation means that the structural effects which influence the entropies also influence the heats and free energies.

Wood⁵ has shown that the entropies of dilution of many 1-1 electrolytes can be correlated with a single parameter for each ion. In the case of the negative ions the parameter is related to the size of the ion. The regularities present in the entropies indicate that a theoretical understanding should be less complicated for the entropies than for the free energies. The fact that there is only one parameter for each ion means that any specific interactions between the ions do not affect the entropy to any great extent. The regularity in the entropies also indicates that it is possible in some cases to predict the entropies of dilution. This should be particularly useful in correcting the entropies of formation of complex ions for the influence of the other ions present. This is often necessary because the entropies of formation often must be measured at very high ionic strengths.⁶ At present the correlation cannot be used to predict the entropies of dilution of com-

plex ions because this kind of ion does not seem to fit the correlation very well. For instance, of the 1-1 electrolytes which contain oxy-anions and for which data are available, only HNO_3 and LiNO_3 fit the correlation while NaNO_3 , KNO_3 , RbNO_3 , CsNO_3 , NaClO_3 , KClO_3 , and NaClO_3 do not fit the correlation.^{7,8}

Since LiNO_3 behaves normally, it was of interest to see if the combination of lithium ion with the perchlorate ion would also behave normally.

Experimental

Heats of dilution were measured in a calorimeter of the twin Joule type.⁹ The calorimeter vessel was made from stainless steel coated with Teflon and had a capacity of about 1850 ml. The lid was brass coated with polyethylene. Temperature differences between the two vessels were measured with a 50 junction chromel-constantan thermopile connected to an electronic chopper amplifier. The noise level was about 0.04 u.v. ($1.3 \times 10^{-5}^\circ$) peak to peak. Glass pipets of 10, 25, and 50 ml. volume were used. The vessels were held in a submarine immersed in a constant temperature bath (constant to better than 10^{-3}°). Electrical calibration was used in all runs. The results are expressed in terms of defined calories (1 cal. = 4.1840 absolute joules).

The results were corrected for the heat losses of the vessels. van der Waals and Hermans¹⁰ have described a method of making this correction when the heat leak from one vessel to the other and the heat of stirring are negligible. A derivation of the heat leak correction for the general case has been made and will be published elsewhere.

The over-all performance of the calorimeter was checked by measuring the known¹¹ heat of dilution of 0.6432 *M* hydrochloric acid (50 ml. diluted to 1850 ml.). The results of four measurements were 8.79, 8.69, 8.68, and 8.67 cal. while the calculated value is 8.68 cal.

The lithium perchlorate was supplied through the courtesy of HEF, Inc.¹² Analysis for sodium and potassium using a Beckman flame photometer gave 0.01% sodium and 0.0% potassium. Gravimetric analysis for heavy metal oxides as R_2O_3 gave less than 0.006% R_2O_3 as Fe_2O_3 . A 4 *M* solution showed no turbidity

(7) Enthalpies of dilution have been taken from the following; for NaClO_3 and NaClO_4 : M. Colomina and J. Nicolas, *Anales real soc. espan. fis. quim.* (Madrid), **B45**, 137 (1949); for all other salts: F. D. Rossini, *et al.*, National Bureau of Standards Circular 500, U. S. Govt. Printing Office, Washington, D. C., 1952.

(8) Activity coefficients have been taken from R. A. Robinson and R. H. Stokes, "Electrolyte Solutions," Academic Press, New York, N. Y., 1955.

(9) A more complete description will be published elsewhere.

(10) J. H. van der Waals and J. J. Hermans, *Rec. trav. chim.*, **69**, 949 (1950).

(11) F. D. Rossini, *et al.*, National Bureau of Standards Circular 500, "Selected Values of Chemical Thermodynamic Properties," U. S. Govt. Printing Office, Washington, D. C., 1952.

(12) HEF, Inc., Philadelphia 44, Pa.

(1) Abstracted in part from the thesis of F. Robert Jones.

(2) H. S. Harned and B. B. Owen, "Electrolytic Solutions," 3rd Ed., Reinhold Publ. Corp., New York, N. Y., 1958.

(3) (a) H. S. Frank and Robinson, *J. Chem. Phys.*, **8**, 933 (1940); (b) H. L. Friedman, *ibid.*, **32**, 1551 (1960).

(4) K. Pitzer and L. Brewer in G. N. Lewis and M. Randall, "Thermodynamics," as revised by K. Pitzer and L. Brewer, McGraw-Hill Book Co., New York, N. Y., 1961, p. 336.

(5) R. H. Wood, *J. Phys. Chem.*, **63**, 1347 (1959).

(6) F. J. C. Rossotti in J. Lewis and R. G. Wilkins, "Modern Coordination Chemistry, Principles and Methods," Interscience Publishers, New York, N. Y., 1960, p. 1.

TABLE I
 CALORIMETER DATA

Concn., mole/kg. water		Moles	No. of expts.	$-\Delta H$ dilution, ^a av., cal./mole	ϕ_L final, cal./mole	ϕ_L initial, cal./mole	Wt. factor	ϕ_L initial av.
Initial	Final							
3.981	0.09159	0.1682	2	420.7 ± 0.2	99.0	519.7	4.0	
3.981	.04570	.08411	3	445.9 ± 1.1	75.3	521.2	3.6	
3.981	.01516	.02775	3	469.0 ± 0.4	47.9	516.9	1.5	
3.981	.01643	.03028	1	469.3	49.6	518.9	0.4	519.8
2.856	.06864	.1262	3	304.9 ± 1.0	88.3	393.2	7.2	
2.856	.03426	.06297	2	326.7 ± 0.0	67.1	393.8	2.4	
2.856	.01129	.02082	2	354.8 ± 1.7	42.2	397.0	1.1	393.7
1.825	.04570	.08412	5	221.1 ± 1.1	75.3	296.4	11.0	
1.825	.02283	.04201	4	238.0 ± 0.5	56.9	294.9	4.4	
1.825	.00753	.01388	2	263.3 ± 1.8	35.3	298.6	0.5	296.1
1.338	.03419	.06297	2	188.4 ± 0.2	67.1	255.5		
0.8747	.02280	.04201	2	159.6 ± .1	56.9	216.5		
.6960	.01825	.03363	2	151.7 ± .3	51.7	203.4		
.5180	.01369	.02523	3	140.3 ± .4	45.8	186.1		
.3430	.00912	.01682	3	125.0 ± 3.0	38.6	163.6		

^a The average value and the maximum deviation from the average are given.

on the addition of silver nitrate. The first stock solution was standardized by evaporating to constant weight at 150° (found 3.976 and 3.974 *M*) and by converting to the sulfate and evaporating to constant weight (found 3.979 and 3.978 *M*). The molality used was 3.975. The second stock solution was standardized by evaporation to constant weight at 150° (found 3.982 and 3.981 *M*). The solutions were prepared by volumetric dilution of the stock solutions. The densities of all solutions were determined at 25° using a Westphal balance. The densities agreed with the results of Geffeken¹³ and Mazzucchelli and Rossi¹⁴ to within 0.1%.

The amount of water vapor in the air space of the calorimeter changes when the salts are mixed. The maximum air space was 10 ml. for the pipets and 110 ml. for the calorimeter vessel. Calculations showed that the correction for the heat of vaporization was less than 0.2 cal. per mole for all experiments.

Results

The results of the calorimetric measurements are given in Table I. In calculating the average of the runs, the results obtained from the first stock solution were weighted by a factor of one-half because several improvements in experimental equipment and technique were made after these runs were complete. The solutions prepared from the first stock solution were 0.15% lower in concentration. The concentrations of the solutions prepared from the second stock solution were used in the calculation of the results, except that the actual number of moles was used to calculate the heat of dilution. The error introduced in this way is less than 0.1%.

The measurements in Table I were combined to give a series of heats of dilution in the 0.1 to 0.007 *m* range. The extended Debye-Hückel equation

$$\phi_L = A\sqrt{m} \left(\frac{1}{1 + a\sqrt{m}} - \frac{\sigma(a\sqrt{m})}{3} \right) + Bm + Cm^{3/2} \quad (1)$$

where

$$\sigma(y) = \frac{3}{y^3} \left[1 + y - \frac{1}{1 + y} - 2 \ln(1 + y) \right]$$

and *A* is the Debye-Hückel slope (688 cal. moles^{-1/2}), was used to extrapolate the data to infinite dilution.

The constants *B* and *C* were evaluated by the method of least squares setting *a* = 1, using the experimental

data and eq. 1 for $\phi_L(m_1) - \phi_L(m_2)$. Owen and Brinkley¹⁵ and Guggenheim and Prue¹⁶ have used similar extrapolations (without the $Cm^{3/2}$ term) and shown that the equations fit the data for sodium chloride up to 0.1 *m*.

The experimental points were weighted according to the estimated accuracy of the data using 0.2% ± 0.03 cal. as the estimated standard deviation of single measurement. The results of the calculations which were performed with the aid of a Bendix G15D digital computer are given in Table II. Repeating the least squares fit with *a* = 1.6 changed the calculated values of apparent relative molal heat content by 0.15 cal./mole or less. Repeating the extrapolation with *a* = 1 and setting all of the weights equal to 1 changed the calculated values of relative apparent molal heat content by 1.0 to 2.5 cal. per mole. The extrapolation is probably good to ±2 cal./mole.

 TABLE II
 EXTRAPOLATION OF ϕ_L TO INFINITE DILUTION

Concn., moles/kg.		$-\Delta H$ dilution, cal./mole		Weighting factor
Initial	Final	Exptl.	Calcd. ^a	
0.09159	0.04570	25.2	23.7	1.90
.09159	.01516	48.3	51.1	1.10
.04570	.01516	23.1	27.4	1.00
.06864	.03426	21.8	21.2	1.80
.06864	.01129	49.9	46.1	0.94
.03426	.01129	28.1	24.9	0.75
.04570	.02283	16.9	18.4	3.10
.04570	.00753	42.2	39.9	0.48
.02283	.00753	25.3	21.5	.45
.09159	.01643	48.6	49.4	.32

^a Calculated by eq. 20 using the values *a* = 1.0, *B* = -318, and *C* = 531 calculated for a least squares fit.

The calculation of the values of ϕ_L at concentrations about 0.1 *m* is given in Table I. The values of the relative apparent molal heat content (ϕ_L) at the final concentrations were calculated from eq. 1 and the values *B* = -318 and *C* = 531 determined by the method of least squares. The values of the relative apparent molal heat content at the initial concentration were calculated from the heat of dilution and the final value of the relative apparent molal heat content.

(15) B. B. Owen and S. R. Brinkley, *Ann. N. Y. Acad. Sci.*, **51**, 753 (1949).

(16) E. A. Guggenheim and J. E. Prue, *Trans. Faraday Soc.*, **50**, 710 (1954).

(13) W. Geffeken, *Z. Physik. Chem.*, **B5**, 81 (1929).

(14) A. Mazzucchelli and A. Rossi, *Chem. Abstr.*, **21**, 3007 (1927).

The weighted averages of all determinations at each concentration are given in Table I.

The values of the relative apparent molal heat content (ϕ_L) and relative partial molal heat content (\bar{L}_2) at even concentrations given in Table III were calculated by a method similar to the one given by Scatchard and Epstein.¹⁷ The data were represented by the formula

$$\phi_L = A\sqrt{m} \left(\frac{1}{1 + a\sqrt{m}} - \frac{\sigma(a\sqrt{m})}{3} \right) + Bm$$

Values of B for $a = 2.0$ and $a = 1.4$ were calculated for each value of the relative apparent molal heat content (ϕ_L) given in Table I. The relative apparent molal heat content was evaluated at even concentrations by reading B from a plot of B vs. m . The average difference between values of the relative apparent molal heat content calculated from the plots for $a = 1.4$ and $a = 2.0$ was 0.6 cal. per mole. The relative partial molal heat content (\bar{L}_2) was evaluated from the same plot and the formula.

$$\bar{L}_2 = \frac{A\sqrt{m}}{1 + a\sqrt{m}} + 2Bm + \frac{m^{3/2}}{2} \left(\frac{dB}{dm} \right)$$

The average difference between values for the relative partial molal heat contents calculated from the plots for $a = 1.4$ and $a = 2.0$ was 3 cal. per mole. The values in Table III below 1 molal are from the $a = 2.0$ plot and the values for 1 molal and above are from the $a = 1.4$ plot.

TABLE III

VALUES OF ϕ_L , \bar{L}_2 , AND $T\Delta\bar{S}^E$ FOR LITHIUM PERCHLORATE AT 25°

Concn., moles/kg. of water	ϕ_L	\bar{L}_2	$T\Delta\bar{S}^E$
0.01	40	57	
.05	78	109	
.10	102	142	389
.20	134	187	460
.30	157	211	488
.40	172	227	494
.50	184	241	494
.60	195	253	489
.80	212	274	464
1.00	228	307	449
1.50	269	395	387
2.00	311	489	314
3.00	408	723	180
4.00	522	1011	93

As a check on this procedure the values of \bar{L}_2 at 0.01 and 0.05 molal were calculated using the least squares fit equation. The results were within ± 0.3 cal. per mole of the values determined from the plot of B vs. \sqrt{m}

(17) G. Scatchard and L. F. Epstein, *Chem. Rev.*, **30**, 211 (1942).

for $a = 2.0$. The values of $T\Delta\bar{S}^E$ given in Table IV were calculated using the activity coefficient measurements of Jones¹⁸ as revised by Robinson and Stokes⁸ and the formula

$$T\Delta\bar{S}^E = \bar{L}_2 - RT \ln (\gamma_{\pm})^{\mu}$$

Where $\Delta\bar{S}^E$ is the relative, non-ideal partial molal entropy, T is the absolute temperature, and γ_{\pm} is the mean molal activity coefficient.

Discussion

The heats of dilution of lithium perchlorate can be checked against the measurement of Austin and Mair,¹⁹ who measured the heat of dilution of 4.178×10^{-3} mole of 1 m LiClO₄ with 0.006267 mole of 0.01515 m LiClO₄. The result of Austin and Mair (167 ± 4 cal. per mole) is just barely consistent with the calculation from our data (153 ± 10 cal. per mole).

A plot of $T\Delta\bar{S}^E$ given in Table III vs. the square root of molality shows that lithium perchlorate is a "normal salt"; i.e., it fits the standard curves for $T\Delta\bar{S}^E$ given by Wood.⁵ The standard curves are characterized by the sum of the ion parameters ($P_+ + P_-$) for the two ions. For lithium perchlorate the sum of the ion parameters necessary to fit the data varies from 1.28 at low concentrations to 1.31 at high concentrations. Taking the average value of the sum of the ion parameters ($P_+ + P_-$) = 1.297 and subtracting the value for the lithium ion $P_- = 0.842^5$ gives a parameter for the perchlorate ion ($P_- = 0.455$). This value checks fairly well with the $P_- = +0.42$ estimated by Wood⁵ from a consideration of the size of the perchlorate ion.

Davies and co-workers²⁰ have collected ample evidence for the occurrence of incomplete dissociation in many aqueous salt solutions. It is just those salts that seem to be incompletely dissociated which do not fit the entropy correlation. The limited data which are available seems to indicate that for the oxy-anions, the smaller cations tend to be completely dissociated and at the same time fit the entropy correlation (HNO₃ and LiNO₃ vs. NaNO₃ and RbNO₃; LiClO₄ vs. NaClO₄; Mg(NO₃)₂ vs. Ba(NO₃)₂). Thus there may be a fairly large family of oxyanion salts of the smaller cations which do have "normal" entropies of dilution.

Acknowledgments.—The authors wish to thank the Research Corporation for a grant and Mr. Huibert Jongenburger for some helpful discussions of the heat leak corrections and Mr. Scott Boice for assistance with calculation of \bar{L}_2 .

(18) J. H. Jones, *J. Phys. Chem.*, **51**, 516 (1947).(19) J. M. Austin and A. D. Mair, *ibid.*, **66**, 519 (1962).

(20) C. W. Davies in W. J. Hamer "The Structure of Electrolytic Solutions," John Wiley and Sons, New York, N. Y., 1959, p. 19.

COMPARATIVE STUDIES OF PYROLYSIS OF ACETYLENE, VINYLACETYLENE, AND DIACETYLENE

By K. C. HOU AND ROBBIN C. ANDERSON

Department of Chemistry, The University of Texas, Austin, Texas

Received November 29, 1962

Since vinylacetylene and diacetylene are both straight-chain unsaturated compounds which might be significant intermediates in the pyrolysis of acetylene, a comparative study of the thermal reactions of these three compounds was made. Reaction patterns were determined in a flow system, using temperatures in the range of 500–800°, and mixtures of 25 mole % hydrocarbon in helium. Products were analyzed chromatographically. A reactor was also designed to discharge directly into a mass spectrometer, so that tests might be made for free radicals and the product gases also analyzed in the mass spectrometer. Good results were obtained in detecting methyl radicals formed in reaction of di-*t*-butyl peroxide and lead tetramethyl, but no evidence was found for any free radical fragments from the acetylenic compounds at temperatures up to 700°. Diacetylene was barely detectable in the low temperature reaction of acetylene, and no evidence was found to indicate it is a likely intermediate in the acetylene reactions under such conditions. Vinylacetylene is readily detected and shows appropriate reactivity, but little tendency to decompose to acetylene. It seems likely that it, like benzene, is a reactive side product rather than a key intermediate.

Certain results in recent years^{1,2} indicate that the pyrolysis of acetylene to form carbon involves straight-chain unsaturates as intermediates rather than aromatics. Since the initial stages of thermal reaction are second order, vinylacetylene is of interest as a possible intermediate in the first stages of reaction. However, hydrogen appears as an early product so diacetylene is another leading possibility; and there is also a question whether these might be secondary products resulting from a free-radical mechanism involving C₂H or C₂H₃. Cherton,³ for example, observed diacetylene bands in the spectra of polymerization products produced by a high-frequency discharge in acetylene, and Munson⁴ found vinylacetylene being formed and then reacting in the pyrolysis of acetylene at 500–850°.

Accordingly, a comparative study of the reactivity of these hydrocarbons was undertaken, with particular attention to mass spectrometric observations which might give some indications of the presence of free radicals. The temperature range (500–800°) and the concentrations (about 25 mole % hydrocarbon in helium) used were such as to span the range in which thermal reaction of acetylene changes from polymerization to decomposition.

Since this was started, Kinney and Slysh⁵ have reported finding diacetylene prominent in a flow system where carbon was formed from acetylene, and Greene, *et al.*,⁶ have found evidence for this also in shock-tube experiments on acetylene, but Skinner⁷ and Bradley and Kistiakowsky⁸ found evidence for vinylacetylene as intermediate in similar shock-tube experiments.

Experimental

Two types of experiments were used to compare reactions of the hydrocarbons.

(1) G. Porter, "Fourth International Combustion Symposium," Williams and Wilkins Co., 1954, p. 248.

(2) F. G. Stehling, J. D. Frazee, and R. C. Anderson, "Eighth Symposium (International) on Combustion," Williams and Wilkins Co., 1962, p. 774. For review of earlier work, see E. W. R. Steacie, "Atomic and Free Radical Reactions," 2nd Ed., Reinhold Publ. Corp., New York, N. Y., 1954; also G. J. Minkoff, *ref. 14*.

(3) R. Cherton, *Bull. soc. roy. sci. Liege*, **10**, 604 (1941).

(4) M. S. B. Munson, Dissertation for the Ph.D. degree, Univ. of Texas, 1959.

(5) C. R. Kinney and R. S. Slysh, "Proc. Fourth Conf. on Carbon," Pergamon Press, 1960, p. 301; *J. Phys. Chem.*, **65**, 1044 (1961).

(6) E. F. Greene, R. L. Taylor, and W. L. Patterson, *ibid.*, **62**, 238 (1958). *Cf. also Combust. Flame*, **5**, 55 (1961).

(7) G. B. Skinner, paper presented at American Chemical Society National Meeting, St. Louis, Mo., March 21–30, 1961.

(8) J. N. Bradley and G. B. Kistiakowsky, *J. Chem. Phys.*, **35**, 264 (1961).

Flow Reactor.—In one series, a flow reactor was used which consisted of a Vycor tube, 2 cm. in diameter and 32 cm. long, wrapped with coils of Nichrome wire and covered with asbestos to give temperature control. Temperature readings were made with a thermocouple in a well at the middle of the tube. These could be held within ±4° up to 1000°.

Flow rates of the gases were checked with capillary-type flowmeters and were reproducible within 2%. Diacetylene was introduced by vaporizing into a stream of helium at controlled temperatures. The total gas flow rate in the reactor was adjusted to 600 cc./min., giving a contact time of 9–10 sec.

The products of reaction were determined with a gas chromatograph. In one set of experiments liquid polymers were collected and analyzed both chromatographically and by mass spectrometer. These showed the usual very complex mixture of product including benzene, toluene, xylene, styrene, indene, naphthalene, biphenyl, and others. However, since the major interest here was in the earlier stages of reaction, usually the gaseous products only were checked.

Product gases were collected in a sampler tube on leaving the reactor and samples for analysis were taken from this by syringe. Three columns were used: with 40–60 mesh charcoal for measuring hydrogen and methane, with silica gel for light hydrocarbons, and with Reoplex 400 (Geigy Chem. Corp., Ardsley, N. Y.) for aromatic compounds (essentially benzene in these experiments).

In the second series of experiments, the mass spectrometer was used in an attempt to detect possible free-radical intermediates.

Reactor in Mass Spectrometer.—For the second series of experiments, a Consolidated Model 21-620 mass spectrometer was modified so as to permit detection of possible free radicals formed in reaction. A small reactor was installed in the sample path so that its exit was only about 2 mm. from the electron beam in the cycloid tube. This reactor was made of alumina tubing 2 mm. in diameter and 2 cm. long. It was heated by means of a resistance wire coil wrapped around the tubing. Johns-Manville refractory cement was used to give thermal insulation. The entire assembly was baked out at 1000° in an electric furnace before installing for a series of tests.

By changing the voltage across the heating coil, any desired temperature up to 800° could be obtained. The temperature in a run was determined from the power supplied to the heating system. This was calibrated by measurements made with a chromel–alumel thermocouple inserted into the reactor.

The electron beam energy of the C.E.C. 21-620 mass spectrometer is 70 v. under normal operating conditions. This is high enough so that any of the reagent and product molecules might be split in reactions occurring on electron impact. A diode clamping circuit was therefore installed to limit the maximum energy of the electron beam. This permitted decreasing the electron energy to as low as 6 v. Thus electron energies great enough to ionize free radicals already formed, but not so great as to give dissociation reactions, could be used. Measurement of the bias voltage, proportional to electron energy, was made with a Tektronix-type oscilloscope.

Materials.—To avoid explosion, mixtures of 25% hydrocarbon

in helium were used. The helium was U. S. Bureau of Mines Grade A. The acetylene was commercial acetylene, purified by bubbling through saturated sodium bisulfite solution and then drying.

The vinylacetylene was obtained commercially and then redistilled, scrubbed with sodium bisulfite and sodium hydroxide, and dried. Mass spectrometric analysis indicated about 95% purity, with ethylene as the other constituent.

The diacetylene was synthesized from 2-butyne-1,4-diol⁹ by a two-step process involving replacement of OH by halogen¹⁰ and dehydrohalogenation.¹¹

For the methyl radical tests, di-*t*-butyl peroxide of minimum purity 99% was supplied by the Lucidol Divis., Wallace and Tiernan, Inc. Tetramethyllead was recrystallized from toluene solution supplied by the Ethyl Corporation.

Results

Data showing the reactivity of the three reagent hydrocarbons in the flow reactor are given in Table I. The general order of decreasing reactivity is diacetylene > vinylacetylene > acetylene.

TABLE I

COMPARISON OF THE REACTIONS OF ACETYLENE, DIACETYLENE, AND VINYLACETYLENE

Temp., °C.	% of reagent pyrolyzing				
	400	500	600	700	800
Acetylene	0	22	48	73	92
Diacetylene	4	68	96	100	100
Vinylacetylene	0	28	66	97	100

Material balance for carbon

Temp., °C.	% of carbon recovered in the exhaust gases				
	400	500	600	700	800
Acetylene	190	97.6	89.2	75.2	41.0
Diacetylene	97.5	35.8	9.4	5.5	4.8
Vinylacetylene	100	99.0	35.0	9.5	6.4

Material balance of hydrogen

Temp., °C.	% of hydrogen recovered in various products in the exhaust gases				
	400	500	600	700	800
Acetylene	100	99.6	98.4	96.0	94.0
Diacetylene	100	42.6	22.6	27.6	34.8
Vinylacetylene	100	91.0	37.5	21.5	27.4

The gaseous products from pyrolysis of acetylene followed familiar patterns—hydrogen, methane, ethylene, acetylene, vinylacetylene, and benzene being the detectable ones. With diacetylene, the amount of gaseous products is less, benzene in particular being definitely decreased. With vinylacetylene, products were similar to those with acetylene, but with less benzene again and with traces of propylene and butadiene appearing.

The same order of reactivity was indicated by the appearance of the exhaust from the reactor. Diacetylene gives a black smoke, indicating appreciable carbon formation, at temperatures for which acetylene and vinylacetylene still give just a yellow or brown mist of polymeric products.

Some comparative data on products of reaction are given in Table II. Results for methane are similar to those for hydrogen and for ethylene to those for benzene.

(9) P. Pomerantz, A. Fookson, T. W. Mears, S. Rothberg, and F. L. Howard, *J. Res. Natl. Bur. Std.*, **52**, 51 (1954).

(10) A. W. Johnson, *J. Chem. Soc.*, 1009 (1946).

(11) J. B. Armitage, H. B. H. Whiting, and M. C. Whiting, *ibid.*, **44** (1951).

TABLE II
PATTERN OF PRODUCTS

Reagent	Mole % hydrogen found			
	500°	600°	700°	800°
C ₂ H ₂	0.0	1.2	2.8	8.4
C ₄ H ₂	0.0	0.5	1.5	3.0
C ₄ H ₄	0.0	0.3	1.8	5.6
Reagent	Mole % vinylacetylene found			
	500°	600°	700°	800°
C ₂ H ₂	1.0	2.0	1.0	0.3
C ₄ H ₂	0.4	0.2	0.0	0.0
C ₄ H ₄		8.5	0.8	0.0
Reagent	Mole % benzene found			
	500°	600°	700°	800°
C ₂ H ₂	0.8	1.2	2.4	2.0
C ₄ H ₂	0.12	0.2	0.5	0.2
C ₄ H ₄	0.0	0.0	0.15	0.1
Reagent	Mole % acetylene found			
	500°	600°	700°	800°
C ₂ H ₂	19.5	13.0	6.8	1.5
C ₄ H ₂	0.1	0.3	0.3	0.1
C ₄ H ₄		0.02	0.1	0.04

Addition of hydrogen increases products such as methane and ethylene and decreases carbon formation.

It is notable that diacetylene was not detected in the pyrolysis of vinylacetylene, and only traces are observed in the acetylene reaction. Benzene also is formed much less extensively by the C₄ hydrocarbons than by acetylene.

The preliminary tests with di-*t*-butyl peroxide and lead tetramethyl in the mass spectrometer gave clear evidence of CH₃ radicals, using an electron voltage of 10 e.v.—above the ionization potential of the methyl radical but not above the appearance potential for formation of CH₃⁺ from the parent molecule by electron impact. Typical results for lead tetramethyl, which seem to be in agreement with those of Hipple and Stevenson¹² are given in Fig. 1. Similar results were obtained with di-*t*-butyl peroxide, in general agreement with those of Lossing and Tickner.¹³ Comparison of the CH₄⁺ and CH₃⁺ peaks indicates that the sensitivity of the mass spectrometer in detecting the free methyl radicals is essentially the same in the present instrument as in theirs.

Thus the unit had sufficient sensitivity to detect free radicals formed from these hydrocarbons, but repeated tests, especially at mass 25, on all three compounds—using 15 v. and gas pressures of 60 μ—simply gave negative results.

Some tests were also made with the electron beam at 70 v. to see whether any unusual pattern of fragments might be observed in the reactor. Comparative values for mass 24 (C₂), mass 25 (C₂H), and mass 27 (C₂H₃) relative to the parent peak were checked carefully. The only possibly significant increase occurring in the reactor was found at mass 27; but it was also found that ethylene could be detected early in the reaction of acetylene and diacetylene as well as of vinylacetylene. Tests in a freshly cleaned reactor gave somewhat more ethylene; so this seems to involve a surface effect rather than the main gas-phase process.

An interesting sidelight is that, in the higher mass ranges in some tests, the amount of mass 52 (C₄H₄) appeared slightly greater than mass 50 (C₄H₂), but

(12) J. A. Hipple and D. P. Stevenson, *Phys. Rev.*, **63**, 121 (1943).

(13) F. P. Lossing and A. W. Tickner, *J. Chem. Phys.*, **20**, 907 (1952).

tests for either were quite faint under the conditions used.

Discussion

It is notable in these results that, although diacetylene and vinylacetylene are more reactive than acetylene, all show patterns indicating that reaction starts under the mild conditions used here by steps which must involve addition rather than decomposition. No evidence is found for any free radical such as C_2H or C_2H_3 .

The results also give no indication of the formation of diacetylene as a first stage in reaction of acetylene under mild conditions. The mass spectrometer tests did not indicate any mass 50 product before mass 52, etc., and in the gas chromatographic studies it may be seen that the production of hydrogen from acetylene is not commensurate with what should appear if the acetylene were reacting to form diacetylene.

At higher temperatures, and with different rates of activation such as can exist in the shock tubes, this pattern could be different. It would be interesting to see what results the shock tubes might give at comparable temperatures.

The general reactivity of vinylacetylene, both in pyrolysis as shown above and in interaction with acetylene,² is not inconsistent with a possible role as intermediate in acetylene reactions. However, if, as indicated by the results of Bradley and Kistiakowsky, there is a dimer (the "A" polymer) which establishes rapid equilibrium with acetylene, this could apparently not be vinylacetylene. The latter shows very little tendency to split to acetylene—even under conditions, such as the 600° tests, where vinylacetylene is clearly reactive and acetylene itself is still observable in readily detectable amounts. Vinylacetylene itself should apparently be considered, like benzene, as a reactive side product but not an essential intermediate. A dimer which is formed without rearrangement of hydrogen and which exists as an activated molecule or free radical is probably the actual intermediate in reaction.

It is also interesting to note that the mass spectrometer tests here give no support to the suggestion of Minkoff¹⁴ that excited states which form on the surface

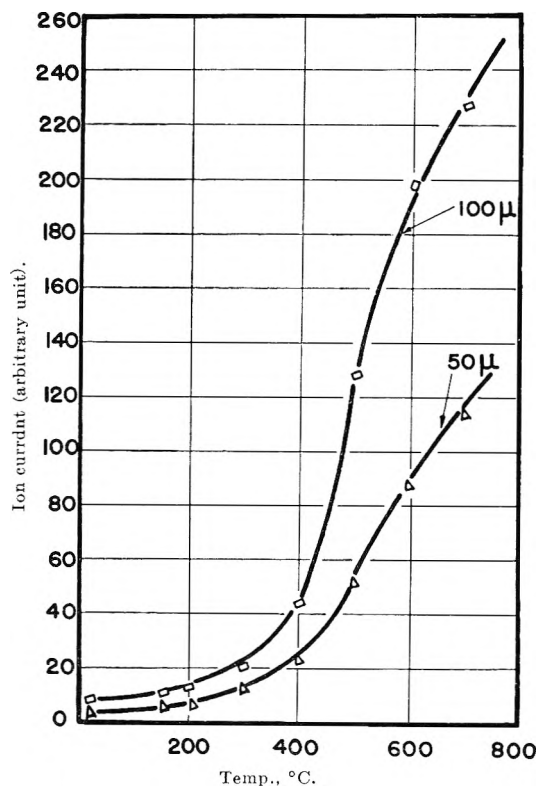


Fig. 1.—Temperature vs. ion current. Mass 15 from $Pb(CH_3)_4$ at 10 e.v.

and diffuse into the gaseous acetylene are essential in reaction. At the very low pressures used in the reactor in the mass spectrometer, there is definite evidence of surface activation and reaction, but with apparently a different pattern of products from that of the ordinary reaction and with no evidence of any active groups appearing in gas phase.

Acknowledgment.—This research was supported in part by a grant from the Petroleum Research Fund administered by the American Chemical Society. Grateful acknowledgment is hereby made to the donors of the fund, and also to the Office of Scientific Research, U. S. Air Research and Development Command, for support of the project in part.

(14) G. J. Minkoff, *Can. J. Chem.*, **36**, 131 (1958).

EFFECTS OF OXYGEN AND CHLORINE ON THERMAL REACTIONS OF ACETYLENE

BY M. S. B. MUNSON¹ AND ROBBIN C. ANDERSON

Department of Chemistry, The University of Texas, Austin, Texas

Received December 18, 1962

The effects of small percentages of added oxygen or chlorine on the thermal reactions of acetylene in the range of 200–800° have been measured in a flow reactor. The pattern of variation in reaction products was determined chromatographically. Variations with time were studied using a multistage reactor. Oxygen in small amounts increases the rate of decomposition. Chlorine decreases the initial rate, particularly of polymerization, but gives secondary reactions which enhance carbon formation.

The reactions of chlorine and oxygen with hydrocarbons have been extensively studied. The chlorine reacts in general to form chlorinated hydrocarbons² and the oxygen to form various oxygenated compounds leading eventually to carbon monoxide or carbon dioxide³.

However, there are still interesting questions about their reactions with a highly unsaturated hydrocarbon such as acetylene, particularly in the early stages. Rates of reaction first increase, then decrease as oxygen is added.⁴ Addition of chlorine and its compounds can increase the rate and extent of carbon formation from hydrocarbons. Halogenated compounds may also be used to extinguish flames⁵; but the presence of either oxygen or chlorine is a well known explosion hazard in the handling of acetylene.

The present experiments on the initial stages of reaction of acetylene with limited amounts of chlorine or oxygen were undertaken to see what further information on the reaction mechanisms might be obtained in particular by using the techniques of gas chromatography now available.

Experimental

The reaction was studied at atmospheric pressure in a flow system using two reactors. One was a flow reactor consisting of a Vycor cylinder 27 cm. long and 2 cm. in diameter, jacketed with a heating coil which could control the temperature within $\pm 4^\circ$ up to 900°. The second was a cylindrical Vycor reactor about 61 cm. long—of total volume of 232 cc.—wrapped in four equal sections with Nichrome wire and insulated with asbestos. Each section had a thermocouple well in the center and a sampling tube at the end, which extended to the center of the reactor. The temperatures were recorded by chromel–alumel thermocouples and were maintained within $\pm 4^\circ$ of the desired temperature by manual control of variable transformers connected to each section.

In this investigation a mixture of 20 mole % acetylene in helium was used as the basic reaction mixture. The helium was Bureau of Mines Grade A and was used without further purification. The acetylene was purified by passing it through an aqueous

sodium bisulfite solution and drying with calcium sulfate. Commercial oxygen was used directly from the cylinder and the chlorine was dried with calcium sulfate. All lines through which the chlorine passed were of copper, glass, or Teflon, and the glass tubing which contained chlorine and acetylene was painted black. The volume of gas going into the reactor was metered with orifice-type flowmeters whose orifices were kept at a constant temperature of $35 \pm 0.2^\circ$.

The samples for analysis were collected with a greased syringe from the flowing gas stream. Most of the products were determined by gas chromatographic methods and positive identification was made by mass spectrometric or infrared analysis except when chromatographic identification was unambiguous. Hydrogen chloride was determined by absorbing it in standard base.

Both reactors were aged by exposure to reacting hydrocarbon to build some surface deposit of carbon, etc., before use and thus to minimize variations due to surface reactions. The mixtures used here, with helium as diluent, gave smooth reaction, with no trouble from explosions. (Chlorine–acetylene mixtures without such a diluent are commonly explosive.)

The various mass spectrometric analyses were kindly done by Dr. F. C. Stehling of the Humble Oil and Refining Company.

Results

The compounds determined in acetylene pyrolysis were acetylene, hydrogen, methane, ethylene, vinylacetylene, and benzene. Mass spectrometric analyses of some high molecular weight polymers gave detectable amounts of hydrocarbons of mass as high as 254. Other compounds—possibly C₄'s—were detected, but not in sufficient quantities to identify. Thus no appreciable amount of diacetylene was found. *cis*- and *trans*-dichloroethylene and vinyl chloride were found, and small amounts of C₄H₂Cl₂ were detected mass spectrometrically. Of the oxygenated products, CO, CO₂, formaldehyde, acetaldehyde, glyoxal, and acrolein were identified.

Typical patterns of reaction products obtained with acetylene alone in helium are summarized in Fig. 1. Typical results obtained in the single-stage reactor with added chlorine or oxygen are given in Table I. This shows the changes in the ordinary products caused by addition of chlorine (or oxygen)

$$\Delta X = \% X \text{ (with Cl}_2\text{)} - \% X \text{ (without Cl}_2\text{)}$$

Effects of Addition of Chlorine.—It may be seen that chlorine inhibits the formation of the gaseous products (the measured disappearance of acetylene itself was also less). Up to 700° these effects are relatively of major importance. Above that, decomposition to hydrogen is not affected markedly, but inhibition of benzene and methane formation is still pronounced. Table II shows some data on the chlorinated products formed. At temperatures less than 400°, traces of free chlorine could also be detected, but none were detectable at higher temperatures.

(1) Research and Development Division, Humble Oil and Refining Company, Baytown, Texas.

(2) See, *e.g.*, E. W. R. Steacie, "Atomic and Free Radical Reactions," Vol. 2, 2nd Ed., Reinhold Publ. Corp., New York, N. Y., 1954, pp. 667, 671, 672, and 697.

(3) See, *e.g.*, B. Lewis and G. von Elbe, "Combustion, Flames, and Explosions of Gases," Academic Press, New York, N. Y., 1951, pp. 125–128.

(4) K. Hellwig, E. A. Westbrook, and R. C. Anderson, "5th Sympos. (Internat.) on Combustion," Reinhold Publ. Corp., New York, N. Y., 1955, p. 631; W. W. Robertson and F. A. Matsen, *Combust. Flame*, **1**, 94 (1957); F. C. Stehling, J. D. Frazee, and R. C. Anderson, "6th Sympos. (Internat.) on Combustion," Reinhold Publ. Corp., New York, N. Y., 1957, p. 247.

(5) R. F. Simmons and H. G. Wolfhard, "The Structure of Chlorine Flames," Tech. Note No. R.P.D. 150, Jan., 1957 (Royal Aircraft Establishment, Farmborough, Hants, England); W. A. Rosser, H. Wise, and J. Miller, "7th Sympos. (Internat.) on Combustion," Reinhold Publ. Corp., New York, N. Y., 1958, p. 175; G. B. Bachman and H. I. Berman, *Ind. Eng. Chem.*, **52**, 621 (1960).

TABLE I
EFFECTS ON PRODUCTS OF PYROLYSIS
(200 cc./min., 20% C₂H₂ in helium)

T, °C.	ΔC ₆ H ₆	ΔC ₄ H ₄	ΔC ₂ H ₄	ΔCH ₄	ΔH ₂
Chlorine (1-2%)					
500	-0.2	-0.1
600	-0.8	-.2
700	-1.6	(+.03)	-0.4	-0.3	-0.3
800	-1.0	(+.01)	+.1	-.5	-.1
Oxygen (3.5%)					
400	+0.1	(+0.03)	+0.1	...	+0.2
500	(+0.02)	(+.01)	+.2	+0.2	+.4
600	-0.3	-.1	+.5	+.4	+.9
700	-1.0	-.1	+.3	+.8	+.9
750	-1.3	-.1	+.2	+.9	+.3

TABLE II
CHLORINATED REACTION PRODUCTS
(200 cc./min., 20% C₂H₂, 1-2% Cl₂ in helium)

T, °C.	% HCl	% C ₂ H ₃ Cl	% <i>trans</i> -C ₂ H ₂ Cl ₂	% <i>cis</i> -C ₂ H ₂ Cl ₂
200	0.84	0.51
25070	.60
300	..	0.04	.54	.68
350	0.25	.07	.51	.67
400	.65	.11	.46	.62
450	.47	.13	.39	.55
500	.96	.14	.37	.48
550	.94	.20	.32	.44
600	1.17	.21	.26	.37
650	1.62	.26	.22	.35
700	2.16	.33	.10	..
750	2.95	.18
800	2.65	.09
850	2.62

At room temperature the reaction proceeded almost entirely to form *trans*-dichloroethylene. Above 350°, the ratio (*cis*-dichloroethylene)/(*trans*-dichloroethylene) was approximately the equilibrium value. At 300° the amounts of *cis*- and *trans*-dichloroethylene were independent of acetylene concentration if the acetylene was in excess of the one-to-one stoichiometric ratio. At 600°, however, the amount of the dichloroethylenes increased markedly with increasing acetylene concentration even after (C₂H₂/Cl₂) = 1.

Since there were relatively large amounts of dichloroethylenes present in the reaction mixtures, the effects of dichloroethylene added initially were studied. An initial concentration of 3.5% *cis*-dichloroethylene prevented benzene formation at 650°. The isomerization equilibrium was nearly achieved and the extent of decomposition was appreciable (*t* ~ 4 sec.). At about 550° for times of 5 to 10 sec., the decomposition of dichloroethylene became noticeable. The presence of acetylene seemed to enhance the rate of isomerization of dichloroethylene at relatively low temperatures.

Effects of Addition of Oxygen.—As shown also in Table I, the effects of oxygen were quite different from those of chlorine. Below 550° oxygen accelerated the entire reaction. Above 550°, oxygen inhibited formation of polymers such as vinylacetylene and benzene, but it still increased decomposition. Table III shows the oxygenated products measured. A very small amount of water was also formed, and there was an appreciable polymeric residue in the form of gum at

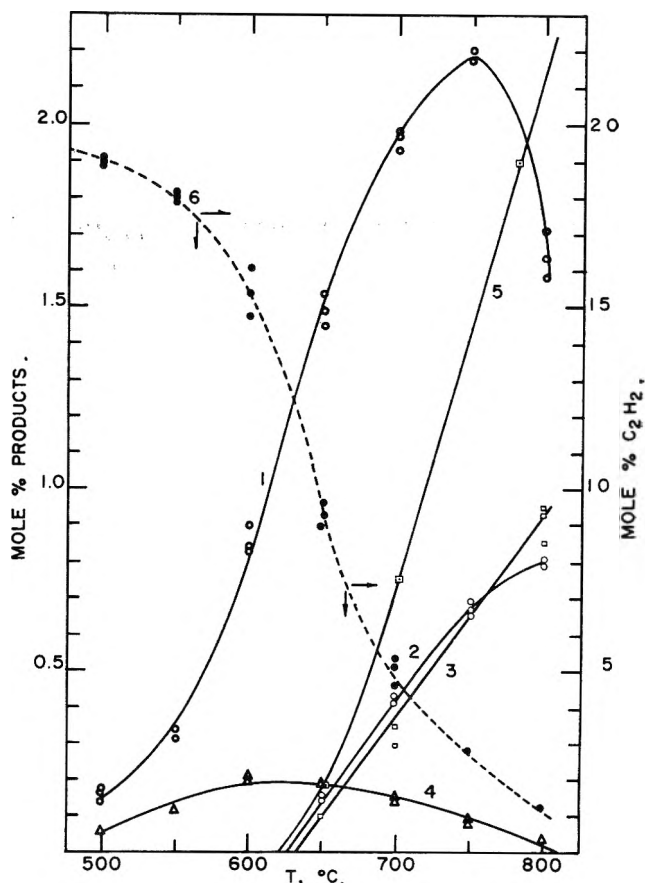


Fig. 1.—Acetylene pyrolysis (20% C₂H₂, 200 cc./min.): 1, C₆H₆; 2, C₄H₄; 3, CH₄; 4, C₂H₂; 5, H₂ (curve 1-5, left scale); 6, C₂H₂ (right scale).

lower temperatures (600°). No evidence for peroxides was found.

TABLE III
OXYGENATED REACTION PRODUCTS
(200 cc./min., 20% C₂H₂ and 3.5% O₂ in helium)

T, °C.	% CO	% CO ₂	% O ₂	A ^a	B ^a
300	..	0.03	3.3	..	0.54
350	1.9	.25	1.5	0.25	0.66
400	4.2	.35	..	.61	1.00
450	5.2	.33	..	.85	0.83
500	5.6	.35	..	.90	.64
550	5.6	.40	..	1.00	.60
600	6.4	.40	..	0.97	.42
650	6.8	.40	..	.62	.20
700	7.0	.35	..	.31	..
750	7.0	.36	..	.10	..
800	6.9	.38

^a A is a mixture of formaldehyde and acetaldehyde—mostly formaldehyde; B is a mixture of glyoxal and acrolein—mostly glyoxal. Relative values; absolute values of the order of tenths of 1%.

Additional experiments were made with some of the oxygenated products as additives—*i.e.*, water, glyoxal, and formaldehyde—to test their effects as possible intermediates. Pyrolysis of acetylene-helium-water mixtures from 600 to 800° gave very little CO, and there was a slight inhibitory effect on the formation of benzene. There was no evidence of appreciable amounts of acetaldehyde (from the addition of water to acetylene).

Addition of glyoxal caused a slight inhibitory effect on benzene formation but accelerated ethylene formation in the pyrolysis of acetylene. Some formaldehyde

apparently was formed from the mixture of acetylene-helium-glyoxal at 700°.

At 600° the effect of formaldehyde on benzene formation was erratic; at 700 and 800°, however, benzene formation was retarded. Under all conditions the addition of formaldehyde promoted the formation of ethylene. There were no appreciable amounts of acrolein (from addition of formaldehyde to acetylene). At 600° formaldehyde-helium mixtures gave little CO, indicating largely polymerization; at 800° large amounts of CO were formed, indicating extensive decomposition.

Experiments in Multistage Reactor.—For the experiments in the multistage reactor, mixtures containing 20.2 ± 0.5 mole % acetylene in helium were used with a constant initial flow rate of 500 cc./min. (at STP), thus giving time intervals of approximately 2 sec. for each stage. Results of these experiments were consistent with others in which the reaction time was varied by changing flow-rates in the single-stage reactor.

The effects of different concentrations of added oxygen at 600° are shown in Table IV. Data on oxygen compounds formed are given in Table V. Very little water was detectable. Here again the relative order of appearance of glyoxal and formaldehyde is interesting.

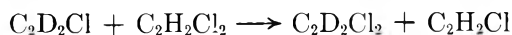
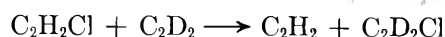
TABLE IV
STAGES IN EFFECTS OF VARIOUS OXYGEN CONCENTRATIONS
 $F_0 = 500$ cc./min., 20% C_2H_2 , 600°

% O ₂	Stage 1	Stage 2	Stage 3	Stage 4
	% C ₄ H ₄			
0.00	0.21	0.24	0.25	0.27
2.5	.20	.21	.21	.21
5.3	.21	.21	.21	.21
	% C ₆ H ₆			
0.00	0.20	0.30	0.37	0.50
2.5	.31	.38	.47	.54
5.3	.37	.48	.54	.60
	% H ₂			
0.00	0.00	0.00	0.00	0.00
2.5	.41	.48	.54	.61
3.9	.79	.84	.90	.96
	% CH ₄			
0.00	0.00	0.00	0.00	0.00
2.5	.10	.14	.16	.18
3.9	.23	.26	.30	.33
5.3	.46	.51	.49	.54

Table VI shows comparative data for the effects of added chlorine and oxygen on formation of benzene and vinylacetylene and data for the chloroethylenes are given in Table VII.

It may be noted again that the chlorine shows an inhibitory effect, in general contrast to oxygen. The pattern is somewhat variable for vinylacetylene, but it is clear-cut in the rate of appearance of benzene and of disappearance of acetylene.

Exchange Experiments.—Because both chlorine and dichloroethylene (under conditions of isomerization and decomposition) inhibited acetylene polymerization and both would be expected to give the C_2H_2Cl radical, a short experiment was done to see if a process such as



occurred.

Two experiments were carried out with a mixture of 53% $C_2H_2Cl_2$ and 47% C_2D_2 at approximately 80 mm. pressure—heating them in a closed tube of about 20–30 cc. total volume at 600° for 15 min. and an hour. There was extensive evidence of reaction under these conditions as evidenced by a shiny black deposit (carbon) on the walls of the tube.

The products after reaction were analyzed mass spectrometrically and the data are summarized in

TABLE V
OXYGENATED REACTION PRODUCTS
20% C_2H_2 , 2.5% O₂

T, °C.	Stage 1	Stage 1	Stage 3	Stage 4
	% CO			
500	2.7	2.8	2.8	2.9
600	3.1	3.2	3.4	3.4
700	4.7	5.1	5.1	5.2
800	5.5	5.7	5.8	5.8
	% CO ₂			
600	0.17	0.17	0.18	0.18
700	.18	.20	.19	.19
800	.14	.15	.16	.16
	A ^a			
500	0.43	0.53	0.54	0.58
600	0.87	.92	.96	.99
700	1.00	.86	.75	.61
800	0.45	.21	.13	.00
	B ^b			
500	0.60	0.81	0.90	1.00
600	0.20	0.14	0.11	0.00

^a A = mostly CH₂O + small amount of CH₃CHO, relative concentrations (actual values of the order of tenths of a per cent).

^b B = mostly $\begin{array}{c} \text{O} \quad \text{O} \\ \parallel \quad \parallel \\ \text{HC}-\text{CH} \end{array}$ + small amount of CH₂=CH-CHO, relative concentrations (actual values of the order of tenths of a per cent). The concentrations of A and B are comparable, so it may be noted that glyoxal appears first.

TABLE VI
TIME DEPENDENCE OF BENZENE AND VINYLACETYLENE
 $F_0 = 500$ cc./min., 20% C_2H_2 , 2.5% O₂, or 1% Cl₂

Stage	C ₂ H ₂ -He	C ₂ H ₂ -He-O ₂	C ₂ H ₂ -He-Cl ₂
	% C ₆ H ₆ , 700°		
1	0.90	0.74	0.34
2	1.71	0.98	.59
3	2.08	1.32	.88
4	2.29	1.38	1.13
	800°		
1	2.33	1.93	1.02
2	2.72	2.22	1.54
3	2.70	2.25	1.64
4	2.68	2.20	1.71
	% C ₄ H ₄ , 700°		
1	0.40	0.28	0.32
2	.27	.22	.33
3	.22	.20	.32
4	.20	.17	.28
	800°		
1	0.34	0.30	0.40
2	.17	.17	.21
3	.09	.12	.16
4	.05	.05	.10

TABLE VII

TIME DEPENDENCE OF DICHLOROETHYLENES

$F_0 = 500$ cc./min., 20% C_2H_2 , 0.5-1% Cl_2

Stage	% <i>trans</i> - $C_2H_2Cl_2$	% <i>cis</i> - $C_2H_2Cl_2$
400°		
1	0.13	0.16
2	.12	.19
3	.12	.18
4	.12	.19
500°		
1	0.10	0.13
2	.11	.14
3	.11	.16
4	.11	.15

Table VIII. The ratio of the concentration of masses 96:98:100 represents the ratio of the concentrations of $C_2H_2Cl^{35}Cl^{35}$: $C_2H_2Cl^{35}Cl^{37}$: $C_2H_2Cl^{37}Cl^{37}$. The theoretical ratio, assuming the natural isotopic distribution for chlorine, is

$$96:98:100 = 1.00:0.652:0.106$$

For the unreacted mixture this ratio was 1.00:0.647:0.106, and no change was found for time up to one hour. No C_2D_2Cl was found, since deuteration would have increased the relative concentration of the 98 and 100 species. Very little DCl was formed, the ratio of DCl/HCl being 0.05 after 15 min. and 0.07 after 1 hr.

TABLE VIII

EXCHANGE EXPERIMENTS

47% C_2D_2 -53% $C_2H_2Cl_2$

600°

	15 min.	1 hr.
96:98:100	1.00:0.644:0.106	1:00:0.648:0.106
C_6H_6		
78:79:80:	0.21:0.54:0.95:	0.18:0.61:1.00:
81:82:83:84	1.00:0.78:0.40:0.10	0.95:0.54:0.16:0.03
C_6H_5Cl	All deuterated products present	All deuterated products present
$C_6H_4Cl_2$	No $C_6D_4Cl_2$; some $C_6H_4Cl_2$	No $C_6D_4Cl_2$; some $C_6H_4Cl_2$

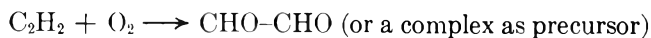
The isotopic distribution of hydrogen and deuterium in the benzene formed complicated the picture even more; the data recorded represent the ratios of concentrations of the various deuterated species and are only slightly skewed from random in favor of H-containing species. Some chlorobenzene was found as well as dichlorobenzene. Fragmentation of the dichloroethylene in the mass spectrometer prevented any analysis of vinyl chloride; there was no $C_4H_4Cl_2$ formed and no methane.

Discussion

The results clearly indicate that the first stage of reaction under relatively mild conditions is addition for both chlorine and oxygen—the chlorine to form dichloroethylenes and the oxygen glyoxal. Chlorine adds more readily than oxygen, reaction being essentially complete in a few seconds even at 300-400°; oxygen addition is measurably slower under these conditions. The basic difference in attack by the two reagents is illustrated by the nature of the ultimate reaction products—carbon and hydrogen chloride for a 1:1 mixture of acetylene with chlorine, and carbon

monoxide and hydrogen for a 1:1 mixture of acetylene with oxygen—and is consistent with the differences in electronic patterns for O_2 and Cl_2 .

The reaction products, etc., for oxygen indicate an intermolecular reaction as suggested by earlier workers^{3,4}



This mechanism can reasonably explain the acceleration of the polymerization and decomposition reactions of acetylene since these tend to be accelerated by any source of free radicals.⁵ In this case a reaction



is a likely factor. At higher concentrations and limited pressures, these reactions should begin to interfere with decomposition of acetylene to form carbon because of splitting of the acetylene molecule. This is consistent with effects observed from addition of oxygen in decomposition flames.⁴ However, if concentrations and pressures increase, they could also cause accelerated reaction and thus explosion.

The tendency for chlorine to react first to form *trans*-dichloroethylene indicates a mechanism of reaction similar to that suggested by Vaughan and Rust for ethylene⁶



The $C_4H_4Cl_2$ observed may then be a product of combination of C_2H_2Cl radicals. *cis*-Dichloroethylene is possibly formed by a slower, molecular reaction of acetylene and chlorine, but it might also involve just a less favorable and slower atomic reaction.

At higher temperatures, step 4 may become a hydrogen-extraction reaction



but the results here indicate that this must have a higher free energy requirement than other possible steps. It is notable also that HCl appears to form by decomposition of halogen compounds. It appears after the chloroethylenes in general; and the experiments with $C_2H_2Cl_2$ and C_2D_2 show HCl rather than DCl even though the isomerization and decomposition reactions occurring are highly likely to involve Cl atoms.⁷

The pronounced inhibitory effect of chlorine—which is 100% effective in stopping benzene formation at 500°, 80% at 750°, and 56% even at 800°—is difficult to explain.⁸ It should be noted that the effect is observed well after molecular chlorine is no longer detectable in the system and that inhibition can also be obtained on addition of dichloroethylene.

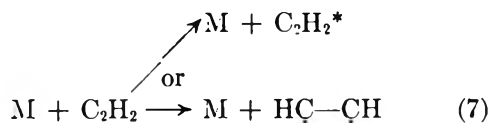
Since the polymerization steps are most strongly

(6) W. E. Vaughan and F. F. Rust, *J. Org. Chem.*, **5**, 449 (1940).

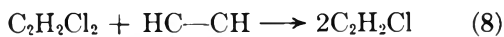
(7) A. M. Goodall and K. E. Howlett, *J. Chem. Soc.*, 3092 (1956).

(8) Cf. also C. F. Cullis, G. J. Minkoff, and M. A. Nettleton, *Trans. Faraday Soc.*, **58**, 1117 (1962).

inhibited, and since these must start from an activation step of the type



some reaction with this activated molecule or diradical is probably involved in the inhibition. Reaction with the dichloroethylene itself



is evidently not significant, because this should give ready exchange in a $\text{C}_2\text{H}_2\text{Cl}_2$ mixture with C_2D_2 and this was not observed. It is more likely therefore that inhibition is caused by the presence of chlorine atoms, either from chlorine or a chloro compound, which form $\text{C}_2\text{H}_2\text{Cl}$ with the diradicals (as in eq. 4) or react with polymeric free radicals and thus interfere with simple polymerization.

At higher temperatures, secondary decomposition reactions such as



should become significant. The chloroacetylene formed should be extremely reactive and decompose readily to Cl atoms and C_2H . Reaction 4—and even more reaction 5—tends to decrease net energy build-up in the acetylene reactions by interfering with combination steps which would release much more energy. If, on the other hand, reaction 6 (or less likely (9)) begins to occur, C_2H radicals, which may be expected to be extremely reactive, are introduced into the system. The fluctuating balance which is possible between such steps for different concentrations and temperatures should serve to explain the difficulties, in practical reaction systems, of predicting whether chlorine may serve as an inhibitor or whether it may cause explosion.

Acknowledgment.—This research was supported in part by a grant from the Petroleum Research Fund administered by the American Chemical Society. Grateful acknowledgment is hereby made to the donors of the fund, and also to the Office of Scientific Research, U. S. Air Research and Development Command, for support of the project in part.

THE VAPOR PRESSURE OF SCANDIUM METAL¹

BY OSCAR H. KRİKORIAN

Lawrence Radiation Laboratory, University of California, Livermore, California

Received December 10, 1962

The vapor pressure of Sc metal was measured by the Knudsen effusion technique at temperatures of 1200 to 1570°. Its enthalpy of sublimation at 298°K. was found to be 91.2 ± 0.3 kcal./g.-atom from a third-law treatment, and 91.1 ± 1.6 kcal./g.-atom from a second-law treatment of the data. High-temperature thermodynamic functions of Sc metal were estimated.

Introduction

Methods have recently been developed for preparation of pure Sc metal, and a number of its properties have been measured.² Its enthalpy of sublimation is of interest for determining the effect of d electrons on bonding energies. The enthalpy of sublimation has been derived previously from vapor pressure measurements by a number of workers. Spedding, Daane, Wakefield, and Dennison² measured the vapor pressure of Sc by the Knudsen effusion technique and determined the ΔH_{298}° of sublimation to be 80.8 kcal./g.-atom. Ackermann and Rauh,³ employing both conventional Knudsen techniques and detection with a mass spectrometer, found ΔH_0° equal to 79.7 kcal./g.-atom. Monatomic Sc was the only detectable species. Karelin, Nesmeyanov, and Priselkov⁴ found 82.3 kcal./g.-atom for ΔH_{298}° from Knudsen studies by using both radioactive and nonradioactive samples. They collected deposits on quartz collectors and analyzed them by radioactive counting or photometric techniques.

Experimental

Scandium metal in the form of arc-melted buttons was procured from American Scandium Corporation. The metal had

(1) Work was performed under the auspices of the U. S. Atomic Energy Commission.

(2) F. H. Spedding, A. H. Daane, G. Wakefield, and D. H. Dennison, *Trans. Met. Soc. AIME*, **218**, 608 (1960).

(3) R. J. Ackermann and E. G. Rauh, *J. Chem. Phys.*, **36**, 448 (1962).

(4) V. V. Karelin, An. N. Nesmeyanov, and Yu. A. Priselkov, *Dokl. Akad. Nauk SSSR*, **144**, 352 (1962).

been purified by vacuum distillation from a Ta crucible and was stated to be 99.8% pure. Spectroanalysis showed the principal metallic impurities to be 0.01% each of Ca, Al, Y, Ta, Fe, Cu, and Pb. Vacuum fusion analysis was performed at 1900° in a Pt bath in graphite on two 80-mg. samples from the Sc ingot used for the vapor pressure determinations. Results were 0.030% H_2 , 0.066% O_2 , and 0.005% N_2 .

The Sc was prepared for use by cutting it into chips 0.5 to 2 mm. across with a steel chisel in an Ar atmosphere drybox. The chips were stored in the box until ready for use. Reactivity of Sc with air was determined by placing a 32-mg. sample of Sc filings having 2 cm.² of surface area on the pan of a semimicro balance and checking the weight over a 16-hr. period. No weight change was detected. The filings then were placed in a drying oven at 110° for an additional 16 hr. A weight gain of 0.08 mg. took place. It was assumed that for the short times required for the handling of Sc in air, oxidation would be negligible.

Three different Knudsen cells were used. They are designated as K-I, K-II, and K-III. Cell bodies for K-I and K-II were made up as cylindrical crucibles formed by drawing from Ta sheet 1.3 mm. thick. Lids for K-I and K-II were made from Ta sheet 1.6 mm. thick. The lids were recessed to allow a snug fit. Knife-edged orifices of 0.2965 and 0.1763-cm. diameter were used for cells K-I and K-II, respectively. The cell body and lid for K-III were machined from Ta bar stock. The lid for K-III was made to telescope all the way down around the outside of the cell body. A small conical protrusion was machined on the center of the bottom of the inside of the cell. This provided a closer approach to blackbody conditions by increasing the contribution of reflected light from the interior of the cell. The orifice for cell K-III was a cylindrical channel, 0.0993 cm. in diameter and 0.019 cm. long. Conical channels were used above and below the orifices for all of the cells. The cone angles were 30° from the orifice planes (see Fig. 1).

An inductively heated Ta assembly was used to heat the cells. The heater was 3.8 cm. in diameter and 3.3 cm. high with walls 1.0 cm. thick. A cell was placed inside of a Ta crucible which in turn was placed in the heater. Contact between crucible and cell was reduced by means of Ta foil spacers. Nine Ta shields were placed above cells K-I and K-II, and two Ta shields were placed above cell K-III. The heater extended over part of the top shield in each case, but the 30° cone angle was left unobstructed. A 2.0-cm. diameter hole was left on the bottom of the heater. The placement of cell K-III in the heater assembly is illustrated in Fig. 1.

The vacuum system was made of brass tubing with an i.d. of 10 cm. It was about 1 m. long and had assorted flanged connections and outlets. Hycar rubber O-rings and gaskets were used. Vacuum was provided by a 300-l./sec. oil diffusion pump backed by a 7-l./sec. mechanical pump. A 10-cm. diameter gate valve and a liquid nitrogen trap were located above the diffusion pump. Pressures were measured with a Bayard-Alpert type ionization gage located between the trap and the furnace section. The base pressure of the system was 2×10^{-7} mm.

The furnace jacket was made of a double-walled quartz tube 28 cm. long with an i.d. of 8 cm. Cooling water was circulated between the walls. The end surfaces of the quartz tube were ground flat, and vacuum seals were made with the rest of the line by using O-rings against the surfaces. The Knudsen cell and heater assembly were supported on a molybdenum stand (see Fig. 1).

A glass prism shielded with a shutter was provided above the cell for temperature sightings. Temperatures were measured with a Leeds and Northrup disappearing-filament-type optical pyrometer. Corrections for the pyrometer were determined with a pyrometric standard lamp certified by the National Bureau of Standards in April, 1960. Corrections for prism transmission were checked before and after the runs, and no appreciable change was noted.

Power for induction heating was supplied by a 15-kw. output, 10,000-c.p.s. motor generator. The power was regulated by sensing the current in the tank circuit with a toroidal coil, and by using a servomechanism to maintain this current constant during a particular run. Regulation was adequate to eliminate short-term fluctuations. Long-term drifts of about $\pm 4^\circ/\text{hr.}$ were compensated for by manual corrections in the power.

Procedure and Results

Heater and cell components were outgassed in several heatings at 1900 to 2100° for about 4 hr. During this treatment, the line pressure dropped from 5×10^{-5} to 5×10^{-6} mm. and the weight loss rate of the cell-crucible assembly decreased from 50 to < 2 mg./hr. The outgassing pressure and outgassing rate both dropped to negligible values at the temperatures of the vapor pressure measurements. During the initial outgassing heatings, the Ta parts had a tendency to stick together. After outgassing, only a slight sticking tendency remained. A sharp rap of the assembly against a flat plate readily separated the sticking parts. The separation had no detectable effect on the weights of the components. After outgassing, heater and cell components were stored *in vacuo* and taken out only for sample loadings and for weighings.

Runs were made by the following procedure. Approximately 0.5 g. of Sc was weighed into a cell. The cell was sealed by forcing the lid on with a manual arbor press. Times and temperatures were selected to allow approximately 10 mg. of weight loss for each heating. The cell was initially heated to $\sim 1000^\circ$ in about 15 min. and then raised to the final heating temperature in about 2 min. The line pressure rose momentarily to $\sim 2 \times 10^{-6}$ mm. as the final temperature was approached, and then dropped off to $\sim 3 \times 10^{-7}$ mm. Heat-up and cool-down rates were noted, and end corrections were applied to the results. Temperatures for each run were averaged on an equal time interval basis. Weight changes were determined on the cell-crucible assembly after removal from the heater. Weight changes of the shields were also checked and found to be negligible.

Cell interiors were examined after each series. Mass transfer to the underside of the lid was noted in all cases. The orifices and channels, however, were free of condensate. The mass transfer was negligible for cell K-I, intermediate for K-II, and extensive for K-III. The trend is believed to be a function of orifice area, since smaller orifices require longer heating times for a given temperature and weight loss. An estimate of the temperature difference between cell lid and bottom may be made for

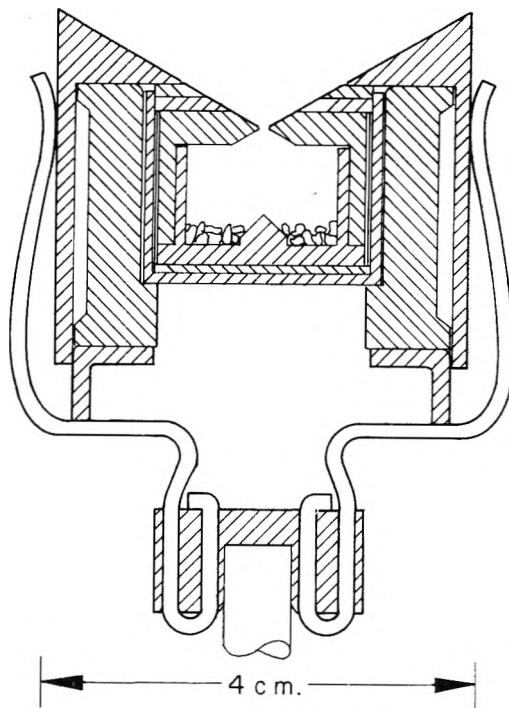


Fig. 1.—Scaled drawing illustrating placement of cell K-III in the heater assembly.

cell K-III. The cell temperature is assumed to be 1700°K. since most of the weight loss occurred at this approximate temperature (see Table I). From the Knudsen relation⁵ and the data of Table I, the vaporization rate of Sc is calculated to be 5.3×10^{-3} g./cm.²-min. at 1700°K. This gives an effective time of 580 min. for the accumulated weight loss of 28.73 mg. The condensate under the lid weighed ~ 280 mg. Using 1.5 cm.² for the cross-sectional area of the cell, this leads to a net transfer rate of 3.2×10^{-4} g./cm.²-min. from cell bottom to lid, and corresponds to a temperature differential of 3.0°K. at 1700°K.

TABLE I
SCANDIUM VAPOR PRESSURE DATA

Temp., °K.	Time, min.	Weight loss, mg.	$-\log p_{\text{atm}}$	ΔH_{298}° , kcal./g.-atom
Cell K-I				
1555.4	110.5	9.57	5.545	89.34 ^a
1797.1	46.1	103.79	4.100	90.85
1795.0	20.4	45.05	4.109	90.83
1525.8	70.6	2.11	6.011	90.96
1585.2	94.0	8.22	5.537	90.95
1583.6	91.1	7.63	5.556	91.00
1477.5	624.2	7.60	6.408	90.85
Cell K-II				
1690.0	49.5	10.49	4.693	90.22 ^a
1731.2	42.8	10.86	4.609	91.69
1686.0	75.7	9.41	4.925	91.81
1507.4	858.2	4.15	6.358	92.29 ^a
1568.1	300.3	4.42	5.866	92.37 ^a
1838.3	21.8	28
Cell K-III				
~ 1600	...	4.29
1719.0	126.1	8.86	4.598	90.97
1685.7	151.3	5.93	4.856	91.26
1593.6	338.1	3.07	5.502	91.17
1761.9	59.9	6.58	4.399	91.55

Av. 91.16 \pm 0.07

^a These runs are given zero weight for reasons discussed in text.

(5) J. L. Margrave, "Vapor Pressure," Chapter 10 in "Physicochemical Measurements at High Temperatures," edited by J. O'M. Bockris, J. L. White, and J. D. MacKenzie, Butterworths Scientific Publications, London, 1959, pp. 225-246.

Tantalum pick-up by Sc was determined by chemical analysis. Tantalum contents of 3.2, 18, and 4.0% were found for Sc in the bottom of cells K-I, K-II, and K-III, respectively. The high value for K-II resulted from melting of the Sc during the last measurement with this cell. An analysis of the condensate beneath the lid of K-III gave 4.6% Ta. Metallographic examination of the cell cross sections showed only a superficial attack of the Ta by Sc. The extensive attack reported by Spedding, *et al.*,² at temperatures above 1475° was not confirmed. It is believed that the preliminary outgassing of the Ta rendered it inert to attack by Sc. Spectroanalysis of a typical sublimate from K-I showed 0.1% Si (probably from the quartz jacket) and 0.01% each of Ca, Cu, and Y. An X-ray diffraction pattern of the sublimate showed h.c.p. Sc present as a single phase.

The effect of oxygen contamination on the volatility of Sc metal has been considered by Ackermann and Rauh.³ They point out that the volatility of ScO is several orders of magnitude lower than for Sc. They also indicate that solution of oxide in the metal or formation of a surface film of oxide may be factors that lower the rate of sublimation of Sc. The effect of solubility is believed to be small. Application of Raoult's law indicates at most a few tenths of 1% decrease in pressure. Large departures from Raoult's law are unlikely because of the small amount of oxide available for solution. Surface oxidation is negligible with the vacuums used. For a cell with 0.01 cm.² orifice area and a sample with 5 cm.² surface area, the oxidation rate is limited by the vacuum to less than a thickness of 10⁻⁸ cm. in 10 hr. Oxidation rates during handling in air are also believed to be small. Since no weight change was detected with a semimicro balance after 16 hr. in room temperature air, the oxidation rate was less than 0.2 μg./cm.²-hr. This does not preclude rapid formation of a thin film of oxide during handling, but such a thin film would not be expected to provide an effective diffusion barrier at 1200° in a Knudsen cell. Indeed, variation of orifice area over an order of magnitude showed no significant change in the apparent vapor pressure of Sc, which indicates that the cell was saturated with the equilibrium vapor pressure of Sc.

Vapor pressures were calculated by the well known Knudsen relation,⁵ and cell pumping speed corrections were applied by the Whitman-Motzfeldt equation.^{5,6} The vaporizing species was taken as monatomic Sc³ (mol. wt. 44.956), and was assumed to have a unit condensation coefficient. Clausing factors were from Dushman,⁷ and corrections for pumping through conical channels were from Iczkowski, Margrave, and Robinson.⁸ Orifice areas were corrected for the thermal expansivity of Ta. A correction factor of 1.02 was applied to the pressure to account for the reduction of Sc activity by dissolved Ta. Total correction factors for the pressures amounted to +2% for the K-I and K-II heatings, and +20% for the K-III heatings.

The vapor pressure results are summarized in Table I. Initial heatings of each series were found to have abnormally high vaporization rates. This is attributed to outgassing of impurities such as Ca, Al, Cu, and Pb. Hence the initial heatings are given zero weight in the calculated results. Toward the end of the fourth heating of cell K-II, the liquid nitrogen trap went dry. The pressure in the system rose above 10⁻⁴ mm. for several minutes. An apparent decrease in vapor pressure was noted in this and in the succeeding run. A blue-gray coloration of the shields indicated that some oxidation had occurred. In the sixth run of cell K-II, the Sc melted and some of it leaked out through the seal between the lid and the cell body. These runs were also given zero weight.

Second-law treatment of the cell K-I data, by using the method of least-squares, gives $\Delta H_{1600}^{\circ} = 88.0 \pm 0.2$ kcal./g.-atom for sublimation of Sc. The uncertainty expresses the indeterminate probable error. The value of ΔC_p° is assumed to be -3.5 e.u. (cal./deg.-mole) for the sublimation reaction. Temperature ranges are too short for the cell K-II and K-III determinations for reliable second-law treatments.

To make a third-law calculation, thermodynamic data on gaseous Sc are taken from Stull and Sinke,⁹ low-temperature

data for Sc metal are taken from Weller and Kelley,¹⁰ and the high-temperature data for Sc metal are estimated. The estimate is made by taking the heat capacity of Sc near its melting point to be 8.7 e.u., and sketching in a curve to join this with the low-temperature data of Weller and Kelley. The derived functions are summarized in Table II. The high-temperature C_p° estimate may be compared with a value of 8.5 e.u. for Ti near its melting point,⁹ and 8.95 e.u. for α -Y at 1758°K.¹¹ A high-temperature transition is reported for Sc,¹¹ but its effect on the thermodynamic functions is assumed to be negligible. The probable error of the C_p° estimate is assumed to range from ± 0.3 e.u. at 1800°K. to zero at room temperature. Results of the third-law calculations for ΔH_{298}° of sublimation of Sc are given in Table I. The mean ΔH_{298}° is 91.16 kcal./g.-atom with an indeterminate probable error of ± 0.07 kcal./g.-atom. Systematic errors are assumed to arise primarily from temperature uncertainties and from uncertainties in the heat capacity estimate. All other errors are assumed to be negligible in comparison. A probable error of $\pm 4^{\circ}$ is assigned for the temperature scale, $\pm 0.5^{\circ}$ for prism corrections, and $\pm 3^{\circ}$ for temperature gradients within the cell. This gives a total probable error of $\pm 5^{\circ}$ in temperature. Combining all errors, a probable error of ± 0.3 kcal./g.-atom is estimated for the third-law result.

TABLE II

ESTIMATED THERMODYNAMIC DATA FOR SCANDIUM METAL				
Temp., °K.	C_p° , e.u.	$H_T^{\circ} - H_{298}^{\circ}$, cal./g.-atom	S_T° , e.u.	$-(F_T^{\circ} - H_{298}^{\circ})/T$, e.u.
298.15	6.10	0	8.20	8.20
400	6.40	637	10.08	8.48
600	6.85	1963	12.76	9.49
800	7.23	3371	14.79	10.57
1000	7.56	4850	16.44	11.59
1200	7.86	6393	17.85	12.52
1400	8.14	7993	19.08	13.37
1600	8.42	9649	20.18	14.14
1800	8.70	11361	21.18	14.87

The derived thermodynamic data may be used to reduce the second-law result to room temperature. Hence, $\Delta H_{298}^{\circ} = 91.1$ kcal./g.-atom. The assumption of a 5° trend in temperature over the working range results in an uncertainty of ± 1.6 kcal./g.-atom in ΔH_{298}° . Since this is by far the greatest uncertainty in the second-law determination, it is taken as the estimate of the probable error.

Discussion

Good agreement is obtained for second- and third-law calculations of ΔH_{298}° of sublimation of Sc in the present work. Comparison of these results with second-law ΔH_{298}° values of previous work (Table III, column 2) shows the previous values to be ~ 10 kcal./g.-atom lower than found here. Treatment of the previous work by

TABLE III

ENTHALPY OF SUBLIMATION OF Sc BY VARIOUS INVESTIGATORS

Temp. range, °K.	ΔH_{298}° second- law, ^a	ΔH_{298}° third-law,	Investigator
	kcal./g.- atom	kcal./g.-atom	
1505-1740	81.8	90.25 \pm 0.10	S, D, W, and D ²
1555-1780	82.3	89.66 \pm 0.12	A and R ³
1420-1720	80.2	A and R
1460-1845	82.3	A and R
1301-1644	83.1	88.91 \pm 0.11	K, N, and P ⁴
1478-1797	91.1	91.16 \pm 0.07	This work

^a ΔH_T° is reduced to 298°K. by using thermodynamic functions from Table II for Sc metal and values from Stull and Sinke⁹ for Sc gas.

(10) W. W. Weller and K. K. Kelley, "Low-Temperature Heat Capacity and Entropy at 298.15°K. of Scandium," U. S. Bur. Mines Rept. of Investigations 5984, 1962.

(11) R. R. Hultgren, "Selected Values for the Thermodynamic Properties of Metals and Alloys," Minerals Research Laboratory, Institute of Engineering Research, University of California, Berkeley, California, 1962.

(6) C. I. Whitman, *J. Chem. Phys.*, **20**, 161 (1952); **21**, 1407 (1953); K. Motzfeldt, *J. Phys. Chem.*, **59**, 139 (1955).

(7) S. Dushman, "Scientific Foundations of Vacuum Technique," John Wiley and Sons, New York, N. Y., 1949, p. 96.

(8) R. P. Iczkowski, J. L. Margrave, and S. M. Robinson, *J. Phys. Chem.*, **67**, 229 (1963).

(9) D. R. Stull and G. C. Sinke, "Thermodynamic Properties of the Elements," American Chemical Society, Washington, D. C., 1956.

the third law (Table III, column 3) gives much better agreement with the present work. It is noted, however, that temperature dependent trends of 1–2 kcal./g.-atom are present in the ΔH_{298}^0 values of prior work. The ΔH_{298}^0 values range from low values at low temperatures to values in agreement with the present work at $\sim 1800^\circ\text{K}$. These trends and the lack of agreement between the second- and third-law treatments are indicative of systematic errors.¹² The discrepancy between second- and third-law treatments was noted by Brewer¹³ for the work of Spedding, *et al.*, and by Ackermann and Rauh³ for their own work. The third-law analysis is very much to be preferred because of the lower uncertainties in the treatment. If the 10-kcal. discrepancy is attributed to uncertainties in the third-law treatment, it requires either a 6 e.u. (>40%) uncertainty in the free energy functions of Sc metal or a 200° uncertainty in temperature. Uncertainties of this magnitude are highly unlikely in either case. The reasons for lack of agreement are not obvious, however. Temperature gradients in the Knudsen cells are believed to be significant, but are difficult to evaluate. It is estimated that 2–6 kcal./g.-atom uncertainty in the second-law enthalpy may result from this factor. Uncertainties in the second-law enthalpy will also arise if impurities with volatilities higher than Sc contribute to the observed weight losses. Thus, 0.1% of volatile impurity would cause a 0.5-mg. weight loss in a 0.5-g. sample. Such impurities would make a greater fractional contribution at lower temperatures and tend to give a lower enthalpy of sublimation.

The mass spectrometric measurements of Ackermann and Rauh³ and the radioactive isotope technique employed by Karelin, *et al.*,⁴ are specific for detection of Sc. A third-law treatment of the mass spectrometer data could not be made, however, because of lack of an absolute pressure measurement. The work of Karelin, *et al.*, is difficult to evaluate because of the small quantities (0.33 to 340 μg .) of material vaporized. Small amounts of impurities may lead to significant side reactions in methods of this type. In similar work by the same authors on Y,¹⁴ vapor pressure values obtained were a factor of ~ 100 higher than those reported by Ackermann and Rauh³ for the same temperatures.

It appears that the presence of systematic errors invalidates the second-law results of the prior work. Third-law treatments of this work, and of the highest temperature results of Spedding, *et al.*, and of Ackermann and Rauh,³ are in agreement, and lead to 91.0 ± 0.5 kcal./g.-atom as the best value for ΔH_{298}^0 of sublimation of Sc.

Enthalpies of sublimation to atoms are compared for a number of elements in Table IV. The value for Sc is seen to be closer to Y than to Al or Ga, and reflects an increase in bonding energy with d electrons as compared with s and p electrons. For groups without d electron bonding, *e.g.*, groups IA or IIIA, there is a decrease in enthalpy of sublimation with increasing atomic number. When d electrons are involved in the bonding, however, there is generally an increase in enthalpy of sublimation with atomic number.¹³ A comparison of sublimation enthalpies of group IIIB elements with group IIIA elements demonstrates the relative increase in bonding energy by d electrons. The sublimation enthalpy of Sc is 20 kcal./g.-atom higher than the average of the Al and Ga values;

the Y value is 40 kcal./g.-atom higher than the average of the Ga and In values; and the La value is 50 kcal./g.-atom higher than the average of the In and Tl values. Similar trends are apparent for other groups of the transition elements. The sublimation enthalpies of the first long row transition elements are affected less by d electron bonding than are those of the later rows. Thus, Ti shows only a 22-kcal. increase over Sc, whereas Zr has a 44-kcal. increase over Y, and Hf has a 48-kcal. increase over La. In group IIA, the high sublimation enthalpy for Ba indicates d electron bonding. Significantly, atomic Ba has a low-lying 6s5d state¹⁸ at 9000 cm^{-1} . This state may be relatively lower in energy in metallic Ba and may contribute to its bonding.

TABLE IV
 ΔH_{298}^0 OF SUBLIMATION TO ATOMS IN KCAL./G.-ATOM FOR VARIOUS ELEMENTS^{9,11}

IA	IIA	IIIA	IIIB ^a	IVB
Na 25.9	Mg 35.6	Al 77.4		
K 21.4	Ca 42.2	Ga 65.3	Sc 91.0	Ti 112.7
Rb 19.5	Sr 39.1	In 58.0	Y 101.7	Zr 146.0
Cs 18.7	Ba 42.5	Tl 43.6	La 100.2	Hf 148.0 ¹⁵

^a Values for Lu¹⁶ and Ac¹⁷ are 95 and 97 kcal./g.-atom, respectively. These are both uncertain by about ± 5 kcal. The Lu value was obtained by a second-law method. The Ac value was derived from a vapor pressure measurement by using a third-law treatment with estimated thermodynamic functions.

Acknowledgment.—The author acknowledges the helpful discussions with Dr. John H. Carpenter and also thanks him for the use of certain furnace components.

(15) R. G. Bedford, 1962, to be published.

(16) D. White, P. N. Walsh, H. W. Goldstein, and D. F. Dever, *J. Phys. Chem.*, **65**, 1404 (1961).

(17) K. W. Foster and L. G. Fauble, *ibid.*, **64**, 958 (1960).

(18) C. E. Moore, "Atomic Energy Levels," Vol. I, II, and III, U. S. National Bur. Standards Circ. 467, 1958.

(12) R. J. Ackermann and R. J. Thorn, "Vaporization of Oxides," Paper 2 in "Progress in Ceramic Science," Vol. I, edited by J. E. Burke, Pergamon Press, New York, N. Y., 1961, pp. 42, 43.

(13) L. Brewer, "Thermodynamic Stability and Bond Mechanisms in Relation to Electronic Structure and Crystal Structure," University of California Lawrence Radiation Laboratory Report UCRL-10012, 1962.

(14) An. N. Nesmeyanov, Yu. A. Priselkov, and V. V. Karelin, "The Vapor Pressure of Metallic Yttrium," paper in "Thermodynamics of Nuclear Materials," International Atomic Energy Agency, Vienna, 1962, pp. 667–673.

NUCLEAR TRANSFER AND ANISOTROPIC MOTIONAL SPIN PHENOMENA: RELAXATION TIME TEMPERATURE DEPENDENCE STUDIES OF WATER ADSORBED ON SILICA GEL. IV

BY D. E. WOESSNER AND J. R. ZIMMERMAN

Socony Mobil Oil Company, Inc., Field Research Laboratory, Dallas, Texas

Received December 14, 1962

An experimental investigation of the temperature dependence of the nuclear magnetic resonance relaxation phenomena of water vapor adsorbed on silica gel is described. Two-component relaxation data are observed. With temperature increase, the longer T_2 value decreases while its fractional population increases. These data are shown to be consistent with nuclear transfers between two state environments possessing distinct relaxation characteristics, and a comparison with theory is made. Evidence of a change of surface characteristics is presented; for early experiments, two-component longitudinal relaxation occurs below a transition temperature; in later experiments, only one-component T_1 behavior is found. A theory for an anisotropic motional model for nuclear magnetic dipole-dipole relaxation on surfaces is presented. The motional model is random reorientation of the interproton vector about an axis normal to the surface which occurs much faster than the time dependence of the angle between the vector and this axis. The relaxation processes are thus related to multiple nuclear correlation times. Consequences of an anisotropic model agree with experimental observations.

I. Introduction

Nuclear magnetic resonance relaxation phenomena are determined by molecular kinetic and structural parameters. Consequently, n.m.r. pulse experiments can be used to study motional phenomena of adsorbed molecules.

Previous room temperature experiments¹⁻³ have shown that the protons of water adsorbed on silica gel exist in two different environmental states characterized by different relaxation times. Strong indications have been observed^{2,3} that protons transfer between these states with an average residence time of approximately 1 msec. Winkler⁴ has presented an excellent review of n.m.r. measurements on adsorbed systems performed heretofore.

The temperature dependence experiments at selected surface coverages of water adsorbed on silica gel, which are reported here, were undertaken to extend our knowledge of the pertinent structural and motional phenomena. These structural and motional phenomena will be first reviewed in terms of dielectric relaxation experiments and later considered in the light of nuclear resonance relaxation data. The effect of a chemical shift on multi-state relaxation behavior⁵ will be considered specifically for the case of water vapor adsorption on silica gel in terms of the relaxation characteristics of the state environments. An anisotropic motional model for relaxation⁶ will form the basis for interpreting the relaxation data of protons of adsorbed molecules. This anisotropic model yields qualitative explanations for relaxation behavior which are unpredictable from and disagree with the conventional isotropic liquid-type motional model.

II. Dielectric Relaxation Experiments

Since both the n.m.r. relaxation times and dielectric relaxation times are affected by the motion of the water molecules, any motional models derived from n.m.r. data must be consistent with the dielectric data and *vice versa*. A considerable amount of study of the di-

electric relaxation of water adsorbed on silica gel has been done. Although a number of different silica gels have been used with different quantitative results, several pertinent features are readily apparent.

Dielectric absorption measurements reflect the reorientation motions of molecules. The dielectric absorption maximum of ice⁷ lies in the range of kilometer wave lengths while that for liquid water⁸ lies in the centimeter wave length region. Using these facts, Freymann and Freymann⁹ attempted to determine the motional state of water adsorbed on silica gel. Since ice has practically no dielectric absorption at 3 cm. while liquid water presents a strong absorption, a measurement at 3 cm. should determine whether water adsorbed on silica gel reorients as does "liquid" water. The amount of absorption actually measured indicated that the water molecules are free to reorient. Furthermore, the dielectric absorption values were proportional to the amount of adsorbed water. Temperature dependence experiments¹⁰ disclosed that no dielectric absorption discontinuity occurs at 0° and that absorption persists down to about -90°. A plot¹⁰ of fusion temperature *vs.* molecular mass for the series H₂Te, H₂Se, H₂S, and H₂O is a straight line except for water: the position of water is abnormal being 0° instead of the linearly extrapolated value of -90°. They suggested that this anomaly is due to the intermolecular hydrogen bonds in water—adsorption destroys the intermolecular hydrogen bonds in water molecules (disassociation). The fusion temperature of adsorbed water is displaced toward the extrapolated value.

A number of experiments¹¹⁻¹⁷ have been performed at low frequencies in the kilocycle per second range. Extensive temperature dependence experiments^{11,13} showed three temperature ranges at which kilocycle

(1) J. R. Zimmerman, B. G. Holmes, and J. A. Lasater, *J. Phys. Chem.*, **60**, 1157 (1956).

(2) J. R. Zimmerman and W. E. Brittin, *ibid.*, **61**, 1328 (1957).

(3) J. R. Zimmerman and J. A. Lasater, *ibid.*, **62**, 1157 (1958).

(4) H. Winkler, *Bull. Ampere.*, 219 (1961), 10th year, special edition.

(5) D. E. Woessner, *J. Chem. Phys.*, **35**, 41 (1961).

(6) D. E. Woessner, *ibid.*, **36**, 1 (1962).

(7) H. Granicher, *Proc. Roy. Soc. (London)*, **A247**, 453 (1958).

(8) C. H. Collie, J. B. Hasted, and D. M. Ritson, *Proc. Phys. Soc. (London)*, **60**, 145 (1948).

(9) M. Freymann and R. Freymann, *Compt. rend.*, **232**, 401 (1951).

(10) M. Freymann and R. Freymann, *ibid.*, **232**, 1096 (1951).

(11) M. T. Rolland and R. Bernard, *ibid.*, **232**, 1098 (1951).

(12) K. I. Kamiyoshi and T. Odake, *J. Chem. Phys.*, **21**, 1295 (1953).

(13) K. I. Kamiyoshi and J. Ripoche, *J. phys. radium*, **19**, 943 (1958).

(14) K. I. Kamiyoshi, M. Freymann, and J. Ripoche, *Arch. sci. (Geneva)*, **11**, 71 (1958).

(15) M. H. Waldman, *J. phys. radium*, **17**, 426 (1956).

(16) W. H. Huekelom and L. L. Van Reijen, *J. chim. phys.*, **51**, 632 (1954).

(17) G. Kaempf and H. W. Kohlschue ter, *Z. anorg. allgem. Chem.*, **294**, 10 (1958).

absorption maxima occur: region I at roughly 80°K., region II at about 170°K., and region III near 270°K. Region I was observed only for samples of small water content. For region II, the frequency at which $\omega\tau_d = 1$ is well described by an activation energy which varies somewhat with the specific silica gel and coverage. Although the τ_d values extrapolated to room temperature are in the range of liquid water values, the activation energies are closer to that of ice⁷ (13.2 kcal./mole) than to that of liquid water⁸ (about 5.1 kcal./mole). This shows that the adsorbed water reorients rapidly but is definitely different from bulk liquid water. For region III, the frequency of the absorption maximum must be described by an apparent activation energy which decreases with temperature increase. This region is likely caused^{12,16} by the Maxwell Wagner effect which results from the heterogeneity of conductivity of the ensemble formed by the silica gel, interstitial air, and the adsorbed water. If this is the case, then region III is not directly related to molecular motion, but to charged particles responsible for electrical conductivity.

Silica gel dehydrated at 100° exhibits region I dielectric absorption with an activation energy of about 5 kcal./mole.¹³ It also exhibits a high frequency absorption^{18,19} at 17,000 Mc./sec. at 293°K. which shifts to 2891 Mc./sec. at 276°K. This corresponds to an activation energy of roughly 12.5 kcal./mole.

LeBot¹⁹ has performed some interesting experiments using 2891 Mc./sec. in the region of room temperature. This frequency at room temperature corresponds to the low-frequency region II data when extrapolated to room temperature. He measured the temperature T_c at which the absorption at this frequency is a maximum as a function of p_0/p , the inverse relative pressure of adsorbed water on silica gel at 19.5°. As p_0/p decreased, T_c also decreased. This means that the motional frequency increases with increasing water content. The slope of the curve changed suddenly at a value of p_0/p which coincides with the monolayer coverage determined from the adsorption isotherm. This was observed for several different silica gels. For all the gels, the T_c values lay in the range 260–320°K. for p_0/p values ranging from 1 to 18. The increase of dielectric absorption was roughly proportional to the increase of water content. Using an activation energy of 12.5 kcal./mole, the room temperature τ_d values decrease from about 2.5×10^{-10} to about 7×10^{-12} sec. as the physically adsorbed water coverage increases from essentially zero to maximum. The 17,000-Mc./sec. absorption at 293°K. for the dehydrated gel mentioned above is evidently a different dielectric absorption.

These experiments show that although adsorbed water is different from liquid water, it nevertheless undergoes rapid reorientation at room temperature with τ_d values almost as small as for liquid water. This is certainly true for one of the environmental relaxation states observed in the n.m.r. experiments and it may be true for both states.

III. Effect of Chemical Shift on Relaxation Measurements

The nuclear resonance chemical shift between the two environmental states of protons adsorbed on silica gel is much smaller than the larger line width of the

two states. This fact together with the nuclear transfer phenomena has precluded accurate chemical shift values from high resolution measurements.^{4,20} Of special importance to interpretation of both previous experiments and those described in this paper is whether the chemical shift value is small enough to yield negligible effects on the relaxation behavior when nuclear transfers occur between the environmental states.

The most tightly bound protons ought to have an extreme shift resulting from interaction with the surface. O'Reilly²¹ has measured the transverse relaxation time and chemical shift for proton dilute silica gel, that is, for silanol protons. The T_2 value is 2.1×10^{-4} sec. and the chemical shift value is -3 ± 2 p.p.m. relative to bulk water protons.

The facts that both environmental states co-exist down to about 0.3 statistical monolayer,^{1,3} that the proton population in both states increase with coverage once this small threshold is reached,³ and that different silica gels behave differently make the characterization of these states qualitatively difficult if not quantitatively unlikely. Nevertheless, several experiments suggest that the water molecules in at least one state do not hydrogen bond with one another but still move freely, Milligan²² has concluded from magnetic susceptibility measurements of water vapor adsorbed on silica gel that for less than a monolayer coverage the water molecules are separated on the surface in a fashion which does not permit hydrogen bonds, or that the adsorption mechanism precludes hydrogen bond formation. Freymann and Freymann⁹ found that the dielectric loss at 3 cm. wave length for water adsorbed on silica gel does not disappear so as to indicate immobile water until the temperature is lowered to about -90° , the expected freezing point for non-hydrogen bonded water. Thorp²³ found that the dielectric constant of the first monolayer is 41, nearly the value expected for non-hydrogen bonded water. Kurosaki²⁴ measured the increase of dielectric polarization with water content. He interpreted an initial slow increase of polarization as caused by water molecules firmly bound to the surface. He found a second adsorption state which has a specific polarization somewhat higher than that of water molecules in the form of vapor or in the dissolved state. Hence, the chemical shift for one environmental state should be near that for gaseous water corrected for bulk magnetic susceptibility. This has been measured²⁵ and it is -4.6 p.p.m. relative to water.

Therefore, if the chemical shift of the other state is equal to that of the silanol OH groups, then the chemical shift between the state environments is in the range 1.6 ± 2 p.p.m. On the other hand if this other state is hydrogen bonded as in liquid water, the chemical shift would be 4.6 p.p.m. The unexciting shift of the silanol proton with respect to water suggests that 4.6 p.p.m. would certainly be a largest possible value.

The relaxation behavior for nuclei undergoing transfers between state environments of different relaxation

(20) V. I. Kvlividze, N. M. Ievskaya, et al., *Kinet. i Kataliz.*, **3**, 91 (1962).

(21) D. E. O'Reilly, H. P. Leftin, and W. K. Hall, *J. Chem. Phys.*, **29**, 970 (1958).

(22) W. Milligan and H. Whitehurst, *J. Phys. Chem.*, **56**, 1073 (1952).

(23) J. M. Thorp, *Trans. Faraday Soc.*, **55**, 442 (1959).

(24) S. Kurosaki, *J. Phys. Chem.*, **58**, 320 (1954).

(25) W. G. Schneider, H. J. Bernstein, and J. A. Pople, *J. Chem. Phys.*, **28**, 601 (1958).

(18) J. LeBot and S. LeMontagner, *Compt. rend.*, **233**, 862 (1951).

(19) J. LeBot, *Ann. phys.*, **1**, 463 (1956).

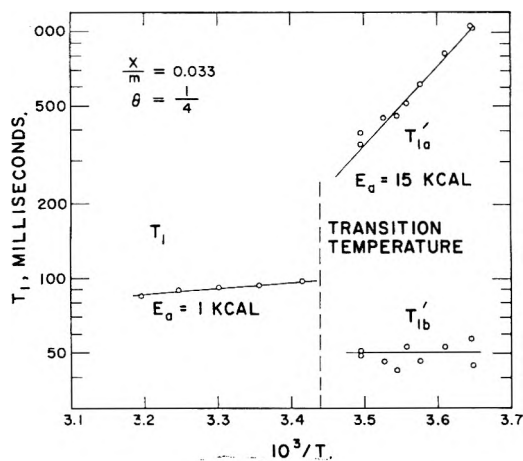


Fig. 1.—Temperature dependences of the apparent proton longitudinal relaxation times for water adsorbed on silica gel in the initial experiments.

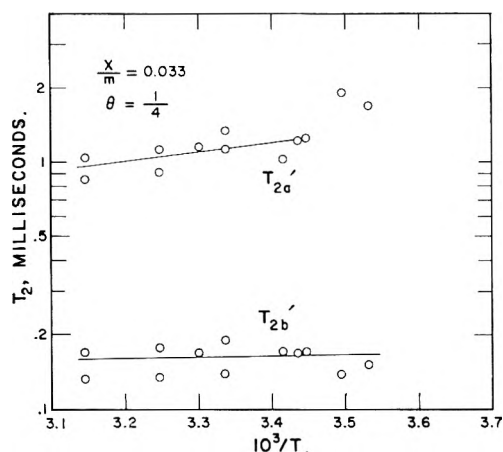


Fig. 2.—Temperature dependences of the apparent proton transverse relaxation times for water adsorbed on silica gel in the initial experiments.

times has been investigated theoretically when a chemical shift between the state environments is absent² and present.⁵ A chemical shift does not affect the relations describing the longitudinal relaxation, but the transverse relaxation relations are greatly increased in complexity. The significant quantity which determines the effect of chemical shift on transverse relaxation⁵ is $T_{2b}(\omega_a - \omega_b)$, the reduced frequency separation; T_{2b} is the shorter relaxation time of the two environmental states; ω is the precessional angular frequency. From arguments which will follow in later paragraphs, $T_{2b} \approx T_{2b}' = 0.135$ msec. Hence, the worst value of reduced frequency separation at a Larmor frequency of 26.5 Mc./sec. would be about 10^{-1} . This value is too small to produce any experimentally observable effect and, hence, the relaxation data to be described in this paper can be interpreted by use of relations which omit the chemical shift.

IV. Experimental

Apparatus.—The relaxation data were obtained from nuclear magnetic resonance pulse (spin-echo) apparatus^{26,27} used in conjunction with a Varian V-4007 research magnet. The resonance frequency was 26.5 Mc./sec. The free decay and spin-echo signal amplitudes were measured visually on a Tektronix Model 536 oscilloscope. These amplitudes were corrected for the observed non-linearity of the receiver.

The silica gel was an especially purified sample²⁸ prepared from ethyl orthosilicate. The material was gelled at pH 7.0 and at a product concentration of 7.3 weight %. After washing, the hydrogel was fired at 280°F. in air and then calcined in air for 8 hr. at 1000°F. to yield the base sample. The surface area of this sample was 463 m.²/g. The sample was then crushed and that fraction which passed through a No. 60 sieve and retained on a No. 200 sieve was used for the experiment.

The pretreatment of the silica gel sample consisted of drying the sample under vacuum ($p < 10^{-6}$ mm.) at 150° for 14 days. The experiments are divided into two groups separated by a one-year interval. The above pretreatment was used immediately preceding each of these two groups.

The water used was distilled under vacuum several times to eliminate dissolved air and was then transferred to a calibrated container. Selected volumes of water were allowed to distill from this container to the silica gel. The sample was then isolated from the rest of the vacuum system by a stopcock placed about 6 in. from the sample.

The sample temperature was controlled by a thermostated, non-hydrogenous liquid flowing through a jacket containing the sample container. The sample container together with the cooling jacket were surrounded by the spin-echo probe.

Data Gathering.—The transverse (T_2) relaxation data were obtained from the spin-echo amplitude $E(2\tau)$ which occurs at time 2τ in two-pulse sequences for pulse separations of τ . In order that all the free precession following the second pulse be from the echo and hence eliminate phase non-coherence effects,⁵ 90–180° pulse sequences were employed. The raw data were analyzed according to the spin-echo amplitude expression²⁹

$$E(2\tau) = E_0 [P_{2a}' \exp(-2\tau/T_{2a}') + P_{2b}' \exp(-2\tau/T_{2b}')] \quad (1)$$

The subscripts a and b refer to components of transverse relaxation having fractional populations (P_2') and transverse relaxation times (T_2'). The shorter relaxation time component is arbitrarily designated b.

The longitudinal (T_1) data were obtained from measurements of the initial amplitudes of the free decay signals which immediately follow each of two 90° pulses which are separated by a time τ . The data were analyzed with the expression

$$F_0 - F(\tau) = F_0 [P_{1a}' \exp(-\tau/T_{1a}') + P_{1b}' \exp(-\tau/T_{1b}')] \quad (2)$$

The fractional populations and components of longitudinal relaxation, P_1' and T_1' , respectively, are identified with subscripts a and b. The shorter longitudinal relaxation time component is arbitrarily designated b. The subscript b does not necessarily correspond to the same group of nuclei in both transverse and longitudinal relaxation time measurements. For instance, a group of nuclei having the shorter T_2' could have the longer T_1' value.

V. Graphical Results

All of these temperature dependence experiments were performed on the same sample. One set of measurements was made about a year before the second set. During this year, the sample was sealed and allowed to stand with about one-third of a statistical monolayer of water. At the beginning of the year, $P_{2a}' = 0.25$ and $T_{2a}' = 1.5$ msec.; but at the end of the year, the corresponding values were 0.65 and 3.0 msec. Clearly, the sample had undergone a change of surface characteristics. Hence the two sets of experiments will be discussed separately.

The data from the first experiments are presented in Fig. 1 and 2. The x/m value was 0.033, corresponding to one-fourth of a statistical monolayer. Above

(26) E. L. Hahn, *Phys. Rev.*, **80**, 580 (1950).

(27) J. C. Buchta, H. S. Gutowsky, and D. E. Woessner, *Rev. Sci. Instr.*, **29**, 55 (1958).

(28) Prepared by the Socony Mobil Research and Development Laboratories at Paulsboro, New Jersey.

(29) The symbols used in this article are chosen to be consistent with the notation in ref. 5 and hence differ with those in ref. 1, 2, and 3.

20°, the longitudinal relaxation data are one-component, but below 18° they are two-component. The data in the 2° transition range are very erratic. The transverse relaxation data are two-component over the entire temperature range. Examples of such relaxation curves have already been presented.¹⁻³ The P_{1a}' and P_{2a}' values are both scattered about 0.2; therefore, the longer T_2 and the longer T_1 values correspond to the same environmental state. These population parameters also exhibit no readily discernible temperature dependence. Several additional measurements performed at the early time for $x/m = 0.045$ showed that the transition in longitudinal relaxation characteristics occurs in the range 25 to 30° at this greater coverage.

The data from the second set of experiments are presented in Fig. 3 through 7. The x/m values used are 0.044 and 0.10, which correspond to one-third and three-fourths of a statistical monolayer, respectively. These data were obtained under more refined instrumentation conditions and are of sufficient precision to establish an increase of P_{2a}' as well as the sizable decrease of T_{2a}' as the temperature increases. The T_{2b}' values exhibit more scatter, but they indicate that the temperature dependence is small, if not actually nil. The transverse relaxation is two-component, but the longitudinal relaxation is one-component over the entire temperature range covered. For the one-third monolayer case, the absence of the longitudinal relaxation transition is additional proof that a change of surface characteristics occurred. The longitudinal relaxation times now increase with temperature rise, in contrast to the decrease of T_1 in the early experiments.

The results for the two different coverages exhibit noticeable differences. The apparent activation energies and T_1 values are greater for the higher coverage. However, for one-third layer the apparent activation energy for T_{2a}' seems to increase at the high temperature end of the experiment. On the other hand, the T_{2b}' values for both coverages are scattered about the same value, 0.135 msec.

VI. Discussion in Terms of Nuclear Transfer Phenomena

General.—In the absence of a chemical shift but with the existence of nuclear transfers, the transverse and longitudinal relaxation curves corresponding to eq. 1 and 2 can both be written in the form⁵

$$F(t) = P_a' \exp(-t/T_a') + P_b' \exp(-t/T_b') \quad (3)$$

where

$$P_a' = 1 - P_b' \quad (4)$$

$$P_b' = \frac{1}{2} - \frac{1}{2} [(P_b - P_a)(1/T_a - 1/T_b) + C_a + C_b] / [(1/T_a - 1/T_b + C_a - C_b)^2 + 4C_a C_b]^{1/2} \quad (5)$$

$$1/T_a' = \frac{1}{2} \{ 1/T_a + 1/T_b + C_a + C_b - [(1/T_a - 1/T_b + C_a - C_b)^2 + 4C_a C_b]^{1/2} \} \quad (6)$$

$$1/T_b' = \frac{1}{2} \{ 1/T_a + 1/T_b + C_a + C_b + [(1/T_a - 1/T_b + C_a - C_b)^2 + 4C_a C_b]^{1/2} \} \quad (7)$$

In these equations the subscripts denoting the type of relaxation, transverse or longitudinal, are omitted. Also, C_a is the probability per second, or rate, for a

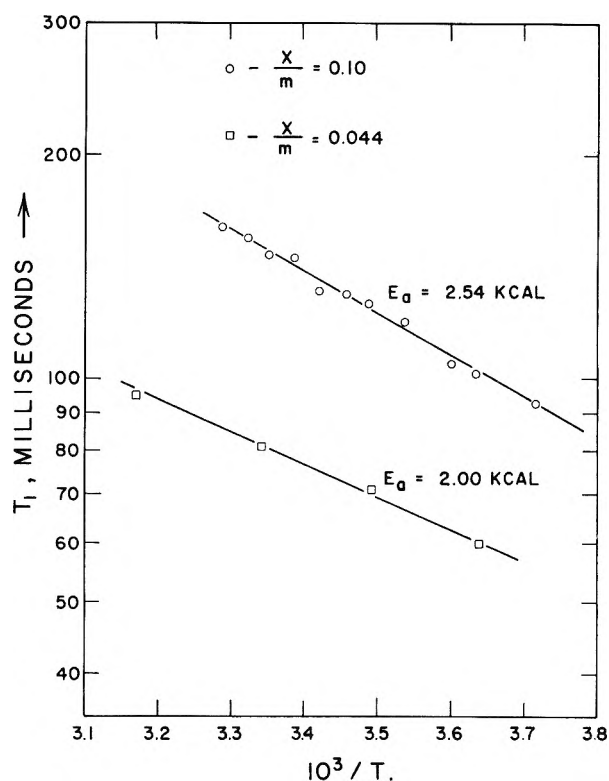


Fig. 3.—Temperature dependence of the apparent proton longitudinal relaxation time for water adsorbed on silica gel in the latter experiments.

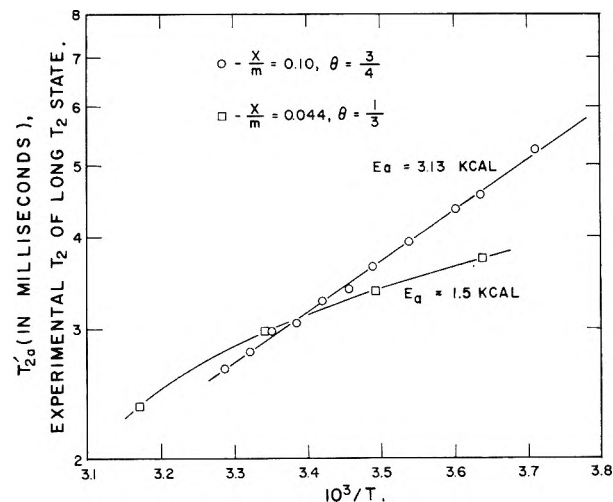


Fig. 4.—Temperature dependence of the apparent proton transverse relaxation time for the long T_2 state of water adsorbed on silica gel in the latter experiments.

given nucleus to leave environmental state a which is characterized by relaxation time T_a and fractional population P_a . In other words, T_a and P_a are the quantities which would be observed when $C_a = 0$. Similar definitions apply for the b state. The state with the shorter relaxation time is designated b regardless of whether one is considering transverse or longitudinal relaxation.

In order to discuss the agreement of the experimental data with this nuclear transfer model, it is informative to consider theoretical plots for a special instance and to inspect the above equations for limiting cases. In the following illustrative discussions, $P_a = P_b$ and $T_a = 10T_b$ or $T_a = 10T_b$.

Figure 8 shows theoretical plots of P_a' as functions of $C_b T_b$, the reduced transfer rate defined for the en-

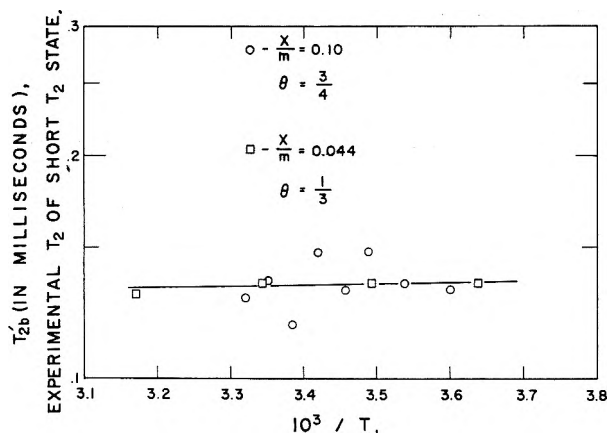


Fig. 5.—Temperature dependence of the apparent proton transverse relaxation time for the short T_2 state of water adsorbed on silica gel in the latter experiments.

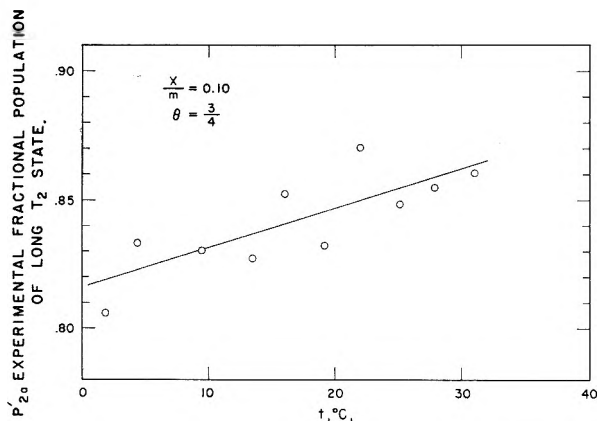


Fig. 6.—Temperature dependence of the apparent fractional population of protons in the long T_2 state of water adsorbed on silica gel in the latter experiments.

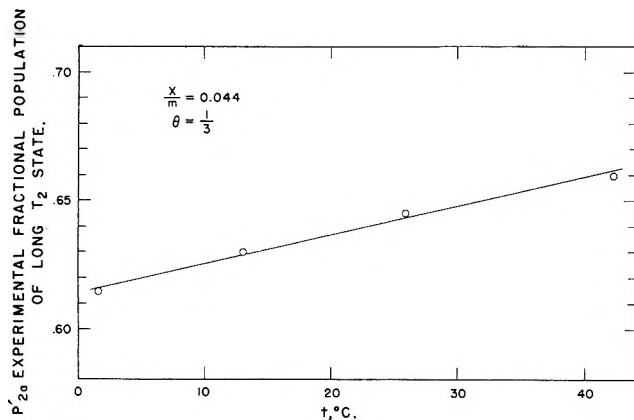


Fig. 7.—Temperature dependence of the apparent fractional population of protons in the long T_2 state of water adsorbed on silica gel in the latter experiments.

environmental state having the shorter relaxation time. Note that for a given T_b value the value of P_a' increases with increase of the nuclear transfer rate. When $C_b T_b = 3$, P_a' is nearly unity; and since $P_a' + P_b' = 1$, P_b' is essentially zero. A curve for infinite T_a (not shown here) differs very little from the one for $T_a = 100T_b$. In experimental practice, the relaxation curve cannot be resolved into two components if $C_b T_b \lesssim 2$. For $C_b T_b = 0.2$, two-component resolution is possible even though for state a the transfer rate C_a is 20 or 2 times its relaxation rate $1/T_a$. Hence, as long as T_a is at least several times larger than T_b , two-com-

ponent relaxation resolution is generally possible unless the shorter relaxation time state b has $C_b \lesssim 1/T_b$.

Figure 9 shows plots of relative relaxation times T'/T as functions of $C_b T_b$. An increase of nuclear transfer rate causes the relative relaxation times for both environmental states to decrease. Simultaneously, the P' values change so that

$$P_a'/T_a' + P_b'/T_b' = P_a/T_a + P_b/T_b \quad (8)$$

Within the range of two-component resolution of relaxation curves, the percentage decrease of T_a'/T_a with increase of $C_b T_b$ is much greater than that of T_b'/T_b . Inspection of Fig. 8 and 9 with $T_a \gg T_b$ reveals that T_a' may be many times smaller than T_a while T_b' may be nearly equal to T_b ; yet P_a' and P_b' may be nearly equal to P_a and P_b , respectively.

Suppose the T_1 values for the environmental states are much greater than the T_2 values. Then the conditions $C_b T_{1b} \gg 1$ for longitudinal and $C_b T_{2b} \ll 1$ for transverse relaxation can occur simultaneously. One-component longitudinal and two-component transverse relaxation behavior would then result. The observable longitudinal relaxation $1/T_1$ would be given by eq. 8. At this point, it is important to note that the equations presented here are independent of the specific models for relaxation in the different environmental states.

Some simple relations can be derived for slow nuclear transfer conditions and different relaxation times. In general, for $C_b T_b \ll 1$ and $T_a/T_b \gg 1$

$$1/T_a' = 1/T_a + C_a \quad (9)$$

$$1/T_b' = 1/T_b + C_b \quad (10)$$

$$P_a' = [P_a + (P_a/P_b)C_a T_b] / \{1 + [(P_a/P_b) - 1]C_a T_b\} \quad (11)$$

Under conditions of a great preponderance of nuclei with a much longer relaxation time so that $T_a \gg T_b$ and $C_a \ll C_b$, the general eq. 6 reduces to

$$1/T_a' = 1/T_a + (P_b/P_a)[T_b + (1/C_b)]^{-1} \quad (12)$$

This reduced expression has also been found by other workers.³⁰

Second Set of Experiments.—The most significant clue to the interpretation of the data described in Fig. 3 through 7 is the observation that the longer transverse relaxation time component T_{2a}' decreases with temperature increase. A temperature rise generally increases T_2 because the increased molecular motion averages out more completely the magnetic dipole-dipole broadening. A possible explanation of this observation is that the temperature increase results in an increase of nuclear transfers between two different environmental states and that this causes nuclei of the long T_2 state to relax more rapidly by placing them in the short T_2 state.

The following experimental observations agree with predictions based on the nuclear transfer model if one makes the reasonable assumption that the nuclear transfer rates increase as the temperature rises: (1) the decrease of T_{2a}' with temperature increase while T_{2b}' remains nearly constant and (2) the increase of P_{2a}' with temperature increase.

(30) H. C. Torrey, J. Koringa, D. O. Seevers, and J. Ueberfeld, *Phys. Rev. Letters*, **3**, 418 (1959).

A quantitative comparison of nuclear transfer theory and experiment is exceedingly difficult because one has no quantitative prior values for the environmental state relaxation times, fractional populations, and transfer rates. However, under limiting conditions, one may infer semiquantitative values. The transverse relaxation data for $x/m = 0.10$ appear most susceptible to this approach. The observation that T_{2a}' is well described by an apparent activation energy suggests that it is predominantly determined by a thermally activated process as nuclear transfer. From the fact that P_{2a}' is roughly 0.8, one may conclude that $C_b T_{2b}$ is no greater than a few tenths (see Fig. 8, for example). This leads to $T_{2b} \approx T_{2b}'$. Then, the observed temperature independence of T_{2b}' suggests that T_{2b} is nearly constant. The low-temperature values then lead to the conclusion that $T_{2a}/T_{2b} \lesssim 39$ for all the temperatures. The conditions for the validity of eq. 9 through 11 are thus fulfilled. Assuming that the nuclear transfer rates are described by an activation energy relationship, the observed T_{2a}' values may be nearly equal to $1/C_a$. If, then, one sets $C_a = 1/T_{2a}'$, the activation energy for the nuclear transfer is 3.13 kcal./mole. The relation $C_a = 1/T_{2a}'$ should be most nearly true at the high temperatures. Another approach is to use the high temperature experimental values and eq. 11 to evaluate P_{2a} and use this value and the observed temperature dependence of P_{2a}' to find the temperature dependence of $C_a T_{2b}$ by use of eq. 11. Use of the 31.1° values $1/C_a = T_{2a}' = 2.65$ msec., $T_{2b}' = T_{2b} = 0.135$ msec., and $P_{2a}' = 0.86$ yields $P_{2a} = 0.79$. From this value, the apparent activation energy of $C_a T_{2b}$ is about 5.2 ± 2 kcal./mole. By use of the exact equations it is found that eq. 11 is very accurate under these values. The plot (including the value $P_{2a}' = 0.83$ at -3.7° which is not shown in Fig. 6) exhibits considerable scatter which includes the line drawn for an activation energy of 3.13 kcal./mole.

The agreement between nuclear transfer theory and experiment for $x/m = 0.10$ is encouraging even though semiquantitative. Equation 9 should be valid but the equality $C_a = 1/T_{2a}'$ may not be good over the whole temperature range. A violation would cause the observed activation energy for T_{2a}' to be smaller than that for C_a . The violation could be great enough to account for a significant part of the difference between 3.13 and 5.2 kcal./mole without producing a noticeable curvature in the $\log T_{2a}'$ vs. $10^3/T$ plot. This would cause the 3.13 kcal. value barrier to nuclear transfer to be too low. Also, T_{2b} could increase somewhat with temperature increase while T_{2b}' remains nearly constant, as examination of eq. 10 shows. This would cause the 5.2 kcal. value to be somewhat too high. In the light of these uncertainties and the scatter of points, the difference of activation energies loses significance as a criterion for establishing disagreement between the theory and experiment. In addition, the nuclear transfer rate may not follow a simple activation energy temperature dependence. Structural parameters of the system may change with temperature so as to cause a temperature dependence of the activation energy and also of the fractional populations. This change of activation energy is suggested by the high-temperature

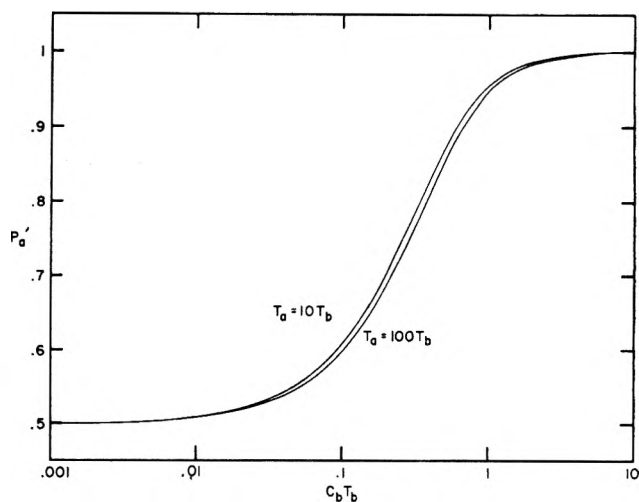


Fig. 8.—Theoretical values of the apparent fractional population of the long relaxation time state as a function of reduced transfer rate when $P_a = P_b$ and $C_a = C_b$ for $T_a = 10T_b$ and $T_a = 100T_b$.

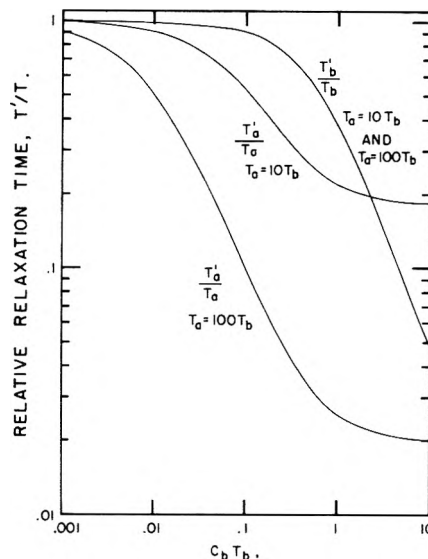


Fig. 9.—Theoretical shortening of the apparent relaxation times vs. reduced transfer rate when $P_a = P_b$ and $C_a = C_b$ for $T_a = 10T_b$ and $T_a = 100T_b$.

point of the T_{2a}' plot for $x/m = 0.044$ (see Fig. 4).

Consider the longitudinal relaxation behavior (Fig. 3). Since only one-component curves are obtained for $x/m = 0.10$ and 0.044 , the weighted-average relaxation is observed. Equation 8 shows that the weighted-average relaxation is unaffected by nuclear transfers. Hence, one can say with certainty that the predominant longitudinal relaxation effect is such that the T_1 values increase with temperature increase. The fact that the $x/m = 0.044$ sample has the larger P_{2b}' values but the shorter T_1 values suggests that the state environment having shorter T_2 values also has the shorter T_1 value. However, it is entirely possible that the T_1 's in the state environments are nearly equal, very different, or even of opposite dependences on temperature.

A little more can be said of the transverse relaxation. Due to the nuclear transfers, the values of T_{2a}' are likely very much shorter than T_{2a} . The consistency of the T_{2b}' values (Fig. 5) indicates that they are reasonably close to T_{2b} even though the scatter is large. Furthermore, the temperature dependence of T_{2b} is likely to be small.

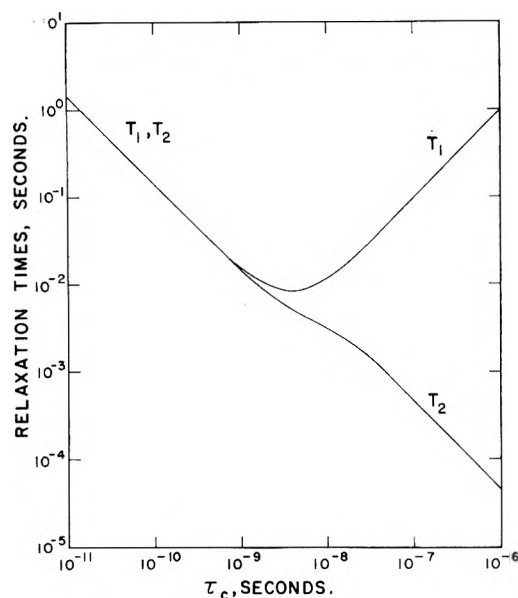


Fig. 10.—Relaxation times at 26.5 Mc. for water molecules calculated on the basis of isotropic rotation.

Consider the effect of the coverage on the transfer probability C_b . For $x/m = 0.10$, the room temperature T_{2a}' is 3.0 msec. Then, if $C_a = 1/T_{2a}'$ and $P_{2a} = 0.79$, one finds $C_b = 1.25 \times 10^3$. Measurements on an aqueous suspension of silica particles with 90 monolayers of water yield $T_{2a}' = 19.5$ msec. Using the reasonable assumptions that only a monolayer is highly effective in relaxation and that $1/T_{a'} \gg 1/T_a$, use of eq. 12 yields $T_{2b} + (1/C_b) = 2.2 \times 10^{-4}$ sec. Then, C_b must be greater than the reciprocal of this quantity, 4.6×10^3 . If $T_{2b} = 0.135$ msec., then $C_b = 1.2 \times 10^4$. These results suggest that the transfer rate increases with increase of coverage.

First Set of Experiments.—The longitudinal and transverse relaxation data are shown in Fig. 1 and 2, respectively. For these experiments, the fact that P_{2a}' is scattered about a value of 0.2 over the entire temperature range and P_{1a}' in the temperature range of two-component longitudinal relaxation is scattered about the same value indicates that the state environment having the longer T_2 value also has the longer T_1 value. The 15 kcal./mole apparent activation energy of T_{1a}' is the combined resultant of nuclear transfer and T_{1a} temperature dependences. It is likely to be predominantly determined by nuclear transfer processes as will be discussed later. It would be tempting to interpret the disappearance of two-component longitudinal relaxation at 19° as the result of T_{1a}' becoming too close to T_{1b}' to allow decomposition of the experimental longitudinal relaxation curve into its two components. Note that T_{1b}' is nearly temperature independent. This mechanism is ruled out because the T_1 value above the longitudinal relaxation transition is much too large to satisfy eq. 8. The weighted average relaxation is observed when the relaxation times are too close to allow resolution. The fact that eq. 8 is radically violated strongly indicates that a transition in molecular arrangement or molecular motion in the state environments has occurred to change the T_1 values. If such a transition occurs, it must be a subtle one because no radical changes in the transverse relaxation times occur. The decrease of T_{2a}' with temperature

increase in the temperature range above the T_1 transition suggests that T_{2a}' is being shortened by nuclear transfers. However the temperature dependence is poorly defined because the data points are widely scattered. A more extensive study of the low temperature transverse relaxation would be very useful. As in the second set of experiments, T_{2b}' is nearly constant. The apparent difference of T_{2b}' values in the two sets of experiments is likely due to improvement of instrumentation in the second set of experiments. This difference is too small to be significant to the interpretations in this paper.

VII. Discussion of Surface Relaxation Mechanism

Relaxation by Isotropic Motion.—In order to discuss the relaxation behavior more fully, recourse to general relaxation theory and to other experimental data is necessary. Assume that the predominant relaxation mechanism involves the magnetic dipole-dipole interaction between the two protons in the same water molecule. This is true for liquid water. The usual expressions for proton pairs in molecules undergoing isotropic tumbling are

$$\frac{1}{T_1} = \frac{3}{10} \gamma^4 \hbar^2 r^{-6} \left[\frac{\tau_c}{1 + \omega_0^2 \tau_c^2} + 4 \frac{\tau_c}{1 + 4\omega_0^2 \tau_c^2} \right] \quad (13)$$

$$\frac{1}{T_2} = \frac{3}{20} \gamma^4 \hbar^2 r^{-6} \left[3\tau_c + 5 \frac{\tau_c}{1 + \omega_0^2 \tau_c^2} + 2 \frac{\tau_c}{1 + 4\omega_0^2 \tau_c^2} \right] \quad (14)$$

where γ is the nuclear gyromagnetic ratio, r is the internuclear distance, ω_0 is the angular resonance frequency, and τ_c is the nuclear correlation time. For isotropic tumbling, only one correlation time is needed. During the time τ_c , a molecular reorientation θ about any axis occurs such that $\langle \theta^2 \rangle_{av} = 1/3$ radian². The expression for T_2 is valid as long as $T_2 \gg \tau_c$. This would be true for the experiments at hand. The relaxation times for isotropic tumbling of water molecules calculated for 26.5 Mc./sec. are shown in Fig. 10. T_1 has a minimum value when $\omega_0 \tau_c = 0.6158$. At this T_1 minimum, $T_1/T_2 = 1.60$. As τ_c decreases from the value at the T_1 minimum, T_1 and T_2 both become inversely proportional to τ_c and equal to each other. As τ_c increases from the value at the T_1 minimum, T_1 becomes proportional to τ_c while T_2 remains roughly inversely proportional to τ_c until τ_c becomes long enough for T_2 to have nearly reached the limiting value for a rigid lattice. Equation 14 does not hold when T_2 becomes near the rigid lattice limiting value.

It is clear that the nuclear correlation time is related to the dielectric relaxation time τ_d for rigid molecules. For isotropic reorientation, $\tau_d = 3\tau_c$.

The present experimental data do not agree with isotropic motion. Consider the state environment having the shorter relaxation times. The experiments reported here indicate that T_{2b}' is very nearly temperature independent. Previous experiments³ show that T_{2b}' is also independent of the total water adsorbed up to two statistical layers. The latter observation suggests that the water molecules in the b state environment do not experience effective intermolecular nuclear interactions insofar as T_2 values are concerned. The temperature independence of T_{2b}' shows that the predominant mechanism determining its value is tempera-

ture independent. The T_2 value for an ensemble of isolated randomly oriented stationary water molecules is calculated as roughly 8.6×10^{-6} sec., much smaller than the observed $T_{2b}' = 135 \times 10^{-6}$ sec. For a water molecule undergoing isotropic reorientation, this T_{2b}' value implies a correlation time $\tau_c = 3.5 \times 10^{-7}$ sec. This value yields $T_{1b} = 0.344$ sec. for water. The T_{1b}' values for the initial experiments (roughly 50 msec.) are nearly temperature independent but are too short. Also, the T_{1b}' values for earlier experiments³ (roughly 5 msec. at one-half monolayer) are strongly dependent on coverage and are much too short for the above isotropic τ_c value. This τ_c value implies a $\tau_d = 1.05 \times 10^{-6}$ sec. Hence the isotropic interpretation would indicate a temperature- and coverage-independent frequency of maximum dielectric absorption of $(2\pi\tau_d)^{-1} = 152$ kc./sec. A dielectric absorption such as this has not been reported. Also, such rapid isotropic motion would conflict with conclusions made from dielectric data that low coverage adsorbed water is immobile.

An isotropic random reorientation which is temperature and coverage independent is difficult to visualize. The dielectric relaxation times in the kilocycle range at room temperature are highly dependent on both temperature and coverage.

It is difficult to make many significant statements about the long relaxation time state a because the relaxation times are so shortened by the nuclear transfers. One could assign the kilomegacycle dielectric absorption peaks to this state. An isotropic motion with dielectric absorption maximum at 2.89 kilomegacycles implies a τ_c of 1.8×10^{-11} sec. This would yield $T_1 = T_2$ and values of roughly a second. The corresponding T_{2a}' value (Fig. 2) is much smaller, of the order of msec.; and it cannot be shortened to this value by nuclear transfers because the T_{1a}' value is too long to permit this. Hence, while the T_{1a}' values agree with a τ_c deduced from dielectric data, the T_{2a}' is too short for an isotropic motion for this τ_c . The decrease of T_{1a}' with temperature increase suggests that T_{1a}' is being shortened by nuclear transfers. The 15 kcal. activation energy is close to the 13 kcal. found for the kilomegacycle dielectric relaxation. Hence, the same motion may be responsible for the nuclear transfers from the low-temperature conditions of the initial experiments.

This discussion has illustrated the grave difficulties encountered in trying to explain the observed relaxation phenomena in terms of isotropic reorientation of water molecules. In the next section, evidence is presented for the existence of anisotropic motion in different systems.

Experimental Indications of Anisotropic Motion.—From nuclear magnetic resonance line-width studies of water sorbed on fibrous materials, Odajima^{31,32} concluded that the relation $\tau_d = 3\tau_c$ is not obeyed for such systems. This led to the suggestion³¹ that water molecules in the sorbed state do not rotate with spherical symmetry (*i.e.*, not isotropically) as in the liquid state. This is basically reasonable. Indeed, one should believe that the directional behavior of the adsorption process for non-spherical molecules would ordinarily not allow isotropic motion. However from T_1 measurements on

the same systems, Sasaki and co-workers³³ suggested that the τ_c determining T_1 agrees with that deduced from dielectric relaxation measurements. Thus, the T_1 and T_2 values seem to be predominantly determined by different nuclear correlation times.

From nuclear magnetic resonance relaxation studies of water on carbon, Kimmel³⁴ also concludes that T_1 and T_2 are determined by different correlation times. He proposed a two-correlation time description of the relaxation times.

Magnetic resonance evidence of anisotropic reorientation has been found from absorption spectra for water adsorbed in zeolites.³⁵⁻³⁷ In single crystals of non-cubic zeolites such as chabazite and edingtonite, the proton resonance of water consists of a doublet whose separation varies with crystal orientation in the magnetic field as

$$\Delta H = k(3 \cos^2 a - 1) \quad (15)$$

where a is the angle between the optical crystal axis and the magnetic field and k is a constant characteristic of the mineral at a given temperature and water content. For instance, k is 0.7 gauss for chabazite and 4.6 gauss for edingtonite. The respective T_1 and T_2 values are 10 and 2 msec. Averbuch and co-workers³⁵ interpret the non-zero k values as the results of rapid molecular rotation which does not result in a spherical symmetry of the proton-proton direction.

Relaxation of Proton Pairs by Anisotropic Motion at Surfaces.—The results of a general treatment^{38,39} of magnetic dipole-dipole nuclear spin relaxation for two nuclei of spin $1/2$ and a singlet resonance line (as is observed in these experiments) may be expressed as linear combinations of spectral energy densities as

$$1/T_1 = (9/8)\gamma^4\hbar^2 [J_1(\omega_0) + J_2(2\omega_0)] \quad (16)$$

$$1/T_2 = (9/32)\gamma^4\hbar^2 [J_0(0) + 10J_1(\omega_0) + J_2(2\omega_0)] \quad (17)$$

The $j_i(\omega)$ are the Fourier intensities of orientation functions $F_i(t)$ of the internuclear separation vector at frequency ω as given by

$$J_i(\omega) = \int_{-\infty}^{\infty} \langle F_i^*(t + \tau) F_i(t) \rangle \exp(i\omega\tau) d\tau \quad (18)$$

These $F_i(t)$ are the following functions of the orientation and magnitude of the internuclear separation vector

$$F_0(t) = (1 - 3n^2)r^{-3} \quad (19)$$

$$F_1(t) = n(l + im)r^{-3} \quad (20)$$

$$F_2(t) = (l + im)^2 r^{-3} \quad (21)$$

where l , m , and n are direction cosines in the laboratory coordinate system of the internuclear separation vector whose magnitude is r . In general, thermal motions cause the $F_i(t)$ to fluctuate by causing l , m , n , and r to vary with time.

A coordinate system suitable for describing motions at a surface is described as follows. Let Δ be the angle between the internuclear vector and an axis which is normal to the surface. The variable azimuth of the

(33) N. Sasaki, T. Kawai, A. Hirai, T. Hashi, and A. Odajima, *J. Phys. Soc. Japan*, **15**, 1652 (1960).

(34) H. Kimmel, *Z. Naturforsch.*, **16a**, 1058 (1961).

(35) P. Averbuch, P. Ducros, and X. Pare, *Compt. rend.*, **250**, 322 (1960).

(36) P. Ducros and X. Pare, *Arch. sci. (Geneva)*, **13**, 383 (1960).

(37) Y. Ayant, P. Ducros, and M. Soutif, *Compt. rend.*, **252**, 550 (1961).

(38) P. S. Hubbard, *Rev. Mod. Phys.*, **33**, 249 (1961).

(39) R. Kubo and K. Tomita, *J. Phys. Soc. Japan*, **9**, 888 (1954).

(31) A. Odajima, *J. Phys. Soc. Japan*, **14**, 308 (1959).

(32) A. Odajima, J. Somha, and S. Watanabe, *J. Chem. Phys.*, **31**, 276 (1959).

internuclear vector about this axis is denoted by ϕ' . Then, let θ be the angle between the axis and the external magnetic field H_0 , and let ϕ be the azimuthal angle. The orientation functions expressed in terms of these coordinates are⁶

$$F_0(t) = r^{-3} [1/2(3 \cos^2 \Delta - 1)(1 - 3 \cos^2 \theta) + 3 \sin \Delta \cos \Delta \sin \theta \cos \theta e^{i\phi} + 3 \sin \Delta \cos \Delta \sin \theta \cos \theta e^{-i\phi} - 3/4 \sin^2 \Delta \sin^2 \theta \times e^{2i\phi} - 3/4 \sin^2 \Delta \sin^2 \theta e^{-2i\phi}] \quad (22)$$

$$F_1(t) = r^{-3} [1/2(3 \cos^2 \Delta - 1) \sin \theta \cos \theta + 1/2 \sin \Delta \cos \Delta (\cos^2 \theta - \sin^2 \theta + \cos \theta) e^{i\phi} + 1/2 \sin \Delta \cos \Delta (\cos^2 \theta - \sin^2 \theta - \cos \theta) e^{-i\phi} - 1/4 \sin^2 \Delta (\sin \theta \cos \theta + \sin \theta) e^{2i\phi} - 1/4 \sin^2 \Delta (\sin \theta \cos \theta - \sin \theta) e^{-2i\phi}] e^{i\phi} \quad (23)$$

$$F_2(t) = r^{-3} [1/2(3 \cos^2 \Delta - 1) \sin^2 \theta + \sin \Delta \cos \Delta (\sin \theta \cos \theta + \sin \theta) e^{i\phi} + \sin \Delta \cos \Delta (\sin \theta \cos \theta - \sin \theta) e^{-i\phi} + 1/4 \sin^2 \Delta (1 + \cos^2 \theta + 2 \cos \theta) e^{2i\phi} + 1/4 \sin^2 \Delta (1 + \cos^2 \theta - 2 \cos \theta) e^{-2i\phi}] e^{2i\phi} \quad (24)$$

Examination of eq. 19 through 24 yields the significant difference between anisotropic and isotropic motions which results in multiple correlation times for anisotropic motion and a single correlation time for isotropic motion. Motion in the direction normal to the surface depends on Δ while that in the plane parallel to the surface depends on both Δ and ϕ' . Each $F_i(t)$ has terms dependent on both Δ and ϕ' and also a term dependent on Δ . For isotropic motion, all the terms have the same time dependence. However, one would expect that for molecules at a surface the time dependence of terms depending on Δ would be different from that of terms depending on both Δ and ϕ' . This would lead to multiple correlation times in the Fourier intensities, an occurrence necessary to interpret relaxation of surface molecules on the basis of nuclear magnetic dipole-dipole interaction. These considerations are valid for relaxation between a nucleus fixed to the surface and one in a molecule moving at the surface and also between two nuclei in the molecule at the surface. In the latter case, r is constant.

To show in a relatively simple fashion how anisotropic motion can cause T_1 to be predominantly determined by one correlation time and T_2 by another, consider the simpler case of constant r . Although some of the following assumptions may be unrealistic in general situations, they allow a simple calculation and yet preserve the qualitative picture. Suppose that the rotation axis is fixed, *i.e.*, θ and ϕ are constant. This axis is normal to the surface. Assume that the Δ and ϕ' values are mutually independent and that the time average of $e^{i\theta'}$ is zero. To keep ϕ' independent of Δ , limit Δ to values from 0 to $1/2 \pi$ while ϕ' varies from 0 to 2π .

Simplify the averages $\langle F_i^*(t + \tau) F_i(t) \rangle$ by making the following definitions

$$g_a = 1 \\ g_b = e^{i\phi'}$$

$$g_c = e^{-i\phi} \quad (25)$$

$$g_d = e^{2i\phi'}$$

$$g_e = e^{-2i\phi'}$$

and

$$f_r = r^{-3} (3 \cos^2 \Delta - 1)$$

$$f_s = r^{-3} \sin \Delta \cos \Delta \quad (26)$$

$$f_t = r^{-3} \sin^2 \Delta$$

Then, $\langle g_j^*(t + \tau) g_k(t) \rangle = 0$ when $k \neq j$; also, $\langle g_c^*(t + \tau) g_c(t) \rangle = \langle g_b^*(t + \tau) g_b(t) \rangle$ and $\langle g_e^*(t + \tau) g_e(t) \rangle = \langle g_d^*(t + \tau) g_d(t) \rangle$. In general, there will be a different relaxation time for each different θ value. However, the sample contains a random distribution of axis orientations and only the average relaxation is observed, and so the average is taken over the θ values to obtain the final result.

For illustrative purposes, consider two different models for the motion of ϕ' . (a) Random jumps occur between the three equilibrium positions ϕ_0' , $\phi_0' \pm 120^\circ$, from any of these positions to either of the two adjacent positions at an average rate of $(3\tau_c)^{-1}$. In this case

$$\langle g_b^*(t + \tau) g_b(t) \rangle = \langle g_c^*(t + \tau) g_c(t) \rangle = \exp(-|\tau|/\tau_c) \quad (27)$$

(b) A stochastic diffusion process describes motion among a very large number of equilibrium positions as given by $\langle (\phi' - \phi_0')^2 \rangle = 2\tau/\tau_c$, where ϕ_0' is the ϕ' value at time t . For this motion

$$\langle g_b^*(t + \tau) g_b(t) \rangle = \exp(-|\tau|/\tau_c) \quad (28)$$

$$\langle g_d^*(t + \tau) g_d(t) \rangle = \exp(-4|\tau|/\tau_c) \quad (29)$$

A model for the time dependence of Δ is required for the completion of the calculation. To keep this discussion simple, one may make the customary assumption that each of the $\langle f_j^*(t + \tau) f_j(t) \rangle$ approaches zero for sufficiently large values of τ as described by the relation

$$\langle f_j^*(t + \tau) f_j(t) \rangle = \langle f_j^*(t) f_j(t) \rangle \exp(-|\tau|/\tau_j) \quad (30)$$

A more complicated stochastic motion could yield a series of exponentials with a number of different τ_j values for each j ; a term with a $\tau_j = \infty$ could occur for some models.

With use of the above assumption for the motion of Δ and model (b) for the motion of ϕ' , one obtains

$$\langle F_i^*(t + \tau) F_i(t) \rangle = K_i \{ 1/4 \langle (3 \cos^2 \Delta - 1)^2 \rangle \times \exp[-|\tau|/\tau_r] + 3 \langle \sin^2 \Delta \cos^2 \Delta \rangle \times \exp[-|\tau|(1/\tau_s + 1/\tau_c)] + 3/4 \langle \sin^4 \Delta \rangle \exp[-|\tau|(1/\tau_t + 4/\tau_c)] \} \quad (31)$$

where

$$K_0 = \frac{4}{5}$$

$$K_1 = \frac{2}{15} \quad (32)$$

$$K_2 = \frac{8}{15}$$

The $j_i(\omega)$ are found by using eq. 31 in 18. The relaxation times are then given by

$$1/T_1 = (3/10)\gamma^4\hbar^2r^{-6} \left\{ \frac{1}{4} \langle (3 \cos^2 \Delta - 1)^2 \rangle \times \left[\frac{\tau_r}{1 + \omega_0^2\tau_r^2} + 4 \frac{\tau_r}{1 + 4\omega_0^2\tau_r^2} \right] + 3 \langle \sin^2 \Delta \cos^2 \Delta \rangle \left[\frac{\tau_1}{1 + \omega_0^2\tau_1^2} + 4 \frac{\tau_1}{1 + 4\omega_0^2\tau_1^2} \right] + \frac{3}{4} \langle \sin^4 \Delta \rangle \left[\frac{\tau_2}{1 + \omega_0^2\tau_2^2} + 4 \frac{\tau_2}{1 + 4\omega_0^2\tau_2^2} \right] \right\} \quad (33)$$

$$1/T_2 = (3/20)\gamma^4\hbar^2r^{-6} \times \left\{ \frac{1}{4} \langle (3 \cos^2 \Delta - 1)^2 \rangle \times \left[3\tau_r + 5 \frac{\tau_r}{1 + \omega_0^2\tau_r^2} + 2 \frac{\tau_r}{1 + 4\omega_0^2\tau_r^2} \right] + 3 \langle \sin^2 \Delta \cos^2 \Delta \rangle \left[3\tau_1 + 5 \frac{\tau_1}{1 + \omega_0^2\tau_1^2} + 2 \frac{\tau_1}{1 + 4\omega_0^2\tau_1^2} \right] + \frac{3}{4} \langle \sin^4 \Delta \rangle \left[3\tau_2 + 5 \frac{\tau_2}{1 + \omega_0^2\tau_2^2} + 2 \frac{\tau_2}{1 + 4\omega_0^2\tau_2^2} \right] \right\} \quad (34)$$

where

$$\tau_1 = [1/\tau_s + 1/\tau_c]^{-1} \quad (35)$$

$$\tau_2 = [1/\tau_t + 4/\tau_c]^{-1} \quad (36)$$

The only change for mode (a) is to evaluate τ_2 as

$$\tau_2 = [1/\tau_t + 1/\tau_c]^{-1} \quad (37)$$

These relaxation time expressions are valid under the stated assumptions as long as $T_2 \gg \tau_r, \tau_1, \tau_2$ and the resonance line is a singlet. Even if assumption (30) fails, each relaxation time relation contains terms independent of the motion of ϕ' .

Anisotropic reorientation allows, in an extreme situation, T_1 to be predominantly determined by a very fast motion and T_2 by a slow motion. Suppose $\omega_0^2\tau_c^2 \ll 1$ while $\omega_0^2\tau_r^2 \gg 1$ and $\tau_r \ll T_2$. Then T_1 may be determined by τ_2 (ϕ' motion) and T_2 by τ_r (Δ motion) such that $T_1 \gg T_2$. Hence, even though T_1 is determined by a very rapid motion, T_2 can be much shorter than that predicted by using the correlation time in an isotropic model. In this case, T_1 is independent of ω_0 . On the other hand, if τ_c is short enough, it can be ineffective in spin lattice relaxation; then both T_1 and T_2 will be determined by τ_r and $T_1 \gg T_2$. However, in this case, T_1 would increase with increase of ω_0 .

Under the conditions $\tau_c \ll \tau_r$, T_1 is given by eq. 33 and T_2 is given by the reduction of 34 to

$$1/T_2 = (9/80)\gamma^4\hbar^2r^{-6} \langle (3 \cos^2 \Delta - 1)^2 \rangle \tau_r \quad (38)$$

For larger values of τ_r such that $\tau_r \lesssim T_2$, a more general relation derived by Kubo and Tomita³⁹ must be used

$$(1/T_2)^2 = [(9 \ln 2)/(20\pi)] \gamma^4\hbar^2r^{-6} \langle (3 \cos^2 \Delta - 1)^2 \rangle \tan^{-1}[(\pi\tau_r)/(4T_2 \ln 2)] \quad (39)$$

Thus, when $\tau_r \lesssim 10T_2$, one finds that T_2 is very nearly constant when τ_r increases. This makes possible the

following circumstance. The value of T_2 can be lengthened considerably from the rigid lattice value ($\tau_c, \tau_r = \infty$) and yet it can remain nearly constant while T_1 may change when motional changes which vary τ_c and τ_r occur. Another way T_1 can change while T_2 remains constant is for τ_r to remain unchanged while τ_c changes.

Application of Anisotropic Model.—The data presently available allow an attempt at an interpretation on the basis of anisotropic relaxation even though some relaxation times are obscured by the nuclear transfer phenomenon.

More recent T_1 measurements on the same silica gel for $\theta = 0.6$ yields a room temperature T_1 of 72 msec. at 25 megacycles and 107 msec. at 56 megacycles. Even though only the weighted average T_1 is measured, this increase of T_1 with frequency indicates that at least one of the correlation times which is effective in determining a T_1 is long enough so that $\omega_0\tau \gtrsim 1$.

Reconsider the state environment having the shorter relaxation times. Dielectric polarization data indicate that low coverage adsorbed water is immobile because the additional polarization caused by the water is much smaller than that expected from the equivalent amount of liquid water.^{17,24} This deficiency of polarization is too great to be explained by a loss of hydrogen bonding between water molecules. Suppose this initial water is predominantly in state environment b which is considered to be the more tightly bound to the surface. Interaction with the surface may possibly decrease the reorientable electric dipole moment of the molecule. Some of this might occur through a shift of the electron distribution of the molecule. If hydrogen bonding occurs with surface OH groups, the interaction could involve a donation of electron charge by the water oxygen to the OH. The water oxygen does not attach to the OH group so that the electric dipole moment is perpendicular to the surface and the proton-proton vector parallel to the surface. If this did occur, an extremely rapid reorientation of the proton-proton vector in the plane parallel to the surface would increase T_2 to only four times the rigid value; the observed T_2 is nearly sixteen times the rigid value. However, if an OH group of the water molecule lies in a plane parallel to the surface and the other OH group lies in a plane roughly perpendicular to the surface while the proton-proton vector reorients rapidly about a line normal to the surface, then the value of $\langle (3 \cos^2 \Delta - 1)^2 \rangle$ for the interaction between the water protons can be much less than unity. The relaxation model illustrated above may yield results which are a reasonable approximation for this motion. This would cause a very marked increase of T_2 over its rigid lattice value and would decrease the reorientable dielectric polarization to 0.4 of that from isotropic motion. The molecular vibrations and reorientations would cause Δ to have a distribution of values. A water molecule in this geometry would have Δ of roughly 52° , which yields $(3 \cos^2 \Delta - 1)^2 = 0.019$. An angle $\Delta = 54.7^\circ$ would yield $(3 \cos^2 \Delta - 1)^2 = 0$. Hence the expected fluctuations of Δ for such a geometry could easily cause $\langle (3 \cos^2 \Delta - 1)^2 \rangle$ to be sufficiently small to yield the observed lengthening of T_2 . Interaction between the water proton nearer to the surface and the silanol proton would have similar geometry as that between the two water protons. The interaction

between the other water proton and the silanol proton would be too small to be effective because of the r^{-6} dependence of the interaction. It may not be too far-fetched for the time dependence of $3 \cos^2 \Delta - 1$ and the value of $\langle (3 \cos^2 \Delta - 1)^2 \rangle$ to be nearly independent of coverage and temperatures in the range 0–40°. This picture, of course, is conjectural; even so it shows how several different kinds of data can be used to synthesize a T_2 model.

The long relaxation time state a exhibits rapid motion. The long T_2 values and the dielectric polarization comparable to that for free water suggest that motion occurs over all directions. The fact that $T_{2a}' \ll T_{1a}'$ for the low temperature initial experiments shows that the motion is anisotropic, at least over some ranges of temperature and coverage. In these initial experiments, the absence of a radical change of T_{2a}' at the longitudinal relaxation transition together with the long T_{2a}' and T_{1a}' values suggests that T_{1a} is predominantly determined by the very rapid motions and that $\omega_0^2 \tau_c^2 \ll 1$. Then, since τ_c would decrease with temperature increase, T_{1a} should increase with temperature. The observed decrease of T_{1a}' may indicate the nuclear transfer effect as discussed in the section on isotropic motion. The relation $\omega_0^2 \tau_c^2 \ll 1$ implies that $\tau_c < 1/\omega_0 = 6 \times 10^{-9}$ sec. The greater T_{2a}' values found in the second set of experiments would indicate a smaller anisotropy effect.

The concept of anisotropic motion does allow a basis for subtle structural and motional changes which result in changes of T_1 and nuclear transfer rate without much change in T_2 . This seems necessary for the explanation of the sudden transition of the longitudinal relaxation at 19° in the initial experiments.

For the second set of experiments, it is conceivable that anisotropy changes with temperature increase could actually decrease the T_{2a} values. The change of population fractions with temperature and the agreement with nuclear transfer theory suggest that this is not predominant for the $3/4$ monolayer experiment. The one-third monolayer data might be affected by a temperature dependent anisotropy parameter.

This section has indicated how anisotropy of motion allows for relaxation phenomena which are incompatible with isotropy; and also it points the way toward evaluating weak structural changes in terms of observable relaxation behavior which is too hard to do with the isotropic model.

VIII. Conclusions

Temperature dependence studies of the proton relaxation times for water adsorbed on silica gel have revealed two observations which indicate the existence of proton

transfers among two state environments having distinct, relaxation characteristics. These observations are (1) the decrease of the apparent T_2 value of the long relaxation time state environment with temperature and (2) the increase of the apparent fractional population of the long T_2 state with temperature increase. A detailed comparison of nuclear transfer theory with experiment is at present precluded by insufficient data. The results of an approximate comparison are encouraging though semiquantitative. The resultant activation energy for nuclear transfer for three-fourths of a statistical monolayer lies somewhere in the range 3.1 to 5.2 kcal./mole.

Evidence of a change of surface characteristics occurring in a one-year interval between experiments was observed. The T_2 value and fractional population of the long relaxation time state increased markedly. Also, a transition from one-component to two-component longitudinal relaxation with temperature decrease disappeared during the interval.

The apparent T_2 value for the short relaxation time state is independent of temperature as well as of surface coverage.

An anisotropic model for nuclear magnetic dipole-dipole relaxation has been developed which is qualitatively consistent with both relaxation time and dielectric constant data. The motional model is random re-orientation of the interproton vector about an axis normal to the surface and a time dependence of the angle between the internuclear vector and this axis. Consideration of nuclear magnetic dipole-dipole interactions are sufficient to give a semiquantitative understanding of the observed relaxation data; it is not necessary to invoke other relaxation agents, such as electron-nuclear dipole interactions which might arise from paramagnetic impurities, for interpreting these silica gel experiments.

The nuclear magnetic resonance relaxation time study of water adsorbed on silica gel is very incomplete. Additional temperature dependence data at both higher and lower temperatures are needed for a better understanding of the nuclear transfer and relaxation mechanism phenomena; such experiments are underway.

Acknowledgments.—The authors are especially indebted to Professor N. Hackerman of The University of Texas for his stimulating discussions on the phenomena of molecular absorption, to Dr. G. L. Hoehn for his valuable technical contributions in instrumentation design, and to Dr. J. A. Lasater for his special efforts in performing the first set of temperature dependence experiments described herein. They also wish to thank the Socony Mobil Oil Company, Inc., for permission to publish this paper.

ION PAIRS. III. GLASS ELECTRODE POTENTIOMETRY IN GLACIAL ACETIC ACID¹

BY ANDREW TEH-AN CHENG, REED A. HOWALD, AND DAVID L. MILLER

Chemistry Departments of Oberlin College, Oberlin, Ohio, and St. John's University, Jamaica, N. Y.

Received December 14, 1962

The behavior of the glass electrode in glacial acetic acid has been investigated by a series of measurements of potentials vs. the Ag-AgCl electrode and by direct comparisons with the Pt-chloranil, tetrachloroquinone electrode in cells without liquid junctions. The conditions necessary for obtaining potentials thermodynamically reliable within 5 mv. were determined. "Acid errors" of up to about 70 mv. due to chloride ion incorporation into the surface layers were found and interpreted in accordance with recent theories.^{2,3} The effect of water on the potentiometric titration of HCl with sodium acetate was measured. To within 5 mv. the effect of water (0.3 to 6 M) on the activities of HCl and sodium acetate in solutions saturated with sodium chloride could be represented by the equations: $\log \gamma_{\text{HCl}} = -0.56C_{\text{H}_2\text{O}} + 0.025C_{\text{H}_2\text{O}}^2$ and $\log [\gamma_{\text{NaAc}}/a_{\text{HOAc}}] = -0.095C_{\text{H}_2\text{O}}$. The equilibrium constant for the titration reaction is $K = 1/a_{\text{HCl}}a_{\text{NaAc}} = 1.4 \times 10^8$.

Introduction

One important aspect of the behavior of ion pairs in solvents of low dielectric constant is the influence of polar molecules and other ion pairs on the thermodynamic activity of the ion pairs. Dipole-dipole forces should be quite strong in such cases, and fairly large "salt effects" may be expected. These equilibrium salt effects may provide insight into the kinetic salt effects observed for certain reactions in the same solvent.^{4,5} This work is primarily an investigation of the suitability of the glass, chloranil, and silver-silver chloride electrodes for such measurements in glacial acetic acid.

There are a large number of experimental observations which indicate the sensitivity of glass electrodes to water. A glass electrode which has not been soaked in water for a long time must be restandardized frequently when used in dilute aqueous solutions. Drying a leached electrode introduces a large asymmetry potential.⁶ Recommendations for particular non-aqueous titrations have included suggestions for soaking the electrode in water before readings,⁷ for working in extremely dry solutions,^{8,9} and for maintaining some water present.¹⁰ However, the most direct measurements showing the effect of water on the potential of the glass electrode are those on the "acid error" of glass electrodes.

It is perhaps unfortunate that the limited data of Dole¹¹ on the "acid error" fit so well the equation $\Delta P = (RT/F) \ln a_{\text{H}_2\text{O}}$, suggesting that the glass electrode responds reversibly to the activity of H₃O⁺ rather than H⁺. This suggestion cannot be completely correct, since in that case measurements under nearly anhydrous

conditions would be erratic and quite unreliable, in sharp contrast to the results obtained in acetic acid in a number of laboratories¹²⁻¹⁴ including the general use of the glass electrode for potentiometric acid-base titrations in glacial acetic acid.^{14,15} Some measure of the accuracy with which the glass electrode provides a direct measure of the hydrogen ion activity is available from direct comparison with the hydrogen electrode over the range 0 to 96% acetic acid in water¹² and from an indirect comparison with the quinhydrone electrode.¹³ These studies indicate that glass electrode potentials are reliable thermodynamically to within 15 and 5 mv., respectively.

This general level of reliability for the glass electrode has been confirmed in this work by repeated measurements over a period of months on the same solution and by direct comparison with the chloranil electrode. However, positive and negative potential errors of the order of 20 mv. were observed temporarily under various conditions, particularly following changes in the water concentration present in the acetic acid. These errors were investigated in detail and shown to be readily interpretable in terms of Izmailov's theory² for the "acid error" of the glass electrode. By deliberately adjusting the conditions, errors as large as 70 mv. could be produced, and conversely the errors could be maintained under 5 mv. Thus, with care, thermodynamic data including equilibrium constants and activity coefficients can be obtained with the glass electrode in acetic acid with an uncertainty of less than 20%. In particular, data on the effect of water on acid-base titrations in acetic acid are reported here, complementing and extending the recent studies of Bruckenstein and Kolthoff¹⁶ and Schwarzenbach and Stensby.¹⁷ Correlations are also possible between this potentiometric data on activities and studies of vapor pressure and freezing point depression.

Experimental

To avoid the uncertainty involved with liquid junction potentials all the electrodes used were placed in the same flask. A

(1) This work was presented at the 140th National Meeting of the American Chemical Society, Chicago, Ill., September, 1961. Address inquiries to Dr. R. A. Howald, Chemistry Department, Montana State College, Bozeman, Montana.

(2) N. A. Izmailov and A. G. Vasil'ev, *Dokl. Akad. Nauk SSSR*, **95**, 579 (1954); *Zh. Fiz. Khim.*, **29**, 1866 (1955); *Chem. Abstr.*, **48**, 13369a (1954); **50**, 6154a (1956).

(3) K. Schwabe and G. Glöckner, *Z. Elektrochem.*, **59**, 504 (1955).

(4) See, for example, S. Winstein, S. Smith, and D. Darwish, *J. Am. Chem. Soc.*, **81**, 5511 (1959).

(5) R. A. Howald, *J. Org. Chem.*, **27**, 2043 (1962) (paper II in this series).

(6) W. S. Hughes, *J. Chem. Soc.*, 491 (1928); D. Hubbard and G. F. Rynders, *J. Res. Natl. Bur. Std.*, **40**, 105 (1948).

(7) R. G. Bates, "Electrometric pH Determinations," John Wiley and Sons, Inc., New York, N. Y., 1954, p. 244.

(8) W. Raehs, Dissertation T. H. Aachen (1951), cited in ref. 9.

(9) K. Cruse, *Arch. tech. Messen*, **245**, 125; **247**, 169; **248**, 203; **249**, 217 (1956).

(10) R. N. Evans and J. E. Davenport, *Ind. Eng. Chem., Anal. Ed.*, **8**, 287 (1936).

(11) M. Dole, "Glass Electrode," John Wiley and Sons, Inc., New York, N. Y., 1941; M. Dole, *J. Am. Chem. Soc.*, **53**, 4260 (1931); **54**, 3095 (1932)

(12) J. A. Cranston and H. F. Brown, *J. Roy. Technical College (Glasgow)*, **4**, 32 (1937).

(13) N. A. Izmailov and A. M. Aleksandrova, *Zh. Obshch. Khim.*, **20**, 2127 (1950); *J. Gen. Chem. USSR.*, **20**, 2207 (1950).

(14) T. Higuchi, M. L. Danguilan, and A. D. Cooper, *J. Phys. Chem.*, **58**, 1167 (1954).

(15) P. C. Markunas and J. A. Riddick, *Anal. Chem.*, **23**, 337 (1951).

(16) S. Bruckenstein and I. M. Kolthoff, *J. Am. Chem. Soc.*, **78**, 2974 (1956); **79**, 1, 5915 (1957).

(17) G. Schwarzenbach and P. Stensby, *Helv. Chim. Acta*, **42**, 2342 (1959).

100-ml. flask was fitted with four long necks. The central vertical neck was fitted with a mechanical stirrer operating through a loose fitting cork. A glass electrode, Beckman 1190-80 or 40498, and Ag-AgCl electrode, Beckman 1264 or 39261, were each sealed with picein cement into one of the necks. The fourth neck was used for the introduction of a long capillary buret tip as well as for platinum electrodes and hydrogen when they were used. This neck was loosely stoppered with a suitable bored cork. The two necks which were not tightly sealed were about 20 cm. long, sufficient so that the pickup of moisture from the air by the solution in the flask was negligible. The flask was immersed in a water bath adjusted to 25°. A second similar flask was constructed from a 50-ml. flask and fitted with a second pair of electrodes.

An ordinary run consisted of a series of about 25 potential readings taken over a period of several hours as portions of a sodium acetate solution were added from the buret to an initially acid solution. The potential measurements were made with a Beckman Model G pH-voltmeter. When three electrodes were used, measurements were made comparing both of the other electrodes to the glass electrode. In a few cases the other electrodes were compared directly, giving a reading negligibly different from the difference of the other two values. In other runs portions of water, a solution of sodium chloride in water, or a solution of water in acetic acid were added to HCl or sodium acetate solutions.

Solutions of HCl in acetic acid were prepared by adding concentrated aqueous hydrochloric acid and acetic anhydride to glacial acetic acid. These solutions lost HCl on standing and when they were poured into the flask containing the electrodes. On standing in this flask there were additional smaller losses of HCl, as much as 70% of the HCl present being lost in 3 days. The concentrations of HCl present were calculated from the amount of sodium acetate solution required to reach the equivalence point of the titration as determined from a plot of potential *vs.* volume of sodium acetate solution added. All other concentrations were calculated from the initial concentrations of the solutions used assuming negligible volume changes on mixing. The water content of each original solution was determined by Karl Fischer titration. In a number of the runs the water content of the final solution was also determined. This was generally somewhat higher than the value calculated from the water contents of the component solutions, corresponding to the pickup of one to three extra milliequivalents of water in the process of filling the cell. In calculating the water concentrations it was assumed that this extra water was present at the beginning of the series of measurements.

Standard C.P. and reagent grade chemicals were used throughout. The glacial acetic acid used generally contained 0.05 to 0.10 *M* water. Sodium acetate solutions were prepared from anhydrous material or from the trihydrate, adding acetic anhydride and refluxing for at least 10 hr. when lower water concentrations were desired. These solutions were standardized by potentiometric titration *vs.* a solution of HClO₄ in glacial acetic acid using Na₂CO₃·H₂O as a primary standard. A 0.643 *M* sodium perchlorate solution was prepared by weighing the anhydrous salt which was obtained by storing the monohydrate on a watch glass in a desiccator over Drierite for 7 weeks. Portions of glacial acetic acid and sodium perchlorate were dried further by refluxing with acetic anhydride, but in most of the work no attempt was made to operate with water concentrations of less than 0.1 *M*.

The initial solution was saturated with sodium chloride before some of the titrations. For this purpose finely divided sodium chloride was prepared by the addition of HCl to a solution of sodium acetate in acetic acid. The slurry was used directly or the precipitated sodium chloride was collected and washed with methanol. Distillation Products Industries tetrachloro-hydroquinone (White Label) and chloranil (practical) were recrystallized from acetic acid before use.

Results and Discussion

Calibration of the Glass Electrode.—Glass electrodes are sensitive to strong electrostatic charges and electrodes used outside the meter are ordinarily equipped with some internal shielding and a coaxial lead. These difficulties are somewhat enhanced on working in glacial acetic acid and in order to get steady potential

readings it was necessary to take special precautions to see that the water bath, the case of the pH meter, and the shielding of the coaxial cable were all well grounded.

Another characteristic feature of glass electrodes is the presence of an asymmetry potential, a potential difference independent of the hydrogen ion activity in the solutions tested. It changes only slowly with time and is ordinarily compensated for by using a standard buffer solution. In order to correct for any small changes in asymmetry potentials, such as a change of 25 mv. over the first month of use of the second glass electrode, repeated measurements were made on reference solutions of known sodium acetate and water concentrations saturated with NaCl.

The glass electrode responded rapidly to changes in the acidity of the acetic acid solutions. On taking alternate readings on solutions of HCl and sodium acetate saturated with sodium chloride, after each change the readings were nearly constant after 3 min. Nevertheless slow drift of the potential readings was observed under certain conditions, depending on the nature of the solution and the past history of the electrodes. The first reference solution was used with the first glass-(Ag-AgCl) electrode pair over a period of almost 4 months. About 90% of the potential readings with this combination at 25° were within the range 352 ± 4 mv., but values as high as 379 mv. were obtained immediately following measurements on solutions with water concentrations of around 8 *M*. This reference solution was itself approximately 1.4 *M* in water. In these cases the readings dropped on prolonged standing with the reference solution, but as much as 24 hr. was sometimes required for apparently complete recovery. An attempt was made to get larger transient effects by changing from an aqueous solution to a reference solution 0.43 *M* in water, but the drift following this change was less than 10 mv.

An attempt was made to calibrate the glass electrode by direct measurement *vs.* a hydrogen electrode. The hydrogen electrode has been used successfully in glacial acetic acid^{12,18,19}; however, these publications indicate that extreme precautions are necessary to obtain reliable potentials in dry solutions. A number of glass *vs.* hydrogen electrode readings were obtained in the range 680 to 695 mv. using one of the wet reference solutions. This is a reasonable range for variation in the glass electrode in the light of the other data. However, with the electrodes and apparatus for hydrogen purification which we used, it was impossible to obtain reproducible potentials with the hydrogen electrode in drier HCl solutions. The observed potentials *vs.* the glass electrode ranged from 385 to 677 mv.

In view of these difficulties with the hydrogen electrode, the glass electrodes were calibrated by comparison with the chloranil electrode. Since both chloranil, C₆Cl₄O₂, and tetrachloro-hydroquinone, C₆Cl₄O₂H₂, are only moderately soluble in acetic acid, it is quite simple to keep the solution saturated and their activities constant. Thus the chloranil electrode is sensitive only to the activity of hydrogen ions. As long as the solid phases are the acetic acid solvates, the potential of a chloranil electrode *vs.* a hydrogen electrode should be

(18) J. Russell and A. E. Cameron, *J. Am. Chem. Soc.*, **68**, 774 (1936); **60**, 1345 (1938).

(19) O. Tomicek and A. Heyrovsky, *Collection Czech. Chem. Commun.*, **15**, 984 (1950).

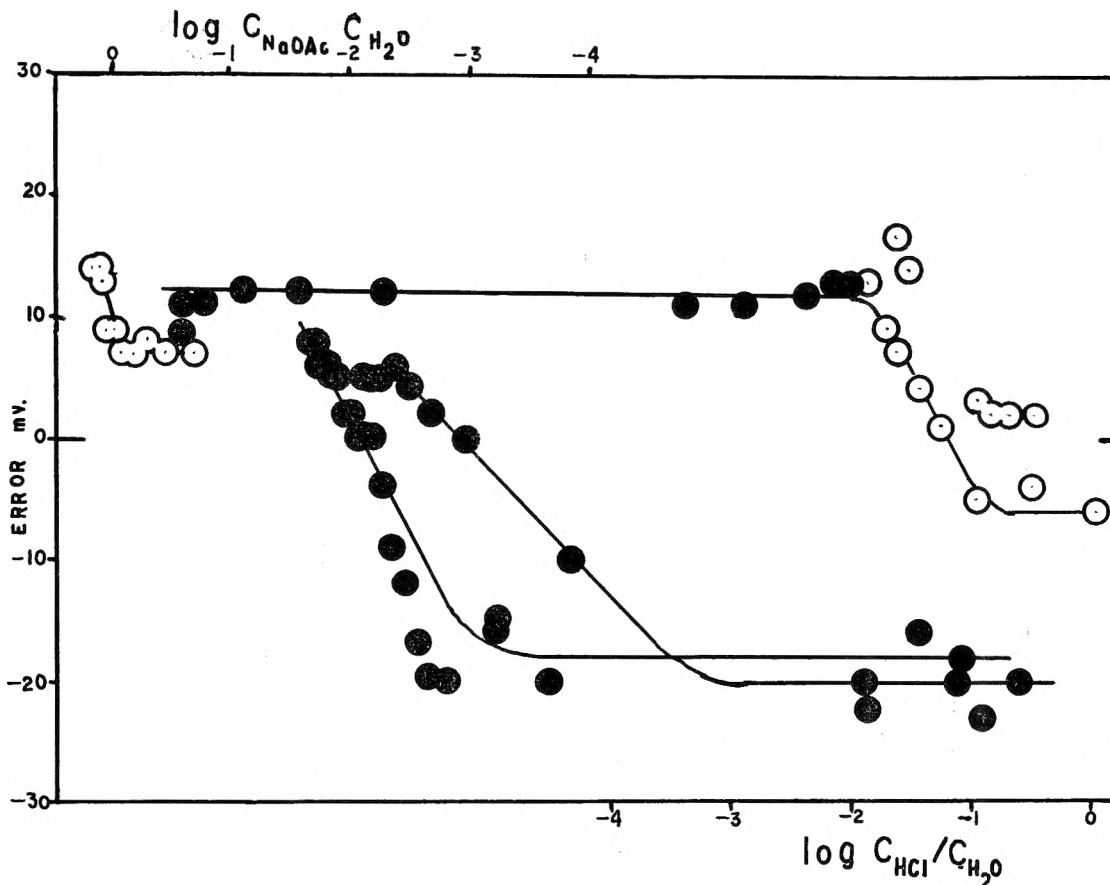


Fig. 1.—Acid error of the glass electrode as measured vs. the chloranil electrode under various conditions. The filled circles represent titrations with sodium acetate, the open circles represent additions of successive portions of water. In all four runs the first of the series of measurements is toward the right side.

680 mv., the E^0 value reported by Heston and Hall.²⁰ The chloranil electrode is susceptible to poisoning, but much less so than the hydrogen electrode. Twice in the course of this work the glass vs. chloranil readings suddenly increased by about 500 mv., but the original reading was restored by replacing the platinum electrode. The principal disadvantage of the chloranil electrode is the sensitivity of the Ag–AgCl electrode to the presence of chloranil and tetrachlorohydroquinone. The presence of these materials introduced an error in the Ag–AgCl potentials of from 0 to 80 mv. depending on the solution and the condition of the Ag–AgCl electrode. Thus, while the chloranil electrode could be used to check the glass electrode in a particular type of titration, any quantitative conclusions must be based on similar titrations with chloranil absent.

As expected from the drift effects described above for the glass electrode, the glass vs. chloranil electrode measurements were not entirely reproducible. Readings with the first glass electrode in solutions which had been stirred with chloranil and tetrachlorohydroquinone in the presence of the electrodes for an hour or more fell into two groups, -10 ± 2 and -28 ± 6 mv. The lower values were mostly obtained following measurements at exceptionally high water concentrations.

The acid error in these HCl solutions is expected to be negative, and it is clear that the best value is -10 mv., corresponding to an E^0 for this glass electrode of 670 ± 2 mv. The second glass electrode gave higher readings. These values increased still more during the first month and the readings on the reference solution

rose correspondingly. The difference between these two types of readings was nearly constant at about 326 mv. The changes are clearly due to variation in the asymmetry potential of the electrode. Considering both reference solution and chloranil values, this glass electrode started with an E^0 of 721 mv. which rose to 742 mv. When this electrode was reused after standing for a year the E^0 was 770 mv.

The Acid Error.—In aqueous HCl solutions the glass electrode gives low readings in concentrated solutions, above 1 *M*, where the ratio $C_{\text{HCl}}/C_{\text{H}_2\text{O}}$ is greater than 0.02. Similar negative errors were observed in glacial acetic acid solutions in this work at similar values of the ratio of concentrations. Various studies of the acid error in concentrated aqueous solutions have established certain features of this error which also appear to be applicable to acetic acid solutions. Thus, a downward drift of readings on standing in HCl solutions similar to that found in aqueous HCl^{3,21} was observed in this work. A small fraction of the drift is explainable by loss of HCl from the solution, but mostly it is due to the effect of HCl on the glass electrode. The initial rate of drift, several millivolts per hour, was comparable to that found in aqueous HCl solutions; however, the rate of change decreased more rapidly than predicted by the equation given by Schwabe and Glöckner.³

It has also been established by earlier workers that the acid error is dependent on the composition of the glass^{21,22} and on the previous treatment of the surface,³ and that it can be correlated with chemical attack

(21) E. E. Sinclair and A. E. Martell, *J. Chem. Phys.*, **18**, 224, 992 (1950).

(22) B. Lengyel and J. Vincze, *Glastechn. Ber.*, **19**, 359 (1941).

(20) B. O. Heston and N. F. Hall, *J. Am. Chem. Soc.*, **55**, 4729 (1933).

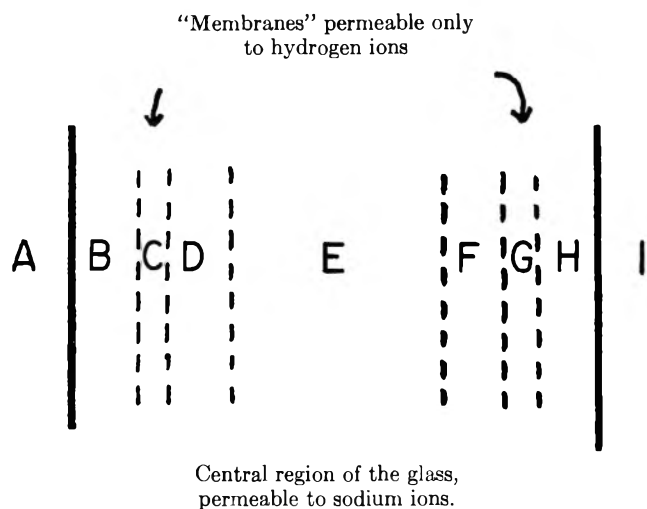


Fig. 2.—Postulated structure of the glass electrode. A and I represent the solutions, B and H are surface layers of hydrated silica gel, and C and G represent regions which act as membranes permeable only to hydrogen ions.

on the glass.²³ Early speculation²⁴ that anions were involved in the acid error has been confirmed and explicitly formulated by Izmailov and co-workers.^{2,25} Other related papers are summarized in recent review articles.^{9,26}

In the ordinary pH range including 0.1 *M* HCl the glass electrode agrees with the hydrogen electrode in 95% alcohol solutions^{27,28}; however, with more concentrated acid or drier solutions negative acid errors have been observed.²⁹ The present work in acetic acid solutions is unique in that substantial positive errors have been observed as well as negative ones. As outlined in the following section, it is expected that if reaction with HCl gives negative errors, the reverse reaction on adding H₂O or decreasing the HCl concentration should give positive errors, but apparently with aqueous solutions and the alcohols this effect is too small to be detected. Quite substantial positive errors are produced on adding either water or sodium acetate to HCl solutions as shown by runs comparing the glass and chloranil electrodes, some of which are shown in Fig. 1. The curves of error *vs.* log ($C_{\text{HCl}}/C_{\text{H}_2\text{O}}$) have a characteristic and reproducible shape with constant regions and a roughly linear portion where the error changes sign. On adding H₂O there are some transient effects giving considerable experimental scatter, but the general shape is clear with a sign change somewhere around ($C_{\text{HCl}}/C_{\text{H}_2\text{O}}$) 10^{-1} to 10^{-3} . In titrations with sodium acetate the sign of the error changes shortly beyond the equivalence point. The shape of these curves is very easily reproduced; however, the slope and intercept vary from run to run. Some titrations

showed much smaller errors than the runs in Fig. 2, often less than 10 mv. These runs showed the same general pattern but with proportionately larger scatter. On the addition of sodium acetate to a solution of HCl containing 6.8 *M* H₂O, the errors were positive throughout and essentially constant. The addition of H₂O to sodium acetate solutions had very little effect on the error. The run of this type in Fig. 2 shows an essentially constant error up to 6 *M* H₂O with a rise of 7 mv. as still more water was added. In some cases the addition of water reduced the error, but in all cases the changes were small. The chloranil data clearly show that in these titrations the glass electrode is reliable to ± 15 mv. However, substantial positive errors were obtained when the solution in the flask was replaced by a drier one. Thus, whenever a run introduced some acid error and also involved some measurements in the range of 5–8 *M* H₂O, subsequent readings on the reference solution were 20 to 30 mv. too high. These errors decreased slowly on standing and were generally negligible the next day. Even larger errors could be produced deliberately. The largest errors observed in this work, around 70 mv., were obtained in a reference solution 0.44 *M* in H₂O after first letting dry HCl stand in the flask for 3 days and then taking readings in solutions of about 3 *M* H₂O just prior to the reference solution.

Negative errors were consistently observed in dry HCl solutions. The presence of some water, 0.3 to 1 *M*, generally increased the rate at which the error appeared so that very little acid error was present in rapid titrations of dry HCl solutions. It was possible to estimate the amount of error in particular runs independently using the measured values for the reference solution obtained following the run. In this way data accurate within 5 mv. can be selected from the various runs which were made. The acid error in glacial acetic acid can presumably be avoided if no solutions with $C_{\text{HCl}}/C_{\text{H}_2\text{O}}$ greater than 10^{-4} are used, but once introduced it is very difficult to remove. While it decreases on standing in a particular solution, it can reappear following an increase and decrease of the water concentration. The work of Schwabe and Glöckner³ indicates that as much as 14 days soaking in water would be necessary to remove the error completely. These various experimental observations on the acid error can be fitted neatly into current theories on the operation of the glass electrode and on the nature of the acid error.

Glass Electrode Theory.—The simplest theory explaining the response of the glass electrode to hydrogen ion activity regards the glass as a membrane permeable only to H⁺ ions, and Donnan membrane equilibrium in proton transfer leads to a balancing electrostatic potential difference between the solutions. This theory is inadequate since it has been clearly shown that in the central portions of the glass the current is carried by Na⁺ ions instead of H⁺.^{30–32} The operation of the glass electrode is, however, explainable in terms of the three layer theory of Haugaard³⁰ which considers two layers near the outer surfaces of the glass where Na⁺ ions have been replaced by H⁺ by exchange with water so that these regions act as membranes permeable only to H⁺ while the central region is permeable only to Na⁺

(23) D. Hubbard, E. H. Hamilton, and A. N. Finn, *J. Res. Natl. Bur. Std.*, **32**, 339 (1939); D. Hubbard and G. F. Rynders, *ibid.*, **39**, 561 (1947).

(24) D. A. MacInnes and D. Belcher, *J. Am. Chem. Soc.*, **53**, 3315 (1931).

(25) N. A. Izmailov and A. M. Aleksandrova, *Sb. Statei Obshch. Khim., Akad. Nauk SSSR.*, **1**, 173 (1953); *Chem. Abstr.*, **48**, 12589d (1954); *Dokl. Akad. Nauk SSSR*, **71**, 311 (1950); *Chem. Abstr.*, **44**, 6304f (1950).

(26) Z. Boksay, B. Csakvari, and B. Lengyel, *Z. physik. Chem. (Leipzig)*, **207**, 223 (1957).

(27) A. L. Bacarella, E. Grunwald, H. P. Marshall, and E. L. Purlee, *J. Phys. Chem.*, **62**, 856 (1958).

(28) J. P. Morel, P. Seguela, and J. C. Pariaud, *Compt. rend.*, **253**, 1326 (1961).

(29) N. A. Izmailov and A. M. Aleksandrova, *Tr. Komiss., Anal. Khim. Akad. Nauk SSSR, Otd. Khim. Nauk*, **4** [7], 149 (1952); *Zh. Obshch. Khim.*, **19**, 1403 (1949); *J. Gen. Chem. USSR*, **19**, 1405 (1949); *Chem. Abstr.*, **44**, 1345 (1950); **48**, 1857 (1954).

(30) G. Haugaard, *J. Phys. Chem.*, **45**, 148 (1941).

(31) K. Schwabe and H. Dahms, *Monatsh. Deut. Akad. Wiss.*, **1**, 279 (1959).

(32) P. R. Hammond, *Chem. Ind. (London)*, 311 (1962).

ions. It is clear that H^+ carries the current in the outer portions of the glass except in strongly basic solutions,³³ but on prolonged electrolysis after one of the outer regions is exhausted, sodium ions are supplied to the solution on this side.³⁰

It is convenient and consistent with common usage to define the activity of ions to be dependent on the composition of a phase but not its electrostatic potential. In the notation of Guggenheim,³⁴ activities so defined would be equal to $i^0 m_i \gamma_i$, and by definition

$$RT \ln a_{H^+,D} = f(\text{comp. D})$$

and

$$RT \ln a_{Na^+,D} = f'(\text{comp. D})$$

The electrochemical potential³⁴ of an ion, μ_i , can then be written as

$$\mu_{H^+}^A = \mu_{H^+}^0 + RT \ln a_{H^+,A} + \mathfrak{F}P(A)$$

where $P(A)$ represents the electrostatic potential of phase A. Then, if the regions between the H^+ and Na^+ permeable regions are designated as in Fig. 2, one can equate the chemical potentials of an ion on opposite sides of a membrane permeable to that ion, obtaining

$$RT \ln a_{H^+,A} + \mathfrak{F}P(A) = RT \ln a_{H^+,D} + \mathfrak{F}P(D)$$

$$RT \ln a_{Na^+,D} + \mathfrak{F}P(D) = RT \ln a_{Na^+,F} + \mathfrak{F}P(F)$$

$$RT \ln a_{H^+,F} + \mathfrak{F}P(F) = RT \ln a_{H^+,I} + \mathfrak{F}P(I)$$

These equations can be rearranged to give

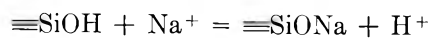
$$\begin{aligned} \mathfrak{F}(P(A) - P(I)) &= RT \ln a_{H^+,I} - RT \ln a_{H^+,A} + \\ f(\text{comp. D}) - f'(\text{comp. D}) - f(\text{comp. F}) + \\ & f'(\text{comp. F}) \end{aligned}$$

Since small currents do not appreciably change the composition of the interior regions D and F, the composition terms contribute only to the asymmetry potential of the electrode. Haugaard,³⁰ in an attempt to explain Dole's equation¹¹ for the acid error, equated the H^+ permeable regions C and G with the hydrated silica gel surface regions B and H, but tritium exchange experiments³² show that hydrogen ions carry the current considerably deeper into the glass than the outer layers which can exchange hydrogen with boiling water.

In the light of this consideration, it is failure to establish equality of the chemical potential of hydrogen ions between phase D and the solution A which leads to the principal errors of the glass electrode. Failure to establish this equilibrium may be due to any layer impermeable to hydrogen ions between region D and the solution, including coatings of SiO_2 , Ag, petrolatum, or stopcock grease.³⁵

Extensive chemical attack, as by HF, may destroy region D giving very large errors²³; however, the acid errors ordinarily encountered appear to be due to diffusion potentials due to exchange processes in the gel layer, B.

Izmailov and Vasil'ev² have shown that the major errors of the glass electrode are related to the amphoteric nature of SiOH groups in the outer hydrated gel layer.



The alkali error is of no direct concern in acetic acid solutions since even in 1 M sodium acetate in acetic acid the ratio a_{H^+}/a_{Na^+} is greater than one. However, the formation of SiCl bonds appears to be a major factor in the acid errors observed in this work. As they are formed there is a net flux of H^+ into the gel layer so

$$\mu_{H^+}^A > \mu_{H^+}^D$$

and a negative error is observed in the potential. In the limit of very high C_{HCl}/C_{H_2O} the concentration of SiOH groups will be very small, so that most of the current is carried through this region by Cl^- rather than H^+ ions, approximating a membrane permeable only to Cl^- . Such limiting behavior with the potential responding to the activity of chloride ions was observed by Izmailov and Vasil'ev² in extremely concentrated aqueous HCl solutions; however, it was not approached in the present work.

The derivative, $d\mu_{H^+}/dx$, and hence the error, can be evaluated using the Nernst-Planck equation for the diffusion of electrolytes in a treatment analogous to the Wagner theory^{36,37} of diffusion controlled reactions, the kinetics of substitution in ion-exchange resins,³⁸ and theories of the alkali error and alkali ion response of glass electrodes.³⁹⁻⁴⁴ Eliminating dP/dx from the equations by setting $J_{H^+} = J_{Cl^-}$ one obtains

$$\begin{aligned} \frac{d(\text{error})}{dx} &= \frac{1}{\mathfrak{F}} \frac{d\mu_{H^+}}{dx} = \\ & \frac{RT}{\mathfrak{F}} \left[\frac{C_{Cl^-} - D_{Cl^-}}{C_{Cl^-} - D_{Cl^-} + C_{H^+} \cdot D_{H^+}} \right] \frac{d \ln a_{HCl}}{dx} \end{aligned}$$

The quantitative application of this equation, which requires information on the concentration dependence of the diffusion coefficients, is beyond the scope of this paper; however, the qualitative effects observed in this work are readily interpreted in terms of this equation with the recognition that water strongly affects the diffusion coefficient of the H^+ ion, D_{H^+} . In ordinary glass $C_{Cl^-} - D_{Cl^-}$ is extremely small compared to $C_{H^+} \cdot D_{H^+}$, and the term in brackets is nearly zero. Thus the error arises only in a "chlorinated" zone in the glass. Even here the error is almost inversely proportional to $C_{H^+} \cdot D_{H^+}$, and hence markedly dependent on the degree of hydration of the glass. Schwabe and Glöckner³ found it necessary to soak electrodes for 14 days to obtain reproducibility in the time dependence of the acid error.

(36) C. Wagner and K. Grunewald, *Z. physik. Chem.*, **B40**, 455 (1938).

(37) W. Jost, "Diffusion in Solids, Liquids, Gases," Academic Press, New York, N. Y., 1960, pp. 383, 393.

(38) F. Helfferich, "Ion Exchange," McGraw-Hill Book Co., Inc., New York, N. Y., 1962, p. 268.

(39) G. Eisenman and G. Karreman, Abstracts of Papers, 141st National Meeting of the American Chemical Society, Washington, D. C., 1962, p. 91.

(40) E. A. Materova, V. V. Moiseev, and A. A. Belyustin, *Zh. Fiz. Khim.*, **35**, 1258 (1961).

(41) K. Schwabe and H. Dahms, *Z. Elektrochem.*, **65**, 518 (1961).

(42) B. Lengyel, B. Csakvari, and Z. Boksay, *Acta Chem. Hung.*, **25**, 225 (1960).

(43) N. A. Izmailov and A. G. Vasil'ev, *Zh. Fiz. Khim.*, **29**, 2145 (1955).

(44) B. P. Nikolskii, *ibid.*, **27**, 724 (1953).

(33) F. Quittner, *Ann. Physik*, **85**, 745 (1928).

(34) E. A. Guggenheim, "Thermodynamics," 4th Ed., North Holland Publishing Co., Amsterdam, 1959, p. 371.

(35) D. Hubbard and G. F. Rynders, *J. Res. Natl. Bur. Std.*, **41**, 163 (1948).

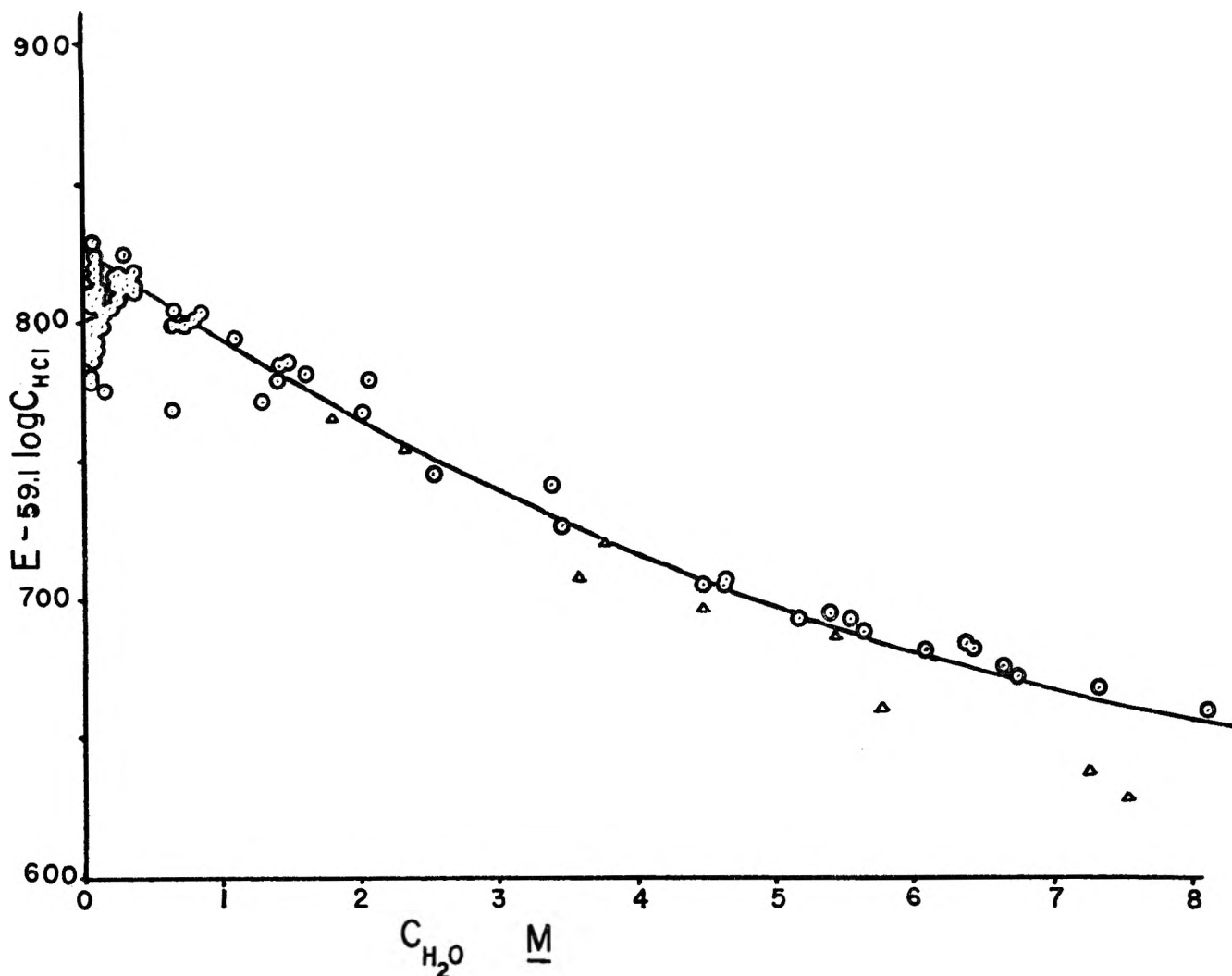


Fig. 3.—The effect of water on the potential in HCl solutions. About one third of the points from each run are shown. The open circles represent data for solutions saturated with sodium chloride while the small triangles stand for solutions with no sodium chloride present.

On reversing the chloride exchange reaction by adding water or removing HCl the negative error may persist briefly, but in a short time a distribution with a maximum of $\ln a_{\text{HCl}}$ at some position within the chlorinated zone will be established. The regions of positive and negative $d \ln a_{\text{HCl}}/dx$ will give errors which will tend to cancel. If the exchange is diffusion controlled, as it appears to be, the activities of HCl at the two boundaries of the chlorinated zone will be determined by equilibrium in the exchange reaction, $\equiv\text{SiCl} + \text{H}_2\text{O} = \equiv\text{SiOH} + \text{HCl}$, and it will not be greatly different at the two boundaries. Thus the relative contributions of the two regions and the sign of the resulting error will depend primarily on the values of $C_{\text{H}} \cdot D_{\text{H}^+}$, and hence on the degree of hydration of the two regions. In aqueous solutions $C_{\text{H}} \cdot D_{\text{H}^+}$ is highest in the outer region, and no net positive errors have been reported. The data presented here clearly show positive errors for acetic acid solutions with water concentrations from 0.05 to 8 M. Ordinarily changes in the water concentration do not have large immediate effects on D_{H^+} over enough of the chlorinated zone to affect the error drastically, and under most conditions encountered in this work there is a limit of about 20 mv. to the error observed. However, at relatively high water concentrations, where the hydrolysis of the chlorinated zone is proceeding rapidly, the region of positive $d \ln a_{\text{HCl}}/dx$

is concentrated near the outer edge of the zone. Then a sudden decrease in the water concentration can give the combination of large $d \ln a_{\text{HCl}}/dx$ and small D_{H^+} necessary for large positive errors. The errors greater than +20 mv. in this work invariably followed such a sharp change to a lower water concentration.

Solutions of HCl. The Effect of Water.—The dependence of the glass vs. Ag–AgCl potentials on the concentration of HCl was given within experimental error by the equation $E = Z + 59.1 \log C_{\text{HCl}}$. Thus Henry's law is followed within experimental error by solutions of HCl in acetic acid over the concentration range from 0.003 to 0.18 M, and ionization and association of the HCl must both be small. This agrees well with the direct experimental test of Henry's law,⁴⁵ and with the generally low values (*ca.* 10^{-7}) found for ionization constants in acetic acid generally.⁴⁶ Moreover, HCl is a weak acid in glacial acetic acid with an ionization constant even smaller than 10^{-7} .⁴⁷ The potentiometric data of Mukherjee⁴⁸ on HCl solutions in acetic acid are inconsistent with these considerations and with the data reported here, apparently because of the failure

(45) W. H. Rodebush and R. H. Ewart, *J. Am. Chem. Soc.*, **54**, 419 (1932).

(46) M. M. Jones and E. Griswold, *ibid.*, **76**, 3247 (1954).

(47) I. M. Kolthoff and A. Willman, *ibid.*, **56**, 1007 (1934).

(48) L. M. Mukherjee, *ibid.*, **79**, 4040 (1957).

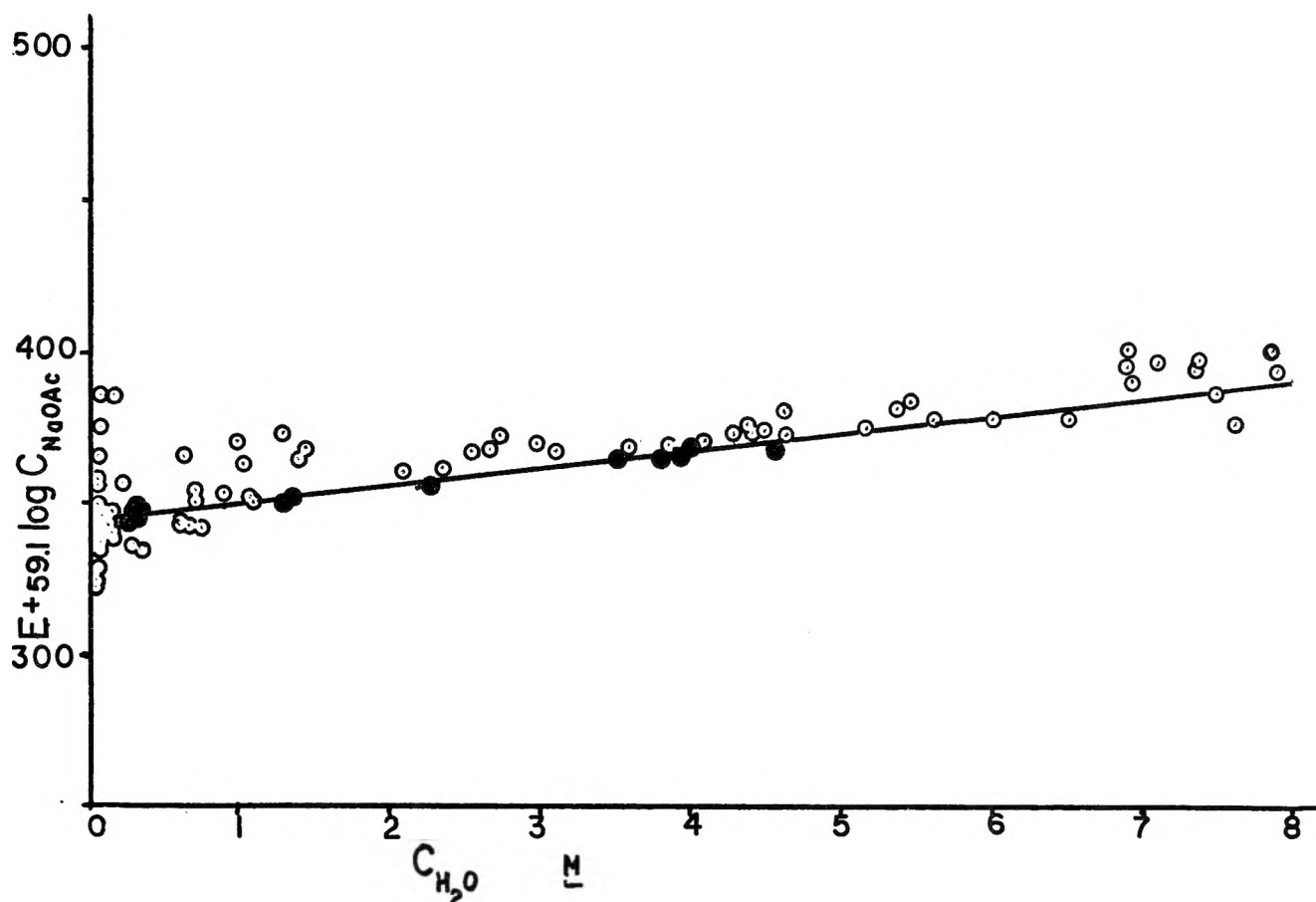


Fig. 4.—The effect of water on the glass vs. Ag-AgCl potential in sodium acetate solutions saturated with sodium chloride. About one third of the points from each run are shown. The dark circles represent data from runs with minimal "acid error." The straight line is given by $345 + 5.6C_{H_2O}$.

of his hydrogen electrode to give reliable potentials in this solvent.

The addition of water lowers the activity of HCl and the observed potentials. Thus the quantity "Z" from the above equation, the potential corrected for the HCl concentration, is a function of the water concentration of the solution as well as the standard electrode potential of the particular glass electrode being used. Comparable values can be obtained by correcting the potentials to an E^0 value of 700 mv. for the glass electrode. Some of these corrected "Z" values from a number of different runs are plotted against the water concentration in Fig. 1. The irreproducibility of the values at the lowest water concentrations is evident. However, the agreement in most runs over the concentration range from 0.3 to 6 M water is excellent. This data cannot be fitted by the formation of a single complex species such as H_3OCl , and there is no appreciable linear region with any integral slope in a plot of Z_{cor} vs. $\log C_{H_2O}$. Thus it appears best to treat the effect of water as a medium effect.

About a third of the experimental values for each run except those with deliberately introduced errors are shown in Fig. 3. The data are in excellent agreement with the equation

$$Z_{cor} = 827 - 33.1C_{H_2O} + 1.5C_{H_2O}^2$$

shown as a solid line in the figure. Thus the potentials corrected to $E^0 = 700$ are given by the equation

$$E_{cor} = 827 + 59.1 \log C_{HCl} - 33.1C_{H_2O} + 1.5C_{H_2O}^2$$

Since $E_{cor} = 827 + 59.1 \log a_{HCl}$ if one chooses a

hypothetical ideal undissociated unit concentration solution of HCl in dry acetic acid as the standard state for its activity, one obtains the equation $\log \gamma_{HCl} = -0.56C_{H_2O} + 0.025C_{H_2O}^2$ for the activity coefficient of HCl in these solutions.

At the higher water concentrations the solubility of sodium chloride is high enough to have an appreciable effect on the potentials. The data obtained on HCl solutions with no sodium chloride present are represented in Fig. 3 by small triangles. It is adequately fitted by the equation

$$Z_{cor} = 827 - 33.1C_{H_2O} + 0.9C_{H_2O}^2$$

A check of the E^0 values used for the glass electrodes is possible using the value 827 mv. for the potential difference in dry acetic acid at unit activity of HCl. This corresponds to the value 127 mv. for the potential between a hydrogen electrode and the Ag-AgCl electrode under these conditions. This is in excellent agreement with the value of 123 mv. calculated from the equation given by Aston and Gittler,⁴⁹ $E = 150.8 + 59.1 \log P_{HCl}$ using the Henry's law constant, 0.334 atm. l. moles⁻¹, measured by Rodebush and Ewart.⁴⁵

Sodium Acetate Solutions. The Effect of Water.—After excess sodium acetate has been added in a titration the electrodes still respond to the activity of HCl. However, the concentration of HCl is no longer directly measurable, and its activity is determined by the equilibrium $HCl + NaOAc = NaCl(s) + HOAc$. The activity of sodium chloride thus has a very great in-

(49) J. G. Aston and F. L. Gittler, *J. Am. Chem. Soc.*, **77**, 3173 (1955).

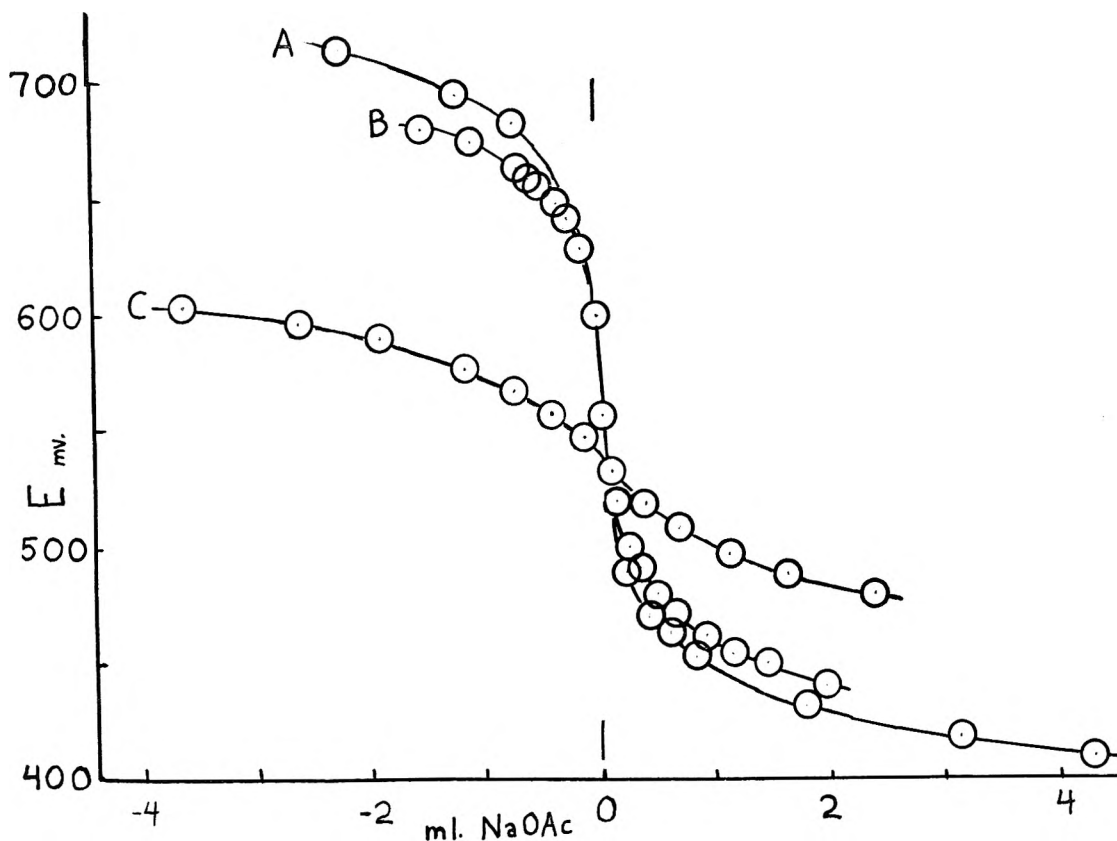


Fig. 5.—Acid-base titration curves, HCl titrated with 0.43 *M* sodium acetate. Potential corrected to $E^0 = 700$ mv. plotted against excess volume of base.

Curve	Ca. concn. of water, <i>M</i>	Vol. at equiv. point, ml.
A	0.3	29
B	1.4	28
C	6.2	32

fluence on the readings, and failure to achieve solubility equilibrium can introduce considerable error in the observed potentials. Thus the somewhat increased experimental scatter shown by these results in basic solutions is not unexpected. When solubility equilibrium is established, the potential should be given by the equation

$$E_{\text{cor}} = 827 + 59.1 \log [K a_{\text{HOAc}} / a_{\text{NaOAc}}]$$

Since the activity of sodium acetate is at least approximately proportional to its concentration, with the proportionality constant γ_{NaOAc} , this can be rearranged to give

$$Z_{\text{cor}}^* = E_{\text{cor}} + 59.1 \log C_{\text{NaOAc}} = 827 + 59.1 \log K a_{\text{HOAc}} / \gamma_{\text{NaOAc}}$$

Z^* may be somewhat dependent on the sodium acetate concentration, but such effects over the concentration range 0.005 to 0.09 *M* are not clearly larger than the experimental uncertainty. In dilute solutions with water concentrations above 3 *M*, the disproportionation of sodium chloride to give HCl and sodium acetate becomes appreciable. However, ionization of the sodium acetate does not appear to be an important factor below 10 *M* water. This can be substantiated from conductance data which yield an ionization constant of 2×10^{-7} for sodium acetate in dry acetic acid⁴⁶ and indicate that it is only about twenty times more ionized in the presence of 15 *M* water.⁴⁷ Also the presence of sodium chloride should repress the ionization of sodium acetate.

The addition of water raises the potential readings in these basic solutions, Z^* values from a number of runs including some in which either or both the water and sodium acetate concentrations were varied are shown in Fig. 4. Again the experimental scatter is worst for the driest solutions.

As noted above, in the course of titrations some negative acid errors were observed on the sodium acetate side of the end point as well as positive errors. This further accounts for the scatter of the experimental points. The runs where the acid error was smallest are shown in Fig. 4 by black circles. These points are clearly all within ± 5 mv. of the line $Z^* = 345 + 5.6 C_{\text{H}_2\text{O}}$. This gives the equation

$$\log \gamma_{\text{NaOAc}} / a_{\text{HOAc}} = -0.095 C_{\text{H}_2\text{O}}$$

for the effect of water on the activity of sodium acetate.

The Titration of HCl with Sodium Acetate.—The equations for Z and Z^* given above summarize the behavior of the potential through the course of a titration. The difference between the constant terms gives a value of 1.4×10^{-8} for the equilibrium constant K . The addition of water shifts the equilibrium markedly toward the left and reduces the sharpness of the potential change at the equivalence point. The concentration equilibrium constant, $1/C_{\text{HCl}}C_{\text{NaOAc}}$, is given by the equation

$$\log K \gamma_{\text{HCl}} \gamma_{\text{NaOAc}} / a_{\text{HOAc}} = 8.15 - 0.66 C_{\text{H}_2\text{O}} + 0.025 C_{\text{H}_2\text{O}}^2$$

The effect of water is large enough that the end point becomes quite indistinct above 6 *M* water in titrations with 0.43 *M* sodium acetate. Since water lowers the potentials of acid solutions more than it raises those of basic solutions, the potential at the equivalence point is lowered somewhat. Several of the titrations with 0.43 *M* sodium acetate are shown in Fig. 5 to illustrate these points. Figures 3 and 4 illustrate the increased experimental error found on working at very low water concentrations, and in the driest solutions the acid error is more persistent. Soaking the electrodes in moist acetic acid solutions, as was done in this work, is quite satisfactory; however, the water content of this solution should not be much greater than in the solutions to be measured. Soaking for short periods in water should probably be avoided, but prolonged soaking in water appears³ to be the best treatment whenever any acid error has been produced. To avoid prolonged exposure of the glass electrode to acids it is probably best to add acid to base in potentiometric titrations, but since HCl is easily lost from solution this was not practicable in this work. For analytical purposes some compromise must be reached between the problems due to acid error which are worst in drier solutions and the effect of

water in reducing the sharpness of the end point. Some value in the range 0.4 to 1.5 *M* water appears to be best for routine work.

Summary.—Potential measurements with the glass electrode in glacial acetic acid can be readily obtained accurate to within ± 5 mv. Still higher accuracy is presumably obtainable in "basic" sodium acetate solutions, but when an electrode has been exposed to dry HCl solutions it will show some "acid error" until all the Si-Cl bonds have been hydrolyzed. These errors are negative in sign in dry acid solutions, but they become positive at higher concentrations of water and in sodium acetate solutions. This type of error is presumably responsible for the measurably low slope of *E* vs. pH found by Izmailov and Aleksandrova.² The errors are ordinarily small, under 20 mv., but by prolonged standing in dry acid solutions and appropriate manipulation of the water concentration much larger errors can be introduced. These effects are understandable in terms of a diffusion potential added to the normal hydrogen electrode response. The possibility of such acid errors should be considered along with the effect of water on the activities of acids and bases in choosing appropriate titration conditions as described above.

THE REACTION OF H ATOMS WITH OH⁻ IN THE RADIATION CHEMISTRY OF AQUEOUS SOLUTIONS

BY SHLOMO NEHARI AND JOSEPH RABANI¹

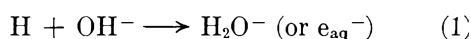
Department of Physical Chemistry, The Hebrew University, Jerusalem, Israel

Received December 21, 1962

Using 200-kvp. unfiltered X-rays, the effect of pH on reduction and dehydrogenation reactions of H atoms was studied. It is concluded that the reducing radicals in water radiolysis include H atoms with a yield of about 0.48 ± 0.05 . This yield is independent of pH between 2 and 13. In the alkaline solutions, H atoms are converted into a species which reacts with scavengers in the same manner as radiation produced e_{aq}^- . The reactivity of H atoms with nitrate, acetate, acetone, OH⁻, and bicarbonate was studied.

Introduction

Hydrogen atoms generated in the gas phase² by an electric discharge and introduced into basic aqueous solutions of chloroacetate³ appear to react with OH⁻, according to reaction



The product of reaction 1 reacts in basic solutions with chloroacetate ions yielding chloride, while H atoms in neutral solutions react mainly *via* dehydrogenation.^{3a,4,5}

The purpose of this work is to provide further evidence that hydrogen atoms as well as electrons are formed in the radiation chemistry of neutral and alkaline water and to yield independent support for reaction 1. This was accomplished by studying the effects of OH⁻ ions in the reactions of H atoms formed in irradiated aqueous solutions.

The primary action of X-rays on aqueous solutions

(1) Chemistry Division, Argonne National Laboratory, Argonne, Illinois.

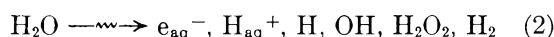
(2) G. Czapski and G. Stein, *J. Phys. Chem.*, **63**, 850 (1959).

(3) (a) J. Jortner and J. Rabani, *ibid.*, **66**, 2081 (1962); (b) *J. Am. Chem. Soc.*, **83**, 4868 (1961).

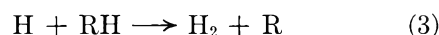
(4) E. Hayon and A. O. Allen, *J. Phys. Chem.*, **65**, 2181 (1961).

(5) E. Hayon and J. Weiss, *Proc. Intern. Conf. Peaceful Uses At. Energy*, **29**, 80 (1958).

may be presented schematically by⁶⁻⁸



The small primary yield of hydrogen atoms ($G_H \approx 0.5$)⁶⁻⁸ is responsible for the dehydrogenation of many organic solutes in neutral solutions according to



In the presence of both RH and a solute which scavenges all the e_{aq}^- without yielding H₂, the hydrogen yield in neutral aqueous solutions will be $G_{H_2} + G_H$. It is to be noted that RH also scavenges all OH.

In this work the effects of OH⁻ on the yield of hydrogen were investigated using acetone or NO₃⁻ as electron scavengers and formate, acetate, or acetone as H atom scavengers.

Experimental

The experimental procedure was similar to that described previously.⁹ The hydrogen produced was collected and its pressure was determined by a thermal conductivity method.⁹

(6) J. T. Allan and G. Scholes, *Nature*, **187**, 218 (1960).

(7) J. Rabani and G. Stein, *J. Chem. Phys.*, **37**, 1865 (1962).

(8) J. Rabani, *J. Am. Chem. Soc.*, **84**, 868 (1962).

(9) G. Czapski, J. Rabani, and G. Stein, *Trans. Faraday Soc.*, **58**, 2160 (1962).

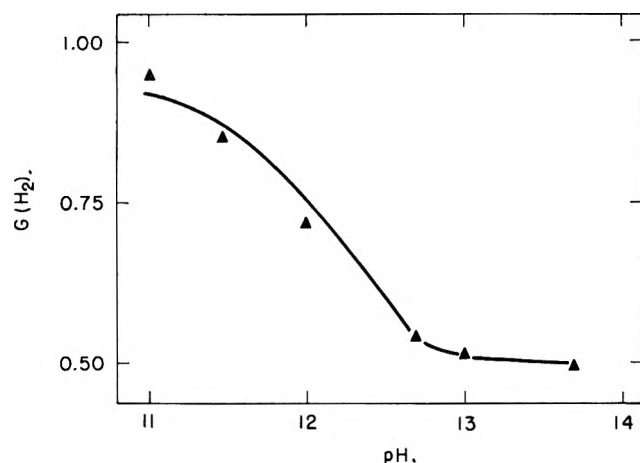


Fig. 1.—The effect of pH on $G(\text{H}_2)$ in solutions containing sodium formate ($10^{-3} M$) and acetone ($2.6 \times 10^{-2} M$).

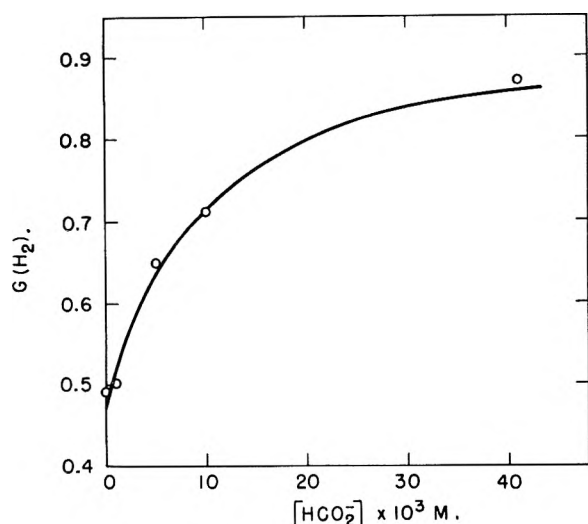


Fig. 2.—The effect of sodium formate concentration on $G(\text{H}_2)$ in solutions containing acetone ($2.6 \times 10^{-2} M$) at pH 13.0.

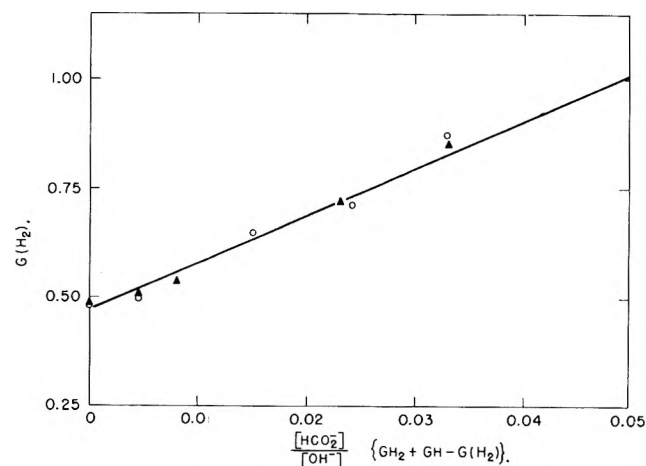


Fig. 3.— $G(\text{H}_2)$ as a function of $[\text{HCO}_2^-]/[\text{OH}^-]$ in $2.6 \times 10^{-2} M$ acetone: \blacktriangle , results of Fig. 1; \circ , results of Fig. 2.

The conductivity tube was kept at constant temperature (ice-water) in order to increase the accuracy of the measurements. Unfiltered X-rays (200 kvp.) were used. The dose rate, 1000 rads min^{-1} , was determined using the Fricke dosimeter: $10^{-3} M \text{FeSO}_4$ in $0.1 N \text{H}_2\text{SO}_4$, taking $G_{\text{Fe}^{3+}} = 14.5$. For most of the experiments NaOH was used to adjust the pH, here defined by $10^{\text{pH}} = 10^{14} [\text{OH}^-]$. The experimental G values reported are the average of at least two determinations. The gas volume above the solution (30 cc.) was about 100 cc.

Results

Solutions Containing Formate and Acetone.—The radiation chemistry of formic acid and formate has been investigated extensively.^{9,10} The formate anion reacts with H atoms^{10d} forming H_2 with a rate constant^{9,11} of $(k_{\text{H} + \text{HCO}_2^-}/k_{\text{H} + \text{O}_2})^{12} 1.3 \times 10^{-2}$. The rate constant of e_{aq}^- with formate is lower by a factor of at least 10^3 than that of e_{aq}^- with acetone.⁷ At the concentrations of formate and acetone employed by us, all the e_{aq}^- react with the acetone to reduce it. It will be shown later that the reaction of H atoms with acetone may be neglected.

Using $10^{-3} M$ sodium formate and $2.6 \times 10^{-2} M$ acetone (without buffer) the experimental yield of hydrogen, $G(\text{H}_2)$, is 0.95 at pH 7. This value is in fair agreement with that obtained previously⁷ in the isopropyl alcohol-acetone aqueous system. As the pH increases above 11, the hydrogen yield decreases rapidly (Fig. 1) to a value of $G(\text{H}_2) \cong 0.50$ at 0.1 – $0.5 M$ hydroxide. (LiOH was used at the concentration of $0.5 M$ to minimize possible changes in the absorption of radiation.) This change in $G(\text{H}_2)$ with pH is due to the competition of reaction 1 with reaction 3. The species produced in reaction 1 reacts with acetone without hydrogen evolution. The limiting value of $G(\text{H}_2) \cong 0.50$ which is reached at the higher pH values is the molecular yield of hydrogen, G_{H_2} . The difference between the two extreme values of $G(\text{H}_2)$ should equal G_{H} in agreement with the value of 0.5 ± 0.1 reported previously.⁶⁻⁸ In Fig. 2 it is seen that at pH 13 $G(\text{H}_2)$ increases with the formate concentration from $G(\text{H}_2) = G_{\text{H}_2} = 0.49$ in the absence of formate to $G(\text{H}_2) = 0.87$ with $4.1 \times 10^{-2} M$ formate.

The competition between reactions 1 and 3 leads to the expression (all electrons being scavenged by acetone)

$$G(\text{H}_2) = G_{\text{H}_2} + \frac{G_{\text{H}}}{1 + \frac{k_3[\text{RH}]}{k_1[\text{OH}^-]}} \quad (4)$$

If $G(\text{H}_2)$ is plotted vs. $([\text{HCO}_2^-]/[\text{OH}^-])[G_{\text{H}_2} + G_{\text{H}} - G(\text{H}_2)]$, a straight line should be obtained with G_{H_2} as intercept and slope k_3/k_1 . The analysis of the results in Fig. 1 and 2 taking $G_{\text{H}_2} + G_{\text{H}} = 0.95$ gives (Fig. 3) $k_3/k_1 = 11$, $G_{\text{H}_2} = 0.47$ and $G_{\text{H}} = 0.48$.

Competition for H Atoms between Acetone and OH^- .

a. The Reaction of Acetone with H Atoms.—In previous work^{10d} it was shown that acetone is dehydrogenated by H atoms



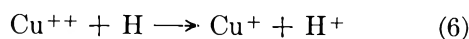
reaction 5 being relatively slow.¹³ In order to determine the value of k_5 , competition experiments with CuSO_4 were carried out in $0.1 N \text{H}_2\text{SO}_4$. Cu^{++} was added as it was found¹³ to react with H atoms, being reduced to the Cu^+ ion, with a rate constant of¹¹ $k_{\text{H} + \text{CuSO}_4}/k_{\text{H} + \text{O}_2} = 3.2 \times 10^{-3}$.

(10) (a) D. Smithies and E. J. Hart, *J. Am. Chem. Soc.*, **82**, 4775 (1960); (b) E. J. Hart, *ibid.*, **73**, 68 (1951); (c) **76**, 4198 (1954); (d) H. Fricke, E. J. Hart, and H. P. Smith, *J. Chem. Phys.*, **6**, 229 (1938); (e) T. J. Hardwick, *Radiation Res.*, **12**, 5 (1960).

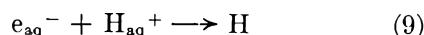
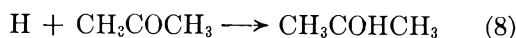
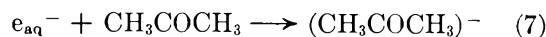
(11) J. Rabani, *J. Phys. Chem.*, **66**, 361 (1962).

(12) In this paper rate constants are given relative to $k_{\text{H} + \text{O}_2}$ to enable direct comparison with previous results.^{9,7,11}

(13) J. H. Baxendale and D. H. Smithies, *Z. physik. Chem. (Frankfurt)*, **7**, 242 (1956).



Using $2.6 \times 10^{-2} M$ acetone in $0.1 N \text{H}_2\text{SO}_4$ (total dose, 1000 rads) a value of $G(\text{H}_2) = 2.8$ was obtained. This value is considerably lower than the sum⁷ $G_{e^-} + G_{\text{H}} + G_{\text{H}_2}$. This is due to the competition of reaction 7 and, as will be shown later, of reaction 8 with reactions 5 and 9



In the presence of both acetone and CuSO_4 , neglecting the reaction of CuSO_4 with e_{aq}^- we obtain

$$G(\text{H}_2) = G_{\text{H}_2} + \frac{G_{\text{E}}}{1 + \frac{k_6[\text{Cu}^{++}] + k_8[\text{CH}_3\text{COCH}_3]}{k_5[\text{CH}_3\text{COCH}_3]}} + \frac{G_{e^-}}{\left\{1 + \frac{k_6[\text{Cu}^{++}] + k_8[\text{CH}_3\text{COCH}_3]}{k_5[\text{CH}_3\text{COCH}_3]}\right\} \times \left\{1 + \frac{k_7[\text{CH}_3\text{COCH}_3]}{k_9[\text{H}^+]}\right\}} \quad (10)$$

The ratio $k_7/k_9 = 0.5$ is known⁷ for $0.1 N \text{H}_2\text{SO}_4$. Taking $G_{\text{H}_2} = G_{\text{H}} = 0.5$ and $G_{e^-} = 3.0$ for $0.1 N \text{H}_2\text{SO}_4$, $k_8/k_5 = 0.3$ is obtained from the experiments in the absence of CuSO_4 according to eq. 10. Values of $G(\text{H}_2) = 2.3, 1.8,$ and 1.25 were obtained in solutions containing $1 \times 10^{-4}, 3 \times 10^{-4},$ and $10^{-3} M \text{CuSO}_4$, respectively. Defining $A = 1 + k_7[\text{CH}_3\text{COCH}_3]/k_9[\text{H}^+]$ plot of $(G_{\text{H}} + G_{e^-}/A)/(G(\text{H}_2) - G_{\text{H}_2})$ vs. $[\text{CuSO}_4]/[\text{CH}_3\text{COCH}_3]$ should give a straight line with $(1 + k_8/k_5)$ as an intercept and k_6/k_5 as a slope. The analysis of these results shows an agreement with $k_8/k_5 = 0.3$ and $k_6/k_5 = 70$. Reaction 8 is also supported by the result that addition of $10^{-2} M$ isopropyl alcohol to a solution of $2.6 \times 10^{-2} M$ acetone in $0.1 N \text{H}_2\text{SO}_4$ increases $G(\text{H}_2)$ from 2.8 in the absence of isopropyl alcohol to 3.5. In these experiments H atoms react with isopropyl alcohol⁶ according to reaction 3, but do not react with acetone, while the e_{aq}^- are shared between H_{aq}^+ and acetone. Thus the increase in $G(\text{H}_2)$ due to isopropyl alcohol should be equal to G_8 , the yield of reaction 8 when acetone only is present. From this result the value $k_8/k_5 = 0.3$ is obtained again.

b. The Effect of Varying pH on $G(\text{H}_2)$ in Acetone Solutions.—In neutral solutions of $2.6 \times 10^{-2} M$ acetone, $G(\text{H}_2) = 0.87$ (total dose 3000 rads). This value is lower by 0.08 than that obtained in the presence of $10^{-3} M$ formate, because of reaction 8. Assuming $G_{\text{H}_2} = 0.47$ and $G_{\text{H}} = 0.48$ as in the formate experiments, $k_8/k_5 = 0.2$ in agreement, within experimental error, with the value found in the acid solutions.

Adding 10^{-3} and $10^{-1} M \text{NaOH}$, $G(\text{H}_2)$ decreased to 0.79 and 0.49, respectively, showing again competition of reaction 1 with reactions 5 and 8. The equation derived to express this competition is

$$G(\text{H}_2) = G_{\text{H}_2} + \frac{G_{\text{H}}}{1 + \frac{k_1[\text{OH}^-] + k_8[\text{CH}_3\text{COCH}_3]}{k_5[\text{CH}_3\text{COCH}_3]}} \quad (11)$$

By the use of eq. 11 we get $k_1/k_5 = 12$. Using this value it is possible to calculate $k_{\text{H}+\text{HCO}_2^-}/k_1 = (k_5/k_1 \times k_6/k_5 \times k_{\text{H}+\text{HCO}_2^-}/k_6)^{11}$ which agrees with the ratio $k_{\text{H}+\text{HCO}_2^-}/k_1$ measured by direct competition of formate and OH^- for the H atoms.

Competition for H Atoms between Acetate, Nitrate, and OH^- .—Experiments in which acetate and nitrate were used as H atom and e_{aq}^- scavengers, respectively, were carried out. In these experiments, all e_{aq}^- in the bulk probably react with NO_3^-

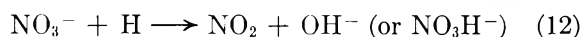
$$\left(\frac{k_{e^- + \text{NO}_3^-}}{k_{e^- + \text{H}_3\text{O}^+}} \cong 1\right)^{14}$$

without forming H_2 . H atoms may react with acetate to form H_2 according to reaction 3 and with nitrate to form reduction products.

TABLE I

HYDROGEN YIELDS IN SOLUTIONS OF ACETATE-NITRATE AT VARIOUS pH VALUES
Total dose 4000 rads

Expt.	pH	$G(\text{H}_2)$	k_1/k_5
1	Neutral [$5 \times 10^{-2} M \text{NaHCO}_3$]	0.86	..
2	11.0	.74	90
3	11.3	.73	50
4	11.6	.65	60
5	12.0	.62	50
6	13.0	.54	..



The effect of pH on $G(\text{H}_2)$ in acetate-nitrate aqueous solutions is shown in Table I. $G(\text{H}_2)$ in experiment 1 is determined by the competition of reactions 3 and 12 neglecting reaction 1. From this experiment $k_{12}/k_3 = 25$ can be calculated according to the procedure employed previously. In a solution containing $10^{-3} M \text{NaNO}_3$ without RH, we found $G(\text{H}_2) = G_{\text{H}_2} = 0.52$. This value and $G_{\text{H}} = 0.48$ were used in the calculations.

The calculated values of k_1/k_3 at pH 11, according to eq. 13

$$G(\text{H}_2) = G_{\text{H}_2} + \frac{G_{\text{H}}}{1 + \frac{k_1[\text{OH}^-] + k_{12}[\text{NO}_3^-]}{k_3[\text{acetate}]}} \quad (13)$$

are given in the last column of Table I. All the values agree within a factor of 2.

Since

$$\frac{k_{\text{H}+\text{HCO}_2^-}}{k_{\text{H}+\text{Fe}(\text{CN})_6^{-3}}}, \frac{k_{\text{H}+\text{NO}_2^-}}{k_{\text{H}+\text{Fe}(\text{CN})_6^{-3}}}, \text{ and } \frac{k_{\text{H}+\text{acetate}}}{k_{\text{H}+\text{NO}_2^-}}$$

are known,^{7,11} it is possible to show that k_3/k_1 in the acetate system is consistent with the results obtained in the formate and acetone systems.

The Reactivity of Bicarbonate toward H Atoms.—The rate constant of the reaction of bicarbonate with H atoms (probably forming an intermediate addition product) was found by studying the competition between bicarbonate and methanol. The results are shown in Table II.

(14) J. Jortner, M. Ottolenghi, J. Rabani, and G. Stein, *J. Chem. Phys.* **37**, 2488 (1962).

TABLE II

 $G(\text{H}_2)$ IN SOLUTIONS CONTAINING BICARBONATE AND METHANOLDose 4000 rads, $[\text{NaHCO}_3] = 5 \times 10^{-2} M$

$[\text{CH}_3\text{OH}], M$	$G(\text{H}_2)$	$\frac{k_{\text{H}+\text{CH}_3\text{OH}}}{k_{\text{H}+\text{NaHCO}_3}}$
.....	0.67	...
3.0×10^{-4}	.78	150
1.0×10^{-3}	.81	60
3.0×10^{-3}	.91	50
1.0×10^{-2}	.99	60
1.0×10^{-1}	1.03	...

The value of $G(\text{H}_2) = 0.67$ in $0.05 M$ NaHCO_3 without methanol seems to be higher than the molecular hydrogen yield, G_{H_2} . This is probably due to the low rate of the reaction of bicarbonate with H atoms, so that recombination of H atoms may occur to some extent. In $0.1 M$ methanol $G(\text{H}_2)$ is interpreted as equal to $(G_{\text{H}_2} + G_{\text{H}})$. Assuming as previously that $G_{\text{H}} = 0.48$ and neglecting H atom recombination in the methanol solutions, $k_{\text{H}+\text{methanol}}/k_{\text{H}+\text{bicarbonate}}$ could be calculated (last column of Table II).

The higher value found in $3.0 \times 10^{-4} M$ methanol may be due to the neglect of H atom recombination, which probably occurs at this low scavenger concentration.

From the results of Table II, taking $k_{\text{H}+\text{CH}_3\text{OH}}/k_{\text{H}+\text{O}_2} = 8.5 \times 10^{-5}$ ¹¹ it is found that $k_{\text{H}+\text{bicarbonate}}/k_{\text{H}+\text{O}_2} = 1.5 \times 10^{-6}$. This value is also confirmed by experiments with $5 \times 10^{-2} M$ sodium acetate and $5 \times 10^{-2} M$ sodium bicarbonate. At 4000 rads, $G(\text{H}_2) = 0.87$ was found. From this one may obtain $k_{\text{H}+\text{bicarbonate}}/k_{\text{H}+\text{O}_2} = 1.0 \times 10^{-6}$.

Reactions with e_{aq}^- .—It is known^{10d} that the hydrogen yield in neutral solutions of RH is in many cases higher than the sum of $G_{\text{H}_2} + G_{\text{H}}$. This excess yield seems to be due to reactions of e_{aq}^- , since electron scavengers such as acetone,⁶ ferricyanide,^{7,8} and bicarbonate⁸ decrease $G(\text{H}_2)$ in such solutions. The actual mechanism by which e_{aq}^- is converted to H_2 is not known. This may be by recombination of e_{aq}^- with itself or by its reaction with water.

TABLE III

 $G(\text{H}_2)$ IN SODIUM FORMATE SOLUTIONS. EFFECT OF ACETONE AND BICARBONATEDose 1000 rads, $[\text{formate}] = 1.0 \times 10^{-3} M$ in $10^{-4} M$ Na_3PO buffer

$[\text{Acetone}], M$	$[\text{Bicarbonate}], M$	$G(\text{H}_2)$	Initial pH
.....	1.58	8.5
.....	1.0×10^{-6}	1.62	Not determined
1.0×10^{-5}	1.30	Not determined
.....	1.0×10^{-3}	1.27	7.6
5.0×10^{-5}	1.18	8.2
.....	5.0×10^{-3}	1.17	8.5

In Table III the effect of acetone on $G(\text{H}_2)$ in $10^{-3} M$ formate solution is compared to the effect of sodium bicarbonate.

During the irradiation the pH was increased by about 0.5 pH unit.

The results show that in order to obtain the same decrease in $G(\text{H}_2)$, $[\text{HCO}_3^-]$ should be about 100 times [acetone]. These experiments do not exclude the possibility that e_{aq}^- is scavenged by the CO_2 presented in equilibrium with the HCO_3^- at this pH. ($k_{e^-+\text{CO}_2}/k_{e^-+\text{H}_3\text{O}^+} \cong 1/3$. G. Scholes, private communication.) A value of $k_{e^-+\text{acetone}}/k_{e^-+\text{bicarbonate}} \geq 100$ is obtained

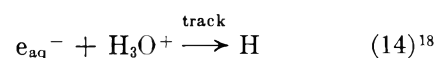
assuming that the scavenging of e_{aq}^- by acetone or bicarbonate is the factor determining $G(\text{H}_2)$ in these solutions.

Discussion

G_{H} .—The present investigation provides further evidence for a small primary product yield of hydrogen atoms⁶⁻⁸ ($G_{\text{H}} \cong 0.5$). k_1 is independent of the source of hydrogen atoms (X-rays or gas phase generated hydrogen atoms).¹⁵ This supports the idea that G_{H} is the yield for primarily produced H atoms. The value $G_{\text{H}} \cong 0.5$ was previously found⁷ constant from pH $\cong 2$ to pH $\cong 8$. This range is now extended up to pH 13.

On the Possible Source of G_{H} .—Theoretical considerations¹⁶ as well as experimental evidence^{4-8,14,17} show that the reducing radicals formed primarily by the action of X-rays on water and dilute aqueous solutions are mainly electrons. $G_{e_{\text{aq}}^-}$ is about 85% of the total yield of the reducing radicals.⁶⁻⁸ It was found previously^{7,8} and confirmed here that the measured G_{H} is not due to any reaction of e_{aq}^- in the bulk, since with electron scavengers the limiting G_{H} is found.

In the tracks, two possible reactions which may yield hydrogen atoms are

and⁶

If G_{H} is G_{14} , it should depend on the concentration of e_{aq}^- scavengers as well as on the $[\text{OH}^-]$. In our experiments no such effect has been observed. Further work with pulsed radiolysis techniques is in progress on the rates of homogeneous reactions of e_{aq}^- and the possible species which are originally formed in the tracks.

The Reaction of H with OH^- .—At the higher pH values, when $[\text{OH}^-]$ is sufficient to compete with other solutes for the hydrogen atoms, these atoms are converted to a species which reacts with electron scavengers and does not dehydrogenate the organic solutes RH. The determined k_1 is independent of the system used (acetone, formate-acetone, acetate-nitrate, chloroacetate³), and therefore we conclude that the effect of pH on $G(\text{H}_2)$ is due to reaction 1 and not to any specific pH dependent secondary reactions of the solutes.

The radical species formed by reaction 1 behave in a similar manner to radiation produced e_{aq}^- . Both species react with acetone and with nitrate without forming H_2 and with chloroacetate forming Cl^- rather than H_2 .³⁻⁵ In both cases no evidence has been found for direct dehydrogenation of RH.¹⁹ It is tempting to suggest that

(15) In the case of gas phase generated hydrogen atoms, the choice of parameters (G. Czapski, J. Jortner, and G. Stein, *J. Phys. Chem.*, **65**, 964 (1961)) leads to a value of $k_{\text{H}+\text{O}_2}$ in agreement with the radiation chemical value. Although the "absolute" value for $k_{\text{H}+\text{O}_2}$ is not certain, relative rate constants for H atoms obtained with radiation can be compared to those obtained with gas phase generated H atoms.

(16) (a) H. Frohlich and R. L. Platzman, *Phys. Rev.*, **92**, 1152 (1953); (b) G. Stein, *Discussions Faraday Soc.*, **12**, 227, 289 (1952); (c) J. Weiss, *Nature*, **186**, 751 (1960).

(17) (a) N. F. Barr and A. O. Allen, *J. Phys. Chem.*, **63**, 928 (1959); (b) J. T. Sworski, *J. Am. Chem. Soc.*, **76**, 4687 (1954); (c) F. S. Dainton and D. B. Peterson, *Nature*, **186**, 878 (1960); (d) G. Dobson and G. Hughes, *Trans. Faraday Soc.*, **57**, 1117 (1961); (e) G. Czapski and A. O. Allen, *J. Phys. Chem.*, **66**, 262 (1962); (f) G. Czapski and H. A. Schwarz, *ibid.*, **66**, 471 (1962); (g) A. R. Anderson and E. J. Hart, *ibid.*, **65**, 804 (1961).

(18) G. Lifshitz, *Can. J. Chem.*, **40**, 1903 (1962).

(19) J. H. Baxendale and G. Hughes, *Z. physik. Chem. (Frankfurt)*, **14**, 306 (1958).

the intermediate formed in reaction 1 is identical with e_{aq}^- formed by the primary action of radiation on water.

On the Origin of G_{H_2} .— H_2O_2 ,²⁰ NO_3^- , and OH^- have about the same reactivity for H atoms. If the precursors of G_{H_2} were H atoms, the effect of these three solutes on G_{H_2} would be the same. However, the experimental results show that OH^- has a negligible effect compared with that of H_2O_2 and NO_3^- , while the last

(20) G. Czapski, J. Jortner, and G. Stein, *J. Phys. Chem.*, **65**, 964 (1961).

two substances have similar effects on G_{H_2} ^{17g,21} and similar reactivity for e_{aq}^- .^{14,17e} This is consistent with the view that e_{aq}^- , and not H atoms, is the main precursor of G_{H_2} .

Acknowledgments.—The authors wish to thank Drs. E. J. Hart, M. S. Matheson, G. Scholes, and Prof. G. Stein for valuable comments.

(21) (a) H. A. Mahlman and J. W. Boyle, *J. Chem. Phys.*, **27**, 1434 (1957); (b) J. A. Ghormley and C. J. Hochanadel, *Radiation Res.*, **3**, 227 (1955).

SPECTROPHOTOMETRIC ANALYSIS OF REACTION MIXTURES. II¹

By S. AINSWORTH

Department of Biochemistry, University of Sheffield, Sheffield, England

Received December 28, 1962

A method is described whereby the absorption of the k th component in a reaction mixture may be evaluated without prior knowledge of the spectra of the other components. The method requires that among the nm optical density readings that relate to n states of the system and m wave lengths there shall be either $k - 1$ states where the k th component is absent or $k - 1$ wave lengths where it does not absorb light. These data are then used with optical density readings to which the k th component makes a contribution to evaluate its absorption either as a function of the state of the system or of the wave length. The results obtained may be used in the further analysis of the system.

Introduction

In the previous paper of this series² a method was described to give the number of absorbing species in a reaction mixture using spectrophotometric data in matrix form. The method also gives information concerning the possible interrelationships among the components of the mixture. Prior knowledge of the spectra of the pure components is not required.

This paper will describe an extension of the method whereby, if the required experimental criteria are met, the absorption of one or more of the components may be calculated, both as a function of the state of the system and of the wave length.

Calculation of Absorption.—In what follows, the optical density of the reaction mixture will be represented as the sum of products of two parameters x and y , one of which is a function of the wave length and the other a function of the state of the system associated, respectively, with i and j variations but not otherwise identified. Thus

$$d_{ij} = \sum_{k=1}^n x_{ik}y_{jk} \quad (1)$$

where $x_{ik}y_{jk}$ is the optical density of the k th component in the mixture defined by i and j and n is the total number of components. For ij variations, the ij optical density readings may be set out as an absorbance matrix A_{ij}

$$A_{ij} = \begin{vmatrix} d_{11} & d_{21} & \dots & d_{i1} \\ \dots & \dots & \dots & \dots \\ d_{1j} & d_{2j} & \dots & d_{ij} \end{vmatrix} \quad (2)$$

which is the product, taken column by row of the matrices

$$\begin{vmatrix} x_{11} & x_{21} & \dots & x_{i1} \\ x_{1n} & x_{2n} & \dots & x_{in} \end{vmatrix} \begin{vmatrix} y_{11} & y_{12} & \dots & y_{1n} \\ y_{j1} & y_{j2} & \dots & y_{jn} \end{vmatrix} \quad (3)$$

or

(1) This work was supported in part by the Atomic Energy Commission.

(2) S. Ainsworth, *J. Phys. Chem.*, **65**, 1968 (1961).

$$A_{ij} = xy$$

Assuming that the initial concentrations of reactants are arbitrary, a reaction system with n components has an absorbance matrix with rank n

$$\det A_{nn} \neq 0$$

and it can easily be shown that

$$\det A_{nn} = \det yX_{1k}x_{1k} + \det yX_{2k}x_{2k} \dots + \det yX_{nk}x_{nk} \quad (4)$$

where X_{nk} is the coefficient of x_{nk} in $\det x$.

It is possible to suppose, however, that there exist conditions where the k th component does not contribute to the total absorption of the mixture. Such a situation might arise at the beginning or towards the end of the reaction when the concentration of k is either zero or sufficiently small to be negligible. Alternatively, there may be a region of the spectrum examined where k ceases to absorb light. In either case, the rank of $\det A_{nn}$ is reduced to $(n - 1)$.

We will assume that this reduction in rank is associated with variations $i = 1, 2 \dots (n - 1)$ but not with the i th variation. Equation 4 then reduces to

$$\det A_{nn} = \det yX_{ik}x_{ik} = \bar{x}_{ik} \quad (5)$$

Thus, if variations $j = 1 \dots n$ and $i = 1 \dots (n - 1)$ are held unchanged, x_{ik} multiplied by an undetermined constant may be evaluated as a function of i .

This treatment is applicable to any system where a decrease in rank of 1 unit can be brought about by the choice of variations and can be applied more than once to the same reaction system if the required criterion is met.

If n such \bar{x}_{ik} -spectra are available, either through calculation or by independent measurement, the ratios of the y_{jk} constants are uniquely determined for

$$y \propto \bar{x}^{-1} \det A_{nn} \quad (6)$$

where \bar{x}^{-1} is directly proportional to the inverse of x .

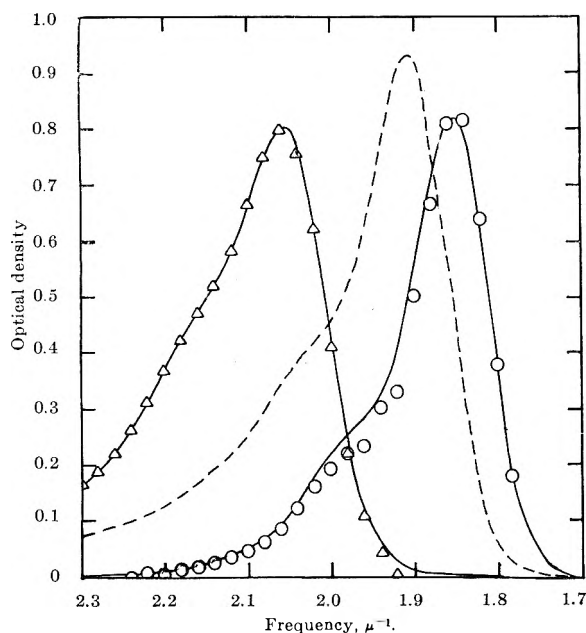


Fig. 1.—The curves are absorption spectra as recorded by the Unicam SP 700. The points are values for \bar{x}_{ik} as calculated by eq. 5 multiplied by constants chosen to give coincidence at the absorption peaks: $-\triangle-\triangle-$, acridine orange; $-\circ-\circ-$, rhodamine B; $-----$, diiodo (R) fluorescein.

TABLE I

k	D:A:R			Frequency, μ^{-1}	
Acridine orange	5:3:2	2:6:2	2:3:5	1.82	1.84 μ^{-1}
Rhodamine B	5:3:2	2:6:2	2:3:5	2.28	2.26 μ^{-1}

TABLE II

μ^{-1}	α			$\bar{\alpha}$	
	D	A	R	A	R
1.98	0.523	0.232	0.257	0.1595	0.2870
2.00	.457	.420	.220	.2975	.2523
2.02	.422	.625	.180	.4471	.2131

μ^{-1}	D:A:R					
	7:2:1	5:3:2	2:6:2	2:3:5	1:2:7	0:3:7
0.438	0.383	0.295	0.295	0.303	0.279	0.250
.426	.399	.387	.327	.284	.280	
.438	.435	.495	.362	.293	.314	

TABLE III

D:A:R	RELATIVE CONCENTRATIONS OF D IN SUCCESSIVE MIXTURES				
	7:2:1	5:3:2	2:6:2	2:5:3	1:2:7
Calcd. by α^{-1}	(7.00)	5.17	2.13	2.43	0.92
Calcd. by $\bar{\alpha}^{-1}$	(7.00)	5.26	2.37	2.66	1.26
Calcd. by eq. 7 and 8	(7.00)	5.16	2.23	2.29	0.58

With $(n - 1)$ \bar{x}_{ik} -spectra, one column of the inverse may still be calculated, thus evaluating the ratios in y of the component whose spectrum is absent from \mathbf{x} .

Further progress can be made if it is possible to assume values for $(n - 1)$ of the terms in eq. 4. As an example, a three component system may be considered where it can be assumed that c_{11} represents the concentration of the first component when $c_{12} = c_{13} = 0$, and where $c_{31} = 0$. The first condition implies knowledge of the absorption spectrum α_{j1} but, in addition, a further α_{jk} spectrum must be known, either by calculation or measurement. Equation 4 gives

$$\det \mathbf{A}_{33} = c_{11} \begin{vmatrix} \alpha_{11} & d_{11} & d_{31} \\ \alpha_{21} & d_{12} & d_{32} \\ \alpha_{31} & d_{13} & d_{33} \end{vmatrix} + c_{11} \begin{vmatrix} d_{11} & \alpha_{11} & d_{31} \\ d_{12} & \alpha_{21} & d_{32} \\ d_{13} & \alpha_{31} & d_{33} \end{vmatrix} + c_{31} \begin{vmatrix} d_{11} & d_{12} & \alpha_{11} \\ d_{12} & d_{13} & \alpha_{21} \\ d_{13} & d_{13} & \alpha_{31} \end{vmatrix} \quad (7)$$

Equation 7 cannot be solved for c_{11} , because two equal columns appear in its coefficient. This situation may be avoided, however, by adding arbitrary amounts of the k th component to successive reaction mixtures.

The new matrix is defined by

$$\mathbf{A}_{33}^k = \mathbf{A}_{33} + [\Delta_1 \Delta_2 \Delta_3][\alpha_{1k} \alpha_{2k} \alpha_{3k}] \quad (8)$$

where Δ_1 , Δ_2 , and Δ_3 are the arbitrary increments in c of the k th component.

Equation 7 may now be rewritten, employing the elements of \mathbf{A}_{33}^k and solved for c_{11} .

Errors.—It was shown in the previous paper, that the value of a determinant of order n will be in error to the extent $\pm ne\bar{S}_m$ where \bar{S}_m is the average value of the minors of order $(n - 1)$ and e is the error attaching to the elements. This error probably is insufficient to distort gravely the value of \bar{x}_{ik} determined by eq. 5 but, if these values are introduced as elements in succeeding determinants, the error will compound and, in view of the increasing size of the minors, may reach very high levels indeed.

Experimental

Absorption spectra for acridine orange, A, diiodo (R) fluorescein, D, and rhodamine B, R, in alcoholic solution, were measured using the Unicam SP 700 recording spectrophotometer. These are shown in Fig. 1.

Spectra for a series of mixtures of these three dyes were computed, rather than measured, so as to limit the error to that produced by rounding off to three significant figures.

Values of $\bar{\alpha}_A$ and $\bar{\alpha}_R$, proportional to the extinction coefficients of acridine orange and rhodamine B, respectively, were calculated by eq. 5, using data from the matrices shown in Table I.

The calculated values of $\bar{\alpha}$ are also shown in Fig. 1 having been multiplied by constants chosen to match the calculated and observed values at the maxima of the observed curves.

Values of $\bar{\alpha}_A$ and $\bar{\alpha}_R$, obtained above, were employed to provide one column of the inverse determinant $\bar{\alpha}^{-1}$ and hence to evaluate ratios between the concentrations of D in successive mixtures. The data employed and ratios obtained are shown in Tables II and III, the ratios being compared with those provided using independently measured values of the extinction coefficients, α .

Equations 7 and 8 were also tested by calculating ratios between the concentrations of D in successive mixtures. The data employed are shown in Table II, values of α_D and $\bar{\alpha}_A$ being inserted in the equations. The results obtained are given in Table III.

Discussion

Examination of Fig. 1, shows that evaluation of \bar{x}_{ik} as a function of wave length gives a reasonable description of the absorption curve, both in shape and peak location. The accuracy of the fit appears better for acridine orange than for rhodamine B, probably because in the evaluation of \bar{x}_{ik} for the latter dye, some residual absorption persists at $i = 2.28$ and $2.26 \mu^{-1}$.

In spite of the good qualitative agreement, quite large quantitative errors are present, particularly on the slopes of the peaks. This is reflected in the results shown in Table III, the ratios calculated using $\bar{\alpha}^{-1}$ being in error to a greater extent than those obtaining using α^{-1} . Unfortunately, as these errors find their origin in the rounding off of the elements of the computed ij matrix to 3 significant figures, it appears certain that the accuracy of current spectrophotometric

data is too low to give more than qualitative significance to results obtained by the procedures described above.

It will be observed, however, that only a small fraction of the available data has been employed in calculating the various ratios. There is the hope, therefore, that a wider selection of the data might provide greater

accuracy. In this connection, the least squares method applied by Sternberg, Stillo, and Schwendeman³ to the analysis of spectrophotometric data offers a model of the procedures that may be used with advantage.

(3) J. C. Sternberg, H. S. Stillo, and R. H. Schwendeman, *Anal. Chem.*, **32**, 84 (1960).

ENERGY PARTITION IN THE RADIOLYSIS OF AROMATIC MIXTURES¹

BY C. E. KLOTS AND R. H. JOHNSEN

Department of Chemistry, Florida State University, Tallahassee, Florida

Received January 9, 1963

Yields of products from the X-irradiation of liquid benzene, pyridine, and their mixtures have been investigated. These yields may be largely understood on the basis of the generation of precursors to all products in accordance with the electron fraction parameter. This is interpreted as placing limitations on a disproportionate role for direct excitation to low level states leading to selective energy absorption and as indicating a negligible role of intermolecular transfer of chemically consequential excitations in liquid aromatic systems.

The separation of radiolytic effects in binary mixtures into energy transfer processes and chemical interactions has generally been premised upon the electron fraction approximation as dictating the initial partition of energy.² This procedure, while attractive for its simplicity, is without a sound theoretical foundation, being based upon considerations derived for high energy particles. The uncertainty in its applicability arises largely because of the unpredictable character of energy losses from the numerous low velocity components of the prevailing degradation spectrum.³ The non-ideality of W values in gaseous mixtures⁴ has, for example, been attributed to the effects of these low energy components.

A relaxation of the electron fraction dictum can offer a serious challenge to traditional views concerning the importance of subsequent energy transfer processes. In the case of cyclohexane-benzene mixtures, for example, so-called "protective" effects have also been interpreted in terms of an inordinate role of direct excitation to the lowest electronic levels of the benzene.⁵ A potentially direct access to this energy partition problem, based on ion yield measurements, has been developed and will be described in another place.⁶ Some information concerning the abundance of direct excitations to low-lying electronic states, relevant to the present topic, may also be gleaned⁷ from an analysis of scintillation measurements. A third approach, and the one described in this paper, involves the degree of correlation between chemical products and the electron fraction parameter in situations where divergences might be expected to occur. Toward this end, radiolytic products from mixtures of liquid benzene and pyridine have been examined as a function of the electron

fraction. These two species, while sharing many common spectral features, differ substantially in the density of their low-lying electronic states. The results, then, permit certain statements to be made concerning the process of initial energy partition as affected by the presence of such states. The nature of the results also allows a commentary on the extent of subsequent transfer between species of chemically consequential excitations.

Experimental

Four-milliliter samples of Eastman Kodak spectral grade benzene, pyridine, and their mixtures were dried over barium oxide, thoroughly outgassed by a thawing and freezing technique, and distilled into Pyrex ampoules and sealed off under vacuum. The samples were mounted on a turntable and irradiated with X-rays generated by 3-mev. electrons impinging on a tungsten target. Total doses amounted to $1-3 \times 10^{21}$ e.v./g. administered over 2-4 hr. Dosimetry was effected by adopting $G(\text{H}_2) = 0.0378$ from pure benzene⁸ and assuming total energy absorbed was proportional to electron density. Gaseous products volatile at -196° , and then -115° , were measured with a McLeod gage. Gas chromatography confirmed their identity as hydrogen and acetylene, respectively. Polymer yields were determined in separate irradiations: sublimation of the solvent permitted the isolation of non-volatile products in a specially designed tip of the radiation ampoule. This tip could then be broken off and accurately weighed.

Results

The polymer yield for pure benzene was 0.99, in excellent agreement with recent determinations.^{5,9} From pyridine a polymer yield of 3.48 was obtained which is comparable to that from many aliphatic compounds and indicates that generalizations concerning the radiation stability of aromatic molecules¹⁰ will need to be modified. Yields from mixtures revealed, within the experimental error of about 1%, no deviations from values predicted on an electron fraction basis (Fig. 1). This is consistent with the view that precursors to polymer formation are generated on this basis.

Yields of acetylene reveal a similar situation (Fig. 2). We find $G(\text{C}_2)_{\text{benzene}} = 0.0194$ in good agreement with previous workers,^{7,8,11} and $G(\text{C}_2)_{\text{pyridine}} = 0.0341$ with intermediate values linearly proportional to electron

(1) (a) This work was supported in part by the U. S. Atomic Energy Commission under Contract AT-(40-1)-2001; (b) presented at the 142nd National Meeting, American Chemical Society, Atlantic City, N. J., September, 1962.

(2) J. Manion and M. Burton, *J. Phys. Chem.*, **56**, 560 (1952).

(3) R. L. Platzman, "Radiation Biology and Medicine," W. E. Claus, Ed., Addison-Wesley, New York, N. Y., 1958, pp. 15-72.

(4) G. S. Hurst and T. D. Strickler, "Penetration of Charged Particles in Matter," E. A. Uehling, Ed., National Research Council, Washington, D.C., 1960, pp. 134-143.

(5) J. Lamborn and A. J. Swallow, *J. Phys. Chem.*, **65**, 920 (1961).

(6) C. E. Klots, *J. Chem. Phys.*, in press.

(7) W. Van Dusen and W. H. Hamill, *J. Am. Chem. Soc.*, **84**, 3548 (1962).

(8) T. Gauman and R. Schuler, *J. Phys. Chem.*, **65**, 703 (1961).

(9) T. Gauman, *Helv. Chim. Acta*, **44**, 1337 (1961).

(10) V. V. Voevodskii and Y. N. Molin, *Radiation Res.*, **17**, 366 (1962).

(11) W. G. Burns, *Trans. Faraday Soc.*, **58**, 961 (1962).

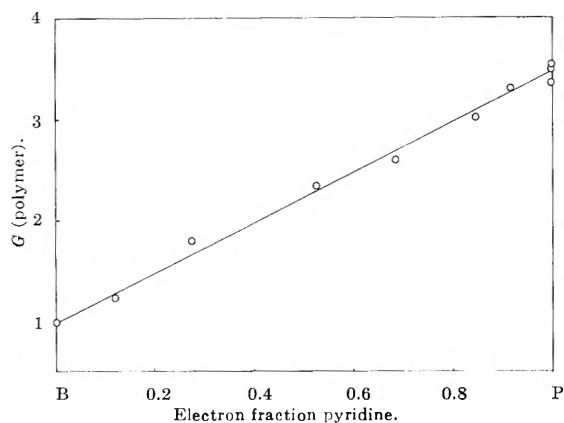


Fig. 1.—Yields of polymer from benzene-pyridine mixtures.

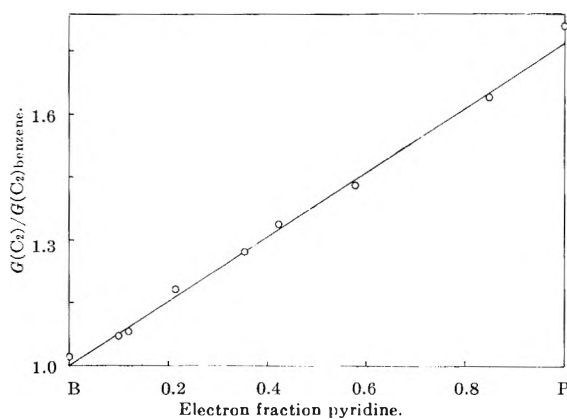


Fig. 2.—Yields of acetylene, normalized to that from pure benzene.

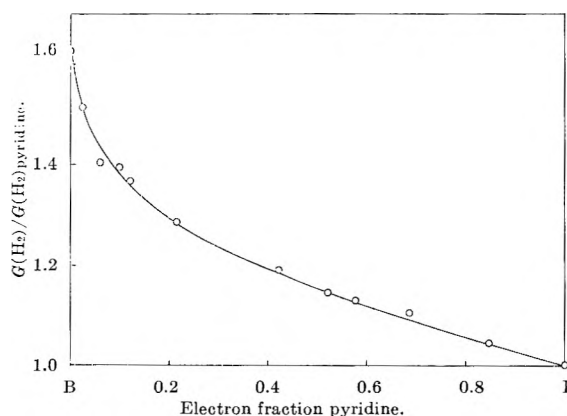


Fig. 3.—Yields of hydrogen, normalized to that from pyridine.

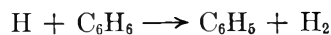
fraction. The validity of this parameter with respect to formation of precursors to these products thus also is indicated.

There is some evidence that acetylene and hydrogen share a common precursor in the case of benzene.^{8,11} Superficially, a comparison of Fig. 2 and 3 would seem to deny this. It is necessary, however, to consider the role of chemical interaction in determining the production of hydrogen. Measurements in a cyclohexane medium¹² with a scavenger technique¹³ indicate that pyridine reacts with H atoms about three times as efficiently as does benzene, in good agreement with their relative methyl affinities.¹⁴ This value may be used, along with arbitrarily assigned rate constants for reactions of the type

(12) C. E. Klots and R. H. Johnsen, to be published.

(13) T. J. Hardwick, *J. Phys. Chem.*, **65**, 101 (1961).

(14) M. Szwarc and J. H. Binks, "Theoretical Organic Chemistry," International Union of Pure and Applied Chemistry, Butterworths, London, 1959.



to reproduce Fig. 3 while retaining the electron fraction basis, indicating that hydrogen yields are also not inconsistent with this parameter.

Discussion

The presence of low energy components in the degradation spectrum must necessarily enhance excitation to low-lying states beyond the extent anticipated from high velocity considerations. Forbidden transitions may be similarly induced.¹⁵ An extreme point of view is that such low energy excitation predominates.^{16,17} Reference to the energy level diagram of pyridine¹⁸ indicates a manifold of electronic transitions in the ultraviolet, involving lone pair electrons, in addition to those found in benzene. Two such transitions are found within the long wave length band (~ 2500 Å.) containing the first $\pi-\pi^*$ transition¹⁹ and contribute to the twenty fold enhancement of oscillator strength in this region over that of benzene.^{20,21} Nevertheless, our results, revealing no evidence for selective energy absorption, show that transitions to within this photochemically inert band²² do not significantly distract energy from transitions to the higher photochemically labile levels of benzene. This conclusion becomes readily understandable, however, if one considers that the "enhanced" 2500 Å. band of pyridine has an oscillator strength of only 0.04. Within the framework of the recently discussed optical approximation,²³ such transitions should then be relatively infrequent. The unqualified identification of low energy transitions as efficient energy sinks, without considerations of their optical properties, is therefore hazardous. A similar conclusion may be drawn from scintillation measurements, as has been pointed out,⁷ which indicate that direct excitation to low levels may be a relatively rare process.

Our failure to observe effects which might be attributed to energy transfer between species is also of considerable interest. The excitation spectra of benzene and pyridine are remarkably similar as indicated by their polarizabilities, ionization potentials,²⁴ and known optical spectra.^{20,21} The apparent lack of coupling between these two species, indicated by a failure of migration of chemically important excitation to compete with chemical reaction, then suggests a similar absence in pure benzene. Such a view is consistent with the hitherto disjointed observations from luminescence measurements that supposedly efficient scintillators do not protect benzene,²⁵ and of LET effects, if these latter are interpreted in terms of track expansion parameters reflecting the diffusion of primary excitations.²⁶ The abrupt decrease in product yields from benzene upon

(15) E. N. Lassettre, *Radiation Res. Suppl.*, **1**, 530 (1959).(16) M. Burton, J. L. Magee, and A. H. Samuel, *J. Chem. Phys.*, **20**, 760 (1952).(17) M. Inokuti, *Isotopes Radiation* (Tokyo), **1**, 82 (1958).(18) M. Kasha, *Radiation Res. Suppl.*, **2**, 243 (1960).

(19) D. D. Pant and M. Kasha, "Symposium on Molecular Structure and Spectra," Ohio State University, Columbus, Ohio, 1961.

(20) L. W. Pickett, et al., *J. Am. Chem. Soc.*, **73**, 4862 (1951).(21) L. W. Pickett, et al., *ibid.*, **75**, 1618 (1953).(22) R. H. Linnell and W. A. Noyes, *ibid.*, **73**, 3986 (1951).(23) R. L. Platzman, *The Vortex*, **23** (1962).(24) M. F. A. El Sayed, M. Kasha, and Y. Tanaka, *J. Chem. Phys.*, **34**, 334 (1961).(25) M. Burton, *Z. Elektrochem.*, **64**, 975 (1960).(26) W. G. Burns, *J. Phys. Chem.*, **65**, 2261 (1961).

freezing²⁷ might then be taken as an indication of the enhancement of such migration in the solid phase. There is some recent evidence that energy transfer to solutes in aromatic media is indeed accelerated by crystallization.²⁸ Conversely, the absence of LET effects²⁹ and indifference to phase boundaries of product yields from aliphatic media³⁰ are possibly then symptomatic of rapid energy migration even in their liquid phases. That the liquid aliphatics should be superior to their aromatic counterparts in this respect is contrary to one's intuitive expectations, grounded in small quantum phenomena. It is further consistent, however, with other evidence of apparently facile energy transfer in aliphatic solutions.^{31,32}

Paradoxically, those excitations having high oscillator strengths and thus most likely to be induced (*vide infra*) are also just those, in most theories of energy transfer³³ and collective excitations,³⁴ which should

(27) J. Y. Chang and M. Burton, 137th National Meeting, American Chemical Society, Cleveland, Ohio, 1960.

(28) E. Collinson, J. J. Conlay, and F. S. Dainton, *Nature*, **194**, 1074 (1962).

(29) H. A. Dewhurst and R. H. Schuler, *J. Am. Chem. Soc.*, **81**, 3210 (1959); R. H. Schuler, *J. Phys. Chem.*, **63**, 925 (1959); R. H. Schuler and A. O. Allen, *J. Am. Chem. Soc.*, **77**, 507 (1955).

(30) H. Hamashima, M. P. Reddy, and M. Burton, *J. Phys. Chem.*, **62**, 246 (1958).

(31) T. J. Hardwick, *ibid.*, **66**, 2132 (1962).

(32) P. J. Dyne and J. Denhartog, *Can. J. Chem.*, **40**, 1616 (1962).

couple most readily with the surrounding medium. A resolution will necessarily require a detailed understanding of intramolecular processes. Tentatively, one may ascribe the apparent lack of coupling in aromatic systems to their expectedly efficient predissociative and internal conversion mechanisms.³⁵

A parenthetical remark may be made concerning reaction mechanisms in these mixtures. To account for LET and isotopic distribution effects, various authors^{11,36} have envisaged hydrogen and acetylene production as arising through bimolecular reactions of the type



Such a mechanism probably is incompatible with the apparent first-order dependence of acetylene production on precursor generation (Fig. 2) and with the likely role of hydrogen atoms in the production of hydrogen gas, as discussed above. The concurrent LET effects on hydrogen and acetylene formation must arise then through other, more complicated, track reaction sequences or through track-associated thermal effects.

(33) M. Burton, *et al.*, Ed., "Comparative Effects of Radiation," John Wiley and Sons, Inc., New York, N. Y., 1960.

(34) U. Fano, *Phys. Rev.*, **118**, 451 (1960).

(35) H. Sporer, *Radiation Res. Suppl.*, **1**, 558 (1959).

(36) J. M. Scarborough and J. G. Burr, *J. Chem. Phys.*, **37**, 1890 (1962).

A KINETIC AND SPECTROPHOTOMETRIC EXAMINATION OF SILVER(II) IN PERCHLORATE MEDIA

BY J. B. KIRWIN, F. D. PEAT, P. J. PROLL, AND L. H. SUTCLIFFE

Donnan Chemical Laboratories, University of Liverpool, Liverpool, England

Received January 9, 1963

The absorption spectra of solutions of Ag(II) in perchloric and nitric acids have been determined in the region 350 to 750 m μ . A change in the spectra with anion concentration provides evidence for complex formation. The kinetic data obtained for the decomposition of Ag(II) in perchloric acid also indicate the participation of perchlorate complexes. A mechanism is proposed for the reduction of Ag(II) to Ag(I).

Introduction

As part of a detailed study of the silver(I)-catalyzed reaction between cobalt(III) and chromium(III) in perchloric acid media, it became necessary to study reactions of silver(II). This paper reports the results obtained from a detailed spectrophotometric and kinetic decomposition study of divalent silver in perchloric acid along with a spectrophotometric examination of divalent silver in nitric acid.

Previous work in this field includes the pioneer work of Noyes, *et al.*,^{1,2} who studied the decomposition of silver(II) in nitric acid media and also investigated the possibility of the occurrence of silver(II)-nitrate complexes. They found, from e.m.f. measurements, that between one and two nitrate ions are bound to the silver ions,² which suggests the occurrence of both AgNO₃⁺ and Ag(NO₃)₂ species; this conclusion is based upon the assumption that silver(II) in perchlorate media is uncomplexed which, as will be shown later in this paper, may be incorrect.

(1) A. A. Noyes, C. D. Coryell, F. Stitt, and A. Kossiakoff, *J. Am. Chem. Soc.*, **59**, 1316 (1937).

(2) A. A. Noyes, D. De Vault, C. D. Coryell, and J. J. Deahl, *ibid.*, **59**, 1326 (1937).

Probably because of the difficulties in handling the very reactive silver(II) solutions, no previous work of a quantitative nature has been reported on the absorption spectra of this valency state in any medium. High acid concentrations are essential to keep the rate of decomposition in control. Since silver(II) is a d⁹ system, it should, in addition to any charge transfer bands, contain an internal d ← d transition the strength of which will depend upon the configuration of the ligands around the metal ion, and it should be possible to suggest from this band if any Jahn-Teller distortion, as found for other d⁹ systems, is present.

Experimental

Materials. Silver(I) Perchlorate.—The B. Newton Maine commercial product was used. The silver concentration was estimated by titration with thiocyanate in the usual manner.

Perchloric Acid.—The British Drug Houses Analar reagent was used, the concentrations being estimated by titration with standard caustic soda or sodium bicarbonate solution in the usual manner.

The Perchlorates of Sodium, Barium, Calcium, Lithium, Magnesium, and Lanthanum.—The above perchlorates were prepared by the action of perchloric acid on the metal carbonates (the carbonates of the first three elements being Analar).

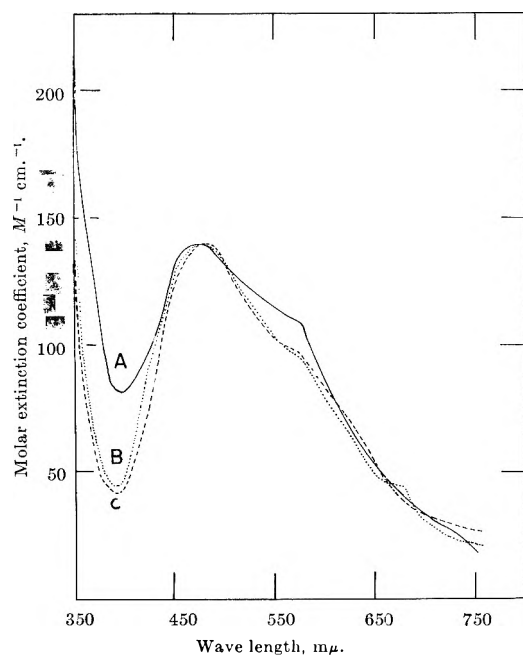


Fig. 1.—The spectrum of Ag(II) in various concentrations of perchloric acid: A, 6.0 *M*; B, 3.0 *M*; C, 1.5 *M* at 25°.

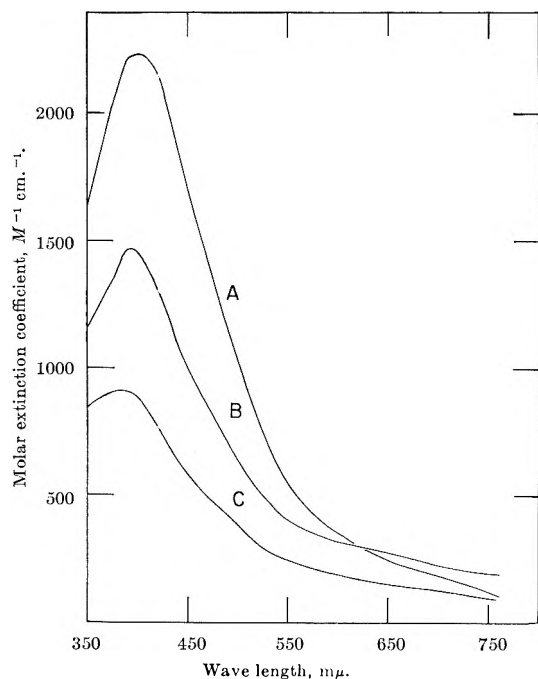


Fig. 2.—The absorption spectrum of silver(II) in nitric acid of concentrations: A, 6.0 *M*; B, 3.0 *M*; C, 1.5 *M* at a temperature of 25.0°.

Nitric Acid and Silver Nitrate.—The Analar Hopkins and Williams products were used.

Silver(II) Perchlorate and Nitrate.—The silver(II) compounds were prepared by ozonolysis of the silver(I) compound (0.15 to 1.2 *M*) in the corresponding acid media. Preliminary ozonolysis was always carried out to remove all traces of impurities which react with the silver(II). A method was evolved for estimating the concentrations of silver(II) by utilizing the oxidation of cerous solutions. The ceric produced was measured either by direct spectrophotometry at 375, 400, 425, and 450 *mμ* or by titration with ferrous sulfate. The ceric produced was always measured relative to the amount produced by cobalt(III) perchlorate or nitrate under identical conditions, since the spectrum of ceric is very dependent upon the anions present.³ The estimation of silver(II) by oxidation of iron(II) to iron(III) as previously used,¹ was found to give very variable results in perchloric

acid media whereas the reaction of Ag(II) with Ce(III) is rapid and gave consistent results.

Spectrophotometry.—The results were obtained from two types of instruments [a] a Unicam S.P. 500 spectrophotometer and [b] a Perkin-Elmer recording spectrophotometer, the latter being used when the rate of decomposition of the silver(II) product was rapid.

Kinetics.—All measurements were made on a Unicam S.P. 500 spectrophotometer at a wave length of 475 *mμ*. The temperatures of solutions were maintained at $\pm 0.05^\circ$ using a cell block through which thermostated water flowed.

Results and Discussion

(1) **Spectrophotometry.**—The absorption spectrum of silver(II) in various concentrations of perchloric acid is shown in Fig. 1. As can be seen from this diagram there is a maximum in the spectrum at a wave length of 475 *mμ* with an extinction coefficient of $140 \pm 7 M^{-1} \text{ cm}^{-1}$, which is clearly an internal ligand field $d \leftarrow d$ transition. There is also a shoulder at 575 *mμ* and the tail of a charge transfer band starting at about 380 *mμ* and increasing sharply in intensity toward the ultraviolet region. The position of the maximum in the visible region at 475 *mμ* shows no change with changing perchloric acid concentrations but there is a slight change in the shape of the band and also large changes in the regions of the shoulder ($\sim 575 \text{ m}\mu$) and the charge transfer band ($\sim 380 \text{ m}\mu$) which is indicative of more than one species being present. This suggests the possibility of silver(II) complexing with ClO_4^- , since any absorption in the visible region must be due solely to Ag(II), as the concentration of Ag(III) present *via* the equilibrium



is very small¹ and Ag(I) absorbs only in the ultraviolet region. Because of this equilibrium, which as will be shown later is established very rapidly, the applicability of the Beer-Lambert law cannot be checked in the normal manner, but it was found that at 475 *mμ* the absorbance over the range 10^{-3} to $10^{-2} M$ Ag(II) was proportional to the oxidizing power. Thus if we assume the concentration of Ag(III) is very small, the above law is applicable to the system.

Since Ag(II) is a d^9 system it should, in addition to being similar to Cu(II), also be similar to Ti(III), hence it should be possible to calculate the position of the absorption maximum relative to that of Ti(III) which is at 490 *mμ*, using the formula

$$\Delta E = \frac{5e\mu\bar{a}^4}{r^6}$$

where ΔE is the splitting of the levels; μ is the dipole moment of surrounding water molecules; r is the distance between ligands and central metal ion; \bar{a}^4 is the average 4th power of the radius of a 4d electron; and e is the effective charge on the nucleus of the central metal ion.

The predicted peak would occur at 460 *mμ* compared with the value of 475 *mμ* that was observed. By analogy with Cu(II), Jahn-Teller distortion effects are the probable reason for the two bands, *i.e.*, that at 475 *mμ* and the shoulder at 575 *mμ*, although the presence of different absorbing species cannot be ruled out. However, if it is assumed that the two bands originate from the Jahn-Teller effect alone, then the distortion produced must be the same order of magnitude as that in the case of Cu(II).

(3) G. Hargreaves and L. H. Sutcliffe, *Trans. Faraday Soc.*, **51**, 1105 (1955).

Figure 2 shows the spectrum of silver(II) in nitric acid of strengths comparable with those of the perchloric acid. As can be seen from this figure a $d \leftarrow d$ transition band again occurs, the position of maximum absorption being at shorter wave lengths than for the perchlorate media, namely, in the region 380–400 $m\mu$, there being a shift in the wave length with nitric acid concentration; this is indicative of complexing. The charge transfer band (not shown in the figure), also begins at shorter wave lengths than for the perchlorate, namely at 330 $m\mu$. Another important feature of the nitric acid spectra is the large over-all increase in extinction coefficients.

Estimates of the oscillator strengths of these transitions are, for the perchlorate 3.8×10^{-2} and for the nitrate, using the spectrum obtained with the 6.0 M nitric acid, 5.5×10^{-2} . These values are very large and hence they both suggest that the observed spectrum is a combination of two bands as is the case for copper(II).⁴ The absorption spectra in the ultraviolet region could not be obtained in a very satisfactory manner, owing to the unavoidable presence of Ag(I).

Figure 3 shows the effect of small amounts of nitric acid on perchloric acid solutions of silver(II), illustrating the stronger complexing nature of the nitrate ion compared to the perchlorate ion, towards silver(II). While the change of extinction coefficient at 400 $m\mu$ with nitrate ion concentration would be sufficiently great for quantitative measurements of complex formation to be made, the difficulty of handling the highly reactive Ag(II) solutions plus the rapid establishment of equilibrium between Ag(II), Ag(I), and Ag(III) militate against reliable measurements being made.

(2) **Kinetics.**—The kinetics of the decomposition of Ag(II) in perchloric acid solution were followed from the disappearance of the silver(II) optical absorption at the wave length of 475 $m\mu$. The results reported here were obtained by a sampling technique, the solution being kept in blackened flasks owing to the light-sensitive nature of the reaction. Light from the spectrophotometer was found to have no effect on the reaction. The disappearance of the silver(II) was found to be second order under all the conditions mentioned in this section (a typical set of rate data is shown in Fig. 4); no trace of the fourth-order term proposed by Noyes, *et al.*,¹ for the reaction in nitric acid solution was observed. Oxidizable impurities, as has been mentioned previously, were removed by a preliminary ozonolysis. The ozone left dissolved in the solution after ozonolysis was removed by passing a stream of oxygen through the solution until no ozone odor could be detected. The products of the decomposition were found to be silver(I) and oxygen. The rates observed were found to be reproducible to within $\pm 5\%$, and all the results presented here are averages of at least three experiments, reactions being followed to not less than 75% completion. No trace of hydrogen peroxide was detected at any time during the reaction.

Figure 5 shows a plot of the rate of decomposition against the inverse of the silver(II) concentration at four temperatures in the range 0 to 30°, with sodium perchlorate being used to replace the silver(I) perchlorate in order to keep the ionic strength constant. The linearity of the plots in Fig. 5 suggests that there is

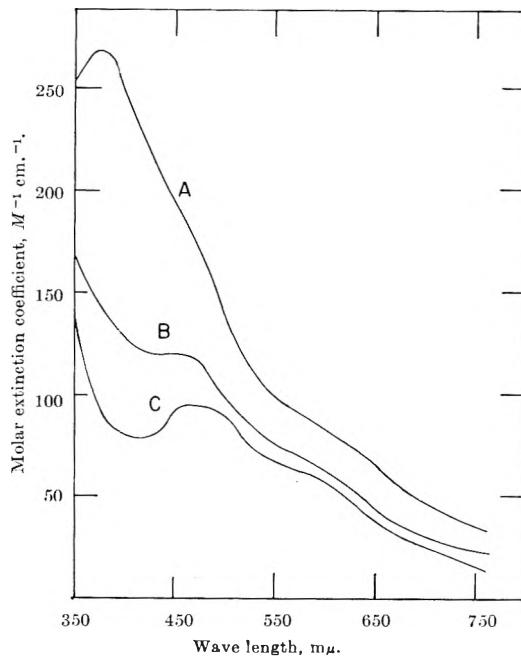


Fig. 3.—The effect of the addition of small amounts of nitric acid to Ag(II) in 3.0 M perchloric acid: A, 0.3 M ; B, 0.12 M ; C, 0.06 M at a temperature of 25.0°.

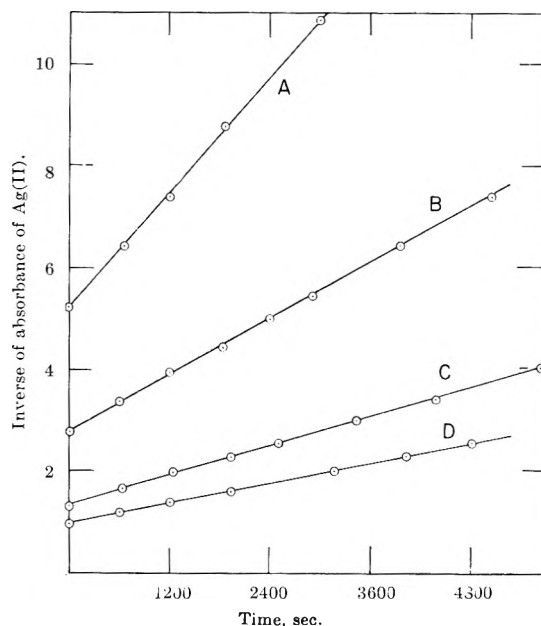


Fig. 4.—The inverse of the absorbance of Ag(II) (measured at 475 $m\mu$) plotted against time for the conditions: Ag(I) concentration = 0.288 M , ionic strength = 4.48 M , temperature = 25.0° and perchloric acid concentrations 1.50 M (A), 2.00 M (B), 3.00 M (C), and 4.20 M (D).

a term $[Ag(II)]^2/[Ag(I)]$ in the rate expression. The over-all activation energy derived from the data shown in the figure is 11 ± 2 kcal. mole⁻¹.

Figure 6 shows the plot of the observed second-order rate constant against the concentration of perchloric acid for a constant concentration of Ag(I) at a temperature of 25°. It can be seen that there is a minimum in the rate at a perchloric acid concentration of 3.0 M . From the shape of the curve, it is obvious that no one effect could produce this variation in the rate: the variation in the perchloric acid concentration must have two effects, one having a retarding and one an accelerating influence.

Since we are forced by the very nature of this reaction to work at very high ionic strengths, in order to find the

(4) J. Bjerrum, C. J. Balhausen, and C. K. Jørgenson, *Acta Chem. Scand.*, **8**, 1275 (1954).

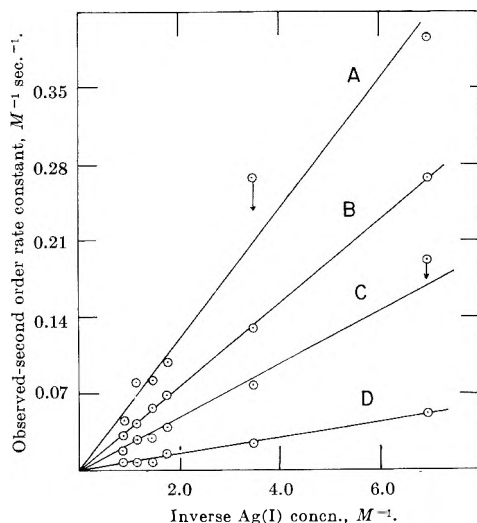


Fig. 5.—The plot of the observed second-order rate constant against the inverse of the Ag(I) concentration at an ionic strength of 7.17 *M* and a constant perchloric acid concentration of 6.0 *M* at temperatures: A, 30.0°; B, 25.0°; C, 17.0°; D, 0.0°.

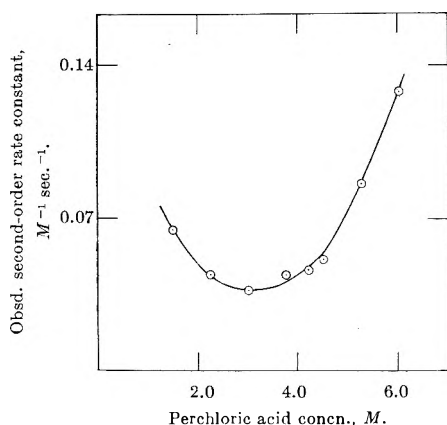


Fig. 6.—The plot of the observed second-order rate constant against the concentration of perchloric acid, at a temperature of 25.0°. The concentration of Ag(I) was kept constant at 0.288 *M*.

variation of the rate with hydrogen ion concentration H^+ must be replaced by Li^+ as this is the nearest replacement one can obtain from the point of view of activity coefficients. Figure 7A shows a plot of the rate against the inverse square of the hydrogen ion concentration at a constant ionic strength of 4.48 *M* and a perchlorate ion concentration of 4.48 *M*. Also shown (in Fig. 7B) is the effect of increasing the perchlorate ion concentration using lithium perchlorate, at a constant concentration of perchloric acid of 1.5 *M*. Unfortunately, the ionic strength cannot be kept constant, since perchlorate affects the rate (see this figure). The results have been plotted as a dependence upon the square of the perchlorate ion concentration although at low concentrations of perchlorate ion a linear dependence is reasonable, and any ionic strength effect is included in this effect.

The dependence of the observed second-order rate constant upon the inverse square of the hydrogen ion concentration is convincing as may be seen from Fig. 7A.

The Mechanism of Decomposition

From the experimental evidence presented above it is obvious that any mechanism proposed to account for the decomposition of Ag(II) must reproduce the following features:

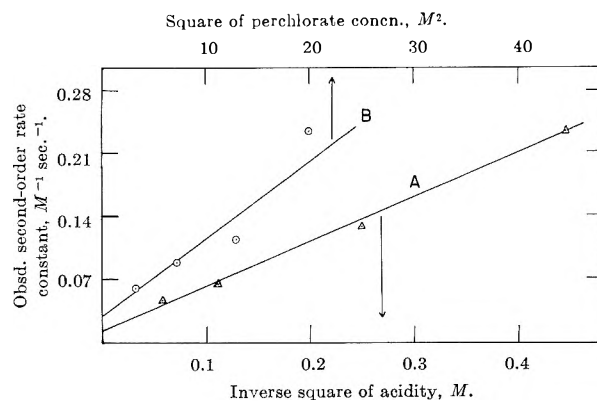


Fig. 7A.—The plot of the observed second-order rate constant against the function $[H^+]^{-2}$, at a constant $[ClO_4^-]$ of 4.48 *M* and $[Ag(I)]$ of 0.288 *M* at a temperature of 25.0°. 7B.—The plot of the observed second-order rate constant against the function $[ClO_4^-]^2$ at a constant $[HClO_4]$ of 1.5 *M* and a constant $[Ag(I)]$ of 0.288 *M* at a temperature of 25.0°.

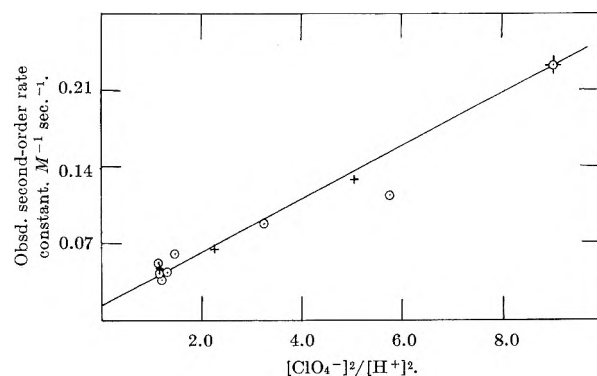
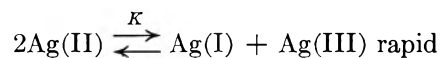


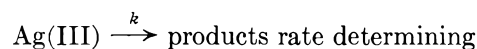
Fig. 8.—The plot of the observed second-order rate constant against the function of $[ClO_4^-]^2/[H^+]^2$ at 25.0° for a Ag(I) concentration of 0.288 *M*, + are for a constant ionic strength of 4.48 *M*; ○ are for a variable ionic strength of between 1.8 and 4.80 *M* obtained from Fig. 5 and 6.

- [a] second order with respect to silver(II)
- [b] an inverse dependence upon silver(I)
- [c] an inverse square dependence upon the acidity
- [d] a dependence upon perchlorate ion concentration of either power two or powers two plus one

By analogy with other silver(II) systems studied^{1,5} [a] and [b] must obviously enter into the rate expression *via* an equilibrium of the type



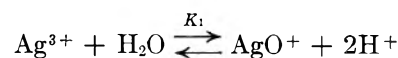
followed by the rate-determining decomposition of silver(III)



Since the concentration of Ag(III) is small and can also be assumed to be stationary, the following rate law can be derived

$$\frac{-d[Ag(II)]}{dt} = \frac{kK[Ag(II)]^2}{[Ag(I)]}$$

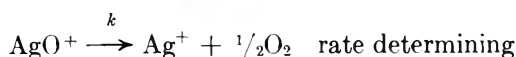
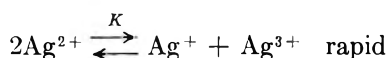
Considering observation [c], the most probable reason for this inverse square dependence upon the acidity is the presence of an equilibrium of the type



which has been postulated already⁶ to account for the effect of pH on the rate of electron exchange between the valency states of silver.

Considering [d], the effect of the perchlorate ion on the rate is most likely to be combination specific complexes of Ag(II) and an ionic strength variation. Evidence for the former conclusion comes from slight changes observed in the spectrum of Ag(II) on addition of the perchlorate ion. Attempts were made to keep the ionic strength constant while varying the perchlorate ion concentration by using di- and trivalent perchlorates as well as monovalent ones. Barium, calcium, magnesium, lanthanum, sodium, and lithium perchlorates were employed. Unfortunately, the ionic strength could not be kept constant due to the large variation in the activity coefficients of the various cations at the necessarily high values of ionic strength.

The detailed mechanism probably is



Again, assuming a stationary state for the concentration of silver(III), the rate law is

(6) J. A. McMillan, *Chem. Rev.*, **62**, 65 (1962).

$$\frac{-d[\text{Ag}^{2+}]}{dt} = \frac{k\kappa\kappa_1[\text{Ag}^{2+}]^2}{[\text{Ag}^+][\text{H}^+]^2}$$

No satisfactory mechanistic explanation for the perchlorate effect can be put forward. The experimental dependence of the rate on $[\text{ClO}_4^-]^2/[\text{H}^+]^2$ is shown in Fig. 8, hence the full rate law should include this function.

Presumably the addition of nitrate ions would replace perchlorate by nitrate complexes hence the form of the rate law would remain unchanged. However, the reactivity of nitrate complexes might be very different and the stationary state assumption might no longer be strictly applicable to the data obtained by Noyes, *et al.*¹; this might account for the introduction of a fourth-order term in the rate expression by these workers. The suggestion could be tested by studying the influence of nitrate ions on the electron exchange reaction. The effect of varying the perchlorate ion concentration on this reaction would also be interesting.

We have found that the addition of small amounts of nitrate ions to the reaction causes a decrease in the rate of reaction, while larger amounts of nitrate ions to the reaction causes an increase in the rate of reaction. These effects are only possible if at least two complexes of silver(II) exist, which supports the suggestion made previously by Noyes, *et al.*²

Acknowledgment.—P. J. P. wishes to thank D. S. I. R. for the award of a postdoctoral fellowship during the tenure of which the work was completed.

AN INFRARED SPECTROSCOPIC STUDY OF THE ADSORPTION OF WATER AND CARBON DIOXIDE BY LINDE MOLECULAR SIEVE X¹

BY L. BERTSCH² AND H. W. HABGOOD

Research Council of Alberta, Edmonton, Canada

Received January 16, 1963

Infrared spectra at 20° are reported for small amounts of water and carbon dioxide (up to 1 molecule per cavity) adsorbed on Li-, Na-, and KX-zeolites. The water spectra show no evidence of structural surface hydroxyl but may be interpreted in terms of isolated water molecules adsorbed simultaneously by an ion-dipole interaction with the exchangeable cation and by hydrogen bonding of one of the hydrogens to an oxygen of the zeolite surface. The remaining hydroxyl is free and gives a sharp OH band around 3700 cm.⁻¹. Carbon dioxide is both physically adsorbed in a linear configuration at a cation and also chemisorbed in one or more bent configurations which are assumed to be carbonate ions formed by interaction with surface oxide ions adjacent to exchangeable cations. One such species common to all three zeolites gives bands around 1700 and 1340 cm.⁻¹. On NaX a second species with bands at 1485 and 1425 cm.⁻¹ is more strongly held at low pressures but is readily converted to the first form in the presence of any additional physically adsorbed molecules. Additional bands are also present at different frequencies for carbon dioxide adsorbed on LiX and KX but these do not show such behavior. Small amounts of preadsorbed water greatly accelerate the rate of carbon dioxide adsorption—presumably by catalyzing the chemisorption step.

Introduction

In studies of the surface chemistry of ionic solids, the dehydrated crystalline zeolites are of interest both in their own right as solids possessing crystallographically well defined surfaces and also as examples of possible limiting structures approached by local regions of silica-alumina cracking catalysts. As part of a general study of the adsorptive and catalytic properties of these substances we have examined, using a pressed disk technique, the infrared spectra of the lithium, sodium, and

potassium forms of Linde Molecular Sieve X containing small amounts of adsorbed water and carbon dioxide.

Zeolite X is the most open-structured of the various synthetic zeolites commercially available. According to the crystallographic study of Broussard and Shoemaker³ the aluminosilicate framework encloses a cavity network in which cavities of approximately 12 Å diameter are interconnected by 9-Å windows in a diamond configuration. Apart from the negligibly small contribution by the external crystal surface, the adsorptive surface is made up of the internal surfaces of these

(1) Contribution No. 202 from the Research Council of Alberta. Presented to the 142nd National Meeting of the American Chemical Society, Atlantic City, N. J., September, 1962.

(2) Research Council of Alberta Postdoctoral Fellow, 1960-1962.

(3) L. Broussard and D. P. Shoemaker, *J. Am. Chem. Soc.*, **82**, 1041 (1960).

cavities and consists entirely of oxygen and sodium ions (or ions of lithium or potassium in the exchanged forms).

Observations of the infrared spectra of partially hydrated zeolite X have been reported by Szymanski, Stamires, and Lynch.⁴ These authors used a combination of mull, pellet, and dispersed powder techniques and were able to cover a wide range of water contents and observational temperatures. They did not, however, carry out measurements at room temperatures for coverages as low as those to be reported here. Frohnsdorff and Kington⁵ have examined by a mull method the infrared spectra of Molecular Sieve A, a related zeolite which would be expected to have similar surface properties, for water coverages between 30% and complete saturation. No previous measurements have been reported for the spectra of carbon dioxide adsorbed on these zeolites.

These earlier investigations of adsorbed water showed the expected broad band for the stretching vibration of hydrogen-bonded OH groups in the 3400–3200 cm^{-1} region and the corresponding bending vibration around 1650 cm^{-1} with some suggestion of a variation of hydrogen bond strength with the degree of water coverage. Szymanski, Stamires, and Lynch reported indications of the presence of structural OH and, at higher coverages, of H_3O^+ .

Whether or not H_3O^+ or isolated OH groups are actually present on the surface, the chemical nature and orientation of the surface water molecules under conditions approaching complete dehydration are of interest because of the very pronounced accelerating effect such water has on the catalytic isomerization of cyclopropane⁶—a reaction which appears to proceed by a carbonium ion intermediate.

The measurements with adsorbed carbon dioxide grew out of observations suggesting that carbon dioxide could be chemisorbed on zeolite X and an unexpected complexity of behavior was found to occur.

Experimental

Materials.—The zeolite used was a sample of Linde Molecular Sieve 13X kindly provided in powder form by the Linde Company Division of Union Carbide Corporation. This material, which will be designated as NaX, was assumed, for calculations of the number of cavities, to have the formula $(\text{Na}_2\text{O})_{40}(\text{Al}_2\text{O}_3)_{40}(\text{SiO}_2)_{112}$ per unit cell³ or one-eighth of this per large cavity. The amount of water is variable under normal laboratory conditions and a figure of 20% of the weight in air was used to calculate the dry weight of the pellets.

Howell⁷ and Szymanski, Stamires, and Lynch⁴ have reported that the normal structure is deficient in sodium to the extent of about 8%, the missing sodium presumably being replaced by hydrogen. Attempts to confirm this sodium deficiency standard mineralogical analyses performed in these laboratories were inconclusive and values of the Na:Al ratio ranging from 0.94 to 1.07 with an average of 1.01 were obtained in five determinations. However, the range of error in silicate analysis by normal methods such as used here⁸ is sufficiently large to encompass a ratio such as reported by these other authors.

Carbon dioxide from Matheson Co., Inc., (99.8%), was purified by repeated bulb-to-bulb distillation over liquid nitrogen. Heavy water, reagent grade, was used as supplied by Merck.

Preparation of Pellets.—The powder as received was fraction-

ated by sedimentation in water in an attempt to remove agglomerates and amorphous material. The fraction retained exhibited under the microscope well defined crystals with an average particle size of 8 μ .

The lithium and the potassium forms, LiX and KX, were prepared by percolation of a large excess of 1 *M* solutions of the respective chlorides through a column of NaX powder for 5 hr. at 50°. This was followed by washing with a dilute solution of the hydroxide (pH 9.5) to minimize "hydrolysis" of the exchanged zeolites. Finally the powder was fractionated by sedimentation in the same manner as with the parent zeolite.

Analyses of similar previous preparations had shown that by this procedure an exchange of approximately 70% could be achieved.

The selected fractions from the sedimentation were ground in a mortar to an average size of 2 μ before being pelletized in a simple 0.75 in. diameter die under a force of 40 tons. This yielded self-supporting pellets weighing about 25 mg. (≈ 10 mg. per cm^2) with transmissions ranging from around 5% at 3500 cm^{-1} to 60% at 2000 cm^{-1} . The low temperature nitrogen adsorptive capacity of the zeolite was found unchanged by the pressing operation.

Equipment.—The spectra were determined on a Perkin-Elmer 221 prism-grating double beam spectrometer and the zeolite pellet was contained in a simple cell fitted with IRTRAN-2 windows (Eastman Kodak Co., Rochester, N. Y.). The cell was constructed from a length of 30-mm. Pyrex tubing, flattened at one end to accommodate the two 25-mm. diameter windows which were cemented in place with an epoxy resin cement. The total path length was 15 mm. A section of the cell back from the windows was wound as a furnace and the pellet could be slid back and forth as required for heat treatment or observation. Since the pellet was freely mobile, its exact position and orientation in the light beam was never completely reproducible. However, the pellets were so uniform that, provided they were sufficiently in position to intercept completely the light beam, their exact position and the precise orientation of the cell were not critical and fully reproducible spectra were obtained. In order to minimize the interference of stopcock grease the cell was completely sealed except for one stopcock at the connection to the vacuum line and pellets were inserted and removed by directly opening the main body of the cell. A similar though much simpler cell was placed in the reference beam.

For quantitative adsorption measurements with CO_2 , known amounts of gas were introduced from a calibrated volume and pressures were measured with a Pirani gage calibrated for CO_2 over the range 1–1000 μ .

Known amounts of water vapor could be admitted to the infrared cell from a calibrated doser which consisted of a short piece of glass tubing between two stopcocks and which was connected to a thermostated water reservoir. At a pressure of 4.579 cm. one dose contained 0.96×10^{-5} g. of water vapor.

The transparency of a pellet was sufficient that the standard slit program of the spectrometer could be used. At 3200 cm^{-1} the slit opening was 0.125 mm. and at 1428 cm^{-1} (prism-grating interchange) it was 0.060 mm.

However in the OH-stretching region, wider slits and a scale expansion were frequently desirable. The slit openings were doubled and a 5-fold expansion of the bands was made.

Procedures.—Prior to any series of measurements the pellet was completely dehydrated by heating at 500° for at least 4 hr. Figure 1 shows two typical spectra of NaX and LiX in a partly dehydrated stage with the spectra of the completely dehydrated material indicated by dashed lines.

During the dehydration process the entire cell, except the windows, was heated to 200° by heating tape in order to remove water from the glass walls as much as possible. Measured amounts of adsorbate, water, or carbon dioxide were then admitted to the pellet in successive doses. In the case of water the uptake was complete and the equilibrium pressure was always below the sensitivity of the Pirani gage; with carbon dioxide the course of the adsorption could be followed by the pressure reading. Spectra were measured at intervals. The spectra were taken at a room temperature of $20 \pm 1^\circ$, but apart from the short time needed for running a spectrum it was possible to keep the pellet at any desired temperature.

With this particular experimental arrangement the full infrared beam passes through the pellet and some heating of the pellet results. This was evidenced, in the case of carbon dioxide, by a distinct rise in pressure resulting from some desorption from the pellet. In spite of the relatively slow over-all adsorption process,

(4) H. A. Szymanski, D. N. Stamires, and G. R. Lynch, *J. Opt. Soc. Am.*, **50**, 1323 (1960).

(5) G. J. C. Frohnsdorff and G. L. Kington, *Proc. Roy. Soc. (London)*, **A247**, 469 (1958).

(6) D. W. Bassett and H. W. Habgood, *J. Phys. Chem.*, **64**, 769 (1960); also unpublished observations.

(7) P. A. Howell, *ibid.*, **64**, 364 (1960).

(8) R. E. Stevens and W. W. Niles, *U. S. Geol. Surv. Bull.*, 1113 (1960).

a steady value in the beam was obtained within one minute and once the cell was removed from the beam the previous value was again found. It appeared therefore that the short periods of heating while the measurements were being made did not significantly modify the slow adsorption processes. The uptake of carbon dioxide was followed at 20° and it is not felt that the brief periods during which the pellet was in the spectrometer have significantly affected the uptake curves except perhaps in their very early stages.

Results

Water.—The maximum water capacity of NaX is 30 molecules per cavity.⁹ Infrared absorption spectra were obtained for various coverages up to 1 molecule per cavity of adsorbed water on NaX both during hydration and during dehydration, and more limited observations were made of water on LiX and KX and of D₂O on all three forms. Higher coverages were not possible due to the resultant decrease in transparency of the pellet. The rates of water adsorption were too high to follow and the uptake was essentially complete; accordingly only the equilibrium water spectrum was attempted.

Most of the water adsorptions were carried out at 110° in the hope that a relatively uniform coverage would be attained rather than a high concentration in the outermost cavities of the crystal. At these coverages negligible additional water is taken up in cooling from 110 to 20°. The fact that extended annealing at 110° did not result in any changes in the spectra suggests that a reasonable uniformity was achieved.

TABLE I

INFRARED ABSORPTION FREQUENCIES FOR ADSORBED WATER

Vibration type	Isolated OH stretching	Bonded OH stretching	H ₂ O bending	Isolated OH stretching
				ing
Observed				
LiX	3720	3400, 3200	1643	2748
NaX	3687-3695	3400, 3250	1645-1660	2730
KX	3648	3400, 3250	1670	2695
Literature				
NaX ^a	3550	3400	1670, 1645	
NaA ^a		3500, 3400	1710, 1660	
NaA ^b		3486-3425	1660	
Heulandite ^c	3610	3400, 3250		
Mesotype ^c	3832, 3730, 3667, 3602			
Porous glass ^d	3740			2761
Pure water	3756, ^e 3652 ^e	3428, ^f 3256 ^{f,g}	1644, ^g 1637 ^g , 1595 ^e	2789

^a H. A. Szymanski, D. N. Stamires, and G. R. Lynch, *J. Opt. Soc. Am.*, **50**, 1323 (1960). ^b G. J. C. Frohnsdorff and G. I. Kington, *Proc. Roy. Soc. (London)*, **A247**, 469 (1958). ^c C. Duval and J. Lecomte, *J. chim. phys.*, **50**, C64 (1953). ^d A. N. Terenin in "Surface Chemical Compounds and their Role in Adsorption," A. V. Kiselev, Ed., Moscow Univ. Press, 1957; AEC Transl. 3750, O.T.S. Dept. of Commerce, Washington, D. C., 1959, p. 227. ^e Vapor. ^f Liquid. ^g Ice. G. Herzberg, "Infrared and Raman Spectra of Polyatomic Molecules," D. Van Nostrand, New York, N. Y., 1945.

In all cases a single sharp band typical of an isolated OH stretching vibration, a broad band characteristic of a hydrogen-bonded OH stretching vibration, and the usual band due to the H-O-H bending vibration were observed. In the case of D₂O absorption due to the D-O-D bending vibration was not visible since it would be expected in the opaque region of the pellet spectrum below 1250 cm.⁻¹. The various band frequencies ob-

(9) R. M. Barrer and G. C. Bratt, *J. Phys. Chem. Solids*, **12**, 130 (1959).

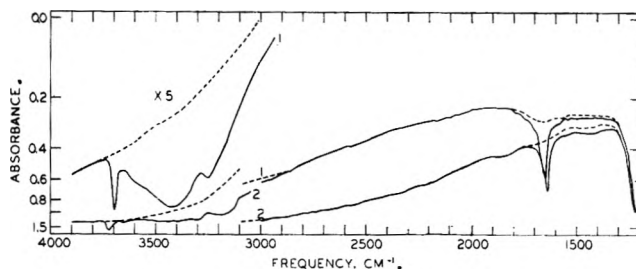


Fig. 1.—Spectra of slightly hydrated zeolites. Dashed lines correspond to complete dehydration: (1) NaX; (2) LiX.

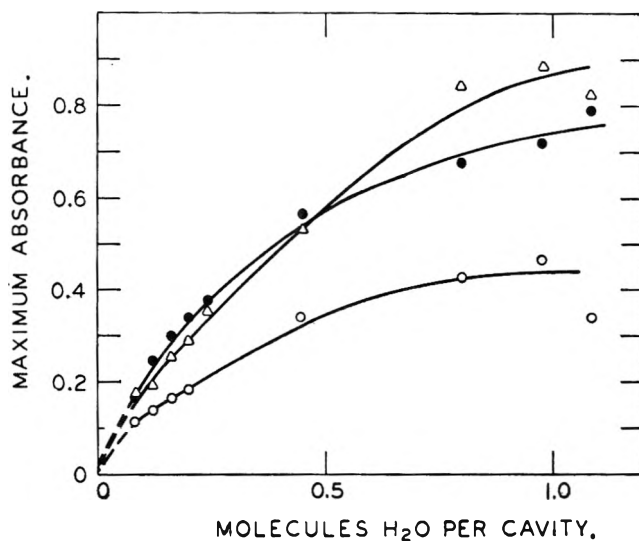


Fig. 2.—Maximum absorbance as a function of water concentration on NaX: O, 3695 cm.⁻¹; Δ, 3400 cm.⁻¹; ●, 1650 cm.⁻¹.

served are summarized in Table I and compared with selected findings of previous workers for related adsorbents. The frequencies are virtually independent of coverage and the increase in absorbance with concentration of adsorbed water is shown in Fig. 2 for the three major bands.

At 1.1 molecules per cavity the absorption band due to the isolated OH groups was initially broadened and displaced from 3695 to 3687 cm.⁻¹ but after the pellet had been kept at 110° for several hours the band became sharper and returned to 3695 cm.⁻¹.

Pumping at 100° for 20 hr. reduced the water content to approximately 0.1 molecule/cavity according to the spectral intensities. Heating under vacuum at 200° for 20 hr. considerably reduced the 3400 cm.⁻¹ band and eliminated the 3695 cm.⁻¹ band completely while the 1650 cm.⁻¹ band was hardly detectable.

Traces of water appear to remain to higher temperatures but may be completely removed by pumping at 500° or higher. For example, based on the intensity of the 3400 cm.⁻¹ band, up to 0.04 molecule per cavity was estimated from the spectrum, corresponding to heating at 400° under vacuum for 30 hr.

More limited experiments were made with LiX and KX. Figure 1 shows the spectrum of a partly hydrated LiX pellet. The shifts in frequency for the free OH stretching vibration and for the H-O-H bending vibration are shown in Table I. A shift of the 3400 cm.⁻¹ band could not be determined. On all forms, water was easily exchanged for D₂O and the observed frequency shifts as listed in Table I all correspond to $\nu_H/\nu_D = 1.35$.

Carbon Dioxide.—It was found that the adsorption of carbon dioxide by Molecular Sieve X is a slow

TABLE II
 INFRARED ABSORPTION BANDS FOR ADSORBED CARBON DIOXIDE

Obsd.—Zeolites			Lit.							
LiX	NaX	KX	Al ₂ O ₃ ^a	Al ₂ O ₃ Cr ₂ O ₃ ^a	ZnO ^b	ZnO ^c	TiO ₂ ^d	NiO ^e	NiO ^f	Gas ^g
2368	2355	2348	2350	2350	2364			2345	2345	2349
		1690								
1728	1715	1670	1750							
1660		1640	1635	1620	1618	1640		1640	1620	
	1580	1570		1580	1600	1570	1580			
	1485		1500	1480			1500			
1446	1425				1431	1430				
1380	1380	1380						1390	1360	1388(R)
1302	1365	1340					1320			
		(1235)	1235	1230	1230	1230				1265(R)

^a L. H. Little and C. H. Amberg, *Can. J. Chem.*, **40**, 1957 (1962). ^b J. H. Taylor and C. H. Amberg, *ibid.*, **39**, 535 (1961). ^c S. Matsushita and T. Nakata, *J. Chem. Phys.*, **36**, 665 (1962). ^d D. J. C. Yates, *J. Phys. Chem.*, **65**, 746 (1961). ^e R. P. Eischens and W. A. Pliskin, *Advan. Catalysis*, **9**, 662 (1957). ^f M. Courtois and S. J. Teichner, *J. Catalysis*, **1**, 121 (1962). ^g G. Herzberg, "Infrared and Raman Spectra of Polyatomic Molecules," D. Van Nostrand Co., Inc., New York, N. Y., 1945.

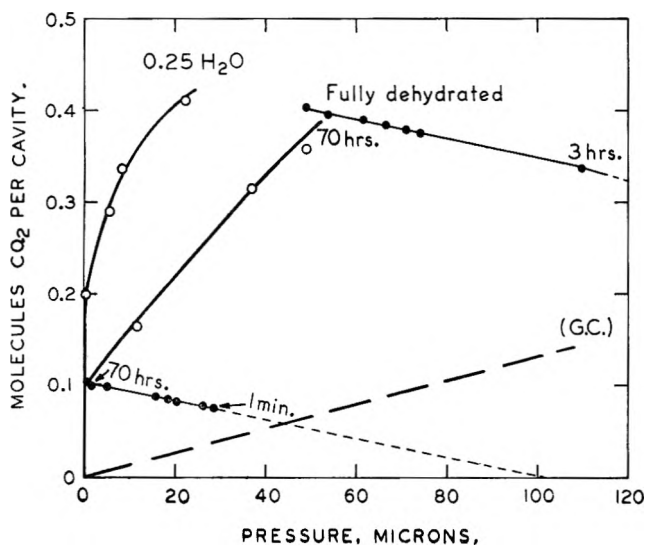


Fig. 3.—Adsorption of CO₂ on NaX. In the presence of 0.25 molecule of H₂O per cavity equilibrium was reached immediately. In the absence of water a pseudo-equilibrium was reached after about 70 hr. for each step, two of which are shown by the solid circles. GC: Isotherm as estimated by gas chromatography, fully dehydrated zeolite.

process and the development of the spectrum follows even more slowly. The presence of some water initially on the adsorbent results in a marked acceleration of the adsorption. Experiments were conducted therefore with the dehydrated zeolite and with a zeolite containing small amounts of preadsorbed water. The general adsorption characteristics of NaX are summarized in Fig. 3. This shows the isotherm at 25° for carbon dioxide on NaX containing approximately 0.25 molecule water per cavity; each value was achieved within a few minutes and appears to be a true equilibrium condition. The figure also shows a pseudo isotherm for carbon dioxide on dehydrated NaX wherein each point was allowed 60 hr. to equilibrate. A separate experiment on the same dehydrated pellet consisted of two successive sets of rate measurements and these are shown by the dashed lines. The isotherm measurements were limited to relatively low concentrations because of the limitations of the Pirani gage although some spectral measurements were taken with higher pressures. Finally, the initial slope of the isotherm as estimated¹⁰ by gas chromatography is shown by the heavy dashed line. This is based on an extrapolation

(10) H. W. Habgood and J. F. Hanlan, *Can. J. Chem.*, **37**, 843 (1959).

to 25° of gas chromatographic retention volumes measured between 235 and 375° and would be expected to represent only rapid adsorption processes.

The various frequencies observed in the spectra of adsorbed carbon dioxide are summarized in Table II. Several bands were found in addition to the band near 2360 cm.⁻¹ produced by the asymmetric stretching vibration which is the major infrared active frequency for carbon dioxide in the region accessible to these experiments. These new bands are in the general region 1800–1200 cm.⁻¹ where other investigators, as summarized in the table, have observed bands attributed to chemisorbed carbon dioxide. It can also be seen that the frequencies in this region are markedly different for the three different zeolite forms. Spectra are compared in Fig. 4 for three different experimental conditions: immediately after admission of a dose corresponding to approximately 0.1 molecule per cavity, 70 hr. later when adsorption was essentially complete, and after admission of a relatively large pressure of carbon dioxide.

The greatest complexity of behavior was found with the sodium form of the zeolite and more extensive investigations were carried out with this form. The spectral changes accompanying the adsorption of carbon dioxide by fully dehydrated NaX at 20° are summarized in Fig. 5, which shows the changes in amounts adsorbed and in absorbance for the various bands as a function of time for two successive adsorption steps. The chemisorption bands in the NaX case tended to vary in pairs, one being the 1715 and the 1365 cm.⁻¹ bands and the other being the 1485 and 1425 cm.⁻¹ bands. They appeared immediately after admission of the carbon dioxide in addition to the 2355 cm.⁻¹ band, which was assumed to represent physical adsorption. Of the 1715–1365 cm.⁻¹ pair of bands, the 1365 cm.⁻¹ band was a little slower in developing and is not noticeable in spectrum (A) of Fig. 4 taken at a time of 1 min.

The 2355 cm.⁻¹ band decreased slowly during the first step but even after it had completely disappeared (30 hr.), an additional major change took place in the spectrum involving the growth of the 1485–1425 cm.⁻¹ pair of bands at the expense of the 1715–1365 cm.⁻¹ pair. It would appear from Fig. 5 that further growth of the 1485–1425 cm.⁻¹ pair of bands would be expected after even longer times. However, a second dose of carbon dioxide was added after 70 hr. and the observations continued for a further 66 hr. at 20°. There was a rather slower build-up of the 2355 cm.⁻¹ band which

later slowly decreased to a steady value. The 1485–1425 cm^{-1} pair of bands which had increased so strongly in the first dose fell sharply and continued to decrease slowly while the 1715–1365 cm^{-1} pair of bands increased steadily and a shoulder appeared on the high frequency side of the 1365 cm^{-1} band. In the final spectrum in this series, 66 hr. after the admission of the second dose, the 1715 cm^{-1} peak was too intense for exact measurement and a new band appeared at 1580 cm^{-1} .

It was found in separate experiments that higher pressures of carbon dioxide up to 150 mm. resulted in the complete disappearance of the 1485–1425 cm^{-1} pair of bands as shown in spectrum (C) of Fig. 4. These high pressures of carbon dioxide gave only very minor further increases in the 1715 and 1365 cm^{-1} bands. It was also found that similar although less complete elimination of the 1485–1425 cm^{-1} pair could be achieved by using other gases such as ethylene, oxygen, or water vapor in relatively large amounts. These effects were very rapid.

Following upon the two-stage adsorption of Fig. 5 the pressure in the cell was brought up to 9.5 mm. of CO_2 and almost complete elimination of the 1485–1425 cm^{-1} pair was obtained. Desorption was then carried out by successive expansions into vacuum, and later by heating under vacuum, and the spectral changes tended to be the reverse of those observed during adsorption. The 1715–1365 cm^{-1} pair of bands were markedly decreased and the 1485–1425 cm^{-1} pair of bands strongly increased. It is noteworthy that pumping at room temperature produced a spectrum closely similar to (B) for NaX in Fig. 4. Such a spectrum could be obtained with only 10-min. pumping of a system initially containing up to 150 mm. CO_2 above the pellet and the spectrum was then unchanged by further pumping at room temperature for periods ranging to 16 hr.

Pumping at elevated temperatures up to 100° brought about the removal of the 1715–1365 cm^{-1} pair but removal of the 1485–1425 cm^{-1} pair could be achieved only by prolonged evacuation at temperatures above 300°.

As stated earlier, the presence of small amounts of preadsorbed water was found greatly to accelerate the adsorption of carbon dioxide. A series of experiments was carried out with a NaX pellet containing about 0.25 molecule of water per cavity—the residual water content remaining after pumping the fully hydrated pellet for 80 hr. at room temperature. Several doses of carbon dioxide were added up to a pressure of 40 μ in the cell in equilibrium with a concentration of 0.41 molecule per cavity. The corresponding spectra for the region between 1700 and 1300 cm^{-1} are shown in Fig. 6. In general these may be characterized as “mature” spectra, *i.e.*, corresponding to those achieved after a long time on the dehydrated zeolite. The 2355 cm^{-1} band of physically adsorbed carbon dioxide behaved in a similar fashion in the sense that it was observed only for spectrum 5, the final dose of the series. The strong decrease in the 1485–1425 cm^{-1} pair of bands was observed only when the 2355 cm^{-1} band was present. The spectral changes on desorption from the slightly hydrated pellet were much more similar to those with the dehydrated zeolite than during adsorption and the presence of water appeared to have less effect on the

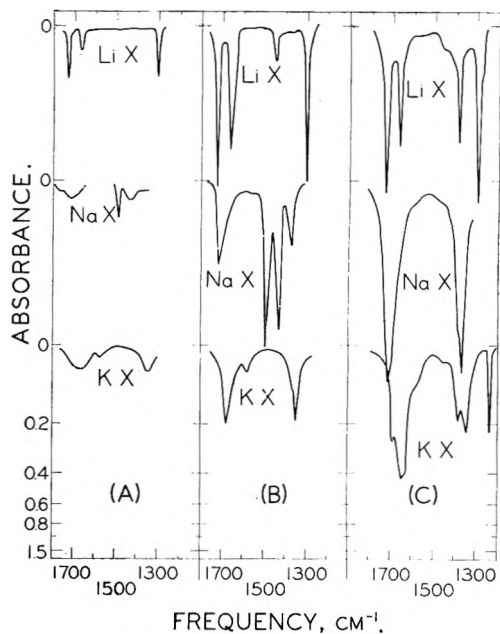


Fig. 4.—Comparison of spectra of carbon dioxide adsorbed on anhydrous LiX, NaX, and KX: (a) 1 min. after admission of 70 μ CO_2 ; (b) 70 hr. later; (c) after further addition of 100 mm. of CO_2 .

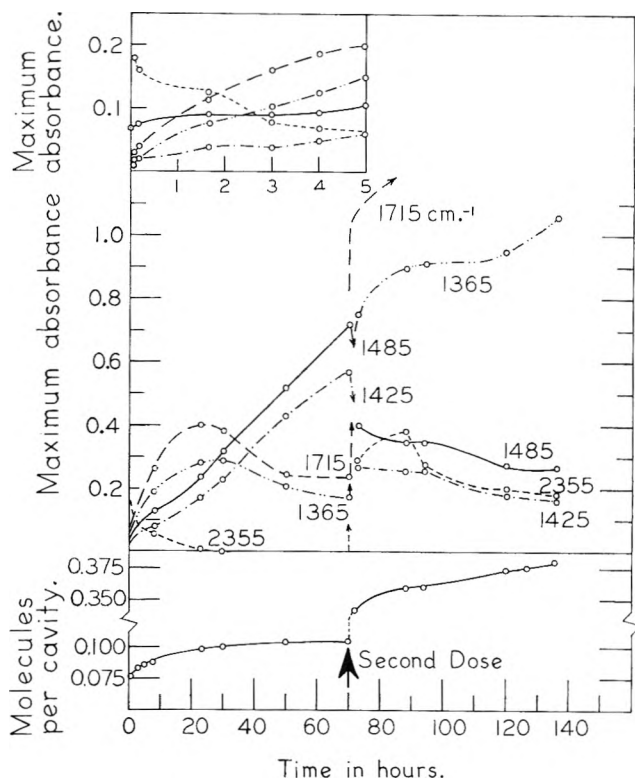


Fig. 5.—Variations in carbon dioxide concentration and band intensities with time during two successive adsorption steps for fully dehydrated NaX at 20°.

rate of desorption. Spectrum 7 of Fig. 6 shows that none of the water was removed by pumping at 100° and the carbon dioxide spectrum here is almost identical with that obtained by pumping the dehydrated pellet at 100°. Pumping at higher temperatures eliminated the 1650 cm^{-1} water band before the 1485–1425 cm^{-1} bands were completely removed.

The OH stretching region was not affected by the adsorption of carbon dioxide except for a slight increase in absorption on the high frequency side of the 3400

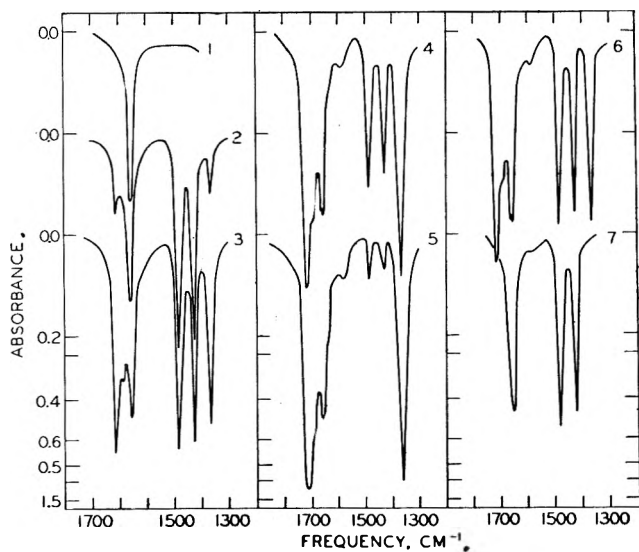


Fig. 6.—Spectra of carbon dioxide and water on slightly hydrated NaX at 20°: (1) 0.25 molecule of H₂O per cavity; (2) 0.10 of molecule CO₂ per cavity added, $p = 0$; (3) 0.20 molecule per cavity, $p = 0$; (4) 0.29 molecule per cavity, $p = 5 \mu$; (5) 0.38 molecule per cavity, $p = 40 \mu$; (6) pumped 2 hr. at room temperature; (7) pumped 1 hr. at 100°. Spectra 2–4 were taken immediately after admission of the carbon dioxide.

cm.⁻¹ band, caused by superposition of the 3609 cm.⁻¹ carbon dioxide band.

Similar though less extensive observations were carried out for carbon dioxide adsorbed on pellets of LiX and KX. As shown in Table II and Fig. 4 band frequencies in the chemisorption region are markedly different from those found with NaX. One exception is the band at 1380 cm.⁻¹ present on all forms at high carbon dioxide concentration and clearly seen in spectra 4(C). The ν_3 band near 2350 cm.⁻¹ shows a cationic shift of magnitude similar to those found in the water spectra.

With neither LiX nor KX was any decrease in band intensity observed to accompany further adsorption such as found with the 1485–1425 cm.⁻¹ pair on NaX. The various bands merely increased in intensity although for KX at high carbon dioxide pressures the 1670 cm.⁻¹ band split into a number of bands ranging from 1690 to 1640 cm.⁻¹ as seen in spectrum (C). In the case of KX spectrum (C) a small amount of D₂O had been added to speed up the equilibration and the sharp band observed at 1235 cm.⁻¹ is in the position of the D–O–D bending vibration although considerably more intense than would have been expected.

Small amounts of preadsorbed water produced a similar acceleration of the adsorption of carbon dioxide as found with NaX.

All bands were removed by pumping at 140° and this is in contrast to the case of NaX where the 1485–1425 cm.⁻¹ pair resisted pumping at temperatures up to 260°.

Discussion

Water.—In an ideal zeolite crystal the internal surfaces of the cavities are complete without the necessity of structural hydrogen to compensate for broken bonds or charge imbalance as is the case for alumina and silica. Thus the surface should not contain any structural hydroxyl groups and the spectrum in the water region should be entirely due to molecular water. In reality, however, the hydrated crystals appear to undergo some "hydrolysis" in which the exchangeable cations are

replaced by H₃O⁺ ions. It is this process which causes the high pH (around 9.5) of aqueous suspensions of zeolites. Upon dehydration, the extra portion of the H₃O⁺ would probably form a surface hydroxyl with one of the lattice oxygens. These surface OH groups would be similar to those observed on silica and alumina and the question is to what extent they are actually present on the zeolite surface.

The chemical analyses of Howell⁷ and Szymanski⁴ suggest that surface hydroxyls to the extent of 8 atom % of the aluminum content are present on zeolite X since the atom concentration of sodium was found to be 8% less than that of aluminum. While our analyses were not of sufficient accuracy to give an unambiguous answer they strongly support a 1:1 sodium:aluminum ratio and hence the absence of appreciable surface OH.

More conclusive evidence is to be expected from the infrared spectra which should show the presence either of H₃O⁺ or of isolated OH. The spectra of H₃O⁺ in solid crystals¹¹ and in solution¹² are characterized by bands around 2900 and 1700–1750 cm.⁻¹. Szymanski, Stamires, and Lynch⁴ reported such bands at high water concentrations but did not give any details of their observations. Under conditions of high dehydration any H₃O⁺ should be converted to surface OH groups which would produce sharp bands in the region 3700–3790 cm.⁻¹ such as are found in the spectra of aluminas,¹³ silica gel,¹⁴ and porous glass.¹⁵ Such groups are further identified by the absence of the ν_2 bending vibration near 1600 cm.⁻¹, since the bending vibration for a single OH occurs at a much lower frequency.¹⁶ Szymanski, *et al.*, concluded that the sharp band they observed at 3550 cm.⁻¹ for water contents below 15% of saturation was due to surface hydroxyls. However, this band was always accompanied by a band between 1600 and 1700 cm.⁻¹ as would be expected for molecular water so that such an interpretation seems unreasonable.

The water coverages of the present study are considerably lower than those employed by Szymanski, Stamires, and Lynch⁴ and at these low concentrations a sharp band is observed at frequencies between 3720 and 3648 cm.⁻¹, depending on the nature of the cation. This band may correspond to the 3550 cm.⁻¹ band of Szymanski, *et al.*, which would occur at a lower frequency because of hydrogen bonding. As shown in Fig. 2, this OH band is uniformly accompanied by the ν_2 band of molecular water and hence cannot represent surface hydroxyls. Furthermore while the surface hydroxyls of alumina and silica resist dehydration at temperatures above 500°, the zeolite band is removed at 200°. It is, of course, possible that small amounts of structural OH could still be present in some strongly hydrogen-bonded form after dehydration to 500° and that the resultant band due to OH stretching would be so broad as to be indistinguishable from the background. This is unlikely to any significant extent, both because the intensity of absorption due to hydrogen-bonded

(11) C. C. Feriso and D. F. Hornig, *J. Chem. Phys.*, **23**, 1464 (1955).

(12) M. Falk and P. A. Giguere, *Can. J. Chem.*, **35**, 1195 (1957).

(13) J. B. Peri, *Actes Congr. Intern. Catalyse 2^e Paris*, 1333 (1960).

(14) R. S. McDonald, *J. Phys. Chem.*, **62**, 1168 (1958).

(15) A. N. Terenin in "Surface Chemical Compounds and their Role in Adsorption Phenomena," A. V. Kiselev, Ed., Moscow Univ. Press, 1957; AEC Transl. 3750 O.T.S., Dept. of Commerce, Washington, D. C., 1959, p. 227.

(16) L. J. Bellamy, "The Infrared Spectra of Complex Molecules," 2nd Ed., John Wiley and Sons, Inc., New York, N. Y., 1958, p. 108.

stretching vibrations is so great that it could hardly escape notice and also because a favorable steric configuration for internal hydrogen bonding by structural OH is unlikely within the zeolite structure. All observations of the present work are consistent, therefore, with the absence of structural surface hydroxyls to any detectable extent.

We must therefore consider these spectra in terms of adsorbed molecular water. Adsorption may occur in either of two ways: by hydrogen bonding to the surface oxygens or by an interaction of the lone pair electrons of the oxygen atom with the surface cations—in effect an ion-dipole interaction. The former would give rise to a strong broad hydrogen-bonded OH stretching band around 3500 cm.^{-1} or lower. The latter type of adsorption would, if both hydrogens were left free, give two sharp bands in the OH region such as observed in dilute solutions of water in non-donor solvents.¹⁷ The observed spectra which contain one sharp band together with a typical hydrogen-bonded band suggest a configuration of the initially adsorbed water which involves a combination of both types of binding; *viz.*, simultaneous adsorption *via* one set of lone pair electrons to the exchangeable cation and *via* one hydrogen to a surface oxide ion leaving the other hydrogen projecting freely into the cavity. Such water would be expected to show the parallel development of the three bands as in Fig. 2. Additional supporting evidence for this assignment will be given in the following paragraphs.

The cation positions are not known completely for zeolite X but it appears³ that there are three different types of cation sites. One of these is at the junction of two "sodalite" units and, in effect, is buried in the wall of the large cavities and unlikely to be exposed for adsorption. Four cations per cavity are located in the six-membered rings and tend to lie in the plane of the ring so that they do not project very much into the cavity, although it is probable that the potassium ion would be too large to fit the ring and would project to a considerable extent. Finally, four cations have not been definitely located and are assumed to be rather freely mobile on the surface with a number of alternative minimum potential sites. The proposed combined bonding of water by an electron pair and a hydrogen would be easiest from a steric point of view with a cation of the last group but could probably also occur with cations of the second group as well.

The very high heats of adsorption which have been observed also support direct bonding to a cation. Barrer and Bratt¹⁸ have reported the isosteric heat of adsorption to approach 30 kcal. per mole at low coverage. The maximum heat of interaction to form two hydrogen bonds is not likely to be more than 15 kcal. per mole but interaction with an unscreened ion, even a noble gas type ion, should involve considerably larger energies.

Finally, direct bonding to the cations is indicated by the shift of the sharp band due to isolated OH stretching from 3720 cm.^{-1} for LiX to 3648 cm.^{-1} for KX. This shift is remarkably similar to that for the OH stretching vibration in solid hydroxides from 3678 cm.^{-1} for LiOH to 3611 cm.^{-1} for KOH.¹⁹ A similar

displacement is found in the spectra of water adsorbed on alkali halides.²⁰

These conclusions are not in disagreement with earlier workers since at higher coverages the free hydrogen would probably become bonded increasingly to adjacent water molecules and a greater proportion of the water would be hydrogen bonded to the oxide surface as suggested by Frohnsdorff and Kington.⁵

Carbon Dioxide.—The adsorption of carbon dioxide appears to involve both physical adsorption and chemisorption. We may consider the physical adsorption to be roughly that indicated by the gas chromatographic isotherm in Fig. 3 (and also the major part of the adsorption which occurs at higher pressures²¹) which produces the infrared band near 2350 cm.^{-1} . This band corresponds to the ν_3 vibration of linear carbon dioxide and the cationic variation in frequency over a range of 20 wave numbers suggests that the carbon dioxide is adsorbed linearly on a cation site. One would expect the adsorption to occur at the oxygen end of the molecule and to produce an asymmetry which might result in the ν_1 vibration becoming infrared active. This assignment is suggested for the band at 1380 cm.^{-1} observed on all three zeolites at higher pressures and which is close to the value 1388 cm.^{-1} listed in Table II for the free molecule. The absence of Fermi resonance with $2\nu_2$ such as is found in the gas phase Raman spectrum and the absence of any significant cation shift leaves some uncertainty about such an assignment.

The remaining bands in the region $1750\text{--}1250\text{ cm.}^{-1}$ may be compared with the numerous reports of spectra of carbon dioxide adsorbed on various oxides as summarized in Table II. These bands are usually assigned by other authors to carboxylate- or carbonate-like structures. While general conclusions of this sort can be strongly supported, detailed comparisons are uncertain because of the great differences in environment between a solid surface and any bulk phase. The formation of a carbonate-like species on a sodium aluminosilicate surface is inherently plausible. It may be considered to result from a carbon dioxide molecule lying on the surface in a bent configuration with the carbon bonded to a surface oxygen. Such a reaction, while it would undoubtedly weaken the bonding between the surface oxygen and the silicon and aluminum with which it is normally coordinated, would not require any major change in the position of the surface oxygen in the lattice. Such a reaction would be most likely with a surface oxygen adjacent to a sodium ion whose positive field extending out into the cavity would stabilize the resultant carbonate. In effect a surface oxide ion would be replaced by a carbonate ion and the negative charge would be distributed in part over the other two oxygens.

Investigations of the spectra of carbonate ion in various environments²²⁻²⁴ have shown that the single frequency around 1440 cm.^{-1} given by carbonate in a

(20) W. C. Price, F. Sherman, and C. R. Wilkinson, *Proc. Roy. Soc. (London)*, **A247**, 467 (1958).

(21) Linde Company, Isotherm Data Sheet No. 25, Carbon Dioxide Adsorption (1959).

(22) F. A. Miller and C. H. Wilkins, *Anal. Chem.*, **24**, 1253 (1952).

(23) B. M. Gatehouse, S. E. Livingstone, and R. S. Nyholm, *J. Chem. Soc.*, 3137 (1958).

(24) K. Buijs and C. J. H. Schutte, *Spectrochim. Acta*, **17**, 917, 921, 927 (1962).

(17) E. Greinacher, W. Luttko, and R. Mecke, *Z. Elektrochem.*, **59**, 23 (1955).

(18) R. M. Barrer and G. C. Bratt, *J. Phys. Chem. Solids*, **12**, 146 (1959).

(19) R. A. Buchanan, *J. Chem. Phys.*, **31**, 870 (1959).

symmetrical environment is split into two bands when the three oxygen atoms are no longer equivalent. The splitting may range from 70 cm.^{-1} for the rhombic environment in $\text{Na}_2\text{CO}_3 \cdot 7\text{H}_2\text{O}$ ²⁴ to some 500 cm.^{-1} in the case of organic carbonates.²³ Carboxylate ion shows a similar pair of bands in this general frequency range.²⁵ Both the organic carbonates and the carboxylate ion have two relatively "free" oxygens, and the third oxygen in the organic carbonate is bound to the rest of the molecule. While there will be significant differences in charge distribution one would expect the carbonate-like structure postulated here to be most like an organic carbonate in having one oxygen much more tightly bound than the other two. Examination of the spectra of carbon dioxide on the zeolites, *e.g.*, Fig. 4B, suggests a similar pair of bands of equal intensity on each zeolite which may be assigned to such a relatively unsymmetrical carbonate structure: 1728 and 1302 cm.^{-1} on LiX, 1715 and 1365 cm.^{-1} on NaX, and 1670 and 1340 cm.^{-1} on KX.

It is difficult to reach any firm conclusions concerning the other bands. Perhaps most remarkable is the 1485–1425 cm.^{-1} pair on NaX and we can do no more than draw attention to its special features. The frequency difference between the two bands is so small as to suggest a carbonate ion in an almost symmetrical environment. It is difficult to see how this might be achieved in terms of the zeolite structure and would probably involve a considerable displacement of the surface oxide ion involved. This structure appears to be the most stable configuration for small amounts of carbon dioxide as shown by the growth of the 1485–1425 cm.^{-1} bands at the expense of the 1715–1365 cm.^{-1} pair and also by the persistence of the 1485–1425 cm.^{-1} pair to higher temperatures of outgassing than any other bands. On the other hand, the configuration is very sensitive to physically adsorbed gas molecules of any sort whose presence causes it to revert instantly to the "normal" 1715–1365 cm.^{-1} structure. It would seem therefore that the 1485–1425 cm.^{-1} structure is closely related to the normal structure and its existence on the surface of only NaX is the result of a nice balance of cation geometry and energetics.

On LiX the 1660–1446 cm.^{-1} pair might be assigned

(25) Reference 16, p. 174.

to a carbonate structure in a somewhat more symmetrical environment than that of the 1728–1302 cm.^{-1} set, although the two components are markedly different in intensities. The 1570 cm.^{-1} band on KX may then be the more intense member of a similar pair.

Finally, there are some bands which are found only at high carbon dioxide pressures but which it is difficult to assign to physically adsorbed gas. These include the band at 1580 cm.^{-1} on NaX and the extra bands around 1670 cm.^{-1} on KX and no suggestions are offered for these bands at this time.

A further question of interest is the interaction of water and carbon dioxide on the zeolite surface. In these low concentration ranges the presence of roughly equivalent amounts of water greatly increases the rate of carbon dioxide chemisorption. There was no observable change in the appearance of the water bands as carbon dioxide is adsorbed. One possible explanation for these rate effects is in terms of a slow process of diffusion into the lattice; this might be speeded up by water adsorbing preferentially on the high energy sites permitting the carbon dioxide to by-pass these. However, the large pore diameter of the X zeolites favors a rapid diffusion of these small molecules and furthermore the very rapid response of the 1485–1425 cm.^{-1} pair of bands to an increase in gas pressure is also indicative of rapid diffusion. It would appear therefore that we must associate the water with the chemisorption step itself, *i.e.*, the formation of carbonate from a surface oxide ion and a physically adsorbed carbon dioxide molecule. The water molecule presumably acts as a catalyst for this reaction but does not enter into any permanent combination with the resultant structure.

While no detailed investigation has been made, it would appear from the few spectra obtained under carbon dioxide pressures of several cm. that there is little further chemisorption, beyond approximately 0.5–1 molecule per cavity and consequently the chemisorption would not be too readily detectable from normal isotherm measurements.²¹

Acknowledgments.—We wish to thank S. Warchola for assistance with the chemical analysis of the zeolites. Helpful discussions with Drs. R. M. Eloffson and J. W. Ward of this institution are gratefully acknowledged.

MASS SPECTRA OF VALENCE TAUTOMERS

BY CHAVA LIFSHITZ AND S. H. BAUER

*Department of Chemistry, Cornell University, Ithaca, New York**Received January 18, 1963*

The mass spectra of two pairs of valence tautomers were compared: cycloheptatriene and Δ^6 -bicyclo[3.2.0]heptene; cycloheptadiene and $\Delta^{2,6}$ -bicyclo[3.2.0]heptadiene. Appearance potentials were determined for the principal ions in each spectrum and the spectra were run at several low ionizing voltages. The following heats of formation were estimated: ΔH_f  = 2.7 ± 0.2 e.v., ΔH_f  = 1.3 ± 0.2 e.v., and ΔH_f ($C_7H_7^+$) ≤ 9.71 e.v. The results are discussed in terms of the differences in the products of excitation by electron impact of closely similar molecular systems.

Introduction

The reversible isomerism in which no atoms or groups shift is termed "valence tautomerism."¹ A current interesting example of such a pair is 1,2,4-tri-*t*-butylbenzene and its bicyclo[2.2.0]hexa-2,5-diene tautomer.² The distinction between *cis-trans* isomers, *endo-exo* isomers, and valence tautomers can be made only in terms of an accepted assignment of electron configurations. Valence tautomers do differ in the disposition of bond types. The structural representation of these molecules in their ground electronic states is unique even though the relationship between valence tautomer pairs is more easily illustrated than defined. However, the specific interest in such isomers is based on the belief that as these molecules are excited to higher vibrational and electronic states, the interconversion becomes very rapid because the structural differences between them become less and less distinct. Clearly, at sufficiently high excitations the distinction between all isomers becomes unclear. However, it is meaningful to inquire whether valence tautomers are indeed of closer kin than are other isomers, given a specific type of excitation. For example, in the statistical theory of mass spectra³ it is assumed that a polyatomic molecule dissociates solely *via* the vibrationally excited molecule ion in its lowest electronic state. How dissimilar must isomers be in molecular geometry and in electron configurations so that their mass spectral breakdown patterns will show recognizably different fragmentation paths? For a hydrocarbon, is a substantial difference in the intercarbon atom distances (as is the case for valence tautomers) more or less important than differences in the complexity of the hydrocarbon atoms?

In this paper the mass spectra and appearance potentials of the main fragments from the C_7H_{10} and the C_7H_8 valence tautomers will be presented and the results will be discussed. Cycloheptadiene and Δ^6 -bicyclo[3.2.0]heptene is one of the pairs studied; the other pair is cycloheptatriene and $\Delta^{2,6}$ -bicyclo[3.2.0]heptadiene.⁴ It has been shown that the monocyclic compounds isomerize photochemically into the bicyclic isomers while the latter are transformed into the former upon mild heating.

Mass spectra of various isomers were studied previously. These were found to be quite similar,⁵ al-

though some differences were observed^{6,7} which are especially pronounced at low ionizing voltages. Several of the isomer pairs studied were valence tautomers; for example, perfluoro-1,3-butadiene and perfluorocyclobutene.⁶ The mass spectrum of cycloheptatriene as well as the appearance potentials of the parent and $C_7H_7^+$ ions were recorded and compared with those of toluene⁸ and $\Delta^{2,5}$ -bicyclo[2.2.1]heptadiene.⁹ Furthermore, the spectrum, energetics, and structure of the tropylium radical ion ($C_7H_7^+$), which is formed from all the C_7H_8 isomers, have been widely investigated.¹⁰⁻¹³ The similarity between the spectra of three C_7H_8 isomers studied was taken as evidence for the redistribution of energy in the parent ion before fragmentation and was cited as support for the statistical theory of mass spectra.¹⁴

Experimental

The spectra were obtained with a C.E.C. mass spectrometer, Model 21-401, which had been modified, as previously described. Appearance potentials were determined by the vanishing current method, using argon or xenon as calibrating gases.^{15,16} The semi-log matching technique^{17,18} was also followed for the estimation of appearance potentials, using one of the main ions in the hydrocarbon spectrum as a reference, in order to compare values with those obtained by the vanishing current method. Mass spectral patterns were recorded at low electron voltages and the dependence of the percentage yields of the different ions upon the ionizing voltage was determined. The magnitudes of these low voltages were deduced from calibrations relative to the ionization potential of the parent molecules.

1,3-Cycloheptadiene was prepared by Dr. Y. Meinwald, by a modification of the method of Pesch and Friess,¹⁹ in which a Cope N-oxide pyrolysis (*cf.* J. Meinwald, *et al.*²⁰) was substituted for the Hofmann elimination.

Δ^6 -Bicyclo[3.2.0]heptene was kindly furnished by Dr. Orville L. Chapman and was $\sim 95\%$ pure (gas chromatography).

Cycloheptatriene was a sample obtained from Shell Develop-

(5) F. L. Mohler, *J. Wash. Acad. Sci.*, **38**, 667 (1952).(6) F. L. Mohler, V. H. Dibeler, and R. M. Reese, *J. Res. Natl. Bur. Std.*, **49**, 343 (1952).(7) (a) P. Natalis, *Bull. soc. chim. Belges*, **66**, 5 (1957); (b) J. Momigny and P. Natalis, *ibid.*, **66**, 26 (1957); (c) J. Momigny, *ibid.*, **70**, 241 (1961).(8) S. Meyerson and P. N. Rylander, *J. Chem. Phys.*, **27**, 901 (1957).(9) S. Meyerson, J. D. McCollum, and P. N. Rylander, *J. Am. Chem. Soc.*, **83**, 1401 (1961).(10) R. F. Pottie and F. P. Lossing, *ibid.*, **83**, 2634 (1961).(11) A. G. Harrison, L. R. Honnen, H. J. Dauben, and F. P. Lossing, *ibid.*, **82**, 5593 (1960).(12) J. M. S. Tait, T. W. Shannon, and A. G. Harrison, *ibid.*, **84**, 4 (1962).(13) (a) P. N. Rylander, S. Meyerson, and H. M. Grubb, *ibid.*, **79**, 842 (1957); (b) S. Meyerson, P. N. Rylander, E. L. Eliel, and J. D. McCollum, *ibid.*, **81**, 2606 (1959).(14) V. Hanus, *Nature*, **184**, 1796 (1959).(15) A. B. King and F. A. Long, *J. Chem. Phys.*, **29**, 374 (1958).(16) R. R. Bernecker and F. A. Long, *J. Phys. Chem.*, **65**, 1565 (1961).(17) R. E. Honig, *J. Chem. Phys.*, **16**, 105 (1948).(18) S. N. Foner and R. L. Hudson, *ibid.*, **25**, 602 (1956).(19) E. Pesch and S. L. Friess, *J. Am. Chem. Soc.*, **72**, 5756 (1950).(20) J. Meinwald, D. W. Dicker, and N. Danieli, *ibid.*, **82**, 4087 (1960).

(1) J. W. Baker, "Tautomerism," George Routledge and Sons, 1934 pp. 201-226.

(2) E. E. van Tamelen and S. P. Pappas, *J. Am. Chem. Soc.*, **84**, 3789 (1962).(3) H. M. Rosenstock, M. B. Wallenstein, A. L. Wahrhaftig, and H. Eyring, *Proc. Natl. Acad. Sci. U. S. A.*, **38**, 667 (1952).(4) W. G. Dauben and R. L. Cargill, *Tetrahedron*, **12**, 186 (1961)

ment Co., Emeryville, California, and was 90-95% pure (gas chromatography).

$\Delta^{2,6}$ -Bicyclo[3.2.0]heptadiene was prepared by Dr. Y. Meinwald as described by Dauben and Cargill⁴ and purified by preparative gas chromatography. It was 90-95% pure (gas chromatography).

Results

C_7H_{10} Isomers.—Table I gives the 70-volt spectra for the C_7H_{10} isomers in terms of percentage yields of the main peaks (the spectra are not isotopically resolved).

TABLE I
70-VOLT SPECTRA

Species				
$C_2H_3^+$	2.6	2.7	1.2	1.5
$C_3H_3^+$	5.9	6.2	5.3	6.4
$C_3H_4^+$			0.7	1.8
$C_3H_5^+$	2.2	2.4		
$C_4H_2^+$			1.3	1.5
$C_4H_3^+$			2.3	2.5
$C_4H_5^+$	2.0	2.2		
$C_5H_3^+$			2.4	2.0
$C_5H_5^+$	2.5	2.5	6.1	5.8
$C_5H_6^+$	5.1	5.8	1.1	6.3
$C_6H_5^+$	10.2	8.3		
$C_6H_7^+$	28.4	31.6		
$C_7H_7^+$	4.4	6.3	42.2	44.7
$C_7H_8^+$	0.5	1.5	20.0	15.6
$C_7H_9^+$	4.0	4.7		
$C_7H_{10}^+$	10.5	3.8		

The temperature of the ion source is usually maintained at 250°. In order to find out whether there is some conversion of the bicyclic to the monocyclic isomer in the ionization chamber we tested the effect of

the source temperature on the spectrum of .

The heater was turned off, the isatron allowed to cool, and the spectra were recorded at varying times after the filament was turned on. The results are given in Table II. $C_6H_7^+$ was taken as the base ion and assigned the nominal value of 31.6 (this is its percentage yield under normal operation conditions, Table I); the other peaks are expressed relative to $C_6H_7^+$. The first spectrum (1 in Table II) was taken at a temperature lower than 90°, the others at increasing temperatures up to 200° (measured with a thermocouple). The recorded trend follows that usually observed. The parent ion yield is higher at lower temperatures (ref. 21, pp. 202-204). There is no evidence, however, for isomerization at high temperatures in the ion chamber.

In Table III there are listed the appearance potentials measured for fragments from the C_7H_{10} isomers by the vanishing current method. Since these compounds contribute to the peak intensity at $m/e = 40$, measurements of appearance potentials relative to Ar may be questioned. The ionization potentials were therefore checked by measurements relative to Xe^+ as the reference ion; the results agree quite well.

In Fig. 1 and 2 semi-log ionization efficiency curves were plotted for ions from the C_7H_{10} isomer pair. The curves are quite parallel over a limited range of ionizing voltages. If one accepts the values obtained by the vanishing current method for the appearance potentials

(21) F. H. Field and J. L. Franklin, "Electron Impact Phenomena," Academic Press, Inc., New York, N. Y., 1957.

TABLE II

TEMPERATURE EFFECT ON THE  SPECTRUM
(Spectra taken at increasing temperatures, as explained in the text)

Species	1	2	3
$C_6H_5^+$	9.1	7.3	7.8
$C_6H_6^+$	2.4	1.8	1.9
$C_6H_7^+$	31.6	31.6	31.6
$C_7H_7^+$	7.1	5.7	6.1
$C_7H_8^+$	2.1	1.7	1.7
$C_7H_9^+$	5.6	4.5	4.7
$C_7H_{10}^+$	7.4	6.0	4.9

TABLE III

Species	APPEARANCE POTENTIALS IN VOLTS			
	Vanishing current method		From Fig. 1 and 2 (based on semi-log plots)	
				
$C_5H_6^+$		10.12 ^a	10.70	10.15
$C_6H_7^+$	10.14 ^a	9.79 ^a	10.14	9.79
			(ref.)	(ref.)
$C_7H_7^+$			13.37	
$C_7H_8^+$		9.41 ^a	10.8	9.4
$C_7H_9^+$			11.30	10.67
$C_7H_{10}^+$	8.75 ^a ; 8.71 ^a	9.34 ^a ; 9.37 ^b	8.40	9.37
	8.60 ^b	9.42 ^b		

^a Relative to Ar. ^b Relative to Xe.

of $C_6H_7^+$ ions, these provide calibrating curves from which one may deduce values for the other A.P.'s from the semi-log curves. They are also listed in Table II. There is some uncertainty in the $C_7H_8^+$ curve from cycloheptadiene; it is not shown in Fig. 1. The agreement between the two methods is quite satisfactory.

Figure 3 shows the dependence of ion yields, expressed as the per cent of total ionization, upon the ionizing voltage. [$V_e - A.P.(C_6H_7^+)$] is the electron accelerating voltage minus the appearance potential of $C_6H_7^+$ from the corresponding C_7H_{10} . The reason for presenting the low voltage data in this manner will be given in the Discussion.

C_7H_8 Isomers.—In Table I there are also listed the 70-v. spectra of the C_7H_8 isomers in terms of percentage yields of the principal ions. Appearance potentials were measured relative to Xe. Results by the vanishing current method are given in Table IV. Figures 4 and 5 consist of semi-log ionization efficiency curves for ions from the C_7H_8 isomer pair. Appearance potentials determined by the semi-log matching technique are also given in Table IV. The $C_5H_6^+$ ionization efficiency

curve from  shows a long tail. This is probably the cause for the discrepancy between the values as estimated by the vanishing current and semi-log methods. Under such circumstances, the estimated value based on the vanishing current method is preferred.

In Fig. 6 the dependence of ion yields, expressed as per cent of the total ionization, upon ionizing voltage was plotted. The abscissa is [$V_e - A.P.(C_7H_7^+)$], the electron voltage minus the appearance potential of

$C_7H_7^+$ from either  or . The yield of the

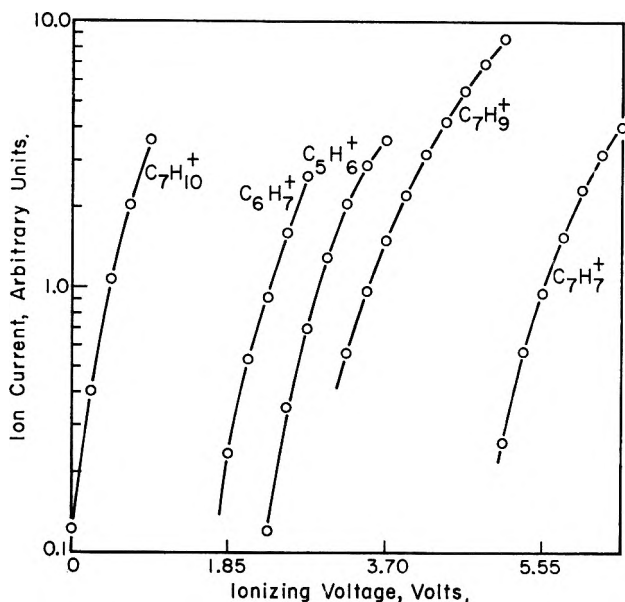


Fig. 1.—Semi-log ionization efficiency curves for fragment ions from cycloheptadiene. The logarithm of the recorded ion current is plotted vs. the ionizing electron voltage. The zero of the voltage scale is arbitrarily set.

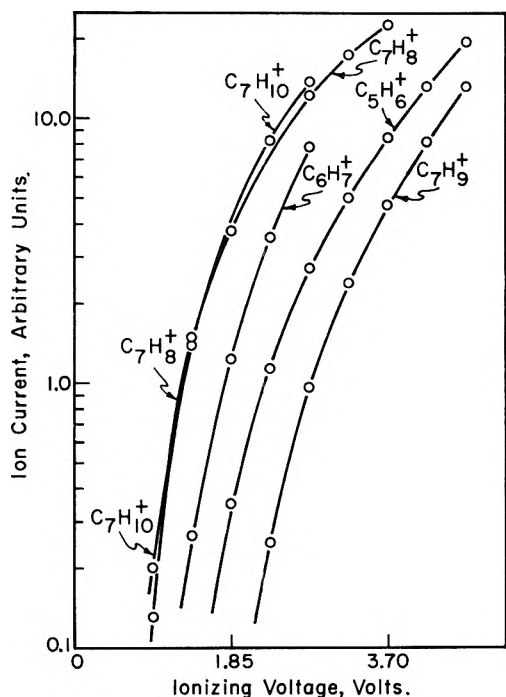


Fig. 2.—Semi-log ionization efficiency curves for fragment ions from Δ^6 -bicyclo[3.2.0]heptene. The zero of the voltage scale is arbitrarily set.

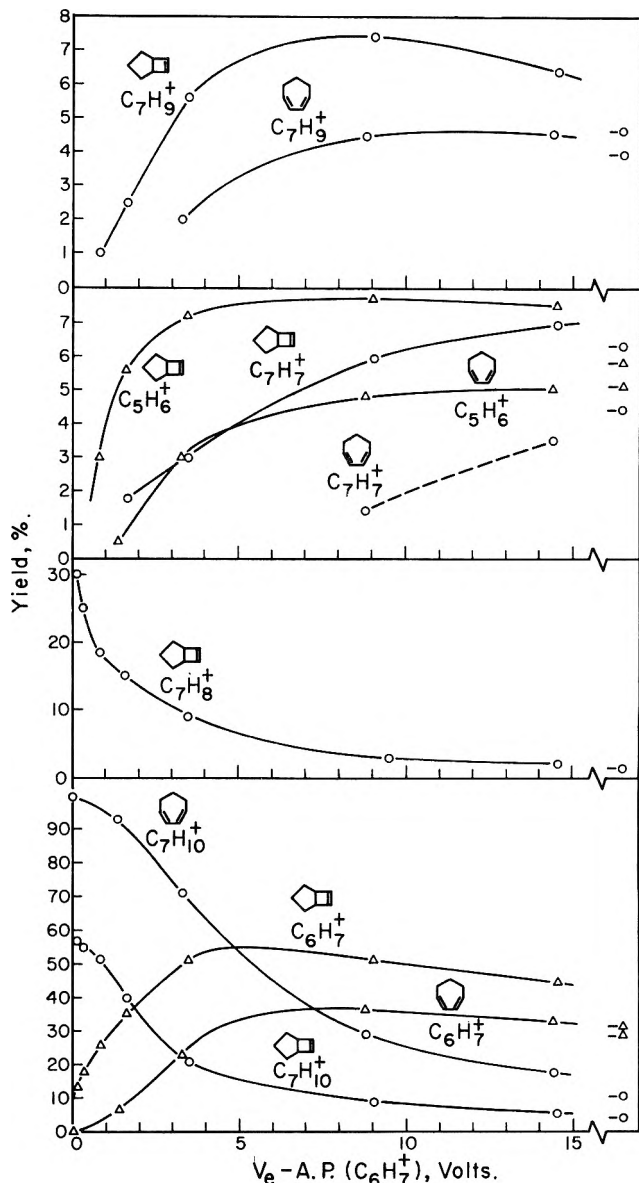


Fig. 3.—Low voltage spectra of C_7H_{10} isomers. The yields of the principal ions (in terms of per cent of total ionization) are plotted vs. the ionizing voltage. The formulas of each ion and its parent molecule are shown beside the curve for that ion. The zero of the voltage scale is set by the appearance potential of $C_6H_7^+$ as explained in the text. The points at high voltage (beyond the break in the voltage scale) are the 70-e.v. yields.

TABLE IV
APPEARANCE POTENTIALS IN VOLTS

Species	Vanishing current method		From Fig. 4 and 5 (based on semi-log plots)	
<chem>C5H5+</chem>			16.0	14.89
<chem>C6H6+</chem>		9.77; 10.27		10.45
<chem>C7H7+</chem>	10.68	9.66	10.73	9.88
<chem>C7H8+</chem>	8.56; 8.38	8.93; 8.92	8.52	8.92

metastable peak at $m/e = 90$, which is due to the transition



is larger in C7H8+ than in C7H7+ and is particularly prominent at low ionizing voltages where it attains $\sim 4\%$ of the total ionization in the former and 1% in the latter.

Comparison with Previous Results. Thermochemical Calculations

The appearance potentials for the C_7H_{10} isomer pair were not measured previously. For comparison, the ionization potential of cyclopentadiene is I.P. (C_5H_6) = 8.58 v.,²¹ although some higher values have been reported.¹¹ The appearance potentials of $C_7H_8^+$ and $C_7H_7^+$ from cycloheptatriene were measured previously. These are compared with the present values in Table V. A summary of the best values available for the appearance potentials of the principal ions from C_7H_8 isomers is given in Table VI. For $C_5H_6^+$ one measure-

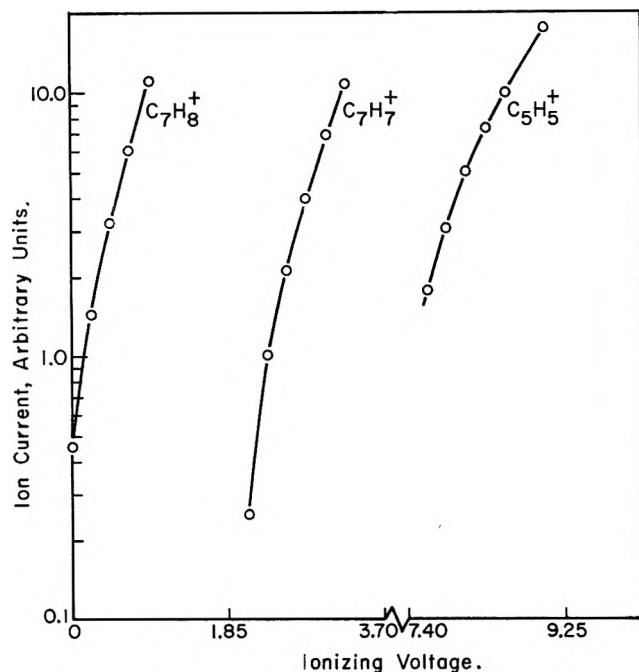


Fig. 4.—Semi-log ionization efficiency curves for fragment ions from cycloheptatriene. The zero of the voltage scale is arbitrarily set.

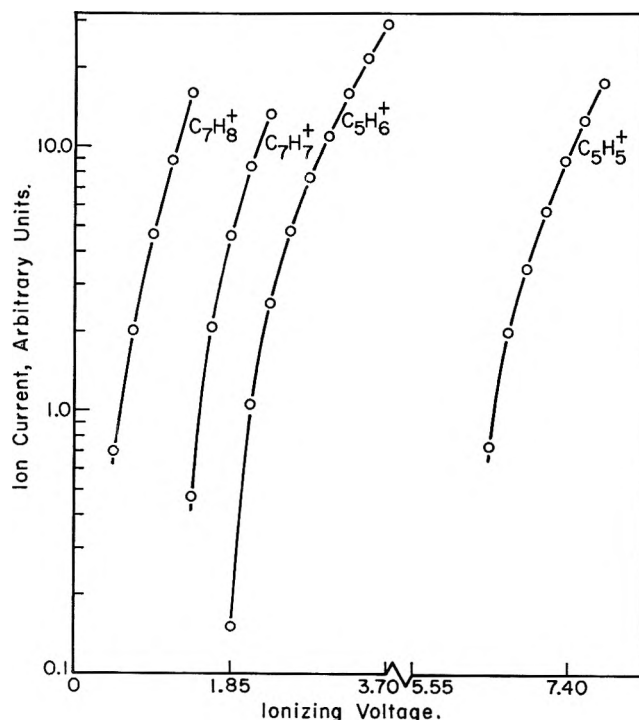


Fig. 5.—Semi-log ionization efficiency curves for fragment ions from $\Delta^{2,6}$ -bicyclo[3.2.0]heptadiene.

ment on bicyclo[2.2.1]heptadiene was also included. The values for the parent ions are probably reliable to ± 0.1 e.v., while those for the fragments are not better than ± 0.2 e.v.

For the molecules studied heats of formation have been measured only for the monocyclic compounds and for bicyclo[2.2.1]heptadiene. These are summarized in Table VII. Values for the heats of formation of the cycloheptadiene, cycloheptatriene, and tropylium ions are also cited (best values given by Harrison, *et al.*¹¹). There is some uncertainty in the estimates for $C_5H_6^+$ ^{11,21} and $C_7H_7^+$ ¹¹. If one assumes that the $C_6H_7^+$, $C_7H_9^+$,

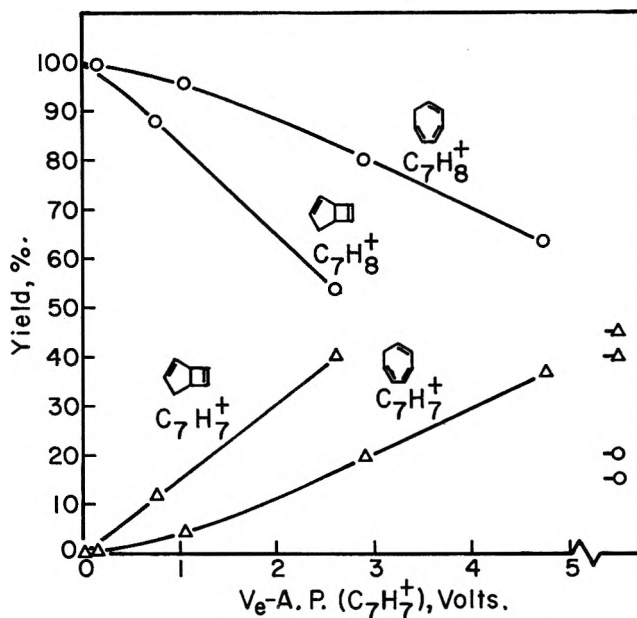


Fig. 6.—Low voltage spectra of C_7H_8 isomers. The yields of the two principal ions (in terms of per cent of total ionization) are plotted vs. the ionizing voltage. The formulas of each ion and its parent molecule are shown beside the curve for that ion. The zero of the voltage scale is set by the appearance potential of $C_7H_7^+$, as explained in the text. The points at high voltage (beyond the break in the voltage scale) are the 70-e.v. yields.

TABLE V
APPEARANCE POTENTIALS (VOLTS) FROM CYCLOHEPTATRIENE

Species	A.P.	Ref.
$C_7H_7^+$	10.4 ± 0.1	8
	10.1 ± 0.2	11
	10.61; 10.38; 10.38	9
	10.68; 10.73	Present data
	10.5	Accepted value
$C_7H_8^+$	8.55 ± 0.1	11
	8.52; 8.52; 8.51; 8.48;	9
	8.38; 8.52; 8.56	Present data

TABLE VI
APPEARANCE POTENTIALS FOR PRINCIPAL IONS FROM C_7H_8 ISOMERS

Species	Toluene	Cycloheptatriene	Bicyclo[2.2.1]-heptadiene	Bicyclo[3.2.0]-heptadiene
$C_5H_6^+$			10.0	10.0
$C_7H_7^+$	11.8 ⁹	10.5	9.6 ⁹	9.7
$C_7H_8^+$	9.0 ⁹	8.5	8.7 ⁹	8.9

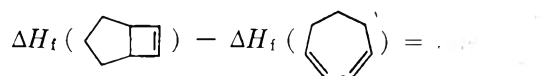
TABLE VII

HEAT OF FORMATION (E.V.)		
Compound	ΔH_f	Ref.
Cycloheptadiene	0.96	22
Cycloheptatriene	1.88	23
Bicyclo[2.2.1]heptadiene	2.90	9
$C_5H_6^+$	10.39	11
$C_7H_7^+$	9.74	11
$C_7H_8^+$	10.48	11

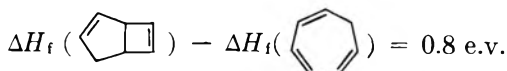
and $C_5H_6^+$ ions formed from either of the C_7H_{10} isomers are identical and that the accompanying neutral species are also the same, he may calculate the following values for the difference in the heats of formation of the parent molecules

(22) H. J. Dauben, private communication.

(23) H. L. Finke, D. W. Scott, M. E. Gross, J. F. Messerly, and G. Waddington, *J. Am. Chem. Soc.*, **78**, 5469 (1956).

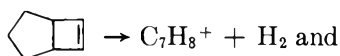
0.35 e.v. (from the difference in A.P. of $C_6H_7^+$)0.65 e.v. (from the difference in A.P. of $C_7H_9^+$)0.55 e.v. (from the difference in A.P. of $C_6H_6^+$)

Similarly, if one assumes that the $C_7H_7^+$ ion is the same whether formed from cycloheptatriene or from bicyclo[3.2.0]heptadiene, then

(from the difference in A.P. of $C_7H_7^+$)

In the above calculations the assumption was made that if there is any rearrangement energy (ref. 21, p. 88) involved in these molecule-ion decompositions, it is the same for each pair of isomers. This has been shown to be the case for $C_7H_7^+$ as derived from several C_7H_8 isomers^{8,9} but may not be generally valid.

The heats of formation of the bicyclic compounds may be estimated from the appearance potentials of ions absent in the spectra of their valence tautomers. For example, from A.P. ($C_7H_8^+$) (Table III), if this ion is the cycloheptatriene ion listed in Table VII, then



$$H\Delta_f(\text{bicyclo[3.2.0]heptadiene}) = 10.48 - 9.41 = 1.07 \text{ e.v.}$$

This is a lower limit since the elimination of H_2 from C_7H_{10} may involve excess rearrangement energy. Similarly from the appearance potential of $C_6H_6^+$ in bicyclo[3.2.0]heptadiene and the heats of formation of the cyclopentadiene ion (Table VII) and of C_2H_2 ^{9,24} one calculates



$$\Delta H_f(\text{bicyclo[3.2.0]heptadiene}) = 10.39 + 2.25 - 10.0 = 2.74 \text{ e.v.}$$

(Because of the uncertainty in the appearance potential of $C_5H_6^+$ this value should be quoted as ΔH_f

(bicyclo[3.2.0]heptadiene) = 2.7 ± 0.2 e.v.). This is in good agreement with the value deduced from the difference in the

A.P.'s of $C_7H_7^+$ from cycloheptatriene and bicyclo[3.2.0]heptadiene. It is also in agreement with the difference of zero to one-tenth

e.v. in A.P. of $C_5H_6^+$ and $C_7H_7^+$ from bicyclo[3.2.0]heptadiene and

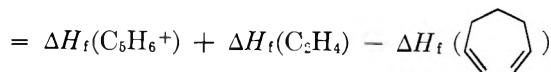


(Table VI), if one takes into account the

heat of formation of bicyclo[2.2.1]heptadiene (Table VII).

The data for C_7H_{10} pairs are not so self-consistent. The greatest weight should be given to the difference of 0.35 e.v. calculated from the $C_6H_7^+$ appearance

potentials. $C_6H_7^+$ occurs frequently in the mass spectra of aromatic compounds and, like $C_7H_7^+$, is probably a rearrangement ion possessing the stable benzene electron system (ref. 21, p. 188). The mechanism of formation of $C_6H_6^+$ ions from the C_7H_{10} isomer pair is uncertain. If $C_6H_6^+$ is a primary ion formed together with C_2H_4 , its appearance potential from cycloheptatriene should be



$$10.39 + 0.54 - 0.96 = 9.97 \text{ e.v.}$$

(the heat of formation of C_2H_4 is from ref. 24) provided $C_5H_6^+$ is indeed the cyclopentadiene ion. This should be compared to the experimental value of 10.7 e.v., (Table III). Apparently, there is excess energy involved in the above process. The appearance potential calculated on the assumption that, concurrently with $C_6H_6^+$, C_2H_2 and H_2 are formed, is 1.1 volts higher than the experimental value ($10.39 + 2.35 - 0.96 = 11.78$ e.v.). The activation energy for the loss of C_2H_4 from the monocyclic compound may be bigger than that for the bicyclic compound.

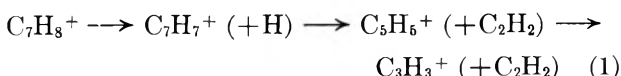
The "best" values for the heats of formation of the two pairs of tautomers are summarized in Table VIII. From the heats of formation of cycloheptatriene and CH_3 and from the appearance potential of $C_6H_7^+$ one calculates the heat of formation of this ion to be ≤ 9.71 e.v.

TABLE VIII
HEATS OF FORMATION (E.V.) OF VALENCE TAUTOMERS

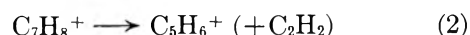
C_7H_8		
	1.88	2.7 ± 0.2
C_7H_{10}		
	0.96	1.3 ± 0.2

Breakdown Patterns

Breakdown patterns have been implied in the above discussion. Cycloheptatriene was considered previously^{8,9} in conjunction with other C_7H_8 isomers. The decomposition sequence is presumed to be

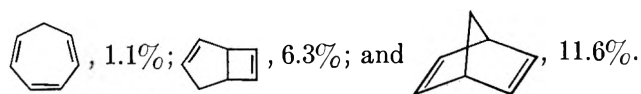


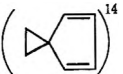
However, as has been noted,⁹ in the case of bicyclo[2.2.1]heptadiene, a parallel decomposition of the parent bicyclo[3.2.0]heptadiene ion takes place



This is of negligible probability in the cycloheptatriene. In (2) there is also some indication for a second step: $C_5H_6^+ \rightarrow C_3H_4^+ (+C_2H_2)$. We ran the spectrum of bicyclo[2.2.1]heptadiene to compare under our operating conditions its $C_5H_6^+$ yield with that from bicyclo[3.2.0]heptadiene and found it to be 11.6% of the total ionization. The yields of $C_5H_6^+$ from the three C_7H_8 isomers studied are

(24) F. D. Rossini, D. D. Wagman, W. H. Evans, W. H. Levine, and I. Jaffe, Natl. Bur. Stds., Circ. No. 500 (1952).



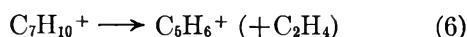
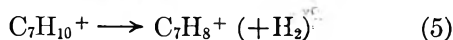
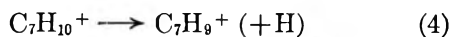
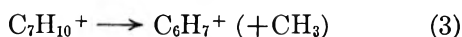
Two other C_7H_8 isomers, toluene⁸ and spiro-(2,4)-cycloheptadiene-(1,3) (¹⁴) exhibit the general

decomposition patterns (1) but show only small amounts of decomposition *via* (2), with yields comparable to those observed for cycloheptatriene. The species which show appreciable decomposition *via* (2) have in common the occurrence of the C_5H_6 ring within the parent mole-

cule. In fact,  has two such rings compared

to the one in  and its yield of $C_5H_6^+$ is about twice as large. In this respect the similarity in the C atom frame structure rather than the disposition of the H atoms is the significant factor.

The C_7H_{10} isomers break down in several parallel sequences of which the first stages are



Reaction 3 is the principal decomposition path. This is seen from the low energy patterns in Fig. 3 as well as from the energetics of the processes. $C_6H_5^+$ is probably formed as a secondary from $C_6H_7^+$ as found for cyclohexadiene.²⁵

The occurrence of $C_7H_8^+$ at very low electron energies in one valence tautomer but not in the other is puzzling. From the appearance potentials of $C_7H_8^+$ in the two compounds, it is plausible to assume that these ions have different structures. The formation of $C_7H_8^+$ may

be favored in , because of a favorable structural

configuration relative to . The loss of H_2 is not

very common, either among the cycloalkanes or among the cycloalkadienes.²⁵

In both pairs of valence tautomers one sees a similar decomposition sequence [in the C_7H_8 isomers it is sequence (1) and in the C_7H_{10} isomers reactions 3, 4, and 6]. In addition there is a reaction which is unique to one of the isomers in each pair—formation of $C_5H_6^+$ from  and $C_7H_8^+$ from .

Concluding Remarks

The ionization potentials are higher and the appearance potentials of the fragments are lower in the bicyclic compounds than they are in the monocyclic

species. The energies required to convert the parent molecule ion to the fragment ions is appreciably smaller in the bicyclic compounds. This may be the cause for the greater degree of decomposition of the latter. A similar trend was observed for the pair toluene and cycloheptatriene.⁸ On the other hand, the

occurrence of $C_5H_6^+$ in  and of $C_7H_8^+$ in 

but not in their valence tautomers cannot be explained on the basis of energetic considerations. In the strict application of the statistical theory of mass spectra³ one should incorporate characteristic frequency factors which are related to the structure of the molecule ions. In other words, one must assume different structures for the molecule-ions of two valence tautomers. In the case of the C_7H_8 isomers, the five-membered ring structure is apparently retained up to quite high states of excitation by electron impact.

It seems plausible to assume that $C_6H_7^+$ has the same structure from both of the C_7H_{10} isomers. This is the case also for the $C_7H_7^+$ ion from the C_7H_8 isomers. In Fig. 3 and 6, we have plotted percentage yields of ions *vs.* the electron voltage above the appearance potentials of these two ions. If energetic considerations only were operative one should get similar dependencies for each pair of valence tautomers. Experimentally, considerable differences are observed. We are forced to the conclusion that the same intermediate ions are not formed. The parent ions are certainly different at the threshold of their formation, since the ionization is a Franck-Condon process. But, for instance in the C_7H_{10} pair, $C_6H_6^+$ as well as $C_6H_7^+$ could be formed from the same intermediate vibrationally excited parent ion. If this were the case, then the curves for each ionic species (Fig. 3) would have been the same for the two tautomers. Actually, the bicyclic compound, although with apparently the same energy content, demonstrates a greater degree of decomposition. Hence, either the structures of the excited parent ion molecules are different and frequency factors favor the greater decomposition of the bicyclic compound, or the structures are very similar, but they have different energy contents (*i.e.*, are in different excited states) since the electron energy is not the actual energy imparted to the molecule upon ionization.²⁶

The data on the relative ionization efficiencies appear to support the assumption that the isomers produced different excited molecules upon electron impact. The constancy of the sum [heat of formation of C_7H_8 + A.P.($C_7H_7^+$)] for toluene, cycloheptatriene, and bicyclo[2.2.1]heptadiene was considered evidence^{8,9} for the formation of the same $C_7H_8^{+*}$ intermediate ion in all three cases. However, it has been pointed out by Meyerson and co-workers^{8,9} that this constancy merely reflects a constant activation energy for the reaction $C_7H_7^+ + H$, and that the $C_7H_8^{+*}$ need not be identical for all the C_7H_8 isomers. Whatever the explanation, these observations again indicate that the details of molecular fragmentation by electron impact depend more specifically on the geometry of the carbon skeleton than on the disposition of multiple bonds or of hydrogen atoms. The feature which

(25) Catalog of Mass Spectral Data, American Petroleum Institute Research Project 44, National Bureau of Standards (1957).

(26) For a discussion of energy distributions in parent molecule ions see, for example: (a) L. Friedman, F. A. Long, and M. Wolfsberg, *J. Chem. Phys.*, **27**, 613 (1957); (b) W. A. Chupka and M. Kaminsky, *ibid.*, **35**, 1991 (1961).

characterizes the relationship between valence tautomers is the comparatively high rate of conversion from the less to the more stable form. This implies a lower activation energy for this unimolecular process than for other types of isomerization. It does not involve excited electronic states. The rationale for this is that the adjustment of the skeleton geometry and the re-shuffling of multiple bonds occur simultaneously. A reasonable estimate for the activation energy is

$$2/3(D_{C=C} - D_{C-C})$$

In contrast, for a *cis-trans* isomerization about a double bond the activation energy is considerably higher, being that required to convert a C=C double bond to a single bond as when compressed to 1.33 Å. Other isomerizations require the rupture of a C-H bond concurrent with changes in the bonding between the carbon atoms.

Finally, the appearance potentials of $C_7H_7^+$ in toluene and cycloheptatriene (Table VI) were not found to be in considerable excess of the thermochemi-

cally calculated values based on the heats of formation of the C_7H_8 isomers. However, if the difference in appearance potentials of the parent $C_7H_8^+$ and product $C_7H_7^+$ is assumed to be the activation energy for the process³



an unexpectedly high activation energy is deduced for this reaction (2.8 e.v. in one case 2.0 e.v. in the other). For molecules with 39 oscillators, such as these are, calculations based on the statistical theory would give a small rate constant for the reaction at the theoretical lower limit of excitation.²⁷ These processes appear to be sufficiently probable so that the threshold energies are not considerably in excess of the theoretical lower limits.

Acknowledgments.—We wish to thank Professor F. P. Lossing and Professor M. J. Goldstein for valuable discussions and Drs. O. L. Chapman and Y. Meinwald for the compounds used.

(27) M. Wolfsberg, *J. Chem. Phys.*, **36**, 1072 (1962).

ELECTROKINETIC PHENOMENA IN CHARGED MICROCAPILLARIES¹

BY LAWRENCE DRESNER

Oak Ridge National Laboratory, Oak Ridge, Tennessee

Received January 19, 1963

Electrokinetic phenomena in small surface-charged capillaries have been studied. Fluid flow has been described by the Navier-Stokes equation, diffusion by coupled equations linear in the electrochemical potentials, and the electric field by Poisson's equation. In the case of good co-ion exclusion from the capillary, the coefficients in the linear laws relating solution flow and counter-ion current to pressure, concentration, and electrical gradients have been explicitly calculated. Some numerical calculations of interest in water desalination are reported.

1. Introduction

Electrokinetic phenomena have been known for more than a century and a half—electroosmosis, for example, was discovered in 1807. The first theory of these phenomena was the work of Helmholtz,² who introduced the concept of the electrical double layer. Helmholtz's theory was later refined by the introduction of a diffuse double layer in the researches of Gouy,^{3a,3b} Chapman,⁴ and Stern.⁵

When electrokinetic phenomena are produced in macroscopic capillaries, the double layer thickness is small compared to the capillary diameter, and charge separation in the fluid filling the capillary occurs only in a thin layer near the wall. Thus the bulk of the fluid is electrically neutral. In microcapillaries, on the other hand, the double layer thickness is comparable to the capillary diameter and the bulk fluid is charged. In general, the radial distribution of the fluid charge is strongly nonuniform. As Mackay and Meares⁶ first pointed out, the details of the spatial nonuniformity of the fluid charge affect electrokinetic phenomena in the

microcapillary. Mackay and Meares studied the effects of charge nonuniformity on electroosmosis in capillaries by assuming a power series with unspecified coefficients for the radial charge distribution in the capillary. In the present work, a consistent theory is used to calculate the radial co- and counter-ion distributions and so to remove the arbitrariness present in Mackay and Meares' work. This theory is based on the use of the Navier-Stokes equation to describe fluid flow, coupled equations linear in the gradients of the electrochemical potentials to describe diffusion, Poisson's equation to describe the electric field, and various appropriate equations of continuity and electroneutrality.

In sections 2, 3, and 4 the theory is developed in the case where there are no concentration gradients along the length of the microcapillary and only electrical and pressure gradients are considered. In section 5, a variety of numerical results are displayed and discussed, so that the reader may get some idea of the size of the various effects. Following section 5, the theory is generalized to admit axial concentration gradients in the microcapillary.

2. The Equations for the Streaming Potential.—

Let us consider a long cylindrical microcapillary of radius R upon whose inner surface a charge of surface density σ resides. Let r measure the radial distance of a point from the capillary axis; let x measure the distance along the axis. Suppose now that the ends of

(1) Work performed for the Office of Saline Water, U. S. Department of the Interior, at the Oak Ridge National Laboratory, Oak Ridge, Tennessee, operated by Union Carbide Corporation for the U. S. Atomic Energy Commission.

(2) H. Helmholtz, *Wid. Ann., N.F.*, **7**, 339 (1879).

(3) (a) G. Gouy, *J. Phys.*, [4] **9**, 357 (1910); (b) *Ann. Physik*, [9] **7**, 129 (1917).

(4) D. L. Chapman, *Phil. Mag.*, [6] **25**, 475 (1913).

(5) O. Stern, *Z. Elektrochem.*, **30**, 508 (1924).

(6) D. Mackay and P. Meares, *Trans. Faraday Soc.*, **55**, 1221 (1959).

the microcapillary are immersed in two reservoirs of electrolyte of equal concentration c and fluid is allowed to enter it. After a time thermodynamic equilibrium will be reached.

Suppose now that we create a pressure difference Δp between the two reservoirs. Fluid then flows through the capillary in the opposite direction to the pressure gradient. This produces a separation of charge, the high pressure reservoir taking the charge of the co-ions and the low pressure reservoir taking the charge of the counter-ions. This separation of charge creates an electric field E that causes diffusion of the counter-ions oppositely directed to the flow of the fluid. When a steady state is reached, the velocity profile of the fluid flow and the magnitude of the electric field E have adjusted themselves so that the effluent fluid is electrically neutral. The potential difference across the capillary created by the electric field is called the streaming potential.

Equations describing transport processes in multi-component systems have been given by Bearman and Kirkwood^{7a} and by de Groot.^{7b} These equations describe (i) diffusion of the various components with respect to the local center of mass and (ii) the motion of the local center of mass. The isothermal diffusion of co- and counter-ions and water with respect to the local center of mass in the presence of an external electric field is specified by the equation

$$\dot{j}_i = - \sum_{k=1}^3 \mathfrak{M}_{ik} N_k (z_k e \nabla \phi + \nabla \mu_k) \quad i = 1, 2, 3 \quad (1')$$

where

\dot{j}_i is the vector mass-current of component i (g. cm.⁻² sec.⁻¹) with respect to the local center of mass and is defined by

$$\dot{j}_i = \rho_i (\mathbf{v}_i - \mathbf{v})$$

ρ_i is the local density (g. cm.⁻³) of component i
 \mathbf{v}_i is the local velocity (cm. sec.⁻¹) of component i
 \mathbf{v} is the velocity of the local center of mass, given by $\mathbf{v} = \frac{\sum_{k=1}^3 \rho_k \mathbf{v}_k}{\sum_{k=1}^3 \rho_k}$

\mathfrak{M}_{ik} is a phenomenological coefficient

N_k is the number of particles (ions or molecules) per g. of component k

z_k is the valence of component k

e is the charge of the proton

ϕ is the electrical potential

μ_k is the chemical potential per particle of component k , and $i = 1$ denotes counter-ions, $i = 2$ denotes co-ions, and $i = 3$ denotes water.

According to Onsager's theorem,^{7b} the coefficients in eq. 1' are symmetric, *i.e.*, $\mathfrak{M}_{ik} = \mathfrak{M}_{ki}$. Furthermore, since $\sum_{i=1}^3 \dot{j}_i = 0$, it can easily be shown that $\sum_{i=1}^3 \mathfrak{M}_{ik} = 0$ for all k . If we replace \dot{j}_i by \mathbf{j}_i/N_i , where \mathbf{j}_i is the particle current (ions or molecules cm.⁻² sec.⁻¹), eq. 1' can be rewritten as

$$\mathbf{j}_i = - \sum_{k=1}^3 M_{ik} (z_k e \nabla \phi + \nabla \mu_k) \quad i = 1, 2, 3 \quad (1)$$

where

$$M_{ik} = N_i \mathfrak{M}_{ik} N_k \quad (1a)$$

$$M_{ik} = M_{ki} \quad (1b)$$

(7) (a) R. J. Bearman and J. G. Kirkwood, *J. Chem. Phys.*, **28**, 136 (1958); (b) S. R. de Groot, "Thermodynamics of Irreversible Processes," North-Holland Publishing Co., Amsterdam, 1958.

and

$$\sum_{i=1}^3 M_{ik}/N_i = 0 \quad (1c)$$

The motion of the local center of mass is given by a form of the Navier-Stokes equation, *viz.*

$$\rho \left(\frac{\partial \mathbf{v}}{\partial t} + \mathbf{v} \cdot \nabla \mathbf{v} \right) = - \nabla p + \eta \nabla^2 \mathbf{v} - e \nabla \phi \sum_{k=1}^3 z_k c_k \quad (2')$$

where

$$\rho \text{ is the total fluid density, given by } \rho = \sum_{k=1}^3 \rho_k$$

p is the pressure

η is the fluid viscosity

c_k is the concn. of component k in particles (ions or molecules) per cubic centimeter

In steady-state flow in the microcapillary, the left-hand side of eq. 2' vanishes. The derivative $\partial \mathbf{v} / \partial t$ vanishes by definition of the steady state; the term $\mathbf{v} \cdot \nabla \mathbf{v}$ vanishes because \mathbf{v} is everywhere axially directed but only changes in the radial direction. Thus in all the applications made of it in this paper, eq. 2' takes the form

$$- \frac{dp}{dx} + \frac{\eta}{r} \frac{d}{dr} r \frac{dv}{dr} - e \frac{d\phi}{dx} (z_1 c_1 + z_2 c_2) = 0 \quad (2)$$

In a steady state, the various flows \mathbf{j}_i and the velocity \mathbf{v} are connected by conditions of continuity. Since only two of the flows \mathbf{j}_i are independent, there are three independent continuity conditions, which in the case of axial flow in a microcapillary, we take as

$$\nabla \cdot \mathbf{v} = 0 \quad (3a)$$

$$\nabla \cdot (\mathbf{j}_1 + c_1 \mathbf{v}) = 0 \quad (3b)$$

$$\nabla \cdot (\mathbf{j}_2 + c_2 \mathbf{v}) = 0 \quad (3c)$$

The electric potential is related to the ionic concentration through Poisson's equation

$$\nabla^2 \phi = -(z_1 e c_1 + z_2 e c_2) / \epsilon \quad (4)$$

where ϵ is the dielectric constant. The electroneutrality of the fluid leaving the microcapillary can be written

$$\langle [z_1 e (\mathbf{j}_1 + c_1 \mathbf{v}) + z_2 e (\mathbf{j}_2 + c_2 \mathbf{v})] \cdot \mathbf{n} \rangle = 0 \quad (5)$$

where \mathbf{n} is a unit vector parallel to the capillary axis, and the braces denote an average over the capillary cross section. Finally, the over-all electro-neutrality of the capillary interior can be written as

$$\langle z_1 e c_1 + z_2 e c_2 + z_0 e c_0 \rangle = 0 \quad (6)$$

Here the subscript zero denotes the fixed charges residing on the capillary wall. They must be taken into account in eq. 6, but they do not enter eq. 4 directly since they are not present in the bulk of the fluid in the microcapillary. They do, however, affect the electrical potential ϕ by influencing the boundary condition the electric field must satisfy at the capillary wall.

If a suitable boundary condition is added to eq. 1-6, a unique solution will be specified. For this boundary condition the requirement has been taken that the fluid

in either end of the capillary is in thermodynamic equilibrium with the fluid of the reservoir into which it intrudes.

3. Solution of the Equations.—If $\mathbf{j}_i = \nabla p = \mathbf{v} = 0$, the concentrations and the electric potential are given by

$$c_i = c_i^{(0)}(r) \tag{7a}$$

$$\phi = \phi^{(0)}(r) \tag{7b}$$

where the superscript zero denotes the equilibrium value of the quantity being considered. Now choose as solutions in the steady-state case under consideration the values

$$c_i = c_i^{(0)}(r) \tag{8a}$$

$$\phi = \phi^{(0)}(r) - Ex \tag{8b}$$

where E is the constant value of the axial electric field. The choice (8b) of E constant and pointing along the axis is based on imagining the microcapillary to be one of many parallel pores through a thin membrane. It is plausible to suppose that the initially separated charges, both signs being mobile, will spread themselves uniformly over the membrane surfaces, producing a constant field within.

In thermodynamic equilibrium only eq. 4 and 6 are nontrivial⁸; since the equilibrium solutions (7) simultaneously satisfy these equations, the assumed solutions (8) also do. The solutions (8a) moreover satisfy the boundary condition given at the end of section 2. The continuity equations (3a,b,c) will be satisfied if we choose \mathbf{v} and \mathbf{j}_i to be axially directed and functions of r only. Such an assumption for \mathbf{j}_i is consistent with eq. 1, since substitution of solution (8) into eq. 1 yields the result

$$j_i = eE \sum_{k=1}^2 M_{ik} z_k - \sum_{i=1}^3 M_{ik} \left(\frac{\partial \mu_k}{\partial p} \right) \left(\frac{dp}{dx} \right) \tag{9'}$$

in the axial direction, while in the radial direction both sides of eq. 1 vanish identically.

In this paper we shall only be interested in the case of good Donnan exclusion of the co-ions from the capillary.⁹ If we make the idealization that $c_2 = 0$ in the microcapillary, then with the help of eq. 1b,c eq. 9' can then be written

$$j_1 = \frac{c_1^{(0)} \mathfrak{D}_1}{kT} \left(z_1 e E - w \frac{dp}{dx} \right) \tag{9}$$

$$j_3 = - \frac{N_3}{N_1} j_1 \tag{9''}$$

where

(8) In equilibrium, eq. 3 and 5 are trivially satisfied. Equation 2 is likewise trivially satisfied in the axial direction, there being no axial flow, no axial pressure gradient, and no axial electric field. Equation 2 must also be satisfied in the radial direction; this means that a radial pressure gradient exists equal to $-e \nabla \phi (z_1 c_1 + z_2 c_2)$. In equilibrium, the electrochemical potential of any component must be constant from point to point in the microcapillary. This means that the parentheses in eq. 1 vanish, so that it, too, is trivially satisfied. The constancy of the electrochemical potential requires a connection between the concentration and the electric potential which in the case of ideality is equivalent to the proportionality of the concentration to the Boltzmann factor $\exp(-z_i e \phi / kT)$. This proportionality, together with eq. 4 and 6 and the boundary conditions, serves to determine the equilibrium concentrations and the equilibrium electric field (see ref. 9).

(9) L. Dresner and K. A. Kraus, *J. Phys. Chem.*, **67**, 990 (1963).

$w_i = \partial \mu_i / \partial p$ is the specific volume per particle of component i
 $w = w_1 - (N_3 / N_1) w_3$
 $M_{11} = c_1^{(0)} \mathfrak{D}_1 / kT$
 \mathfrak{D}_i is the diffusion constant of the counter-ions in the fluid (cm.² sec.⁻¹)
 k is Boltzmann's constant
 T is the temperature

If we now substitute solution (8) into eq. 2 we get

$$z_1 e E c_1^{(0)}(r) - \frac{dp}{dx} + \frac{\eta}{r} \frac{d}{dr} r \frac{dv}{dr} = 0 \tag{10}$$

From (10) it follows that

$$\eta v = \int_r^R \frac{dr'}{r'} \int_0^{r'} \left(z_1 e E c_1^{(0)}(r'') - \frac{dp}{dx} \right) r'' dr'' \tag{11}$$

By substitution of eq. 9 and 11 into eq. 5 and some re-writing, the following solution for the field E is obtained

$$z_1 e E = \frac{dp}{dx} \times \frac{\frac{2}{R^2} \int_0^R c_1^{(0)}(r) [(R^2 - r^2)/4 + \eta \mathfrak{D}_1 w / kT] r dr}{\frac{2}{R^2} \int_0^R \frac{dr}{r} \left(\int_0^r c_1^{(0)}(r') r' dr' \right)^2 + \frac{\eta \mathfrak{D}_1}{kT} \frac{2}{R^2} \int_0^R c_1^{(0)}(r) r dr} \tag{12}$$

Dresner and Kraus⁹ have derived the formula

$$c_1^{(0)}(r) = \langle c_0 \rangle \left(a - \frac{\xi^2}{8a} \right)^{-2} \tag{13}$$

for $c_1^{(0)}(r)$ in the case of good co-ion exclusion, where

$$a^2 = 1 + \xi_R^2 / 8$$

$$\xi_R = \kappa R$$

$$\xi = \kappa r$$

$$\kappa^2 = e^2 \langle c_0 \rangle / kT \epsilon$$

With this formula for $c_1^{(0)}(r)$ the integrals in eq. 11 and 12 are simple ones. Carrying them out leads to the results

$$\frac{z_1 e E}{dp/dx} = \frac{\frac{\eta}{2kT} \kappa^2 \mathfrak{D}_1 w + [(1 + 8/\xi_R^2) \ln(1 + \xi_R^2/8) - 1]}{\frac{\eta}{2kT} \mathfrak{D}_1 \kappa^2 + \langle c_0 \rangle [1 - (8/\xi_R^2) \ln(1 + \xi_R^2/8)]} \tag{14a}$$

$$\frac{\eta v}{dp/dx} = \frac{2}{\kappa^2} \left\{ \frac{z_1 e E}{dp/dx} \langle c_0 \rangle \ln(1 + [\xi_R^2 - \xi^2]/8) - \frac{[\xi_R^2 - \xi^2]}{8} \right\} \tag{14b}$$

4. Other Phenomena.—In addition to the streaming potential, various other electrokinetic quantities such as the streaming current and the electroosmosis are of interest.^{7b} These quantities are calculable on the basis

of the model described in sections 2 and 3, but such calculations are unnecessary since all isothermal electrokinetic quantities can be obtained from the results given in eq. 14 by use of the laws of irreversible thermodynamics.^{7b}

Suppose that q represents the total *volumetric* flow through the microcapillary and J represents the total counter-ion current. The entropy production dS/dt in the capillary is given by

$$-T(dS/dt) = q\Delta p + Jz_1e\Delta\phi \quad (15)$$

where henceforth ϕ is the potential of either reservoir and Δ denotes the difference between the two reservoirs. The linear laws relating the flows and forces are

$$q = L_{11}\Delta p + L_{12}z_1e\Delta\phi \quad (16a)$$

$$J = L_{21}\Delta p + L_{22}z_1e\Delta\phi \quad (16b)$$

$$L_{12} = L_{21} \quad (16c)$$

Equation 16c is Onsager's relation.^{7b} Equations 16 constitute a full thermodynamic description of the microcapillary system in the case of good co-ion exclusion from which all electrokinetic quantities can be obtained. The important L -coefficients can be obtained from the results of eq. 14 as follows.

When $\Delta\phi = 0$, $E = 0$ and the velocity v is given by the second term in eq. 14b. q is always given by

$$q = \int_0^R [(j_1 + c_1v)w_1 + (j_3 + c_3v)w_3]2\pi r dr \quad (17)$$

Substituting eq. 9 and 9'' for j_1 and j_3 and using the identity $c_1w_1 + c_3w_3 = 1$ (Gibbs-Duhem equation) this becomes

$$q = - \left(\frac{dp}{dx} \right) \left(\frac{\pi R^4}{8\eta} + \frac{\pi R^2 \langle c_0 \rangle \mathcal{D}_1 w^2}{kT} \right) \quad (18)$$

From (18) it follows that

$$-L_{11} = \frac{\pi R^4}{8\eta d} + \frac{\pi R^2 \langle c_0 \rangle \mathcal{D}_1 w^2}{kTd} \quad (19)$$

where d is the length of the capillary. The first term in eq. 19 is Poiseuille's law; the second term arises from *diffusion* relative to the local center of mass caused by the pressure gradient.

J is always given by

$$J = \int_0^R (j_1 + c_1v)2\pi r dr \quad (20a)$$

which in the case $\Delta\phi = 0$ becomes

$$J = - \frac{dp}{dx} \int_0^R c_1^{(0)}(r) \left[\frac{\pi}{2\eta} (R^2 - r^2) + \frac{w\mathcal{D}_1}{kT} \right] 2\pi r dr \quad (20b)$$

$$= - \frac{2\pi}{\eta} \left(\frac{dp}{dx} \right) \frac{R^2 \langle c_0 \rangle}{\kappa^2} \left[(1 + 8/\xi_R^2) \ln(1 + \xi_R^2/8) - 1 + \frac{\eta \mathcal{D}_1 w \kappa^2}{2kT} \right] \quad (20c)$$

Thus

$$-L_{21} = \frac{2\pi R^2 \langle c_0 \rangle}{\eta \kappa^2 d} \left[(1 + 8/\xi_R^2) \ln(1 + \xi_R^2/8) - 1 + \frac{\eta \mathcal{D}_1 w \kappa^2}{2kT} \right] \quad (21)$$

If $\Delta p = 0$ and an external potential difference is supplied, E is different from zero, and the appropriate expression for v belonging in (17) is given by the first term of (14b). Thus

$$q = z_1eE \int_0^R \left[\frac{2\langle c_0 \rangle}{\kappa^2 \eta} \ln(1 + [\xi_R^2 - \xi^2]/8) + \frac{c_1^{(0)}(r)\mathcal{D}_1 w}{kT} \right] 2\pi r dr \quad (22a)$$

$$= z_1eEd \frac{2\pi R^2 \langle c_0 \rangle}{\eta \kappa^2 d} \left[(1 + 8/\xi_R^2) \ln(1 + \xi_R^2/8) - 1 + \frac{\eta \mathcal{D}_1 w \kappa^2}{2kT} \right] \quad (22b)$$

Since $z_1eEd = -z_1e\Delta\phi$ in the case at hand, comparison of eq. 16, 21, and 22 shows that $L_{21} = L_{12}$, as it must.

Finally, when $\Delta p = 0$

$$J = \int_0^R [j_1 + c_1^{(0)}(r)v] 2\pi r dr = \int_0^R \left[\frac{\mathcal{D}_1 c^{(0)}(r)}{kT} z_1eE + c_1^{(0)}(r)v \right] 2\pi r dr \quad (23)$$

where v is again given by the first term in eq. 14b. Thus

$$J = \frac{\pi R^2 \mathcal{D}_1}{kT} \langle c_0 \rangle z_1eE + \int_0^R c_1^{(0)}(r) \times \left[\frac{2\langle c_0 \rangle}{\eta \kappa^2} z_1eE \ln(1 + [\xi_R^2 - \xi^2]/8) \right] 2\pi r dr \quad (24a)$$

$$= \frac{\pi R^2 \mathcal{D}_1}{kT} \langle c_0 \rangle z_1eE + \frac{2\pi \langle c_0 \rangle^2 R^2}{\kappa^2 \eta} z_1eE [1 - (8/\xi_R^2) \ln(1 + \xi_R^2/8)] \quad (24b)$$

so that

$$-L_{22} = \frac{\pi R^2 \mathcal{D}_1 \langle c_0 \rangle}{kTd} + \frac{2\pi \langle c_0 \rangle^2 R^2}{\kappa^2 \eta d} [1 - (8/\xi_R^2) \ln(1 + \xi_R^2/8)] \quad (25)$$

If in eq. 16b J is set equal to zero, the result of eq. 14a for E is recovered.

5. Discussion and Numerical Examples.—In his discussion of electrokinetic phenomena de Groot^{7b} mentions eight quantities all of which are studied experimentally. The names and definitions of these quantities, as well as their expression in terms of the L -coefficients of eq. 16, are shown in the first eight lines in Table I. Two other quantities not mentioned by de Groot are shown in the last two lines.

Because of Onsager's relation (16c), the first eight quantities in Table I are equal by pairs, save for a possible sign change. Thus the streaming current equals (minus) the electroosmotic pressure, the streaming potential equals (minus) the electroosmosis, the second streaming current equals the second electroosmosis, and the second electroosmotic pressure equals the second streaming potential.

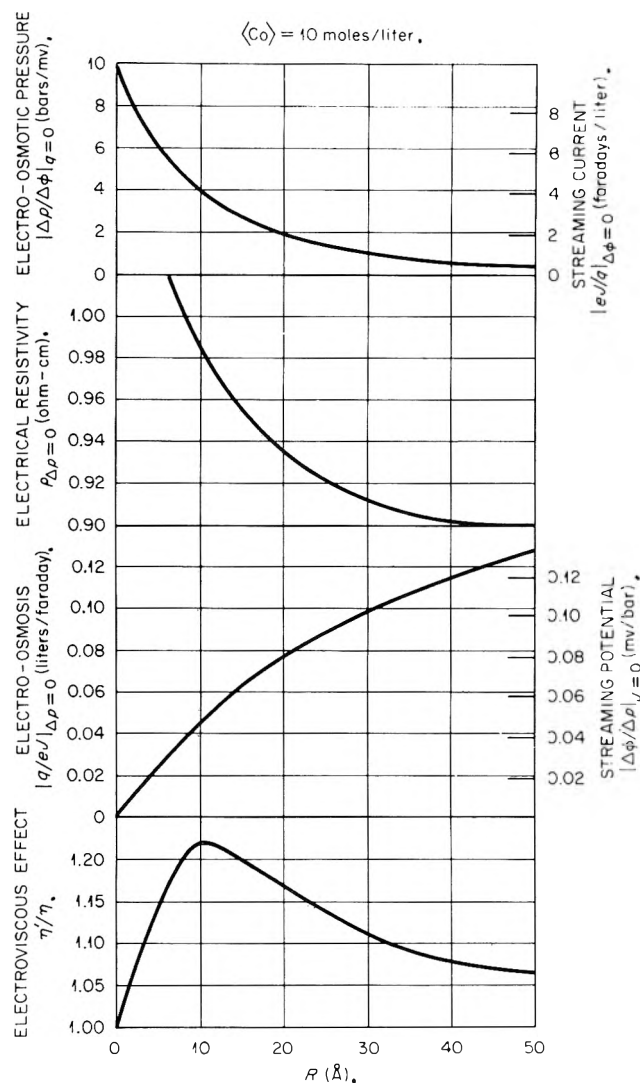


Fig. 1a.—Various electrokinetic quantities plotted against the capillary radius R in the case of constant fixed charge density (c_0).

TABLE I

THE NAMES AND DEFINITIONS OF THE VARIOUS ELECTROKINETIC QUANTITIES, AS WELL AS THEIR EXPRESSION IN TERMS OF THE L -VALUES OF EQ. 16

Name	Definition	Expression in terms of the L 's
Streaming current	$(eJ/q)_{\Delta\phi=0}$	eL_{21}/L_{11}
Electroosmotic pressure	$(\Delta p/\Delta\phi)_{q=0}$	$-eL_{12}/L_{11}$
Streaming potential	$(\Delta\phi/\Delta p)_{J=0}$	$-L_{21}/eL_{22}$
Electroosmosis	$(q/eJ)_{\Delta p=0}$	L_{12}/eL_{22}
Second streaming current	$(eJ/\Delta p)_{\Delta\phi=0}$	eL_{21}
Second electroosmosis	$(q/\Delta\phi)_{\Delta p=0}$	eL_{12}
Second electroosmotic pressure	$(\Delta p/eJ)_{q=0}$	$(eL_{21})^{-1} \left(1 - \frac{L_{22}L_{11}}{L_2 L_{12}} \right)^{-1}$
Second streaming potential	$(\Delta\phi/q)_{J=0}$	$(eL_{12})^{-1} \left(1 - \frac{L_{22}L_{11}}{L_{21}L_{12}} \right)^{-1}$
Hydrodynamic resistance	$(q/\Delta p)_{J=0}$	$L_{11} \left(1 - \frac{L_{12}L_{21}}{L_{11}L_{22}} \right)$
Electrical resistance	$(\Delta\phi/eJ)_{\Delta p=0}$	$(e^2L_{22})^{-1}$

Plotted against the capillary radius in Fig. 1a,b are values of the various electrokinetic quantities calculated for the following typical choice of parameters

- $\langle c_0 \rangle = 10$ moles/l.
- $\epsilon/\epsilon_0 = 80$
- $\epsilon_0 =$ dielectric constant of a vacuum (8.854×10^{-12} farads/m.)

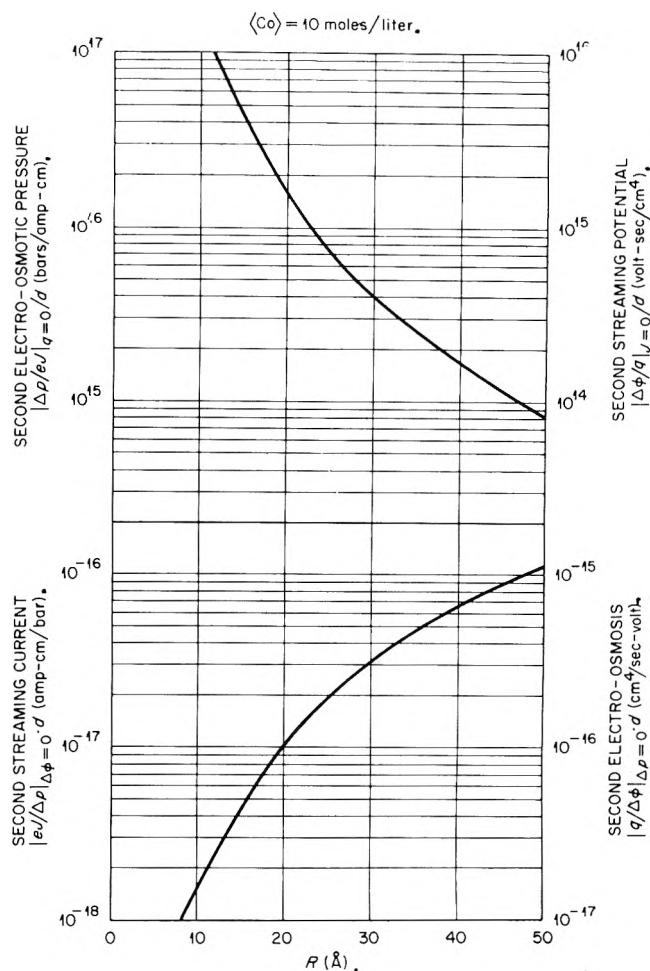


Fig. 1b.—Various electrokinetic quantities plotted against the capillary radius R in the case of constant fixed charge density (c_0).

$$\begin{aligned} \mathfrak{D}_1 &= 2 \times 10^{-5} \text{ cm.}^2 \text{ sec.}^{-1} \\ T &= 15^\circ \\ \eta &= 0.01 \text{ g. cm.}^{-1} \text{ sec.}^{-1} \\ w &= 0 \end{aligned} \tag{26}$$

The radii have been limited to values $\leq 50 \text{ \AA}$. because this is the region in which one must work to achieve good exclusion ($\langle c_2 \rangle/c < 10\%$) with reservoir electrolyte concentrations ≥ 0.02 mole/l. (such as are of interest in the desalination of brackish waters).⁹ w has been taken to be zero for simplicity, but extensive numerical calculations have shown that when w varies in the range from 0 to 30 \AA ,³ the various electrokinetic quantities change only by amounts of the order of 20%.

In Fig. 2 velocity profiles for $R = 10, 25,$ and 50 \AA . are shown which correspond, respectively, to the situations $J = 0$ and $\Delta p = 0$, *i.e.*, to the processes of reverse osmosis and electro dialysis. In Table II the quantities $L_{11}d, L_{12}d,$ and $L_{22}d$ for the same three radii are given.

An average fixed charge concentration $\langle c_0 \rangle$ of 10 moles/l. in a microcapillary with a radius R_0 of 10 \AA . can be produced by a surface charge density $\sigma = (1/2)R_0 \langle c_0 \rangle$ of about 3×10^{14} monovalent ions per cm.^2 . If this charge density is kept fixed, in a capillary with a 25 \AA . radius the average fixed charge concentration will only be 4 moles/l. The data in Fig. 1 do not apply to such a microcapillary. However, when $w = 0$, these data can be interpreted as follows.

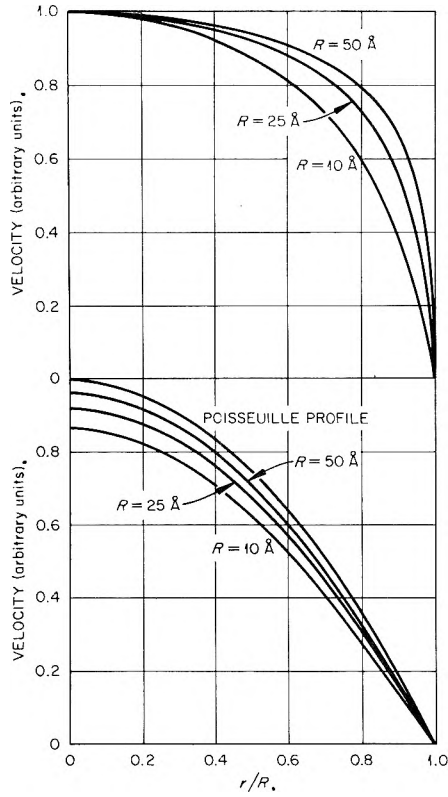


Fig. 2.—Velocity profiles in reverse osmosis (lower figure: $J = 0$) and electroosmosis (upper figure: $\Delta p = 0$).

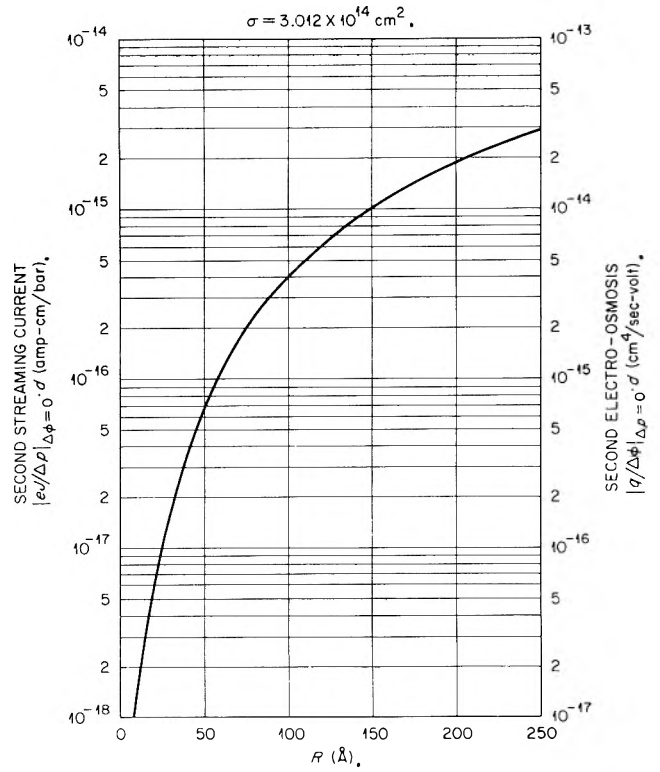


Fig. 3b.—Various electrokinetic quantities plotted against the capillary radius R in the case of constant surface charge density σ .

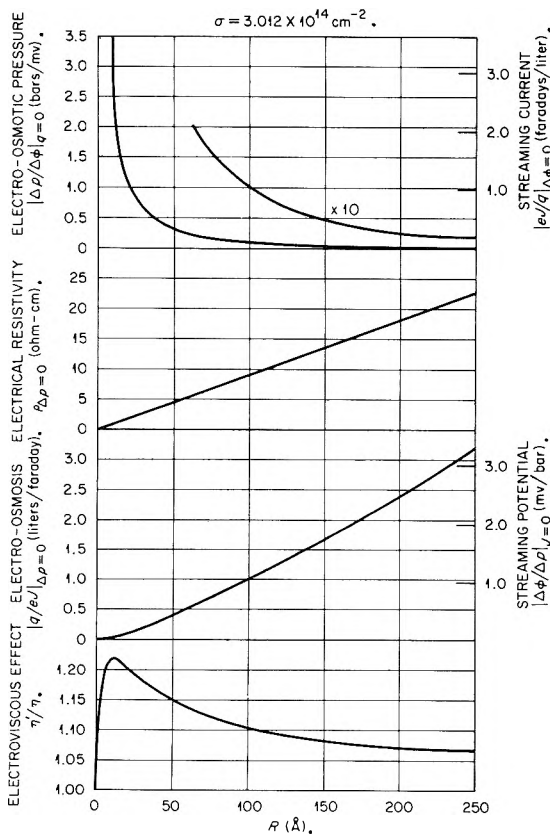


Fig. 3a.—Various electrokinetic quantities plotted against the capillary radius R in the case of constant surface charge density σ .

Let us consider one series of capillaries with radii denoted by R' for which σ is held fixed and a second series with radii denoted by R for which $\langle c_0 \rangle$ is held fixed. Let $\langle c_0 \rangle = 2\sigma/R_0$. If $R' = R^2/R_0$, then

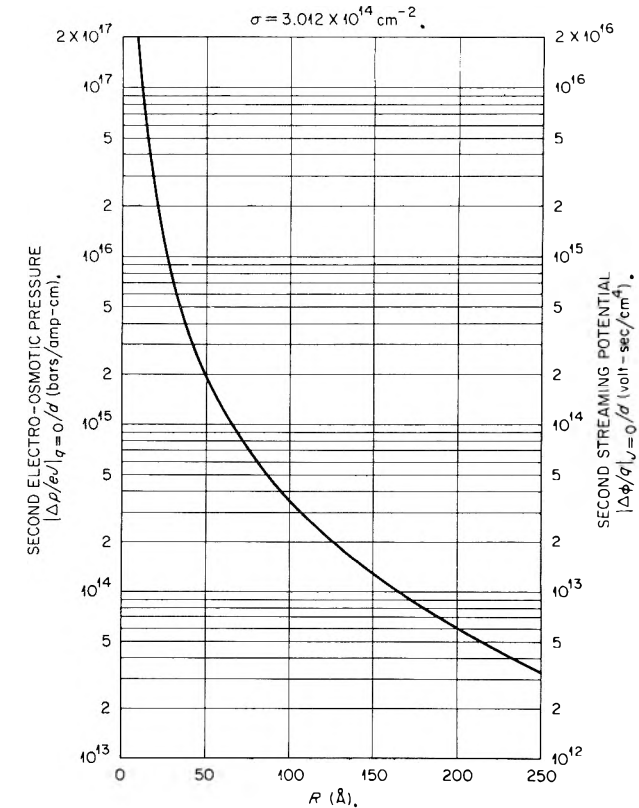


Fig. 3c.—Various electrokinetic quantities plotted against the capillary radius R in the case of constant surface charge density σ .

$$\xi_{R'}^2 = \frac{e^2 \langle c_0 \rangle}{kT\epsilon} R^2 = \frac{e^2}{kT\epsilon} \frac{2\sigma}{R_0} R' R_0 = \frac{e^2}{kT\epsilon} \frac{2\sigma}{R'} R'^2 = \xi_R'^2 \quad (27)$$

since in the capillaries with fixed surface charge σ , the average fixed ion concentration is $2\sigma/R'$. Since the constant $\eta\kappa^2\mathcal{D}_1/2\langle c_0 \rangle$ is actually independent of $\langle c_0 \rangle$, it follows from eq. 25, for example, that the same value of L_{22} which refers to a radius R and an average fixed ion concentration $\langle c_0 \rangle$ also refers to a radius $R' = R^2/R_0$ and a fixed surface ion density of $\sigma = R_0\langle c_0 \rangle/2$. This equivalence is only one of several which may be summarized as follows. The quantities shown below in the first column of Table III refer to fixed $\langle c_0 \rangle$. If they are multiplied by the quantities next to them in column 2, corresponding values are obtained which refer to fixed σ , σ and $\langle c_0 \rangle$ being related by $\langle c_0 \rangle = 2\sigma/R_0$. Finally,

$$\xi'^2 = \frac{e^2}{kT\epsilon} \frac{2\sigma}{R'} r'^2 = \frac{e^2\langle c_0 \rangle}{kT\epsilon} R^2 \left(\frac{r'}{R'}\right)^2 = \xi R^2 \left(\frac{r'}{R'}\right)^2 \quad (28)$$

so that when plotted against the fractional radius the velocity profiles of Fig. 2 apply.

Shown in Fig. 3a-c are the data of Fig. 1 replotted to

TABLE II

THE COEFFICIENTS L_{11d} , L_{12d} , L_{22d} CALCULATED FROM EQ. 19, 21, AND 25 FOR THREE RADII AND THE CONSTANTS SHOWN IN EQ. 26

R (Å.)	$-L_{11d}$ (g. ⁻¹ cm. ³ sec.)	$-L_{12d}$ (g. ⁻¹ cm. ² sec.)	$-L_{22d}$ (g. ⁻¹ cm. ⁻¹ sec.)
10	3.927×10^{-27}	9.388×10^{-6}	1.244×10^{17}
25	1.534×10^{-25}	1.236×10^{-4}	8.327×10^{17}
50	2.454×10^{-24}	7.205×10^{-4}	3.391×10^{18}

TABLE III

EQUIVALENCE OF THE CASE OF FIXED $\langle c_0 \rangle$ AND THE CASE OF FIXED σ WHEN $w = 0$.

The quantities in the first column refer to fixed $\langle c_0 \rangle$. If they are multiplied by the ratios next to them in the second column, corresponding values are obtained which refer to fixed σ , σ and $\langle c_0 \rangle$ being related by $\langle c_0 \rangle = 2\sigma/R_0$.

R	R/R_0
L_{11}	$(R/R_0)^4$
L_{12}	$(R/R_0)^2$
L_{22}	1
$(eJ/q)_{\Delta\phi=0}$	$(R/R_0)^{-2}$
$(\Delta p/\Delta\phi)_{q=0}$	$(R/R_0)^{-2}$
$(\Delta\phi/\Delta p)_{J=0}$	$(R/R_0)^2$
$(q/eJ)_{\Delta p=0}$	$(R/R_0)^2$
$(eJ/\Delta p)_{\Delta\phi=0}$	$(R/R_0)^2$
$(q/\Delta\phi)_{\Delta p=0}$	$(R/R_0)^2$
$(\Delta p/eJ)_{q=0}$	$(R/R_0)^{-2}$
$(\Delta\phi/q)_{J=0}$	$(R/R_0)^{-2}$
$(q/\Delta p)_{J=0}$	$(R/R_0)^4$
$(\Delta\phi/eJ)_{\Delta p=0}$	1

apply to the case of $\sigma = 3.012 \times 10^{14}$ cm.⁻². In this case, the radii extend to 250 Å., but, as before, only for radii up to 50 Å. can 90% or better exclusion be achieved with electrolyte concentrations $\gtrsim 0.02$ mole/l. For the larger radii smaller values of c are required to produce good exclusion; when $R = 250$ Å., c must not exceed 6×10^{-4} mole/l. in order to have $\langle c_2 \rangle/c < 10\%$.

6. Reservoirs with Unequal Electrolyte Concentrations.—In case the electrolyte concentrations in the two reservoirs are not equal, axial concentration gradients appear along the length of the capillary. The set of eq. 16 is then no longer adequate to describe the flow of counter-ions and water. However, if the concentration gradients are not too large, linear phenomenological equations can be written down whose coefficients are uniquely determined by the L_{ik} already calculated.

If we again ignore the presence of co-ions, the entropy production in the capillary can be written^{7b}

$$-T(dS/dt) = J_w\Delta\mu_3 + J\Delta\bar{\mu}_1 \quad (29)$$

where as before J is the total counter-ion current, J_w is the total current of water molecules, $\Delta\bar{\mu}_1$ is the difference in the electrochemical potential per counter-ion between the ends of the capillary, and $\Delta\mu_3$ is the difference in the chemical potential per water molecule between the ends of the capillary. Appropriate linear laws relating the flows and forces are

$$J_w = K_{11}\Delta\mu_3 + K_{12}\Delta\bar{\mu}_1 \quad (30a)$$

$$J = K_{21}\Delta\mu_3 + K_{22}\Delta\bar{\mu}_1 \quad (30b)$$

$$K_{12} = K_{21} \quad (30c)$$

In the case of *identical* reservoirs

$$\Delta\bar{\mu}_1 = w_1\Delta p + z_1e\Delta\phi \quad (31a)$$

$$\Delta\mu_3 = w_3\Delta p \quad (31b)$$

If these equations are substituted into eq. 30, the latter becomes identical in content with eq. 16. If we note that

$$q = w_1J + w_3J_w \quad (32)$$

we can determine the K_{ij} in terms of the L_{ij} . The result of this determination is

$$K_{11} = (L_{11} - 2w_1L_{12} + w_1^2L_{22})/w_3^2 \quad (33a)$$

$$K_{12} = K_{21} = (L_{12} - w_1L_{22})/w_3 \quad (33b)$$

$$K_{22} = L_{22} \quad (33c)$$

SOLUTIONS OF N-SUBSTITUTED AMINO ACIDS. I. THE SOLUBILITY OF N,N-DIETHYL- β -AMINOPROPIONIC ACID IN BENZENE

BY CHARLES P. NASH, EARL L. PYE, AND DON B. COOK

Department of Chemistry, University of California, Davis, California

Received January 23, 1963

The two-component system N,N-diethyl- β -aminopropionic acid-benzene is characterized by gross positive deviations from Raoult's law and by an unusually large temperature coefficient of the solubility of the solid. These results can be explained by considering a model in which substantial aggregation of the dipolar ion tautomer is presumed to occur.

Introduction

It has been suggested recently by Barrow,¹ on the basis of infrared spectroscopic evidence, that nitrogen-substituted β -amino acids in solutions of low dielectric constant exist principally as chelated monomers having two tautomeric forms—a hydrogen-bonded complex and a dipolar ion species. Since most of Barrow's studies were made in solvents which are well known to form hydrogen bonds, we have elected to examine the behavior of amino acids in more inert media. In this paper we report the results of solubility and ebullioscopic studies, as well as infrared spectroscopic investigations, of benzene solutions of N,N-diethyl- β -aminopropionic acid. For the sake of brevity we shall henceforth refer to this compound as N,N-diethyl- β -alanine, or more simply, NDBA.

Experimental

N,N-Diethyl- β -alanine was synthesized by first treating ethyl acrylate with diethylamine. The resulting ester was hydrolyzed in a large excess of distilled water to obtain the desired free acid, m.p. 81–82°, in 65% over-all yield.

Anal. Calcd. for C₇H₁₅O₂N: C, 58.0; H, 10.4; N, 9.6. Found: C, 57.8; H, 10.2; N, 9.6.

Eastman "Spectro Grade" benzene was either distilled from phosphorus pentoxide as required or was distilled from phosphorus pentoxide and stored over sodium ribbon. Identical solubilities were obtained with solvents treated by either method. Eastman White Label biphenyl was recrystallized from 90% methanol-water mixtures, m.p. 69–70°.

A number of years ago Bowman² reported that benzene was a suitable recrystallizing solvent for a similar compound, N,N-diethylglycine. Accordingly we attempted to recrystallize NDBA from benzene solution and thereby first noted a number of the characteristics of this system which prompted the detailed investigations reported herein.

The solubility of NDBA in benzene was studied in two ways. For the more concentrated solutions we employed a modification of the synthetic method,³ in which weighed samples of NDBA and benzene were sealed into tubes, attached to a rocker arm, and immersed in a temperature bath. The temperature of the bath was increased at a rate of about 1° in 30–40 min. The bath temperature at which the last portion of solid phase disappeared was taken to be the solubility temperature. In all cases the compositions were corrected for vaporization of the benzene. In order to assure that no appreciable thermal lag was present, we verified the reported melting temperature of pure biphenyl in an experiment completely similar to our solubility determinations.

In the dilute solution region the solubility was obtained by equilibrating a large amount of solid with a large amount of solvent in a bath held to within 0.05° of the desired temperature for 2–5 days. Weighed 10–50-ml. portions of the solutions were withdrawn through a filter and the solvent was stripped using a rotary film evaporator until a constant weight of residue was achieved. The melting point of the residue was also measured

and used as a criterion of purity. In the intermediate region of the solubility curve satisfactory agreement between solubilities determined by the two methods was obtained.

Infrared spectra of solid NDBA were taken on potassium bromide pellets of the material. In addition, molten NDBA was spread thinly on sodium chloride blocks and the spectra of the solidified films were recorded. We also have examined the spectra of various solutions of NDBA in benzene at various temperatures. Cell temperatures were monitored with a copper-constantan thermocouple taped into a small well drilled into one of the sodium chloride windows out of the beam. All infrared spectra were taken using the double beam mode of a Beckman Model IR-4 spectrophotometer equipped with sodium chloride optics.

The boiling point elevations of benzene solutions of NDBA or biphenyl were measured by using a specially designed differential ebulliometer⁴ operated at reduced pressure. The principal innovations were the introduction of a magnetic stirring bar immediately below the electrical heater in the boiler chamber and a device for dropping shatterable bulbs containing weighed samples of solute into the solvent without opening the system. The first of these modifications proved to be particularly effective in minimizing superheating and bumping.

In order to obtain the difference between the boiling and condensation temperatures, the two halves of a 10-junction copper-constantan thermel were placed in the two wells of the apparatus. To observe the approach to thermal equilibrium, the thermopile output was suitably amplified and displayed on a 10-mv. recorder. The equilibrium potential difference was measured with a Leeds and Northrup Type K potentiometer.

Results

The solubility of NDBA in benzene as a function of inverse temperature is presented in Fig. 1. Here we have plotted the data in the conventional semilogarithmic fashion so as to emphasize the remarkable behavior of this system. We have included in Fig. 1 two reference lines whose slopes represent the temperature dependence of the ideal solubility of solids having heats of fusion of 10 and 50 kcal./mole. It is evident from the sigmoid shape of the solubility curve that NDBA-benzene solutions are far from ideal. The most noteworthy feature is the unusually large temperature coefficient of solubility in the 10⁻¹–10⁻² mole fraction region.

Further evidence for gross deviations from ideality in this system is provided by the data in Fig. 2. Here we have plotted the boiling point elevation, ΔT_B , (expressed in terms of the thermopile output in microvolts) against the mole fraction of either biphenyl or NDBA. Mole fractions were computed on the basis of the monomeric molecular weights of the solutes.

At temperatures between 45 and 50°, benzene-biphenyl solutions are virtually ideal up to a solute mole fraction of ~ 0.1 .⁵ Since our experiments were carried out at an applied pressure such that pure ben-

(1) G. M. Barrow, *J. Am. Chem. Soc.*, **80**, 86 (1958).

(2) R. E. Bowman, *J. Chem. Soc.*, 1346 (1950).

(3) R. D. Vold and M. J. Vold in A. Weissberger, Ed., "Technique of Organic Chemistry," 2nd Ed., Vol. I, Interscience Publishers, Inc., New York, N. Y., 1949, p. 316.

(4) W. Swietoslawski, ref. 3, p. 118.

(5) Activity coefficients are tabulated in E. A. Guggenheim, "Mixtures," Oxford University Press, London, 1952, pp. 236–238.

zene boiled at 47°, a plot of ΔT_B against mole fraction for biphenyl should be linear. This expectation is confirmed by the results in Fig. 2. Indeed, the slope of the line joining the biphenyl points is within 5% of the theoretical one which can be calculated from the known heat of vaporization of benzene and the temperature coefficient of e.m.f. for the (uncalibrated) thermocouples used.

The boiling point elevation of the NDBA solutions differs markedly from ideal solution behavior. At a "calculated" mole fraction of 0.1, ΔT_B is too small by a factor of seven. These results immediately suggest that NDBA solutions might be amenable to interpretation on the basis of a self-association theory, for it is known that binary solutions in which one component is associated exhibit positive deviations from Raoult's law.⁶

Infrared spectroscopic results are particularly useful in establishing the minimum degree of complexity which must be included in a theoretical model. At room temperature the infrared spectra of potassium bromide pellets containing 0.1–0.2% solid amino acid show a single sharp band in the carbonyl–carboxylate region at 1595 cm^{-1} . As will be shown below, an absorption at this frequency is consistent with the zwitterion form of the molecule. As the pellet was heated a new peak at 1725 cm^{-1} appeared at about 50°. As the temperature was increased to 63° the intensity of the new peak increased markedly. Of the two, however, the 1595 cm^{-1} peak remained the more intense. The pellet was then placed in a desiccator at room temperature for 15 hr. At the end of this period only a faint 1725 cm^{-1} peak was evident in the spectrum. This entire procedure could be carried out repeatedly.

A sequence of operations similar to the above was also carried out using amino acid films supported on sodium chloride plates in order to assure that the high-pressure pelleting process does not alter the state of the solid amino acid. The results of our experiments on these films confirm our findings on the pelleted material.

We infer from these experiments that below about 50° solid NDBA exists principally, if not entirely, in the form of a dipolar ion species. Above 50°, however, a substantial fraction of the molecules probably exist in an uncharged form. An absorption at 1725 cm^{-1} is consistent with a carbonyl group rather than a carboxylate ion.

To confirm our frequency assignments, infrared spectra of potassium bromide pellets of the hydrochloride of NDBA and the sodium salt of NDBA were also taken. In agreement with expectation we find for the hydrochloride an intense absorption at 1730 cm^{-1} with only a small shoulder at 1640 cm^{-1} . In the sodium salt we observe a strong band at 1575 cm^{-1} and there is no evidence for absorption at a higher frequency.

The infrared spectra of supersaturated solutions of NDBA in benzene undergo striking changes as the concentration is varied. It should be emphasized that these supersaturated solutions are stable to a remarkable degree to both thermal and mechanical shock. In very dilute solution ($N_2^a < 10^{-3}$)⁷ only a

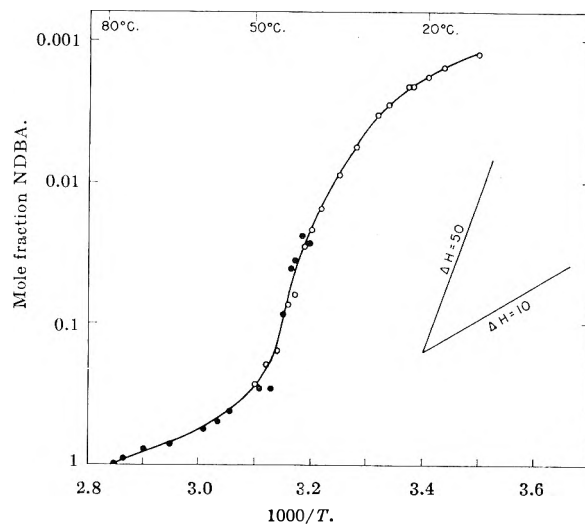


Fig. 1.—Temperature dependence of the solubility of NDBA in benzene: ●, synthetic method; ○, saturation method.

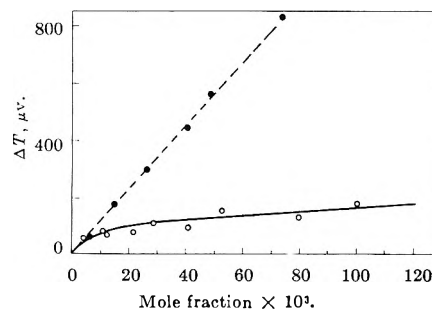


Fig. 2.—Boiling point elevations of benzene solutions of biphenyl (●) and NDBA (○).

single sharp peak appears in the carbonyl–carboxylate region at 1745 cm^{-1} . In very concentrated solutions ($N_2^a \sim 10^{-1}$) two peaks appear at 1720 and 1600 cm^{-1} , the latter being the more intense. By making a series of measurements in the same cell it was possible to investigate in a semiquantitative fashion the way in which the intensities of these two bands varied with concentration.

The usual difficulties encountered in obtaining meaningful absorbances in the infrared region also occur in the present system. As the concentration of amino acid is increased the general opacity of the sample increases so that only ~50% of the incident light is transmitted by the more concentrated solutions, even in regions where no "absorption peaks" are observed. The absorbances are therefore uncertain by at least the uncertainty in the position of the base line, which undergoes a gradual increase in transmittance as the wave length is decreased.

A further complication arises in that the spectrum of solid NDBA suggests that the carboxylate absorption may still be significant in the region where the carbonyl maximum occurs. From the spectrum of the amino acid hydrochloride it appears, however, that the carbonyl peak does not influence the intensity at the carboxylate maximum.

In Fig. 3 we have plotted the absorbance of the carbonyl peak as a function of concentration. We have indicated in the figure realistic error limits for the absorbances based on the considerations mentioned above. Up to a mole fraction of 0.1 the absorbance of the carboxylate peak would be represented on this

(6) I. Prigogine and R. Defay, "Chemical Thermodynamics," Longmans Green and Co., New York, N. Y., 1954, p. 414.

(7) This notation is explained in the Discussion section.

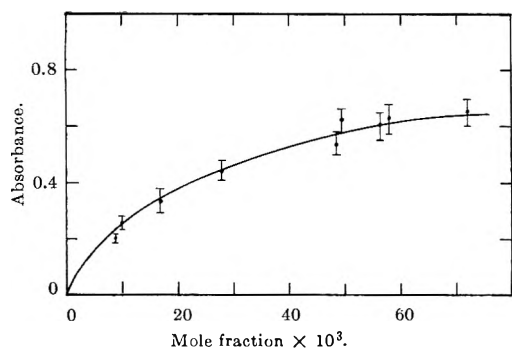


Fig. 3.—Concentration dependence of the intensity of the carbonyl infrared spectral peak of NDBA in benzene solution.

figure by a straight line through the origin which intersects the carbonyl curve at $N_2^a \approx 0.06$.

Discussion

The spectroscopic and colligative results indicate that a working model of NDBA–benzene solutions must include at the very minimum a tautomeric equilibrium between an uncharged form and a dipolar-ion form of NDBA, and some means for the formation of rather large aggregates of solute molecules.

Although the rapidly increasing solubility function in Fig. 1 bears a superficial resemblance to the behavior of systems in which micelle formation occurs, it appears probable that micellization is not taking place in the present instance. When the data pertaining to the several systems studied by Tartar and Wright,⁸ for example, are plotted on the same scale as Fig. 1, the change in slope occurring at the critical micelle concentration is much more abrupt than the rather rounded shape we observe in the NDBA–benzene system.

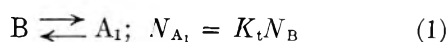
For this reason it seems more plausible to interpret the present solutions in terms of a series of simultaneous equilibria. The general type of treatment we propose has been applied to less complicated systems by Davies and Thomas,⁹ Redlich and Kister,¹⁰ and earlier workers cited in these references.

We treat first the simplest model which, in a qualitative sense, fits the experimental facts, namely, a tautomeric equilibrium superimposed on an infinite sequence of electrostatically-bound zwitterion clusters. This model then is easily modified to include dimerization of the uncharged carboxylic acid, which modification yields results in fair agreement with experiment.

In what follows, we assume that the composite solution is ideal. That is, the vapor pressure of the solvent is proportional to its *real* mole fraction. For convenience we here define the symbols

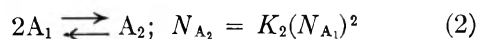
- N_2^a = apparent solute mole fraction—the abscissa in Fig. 2
- N_2^r = real solute mole fraction—that which one calculates from the colligative properties of the soln.
- N_1 = real solvent mole fraction
- N_{A_1} = real mole fraction of monomeric dipolar NDBA
- N_B = real mole fraction of “uncharged” monomeric NDBA
- N_{A_n} = real mole fraction of an n -mer of dipolar NDBA

The tautomeric equilibrium can be written as



The first two polymerization equilibria can be described by the equations

- (8) H. V. Tartar and K. A. Wright, *J. Am. Chem. Soc.*, **61**, 539 (1939).
- (9) M. Davies and D. K. Thomas, *J. Phys. Chem.*, **60**, 763 (1956).
- (10) O. Redlich and A. T. Kister, *J. Chem. Phys.*, **15**, 849 (1946).



In the general case



If we now assume that K_n is a constant independent of n , eq. 1 and 4 combine to yield the simple expression

$$N_{A_n} = K_p^{n-1} (K_t N_B)^n \quad (5)$$

where K_p is the polymerization equilibrium constant. A slightly more sophisticated treatment would recognize that the constant for reaction 2 would be smaller than that for the general reaction 4 owing to the greater relative decrease in the entropy.¹¹

The real mole fraction of solute is given by

$$N_2^r = N_B + \sum_{n \geq 1} N_{A_n} \quad (6)$$

By combining eq. 5 and 6, and by assuming $K_p K_t N_B < 1$, we find, on summing the series

$$\frac{N_2^r}{N_B} = 1 + \frac{K_t}{1 - K_p K_t N_B} \quad (7)$$

The apparent mole fraction of the solute is given by

$$N_2^a = \frac{N_B + \sum_{n \geq 1} n N_{A_n}}{N_1 + N_B + \sum_{n \geq 1} n N_{A_n}} \quad (8)$$

Again, by inserting eq. 5 into eq. 8 (with the assumption that $K_t K_p N_B < 1$) and summing the resulting series

$$N_2^a = [1 + K_t / (1 - K_p K_t N_B)^2] [1 + K_t / (1 - K_p K_t N_B)^2 + N_1 / N_B]^{-1} \quad (9)$$

or, from eq. 7

$$N_2^a = [N_B^2 + (N_2^r - N_B)^2 / K_t] [N_1 N_B + N_B^2 + (N_2^r - N_B)^2 / K_t]^{-1} \quad (10)$$

If molal concentrations are used the formal development is along parallel lines except that the parameter K_p is numerically different (we call the new value K_c) and no denominator is necessary in eq. 8. The molal analogs of eq. 7 and 10 are

$$\frac{M_2^r}{M_B} = 1 + \frac{K_t}{(1 - K_t K_c M_B)} \quad (11)$$

and

$$\frac{M_2^a}{M_B} = 1 + \frac{K_t}{(1 - K_t K_c M_B)^2} \quad (12)$$

Provided that molal concentrations units are employed, it is a simple matter to modify the development to include also dimerization of the nonpolar tautomer B. The starting equations become

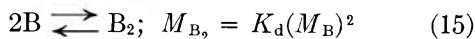
$$M_2^r = M_B + K_d (M_B)^2 + \sum_{n \geq 1} M_{A_n} \quad (13)$$

and

(11) A statistical treatment showing the necessity for using at least two constants for successive association equilibria has been given by L. Sarolea-Mathot, *Trans. Faraday Soc.*, **49**, 8 (1953).

$$M_2^a = M_B + 2K_d(M_B)^2 + \sum_{n \geq 1} nM_{A_n} \quad (14)$$

where K_d is the equilibrium constant for the dimerization of B



With the substitutions and assumptions used above, save that K_p is everywhere replaced by K_c , eq. 14 and 15 reduce to

$$M_2^r = M_B + K_d(M_B)^2 + \frac{K_t M_E}{(1 - K_t K_c M_B)} \quad (16)$$

and

$$M_2^a = M_B + 2K_d(M_B)^2 + \frac{K_t M_E}{(1 - K_t K_c M_B)^2} \quad (17)$$

The point of the entire preceding development is that in eq. 7 and 10, or 11 and 12, or 16 and 17 we should have a complete description of the system in terms of our idealized tautomerization-polymerization model, with or without dimerization of the "uncharged" carboxylic acid.

The equations can be tested in several ways. One could, for example, attempt a two-parameter fit of eq. 7 and 10 to the ebullioscopic data in Fig. 2. Owing to the sensitive nature of these equations to small variations in N_B , no unique fit can be obtained. Rather, constants in the ranges $0.013 < K_t < 0.3$ and $7700 > K_p > 700$ yield a fair representation of the data. Alternatively, a fit may be sought *via* the spectroscopic intensities from Fig. 3.

If it is assumed that the plotted absorbance is proportional to the molality of the B tautomer, then three absorbances yield three molalities whose relative magnitudes are known. In eq. 12 three relative magnitudes of the quantities M_2^a/M_B and $K_t K_c M_B$ result. If these three equations are divided one into another, a pair of independent equations emerges. When the ratio of this pair of equations is taken, the parameter K_t is eliminated and a final equation in the single variable $K_t K_c M_B^0$ results, where M_B^0 is the molality of the B tautomer in the mixture chosen as a reference.

If a solution to this last auxiliary equation can be found, it is possible to return to one of the pair of intermediate equations and determine K_t unambiguously. The entire procedure is extremely sensitive to the actual magnitudes of the absorbances which are used, but a reasonably good value of $K_t \approx 0.25$ can be obtained by this method from the absorbance curve shown in Fig. 3. Although this value lies within the range obtained by fitting the ebullioscopic data, the spectroscopic absorbances also can be used to obtain unambiguous values for both M_B^0 and K_c (or K_p). The spectroscopic value of $K_p \approx 200$ is outside the indicated range by an appreciable factor, and the theoretical boiling-point elevation curve constructed from eq. 7 lies above the experimental one by a factor of three at $N_2^a = 0.06$. In physical terms the simple model predicts far too many particles in solution.

When appreciable dimerization of the uncharged B form is introduced the agreement between theory and experiment is greatly improved. That dimerization should occur seems reasonable in view of the results

of Maryott, Hobbs, and Gross,¹² who cite values for K_d in eq. 15 of about 10^3 kg. mole⁻¹ for cyclic dimerization of aliphatic carboxylic acids in benzene solution.

The first two terms on the right side of eq. 17 represent essentially the total number-density of the non-polar form in solution, and hence their sum, in the revised model, is proportional to the absorbances in Fig. 3. If it is assumed that in the more concentrated solutions the molality of the B dimer can be approximated by one-half the total apparent molality of the B form, then mathematical procedures similar to those just described can be applied to eq. 16 to obtain values of the constants $K_t/(2K_d)^{1/2}$ and K_c . It is noteworthy that this model is still effectively a two-parameter one, since the ratio of two equilibrium constants appears in the working equation. All one need assume to achieve this simplification is that K_d is large.

If K_d is assumed to be 10^3 , we find $K_t = 1$ and $K_c = 65$ ($K_p = 900$). In addition, eq. 17 can be used to construct a theoretical boiling-point elevation curve which now exceeds the experimental one by only 20% at $N_2^a = 0.06$.

It is doubtful whether a further refinement of the model including dimerization is worthwhile at this stage. First, the spectroscopic data from which the constants were evaluated are not of a high order of accuracy. It is probable that small variations in the magnitudes of the absorbances employed in the sensitive equations could improve the agreement by a few per cent. In addition, we expect that some implicit nonideality is also present in the system. Solutions of polar molecules in benzene or carbon tetrachloride almost invariably show positive deviations from Raoult's law,¹³ and the discrepancy between theory and experiment in the present instance is also in this direction. Indeed, nonideality must exist in several of the systems we are currently investigating (*e.g.*, NDBA-carbon tetrachloride) which form two liquid phases, since phase separation cannot be exhibited by an ideal solution.¹⁴

It is possible to deduce from the constants cited above that at $N_2^a = 0.1$ the zwitterionic aggregates contain, on the average, about 12 monomeric units. As regards the shape of the aggregates, a Cortauld model of the monomer in question reveals that a cyclic form is readily accessible, whereby the tautomeric equilibrium can be accomplished by a unimolecular internal proton transfer. The resulting cyclic zwitterion has virtually a hydrocarbon perimeter, and hence it seems plausible that aggregation would occur by placing the charges at the various vertices of a polyhedron to yield a nearly spherical aggregate with a low net dipole moment and effectively a hydrocarbon exterior.

Light-scattering techniques might be useful in testing both this point and another aspect of the model. In its present form, the model predicts a rather broad distribution of polymer sizes, and hence the weight-average molecular weight obtained from light-scattering measurements should exceed the number-average

(12) A. A. Maryott, M. E. Hobbs, and P. M. Gross, *J. Am. Chem. Soc.*, **71**, 1671 (1949).

(13) Some pertinent results are summarized by J. S. Rowlinson, "Liquids and Liquid Mixtures," Academic Press Inc., New York, N. Y., 1959, pp. 173-182.

(14) I. Prigogine and R. Defay, *ref. 6*, pp. 518-519.

value cited above by an appreciable factor. Experiments of this type are currently in progress.

It is a simple and straightforward procedure to obtain the total derivative of eq. 17 with respect to inverse temperature, the result of which may be expressed in the form

$$\frac{d \ln M_2^a}{d(1/T)} - \frac{d \ln M_B}{d(1/T)} = \frac{2(M_B)^2}{M_2^a} \left\{ \frac{K_t^2 K_c}{(1 - K_t K_c M_B)^3} \times \left[\frac{d \ln K_t}{d(1/T)} + \frac{d \ln K_c}{d(1/T)} + \frac{d \ln M_B}{d(1/T)} \right] + K_d \left[\frac{d \ln K_d}{d(1/T)} + \frac{d \ln M_B}{d(1/T)} - \frac{d \ln K_t}{d(1/T)} \right] \right\} + \left(1 - \frac{M_B}{M_2^a} \right) \frac{d \ln K_t}{d(1/T)} \quad (18)$$

In a qualitative way this equation accounts for the form of the observed solubility curve up to about 50°, where we suspect a change in the nature of the solid phase. In very dilute solutions the entire first term on the right of eq. 18 approaches zero, M_B approaches a sizable fraction of M_2^a , and the limiting slope of the solubility curve then yields an "intrinsic" value for $d \ln M_B/d(1/T)$. As the temperature and solubility increase the factor $2(M_B)^2/M_2^a$ approaches K_d , $K_t K_c M_B$ approaches unity, and the temperature coefficient of M_2^a becomes enormous.

The temperature derivatives of the various equilibrium constants which appear in eq. 18 are of interest for their own sakes. A determination of the enthalpy change for the dimerization equilibrium K_d would confirm or deny the existence of a cyclic dimer, since a value near -8.5 kcal./mole has been well established for this process.^{15,16} The tautomeric equilibrium constant will involve both "chemical" contributions (bond energies) and "electrostatic" contributions (dielectric effects) even if more specific solvation (*e.g.*, hydrogen bonding) does not occur. A determination of K_t and its temperature coefficient in a series of "inert" solvents

would yield data to test theories of dipole-dielectric interactions. Further, by extrapolating ΔH_t to unit dielectric constant one could conceivably eliminate dielectric effects and hence obtain the difference between the energies of the O-H and N-H bonds when they are cleaved heterolytically.

From a theoretical standpoint, a study of the role of "inert" solvents having various dielectric constants on the polymerization equilibrium could prove especially fruitful. Consider an idealized system in which an equilibrium is established by purely electrostatic forces and for which the equilibrium constant K can be written

$$\ln K = \frac{A}{DkT} \quad (19)$$

where A is some factor depending on the configuration of charges, D is the dielectric constant of the medium, and kT has its usual significance. As an example, Kirkwood¹⁷ has shown that the interaction between an ellipsoidal dipolar ion and a real ion is of this form.

By differentiating eq. 19 with respect to inverse temperature we find

$$\frac{d \ln K}{d(1/T)} = KT \left[1 + T \frac{d \ln D}{dT} \right] \quad (20)$$

where the factor involving the dielectric constant is intrinsically negative. Evidently for such a system the equilibrium constant can either increase or decrease with increasing temperature, depending on the magnitude of $d \ln D/d \ln T$. At room temperature solvents such as benzene, carbon tetrachloride, anisole, toluene, and bromoform yield a positive value for $d \ln K/d(1/T)$, whereas for acetonitrile, ethylene chloride, acetone, and ethyl bromide a negative value results. It would be of importance, therefore, to study the effect of temperature on the degree of polymerization of zwitterionic aggregates in these two classes of solvents.

(17) J. G. Kirkwood in E. J. Cohn and J. T. Edsall, "Proteins, Amino Acids and Peptides," Reinhold Publ. Corp., New York, N. Y., 1943, pp. 282-283.

(15) G. Allen and E. F. Caldin, *Trans. Faraday Soc.*, **49**, 895 (1953).

(16) F. T. Wall and F. W. Banes, *J. Am. Chem. Soc.*, **67**, 898 (1945).

ENHANCEMENT OF DIFFUSION-LIMITED RATES OF VAPORIZATION OF METALS

BY E. T. TURKDOGAN, P. GRIEVESON, AND L. S. DARKEN

Edgar C. Bain Laboratory for Fundamental Research, United States Steel Corporation Research Center, Monroeville, Pennsylvania

Received January 31, 1963

On a theoretical basis, it is shown that the rate of vaporization of metals in a stream of a neutral atmosphere should increase with increasing partial pressure of a reacting gas, such as oxygen. Considering the vaporization of a metal in a stream of argon + oxygen, the enhanced vaporization is basically a vaporization-oxidation process involving the counter diffusion of oxygen (or oxidizing species) and metal vapor within the gaseous boundary layer. These interact to form a metal oxide mist in the gas close to the metal-gas interface. As a result of this reaction, the partial pressure of oxygen influences the rate of vaporization of the metal. As the partial pressure of oxygen in the gas stream increases, the thickness of the boundary diffusion layer for metal vapor decreases, resulting in an increased rate of vaporization. At a critical partial pressure of oxygen, the vaporization of the metal is close to the maximum rate obtainable *in vacuo*. When the oxygen pressure exceeds this critical value, the flux of oxygen toward the surface is greater than the counter flux of the metal vapor, and consequently a liquid or a solid oxide layer forms on the metal surface and vaporization practically ceases. The experimental results obtained on the rate of vaporization of copper, nickel, cobalt, iron, manganese, and chromium in argon + oxygen mixtures verify the validity of the above theoretical consideration. Similarly, it is shown that the rate of vaporization of molten silicon into argon can be increased by introducing nitrogen into the stream. In this system, the formation of silicon nitride, by reaction of silicon vapor with nitrogen close to the metal surface, provides a sink for the vapor and gas species; this results in an enhanced rate of vaporization of silicon.

Introduction

Much of the early work on the kinetics of vaporization of metals was confined essentially to the development of the theory of vaporization at reduced pressures. On the other hand, practically no work has been done to discover what possible effects reactive atmospheres can have on the rate of vaporization of metals. It is nevertheless common knowledge that when determining the vapor pressures of metals by the transpiration technique, utmost care has to be taken to ensure that the carrier gas is free of impurities which are likely to react with the metal in the condensed or vapor state. In practice there are many instances where enhanced vaporization is observed under atmospheric pressure. For example, in pyro-metallurgical processes metal-oxide fume is evolved from furnaces at rates much higher than those which can be calculated assuming saturation of the evolved gases with metal vapor.

There are two types of mechanisms responsible for an increased rate of vaporization of metals: a chemical process and a transport process. The chemical process is that involving the formation of volatile metal compounds, *e.g.*, FeCl_3 , WO_3 , SiO , $\text{Fe}(\text{CO})_5$, $\text{Fe}(\text{OH})_2$; in the transport process, which is the subject matter of this paper, enhanced vaporization is brought about by the reaction of the metal vapor with the gas phase very close to the metal-gas interface to form a finely divided condensed phase.

Theory

The effect of a reactive gas on the rate of vaporization of a metal can be considered as a counter flux-transport process. For example, when iron vaporizes in a stream of argon + oxygen, the counter flux of the iron vapor and oxygen is as shown in Fig. 1a. At some short distance from the surface of the metal iron vapor and oxygen react forming an iron oxide mist



where v, g, s, and l indicate vapor, gas, solid, and liquid phases, respectively. For the sake of simplicity, non-stoichiometry in ferrous oxide can be ignored. The formation of an iron oxide, which is in a state of fine sub-

division, in the gas phase provides a sink for the iron vapor and oxygen, resulting in the counter flux of these two gaseous species. When a steady state of counter flux is established under these boundary conditions in an isothermal system, the concentration profiles for iron vapor, C_{Fe} , and oxygen, C_{O} , close to the metal surface will be as shown schematically in Fig. 1b. At a particular distance δ , an iron oxide fog is formed and beyond a particular distance Δ , which is the thickness of the aerodynamic boundary layer, the oxygen partial pressure is considered as being maintained constant; the gas flow within the boundary layer is laminar.

Under the above boundary conditions, by Fick's law, the counter flux of iron vapor and oxygen for a steady state is given by

$$J_{\text{Fe}} = \frac{D_{\text{Fe}}}{\delta RT} (p_{\text{Fe}} - p_{\text{Fe}}') \quad \text{moles/cm.}^2 \text{ sec.} \quad (2)$$

$$J_{\text{O}_2} = - \frac{D_0}{(\Delta - \delta)RT} (p_{\text{O}_2} - p_{\text{O}_2}') \quad \text{moles/cm.}^2 \text{ sec.} \quad (3)$$

where

- D_{Fe} = interdiffusivity of Ar + Fe vapor
- D_0 = interdiffusivity of Ar + O_2
- R = gas constant
- T = temperature in $^\circ\text{K}$.
- p_{Fe} = vapor pressure of iron at $x = 0$
- p_{Fe}' = partial pressure of iron vapor at $x = \delta$
- p_{O_2} = partial pressure of oxygen at $x = \Delta$
- p_{O_2}' = partial pressure of oxygen at $x = \delta$

Since at the distance δ reaction 1 is presumed, the counter flux of iron vapor is twice that of oxygen $J_{\text{Fe}} = -2J_{\text{O}_2}$. Since the partial pressures p_{Fe}' and p_{O_2}' at $x = \delta$ are much lower than the respective values p_{Fe} and p_{O_2} at $x = 0$ and $x = \Delta$ and, furthermore, since the distance δ is much less than Δ , the following simplification can be made

$$J_{\text{Fe}} = -2J_{\text{O}_2} = \frac{2D_0}{\Delta RT} p_{\text{O}_2} \quad \text{moles/cm.}^2 \text{ sec.} \quad (4)$$

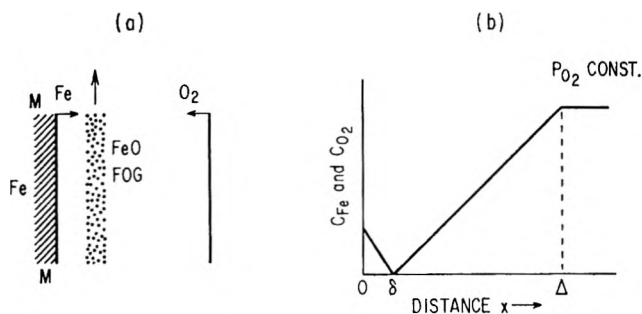


Fig. 1.—Schematic diagram showing the counter flux of iron vapor and oxygen in a neutral atmosphere under isothermal conditions.

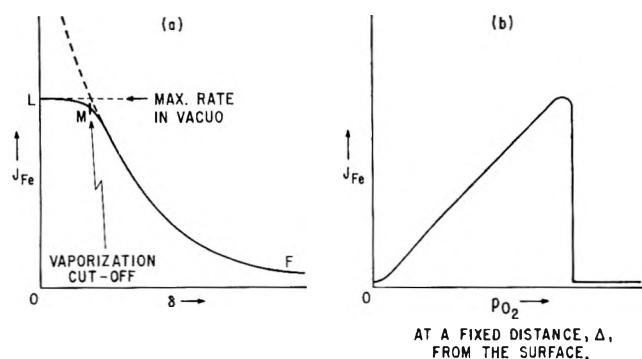


Fig. 2.—Schematic diagram showing the variation of J_{Fe} with δ and p_{O_2} .

$$J_{Fe} = 2h \frac{p_{O_2}}{RT} \quad \text{moles/cm.}^2 \text{ sec.} \quad (5)$$

where $h = D_0/\Delta$ is the average film mass-transfer coefficient for the transport of oxygen through the aerodynamic diffusion boundary layer which is calculable for known flow conditions.

In the above considerations it has been assumed that the formulation of a layer of an iron oxide fog at δ does not interfere with the suggested mechanism; in practice there is sufficient forced or free convection to remove this layer of fog (by vertical motion as shown in Fig. 1a).

According to eq. 5, for a given temperature and film mass-transfer coefficient, the rate of vaporization of iron is expected to increase linearly with increasing partial pressure of oxygen. In other words, increasing oxygen partial pressure decreases the distance δ through which the iron vapor is transported. However, there are two serious restrictions to this mechanism of increasing the rate of evaporation by increasing oxygen partial pressure: (I) maximum free vaporization cannot be exceeded and (II) for a given metal and temperature, there is a minimum oxygen partial pressure below which the metal oxide fog does not form.

(I) **Maximum Rate of Vaporization.**—Under no condition can the rate of evaporation exceed that *in vacuo*. Using the Langmuir equation, the rate of evaporation *in vacuo* is given by

$$J_{max} = \frac{p_i}{\sqrt{2\pi RT M_i}} \quad (6)$$

where p_i and M_i are the vapor pressure of metal (i) and molecular weight of the metal vapor, respectively. When this limiting value of the flux is approached, the form of Fick's law used will not apply. Near this value

of the flux, the vapor in contact with the metal surface is no longer saturated and thus the boundary condition assumed is no longer maintained; also δ approaches the mean free path, thus leading to incipient failure of Fick's law. Therefore, the plot of J_{Fe} against δ will be as shown by curve FML in Fig. 2a. On further increase in oxygen partial pressure at Δ , *i.e.*, decrease of δ , the flux of oxygen toward the surface of the metal is greater than the equivalent counter flux of metal vapor, resulting in the oxidation of the metal surface. In the case of iron, at temperatures above 1400° the surface of the metal will be covered by a layer of liquid iron oxide, when this critical value of δ is reached. Since this iron oxide layer is in contact with iron at one interface and in contact with the oxygen-bearing gas at the other interface, there is a sharp decrease in the vapor pressure of iron across the oxide layer. For example, according to the data of Darken and Gurry,¹ at 1600° the vapor pressure of iron decreases by a factor of about 10^6 when the oxide is in equilibrium with pure oxygen. Consequently, at oxygen partial pressures in the gas stream above the critical value, the surface of the iron is coated with a layer of iron oxide and the rate of vaporization should become vanishingly small.

(II) **Minimum Rate of Vaporization.**—Depending on the oxygen potential of the oxide (fog) formed at δ , there is a minimum critical oxygen partial pressure below which an oxide fog cannot be formed. Although at $x = \delta$, $p_i' < p_i$ for the metal *i* and $p_{O_2}' < p_{O_2}$, for the purpose of estimating approximately this minimum critical value of p_{O_2} from the thermodynamic data, the activity of the metal at δ may be taken as unity. For example, for Fe-FeO the minimum critical pressure is $p_{O_2} = 4.13 \times 10^{-6}$ mm. and for Cu-Cu₂O at 1200°, $p_{O_2} = 1.65 \times 10^{-2}$ mm. Below the critical oxygen partial pressure, the rate of vaporization of the metal in a laminar gas stream is given by the equation

$$J_{min} = \frac{D_i}{\Delta} \frac{p_i}{RT} \quad (7)$$

where the symbols have the same significance as before. This equation is for the condition that gas flow is laminar over the surface of the metal and at $x = \Delta$, $p_i = 0$.

Taking the above two restrictions into account, the relationship between J_{Fe} and p_{O_2} , expected from eq. 5 is shown in Fig. 2b.

Experimental

Qualitative Experiments.—In the initial qualitative experiments, about 20 g. of pure iron was melted by levitation in each of several helium + oxygen mixtures. As seen from the photographs in Fig. 3, the rate of vaporization, enhanced by oxidation, initially increases with increasing partial pressure of oxygen in the atmosphere. The photograph on the extreme right in Fig. 3 was taken when the iron melt was levitated in pure oxygen at 1 atm. pressure; under these conditions iron oxide fumes were not formed and the surface of the melt was coated with molten iron oxide. (The background fog here is due to some fume from the previous experiment which is well illuminated on account of the high emissivity of the liquid iron oxide.) Though qualitative, the results of these initial experiments are in agreement with the theoretical prediction as illustrated in Fig. 2b.

Quantitative Experiments.—The rates of vaporization of liquid copper, nickel, cobalt, iron, manganese, and solid chromium in streams of argon + oxygen mixtures were measured using the apparatus shown schematically in Fig. 4. The transparent silica reaction tube consisted of three parts: gas preheater, vaporization chamber, and condenser.

(1) L. S. Darken and R. W. Gurry, *J. Am. Chem. Soc.*, **68**, 798 (1946).

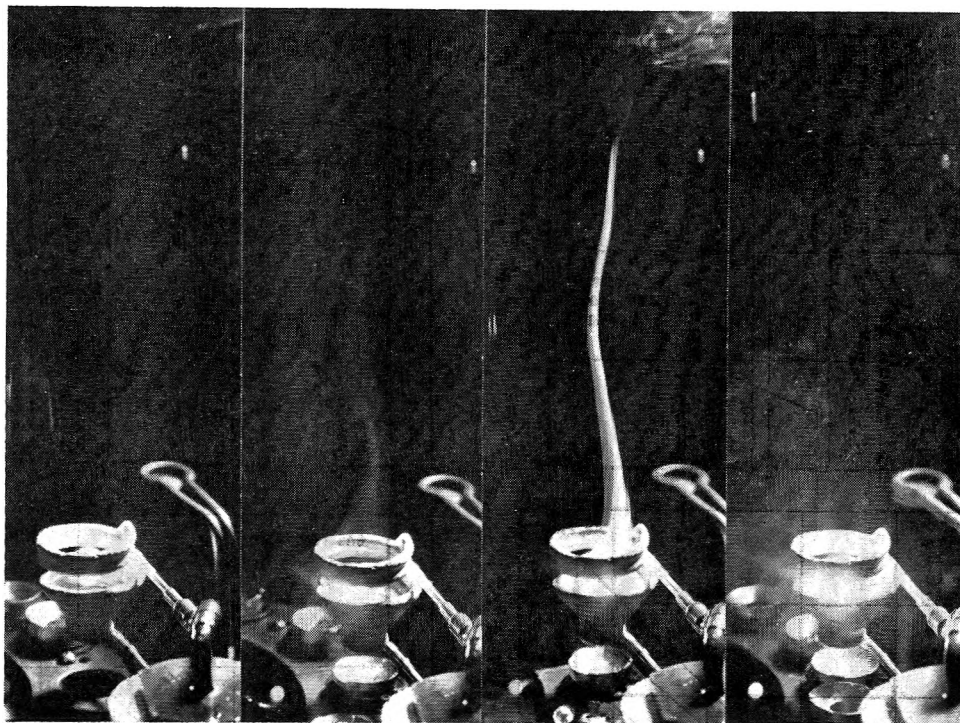


Fig. 3.—Vaporization of levitated iron melts in helium + oxygen atmospheres.

The gas preheater was made of $\frac{5}{8}$ in. diameter closed end recrystallized alumina tube wound with Pt-10% Rh wire.

The vaporization zone is shown in Fig. 4 on an enlarged scale and requires no further description, except to point out that care was taken to keep the surface of the melt almost level with the edge of the alumina boat so that the flow of gas over the surface of the melt was laminar. The alumina boat was separated from the silica reaction tube by a layer of alumina powder about $\frac{1}{4}$ in. deep to cut down heat losses from the boat and to reduce the temperature gradient within the melt. The metal sample was heated by an induction coil and the temperature of the sample was maintained within $\pm 10^\circ$ by manual operation of the input power to the radiofrequency generator.

The colloidal metal oxide fumes were collected in a condenser tube filled with glass wool.

The sequence of events for each experiment was as follows. Before each set of experiments, a dummy experiment was first carried out with the thermocouple placed above the metal sample (through the condenser tube, not shown in Fig. 4) and adjusting the power input to the preheater until the gas and metal were at the same temperature. The vaporization experiments were started by heating the sample to the desired temperature in a stream of pure argon. When the sample reached the required temperature an argon + oxygen mixture of known composition and flow rate was introduced into the reaction vessel. In order to ensure constant temperature of the metal sample, several temperature readings were taken at time intervals depending upon the duration of the experiment. At the end of the experiment the specimen was quenched in a stream of pure argon; the condenser tube was removed and condensate which had deposited on the cool parts of the silica tube was collected and analyzed by the usual analytical techniques. It is estimated that greater than 95% of the condensate was collected for chemical analysis.

Results

In all cases, except that of chromium, the metal was molten and in all cases, except that of iron, the metal oxide formed was solid. In experiments with oxygen partial pressures above the critical values for maximum vaporization, a continuous oxide layer was observed on the surface of the metal after quenching in pure argon. The time of vaporization varied from a few minutes to about 2 hr., depending on the rate of vaporization of the metal. The amount of metal collected in the form of oxides was within the range 0.01 to 0.4 g., except in the case of manganese where 0.3 to 3.0 g. vaporized.

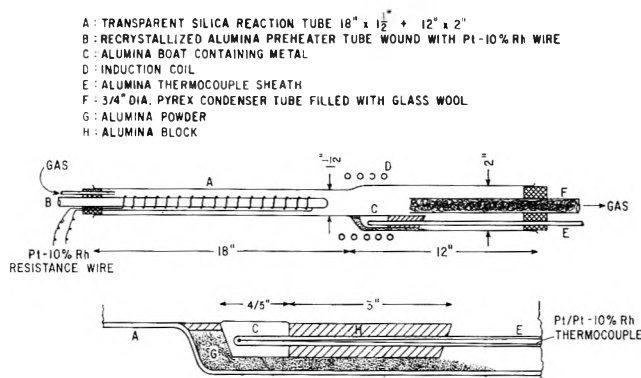


Fig. 4.—Apparatus used to measure rates of vaporization of metals in argon + oxygen mixtures flowing parallel to the surface of the melt.

All the experimental results are given graphically in Fig. 5 where rates of vaporization in $\text{g./cm.}^2 \text{ hr.}$ are plotted against the partial pressure of oxygen in mm. for three rates of gas flow. The experimental data are in complete agreement with the theory, *i.e.*, eq. 5 and Fig. 2b. That is, for a given temperature the rate of vaporization increases with increasing gas flow rate or with increasing partial pressure of oxygen in the atmosphere until a critical value is reached, above which the metal surface is covered with a layer of liquid or solid oxide and vaporization virtually ceases. The maximum rate of vaporization obtained for copper seems to decrease with increasing flow rate; no particular significance is attached to this, since it may well be attributed to experimental difficulties. In the case of manganese, the vaporization cut-off was observed at 95% $\text{O}_2 + 5\% \text{ Ar}$ mixture independent of the rate of gas flow. It may well be that in the case of such a volatile metal, where the oxide "fog" formation is copious, some of the oxide particles contact the metal surface giving rise to a film and hence a premature cut-off of vaporization.

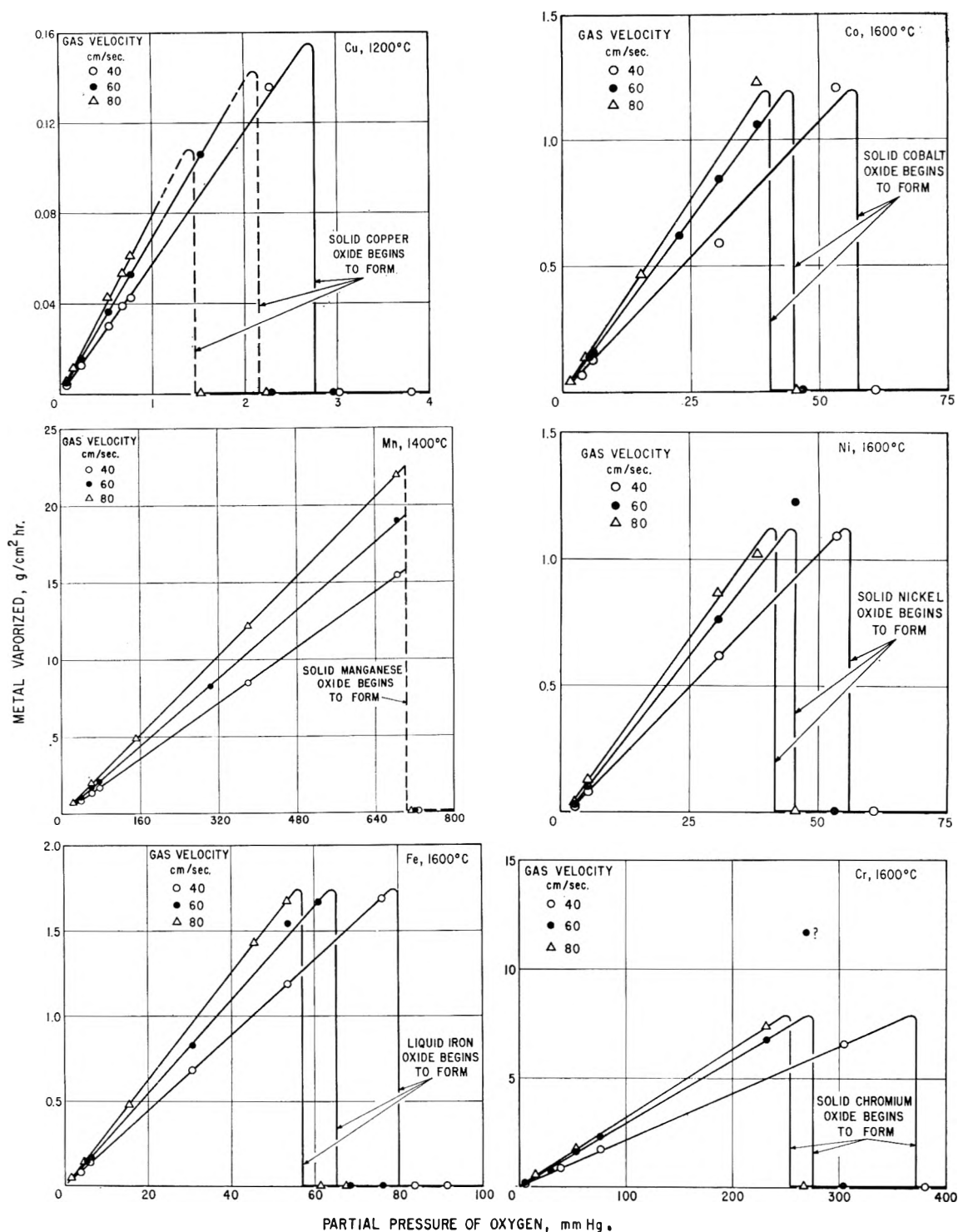


Fig. 5.—Relationship showing the effects of oxygen partial pressure of Ar + O₂ mixtures and the velocity of gas stream on the rate of vaporization of metals.

Discussion

When there is a mass transfer between a condensed phase and a gas stream there is a velocity and a concentration profile near the interface. In order to interpret the results on the rate of vaporization, the film mass-transfer coefficient should be evaluated.

Film Mass-Transfer Coefficient.—For laminar flow of gas over a flat surface the following dimensionless expression can be used (Eckert and Drake²)

$$\frac{hl}{D} = 0.664 (Sc)^{1/2} (Re)^{1/2} \quad (8)$$

where

- h = average film mass-transfer coefficient
- l = length of the surface in the direction of gas flow
- Sc = Schmidt number
- Re = Reynolds number
- D = interdiffusivity

The dimensionless Schmidt and Reynolds numbers are given by

$$Sc = \frac{\nu}{D} \quad (9)$$

$$Re = \frac{vl}{\nu} \quad (10)$$

(2) E. R. G. Eckert and R. M. Drake, "Heat and Mass Transfer," McGraw-Hill Book Co., New York, N. Y., 1959.

where

ν = kinematic viscosity = coefficient of viscosity/density
 v = Uniform linear velocity of gas away from the interface

From the above equations the average film mass-transfer coefficient is given by

$$h = 0.664 \left(\frac{D^4}{\nu} \right)^{1/4} \left(\frac{v}{l} \right)^{1/2}, \text{ length/time} \quad (11)$$

Kinematic Viscosity.—The viscosity coefficients of most common gases have been measured over a wide temperature range; in the present work, the data compiled by Hirschfelder, Bird, and Spotz³ are used. The kinematic viscosities of argon and oxygen are similar, e.g., at 1600° $\nu = 2.92 \text{ cm}^2/\text{sec.}$ for argon and $\nu = 3.36 \text{ cm}^2/\text{sec.}$ for oxygen. For convenience, therefore, an average value is used for all argon + oxygen mixtures.

Interdiffusivity.—In the vaporization-oxidation process already discussed, there are two binary interdiffusivities to be considered: argon + oxygen and argon + metal vapor. Although the self- and interdiffusivities of gases have not been measured at elevated temperatures, the diffusivities of common gases can readily be calculated. As discussed in detail by Chapman and Cowling,⁴ the following expression can be derived as a first approximation of the coefficient of diffusion in binary non-polar gas mixtures from the rigorous kinetic theory of gases developed by Enskog and Chapman for monatomic gases.

$$D_{12} = 0.0018583 \frac{T^{3/2}}{P(\sigma_{12})^2 (\Omega^{1,1*})_{T_{12}^*}} \sqrt{\frac{1}{M_1} + \frac{1}{M_2}} \quad (12)$$

where

D_{12} = interdiffusion coefficient in $\text{cm}^2/\text{sec.}$
 T = temperature in °K.
 P = pressure in atm.
 M_1, M_2 = molecular weights of species 1 and 2
 σ_{12} = collision diameter in Å.; arithmetical mean of collision diameters of species 1 and 2
 $(\Omega^{1,1*})_{T_{12}^*}$ = Dimensionless collision integral for mixtures of 1 and 2 at a given reduced temperature T_{12}^*
 T_{12}^* = $(k/\epsilon)_{12}T$, where k is Boltzmann's constant and ϵ is the maximum energy of attraction, i.e., potential well; $(k/\epsilon)_{12}$ is the geometrical mean of force constants for species 1 and 2

The collision diameter and the collision integral in eq. 12 for the coefficient of diffusion are based on the intermolecular Lennard-Jones (6-12) potential energy function $\varphi(r)$. For spherical and non-polar molecules

$$\varphi(r) = 4\epsilon \left[\left(\frac{\sigma}{r} \right)^{12} - \left(\frac{\sigma}{r} \right)^6 \right] \quad (13)$$

where

$\varphi(r)$ = intermolecular potential energy
 r = distance of separation of molecular or atomic species
 σ = the collision diameter for low energy collisions, i.e., the value of r at $\varphi(r) = 0$

The term $4\epsilon(\sigma/r)^{12}$ is the inverse 12th-power energy of molecular repulsion and $4\epsilon(\sigma/r)^6$ is the inverse 6th-power energy of molecular attraction.

(3) J. O. Hirschfelder, R. B. Bird, and E. L. Spotz, *Trans. Am. Soc. Mech. Eng.*, **71**, 921 (1949).

(4) S. Chapman and T. G. Cowling, "The Mathematical Theory of Non-uniform Gases," Cambridge University Press, 1939.

For collisions between unlike molecules of species 1 and 2, the maximum energy of attraction is approximated as the geometrical mean of the pure components, thus

$$\epsilon_{12} = \sqrt{\epsilon_1 \epsilon_2} \quad (14)$$

and the collision diameter is taken as the arithmetical mean of the components, thus

$$\sigma_{12} = \frac{\sigma_1 + \sigma_2}{2} \quad (15)$$

Using the force constants σ and k/ϵ and the collision integrals compiled by Hirschfelder, Curtiss, and Bird,⁵ interdiffusivities in binary gas mixtures can be calculated.

The force constants for metal vapors are not known, but as shown by Turkdogan,⁶ the force constants may be estimated with a reasonable degree of accuracy using the empirical relationships

$$\epsilon/k = 0.77T_c \quad \text{in } ^\circ\text{K.} \quad (16a)$$

$$\epsilon/k = 1.15T_b \quad \text{in } ^\circ\text{K.} \quad (16b)$$

$$\epsilon/k = 1.92T_m \quad \text{in } ^\circ\text{K.} \quad (16c)$$

$$\sigma = 0.841(V_c)^{1/3} \quad \text{in } \text{Å.} \quad (17a)$$

$$\sigma = 1.166(V_b)^{1/3} \text{ (liq.)} \quad \text{in } \text{Å.} \quad (17b)$$

$$\sigma = 1.221(V_m)^{1/3} \text{ (sol.)} \quad \text{in } \text{Å.} \quad (17c)$$

where T_c , T_b , and T_m are critical, boiling, and melting temperatures; V_c and V_b are molar volumes of liquid metals at critical and boiling temperatures; and V_m is the molar volume of solid metal at its melting temperature. The recent experimental work of Grieveson and Turkdogan⁷ indicates that the interdiffusivities computed using eq. 12, 16, and 17 are within $\pm 10\%$ of the values obtained experimentally at elevated temperatures.

Critical Conditions for Maximum Rate of Enhanced Vaporization.—The experimental evidence already given illustrates the validity of the theory that below the maximum rate of vaporization (and well above the minimum rate), for a given gas flow rate and temperature, the rate of vaporization of metals is directly proportional to the oxygen partial pressure. That is, writing eq. 5 in a general form

$$J_i = \frac{\alpha h}{RT} p_{O_2} \quad (18)$$

where α is the number of gram-atoms of metal vapor required to combine with one mole of oxygen at the distance $x = \delta$ very close to the surface of the metal. This relationship is valid for any metal; it will be noted that J_i is independent of the vapor pressure of the metal and that this rate of vaporization can be predicted by calculating the value of the average film mass-transfer coefficient of oxygen, h , for known boundary conditions and flow patterns, by using eq. 11. Temperature has a twofold effect: the first effect is as shown in eq. 18 and the second effect is that due to

(5) J. O. Hirschfelder, C. F. Curtiss, and R. B. Bird, "Molecular Theory of Gases and Liquids," John Wiley and Sons, Inc., New York, N. Y., 1954.

(6) E. T. Turkdogan, "Symposium on Physical Chemistry of Steelmaking," Mass. Inst. of Tech., in press.

(7) P. Grieveson and E. T. Turkdogan, to be published elsewhere.

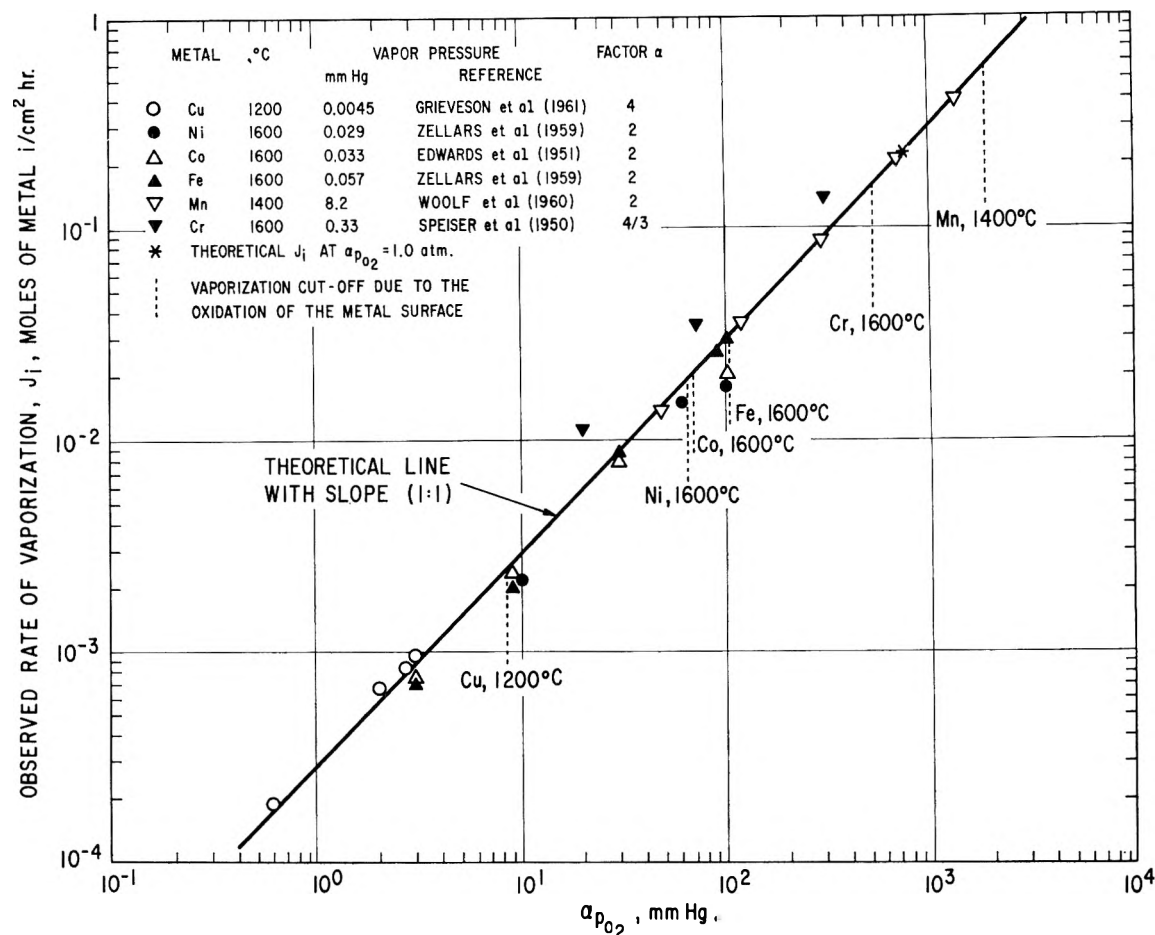


Fig. 6.—Experimental verification of the theoretical eq. 19 showing the rate of vaporization, J_i , as a function of oxygen partial pressure, αp_{O_2} , for gas (Ar + O₂) velocity $v = 80$ cm./sec. References: J. W. Edwards, H. L. Johnston, and W. E. Ditmars, *J. Am. Chem. Soc.*, **73**, 4729 (1951); P. Grievson, G. W. Hooper, and C. B. Alcock, "Physical Chemistry Process Metallurgy," Vol. 7, Interscience Publishers, Inc., New York, N. Y., 1961, p. 341; R. Speiser, H. L. Johnston, and P. Blackburn, *J. Am. Chem. Soc.*, **72**, 4142 (1950); P. L. Woolf, G. R. Zellars, E. Foerster, and J. P. Morris, U. S. Bureau of Mines Report No. R15634, 1960; G. R. Zellars, S. L. Payne, J. P. Morris, and R. L. Kipp, *Trans. Met. Soc. AIME*, **215**, 181 (1959).

increase in the value of h with increasing temperature. The net result is that, for a given gas velocity and oxygen partial pressure, the effect of temperature on the rate of enhanced vaporization, J_i , is practically negligible.

It will be noted that by taking the logarithm of each side of eq. 18, it follows that

$$\log J_i = \log(\alpha p_{O_2}) + \log \frac{h}{RT} \quad (19)$$

It is thus convenient, for a large range of data, to plot $\log J_i$ vs. $\log(\alpha p_{O_2})$ as suggested by this equation. All the data on vaporization in argon + oxygen mixtures for the flow rate of $v = 80$ cm./sec. are collated in such a plot, Fig. 6. The value of α chosen is that for the formation of the lowest stable oxide, e.g., $\alpha = 2$ for Ni, Co, Fe, and Mn and $\alpha = 4$ for Cu. In Fig. 6 it is clearly seen that all the data for the various metals, at varying temperatures, fall on the same straight line with unit slope and the theoretical intercept in accord with eq. 19. It will be noted that it is only the position of the cut-off that is determined by the specific metal and its vapor pressure.

From the known vapor pressure data (given in Fig. 6) the maximum rate of free vaporization can be calculated using the Langmuir eq. 6 for the accommodation coefficient of unity, and as seen from Fig. 7, the observed

maximum rates at the vaporization cut-off are in accordance with the theoretical maximum rates.

The critical partial pressure of oxygen corresponding to the vaporization cut-off can be calculated by equating eq. 6 and 18, from which the following is obtained for $(p_{O_2})_{\max}$.

$$(p_{O_2})_{\max} = \frac{p_i}{\alpha h} \sqrt{\frac{RT}{2\pi M_i}} \quad (20)$$

Therefore, for any given metal of known vapor pressure, p_i , the value of $(p_{O_2})_{\max}$ can be computed for a given temperature and gas velocity. In Fig. 8, the observed and theoretical values of $(p_{O_2})_{\max}$ are compared.

Since the partial pressure of the metal vapor, p_i' , at $x = \delta$ is much smaller than the vapor pressure of the metal, p_i , the flux of metal vapor within the boundary layer δ may be written in a general form

$$J_i = \frac{D_i}{\delta} \frac{p_i}{RT} \quad (21)$$

where D_i is the metal vapor + inert gas interdiffusivity. The ratio D_i/δ is of course the velocity of the vapor diffusing. At maximum rate of vaporization, the velocity D_i/δ reaches a maximum and from the sum of eq. 6 and 21, this maximum velocity is given by

$$\frac{D_i}{\delta} = \sqrt{\frac{RT}{2\pi M_i}} = \frac{1}{4} \bar{v}_i \quad (22)$$

where \bar{v}_i is the mean velocity of the vapor due to its kinetic energy. The significance of $D_i/\delta = \bar{v}_i/4$ is obvious from the derivation of the Langmuir equation which is based on the fact that the number of molecules striking unit surface area of the walls of the container per unit time is $n\bar{v}_i/4$, where n is the number of molecules per unit volume.

The critical thickness, δ , of the diffusion boundary layer at the vaporization cut-off can be derived using equations based on the kinetic theory of gases. Based on the simple theory of the kinetics of gases, the interdiffusivity D_i for metal vapor (i) + inert gas (j), at dilute solution of the vapor (i), is given by

$$D_i = \frac{\pi}{8} \bar{v}_j l_j \quad (23)$$

where \bar{v}_j and l_j are the mean velocity and mean free path of the gas j, respectively. By substituting D_i from eq. 21 in 22, the value of δ is obtained

$$\delta = \frac{\pi \bar{v}_j}{2 \bar{v}_i} l_j \quad (24)$$

i.e.

$$\delta = \frac{1}{\sqrt{8n_j\sigma_j^2}} \sqrt{\frac{M_i}{M_j}} \quad (25)$$

where n_j is number of molecules in a unit volume of gas, σ_j the collision diameter and M_j the molecular weight of the inert gas j, and M_i is the molecular weight of the metal vapor.

The theory of homogeneous nucleation of droplets from vapor originally developed by Volmer and Weber⁸ and Becker and Döring⁹ has recently been modified by Lothe and Pound¹⁰ and Oriani and Sundquist.¹¹ However, the theory so far developed is applicable only to the homogeneous nucleation involved in the condensation of vapor of a single species, e.g., H₂O, Hg. The theory cannot be applied with any reasonable degree of certainty to the condensation of, for example, a metal oxide formed from a metal vapor and oxygen, as encountered in enhanced vaporization. Since the decrease in free energy accompanying the formation of the metal oxides is large, e.g., 50 to 150 kcal./mole for the systems studied in this work, the extent of supersaturation of metal vapor and oxygen in the "gas" embryo by about an order of magnitude cannot be detected by the experimental technique used in the present investigation. In fact, the good agreement obtained between the observed and theoretical rate of vaporization (Fig. 7) supports the view that the partial pressures p_i' and p_{O_2}' at $x = \delta$ are negligible compared with the vapor pressure of the metal and the oxygen partial pressure of the gas stream.

Generalization of the Effect of Reactive Gases on the Rate of Vaporization.—If the carrier gas contains, for example, carbon dioxide instead of oxygen the effect on the rate of vaporization of metals will be the same as

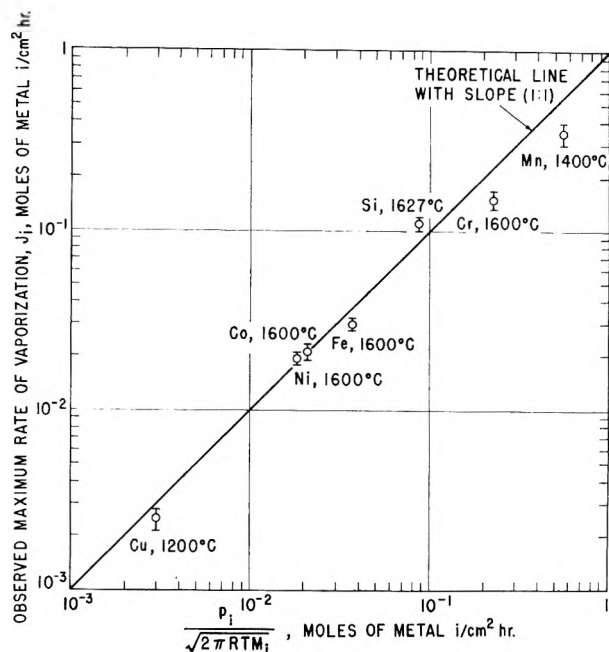


Fig. 7.—Observed maximum rate of vaporization in Ar + O₂ mixtures related to the Langmuir equation for vaporization *in vacuo*.

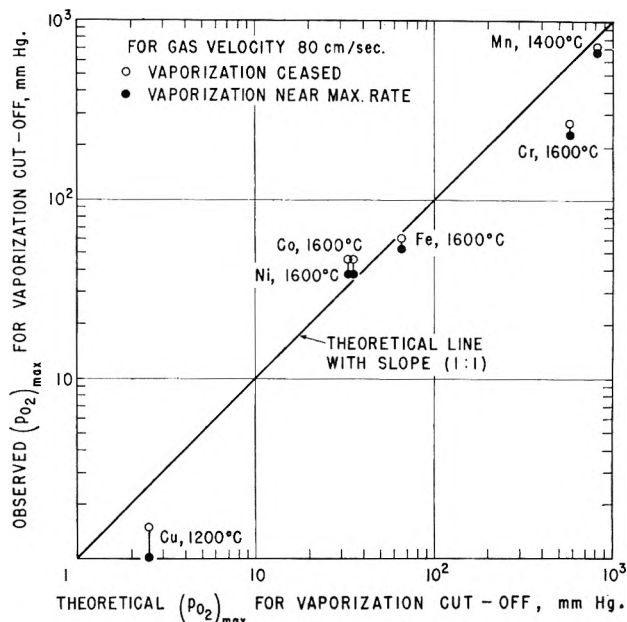


Fig. 8.—Comparison of the observed and theoretical $(p_{O_2})_{\max}$ at which vaporization cut-off occurs.

those discussed above for argon + oxygen mixtures. For the vaporization of liquid iron in argon + carbon dioxide mixtures, the reaction at $x = \delta$ is



for which $\alpha = 1$ and the flux of iron vapor is given by

$$J_{\text{Fe}} = \frac{h}{RT} p_{\text{CO}_2} \quad (27)$$

As seen from Fig. 9, the observed rate of vaporization of iron at 1600° and $v = 40$ cm./sec. agrees well with that calculated using eq. 27.

Enhanced vaporization can be brought about by the presence of suitable reactive gases other than the oxygen-bearing species. For example, in a series of experiments the rates of vaporization of molten silicon in argon + nitrogen gas streams were measured, and as

(8) M. Volmer and A. Weber, *Z. physik. Chem.*, **119**, 277 (1925).

(9) R. Becker and W. Döring, *Ann. Physik*, **24**, 719 (1935).

(10) J. Lothe and G. M. Pound, *J. Chem. Phys.*, **36**, 2080 (1962).

(11) R. A. Oriani and B. E. Sundquist, private communication, 1962.

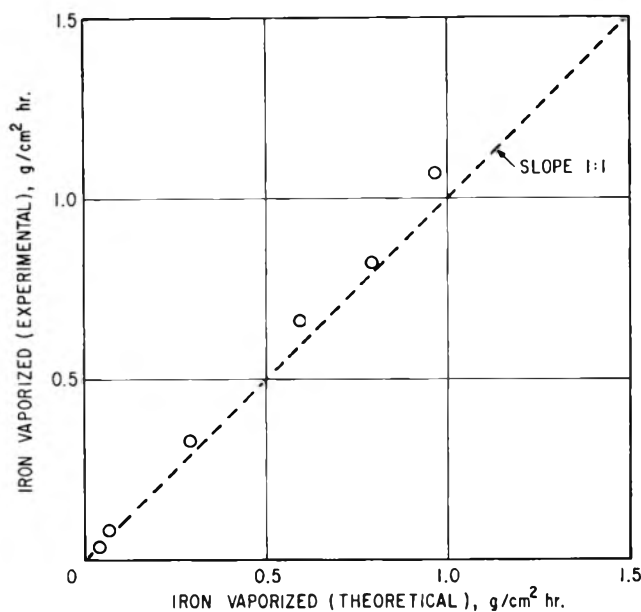


Fig. 9.—Comparison of experimental and theoretical rate of vaporization of liquid iron in Ar + CO₂ mixtures flowing parallel to the surface of the melt at 40 cm./sec. at 1600°.

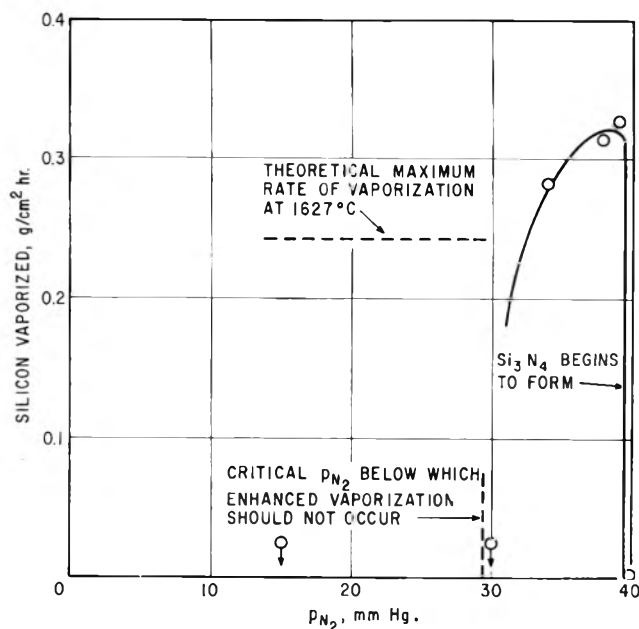


Fig. 10.—Relationship showing the effect of nitrogen partial pressure of Ar + N₂ mixtures ($v = 40$ cm./sec.) on the rate of vaporization of liquid silicon at 1627°.

shown in Fig. 10, there is a marked increase in the vaporization rate with increasing nitrogen partial pressure. In this instance, the sink for silicon vapor and nitrogen at $x = \delta$ is provided by the formation of Si₃N₄, which was identified from its X-ray diffraction pattern indicating the presence of both α and β forms of Si₃N₄ (Turkdogan, Bills, and Tippett¹²). At unit

(12) E. T. Turkdogan, P. M. Bills, and V. A. Tippett, *J. Appl. Chem.*, **8**, 296 (1958).

silicon activity, the equilibrium nitrogen partial pressure of silicon nitride is 27 mm. at 1627° (Hincke and Brantley¹³; Pehlke and Elliott¹⁴); in fact no enhanced vaporization was observed at nitrogen partial pressures below 30 mm. As indicated in Fig. 10, the observed maximum rate of vaporization prior to the cut-off is much higher than that calculated for free vaporization at 1627° using the vapor pressure data of Grieveson and Alcock.¹⁵ This discrepancy can be accounted for if the real temperature were about 30° higher than that measured.

In the light of the present theory explaining the effect of oxygen in the atmosphere on the rate of vaporization of metals, an explanation is given by the authors (Turkdogan, Grieveson, and Darken¹⁶) to account for the apparent association between decarburization of iron and the formation of iron oxide fumes.

The concept of enhanced vaporization considered here is applicable to other systems where the counter diffusion of reacting species occurs. For example, Mullaly and Jacques¹⁷ measured the interdiffusivities of N₂ + Hg vapor and N₂ + I₂ vapor by a counterflux method. The mercury and iodine vapors were allowed to diffuse from the free elements situated at the opposite ends of a closed glass tube containing nitrogen at a reduced pressure. At a particular distance from the ends of the tube, the two vapors react forming iodides of mercury which deposit on the inner walls of the glass tube. By measuring the counterflux of both vapors deposited and their diffusion distances, and using the known vapor pressure data for mercury and iodine, the interdiffusivities were evaluated.

In the study of the kinetics of reaction between sulfur trioxide and water vapor, Goodeve, Eastman, and Dooley¹⁸ considered the counterflux whereby sulfuric acid mist was formed in the gas phase.

Another example is the formation of a "Liesegang ring" arising from the counter diffusion of ammonia and hydrogen chloride in air, studied by Spatz and Hirschfelder.¹⁹

Similar phenomena have been observed and treated in condensed systems, for example in the ring test for nitrates, in the formation of Liesegang bands in gels and in the formation of subscale in solid metals (Darken²⁰).

Acknowledgment.—The authors wish to thank B. F. Oliver of this Laboratory for the experiments by levitation melting.

(13) W. B. Hincke and L. R. Brantley, *J. Am. Chem. Soc.*, **52**, 48 (1930).

(14) R. D. Pehlke and J. F. Elliott, *Trans. Met. Soc. AIME*, **215**, 781 (1959).

(15) P. Grieveson and C. B. Alcock, "Special Ceramics," Heywood and Co. Ltd., London, 1961, p. 183.

(16) E. T. Turkdogan, P. Grieveson, and L. S. Darken, *Proc. Natl. Open Hearth Steel Con.*, 470 (1962).

(17) J. M. Mullaly and H. Jacques, *Phil. Mag.*, **48**, 1105 (1924).

(18) C. F. Goodeve, A. S. Eastman, and A. Dooley, *Trans. Faraday Soc.*, **30**, 1127 (1934).

(19) E. L. Spatz and J. O. Hirschfelder, *J. Chem. Phys.*, **19**, 1215 (1951).

(20) L. S. Darken, *Trans. AIME*, **150**, 157 (1942).

AMIDINIUM IONS. I. HINDERED INTERNAL ROTATION¹BY GEORGE S. HAMMOND AND ROBERT C. NEUMAN, JR.²

Contribution No. 2939 from the Gates and Crellin Laboratories of Chemistry, California Institute of Technology, Pasadena, California

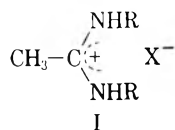
Received February 1, 1963

N.m.r. spectra of unsubstituted and symmetrically substituted aliphatic amidinium salts in dimethyl sulfoxide or water showed that rotation about the C-N bonds of the amidinium groups is hindered. The magnetic resonance characteristics of protons bonded to N in these amidinium salts are discussed.

In the course of an investigation of the thermal decomposition of azobisamidinium salts,³ an independent n.m.r. study of amidinium ions in solution was initiated. Results elucidating the stereochemistry of these ions in solution and the n.m.r. spectral properties of protons bonded to N in amidinium ions are discussed in this paper. The mechanisms of nitrogen-proton exchange in dilute and strong aqueous acid solutions are presented in part II of this series⁴ and are compared with those of ammonium ions.

Results and Discussion

Hindered Rotation.—The proton magnetic resonance spectra of the amidinium salts I-III have been recorded at a spectrometer frequency of 60 Mc.p.s.



Ia, R = H, X = Cl⁻
 b, R = H, X = NO₃⁻
 c, R = CH₃, X = Cl⁻

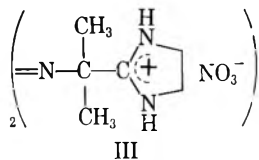
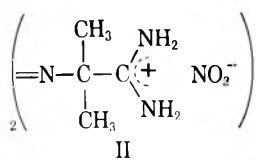


(Table I). Assignment of N-H and N-CH₃ protons is based on integrated relative intensities of the signals and agrees with the generally observed order $\nu_{\text{C-CH}_3} < \nu_{\text{N-CH}_3} < \nu_{\text{N-H}}$. The chemical shifts of the N-H protons correspond closely to those of amides^{5,6} and ammonium salts.⁷

Two nitrogen-proton signals are observed for the unsubstituted amidinium salts Ia, Ib, and II in anhydrous DMSO. Integrated signal areas are in the ratio 1:1. These results are consistent with the view that rotation about the C-N bonds is slow in comparison with the difference between the absorption frequencies of protons in the magnetically non-equivalent "inside" (H(a)) and "outside" (H(b)) positions in IV. Restricted rotation in the amidinium systems is no doubt due to the partial double bond character associated with each C_N-N bond. Because of the symmetry of the

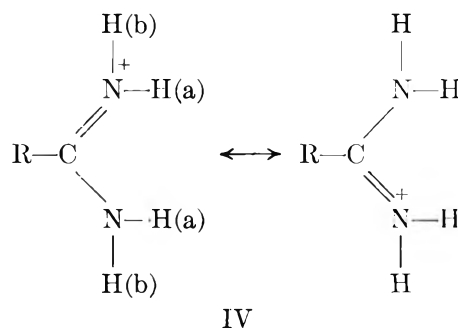


TABLE I
 N.M.R. SPECTRAL RESULTS FOR AMIDINIUM IONS IN SOLUTION;
 30°, 60 Mc.p.s.

Compd.	Solvent	$\nu_{\text{N-H}}^a$ (c.p.s.)	$\Delta\nu^{1/2}$ (N-H) ^b (c.p.s.)	$\nu_{\text{N-CH}_3}^a$ (c.p.s.)	$J(\text{N-H}, \text{N-CH}_3)^c$ (c.p.s.) ^c
Ia	DMSO ^d	530	10
		560	11
Ib	DMSO	530	10
		560	11
Ic	DMSO	554	13	171.5	5.0
		609	16	176.5	5.0
Ic	H ₂ O	177.5	0
		187.0	0
Ic	14% H ₂ SO ₄	~425	..	179.0	5.0
		~455	..	188.5	5.0
Ic	60% D ₂ SO ₄	184.0	0
		194.0	0
II	DMSO	534	9
		547	9
III	DMSO	608	15
	

^a Chemical shift in c.p.s. referenced to external tetramethylsilane (0 c.p.s.). Positive values of ν represent downfield shifts. No corrections have been made for bulk susceptibility effects.
^b Signal width at half-height. ^c Spin-coupling constant obtained from the observed splitting in the N-CH₃ signals (see below).
^d Anhydrous methyl sulfoxide (dimethyl sulfoxide).

(1) R. C. Neuman, Jr., G. S. Hammond, and T. J. Dougherty, *J. Am. Chem. Soc.*, **84**, 1506 (1962).

(2) National Institutes of Health Predoctoral Fellow (1960-1962).

(3) G. S. Hammond and R. C. Neuman, Jr., *J. Am. Chem. Soc.*, **85**, 1501 (1963).

(4) R. C. Neuman, Jr. and G. S. Hammond, *J. Phys. Chem.*, **67**, 1659 (1963).

(5) J. A. Pople, W. G. Schneider, and H. J. Bernstein, "High Resolution Nuclear Magnetic Resonance," McGraw-Hill Book Co., Inc., New York, N. Y., 1959, p. 272.

(6) L. M. Jackman, "Nuclear Magnetic Resonance Spectroscopy," Pergamon Press, Inc., New York, N. Y., 1959, p. 73.

(7) E. Grunwald, A. Loewenstein, and S. Meiboom, *J. Chem. Phys.*, **25**, 382 (1956); **27**, 630 (1957).

ion, a bond number⁸ of 1.5 can be assigned to each C_{CN}-N bond. For maximum π overlap, the group should be planar. Hindered rotation about C_{CO}-N bonds in amides has been extensively investigated and attributed to a similar restriction of rotation about the C-N bond.⁹

That a single N-H proton signal is observed for III in DMSO (Table I) is in agreement with the above hypothesis since the nitrogen protons are restricted to the magnetically equivalent "outside" positions.

The amidinium group in N,N'-dimethylacetamidinium chloride (Ic) could conceivably assume three possible conformations, Va-c.

Spectra of this compound in a series of solvents are given in Table I and indicate that the conformation Va is the only detectable form present in solution. In each

(8) L. Pauling, "The Nature of the Chemical Bond," 3rd Ed., Cornell University Press, New York, N. Y., 1960, p. 239.

(9) See, for example, ref. 5, p. 365.

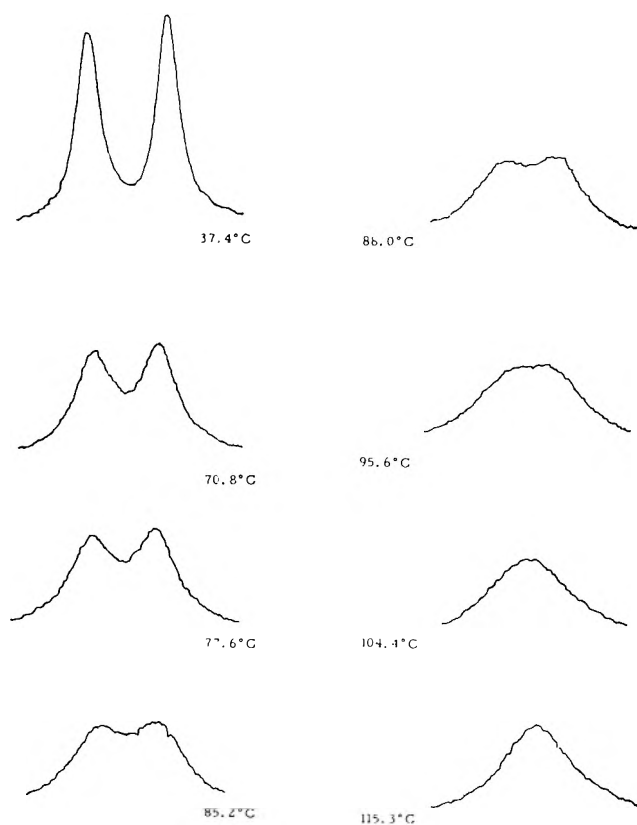
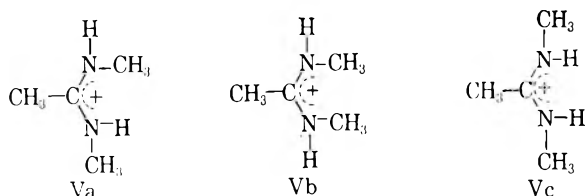


Fig. 1.—N-H signals of acetamidinium chloride in DMSO as a function of temperature.



solvent two separate N-CH₃ resonances of equal area are observed. In DMSO and 14% H₂SO₄, in which two N-H resonances of equal area are observed, each N-CH₃ signal is split into a doublet ($J = 5$ c.p.s.). The N-H resonance signals in water and D₂SO₄ are not observed, due, respectively, to rapid proton exchange and deuterium replacement of nitrogen protons.⁴ Correspondingly, the N-CH₃ signals are singlets in these solvents.¹⁰ The magnitude of J in DMSO and in 14% H₂SO₄ implies that the splitting of the N-CH₃ signals is due to the adjacent proton on the same nitrogen atom.¹¹

The spectra could alternatively be interpreted as arising from equal amounts of the "inside-inside" and "outside-outside" conformations Vb and Vc; however, models indicate that steric interactions between the "inside" N-CH₃ groups in Vb are very unfavorable. A statistical mixture of the three conformations would give the results only if the chemical shift of the "inside" N-CH₃ group of Va were identical with that of the "inside" N-CH₃ groups of Vb. This is considered very unlikely. Although conformation Vc may appear at

(10) The difference in chemical shifts for N-CH₃ protons and N-H protons in the different solvents is due to a solvent effect on the shielding of these protons.

(11) N-H, N-CH₃ coupling constants of 4 and 4.8 c.p.s. are observed for N-methylacetamide and N-methylformamide, respectively.¹² The corresponding N-H quartet is not resolved because of the broadness of the N-H signal (*vide infra*).

(12) G. Fraenkel and C. Franconi, *J. Am. Chem. Soc.*, **82**, 4478 (1960).

first glance to be the most sterically favorable, the three methyl groups are approximately as crowded as the three methyl groups in 1,2,3-trimethylbenzene in which steric strain is obvious.¹³

The results thus demonstrate the predominant presence of the unsymmetrical conformation Va in solution.¹⁴

The possibility of formation of unsymmetrical ion-pairs between the amidinium cation and an anion had been considered as an alternate rationale for the magnetic non-equivalence of N-H protons in Ia, Ib, and II in DMSO. However, the magnetic non-equivalence of the N-CH₃ groups of Ic in water (where ion-pair formation is expected to be negligible) and the magnetic-equivalence of the two N-H protons of III in DMSO make this explanation untenable.¹⁵

The barrier to rotation about the C-N partial double bonds of Ia in DMSO has been estimated. The effect of temperature on the N-H signals is shown in Fig. 1. The kinetic data for the coalescence of these signals are given in Table II. The observed signal separation as a

TABLE II

VARIATION OF THE N-H PROTON RESONANCE SIGNALS OF ACETAMIDINIUM CHLORIDE WITH TEMPERATURE OF DMSO

T , °K.	$10^3/T$, °K.	$\delta\nu_c/\delta\nu_\infty^a$	$1/2\pi\tau\delta\nu$	
			$T_2 = 0.03$ sec.	$T_2 = 0.01$ sec.
310.6	3.22	1.00	0	0
344.0	2.91	0.85 ± 0.03	0.24 ± 0.03	0.02 ± 0.03
350.8	2.85	$.82 \pm .03$	$.28 \pm .03$	$.06 \pm .02$
358.4	2.79	$.68 \pm .03$	$.37 \pm .02$	$.14 \pm .01$
361.2	2.77	$.62 \pm .03$	$.42 \pm .02$	$.17 \pm .01$

^a $\delta\nu_c$ = observed signal separation, $\delta\nu_\infty$ = signal separation at 37.6°. ^b τ = mean lifetime of protons in the two environments, T_2 = transverse relaxation time.

function of temperature has been corrected for overlap of the signals by the method of Gutowsky and Holm.¹⁷ Their treatment requires that the transverse relaxation times of the signals be invariant with temperature. This was not true for the N-H signals of Ia. A qualitative inspection of Fig. 1 shows that at about 20° above the coalescence temperature the single signal is much broader than the initial signals at 37°. Further increase of temperature did not noticeably sharpen this signal. The initial signals (37°) give a value $T_2 \cong 0.03$ sec., while the final signal (115°) gives $T_2 \cong 0.01$ sec. Using the data in the last two columns of Table II, activation parameters were calculated for each of these values of T_2 from the graphical plots shown in Fig. 2 and 3. They are: $T_2 = 0.03$ sec. (Fig. 2), $E_a = 9 \pm 2$ kcal. mole⁻¹, $k_0 = 10^5$ - 10^7 sec.⁻¹; $T_2 = 0.01$ sec. (Fig. 3), $E_a = 25 \pm 8$ kcal. mole⁻¹, $k_0 = 10^{11}$ - 10^{21} sec.⁻¹. Since T_2 probably decreases in some regular manner with increase in temperature the true activation parameters lie somewhere between these extreme values. The dependence of T_2 for the N-H signals on temperature is probably due to the effect of temperature on the

(13) H. C. Brown, G. K. Barbaras, H. L. Berneis, W. H. Bonner, R. B. Johannesen, M. Grayson, and K. L. Nelson, *ibid.*, **75**, 1 (1953).

(14) Small amounts of the other conformers may be present, but are not detected by the n.m.r. method. Rapid interconversion between the conformers would require the spectra to show only one N-CH₃ signal and one N-H signal.

(15) The effect of ion-pairing in DMSO on the magnetic shields of ring protons in anilinium ions has been discussed,¹⁶ but appears to have no apparent consequences in these studies of amidinium ions.

(16) G. Fraenkel, Abstracts of the Symposium on High Resolution N. m.r. Spectroscopy, July 2-4, 1962, Boulder, Colorado.

(17) H. S. Gutowsky and C. H. Holm, *J. Chem. Phys.*, **25**, 1228 (1956).

quadrupole broadening of protons bonded to ^{14}N (*vide infra*).

Although the barrier to rotation in Ia is not known with high precision, it is interesting that the value is in the same range as those of amides (7–18 kcal./mole).^{9,18,19}

It might be expected that barriers to rotation in amidinium ions would be consistently higher than those in simple amides due to the greater double bond character associated with an amidinium $\text{C}=\text{N}$ bond. It is reasonable to assign a bond order of ~ 1.5 to each $\text{C}=\text{N}$ bond in symmetric amidinium ions (*vide supra*) whereas the corresponding bond order for the $\text{C}-\text{N}$ bonds in amides should be smaller.^{9,12} The existing data for amidinium ions is insufficient to test this hypothesis.

Absolute Spectral Assignments.—A tentative absolute spectral assignment can be made by a comparison of the spectra of Ic and III in DMSO (Table I). The similarity between the chemical shift of the "outside" proton in III (608 c.p.s.) and the lower field N-H signal in Ic at 609 c.p.s. suggests that this latter resonance is due to the "outside" protons; therefore, the signal at 554 c.p.s. is due to the "inside" proton. Rationale for this comparison lies in the similarity of substitution of each nitrogen in Ic and III. It is reasonable to assume that the relative screening of "inside" and "outside" nitrogen protons is similar in each amidinium ion and is determined by the position of the proton relative to the $\text{N}=\text{C}=\text{N}$ linkage. Thus it can be tentatively assumed that the lower field N-H signals in Ia-c and II correspond to "outside" protons and the higher field N-H signals to "inside" N-H protons.

This conclusion is further strengthened by an analysis of the $\text{N}-\text{CH}_3$ signal shapes of Ic. In all solvents, the lower field $\text{N}-\text{CH}_3$ resonance pattern is much sharper than the high field $\text{N}-\text{CH}_3$ resonance. For example for Ic in water, values of $\Delta\nu_{1/2}$ for the signals are: $\text{N}-\text{CH}_3$ (low field) 1.0 c.p.s.; $\text{N}-\text{CH}_3$ (high field) 1.7 c.p.s.; and $\text{C}-\text{CH}_3$, 1.6 c.p.s. The relative line widths may be attributed to unequal (unresolved) spin coupling between the $\text{C}-\text{CH}_3$ protons and the conformationally different $\text{N}-\text{CH}_3$ protons. Thus the strongest coupling is between the $\text{C}-\text{CH}_3$ protons and the high field $\text{N}-\text{CH}_3$ group. In amides²⁰ and other systems^{21,22} 1,4-coupling between methyl group protons has established the relationship $J_{trans} > J_{cis}$. This leads to the conclusion that the high field $\text{N}-\text{CH}_3$ group is *trans* to the $\text{C}-\text{CH}_3$ group or in the "inside" position. Data to be given in the second paper of this series⁴ show that the high field member of the two $\text{N}-\text{CH}_3$ resonances and the low field member of the two N-H resonances of Ic are due to groups attached to the same nitrogen. Thus, the assignment of the high field $\text{N}-\text{CH}_3$ resonance to the "inside" proton requires the low field N-H resonance to be assigned to the "outside" proton. This is in agreement with the previously discussed assignments based on comparison of Ic and III. Analogous assignments

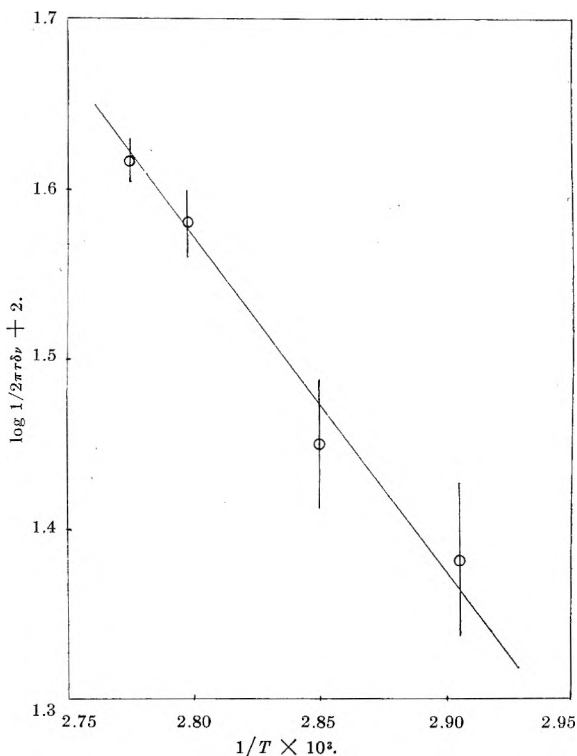


Fig. 2.—Estimation of activation energy for rotation in acetamidinium ion assuming $T_2 = 0.03$ sec.

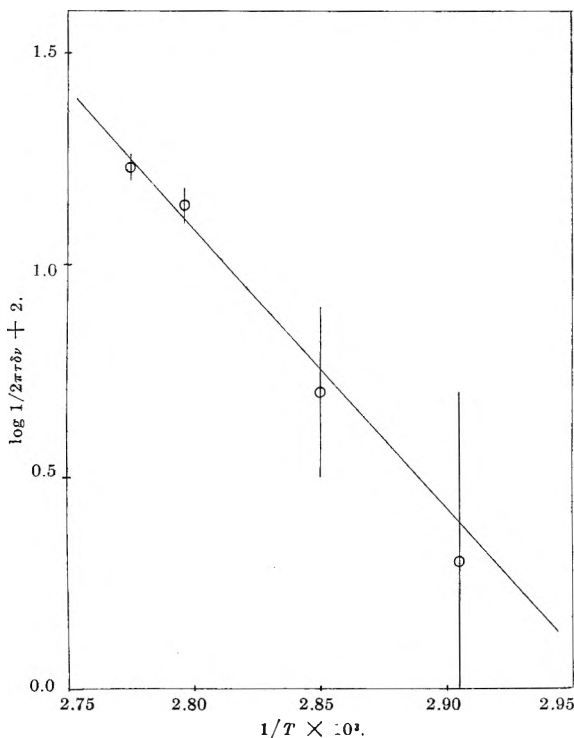


Fig. 3.—Estimation of activation energy for rotation in acetamidinium ion assuming $T_2 = 0.01$ sec.

using the above arguments have been made for *N,N*-dimethylamides.^{18,20}

Spectral Characteristics of Amidinium Nitrogen Protons.—The shapes of the N-H resonance signals are also of interest. This discussion will be limited to the results obtained in DMSO solutions. In general, the spectral properties of N-H protons are strongly dependent on whether or not they are involved in exchange processes.²³ Care was taken to assure that

(18) M. T. Rogers and J. C. Woodbrey, *J. Phys. Chem.*, **66**, 540 (1962).

(19) B. Sunners, L. H. Piette, and W. G. Schneider, *Can. J. Chem.*, **38**, 681 (1960).

(20) V. J. Kowalewski and D. G. de Kowalewski, *J. Chem. Phys.*, **32**, 1272 (1960); *Arkiv Kemi*, **16**, 373 (1961).

(21) R. R. Fraser, *Can. J. Chem.*, **38**, 549 (1960).

(22) J. H. Richards and W. F. Beach, *J. Org. Chem.*, **26**, 623 (1961).

(23) Reference 6, p. 72.

the DMSO used in these studies was anhydrous and the observable N-H, N-CH₃ spin-spin coupling for Ic in DMSO (Table I) indicates that proton exchange is not occurring at a significant rate in this solvent. Further proof for the anhydrous nature of this solvent lies in the observation that addition of small amounts of water to DMSO solutions of Ia causes the two separate N-H signals to coalesce into a broad singlet. Under such non-exchanging conditions various types of N-H signals have been observed. Ammonium salts²⁴ customarily show the triplet pattern arising from coupling of the protons with ¹⁴N (*I* = 1) as do anhydrous ammonia²⁵ and certain amides at elevated temperatures.²⁶ On the other hand, certain amides at room temperature show only broad singlets with values of $\Delta\nu_{1/2}$ of 10–75 c.p.s.²⁶ Tiers²⁷ has examined a series of N-acylamino acids and guanidinoacetic acid under non-exchanging conditions and finds values of $\Delta\nu_{1/2}$ in the range of 6–10 c.p.s. All of these results are explained in terms of the effect of the symmetry of the electrical field on the coupling of the ¹⁴N quadrupole moment with proton magnetic moment.^{23,26–28} Coupling of this electric field with the ¹⁴N nuclear moment results in efficient relaxation if the field is highly asymmetric; relaxation is relatively inefficient if the field is highly symmetrical. The former case gives rise to a relatively sharp singlet and the latter to the triplet pattern. Broad N-H singlets are taken as indicative of electric fields of intermediate symmetry about the nitrogen atoms.

Inspection of values of $\Delta\nu_{1/2}$ for the N-H protons of amidinium ions in DMSO (Table I) and comparison with the narrow N-H signals observed by Tiers²⁷ for α -amino acids and the broad N-H signals for amides²⁶ leads to the conclusion that amidinium nitrogen atoms are surrounded by relatively asymmetric fields. Roberts²⁶ has shown that the broad singlets observed for N-H protons of certain amides undergo transitions to triplets at elevated temperatures and concluded that increased molecular motion effectively symmetrizes the field surrounding the ¹⁴N atoms. The transition temperatures were dependent on structures of the amides but in general were above 175°. We conclude that the increased width of the coalesced N-H signal for Ia in DMSO at 115° is a result of the same process and that at still higher temperatures further broadening would occur and eventually a triplet pattern would arise.

Dihedral Angles and N-H, C-H Proton Coupling.—Azo-bis-(N,N'-dimethylene)-isobutyramidinium nitrate (III) deserves special mention. Spin-spin coupling between the nitrogen protons and protons on the adjacent N-methylene groups in this molecule has not been observed in anhydrous DMSO or sulfuric acid solutions. Rapid nitrogen-proton exchange does not satisfactorily explain these results since it has been demonstrated for other amidinium salts that exchange of nitrogen protons in sulfuric acid solutions of appropriate composition⁴ and in anhydrous DMSO (*vide supra*) is extremely slow.

We postulate that the absence²⁹ of spin-spin coupling is due to the magnitude of the dihedral angle (probably

close to 60°) between the methylene protons and adjacent nitrogen protons in this rigid ring system. Karplus³⁰ and Conroy³¹ have discussed the effect of dihedral angle on vicinal proton coupling constants for saturated carbon systems. Maximum coupling is observed at $\phi = 0^\circ$ and $\phi = 180^\circ$ and minimum coupling occurs at $\phi \approx 80^\circ$. For these saturated carbon systems, J_{12} at $\phi = 60^\circ$ is predicted to be about 30% of the value found in open-chain systems such as ethyl and isopropyl groups. Since the N-H, N-CH₃ 1,2-coupling constant for Ic has been found to be 5 c.p.s., while J_{12} for N-methylamides is ~ 4 –5 c.p.s., a rough approximation of the expected magnitude of coupling in III is $J_{12} = 1$ –1.5 c.p.s.

It is not necessary to discuss the lack of resemblance of an amidinium group to a saturated carbon system but it is perhaps significant to observe that no resolvable coupling is observed in III which possesses a geometry similar to that expected to minimize coupling in the saturated carbon systems.

Experimental

Materials.³²—Dimethyl sulfoxide (DMSO), Crown-Zellerbach, was distilled at reduced pressure, shaken with Molecular Sieve, Linde Co., Type 4A, filtered through Celite in a drybox under nitrogen, and redistilled. The middle fraction, b.p. 45° at 0.2 mm., was collected for use. Sulfuric acid, DuPont reagent grade, was used without further purification. Sulfuric acid-d₂ was prepared³³ from Baker and Adamson "Sulfan B" (sulfur trioxide) and deuterium oxide (99.5%), General Dynamics Corporation.

Acetamidinium chloride (Ia) was prepared according to the method of Pinner,³⁴ recrystallized from absolute ethyl alcohol, and dried over phosphorus pentoxide *in vacuo*; m.p. 165–168° (lit. m.p. 164–166°,^{34a} 166–167°^{34b}).

Acetamidinium nitrate was prepared from an aqueous solution of the corresponding chloride (Ia) by addition with stirring of an equivalent amount of aqueous silver nitrate. The resultant silver chloride precipitate was filtered off and the amidinium nitrate was precipitated from solution by addition of a large quantity of acetone, recrystallized from absolute ethyl alcohol, and dried over phosphorus pentoxide *in vacuo*; m.p. 189–190°. *Anal.* Calcd. for C₂H₇N₃O₃: C, 19.83; H, 5.83; N, 34.70; O, 39.64. Found: C, 18.44, 18.22; H, 5.83, 5.97; N, 35.07, 34.88. The microanalyst (Spang) reported violent explosion during combustion under oxygen.

N,N'-Dimethylacetamidinium chloride (Ic) was prepared according to the method of Pinner,³⁵ recrystallized from absolute ethyl alcohol, and dried over phosphorus pentoxide *in vacuo*; m.p. 214.5–215.5° (lit.³⁵ m.p. 218°). Ic is very hygroscopic. Hydrolysis of Ic in 1 *N* sodium hydroxide solution gave equivalent amounts of methylamine and N-methylacetamide. This was shown by n.m.r. analysis and confirms the symmetrical structure.

Azobisisobutyramidinium nitrate (II) was prepared from the corresponding chloride by a procedure identical with that given for the preparation of acetamidinium nitrate (Ib). The chloride was obtained from the Yerkes Research Laboratory, E. I. du Pont de Nemours and Co., and had been recrystallized from water. *Anal.* Calcd. for C₈H₂₀N₈O₆: C, 29.63; H, 6.22; N, 34.55; O, 29.60. Found: C, 29.75; H, 6.30; N, 34.45; m.p., 162.5° dec.

Azobis-(N,N'-dimethylene)-isobutyramidinium Nitrate (III). A 10-g. sample of unrecrystallized azobisisobutyramidinium chloride, obtained from DuPont, was dissolved in 100 ml. of 98% ethylenediamine, Matheson, Coleman and Bell, with stirring. Upon stirring the solution for several minutes at room temperature a white solid precipitated, was filtered off, and recrystallized first from chloroform and then absolute methyl alcohol; m.p.

(30) M. Karplus, *J. Chem. Phys.*, **30**, 11 (1959).

(31) H. Conroy, *Advan. Org. Chem.*, **2**, 308 (1960).

(32) Melting points are uncorrected. Microanalyses were done by Elek Micro Analytical Laboratories, Los Angeles, Calif., and Spang Microanalytical Laboratory, Ann Arbor, Michigan.

(33) A. P. Best and C. L. Wilson, *J. Chem. Soc.*, 239 (1946).

(34) (a) A. W. Dox, "Organic Syntheses," Coll. Vol. I, John Wiley and Sons, Inc., New York, N. Y., 1941, p. 5; (b) A. Pinner, *Ber.*, **16**, 1643 (1883); **17**, 171 (1884).

(35) A. Pinner, "Die Imidoather und ihre Derivate," Berlin, 1892, p. 112.

(24) See for example: M. T. Emerson, E. Grunwald, and R. A. Kromhout, *J. Chem. Phys.*, **33**, 547 (1960).

(25) R. A. Ogg, *ibid.*, **22**, 560 (1954).

(26) J. D. Roberts, *J. Am. Chem. Soc.*, **78**, 4495 (1956).

(27) G. V. D. Tiers and F. A. Bovey, *J. Phys. Chem.*, **63**, 302 (1959).

(28) Reference 5, pp. 102, 227.

(29) Coupling of less than 1 c.p.s. probably would not be resolved under our spectral conditions.

122.5° dec. *Anal.* Calcd. for azobis-N,N'-dimethyleisobutyramidine (C₁₂H₂₂N₆): C, 57.56; H, 8.86; N, 33.57. Found: C, 57.65; H, 8.97; N, 33.46. The hydrochloride of C₁₂H₂₂N₆ was prepared. *Anal.* Calcd. for C₁₂H₂₂N₆Cl₂: C, 44.58; H, 7.49; N, 26.00; Cl, 21.94. Found: C, 44.48; H, 7.51; N, 25.88; Cl, 21.86. The nitrate was prepared by addition of an equivalent amount of concentrated nitric acid to an absolute ethyl alcohol solution of the amidine, C₁₂H₂₂N₆, and recrystallized from water; m.p. 146.5° dec. *Anal.* Calcd. for C₁₂H₂₄N₆O₆: C, 38.29; H, 6.43; N, 29.77; O, 25.51. Found: C, 38.27; H, 6.29; N, 29.82; O, 29.66. Thermal decomposition of this nitrate salt in DMSO gives a stoichiometric quantity of nitrogen gas based on the structural formula III. The microanalyst (Spang) reported a violent explosion during combustion under oxygen.

N.m.r. Spectrometers.—The nuclear magnetic resonance spectrometers used in this study were a Varian Model V-4300 B(HR-60) spectrometer, equipped with a Super-stabilizer, operating at $\nu_0 = 60$ Mc.p.s.; and a Varian A-60 spectrometer operating at $\nu_0 = 60$ Mc.p.s. The majority of the spectra were taken with the A-60 spectrometer used without modification. The variable temperature experiment was performed using the HR-60 spectrometer with suitable modifications as described below.

N.m.r. Sample Tubes.—Standard Varian analytical sample tubes (4.28 mm. i.d.) were used for all spectra taken with the A-60 spectrometer. Sample tubes for use with the HR-60 spectrometer were made from Pyrex glass tubing (5-mm. o.d.). All tubes were thoroughly cleaned and dried before use.

Temperature Dependence Study—Acetamidinium Chloride in DMSO.—The sample used in this study was prepared by dissolving acetamidinium chloride (Ia), recrystallized from ethyl alcohol and dried *in vacuo*, in anhydrous DMSO. The solution contained approximately 15% of Ia and was sealed in a Pyrex n.m.r. tube. A variable temperature probe with a Pyrex dewar encasing the insert was used.³⁶ The temperature in the probe insert was measured by means of a copper-constantan thermocouple placed within the probe insert in conjunction with a Leeds-Northrup precision potentiometer. The temperature was determined both before and after the spectrum was taken. The peak separation was determined by the audio side-band technique³⁷ using a Hewlett-Packard Model 200 AB audio oscillator and Model 521-C frequency counter. The values $^{1/2}\pi\tau\delta\nu$ were calculated by the method of Gutowsky and Holm¹⁷ using the parameters $\delta\nu_\infty = 29$ c.p.s., (a) $T_2 = 0.03$ sec., and (b) $T_2 = 0.01$ sec. The two values of T_2 were obtained from the relationship $2/T_2 = 2\pi\Delta\nu^{1/2}$ where $\Delta\nu^{1/2}$ is the width at half-height of the nitrogen-proton resonance signal. The value $T_2 = 0.03$ sec. was calculated from the average value $\Delta\nu^{1/2} = 10.5 \pm 0.5$ c.p.s. for the two signals at 37°, and the value $T_2 = 0.01$ sec. was calculated from the value $\Delta\nu^{1/2} = 30$ c.p.s. for the coalesced signal at 115°. The rate expression used for calculating activation parameters is that given in eq. 1.¹⁷

$$\log \frac{1}{2\pi\tau\delta\nu} = \log \frac{k_0}{\pi\delta\nu} - \frac{E_a}{2.3RT} \quad (1)$$

(36) C. Franconi and G. Fraenkel, *Rev. Sci. Instr.*, **31**, 657 (1960).

(37) J. T. Arnold and M. E. Packard, *J. Chem. Phys.*, **19**, 1608 (1951).

AMIDINIUM IONS. II. MECHANISMS OF EXCHANGE OF PROTONS BOUND TO NITROGEN¹

By ROBERT C. NEUMAN, JR.,² AND GEORGE S. HAMMOND

Gates and Crellin Laboratories of Chemistry,³ California Institute of Technology, Pasadena, California

Received February 1, 1963

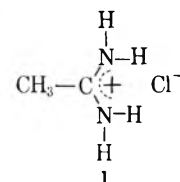
Kinetics of exchange reactions of protons attached to nitrogen in amidinium ions have been studied in dilute hydrochloric acid and in various water-sulfuric acid mixtures. In dilute aqueous acid, the principal mechanism for exchange of protons with the solvent appears to involve reaction of the amidinium ions with hydroxide ion. In concentrated sulfuric acid the exchange of protons between conformationally distinct, "inside" and "outside" positions involves an acid-catalyzed mechanism as does the exchange with solvent. The two nitrogen atoms in N,N'-dimethylacetamidinium ion-exchange hydrogen ions with the solvent at different rates.

The n.m.r. spectra of protons bound to nitrogen of amidinium ions were reported in part I of this series.⁴ It was shown that rotation about the C-N bonds is restricted and that protons in "inside" and "outside" positions are magnetically distinguishable. The results of studies of the kinetics of various exchange reactions of amidinium ions in aqueous acid are reported in this paper. The work was aided substantially by consideration of the reports of very careful studies of the exchange reactions of ammonium ions.⁵⁻⁹

Results and Discussion

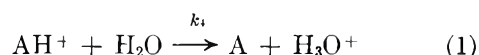
Dilute Aqueous Acid.—Acetamidinium chloride, 1, was used in this study. Preliminary n.m.r. experi-

ments with 1 in dilute hydrochloric acid showed that the nitrogen-proton and water-proton resonance



signals were markedly dependent on the acidity of the solution. As the pH of the solutions is decreased from 5.6 to 3.0 the water-proton resonance changes from a broad to a sharp singlet. The nitrogen-proton resonance, absent at pH 5.6, becomes distinguishable as a very broad singlet as the acidity is increased. The C-CH₃ singlet is sharp and independent of acidity. These results indicate that one or several pH dependent processes effect exchange between N-H groups and protons of the solvent in dilute acid solutions of 1.

Grunwald⁵ and Meiboom⁷⁻⁹ consider several exchange processes, given in eq. 1-4, for ammonium salts in dilute aqueous acid and these have been used in this



(1) R. C. Neuman, Jr., G. S. Hammond, and T. J. Dougherty, *J. Am. Chem. Soc.*, **84**, 1506 (1962).

(2) National Institutes of Health Predoctoral Fellow (1960-1962).

(3) Contribution No. 2940.

(4) G. S. Hammond and R. C. Neuman, Jr., *J. Phys. Chem.*, **67**, 1655 (1963).

(5) (a) M. T. Emerson, E. Grunwald, and R. A. Kromhout, *J. Chem. Phys.*, **33**, 547 (1960); (b) E. Grunwald, P. J. Karabatsos, R. A. Kromhout, and E. L. Purlee, *ibid.*, **33**, 556 (1960).

(6) M. T. Emerson, E. Grunwald, M. L. Kaplan, and R. A. Kromhout, *J. Am. Chem. Soc.*, **82**, 6307 (1960).

(7) E. Grunwald, A. Loewenstein, and S. Meiboom, *J. Chem. Phys.*, **25**, 382 (1956); **27**, 630 (1957).

(8) A. Loewenstein and S. Meiboom, *ibid.*, **27**, 1067 (1957).

(9) S. Meiboom, A. Loewenstein, and S. Alexander, *ibid.*, **29**, 969 (1958).

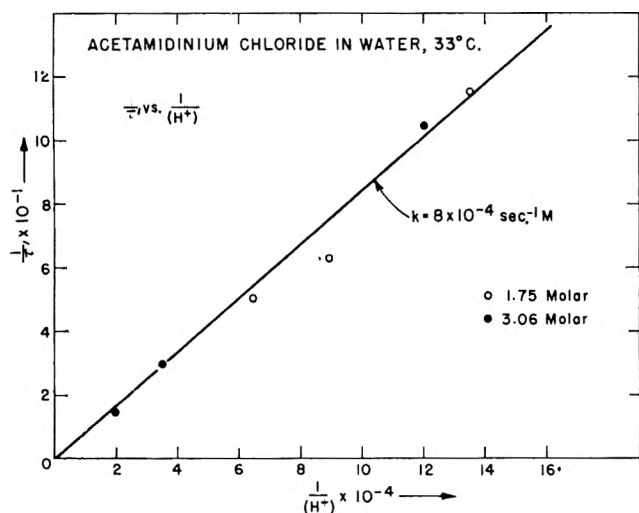


Fig. 1.—Dependence of relaxation times for solvent protons on acidity in solutions of acetamidinium chloride.

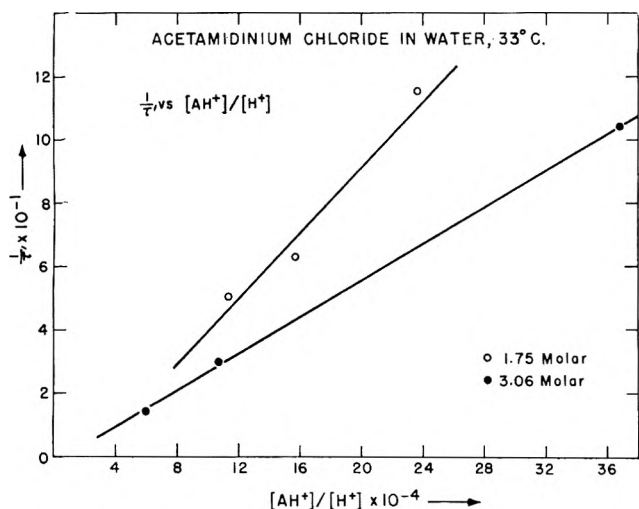
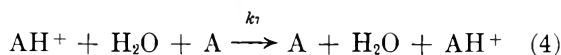


Fig. 2.—Variation of relaxation times of solvent protons on concentration of amidinium ions in solutions of acetamidinium chloride.



study as a basis for consideration of the possible proton exchange reactions of 1. The numbering of specific rate constants is that of the earlier workers and will be maintained here to afford easy comparison of results; AH^+ is the amidinium ion 1 and A is unprotonated acetamidine. Reactions 1, 2, and 4 may all involve more than one intermediary water molecule.^{5a} The resultant rate law for proton exchange is given by eq. 5 in which K_A is the acid dissociation constant for the

$$1/\tau = \text{rate}/(\text{AH}^+) = k_4 + k_5K_w/(\text{H}^+) + (k_6 + k_7)K_A(\text{AH}^+)/(\text{H}^+) \quad (5)$$

AH^+ ion, K_w is the autoprotolysis constant for water, and τ is the mean lifetime of an AH^+ molecule before it exchanges a proton with solvent.^{5a,7}

Only the proton exchange processes involving water molecules (eq. 1, 2, and 4) have been investigated for 1. The exclusion of reaction 3 from kinetic studies was

necessitated by the inability to measure the over-all rate of proton exchange in this system. In studies of methylammonium chloride^{5b,7} it was possible to determine the total rate of proton exchange by observing the effect of acidity on the $\text{CH}_3\text{-N}$ quartet. Since coupling between the $\text{CH}_3\text{-C}$ and N-H proton in 1 is immeasurably small this procedure could not be used in the present case. An analysis of the effect of acidity on the N-H resonance signal^{5a} may not necessarily be reliable because of the magnetic difference between the nitrogen protons in 1.⁴ Kinetic studies were therefore limited to study of the effect of variation of the acidity on the water-proton resonance signal.⁷ Under these conditions the rate law given in eq. 6 applies to reactions 1, 2, and 4; $1/\tau'$ is the mean lifetime of an AH^+ mole-

$$1/\tau' = k_4 + k_5K_w/(\text{H}^+) + k_7K_A(\text{AH}^+)/(\text{H}^+) \quad (6)$$

cule before exchange of a proton with water.

The dependence of $1/\tau'$ on acidity and the concentration of 1, is determined from the relationships given in eq. 7 and 8.

$$\tau' = (\text{AH}^+)\tau_{\text{H}_2\text{O}}/2(\text{H}_2\text{O}) \quad (7)$$

$$1/\tau_{\text{H}_2\text{O}} = 1/T_2' - 1/T_2 \quad (8)$$

The quantity $\tau_{\text{H}_2\text{O}}$ is the mean lifetime of protons bonded in water before transfer to nitrogen, T_2' is the transverse relaxation time for solvent protons under non-exchanging conditions, and T_2 is the transverse relaxation time under slow exchange conditions. Equation 8 is valid only under conditions of relatively slow exchange. Rigorous application of eq. 8 requires that $1/T_2'$ and $1/T_2$ be the "natural line widths" of the water-proton signals¹⁰; however, Meiboom⁷ has shown that even under conditions of relatively inhomogeneous magnetic fields (which determine the magnitude of T_2'), eq. 8 is valid as long as the field remains constant during measurements of both T_2' and T_2 . To assure that this was so in our studies, T_2' was determined with pure water samples before and after each measurement of T_2 for solutions of 1. All transverse relaxation time measurements were made under fast passage conditions.¹¹ The experimental results for acetamidinium chloride (1) in aqueous hydrochloric acid solutions are given in Table I.

The dependence of $1/\tau'$ on acidity and amidinium ion concentration at 33° is shown in Fig. 1 and 2. A plot of $\log \tau_{\text{H}_2\text{O}}$ vs. pH, for each amidinium ion concentration, is correlated by a line of slope 1.0. The mean lifetime of protons bonded to water before transfer to nitrogen is thus directly proportional to (H^+) . It may be seen that $1/\tau'$ is apparently independent of (AH^+) (Fig. 1) and this is further confirmed by the ratio (1.8) of the slopes of the two lines in Fig. 2 as compared to the calculated ratio (1.75) of the concentration of 1. Since, within experimental error, the intercept in Fig. 1 is zero the kinetic equation for proton exchange is that given in eq. 9.

$$1/\tau' = k/(\text{H}^+) \quad (9)$$

Since the rate of exchange is inversely proportional to the hydrogen ion concentration and independent of

(10) J. A. Pople, W. G. Schneider, and H. J. Bernstein, "High Resolution Nuclear Magnetic Resonance," McGraw-Hill Book Co., Inc., New York, N. Y., 1959, p. 219.

(11) Reference 10, p. 40.

TABLE I

MEAN LIFETIMES OF PROTONS ON ACETAMIDINIUM IONS AND WATER IN AQUEOUS SOLUTIONS OF ACETAMIDINIUM CHLORIDE (33°)

(AH ⁺), <i>M</i>	pH	(H ⁺) × 10 ⁵ (<i>M</i>)	Density (g./cc.)	(H ₂ O) (<i>M</i>)	1/τ _{H₂O} (sec. ⁻¹)	1/τ' (sec. ⁻¹)
1.750 ± 0.002	5.130 ± 0.005	0.74 ± 0.01	1.0245 ± 0.0002	47.68 ± 0.02	2.18 ± 0.08	119 ± 4
1.750 ± .002	4.950 ± .005	1.12 ± .01	1.0245 ± .0002	47.68 ± .02	1.16 ± .08	63 ± 4
1.750 ± .002	4.810 ± .005	1.55 ± .02	1.0245 ± .0002	47.68 ± .02	0.93 ± .08	51 ± 4
3.059 ± .005	5.080 ± .005	0.83 ± .01	1.0449 ± .0002	41.94 ± .04	3.86 ± .08	106 ± 2
3.059 ± .005	4.540 ± .005	2.88 ± .04	1.0449 ± .0002	41.94 ± .04	1.15 ± .08	32 ± 2
3.059 ± .005	4.290 ± .005	5.13 ± .06	1.0449 ± .0002	41.94 ± .04	0.59 ± .08	16 ± 2

TABLE II

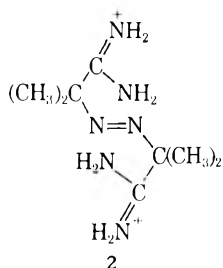
SUMMARY OF RATE CONSTANTS FOR PROTON EXCHANGE. AMMONIUM IONS (25°) AND ACETAMIDINIUM IONS (33°)

Compd.	<i>K_A</i> × 10 ¹⁰ (<i>M</i>)	<i>k₄</i> (sec. ⁻¹)	<i>k₅</i> × 10 ⁻¹⁰ (sec. ⁻¹ <i>M</i> ⁻¹)	<i>k₅K_w</i> × 10 ⁴ (sec. ⁻¹ <i>M</i>)	<i>k₆</i> × 10 ⁻⁸ (sec. ⁻¹ <i>M</i> ⁻¹)	<i>k₇</i> × 10 ⁻⁸ (sec. ⁻¹ <i>M</i> ⁻¹)	<i>k₇K_A</i> × 10 ⁻⁷ (sec. ⁻¹)
NH ₄ ⁺ ^a	5.68	24.4	3.0 (20°)	1.9	11.5	0.9	5.1
CH ₃ NH ₃ ⁺ ^b	0.242	0.90	3.7 (25°)	3.8	4.0	5.3	1.3
			3.2 (19°)	2.0			
(CH ₃) ₂ NH ₂ ⁺ ^c	0.168	0.52	0.5	7.3	1.2
(CH ₃) ₃ NH ⁺ ^c	1.57	4.0	0.0	4.0	6.3
CH ₃ C(NH ₂) ₂ ⁺	(0.001)	<6	3.6	8.0	..	(1)	(0.001)

^a References 4 and 9. ^b References 5 and 7. ^c Reference 8.

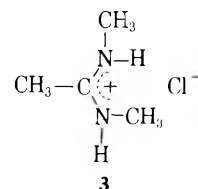
the concentration of AH⁺, we must conclude that of the three mechanisms considered for exchange with solvent, only reaction 2 can be important. Since the intercept of the line in Fig. 1 is zero within experimental error, we conclude that exchange by reaction 1 is negligible. The fact that no term involving second-order dependence of [AH⁺] could be found shows that reactions 3 and 4 must also be negligible. This is a point of special interest since reactions 3 and 4 were found to be dominant in the exchange reactions of ammonium ions. Comparative data for the rates of exchange of various ammonium ions and of 1 with aqueous solvents are shown in Table II.

The contrast between the preferred mechanisms of exchange by ammonium ions on the one hand and acetamidinium ions on the other is easily understood in light of the differences in the acid strengths of the species. The value of *K_A* of 1 in aqueous solution is not known. However, we have attempted to titrate azobisisobutyramidinium chloride, 2, with 0.1 *N* sodium hydroxide in aqueous solution. No inflection point is found in a plot of pH vs. volume of titrant up to pH 12 but some buffering action is observed above that value. Since ammonia is evolved rapidly in solutions of high basicity (because of hydrolysis), no good value of the acidity constant can be obtained. The results indicate that the value of *K_a* for the amidinium ion is of the order of 10⁻¹³.¹² The value of *K_a* for NH₄⁺ is 5.7 × 10⁻¹⁰. Consequently, at a given acidity, the concentration of ammonia in equilibrium with ammonium ion is more than three powers of ten greater than the concentration of an amidine in equilibrium with the related amidinium ion. It is not surprising that reactions 3 and 4 are inconsequential in the latter case.



The rate constant for reaction of ammonium and hydroxide ions has been measured by Eigen and Schoen¹³ and the values of *k₅* have been calculated by Grunwald⁷ on the assumption that the reaction is diffusion controlled. The two values are close enough to encourage the view that reactions such as 2 should be diffusion controlled. The data of Table II yield a value of *k₅* of 3.6 × 10¹⁰ l. mole⁻¹ sec.⁻¹ for acetamidinium chloride. This is in good agreement with the view that exchange occurs by way of reaction 2 and that the reaction is diffusion controlled.

Strong Acid.—It has been previously⁴ shown that the character of the N-CH₃ resonances of aqueous solutions of N,N'-dimethylacetamidinium chloride, 3, is dependent on acidity. Two singlet resonances at 177.5



and 187 c.p.s. (ref. external tetramethylsilane) are observed for these protons in water, while two doublet resonances (*J* = 5 c.p.s.) at 179 and 188.5 c.p.s. arise when the solvent is 14% H₂SO₄. These observations agree with the inverse dependence of nitrogen-proton exchange rate on acidity for 1 (*vide supra*). The splitting of the N-CH₃ resonances is attributed to splitting by adjacent N-H protons and is confirmed by the absence of this splitting in 60% D₂SO₄-D₂O solutions of 3 in which nitrogen protons are replaced by deuterium.⁴

The effect of variation in composition of sulfuric acid-water mixtures on the spectra of the N-methyl proton of 3 is shown in Fig. 3 and 4. The C-CH₃ protons give a sharp singlet resonance independent of acidity. In 14% H₂SO₄, the nitrogen protons give two signals at ~425 and ~455 c.p.s. and a sharp solvent resonance is observed at ~340 c.p.s. Between 15 and 62% H₂SO₄ the N-H protons cannot be observed because

(12) L. Meites and H. C. Thomas, "Advanced Analytical Chemistry," McGraw-Hill Book Co., Inc., New York, N. Y., 1958, p. 91.

(13) M. Eigen and J. Schoen, *Z. Elektrochem.*, **59**, 483 (1955).

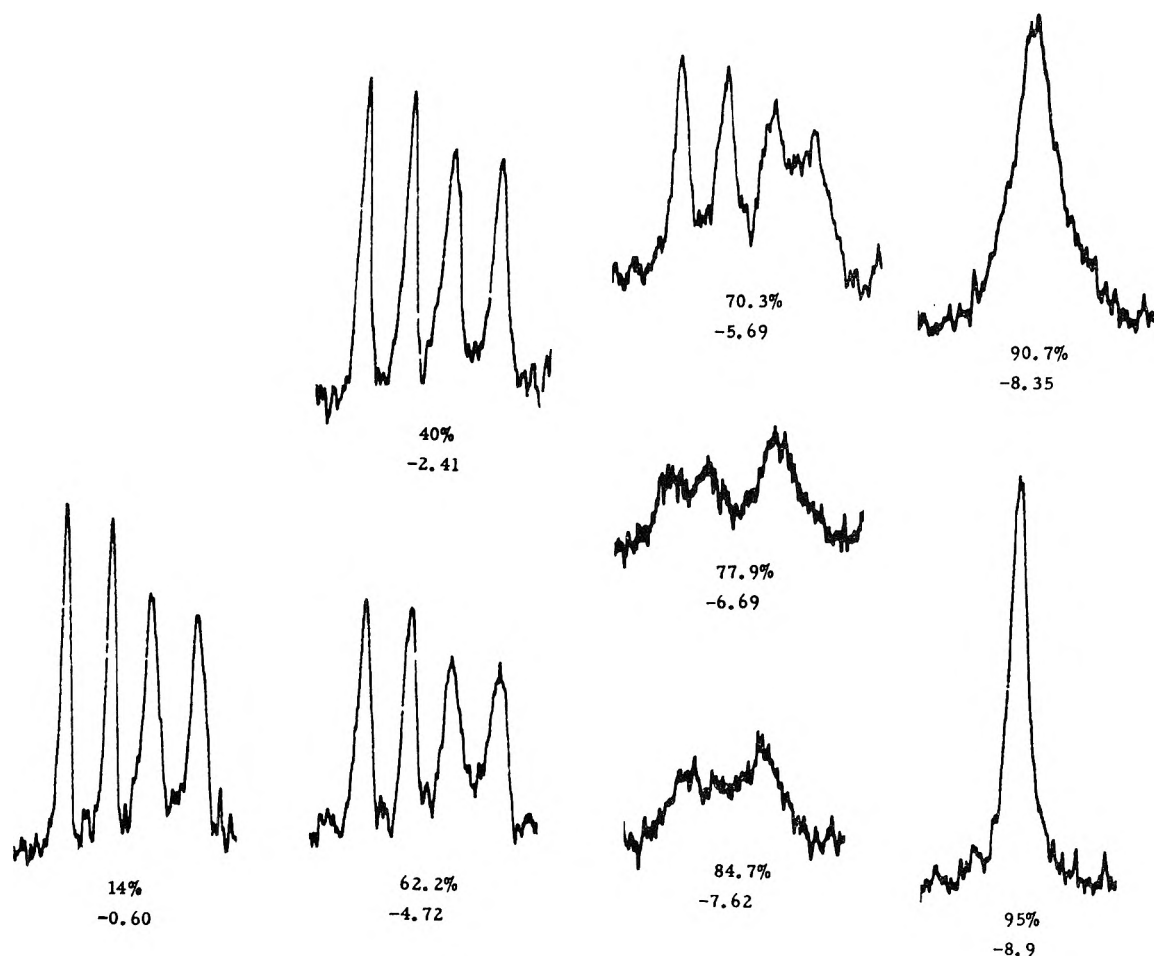


Fig. 3.—Resonance due to N-CH₃ groups of N,N'-dimethylacetamidinium in H₂SO₄-H₂O mixtures. Percentages are weight per cent H₂SO₄.

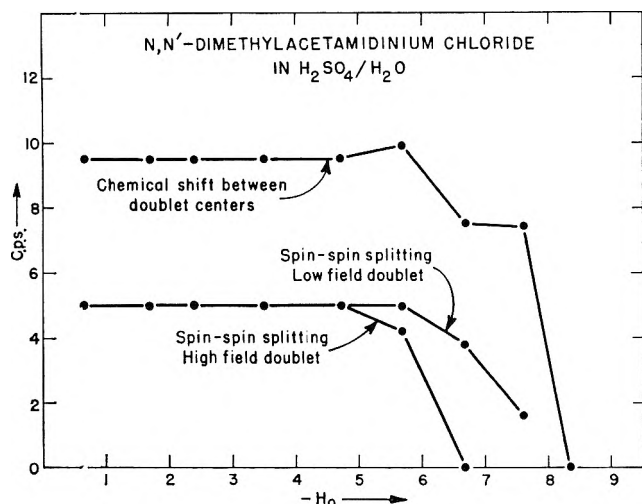


Fig. 4.—Graphical representation of the coalescence of the signals due to N-CH₃ groups in N,N'-dimethylacetamidinium.

the solvent resonance moves downfield obscuring these signals. In 62.2% H₂SO₄ the two N-H signals are again observed at ~433 and ~463 c.p.s. while the solvent signal is a sharp singlet at ~550 c.p.s. In 77.9% H₂SO₄ the lower field N-H signal is quite broad, the higher field signal remains unchanged, and the solvent signal has begun to broaden. In 84.7% H₂SO₄ only the higher field N-H signal at ~410 c.p.s. is visible and the solvent signal is quite broad. In 90.7% H₂SO₄ no N-H signals are observed and the solvent signal is very broad.

The results imply that *two distinct exchange reactions are occurring*. First, the coalescence of the two N-CH₃ doublets into two singlets, and the concomitant changes in the signals from N-H and solvent, must be due to exchange of protons between the cation and the solvent. Second, the coalescence of the N-CH₃ signals into a single, reasonably sharp signal shows that there must be another process which allows methyl groups to pass rapidly between the conformationally different "inside" and "outside" positions in 3. Both reactions are obviously acid-catalyzed. Furthermore, since the two N-CH₃ doublets collapse to singlets in different acidity ranges (Fig. 3), we must conclude that there is a measurable difference in the reactivities of the two nitrogen atoms of 3.

The methyl interchange reaction almost certainly involves rotation about the C-N bonds within the amidinium group. The kinetics of this reaction were studied in 83-88% D₂SO₄-D₂O mixtures. In the deuterated solvent one merely observes the merging of two singlets. The values of 1/τ were determined by the method of Gutowsky and Holm.¹⁴ Figure 5 shows a plot log 1/τ against D₀.¹⁵ The line drawn in Fig. 5 has a slope of 1.1 although the data show too much scatter to permit determination of the slope with much precision. The imprecision arises from the fact that the signals were not cleanly peaked. The concentrations

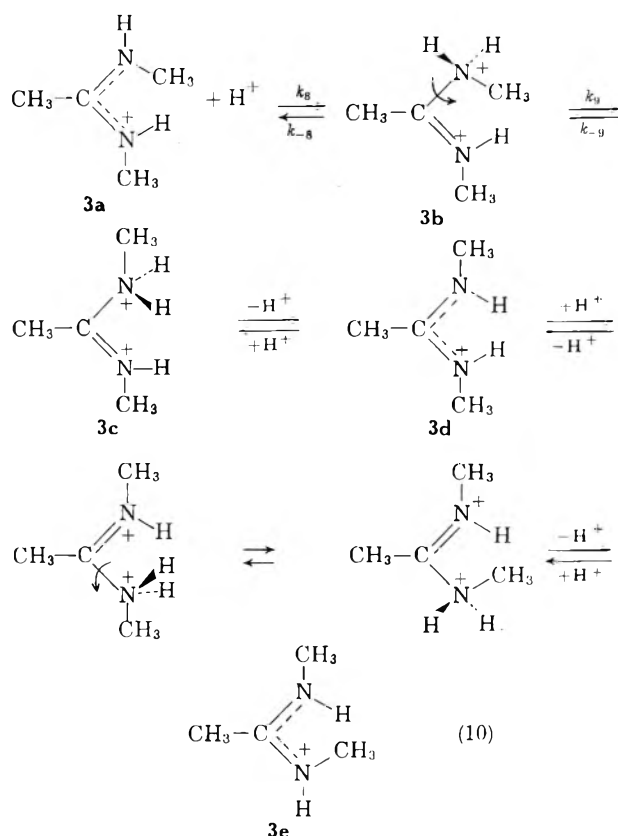
(14) H. S. Gutowsky and C. H. Holm, *J. Chem. Phys.*, **25**, 1228 (1956).

(15) (a) M. A. Paul and F. A. Long, *Chem. Rev.*, **57**, 1 (1957); (b) E. Högfeldt and J. Bigeleisen, *J. Am. Chem. Soc.*, **82**, 15 (1960); (c) D₀ and d₀ are analogous to the Hammett acidity constants H₀ and h₀.

of **3** were only known approximately so it is not possible to assess the possibility that some of the scatter arises from reactions which are second order with respect to the concentration of amidinium ion. Tentatively we conclude that $1/\tau$ shows first-order dependence on d .

$$\frac{1}{\tau} = kd_0^c; 0.8 < c < 1.3$$

It did not seem feasible to study the merging of the methyl doublets into singlets in detail because broadening of the peaks by the methyl exchange reaction begins before the disappearance of the doublets is complete. Since the reaction is obviously acid-catalyzed, we propose the following mechanism which interrelates the two exchange processes.



The rates of the exchange reactions with the solvent are determined by the rates of protonation of **3a** to form **3b** and its isomer in which the extra proton is bound to the other nitrogen atom. Interchange of the positions of the two N-CH₃ groups requires that each nitrogen atom pass through a freely rotating condition and also appears to require the intermediacy of either **3d** or the other symmetrical isomer in which both methyl groups occupy "inside" positions. Involvement of these high energy amidinium ions is consistent with the observation that methyl interchange is slower than exchange of protons with the solvent. We have no way of knowing whether k_9 or some subsequent proton transfer is rate-limiting in the interchange process.

The difference in the rates of conversion of the two doublets to singlets shows that the rates of protonation of the two nitrogen atoms of **3a** are different (Fig. 3 and 4). Values of τ for both N-H resonances in 70.3 and 77.9% sulfuric acid were estimated by the method of Gutowsky and Holm.¹⁴ Assuming that the equa-

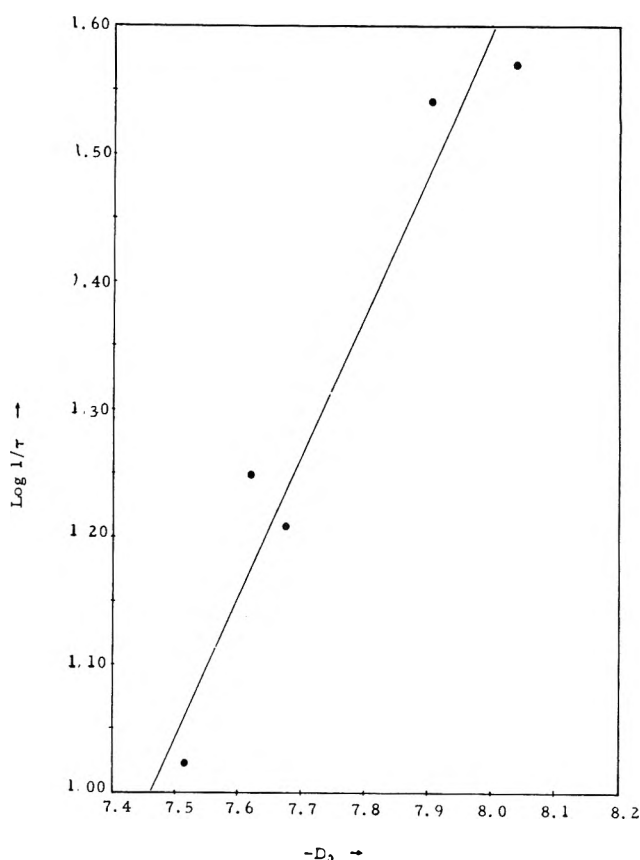


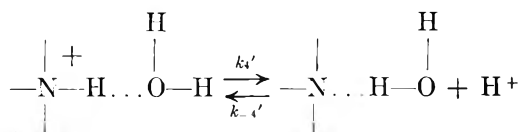
Fig. 5.—Dependence of $1/\tau$ for the methyl interchange reaction of N,N'-dimethylacetamidinium ion on acidity.

tion, $1/\tau = kh_0$, applies to both exchange processes one can calculate that the ratio $k_{\text{high field}}/k_{\text{low field}}$ is 6.4. The result $k_{\text{high field}} > k_{\text{low field}}$ has been confirmed independently. A sample of **3a** was dissolved in 28% D₂SO₄-D₂O and the spectra of the solution then scanned repeatedly with the results shown in Fig. 6. Before the first scan could be completed (~15 sec. after mixing) the high field resonance was almost entirely collapsed to a singlet, indicating that exchange of protons for deuterons was virtually complete. Complete collapse of the low field doublet required almost 100 sec. Since the high field resonance has been assigned to the proton attached to nitrogen bearing an "inside" methyl group, we believe that center is the more reactive of the two basic sites. The effect is probably due to the fact that both protons attached to that nitrogen in **3b** are exposed solvation sites.

The rate constant for the methyl interchange reaction (**3a** → **3e**) was estimated by observing the rate of coalescence of the two N-CH₃ signals in D₂SO₄ and assuming that $1/\tau = k_{\text{interchange}} h_0$. The relative rates are: $k_{\text{high field}}:k_{\text{low field}}:k_{\text{interchange}} \cong 40:6:1$.

Grunwald⁶ has studied the proton exchange reactions of ammonium ions in concentrated sulfuric acid solutions and found an inverse dependence of rate on acidity.

The results were explained in terms of a mechanism involving proton transfer to a water molecule with solvent relaxation (k_H') being the rate-determining step.



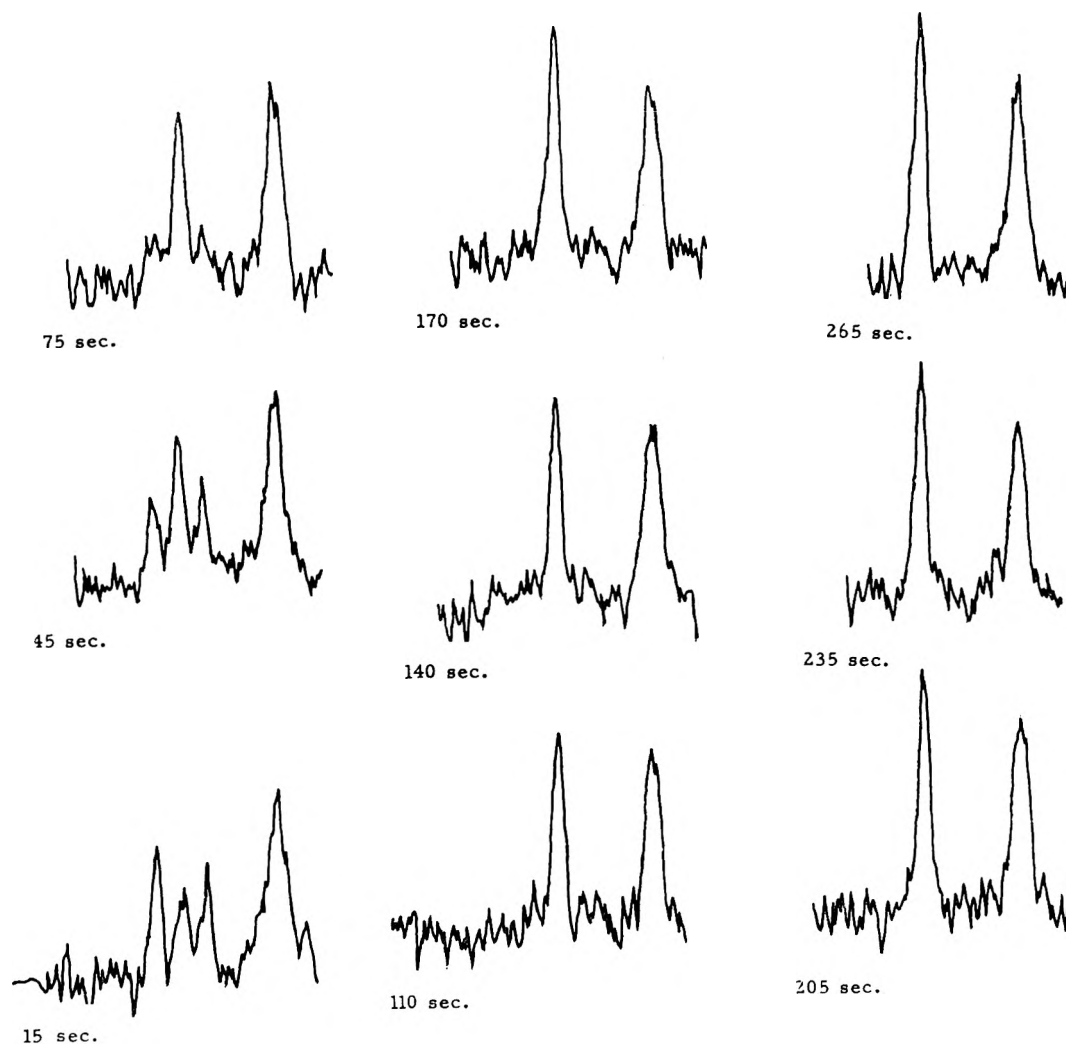
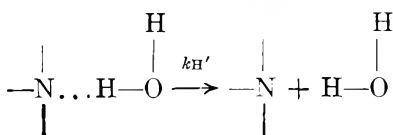


Fig. 6.—Collapse of the N-CH₃ doublets in the spectrum of N,N'-dimethylacetamide in 28% D₂SO₄-D₂O.



The proton addition mechanism observed with amidinium ions is of course impossible for ammonium ions; however, the Grunwald mechanism might well be operative with amidines. However, the ionization constants k_4'/k_{-4}' should be proportional to the acidity constants of the onium ions so one would expect k_4 for an amidinium ion to be about three orders of magnitude smaller than it is for NH₄⁺. The mechanism is superseded in concentrated acid by reaction sequence 10 and in dilute acid by reaction 2. The behavior in concentrated acid would not have been predictable on an *a priori* basis. However, given the observed rates of exchange of amidinium ions in concentrated acid, one would surely conclude that a new mechanism must be involved. For example, the rate constant for exchange of CH₃ND₃⁺ with 34% sulfuric acid at 25° is 2×10^{-3} sec.⁻¹. The half-lives for exchange of the NH groups of 3a with 28% D₂SO₄ were only a few seconds for one proton and perhaps 40–50 sec. for the other. While reaction by the Grunwald mechanism should have been faster in 28% acid than in 34% acid, it is evident that the expected large difference in rate between ammonium and amidinium ions is not observed. The incursion of reaction 2 in dilute acid

could have been anticipated. The rate of such a reaction is probably fixed at the diffusion-controlled rate. The first-order rate constant for ionization of NH₄⁺ in dilute aqueous solution is 24 sec.⁻¹ at 25°. The value is reduced to $\sim 10^{-4}$ sec.⁻¹ for an amidinium ion; at pH 4 the value of $k_5[\text{OH}^-]$ should be of the order 0.1–1.0 sec.⁻¹ so reaction 2 should be dominant.

Experimental

Materials.—Sulfuric acid, DuPont reagent grade, was used without further purification. Sulfuric acid-d₂ was prepared¹⁶ from Baker and Adamson "Sulfan B" (sulfur trioxide) and deuterium oxide (99.5%), General Dynamics Corporation, and shown to be isotopically pure by n.m.r. analysis. Acetamidinium chloride (1) and N,N'-dimethylacetamidinium chloride (3) have been previously described.³ Tap distilled water was used for the H₂SO₄-H₂O mixtures and de-ionized water was used for the studies with dilute hydrochloric acid. Deuterium oxide (99.5%), General Dynamics Corporation, was used in preparation of D₂SO₄-D₂O mixtures.

N.m.r. Spectrometers.—Measurements with sulfuric acid solutions were performed with a Varian A-60 n.m.r. spectrometer operating at 60 Mc.p.s. Those with dilute hydrochloric acid solutions were performed with a Varian Model V-4300 B(HR-60) spectrometer operating at 60 Mc.p.s., equipped with a Superstabilizer and a Sanborn high speed recorder.

Dilute Hydrochloric Acid Studies.—An aqueous solution of acetamidinium chloride 1 of approximate desired concentration was prepared and the concentration determined by titration of chloride ion in aliquots using an adsorption indicator.¹⁷ The

(16) A. P. Best and C. L. Wilson, *J. Chem. Soc.*, 239 (1946).

(17) A. R. Olson, C. W. Koch, and G. C. Pimentel, "Introductory Quantitative Chemistry," Freeman and Co., San Francisco, Calif., 1956, p. 272.

density of the solution was also determined with aliquots of the solution. The pH of the remaining solution was decreased by dropwise addition of concentrated hydrochloric acid with stirring. Aliquots were taken at appropriate pH values (Beckman Model G pH meter with Beckman glass and calomel electrodes) and placed in n.m.r. tubes which were immediately sealed and immersed in a Dry Ice-isopropyl alcohol slurry until spectra were recorded. Spectra of the water-proton resonance were recorded under fast-passage conditions¹¹ using the "saw-tooth" sweep unit of the spectrometer. Care was taken to ensure reproducible homogeneity of the field. All samples were run consecutively and spectra of a sample of pure water were run between each pair of

determinations to ensure that the field remained constant. Results for the pure water sample were $1/\tau_2' = 2.04 \pm 0.06 \text{ sec.}^{-1}$ for six determinations.

Concentrated Sulfuric Acid Solutions.—The compositions of the $\text{H}_2\text{SO}_4\text{-H}_2\text{O}$ and $\text{D}_2\text{SO}_4\text{-D}_2\text{O}$ mixtures were determined by titration of weighed amounts with standardized aqueous sodium hydroxide. Values of H_0 and D_0 were determined from data of Paul and Long.^{15a} Bigeleisen^{15b} has shown that data for H_2SO_4 apply equally well for D_2SO_4 in the composition range involved. Solutions of 3 were prepared with cooling, transferred to n.m.r. tubes, immediately sealed, and immersed in a Dry Ice-isopropyl alcohol slurry until the spectra were recorded.

EXCESS THERMODYNAMIC PROPERTIES OF THE BINARY LIQUID SYSTEM ETHYLENE GLYCOL-METHANOL

By P. D. CRATIN¹ AND J. K. GLADDEN

Chemistry Department, The Agricultural and Mechanical College of Texas, College Station, Texas

Received February 2, 1963

The excess thermodynamic properties of the binary liquid system ethylene glycol-methanol have been determined at 25°. This system shows small positive deviations from Raoult's law. The mixing process is slightly endothermic. The entropy of mixing is negative. There is a small contraction in volume upon mixing. The n.m.r. spectrum of this system shows some very unusual properties. An attempt is made to offer a plausible explanation for the observed behavior of this system.

Introduction

Interest in the ethylene glycol-methanol system was aroused by statements in the literature concerning binary mixtures of monohydric alcohols. In 1924 Parks and Schwenk² reported that mixtures of ethanol and 1-propanol formed ideal solutions throughout the entire composition range at 39.90°. In 1953, Mitchell and Wynne-Jones³ stated that from available literature data, the systems ethanol-methanol and ethanol-1-propanol "form ideal solutions with zero values for all excess functions." Furthermore, these authors seem to imply that all mixtures of monohydric alcohols should exhibit ideal behavior.

A recent American Petroleum Institute compilation of the results from thirty-four laboratories⁴ on the vapor pressure of methanol brought out some inconsistencies. These findings, further substantiated in this Laboratory, show the vapor pressure of methanol to be 2 to 4% higher than the previously accepted value.⁵ If the more recent data are correct, then it is doubtful whether the reported excess free energies for methanol solutions are correct. It has been found⁶ that methanol in contact with boron-containing glass produces trimethyl borate in substantial quantities (as high as 12 mole %). Thus, it is conceivable that some of the reported values for the vapor pressure of methanol were low due to the trimethyl borate present.

Some inconsistencies exist in the literature concerning aqueous solutions of ethylene glycol. Curme⁷ has reported a volume contraction of 1.4% at 50% volume

concentration whereas a recent publication by Fogg⁸ stated that there is almost a linear relationship between the composition and density of aqueous ethylene glycol solutions.

Experimental

Chemicals.—The methanol used in this research was Fisher's reagent grade ("suitable for Karl Fischer reagent"). The methanol was purified by the method outlined by Vogel.⁹ The fraction distilling between 64.45 and 64.55° was collected and used in this investigation. The refractive index, n_D^{25} , of this fraction was 1.3269, and the density at the same temperature was 0.7867 g. ml.⁻¹. The methanol used for the vapor pressure determinations in this research had been stored no longer than a month in a Pyrex container; a flame test as outlined by Scott¹⁰ confirmed the absence of borates in the methanol.

The ethylene glycol used in this work was Matheson, Coleman and Bell reagent grade material, whose normal boiling point had a range of 195 to 197°. Four different methods were employed to purify this reagent grade material. (1) Distillation of the glycol under reduced pressure. The middle fraction which distilled at 110° (28.5 mm.) was collected. (2) Distillation of the glycol at atmospheric pressure. The middle fraction having a boiling point range of ca. 0.3° was collected. (3) Water and other low boiling materials were removed by prolonged heating at 110° and 50 mm. pressure, and the pot charge was saved. (4) The water and other low boiling materials were removed by maintaining a temperature of 25° and a pressure of 5 mm. for a period of 10 to 12 hr. The pot charge was saved and used for this investigation.

No difference could be detected in the refractive index of the products obtained from the above four methods. The refractive index, n_D^{25} , was 1.4302; the density at 25° was 1.1103 g. ml.⁻¹.

Temperature Control.—The temperature control was achieved by means of a Sargent S-83805 Thermostatic, 0.01°, mercurial regulator, reactor controller water bath. A Beckmann differential thermometer, previously calibrated at 20 and 25° with Bureau of Standards thermometers, was immersed in the bath to facilitate temperature readings. The temperature was controlled to $\pm 0.02^\circ$ for all the refractive index, density, and vapor pressure measurements.

(8) E. T. Fogg, A. N. Hixson, and A. R. Thompson, *Anal. Chem.*, **27**, 1609 (1955).

(9) A. I. Vogel, "A Textbook of Practical Organic Chemistry," Longmans Green and Co., London, 1951, pp. 167-168.

(10) W. W. Scott, "Standard Methods of Chemical Analysis," D. Van Nostrand Co., Inc., New York, N. Y., Vol. I, p. 162.

(1) Abstracted from the Ph.D. Dissertation submitted by P. D. Cratin to the Agricultural and Mechanical College of Texas, 1962.

(2) G. S. Parks and J. R. Schwenk, *J. Phys. Chem.*, **28**, 720 (1924).

(3) A. G. Mitchell and W. F. K. Wynne-Jones, *Discussions Faraday Soc.*, **15**, 161 (1953).

(4) "Selected Values of Properties of Hydrocarbons and Related Compounds," American Petroleum Institute Research Project 44, Vol. I.

(5) T. E. Jordan, "Vapor Pressures of Organic Compounds," Interscience Publishers, Inc., New York, N. Y., 1954, p. 65.

(6) R. P. Porter, *J. Phys. Chem.*, **61**, 1260 (1957).

(7) G. O. Curme, "Glycols," A. C. S. Monograph Series Number 114, Reinhold Publ. Corp., New York, N. Y., 1952, p. 36.

Refractive Index-Composition.—The refractive index-composition data were determined by adding weighed samples of purified glycol and methanol from weight burets into 60-ml. Pyrex bottles fitted with ground glass stoppers. The refractive index (using the D-line of sodium) of each freshly-prepared solution was immediately measured with a Bausch and Lomb Abbé 3L refractometer, which was thermostated to $25.00 \pm 0.02^\circ$. By this method, mole fractions to ± 0.001 could be determined. The results of these measurements are given in Table I.

TABLE I
REFRACTIVE INDICES OF ETHYLENE GLYCOL-METHANOL
SOLUTIONS AT 25°

$x_{\text{CH}_2\text{OH}}$	Refractive index, n_D^{25}	$x_{\text{CH}_2\text{OH}}$	Refractive index, n_D^{25}
1.000	1.3269	0.520	1.3900
0.931	1.3383	.469	1.3951
.905	1.3424	.350	1.4058
.878	1.3466	.302	1.4096
.792	1.3589	.292	1.4103
.771	1.3618	.225	1.4155
.728	1.3668	.177	1.4189
.714	1.3688	.126	1.4224
.692	1.3718	.0883	1.4249
.624	1.3793	.000	1.4302

Excess Volume.—Weld specific gravity bottles of approximately 25-ml. capacity were used in all volume determinations. The bottles were fitted with standard taper matched capillaries and caps to minimize evaporation during a determination. The volume of each specific gravity bottle was determined from the accepted values of the density of water. Duplicates fortuitously checked to within four parts in 250,000.

Table II gives the values of the excess volumes V^E for this binary system at 25° .

TABLE II
MOLAR EXCESS VOLUMES OF MIXING OF ETHYLENE GLYCOL-
METHANOL SOLUTIONS AT 25°

$x_{\text{CH}_2\text{OH}}$	V^E (ml. mole ⁻¹)	$x_{\text{CH}_2\text{OH}}$	V^E (ml. mole ⁻¹)
1.000	0.000	0.624	-0.654
0.931	-.252	.520	-.642
.905	-.320	.469	-.605
.878	-.388	.350	-.526
.792	-.536	.302	-.456
.771	-.549	.126	-.206
.728	-.595	.0883	-.152
.714	-.610	.000	.000

The mixing process is accompanied by a contraction in volume; the maximum contraction occurs at approximately 60 mole % methanol. At this maximum V^E is approximately -0.65 ml. mole⁻¹, or about 1.4%.

The over-all accuracy of the excess volume data is estimated to be approximately $\pm 1\%$.

Vapor Pressure Measurements.—The vapor pressures of the ethylene glycol-methanol system were measured by the static method. The bulb which contained the liquid mixture had a volume of approximately 50 ml. The apparatus was constructed entirely of Pyrex glass.

After the charge was placed in the bulb and the apparatus assembled, the bulb was immersed in liquid nitrogen to freeze the contents. The system was then pumped down with a Cenco vacuum pump. Successive freezing-thawing operations were carried out during the evacuation to remove dissolved gases from the solution. Usually, five to seven freezing-thawing operations were required to remove all evidence of dissolved gases. After removal of the dissolved gases, the vacuum stopcock between the apparatus and the vacuum pump was closed and the flask immersed in a constant temperature bath. The absolute vapor pressures were read from a mercury-sealed manometer with a 100-cm. cathetometer calibrated in 0.05 mm.

The liquid solutions were periodically shaken to increase the attainment of liquid-vapor equilibrium. When the pressure variation over a 12-hr. period was no greater than ± 0.05 mm., it was assumed that equilibrium had been established, and the vapor pressure was recorded.

Upon completion of a run, air was carefully bled into the system and the composition of the solution was determined by measuring the refractive index.

The activity coefficients calculated from the measured vapor pressures showed some scattering when plotted *vs.* the composition of the solution. The largest deviations occurred at the higher methanol concentration. Since the reproducibility of the vapor pressure measurements was very good, it was thought that the deviations might be due to the non-ideal behavior of the vapor. An attempt was made to correct for some of the vapor imperfection by means of the equation

$$\ln f = \ln p + Bp/RT \quad (1)$$

Where f is the fugacity, p , the measured pressure, B , the second virial coefficient, and R and T have their usual significance. Kretschmer and Wiebe¹¹ have measured the second virial coefficient, B , of methanol vapor in the temperature range required. They have found that the temperature dependence of B could be expressed by the equation

$$B = -100 - 2.148 \exp(1986/T) \text{ ml. mole}^{-1} \quad (2)$$

When the fugacities were computed, the activity coefficients were calculated; from these values a smooth curve could be drawn through the points.

Activity Coefficients.—From a knowledge of the relative fugacities and mole fraction of methanol, the activity coefficients of methanol were calculated by eq. 3.

$$\gamma_i = f_i/x_i f_i^0 \quad (3)$$

where x_i is the mole fraction of methanol in the solution, f_i^0 is the standard fugacity of pure methanol at a given temperature, and f_i is the measured fugacity of methanol over the solution at the same temperature. In order to determine the activity coefficients of glycol in the solutions, glycol was treated as if it were a non-volatile material. This should be a good approximation since the vapor pressure of pure glycol at 25° is only approximately 0.1 mm.

The activity coefficients of ethylene glycol were determined by the graphical integration of the equation

$$\ln \gamma_2 = - \int_{x_1/x_2=0}^{x_1/x_2} (x_1/x_2) d \ln \gamma_1 = - \sum (x_1/x_2) \Delta \ln \gamma_1 \quad (4)$$

The subscript 1 refers to methanol and the subscript 2 to glycol.

Excess Chemical Potentials.—The excess chemical potentials for methanol and glycol were calculated from the activity coefficients by means of the equation

$$\mu_i^E = RT \ln \gamma_i \quad (5)$$

The results of the above calculations are given in Table III.

The Excess Gibbs Free Energies.—The excess Gibbs free energies of these binary mixtures were calculated from the activity coefficients of the two components from eq. 6

$$g^E = RT \sum_{i=1}^2 x_i \ln \gamma_i \quad (6)$$

As in the case of the excess volumes, the curve of g^E *vs.* mole fraction of methanol is slightly skewed toward the higher methanol concentrations. The maximum appears to lie at approximately 55 mole % methanol where g^E has a value of 55.42 cal. mole⁻¹.

TABLE III

FUGACITIES, ACTIVITY COEFFICIENTS, AND EXCESS CHEMICAL POTENTIALS OF ETHYLENE GLYCOL AND METHANOL AT 25°

$x_{\text{CH}_3\text{OH}}$	$f_{\text{CH}_3\text{OH}}$ (mm.)	$\gamma_{\text{CH}_3\text{OH}}$	γ_{EtG1}	$\mu_{\text{CH}_3\text{OH}}$ (cal. mole ⁻¹)	μ_{EtG1} (cal. mole ⁻¹)
0.00	1.000	0.00
.10	16.71	1.330	1.002	169.06	0.89
.20	31.92	1.270	1.009	141.69	5.31
.30	45.73	1.213	1.025	114.47	14.81
.40	58.26	1.159	1.049	87.47	28.58
.50	69.68	1.109	1.087	61.33	49.45
.60	80.68	1.070	1.135	40.10	75.28
.70	91.58	1.041	1.197	23.82	106.35
.80	102.65	1.021	1.267	12.32	140.43
.90	114.00	1.008	1.335	4.72	171.06
1.00	125.67	1.000	...	0.00

Excess Enthalpies.—A sketch of the calorimeter used in measuring the heats of mixing is shown in Fig. 1. D is a 665-ml. dewar flask; C, an inner glass tube of approximately 230-ml. capacity; B, a machined nylon sleeve; F, a heater with a resistance of 45.93 ohms at 25° and a temperature coefficient of 5.1×10^{-3} ohm per degree. H is a General Electric disk-type (D-203) thermister with a resistance of 1000 ohms ($\pm 10\%$ at 25°). The thermister was calibrated with a Bureau of Standards platinum resistance thermometer between 18 and 30°. The relationship between the temperature and the logarithm of the resistance proved to be linear in this range. The slope calculated by the method of least squares, gave the relationship below.

$$\frac{\Delta T(^{\circ}\text{C.})}{\Delta \log \Omega} = -49.856 \quad (7)$$

where ΔT is the change in temperature in degrees centigrade, and $\Delta \log \Omega$ is the change in the logarithm of the resistance of the thermister. E is a $1/4$ inch o.d. glass tube for transferring the liquid in the outer to the inner compartment. G is the stirrer for mixing. A copper flange was fastened around the upper rim of the dewar flask, and the cover for the flask had a copper sheet which made contact with the flange when the calorimeter was assembled. The shaft from the stirrer motor entered the calorimeter through a mercury seal.

Procedure for Measuring Heats of Mixing.—After the calorimeter was assembled and placed in the constant temperature bath, which was controlled to $\pm 0.015^{\circ}$, 0.25 ml. of mercury was added to form a seal between the inner and outer compartments of the calorimeter. The calorimeter charge was then added by the use of dry compressed air to transfer the pure liquids from flasks to the calorimeter. The calorimeter and charge were then allowed to stand in the constant temperature bath until thermal equilibrium was established (usually 10–12 hr.).

Prior to mixing, the stirrer was started, and a "drift" rate was recorded for 7–10 min.

For runs in which methanol was placed in the outer compartment of the calorimeter, the compressed air used in the transfer process was first dried by passing through a 30-in. silica gel column; it was then sparged through calcium oxide-dried methanol. The air, now saturated with methanol, was allowed to equilibrate in a 10-ft. coil of copper tubing in the constant temperature bath. When ethylene glycol was placed in the outer compartment, the sparging treatment was omitted.

Mixing was effected by placing a piece of polyethylene tubing (attached to the copper coil) over the nozzle leading to the outer compartment. Sufficient air pressure was applied to transfer the liquid in the outer compartment to the inner one. Transfer was adjudged complete when the mercury in a manometer (in series with the system) suddenly fell. One ml. of mercury was immediately injected by a hypodermic syringe into the outer compartment to prevent vapor transfer between the compartments.

As soon as possible, resistance readings were recorded, and a post-mixing "drift" rate was established for 10–15 min.

After the post-mixing "drift" rate, electrical energy was added to bring the calorimeter and contents back to near the pre-mix temperature. In this manner a heat of mixing (usually within 1–2 cal.) could be determined.

When thermal equilibrium had been established (several

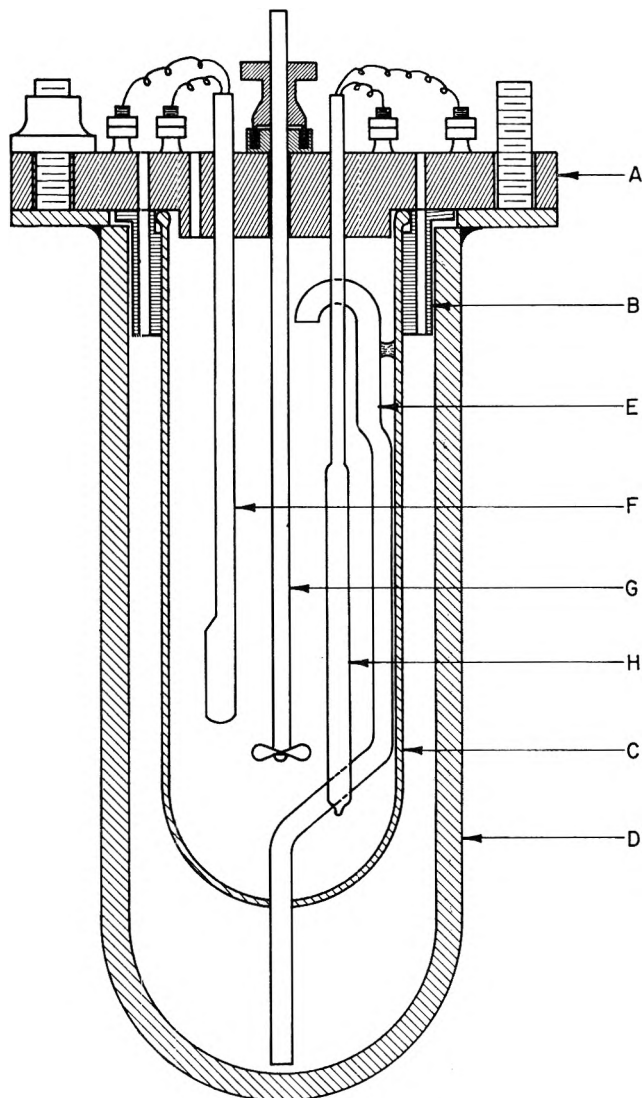


Fig. 1.—Calorimeter.

hours later), the stirrer was again started and another 7–10 min. "drift" rate determined. Sufficient electrical energy was added to change the temperature by approximately 0.2° , and another post-"drift" rate determined. From this information, the heat capacity of the system could be determined. With the change in temperature for the mixing process, and the heat capacity of the system known it was possible to obtain the enthalpy of mixing. In order to obtain the molar heat of mixing it is only necessary to divide the heat of mixing by the number of moles in the mixture.

The thermister was placed in one arm of a Wheatstone bridge circuit; the ratio arms were each 1000 ohms. The detector used in the bridge circuit was a Leeds and Northrup (type E, guarded) d.c. galvanometer (sensitivity of 5×10^{-10} amp./mm.), and this was equivalent to 4.5×10^{-6} deg./mm. scale deflection.

The circuit used for measuring the input of electrical energy to the calorimeter was of the conventional type.

All calorimetric determinations were carried out in a room set at 40% relative humidity, and the temperature of the room was controlled to $25 \pm 0.5^{\circ}$.

It is believed that the accuracy in the heat of mixing measurements was within 1 cal.

The smoothed values for the excess enthalpies, Gibbs free energies, and entropies of mixing for this binary system at 25° are given in Table IV and are depicted graphically in Fig. 2.

N.m.r. Spectra of Ethylene Glycol-Methanol Solutions at 35°.—Proton resonance spectra were measured for the two pure components and twelve solutions. The majority of the solutions were taken directly from the calorimeter after the completion of a run. Thus, these samples were not especially purified for n.m.r. spectral studies, nor was all contact of the solutions with air prevented. A Varian 60 Mc. proton resonance spectrometer was used in making the measurements.

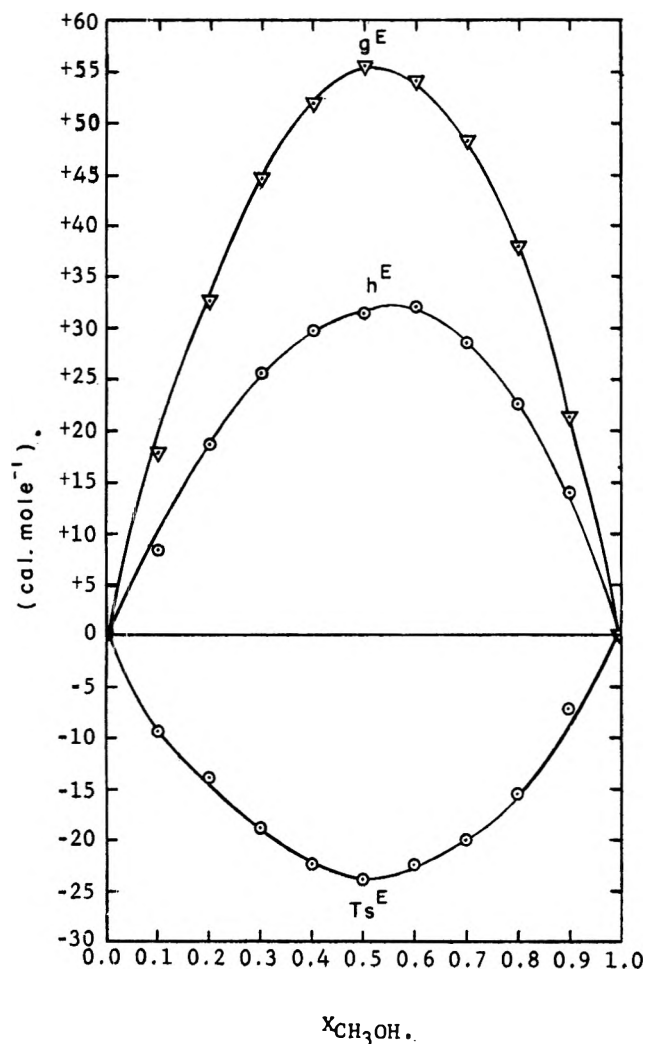


Fig. 2.—Excess enthalpies, Gibbs energies, and entropies of mixing vs. composition at 25°.

TABLE IV
EXCESS ENTHALPIES, GIBBS FREE ENERGIES, AND ENTROPIES OF MIXING AT 25°

$x_{\text{CH}_3\text{OH}}$	h^E (cal. mole ⁻¹)	g^E (cal. mole ⁻¹)	T_s^E (cal. mole ⁻¹)
0.00	0.00	0.00	0.00
.10	8.20	17.72	-9.52
.20	18.63	32.58	-13.95
.30	25.67	44.72	-19.05
.40	29.62	52.13	-22.51
.50	31.47	55.39	-23.92
.60	31.70	54.18	-22.48
.70	28.40	48.48	-20.18
.80	22.35	37.95	-15.60
.90	14.07	21.35	-7.28
1.00	0.00	0.00	0.00

Tetramethylsilane was used as an internal standard in all spectra studies, and all spectral shifts were measured relative to that of tetramethylsilane which is taken as zero.

The proton resonance peak for the methanol hydroxyl occurs at 4.78 p.p.m. to the low magnetic field side of tetramethylsilane, and that of the glycol hydroxyls at 5.18 p.p.m., also to the low field side of the internal standard.

The most interesting spectral region of this system is that section where both the glycol and methanol hydroxyl protons exhibit resonance. Figure 4 shows tracings of this part of the n.m.r. spectra. The two vertical dashed lines in Fig. 3 indicates the positions at which proton resonance spectra of the hydroxyl protons occur in the pure components. The X associated with each spectra refers to the mole fraction of methanol in the solution.

Some of the more prominent features of the n.m.r. spec-

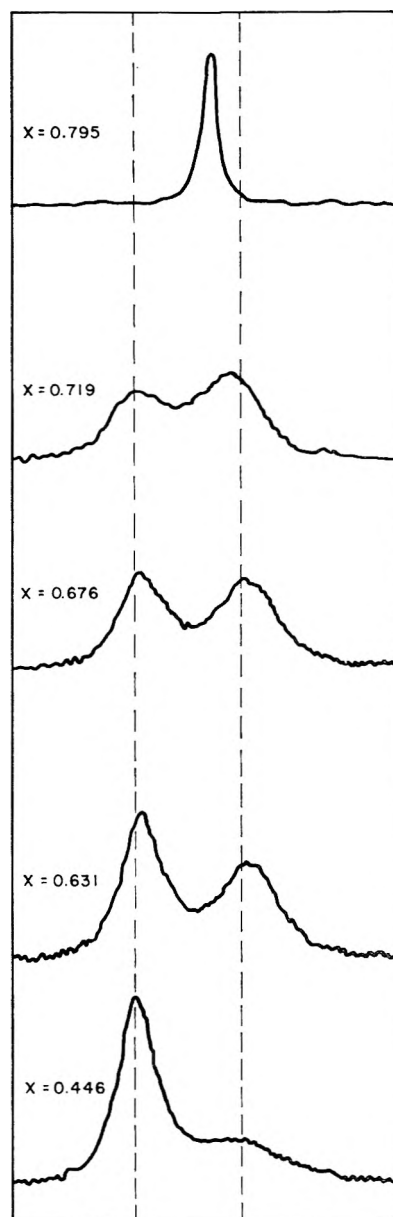


Fig. 3.—N.m.r. spectra of ethylene glycol-methanol solutions at 37°.

tra should be noted: (1) When methanol is added to glycol, only a single resonance OH proton peak is obtained up to a mole fraction of methanol of approximately 0.2. (2) A small "hump," much broadened, begins to appear at methanol mole fractions greater than approximately 0.3. (3) This "hump" continues to increase in height with increase in mole fraction of methanol in the solution, and the two peaks become of approximately the same height at a mole fraction of about 0.67. (At this mole fraction the number of methanol OH groups is equal to the number of glycol OH groups.) (4) Only a single peak is obtained at methanol mole fractions greater than 0.795, and this peak shifts toward that characteristic of the pure methanol as the methanol mole fraction increases.

Discussion

The present state of solution theory and the very limited knowledge which exist about the dependence of the intermolecular potential energy of interaction among associated molecules on distance and orientation make it impossible to give a quantitative description of the observed properties of these highly associated systems. The authors shall, therefore, offer a tentative qualitative explanation which appears to them to be both reasonable and to be in agreement with the observed properties of this binary system.

The evidence from the entropies of vaporization, surface tension, thermal conductivity, coefficient of thermal expansion, isothermal compressibility, sound velocity, and internal pressure indicates that ethylene glycol contains more hydrogen bonds per unit volume than does methanol. The n.m.r. hydroxyl proton shifts would also probably imply that the hydrogen bonds are not only more numerous in glycol but that they might perhaps also be somewhat stronger.

Due to difference in size, shape, strength of hydrogen bond, and number of hydroxyl groups per molecule the average statistical configuration of methanol molecules in the pure liquid state will be different from the average statistical configuration of glycol molecules in the pure liquid state. When a small number of methanol molecules are added to pure glycol the methanol molecules must be incorporated into the glycol configuration. This accommodation could be accomplished by the methanol molecules hydrogen bonding to the oxygen atoms in glycol which are already involved in hydrogen bonds in glycol chains or rings, or by hydrogen bonding in one of two ways with the free hydroxyl groups at the end of glycol chains. In either case the average statistical configuration would be that of the glycol structure. The same argument could be applied to methanol solutions containing a small amount of glycol, except the average statistical configuration would be that characteristic of methanol. As the number of solute molecules is increased in the solution the average statistical configuration of the molecules in the solution must change if the two molecular species differ in size, shape, hydrogen bond strengths, and number of hydroxyl groups per molecule. This new statistical configuration could be one in which the molecules of the two

molecular species were more or less randomly distributed in the solution, or there could be a preference for each of the molecular species to prefer their own configuration environment thus leading to partial "clustering" of the two molecular species into two somewhat different average statistical configurations which coexist in the same solution. These configurations are to be viewed as an assemblage of molecules whose average configuration lifetime is longer than the time required for them to disperse and regroup with new members into a new but similar configuration. The times required for the above processes could very well be of the order of a microsecond or less.

When the "clustering" effect become very large it can lead to phase separation. Measurements of many different types indicate that there is partial "clustering" in solutions which contain alcohols dissolved in non-polar solvents.

The n.m.r. spectra of glycol-methanol solutions would seem to indicate that perhaps there is a tendency for partial "clustering," especially in the concentration range of methanol between mole fractions of 0.5 to approximately 0.72.

The excess thermodynamic properties imply that the binary system glycol-methanol is less stable than would be an ideal solution formed from the same two components, and that this decrease in stability is due both to an energy and entropy factor which make about equal contributions.

Acknowledgment.—The partial financial support of this research by the Chemstrand Corporation is gratefully acknowledged. Appreciation is extended to Mr. W. D. Henderson for his construction of the calorimeter.

A HIGH TEMPERATURE CALORIMETER: THE ENTHALPIES OF α -ALUMINUM OXIDE AND SODIUM CHLORIDE

BY RAPIER DAWSON, ELIZABETH B. BRACKETT,* AND THOMAS E. BRACKETT*

Department of Chemistry, William Marsh Rice University, Houston, Texas

Received February 4, 1963

The construction and operation of a high temperature calorimeter is described. The enthalpy of a sample of α -aluminum oxide furnished by the National Bureau of Standards has been measured from 750 to 1400°K. and found to be about 0.3% higher than the enthalpy reported by the N.B.S. in the region in which it can be compared. The enthalpy of sodium chloride has been measured and found to fit the equations ($H_T - H_{298.15}$) = $10.45T + 0.002442T^2 - 3334$ cal./mole [600°K. < $T \leq 1073.8^\circ\text{K.}$; $\pm 0.2\%$] and ($H_T - H_{298.15}$) = $25.24T - 0.00376T^2 - 5307$ cal./mole [1073.8°K. $\leq T < 1300^\circ\text{K.}$; $\pm 0.1\%$].

Introduction

Recently the high temperature thermodynamic properties of inorganic compounds have become of increasing interest. This is especially true of those relatively simple compounds for which theoretical calculations of thermodynamic properties can be made.

This paper describes the construction and certain operational details of a high temperature drop type calorimeter, as well as measurements on the enthalpies of α -aluminum oxide and sodium chloride.

Experimental

Description of the Apparatus and Operating Procedure.—The general design of the apparatus is similar to the designs of Southard¹ and Olette.²

The inner core of the furnace is a recrystallized alumina tube of 1-in. i.d. and 24 in. long. Around its outside diameter a main heater is wound noninductively 6 turns/in. over a length of 15 in., and an end heater on top of the main heater for the last 4.5 in. of its length on each end. Both heaters consisted of (22 B & S gage) platinum-10% rhodium wire. A nichrome element wound on a coaxial outer core served as an auxiliary heater. The power was at all times distributed between the heaters in such a way that the temperature gradient along the furnace core was less than 0.5°/in. as shown by thermocouples placed along the core for that purpose. The temperature drift was reduced to a value less than 0.1°/min. during a temperature measurement. The platinum-10% rhodium thermocouples were calibrated against the melting points of samples of lead, tin, zinc, aluminum, and copper furnished by the National Bureau of Standards. These

(1) J. C. Southard, *J. Am. Chem. Soc.*, **63**, 3142 (1941).

(2) M. Olette, *Compt. rend.*, **244**, 891 (1957); M. Olette and C. Tuppin, *Silicates Ind.*, **22**, 343 (1957).

* Department of Chemistry, Colgate University, Hamilton, N. Y.

calibrations were checked and found to have changed by about 0.2° over a period of several months.

The sample container was fabricated from platinum-10% rhodium by J. Bishop & Co. Its main feature of interest was the inclusion of a thermocouple well 1 in. long and 0.25 in. in diameter, into which the thermocouple fitted. Thus it was hoped that the thermocouple could be brought into good thermal contact with the sample. In order to investigate this point, a number of experiments were carried out on the melting point of sodium chloride in this sample container. The results were compared with the results of a similar series of experiments carried out in a graphite crucible originally designed for calibration of the thermocouples. The results of each series were self consistent to 0.1°; however, the results of the latter series of experiments (in which extremely good thermal contact was expected) were 0.4° higher than the former. It is believed that the temperature measurements are consistent to within 0.2°; however, the absolute value of the temperature might be in error by as much as 0.1%.

A thermistor used in the measurement of calorimeter temperature was frequently calibrated against a platinum resistance thermometer. Whereas the calibration changed by several thousandths of a degree every few months, temperature differences as measured by the thermistor changed somewhat less rapidly. Thus the thermistor could be used to measure temperature changes to about 0.002° for a period of approximately 3 months between calibrations. It is believed that this source of error is the largest such source in the investigation.

In order to minimize heat leak between the calorimeter and its surroundings, all surfaces exposed to the calorimeter and all electrical leads in thermal contact with the calorimeter are first brought into thermal contact with a water bath whose temperature is controlled so as to be equal to the calorimeter temperature at all times. This control is accomplished by use of a Leeds and Northrup triple action C.A.T. controller in conjunction with a saturable core reactor which could furnish up to 4 kw. to the bath heater. The temperature difference was detected by two matched thermistors compared in a Wheatstone bridge circuit which had an over-all sensitivity of 10^{-4} °. During a rapid rise in temperature of the calorimeter the bath was frequently controlled manually and the temperature difference was held to within 10^{-2} °. This difference was recorded and heat leak calculations were made; however, in all cases the correction was very small, being in the order of 0.1% or less of the total heat input to the calorimeter.

It is interesting to note in connection with corrections of this sort that the enthalpy of the empty sample container was measured in one series of experiments in a pressure of 10^{-4} mm. and in another series of experiments in a pressure of 2 cm. of helium gas. Equilibrium was established between the sample container and the calorimeter after 2.5 hr. in the vacuum experiments whereas only 15 min. was required in the other experiments. Since no consistent difference was found between the results which showed a 0.3% precision, all the results were used in establishing the enthalpy of the empty sample container.

Considering the 0.3% error (which should be reduced by a factor of six in calculating its effect upon the results) in the determination of the empty sample container; the 0.1% error in the high temperature determination; and the error in the temperature rise of the calorimeter which amounts to about 0.15%, the results are estimated to be accurate to $\pm 0.3\%$. The precision of the results is of course somewhat better, the standard deviation being 13 cal./mole.

Results

Table I gives the measured values of the enthalpy of α -aluminum oxide together with those determined by the National Bureau of Standards³ on a similar sample. The results are expressed in defined calories per mole (1 cal. = 4.1840 joules).

The results agree well in the region in which they can be compared. It is interesting to note, however, that all of the measurements lie above those of the N.B.S. Similar results are obtained by other authors,⁴⁻⁶

(3) G. T. Furukama, T. B. Douglas, R. E. McCoskey, and D. C. Ginnings, *J. Res. Natl. Bur. Std.*, **57**, 67 (1956).

(4) J. L. Margrave and R. T. Grimley, *J. Phys. Chem.*, **62**, 1436 (1958).

(5) B. E. Walker, J. A. Grand, and R. R. Miller, *ibid.*, **60**, 231 (1956).

(6) C. H. Shomate and B. J. Naylor, *J. Am. Chem. Soc.*, **67**, 72 (1945).

TABLE I

SUMMARY OF Al_2O_3 DATA

Temp., °K.	$(H_T - H_{298.15})$, cal./mole	$(H_T - H_{298.15})$, cal./mole	% deviation
	This work	N.B.S.	
785.3	12,403	12,356	+0.39
784.1	12,338	12,321	+ .14
770.2	11,957	11,923	+ .28
1031.9	19,648	19,596	+ .26
1173.0	23,918	23,853	+ .27
1162.9	23,636	23,548	+ .37
870.2	14,870	14,812	+ .39
873.9	14,972	14,919	+ .35
1410.1	31,096
			+ .31

although Shomate and Cohen,⁷ and Egan, Wakefield, and Elmore⁸ report results lower than the N.B.S. A statistical analysis of the data of these authors plus the present data shows that one can expect the deviations from the N.B.S. to be positive with 90% confidence. That is to say the probability that the observed difference is due to a random fluctuation in the observations is 0.1. Although more work needs to be done to establish this point, the possibility of a systematic error is suggested.

The data on sodium chloride are given in Table II.

TABLE II

T , °K.	$(H_T - H_{298.15})$, cal./mole	T , °K.	$(H_T - H_{298.15})$, cal./mole
672.2	4,804	1071.3	10,758
672.2	4,804	1071.4	10,768
723.6	5,510	1076.8	13,942
723.5	5,498	1073.4	10,897
775.6	6,231	1157.4	18,868
772.7	6,183	1065.3	10,606
823.8	6,913	1099.1	17,894
825.2	6,950	1098.6	17,897
873.1	7,644	1087.1	17,718
872.1	7,642	1078.7	17,546
923.7	8,383	1131.7	18,455
921.5	8,357	1128.1	18,382
975.5	9,182	1064.7	10,591
974.6	9,159	1172.3	19,104
1024.9	9,951	1219.2	19,889
1021.3	9,846	1221.7	19,913
1071.9	10,751	1271.3	20,712
1070.0	10,707	1279.1	20,827
		1076.6	17,526

A standard four-parameter equation was fitted by the method of Shomate⁹ to the experimental data below the melting point using the heat capacity given by Stull¹⁰ ($C_{p,298.15^\circ\text{K}} = 11.90$ cal./mole deg.). The coefficient of the T^{-1} term fortuitously turned out to be negligible. Above the melting point a three-parameter equation was easily derived by fitting a straight line to a graph of values of $[(H_T - H_m)/(T - T_m)]$ vs. $T^\circ\text{K.}$ (where T_m is the melting point temperature). The resulting equations are $(H_T - H_{298.15})_s = 10.45T + 0.002442T^2 - 3334$ cal./mole [$600^\circ\text{K.} < T \leq 1073.8^\circ\text{K.}; \pm 0.2\%$] and $(H_T - H_{298.15}) = 25.24T - 0.00376T^2 - 5307$ cal./mole [$1073.8^\circ\text{K.} \leq T < 1300^\circ\text{K.}; \pm$

(7) C. H. Shomate and A. J. Cohen, *ibid.*, **77**, 285 (1955).

(8) E. P. Egan, Jr., Z. T. Wakefield, and K. L. Elmore, *ibid.*, **72**, 2418 (1950).

(9) C. H. Shomate, *J. Phys. Chem.*, **58**, 368 (1954).

(10) JANAF Thermochemical Tables (D. R. Stull, Thermal Laboratory, Dow Chemical Company, Midland, Michigan).

TABLE III

$T, ^\circ\text{K.}$	$(H_T - H_{298.15}),$ cal./mole	$(S_T - S_{298.15}),$ cal./mole deg.	$-(F_T - H_{298.15}),$ T cal./mole deg.
600	(3,815)	(8.78)	(19.75)
700	5,178	10.88	20.81
800	6,589	12.76	21.86
900	8,049	14.48	22.87
1000	9,558	16.07	23.84
1073.8(s)	10,703	17.17	24.54
1073.8(l)	17,463	23.47	24.54
1100	17,910	23.88	24.93
1200	19,569	25.32	26.35
1300	(21,153)	(26.59)	(27.65)

TABLE IV

	ΔH fusion, cal./mole	M.p. $T, ^\circ\text{K.}$
This work	6760 ± 30	1073.8
Dworkin and Bredig ¹²	6690	1073

0.1%]. From these equations, their derivatives, and the value $-(F_T - H_{298.15})/T$ at 298.15°K. , equal to 17.33 cal./deg. mole,¹¹ the thermodynamic functions listed in Table III were calculated.

Table IV gives the values of the heat of fusion and the melting point of sodium chloride.

Considering the estimated error of this work and that of Dworkin and Bredig,¹² it is seen the agreement is satisfactory. This is especially true if one considers that the latter authors calibrated their apparatus with a sample of α -aluminum oxide furnished by the N.B.S. This directly accounts for one-third of the difference between their measurements and these reported here.

Acknowledgment.—The authors wish to acknowledge the support of the National Aeronautics and Space Administration for this work. The sample of α -aluminum oxide was furnished through the courtesy of the National Bureau of Standards.

(11) L. Brewer and E. Brackett, *Chem. Rev.*, **61**, 425 (1961).

(12) A. S. Dworkin and M. A. Bredig, *J. Phys. Chem.*, **64**, 269 (1960).

RADIOLYSIS OF *n*-BUTENES¹

BY PRISCILLA CHANG KAUFMAN²

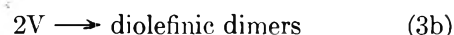
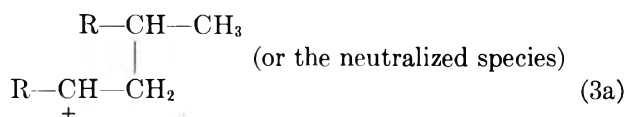
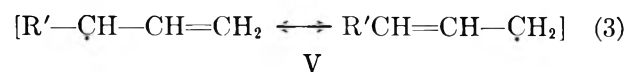
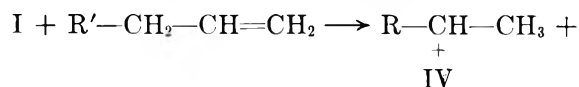
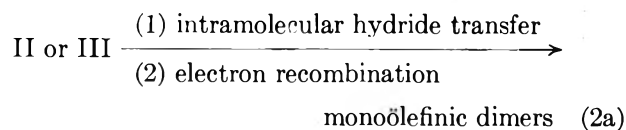
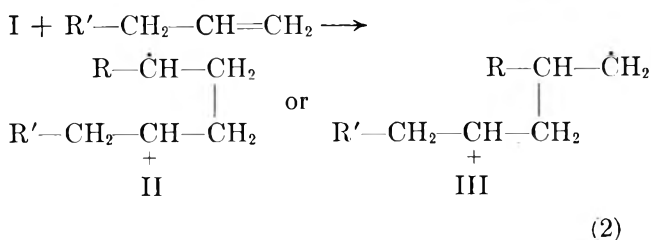
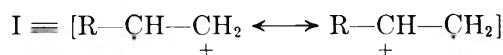
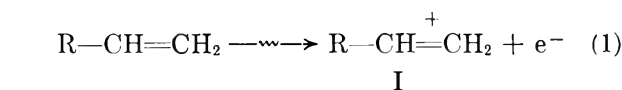
Chemistry Department, Brookhaven National Laboratory, Upton, L. I., New York

Received February 18, 1963

The radiolyses of 1-butene, *cis*-2-butene, and *trans*-2-butene with γ -rays were studied in gas and liquid phases, at -78° and room temperature. In all cases, the major products were the C_8 hydrocarbons, the saturated monomer, the geometric isomer (*e.g.*, *trans*- from *cis*-2-butene), the double-bond isomer (*e.g.*, 1-butene from 2-butene), hydrogen, and unidentified high polymers. Small amounts of C_2 , C_3 , C_5 , C_6 , and C_7 hydrocarbons were also formed. The C_3 hydrocarbons produced were examined for carbon skeleton and extent of unsaturation. Comparison of the present results with the 1-hexene radiolysis led to the conclusion that the ion-molecule mechanism previously proposed is applicable.

Introduction

Detailed studies of the radiolysis of olefins in the liquid phase have been confined to olefins with terminal double bonds. Ion-molecule reactions have been suggested to play an important role in the formation of dimers and higher polymers.³⁻⁵ The following scheme depicts the initial steps



where the positive charge in the molecule-ion I is localized at the double bond and the subsequent reactions occur at this electron-deficient center. Reaction 2 is the direct condensation of I with a parent molecule yielding dimeric molecule-ions II and III. Intramolecular hydride transfer and electron recombination of II and III yield monoolefinic dimers with carbon skeletons as shown. Excess energy resulting from neutralization is believed to be dissipated by collisional

(1) Research performed under the auspices of the U. S. Atomic Energy Commission.

(2) Atlas Chemical Industries, Industrial Reactor Laboratory, Plainsboro, New Jersey.

(3) P. C. Chang, N. C. Yang, and C. D. Wagner, *J. Am. Chem. Soc.*, **81**, 2060 (1959).

(4) C. D. Wagner, *Tetrahedron*, **14**, 164 (1961).

(5) E. Collinson, F. S. Dainton, and D. C. Walker, *Trans. Faraday Soc.*, **57**, 1732 (1961).

TABLE I
 PRODUCTS FROM RADIOLYSIS OF *n*-BUTENES
 Dose rate: 2.4×10^6 R./hr.

Material irradiated	System Phase	Temp., °C.	Total dose, R.	G (products)										Total above C ₄							
				H ₂	CH ₄	C ₂ H ₆	C ₂ H ₄	C ₂ H ₂	C ₃ H ₈	C ₃ H ₆	<i>n</i> -C ₄ H ₁₀	C ₄ H ₈			C ₇	C ₈					
										1-	<i>trans</i> -	<i>cis</i> -									
Butene-1	Liq.	23	6.0 × 10 ⁶	0.57	0.03	0.29	0.17														
			1.2 × 10 ⁷	.57	.04																
			2.4 × 10 ⁷	.64		.21	.18				.07	.09	.29						.02	1.43	17.8
			3.0 × 10 ⁷	.57		.11	.17				.06	.10	.29						.02	1.51	16.6
		-78	4.0 × 10 ⁷	.64	.05	.13	.21	0.30	.06	.13	.30		0.16	0.18			.02	1.72	16.0		
			2.3 × 10 ⁷	.62	.15	.15	.30	.30	.04	.09	.45		.14	.13			.03	1.34	15.6		
			Gas ^a	23	4.0 × 10 ⁷	1.03	.26	.43	4.30	2.92	.22	.13	1.94		.52	.56				0.17	
			Gas ^a	23	4.0 × 10 ⁷	0.99	.17	.09	0.17	0.17	.22	.13	0.95	0.34		4.1				1.03	6.9
<i>trans</i> -Butene-2	Liq.	-78	2.3 × 10 ⁷	.97	.15	.01	.02	.02	.07	.07	.60	.37		3.7				0.90			
			Gas ^a	23	2.5 × 10 ⁷	1.37	.14	.07	.82	1.17	.55	.48	1.51	.62		4.1					
<i>cis</i> -Butene-2	Liq.	-78	2.3 × 10 ⁷	.99	.13	.09	.26	0.26	.22	.26	1.03	.43	4.0					.01	.96	6.9	
			Gas ^a	23	2.6 × 10 ⁷	.79	.13	.01	.04	.03	.01	.13	0.40	.46	3.3					.90	
	Gas ^a	23	4.0 × 10 ⁷	1.15	.09	.09	.86	.86	.09	.52	1.29	.43	3.4								

^a Pressure ranged from 0.5 to 2 atm. *G*-values were found to be independent of pressure in this range.

deactivation. Reaction 3 involves hydrogen transfer from the parent olefin to I yielding the carbonium ion IV and the alkenyl radical V. Reactions of IV or the neutralized species thereof give rise to saturated dimers. Association of two alkenyl radicals V gives rise to diolefinic dimers. The finding that the dimers from 1-hexene³ were mostly monoolefinic and had carbon skeletons of *n*-dodecane and 5-methylundecane suggested that reaction 2 was favored over reaction 3. The dimers obtained from the radiolysis of liquid propene,⁴ however, were found to contain less monoolefins and indicated that reaction 2 was less favorable in propene than in hexene. It was suggested that this difference may be attributed to (a) the larger size of the hexene molecule, and therefore the greater number of modes of energy dissipation in the condensation step and the subsequent electron recombination step and (b) the greater stability of the symmetric allyl radical derived from propene in reaction 3. In the present work, radiolysis of 1-butene was undertaken to study the effect of the size and structure of a terminal olefin on the relative importance of reactions 2 and 3, and the radiolysis of the 2-butenes was studied to test the applicability of the ion-molecule mechanism to non-terminal olefins.

Experimental

The butenes used were Phillips research grade. After the usual degassing by bulb-to-bulb distillations, measured amounts of the middle cut were sealed *in vacuo* at liquid nitrogen temperatures in Pyrex tubes equipped with break-off tips. For irradiations in the liquid phase, the gas/liquid volume ratio in the ampoule did not exceed 1/10. Vapor phase chromatographic (VPC) analysis of the starting materials showed negligible amounts of impurities. The samples were irradiated with γ -rays at the Brookhaven high level gamma facility. After irradiation the sample was degassed in an analysis device comprising a Toepler pump, a McLeod gage, and a modified Saunders-Taylor combustion system for the determination of hydrogen and methane.^{6,7} Products condensable at -196° were then expanded into a reservoir of sufficiently large volume to maintain hydrocarbons up to C₇ in the gas phase. Aliquots of the gaseous mixture were then analyzed by VPC using a dimethylsulfolane column (16 m. × 6 mm.) and a Ucon column (16 m. × 6 mm.) operated at room temperature. Identification of the products up to *n*-hexane was based on the retention times which were distinct and reproducible for all low boiling hydrocarbons. Yields were calculated from the peak areas using the parent compound as an

internal standard. Known mixtures of a butene and as little as 0.01 mole % of another hydrocarbon were used to give calibration curves.

For the analysis of the higher products, a known amount of *n*-nonane (not a radiolysis product) was added to the irradiated sample. The sample was then fractionally distilled at 0° and the residue was analyzed by VPC with a Ucon column (4 m. × 6 mm.) using the added nonane as an internal standard for quantitative calculations. The C₈-C₉ fraction was trapped as it emerged from the column for further analysis. No attempt was made to investigate products higher than C₉.

Yields of all products from the butenes are listed in Table I. Figures in the last column are the *G*-values for conversion of the butene to higher products including the unidentified higher polymers. In all cases, isobutane and isobutene were produced in insignificant amounts and are not listed. The C₅ and C₆ yields could not be determined precisely because the peaks were too broad on the 16-m. columns. Rough estimates from the VPC curves using the short Ucon column showed that the *G*-values for C₅ and C₆ did not exceed 0.01.

To elucidate the nature of the dimers produced, the trapped C₅-C₉ fraction, including the added nonane, was examined by infrared spectroscopy, bromination, hydrogenation, and ozonization. The results are shown in Table II. In all cases, the infrared spectra of the dimers indicated the absence of acetylenes, allenes, and conjugated dienes. Data on the carbon skeletons were obtained by the VPC analysis of the fraction after hydrogenation over Adams' catalyst. It is noteworthy that whereas the original dimers showed at least fifteen overlapping peaks on the VPC tracings, the dimers after hydrogenation gave remarkably simple curves consisting of two major peaks, one being *n*-octane and the other 3,4-dimethylhexane and 3-methylheptane, which were not resolvable by the available packed columns. Quantitative infrared spectroscopy was applied to determine the concentration of 3,4-dimethylhexane, which showed a characteristic and distinct absorption band at 1122 cm.⁻¹. Calibration with authentic mixtures yielded a linear relationship between the concentration of 3,4-dimethylhexane and the optical density at 1122 cm.⁻¹.

To determine the concentrations of saturated, monoolefinic and diolefinic dimers, bromination of the entire dimeric fraction was carried out in carbon disulfide at 0°. Under these conditions, the saturates were not attacked. The bromination mixture was analyzed by VPC without prior purification. The dibromides and tetrabromides were retained on the column and the saturates which emerged were calculated using the nonane standard. Carbon skeleton studies were carried out on the trapped saturates. Determination of the concentrations of the mono- and diolefins was based on the bromination results and quantitative hydrogenation which yielded the average number of double bonds per molecule. A further check was accomplished by degradative ozonolysis applied to the C₅ fraction produced from *trans*-2-butene. Ozonides from the olefins were converted to acids, treatment with diazomethane converted the acids to esters, and the esters were separated by VPC. The diesters arising from diolefins were characterized by their dianilide derivatives. As the peaks

(6) R. C. Petry and R. H. Schuler, *J. Am. Chem. Soc.*, **75**, 3796 (1953).

(7) Some methane dissolved in the hydrocarbon mixture could not be degassed. This showed up later in the VPC analysis and was added to the combustion value.

TABLE II
 NATURE OF C₃ FRACTIONS FROM RADIOLYSIS OF *n*-BUTENES IN LIQUID PHASE

System	Temp., °C.	Total dose, ^a R.	Carbon skeleton, %			Extent of unsaturation, %		
			C-C-C-C	C-C-C-C	C-C-C-C	C ₃ H ₁₈	C ₃ H ₁₆	C ₂ H ₁₄
C-C-C=C	23	4.0 × 10 ⁷	50	9	35	10 ^b	80	10
	-78	2.3 × 10 ⁷	44	10	36	9	81	10
$\begin{array}{c} \text{C} \\ \diagdown \\ \text{C}=\text{C} \\ \diagup \\ \text{C} \end{array}$	23	4.0 × 10 ⁷	24	35	36	17 ^c	59	24 ^d
	-78	2.3 × 10 ⁷	22	74		7	75	18
$\begin{array}{c} \text{C} \quad \text{C} \\ \diagdown \quad \diagup \\ \text{C}=\text{C} \end{array}$	23	4.0 × 10 ⁷	25	26	44	15 ^c	61	26
	-78	2.6 × 10 ⁷	18	73		4	77	19

^a Variation of dose from 6 × 10⁶ to 4 × 10⁷ R. in the radiolysis of 1-butene has no effect on the nature of the C₃ fraction. ^b This fraction consists of C-C-C-C, 2%; C-C-C-C, 3%; C-C-C-C, 4%. ^c This fraction contains no *n*-C₃H₁₈; C-C-C-C, 3-5%; C-C-C-C, 10-12%. ^d After hydrogenation this fraction consists of C-C-C-C, 22%; C-C-C-C and C-C-C-C, 2%.

 TABLE III
 COMPARISON OF RADIOLYSIS OF 1-HEXENE,³ 1-BUTENE, AND PROPENE⁴ IN LIQUID PHASE

Material irradiated	H ₂ <i>G</i>	RCH ₂ CH ₂ <i>G</i>	<i>G</i>	Carbon skeleton, %			Extent of unsaturation, %			Total conversion
				R-C-C	R-C-C	R-C-C	C _n H _{2n+2}	C _n H _{2n}	C _n H _{2n-2}	
1-Hexene	0.7	0.1	1.7	45	..	35	8	85	7	16
1-Butene	.6	.3	1.7	50	9	35	10	80	10	16
Propene	.6	.2	1.1	36	5	51	15	62	16	9

^a R = C₄H₉ for 1-hexene, C₂H₅ for 1-butene, CH₃ for propene.

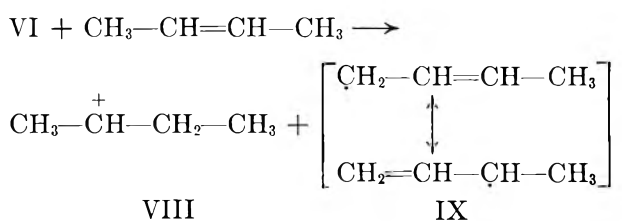
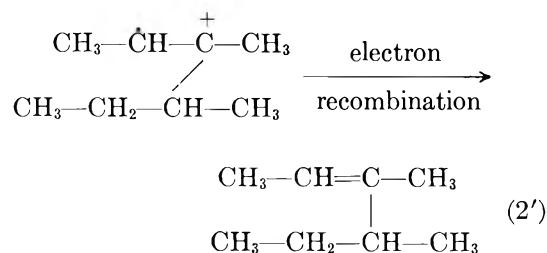
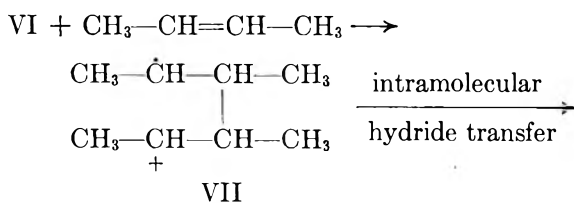
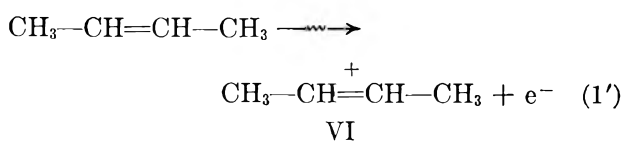
in the C₈-C₉ region formed two distinct groups on VPC, the ozonolysis technique was applied to the separately trapped groups. It was thus shown that the first group consisted of saturates and monoolefins only and the second group consisted of diolefins only. Characterization of the dianilide derivatives of the diolefins indicated the presence of R=C-C-C-C=R', R=C-C-C-C-C=R', and C=C-C-C-C=C. The amount

of diolefinic dimers calculated from the peak areas of the second group agreed with the bromination and hydrogenation data.

Discussion of Results

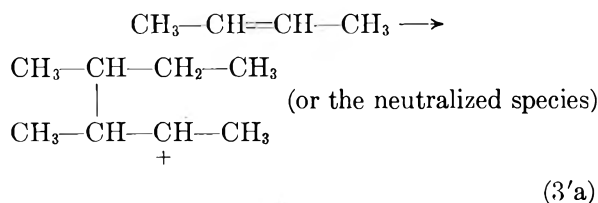
Liquid Phase Radiolysis.—Products obtained in the radiolysis of the *n*-butenes are shown in Tables I and II. Comparison of the main features in terminal olefin systems is shown in Table III which indicates that the radiolysis of 1-butene follows a very similar course to that of 1-hexene, and the ion-molecule scheme previously proposed can therefore be adopted to explain the products formed. In the case of propene the noteworthy deviation in the dimers produced is the presence of smaller amounts of monoolefins, indicating that reaction 2 is less favorable. A plausible explanation for this fact is the increased competition of reaction 3 in propene due to the greater stability of the symmetric allyl radical, V (where R' = H), thus providing a greater driving force for the intermolecular hydrogen transfer reaction.

The effect of structure of the olefin on the relative importance of reactions 2 and 3 was further illustrated in the 2-butene systems. The corresponding mechanism would be reactions 1', 2', and 3'.

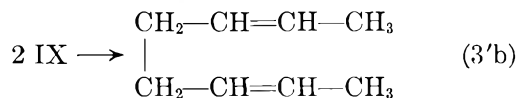


(3')

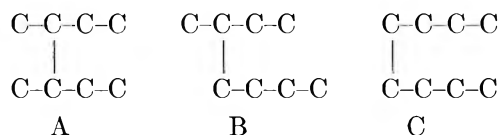
VIII (or the neutralized species) +



(3'a)



Since 2-butene is symmetrical, the direct condensation product VII would yield octenes with carbon skeleton A exclusively.



Dimers resulting from species produced in reaction 3' would be octanes with carbon skeleton A and octadienes with skeleton C. The concentration of A in the monoolefinic dimers could thus be used to determine the extent of reaction 2'. Results from the 2-butenes shown in Table II indicate the presence of ca. 30% A, 40% B, and 25% C. Analysis of the C₈H₁₄ fraction indicated that nearly all the straight chain dimers were *n*-octadienes.⁸ Therefore, the dimers with skeleton A consisted of monoolefins and paraffins only. Subtracting the amount of paraffinic A, 3–5%, from the total amount of A, we arrive at the value of 25–30% for the extent of reaction 2'. A similar conclusion was reached by Wagner⁴ in the radiolysis of propene. Intermolecular hydrogen transfer is more favored in 2-butene than in 1-butene, conceivably because there are six allylic hydrogen atoms in 2-butene. Another manifestation of the increased participation of reaction 3 or

(8) *n*-Octadienes could only arise from the coupling of two CH₂-CH=CH-ĊH₂ radicals. This raises the interesting question of the relative reactivities of the two canonical forms of the resonance hybrid. The present finding of the preponderance of the straight chain skeleton in the diolefins suggests that C=C-Ċ rather than C-Ċ=C is favored in combination reactions. This phenomenon is frequently encountered in polymerization studies and has been attributed to steric effects. C. Walling, "Free Radicals in Solution," John Wiley and Sons, Inc., New York, N. Y., 1957, pp. 228–231.

3' is the lower total conversion of the 2-butenes and propene. Intermolecular transfer of allylic hydrogen is known to inhibit the formation of higher polymers.

Dimers with skeleton B can be formed only by radical reactions such as coupling of a *s*-butyl radical with a butenyl radical or cross association of the butenyl radicals. A possible source of *s*-butyl radicals, in addition to neutralization of the carbonium ion VIII, is the addition of a hydrogen atom to 2-butene, a process with an activation energy of about 5 kcal.⁹ It is conceivable that the difference observed in the radiolysis at -78° is due to this energy requirement.

Comparison of the results from *trans*- and *cis*-2-butene showed that stereochemistry is not a concern in the present interpretation. The VPC curves of the dimers from the two 2-butenes were different but the curves of the dimers after hydrogenation were identical. The original difference is undoubtedly due to different concentrations of geometric isomers which disappear upon hydrogenation. The *cis-trans* isomerization of the parent molecule seemed to be independent of temperature and phase, suggesting a unimolecular mechanism in conformance with the current view on the subject.¹⁰

Gas Phase Radiolysis.—Results listed in Table I show that radiolysis in the gas phase produces significantly larger amounts of fragmentation products, *i.e.*, H₂, C₁-C₃ hydrocarbons, than that in the liquid phase. This can easily be explained by the effect of collisional deactivation which is essential in the steps following condensation and electron recombination steps depicted in reactions 1–3. The present study does not allow any attempt to devise a mechanism, although it can be concluded that the mechanism involving excited molecules undergoing β-C-H and β-C-C bond cleavages suggested in mercury-photosensitized reactions of olefins¹¹ is inadequate to explain the radiolysis results. More detailed studies in a wider pressure region are necessary for further speculation.

Acknowledgments.—The author wishes to express her gratitude to Drs. A. O. Allen and H. A. Schwarz for their encouragement and helpful discussions.

(9) B. deB. Darwent and R. Roberts, *Discussions Faraday Soc.*, **14**, 55 (1953).

(10) S. W. Benson, "The Foundations of Chemical Kinetics," McGraw-Hill Book Co., Inc., New York, N. Y., 1960, pp. 255–257.

(11) J. R. Majer, B. Mile, and J. C. Robb, *Trans. Faraday Soc.*, **57**, 1336 (1960).

CHEMICAL EFFECTS OF (n, γ)-ACTIVATION OF HALOGEN ATOMS IN ALKYL HALIDE-PENTANE SOLUTIONS¹; AUGER ELECTRON REACTION HYPOTHESIS

BY PAUL R. GEISSLER AND JOHN E. WILLARD

Department of Chemistry of the University of Wisconsin, Madison, Wisconsin

Received February 13, 1963

Solutions of methyl iodide, ethyl iodide, amyl iodide, and propyl chloride in pentane were irradiated with neutrons and the organic products formed by the halogen atoms which underwent radiative neutron capture ($I^{127}(n,\gamma)I^{128}$ or $Cl^{37}(n,\gamma)Cl^{38}$) were determined by gas chromatography. In each of the iodide solutions the largest fraction of the I^{128} activity was found in the form of the parent alkyl iodide even in the presence of I_2 scavenger. Evidence from other studies indicates that failure of bond rupture, recombination of parent partners, or exchange of I^{128} with an alkyl iodide molecule following the (n, γ) process is improbable in these systems. The hypothesis is suggested that the recoil I^{128} atoms react with parent-type R radicals which are formed at high localized concentration in their immediate vicinity by reactions such as $RI + e^- \rightarrow R + I^-$ and $RI + H \rightarrow R + HI$ made possible by the localized radiation chemistry induced by the internal conversion and Auger electrons emitted by the recoil atoms. The relative yields of I^{128} products are similar to those of I^{131} products observed in the Co^{60} radiolysis of solutions of alkyl iodides in pentane containing I_2^{131} scavenger. If the hypothesis is correct that the chemical fate of an I^{128} atom as studied in this work is influenced by the decomposition of the immediately surrounding envelope of solvent by conversion electrons and Auger electrons, similar autoradiation processes may be significant in many other systems where chemical activation by nuclear processes has been studied. The organic yield of I^{128} from neutron irradiation of unscavenged alkyl iodide-pentane solutions has been observed to increase from 50 to 90% with time of irradiation from 1 sec. to 1 min. at a neutron flux of about 10^{13} neutrons $cm^{-2} sec^{-1}$ and a γ -dosage rate of about 3×10^{18} e.v. $g^{-1} min^{-1}$. Equivalent γ -radiation administered prior to the neutron irradiation does not cause such an increase.

Introduction

Although a great deal is known² about the processes by which atoms activated by nuclear transformations react chemically with surrounding media and enter stable combination, much more specific knowledge of the several types of elementary processes is needed. Thus, in liquid alkyl halide systems, which have been extensively studied, there remains great uncertainty as to the role of the kinetic energy of the recoil atom relative to the role of the charge generated by internal conversion and Auger transitions. Gas phase experiments have established the fact that recoil halogen atoms can undergo unique bimolecular displacement² reactions and scavenger studies have demonstrated that in solution some of the stable products are formed by combination of a free radical with the recoil atom after the latter has diffused some distance after reaching thermal equilibrium with the medium.² These two processes account for only one third or so of the organic yield in liquid alkyl iodide and bromide solutions, unless the probability of the displacement reaction is much higher in the liquid than the gas. The remaining organic combination, which occurs even in the presence of free halogen scavenger, must be the result of failure of bond rupture, or of combination of the atoms with radicals formed by the atoms in the process of dissipating their energy.

In the present work solutions of alkyl halides in pentane have been activated by neutron capture at dilutions such that the probability of kinetic energy transfer or direct charge transfer from the recoiling atom to a molecule of the parent alkyl iodide is low. High organic yields as the parent molecule have nevertheless been observed. This has suggested the hypothesis that a

major portion of the organic yield in alkyl iodides is due to the combination of I^{128} atoms with radicals formed by the conversion and Auger electrons emitted by the atom itself.

About 41%³ of I^{128} atoms produced by the $I^{127}(n,\gamma)I^{128}$ process in liquid ethyl iodide enter organic combination. Dilution of the ethyl iodide with alkanes increases this yield. At room temperature the limiting values, reached at ethyl iodide concentrations below about 0.1 mole %, are 45% in pentane, 47% in heptane, and 52.5% in decane.⁴ The organic yield in hydrocarbon solutions decreases with increasing temperature (*e.g.*, in decane it is 55% at 0° and 45.5% at 100°). In the presence of iodine scavenger these yields are all lowered, as would be expected, but the yields still decrease with increasing temperature and increase with increasing molecular weight of the hydrocarbon solvent.⁴ The effects of molecular weight of the hydrocarbon and of temperature are such as would be expected if the organic yield is increased by decreasing the ease of diffusion in the system. Since these effects are observed even in the presence of 0.01 mole fraction of I_2 scavenger they concern processes in which the fate of the I^{128} is determined within an average of only 10^2 to 10^3 encounters or so after it has been reduced to an energy and charge where it is capable of entering stable combination.

In the work reported here the organic products formed from the I^{128} produced by the neutron irradiation of solutions of different alkyl halides in pentane have been determined, and compared both with those formed by neutron irradiation of the pure liquid alkyl halide and with those formed⁵ by the γ -radiolysis of alkyl halide-pentane solutions containing $I_2(I^{131})$, $CH_3I(C^{14})$, or $C_2H_5I(I^{131})$.

Experimental¹

Neutron Irradiations.—All samples, contained in thin quartz bulbs about 6 mm. in diameter, were irradiated in the rabbit facility of the CP-5 reactor at Argonne National Laboratory with

(1) Further details may be found in the Ph.D. thesis of Paul R. Geissler, University of Wisconsin, 1962, available from University Microfilms, Ann Arbor, Michigan.

(2) Additional discussion and references dealing with the chemical effects of nuclear transformations in alkyl halide systems are given in: (a) J. E. Willard, *Ann. Rev. Nucl. Sci.*, **3**, 193 (1953); (b) *Ann. Rev. Phys. Chem.*, **6**, 141 (1955); (c) "Chemical Effects of Nuclear Transformations," International Atomic Energy Agency, Vienna, 1961, Vol. I, p. 215; (d) *Nucleonics*, **19**, No. 10, 61 (1961).

(3) G. Levey and J. E. Willard, *J. Am. Chem. Soc.*, **74**, 6162 (1952).

(4) S. Aditya and J. E. Willard, *ibid.*, **79**, 3367 (1957).

(5) P. R. Geissler and J. E. Willard, *ibid.*, **84**, 4627 (1962).

TABLE I
RELATIVE YIELDS^a OF ORGANIC I¹²⁸ COMPOUNDS FORMED BY I¹²⁷(n,γ)I¹²⁸ ACTIVATION OF RI-C₆H₁₂ SOLUTIONS

RI mole %	CH ₃ I	C ₂ H ₅ I	C ₃ H ₇ I	<i>i</i> - C ₃ H ₇ I	<i>n</i> - C ₃ H ₇ I	<i>sec</i> - C ₄ H ₉ I	<i>n</i> - C ₄ H ₉ I	2-Iodo C ₆ H ₁₁ I	3-Iodo C ₆ H ₁₁ I	<i>n</i> - C ₆ H ₁₁ I	Duration of irradiation
C ₂ H ₅ I	5.9	0.97	41.3	0.42	6.9	0.31	1.3	20.4	11.2	11.3	
0.14	5.4	0.78	41.5	.43	6.5	.25	1.5	19.9	11.3	12.6	10 min.
C ₂ H ₅ I											
1.2	5.3	0.99	46.8	.79	5.8	.34	1.4	19.2	7.7	11.6	2 min.
C ₂ H ₅ I											
1.4	5.1	1.00	55.2	.65	5.4	.33	1.3	14.7	6.7	9.3	1 min.
C ₂ H ₅ I											
2.8	6.1	0.90	54.3	.41	5.7	.33	1.5	12.8	7.3	10.3	
	6.3	1.06	51.9	.43	6.9	.37	1.6	13.2	6.8	11.1	30 sec.
C ₂ H ₅ I											
6.7	5.8	1.03	46.8	2.7	6.1	.47	1.5	16.7	7.7	11.2	
	5.8	1.01	57.8	1.1	4.6	.25	1.3	13.8	6.0	8.3	10 sec.
C ₂ H ₅ I											
13.7	5.2	1.2	67.5	0.43	4.3	.31	1.2	8.3	4.5	7.0	
	5.9	1.5	63.2	.39	4.8	.42	1.4	8.9	5.2	8.5	10 sec.
C ₂ H ₅ I											
25.2	5.0	1.8	68.5	.30	4.4	.45	1.3	7.4	3.9	6.8	
	5.2	1.4	69.6	.32	4.2	.37	1.1	7.1	4.3	6.3	5 sec.
C ₂ H ₅ I											
58.8	4.7	2.5	80.1	.13	2.4	.34	0.74	3.7	2.1	3.2	
	4.5	2.7	80.2	.19	2.3	.25	0.67	3.6	2.2	3.4	2 sec.
CH ₃ I											
1.8	44.1	1.07	9.0	.37	6.2	.29	1.6	15.9	10.0	11.6	
	40.8	0.76	9.0	.36	5.8	.31	1.4	19.1	10.3	12.1	1.25 min.
<i>n</i> -C ₆ H ₁₁ I											
0.9	5.6	0.94	8.6	.40	5.7	.33	1.4	18.5	12.3	46.2	
	6.4	0.83	8.9	.37	6.1	.35	1.6	19.2	12.9	43.1	1.75 min.

^a Expressed as per cent of total organic activity.

TABLE II

RELATIVE YIELDS^a OF ORGANIC I¹²⁸ COMPOUNDS FORMED BY I¹²⁷(n,γ)I¹²⁸ ACTIVATION OF C₂H₅I-C₆H₁₂-0.25% I₂ SOLUTIONS

C ₂ H ₅ I, mole %	CH ₃ I	C ₂ H ₅ I	C ₃ H ₇ I	<i>i</i> - C ₃ H ₇ I	<i>n</i> - C ₃ H ₇ I	<i>sec</i> - C ₄ H ₉ I	<i>n</i> - C ₄ H ₉ I	2-Iodo C ₆ H ₁₁ I	3-Iodo C ₆ H ₁₁ I	<i>n</i> - C ₆ H ₁₁ I	Organic yield
6.7	12.5	2.5	59.2	0.39	6.4	0.17	1.6	7.7	3.1	6.6	
	12.9	2.5	69.9	.41	7.5	.16	1.2	2.4	1.0	2.2	35.8
13.7	8.1	2.3	63.0	.36	6.4	.38	1.4	7.4	4.1	6.7	
	7.4	2.8	65.4	.12	6.4	.18	0.33	7.1	3.9	6.4	33.2
25.2	8.3	3.0	64.2	.22	5.8	.36	1.5	6.5	4.1	6.0	
	8.0	2.9	68.2	.23	6.8	.28	1.4	5.0	2.4	4.5	31.2
58.8	6.0	4.0	76.8	.08	3.1	.29	1.2	4.0	1.0	3.5	
	6.0	4.2	79.1	.10	2.8	.21	0.77	2.8	1.2	2.9	30.6

^a Expressed as per cent of total organic activity, except for the last column which shows the per cent of total activity in organic combination.

TABLE III

RELATIVE YIELDS^a OF ORGANIC I¹²⁸ COMPOUNDS FORMED BY I¹²⁷(n,γ)I¹²⁸ ACTIVATION OF I₂-C₆H₁₂ SOLUTIONS

I, mole %	CH ₃ I	C ₂ H ₅ I	C ₃ H ₇ I	<i>i</i> - C ₃ H ₇ I	<i>n</i> - C ₃ H ₇ I	<i>sec</i> - C ₄ H ₉ I	<i>n</i> - C ₄ H ₉ I	2-Iodo- C ₆ H ₁₁ I	3-Iodo C ₆ H ₁₁ I	<i>n</i> - C ₆ H ₁₁ I	Others ^b	Organic yield
0.25	14.4	2.6	17.7	5.7	12.8	1.0	2.5	16.9	7.9	13.4	5.0	36.8
	16.3	2.6	19.6	3.5	13.9	0.7	2.4	16.6	9.0	10.9	4.1	
0.125	11.1	1.7	15.7	2.9	12.5	0.3	1.6	26.0	11.6	14.1	2.7	36.8
	10.3	1.6	16.3	4.8	10.3	1.0	1.9	23.8	11.6	13.6	4.7	

^a Expressed as per cent of total organic activity, except for the last column which shows the per cent of total activity in organic combination. ^b Two additional peaks separated by gas chromatography.

TABLE IV

RELATIVE YIELDS^a OF I¹²⁸ FORMED BY I¹²⁷(n,γ)I¹²⁸ ACTIVATION OF C₂H₅I-I₂ SOLUTIONS

I ₂ , mole %	CH ₃ I	C ₂ H ₅ I	C ₃ H ₇ I	<i>n</i> -C ₃ H ₇ I	<i>n</i> -C ₄ H ₉ I	C ₂ H ₄ I ₂ ^b	CH ₂ I ₂ ^c	Organic yield
0.0	1.3	2.3	94.2	0.20	0.08	1.7	...	
	1.9	2.7	92.5	0.23	0.13	2.5	...	
.0 ^d	4.0	1.4	82.6	—————(3.3)—————			8.7	42.6
.0 ^e	8.0	3.9	81.1	—————(7.0)—————				41.3
.25	2.8	5.1	86.6	0.41	0.10	5.0	...	33.2
	2.6	5.3	87.0	0.57	0.22	4.3	...	

^a Expressed as per cent of total organic activity, except for the last column which shows the per cent of total activity in organic combination. ^b Two peaks of approximately equal areas. ^c No peak observed. ^d (n,2n) activation analyzed by fractional distillation with carriers. ^e (n,γ) activation, analyzed by fractional distillation with carriers.²

the reactor operating at a power level of either 2.2 or 4.6 megawatts. The thermal neutron flux was approximately 10¹³ neu-

trons cm.⁻² sec.⁻¹, and the γ-ray intensity was about 3 × 10¹⁸ e.v. g.⁻¹ min.⁻¹ at the lower power.

Sample Preparation and Analysis.—The methods of purification of chemicals and preparation of degassed samples for irradiation

(6) C. E. McCauley, G. J. Hilsdorf, P. R. Geissler, and R. H. Schuler, *J. Am. Chem. Soc.*, **78**, 3246 (1956).

tion have been discussed earlier.⁵ The alkyl halide products containing radioactive recoil atoms were separated and detected by gas chromatography using a well-type scintillation counter to monitor the effluent stream from the column. Organic yields were determined by the usual technique of extracting the inorganic halogen products from a CCl_4 solution with an aqueous reducing solution and counting the two phases.

Results

Relative Yields of Organic Products Containing I^{128} .—Tables I through IV show the relative percentages of I^{128} in each of the organic products formed by $\text{I}^{127}(\text{n},\gamma)\text{I}^{128}$ activation of solutions of: (I) CH_3I , $\text{C}_2\text{H}_5\text{I}$, and $\text{C}_3\text{H}_7\text{I}$ in C_5H_{12} ; (II) $\text{C}_2\text{H}_5\text{I}$ in C_5H_{12} containing 0.25 mole % added I_2 ; (III) I_2 in C_5H_{12} ; and (IV) I_2 in $\text{C}_2\text{H}_5\text{I}$. Table V gives analogous data for the distribution of Cl^{38} formed by the $\text{Cl}^{37}(\text{n},\gamma)\text{Cl}^{38}$ process in solutions of $n\text{-C}_3\text{H}_7\text{Cl}$ in C_5H_{12} .

TABLE V

RELATIVE YIELDS^a OF ORGANIC Cl^{38} PRODUCTS FORMED BY $\text{Cl}^{37}(\text{n},\gamma)\text{Cl}^{38}$ ACTIVATION OF $n\text{-C}_3\text{H}_7\text{Cl}$ - C_5H_{12} SOLUTIONS

Products	10% $n\text{-C}_3\text{H}_7\text{Cl}$	1% $n\text{-C}_3\text{H}_7\text{Cl}$	0.1% $n\text{-C}_3\text{H}_7\text{Cl}$
CH_3Cl	11.4, 12.2	9.9, 10.3	6.3
$\text{C}_2\text{H}_5\text{Cl}$	6.5, 6.9	5.6, 5.8	3.6
$\text{C}_3\text{H}_7\text{Cl}$	7.5, 6.8	6.4, 7.0	4.7
<i>i</i> - $\text{C}_3\text{H}_7\text{Cl}$	3.2, 2.7	1.9, 2.0	.. ^b
$\text{C}_3\text{H}_5\text{Cl}$	0.34, 0.22	.. ^b , .. ^b	.. ^b
$n\text{-C}_3\text{H}_7\text{Cl}$	15.2, 17.3	11.5, 12.9	8.2
<i>sec</i> - $\text{C}_4\text{H}_9\text{Cl}$	1.5, 1.2	1.3, 1.3	.. ^b
$n\text{-C}_4\text{H}_9\text{Cl}$	5.4, 5.9	5.5, 6.2	5.9
<i>sec</i> - $\text{C}_5\text{H}_{11}\text{Cl}$	27.2, 18.9	32.9, 27.8	54.3
$n\text{-C}_5\text{H}_{11}\text{Cl}$	12.2, 13.1	15.9, 17.4	17.0
Others ^c	9.6, 14.7	9.1, 9.3	.. ^b

^a Expressed as per cent of total organic activity. ^b Peak not observed due to insufficient activity. ^c Includes four unidentified peaks.

Effect of Duration of Irradiation on Fraction of I^{128} Entering Organic Combination in $\text{C}_2\text{H}_5\text{I}$ - C_5H_{12} Solutions.—Organic yields were determined on a series of 1–10 mole % solutions of $\text{C}_2\text{H}_5\text{I}$ in pentane exposed for 1 sec. to 10 min. in the rabbit of the CP-5 reactor. The organic yields for 1 sec. irradiations were in agreement with those observed earlier for relatively low intensity irradiations with an Sb-Be photoneutron source.³ For periods of irradiation longer than 1 sec. the yields rose sharply to about 90% for irradiations of 10 sec. and longer. Samples which were irradiated to a dose of 3.4×10^{19} e.v. g^{-1} with Co^{60} γ -rays prior to neutron irradiation gave organic yields of about 50% for 1 sec. irradiations in the rabbit and this yield increased sharply with duration of pile exposure, as in the case of samples which had not been pre-irradiated. The pre-irradiation dose was equivalent to the dose of ionizing radiation received during about 10 min. in the rabbit. Two of the samples of 13 mole % $\text{C}_2\text{H}_5\text{I}$ which had received the Co^{60} γ -dose were exposed in the thermal column of the reactor for 7 min. where they received 5×10^{15} e.v. of ionizing radiation per g. compared to 5×10^{16} e.v. for 1 sec. in the rabbit. They gave organic yields of 44 and 49%. In another experiment a solution of 1.2 mole % $\text{C}_2\text{H}_5\text{I}$ in C_5H_{12} was irradiated in the rabbit for 10 min. following which the I^{128} activity was allowed to decay completely. When this sample was then exposed in the rabbit for approximately 1 sec. an organic yield of 62% was obtained. These observations seem to demand the conclusion that the increase from about 50 to 90% in organic yield which accompanies an

increase in irradiation time in the rabbit from 1 to 10 sec. or more is dependent on a metastable species which is capable of reacting with some form of I^{128} to incorporate it in organic combination. The data indicate that this species requires about 10 sec. of irradiation at the intensities in the rabbit to reach its steady-state concentration and that it disappears when the sample is removed from the radiation field. It may be estimated¹ that the steady-state concentrations of free radicals in samples in the rabbit are reached in 10 msec. or so if the radicals are formed with a G -value of 10 and disappear with a bimolecular rate constant⁷ the same as that for the recombination of iodine atoms in hydrocarbon solutions. It would appear therefore that if a radical or radicals are responsible for the increase in yield they combine with other radicals in the system with rate constants much smaller than that for the recombination of iodine atoms or are produced with a G -value much less than 10, or both. The nature of these phenomena, which nearly double the organic yield, is made additionally puzzling by the fact that the product distributions shown by the data of Table I, for which most of the irradiations were such as to give organic yields in the 90% range, and those of Table II, where iodine scavenger was used and the yields were in the 35% range, are qualitatively similar. This similarity in distribution of products can be rationalized if the organic yield in the presence of scavenger results from combination of the I^{128} with radicals formed in its immediate solution envelope by its own conversion and Auger electrons, the distribution of radical species in this envelope being the same as that produced in the bulk of the solution by external radiation, as discussed below.

Organic yields were not determined on the samples of Table I. They undoubtedly varied for the samples with short irradiations and were in the high range for those with long irradiation. For this reason the results are given as per cent of total organic activity and any interpretation of their meaning must be conditioned by an awareness that the chemistry of the system is affected by the intensity-duration effect discussed above.

Discussion

High Yield of I^{128} in Form of Parent Iodide.—The most interesting aspect of the data of Tables I and II is the large fraction of the I^{128} activity that appears in the form of the alkyl iodide solute even at low concentrations of alkyl iodide and even in the presence of 0.25 mole % I_2 . Thus 41% of the organic I^{128} is found as $\text{C}_2\text{H}_5\text{I}^{128}$ from 1.4% $\text{C}_2\text{H}_5\text{I}$ in $n\text{-C}_5\text{H}_{12}$, 42% as $\text{CH}_3\text{I}^{128}$ from 1.8% CH_3I in $n\text{-C}_5\text{H}_{12}$, and 44% as $n\text{-C}_5\text{H}_{11}\text{I}^{128}$ from 0.9% $n\text{-C}_5\text{H}_{11}\text{I}$ in $n\text{-C}_5\text{H}_{12}$ (Table I). Likewise some 65% is found as $\text{C}_2\text{H}_5\text{I}^{128}$ in 6.7% solutions of $\text{C}_2\text{H}_5\text{I}$ in $n\text{-C}_5\text{H}_{12}$ containing 0.25% I_2 (Table II). These relative yields in the form of the solute molecule are much higher than the yields of any other organic products and much higher than the yield of any single organic I^{128} product from the neutron irradiation of solutions of I_2 in $n\text{-C}_5\text{H}_{12}$ (Table III).

Among the explanations for the high yields of I^{128} in the form of the parent iodide which must be considered are: (1) failure of the parent C-I bond to rupture following the $\text{I}^{127}(\text{n},\gamma)\text{I}^{128}$ process; (2) primary or secondary recombination of the parent radical and I^{128} atom following rupture; (3) exchange of the I^{128} atom

(7) S. Aditya and J. E. Willard, *J. Am. Chem. Soc.*, **79**, 2680 (1957).

with parent-type alkyl iodide molecules; (4) reaction of the I^{128} atoms, or molecules which they have formed, with radicals of the parent type which have been formed by the processes of radiation chemistry in the system.

Failure of the parent bond to rupture is ruled out by the fact that the organic yields of the parent molecule from radiative neutron capture by alkyl halides in the gas phase are normally very low. Thus yields of 1.09% or less have been observed for seven alkyl iodides and eleven alkyl bromides tested.⁸ Rupture of the parent bond may be caused by the recoil energy imparted to the atom on emission of a γ -ray or by generation of a high positive charge on the halogen atom as a result of internal conversion.

Iyer and Martin⁹ have carried out an ingenious and important experiment to determine experimentally the extent of failure of I^{128} atoms to escape from the parent radical following radiative neutron capture by the iodine in liquid alkyl iodides. This consisted of neutron irradiations of mixtures of CH_3I and C_3H_7I in which the dilute component was synthesized from I^{129} while the major component contained only I^{127} . I^{130} was formed by the $I^{129}(n,\gamma)I^{130}$ process. By determining its yield in the form of the parent molecule in excess of the yield in that form when I_2 was used as the source of I^{129} a value of about 4% was obtained for the fraction of the (n,γ) events in which the recoil atom either failed to rupture the parent bond or recombined with the parent radical.

Photochemical evidence also seems to rule out the possibility that the high yields of the parent species observed in the present work are due to recombination of I^{128} with the parent radical either in the parent cage or after diffusion. When liquid C_2H_5I is exposed to 2537 Å. radiation at 25° the quantum yield for formation of C_2H_5 radicals which do not recombine with iodine atoms with which they were initially bound is 0.32.¹⁰ In this example the maximum kinetic energy of the I atom is ~ 14 kcal. mole⁻¹ and that of the C_2H_5 radical ~ 54 kcal. mole⁻¹. The photochemical dissociation of I_2 with visible light and escape from recombination has a quantum yield of 0.66 in *n*- C_6H_{14} ,¹¹ 0.14 in CCl_4 ,^{11,12} and 0.08 in hexachlorobutadiene at 25°.¹¹ The iodine atoms produced by the visible light have about 20 kcal./mole each of kinetic energy. The yields for escape from recombination would be expected to be much higher for the kinetic energies imparted by the (n,γ) process than for those imparted by absorption of light.

Exchange of thermal I^{128} atoms with the alkyl iodide solute molecules cannot be responsible for the organic yields observed. Experiments¹³ in which solutions of 0.04 *M* C_2H_5I in hexane containing 0.002 *M* I_2 were illuminated for a week with a tungsten lamp indicate a very slow rate of exchange. It has been reported¹⁴ that the rate constant for the exchange of iodine atoms with liquid methyl iodide is 20 ml. mole⁻¹ sec.⁻¹ at 25°, whereas that for the exchange of I atoms with I_2

molecules in hexane¹⁵ is 8×10^{10} ml. mole⁻¹ sec.⁻¹. These data indicate that even low concentrations of iodine would compete very effectively with alkyl iodides for thermalized I atoms. The conclusion that the exchange of thermal I^{128} atoms with alkyl iodide molecules cannot be important in determining the organic yields observed is supported by many qualitative observations in the course of studies of alkyl iodide solutions in this Laboratory.

The evidence reviewed above indicates that the high yields of the I^{128} as the parent alkyl iodide are not the result of failure of bond rupture, primary or secondary recombination with the parent radical, or thermal exchange with the parent molecular species. The only plausible alternative of which we are aware is combination of the I^{128} atoms with radicals formed by the processes of radiation chemistry in the system.

Reaction with radicals formed by the recoil atom in losing its kinetic energy seems to be ruled out as an explanation of the high yield of the I^{128} in the form of the dilute alkyl halide solute. This follows from the fact that such yields are observed even in solutions as dilute as 0.14 mole % (Table I). The hypothesis that radiation-produced radicals are involved is consistent with the fact that in the γ -ray radiolysis of dilute solutions of alkyl iodides in pentane the predominant radicals are the alkyl radicals of the alkyl iodide solute.⁵ It is also consistent with the similarity between the spectrum of products obtained from the γ -ray radiolysis of alkyl iodide-pentane solutions with added $I_2(I^{131})$ ⁵ and the I^{128} products formed by the neutron activation of alkyl iodide-pentane solutions. This is illustrated in Table VI.

Despite these facts it would appear at first that the data of Table II which show that a high yield of I^{128} in the parent alkyl iodide species persists in alkyl iodide-pentane solutions even in the presence of 0.25 mole % I_2 scavenger preclude the possibility that the I^{128} atoms which re-form the parent compound in solutions of alkyl iodides in hydrocarbons do so by encountering radicals formed by radiation. The concentration of iodine in these experiments (0.25 mole %) is high enough to scavenge nearly all radicals produced by the γ -radiation in the system, and also all of the thermalized I^{128} atoms, before these species have an opportunity to encounter each other. (The rate of production of radicals in these systems by ionizing radiation was about 1 per sec. per 10^5 molecules of solution.)

The possibility must be considered, however, that electrons emitted by the I^{128} atom as a result of internal conversion and Auger transitions produce a high localized concentration of radicals so close to the atom that their reactions with the atom are not precluded by the I_2 scavenger. At least 50% of the I^{128} atoms produced by the (n,γ) process are born with a positive charge.¹⁶ This presumably results from an internal conversion process utilizing some of the energy available from the neutron capture. Although the charge spectrum of the I^{128} ions resulting from the Auger transitions following internal conversion has not been measured the spectrum of Xe^{131} ions from the internal conversion accompanying the $Xe^{131m} \rightarrow Xe^{131}$ process has been studied¹⁷ and shown to include Xe ions with charges from +1 to +22

(8) A. A. Gordus and C. Hsiung, *J. Chem. Phys.*, **36**, 954 (1962).

(9) R. M. Iyer and G. Martin, "Chemical Effects of Nuclear Transformations," International Atomic Energy Agency, Vienna, 1961, Vol. I, p. 282.

(10) R. H. Luebke and J. E. Willard, *J. Am. Chem. Soc.*, **81**, 761 (1959).

(11) F. W. Lampe and R. M. Noyes, *ibid.*, **76**, 2140 (1954).

(12) R. L. Strong and J. E. Willard, *ibid.*, **79**, 2098 (1957).

(13) R. M. Noyes, *ibid.*, **70**, 2614 (1948).

(14) T. S. Laurence and D. R. Stranks, "International Atomic Energy Agency Conference on the Use of Radioisotopes in the Physical Sciences and in Industry," Copenhagen, Denmark, 1960.

(15) R. M. Noyes and J. Zimmerman, *J. Chem. Phys.*, **18**, 656 (1950).

(16) S. Wexler and T. H. Davies, *ibid.*, **20**, 1688 (1952).

TABLE VI
COMPARISON OF THE I^{131} ORGANIC PRODUCTS^a FROM THE γ -RADIOLYSIS OF $I_2(I^{131})$ -RI-C₅H₁₂ SOLUTIONS WITH THE I^{128} PRODUCTS^a PRODUCED AS A RESULT OF THE $I^{127}(n,\gamma)I^{128}$ PROCESS IN RI-C₅H₁₂ SOLUTIONS^f

RI mole %	System	CH ₃ I	C ₂ H ₅ I	C ₃ H ₇ I	i-C ₄ H ₉ I	n-C ₅ H ₁₁ I	sec-C ₆ H ₁₃ I	n-C ₇ H ₁₅ I	2-Iodo C ₈ H ₁₇ I	3-Iodo C ₈ H ₁₇ I	n-C ₉ H ₁₉ I
C ₂ H ₅ I	I^{128}	5.7	0.9	41	0.4	6.7	0.3	1.4	20.2	11.3	12.0
0.1%	I^{131}	2.0	0.3	37	0.5	7.0	.3	1.0	26.0	12.8	10.3
C ₂ H ₅ I	I^{128}	5.2	1.0	51	0.7	5.6	.3	1.3	17.0	7.2	10.0
1.2%	I^{131}	2.5	0.4	57	0.4	3.0	.3	0.7	16.4	8.2	5.2
C ₂ H ₅ I	I^{128}	5.8	1.0	52	1.9	5.3	.4	1.4	15.2	6.8	9.8
6.7%	I^{131}	3.8	0.2	66	0.6	2.8	.6	0.4	10.0	6.8	4.9
CH ₃ I	I^{128}	42	0.9	9.0	0.4	6.0	.3	1.5	17.5	10.2	11.8
1.8%	I^{131}	54	... ^b	5.1	0.4	3.3	.5	0.6	17.9	9.5	8.3
I ₂ ^c	I^{128d}	15.3	2.6	18.6	4.6	13.5	.8	2.4	16.7	8.5	12.3
	I^{128e}	10.7	1.6	16.4	3.8	11.4	.6	1.8	24.9	11.6	13.8
	I^{131d}	6.1	... ^b	14.1	0.7	10.2	... ^b	1.0	34.0	17.0	17.0

^a Expressed as per cent of total organic activity. ^b No peak observed. ^c No added RI, only I₂ present. ^d 0.25% I₂. ^e 0.12% I₂. ^f The data for the $I^{127}(n,\gamma)I^{128}$ process are taken from Table I; they include experiments in which the organic yields were as high as 90% as a result of pile irradiations in excess of 10 sec. (see Discussion). The data for the radiolysis experiments are from reference 5; the concentration of $I_2(I^{131})$ in these experiments was 0.25 mole %.

with a maximum yield at +8. The distribution of charge for the 50% or more of the I^{128} atoms which are charged may be expected to be similar. The energies of the electrons emitted by the I^{128} will include the unknown energy of the conversion electron, electrons with the energy of the L \rightarrow K transition minus the L binding energy, *i.e.*, about 20,000 e.v., and, in the case of the more highly charged ions, additional electrons in the range from a few thousand e.v. down. Each of these electrons will excite and ionize molecules of the solution in close proximity to the I^{128} ion from which they come. The linear energy transfer for electrons of 0.1, 1, 10, and 20 kev. is reported^{18a} as 3.3, 1.2, 0.23, and 0.13 e.v. per Å., respectively. Thus an I^{128} ion which has emitted several Auger electrons will find itself in the center of a high localized concentration of species such as those formed along the track of a Compton electron in a similar solution exposed to Co⁶⁰ γ -rays. The multiply-charged I^{128} will be rapidly neutralized by charge transfer with adjacent molecules since even its first ionization potential (10.44) is higher than that of C₂H₅I (9.47) and about the same as that of C₅H₁₂ (10.55) (assuming gas phase values). A probable fate for the atom thereafter will be combination with a radical which has resulted from the activation of the surrounding solution by its own conversion electron or Auger electrons. The result should be a spectrum of I^{128} products similar to the spectrum of I^{131} labeled products observed when solutions of RI in pentane containing $I_2(I^{131})$ are radiolyzed with γ -rays.

If this hypothesis as to the mechanism by which I^{128} atoms enter organic combination is correct it implies either that metastable states of the I^{128} nucleus are sufficiently long lived^{18b} so that internal conversion does not occur until the atom has lost its kinetic energy of recoil or that the length of the recoil path in the condensed phase is short compared to the dimensions of the localized volume of high radical concentration produced by the electrons emitted by the atom. Both possibilities are plausible.

(17) (a) M. L. Perlman and J. A. Miskel, *Phys. Rev.*, **91**, 899 (1953); (b) A. H. Snell, F. Pleasanton, and T. A. Carlson, "Chemical Effects of Nuclear Transformations," International Atomic Energy Agency, Vienna, 1961, Vol. I, p. 147.

(18) (a) D. E. Lea, "Actions of Radiations on Living Cells," Cambridge Univ. Press, 1955, p. 24; (b) J. L. Thompson and W. W. Miller, *J. Chem. Phys.* **33**, 2477 (1963).

At least one mechanism other than the "autoradiation" (or "Auger radiation") mechanism must contribute to the total organic yield observed in condensed iodine-scavenged systems containing organic iodides. This is the displacement type of reaction, which has been observed in the gas phase, whereby the recoil iodine atom or ion replaces a hydrogen atom or a radical from an organic molecule in a bimolecular process. Except when CH₄ is the species attacked by the I^{128} , the total organic yields of this type of process are only a few per cent¹⁹ and so would not contribute appreciably to the total yields observed in condensed systems unless the probability of this type of reaction is greatly altered by change in phase.

The experiments of Table II were carried out with an excess of C₂H₅I (6.7 mole %) over I₂ (0.25 mole %) to ensure that most of the $I^{127}(n,\gamma)I^{128}$ events would occur in I^{127} which was organically bound, in order to give a satisfactory basis for comparison with the C₂-H₅I-C₅H₁₂ solutions of Table I in which no I₂ scavenger was present. On the basis of the Auger radiation hypothesis presented here, it might be speculated that much lower concentrations of C₂H₅I added to solutions of 0.25 mole % I₂ in C₅H₁₂ would lead to high yields of I^{128} as C₂H₅I even though many of the $I^{127}(n,\gamma)I^{128}$ events occurred in I₂ rather than C₂H₅I. As little as 0.1 mole % C₂H₅I added to 0.25 mole % solutions of $I_2(I^{131})$ in pentane prior to Co⁶⁰ radiolysis raised the $G(C_2H_5)$ from 1.16 to 3.3.⁵ There is, however, a difference between the nature of the Co⁶⁰ experiments, in which macro concentrations of I_2^{131} are used to detect and identify all of the free radicals, and the $I^{127}(n,\gamma)I^{128}$ experiments, in which the experimental observations concern the fate of the individual I^{128} atoms as they are formed. In the former case essentially every free radical formed undergoes the reaction $R + I_2 \rightarrow RI + I$ to form an alkyl iodide that is labeled with I^{131} . In the latter case the probability that the I^{128} will first encounter a radical formed from the solvent rather than from the solute increases as the solute concentration decreases even if the total number of radicals formed by the $RI + e^- \rightarrow R + I^-$ process is insensitive to RI concentration in the range studied. Stated another

(19) (a) G. Levey and J. E. Willard, *ibid.*, **25**, 904 (1956); (b) A. A. Gordus and J. E. Willard, *J. Am. Chem. Soc.*, **79**, 4609 (1957); (c) E. P. Rack and A. A. Gordus, *J. Chem. Phys.*, **36**, 287 (1962).

way, the R radicals formed by the electron attachment process by electrons resulting from the "autoradiation" mechanism will be distributed through a larger volume surrounding the I^{128} atom if the RI concentration is lower, and hence the ratio of concentration of these radicals to those formed from the solvent in the volume element immediately surrounding the I^{128} atom will be lower. Experiments made in our Laboratory by Mr. Hong Yol Kang indicate that the presence of CH_3I at 0.1 mole % in solutions of 0.2 mole % I_2 in C_6H_{14} does not increase the relative yield of CH_3I^{128} from the $I^{127}(n,\gamma)I^{128}$ process appreciably.

To further explore the implications of the autoradiation hypothesis Mr. Rolf Hahne of our Laboratory has investigated the organic yields of the $Br^{80m} \rightarrow Br^{80}$ isomeric transition occurring in $BrBr^{80m}$ dissolved in $n-C_6H_{14}$ with and without 1 mole % added $n-C_3H_7Br$, and in $n-C_5H_{12}$ with and without 1 mole % C_2H_5Br . The total organic yields were about 30% in the presence of 1 mole % Br_2 and 39% with 0.16 mole % Br_2 . In each case about 10% of the total Br^{80} appeared as the solvent bromide ($C_6H_{13}Br$ or $C_5H_{11}Br$) and only one or two per cent as the solute bromide (C_3H_7Br or C_2H_5Br). It is known that internal conversion and Auger electron emission occur in the Br^{80m} isomeric transition to produce an average charge of about 10.²⁰ The absence of preferential combination of the Br^{80} with radicals produced by the solute may be due in part to the relative concentration effect discussed in the preceding paragraph. When $n-C_3H_7Br$ is added to solutions of 0.25 mole % $I_2(I^{131})$ in $n-C_5H_{12}$ undergoing Co^{60} radiolysis a preferential yield of $C_3H_7I^{131}$ is observed but the effect is less than when RI is used as the solute. In considering the results of the isomeric transition experiments described above it is important also to note that no evidence is available on the probability of available electrons being scavenged by the process $Br_2 + e^- \rightarrow Br_2^-$ (or $Br + Br^-$) in competition with $RBr + e^- \rightarrow R + Br^-$.

The data of Table V show that in dilute solutions of $n-C_3H_7Cl$ in C_6H_{12} the organic yields of Cl^{38} products from the $Cl^{37}(n,\gamma)Cl^{38}$ process decrease in the order $sec-C_6H_{11}Cl > n-C_6H_{11}Cl > n-C_3H_7Cl > CH_3Cl$ which is the same order as the G -values for the corresponding radicals produced by the Co^{60} radiolysis of similar solutions.⁵ It is notable that the parent propyl radical does not predominate in the products of either the radiolysis or (n,γ) experiments with chlorides whereas the parent alkyl radical is clearly the organic product of greatest yield when the solute is an alkyl iodide or, in

the case of radiolysis, a bromide. As noted earlier⁵ this is consistent with the fact that the appearance potentials of I^- , Br^- , and Cl^- from the methyl halides are 0, 0, and 10 e.v., respectively.²¹

Great similarity in product distributions produced by different nuclear reactions of the same element have been observed in each of several media.²² The nuclear processes compared include for iodine $I^{127}(n,\gamma)I^{128}$, $I^{127}(\gamma,n)I^{126}$, $I^{127}(d,p)I^{128}$, and $I^{127}(n,2n)I^{126}$ in alkyl iodides. For bromine they include $Br^{80m} \xrightarrow{I.T.} Br^{80}$, $Br^{79}(n,\gamma)Br^{80m}$, $Br^{79}(n,\gamma)Br^{80}$, $Br^{81}(n,\gamma)Br^{82}$, $Br^{79}(n,2n)Br^{78}$ in alkyl and aromatic halides. The observations show conclusively that nuclides of a given element activated by drastically different nuclear processes may give both the same organic yield and same product distribution. If all the nuclear processes produce nuclei which pass through low lying metastable levels which decay by internal conversion the similarity of products could be explained in terms of the Auger radiation hypothesis discussed above. The fact that Br^{80} atoms activated by the isomeric transition which gives the atom no kinetic energy (except from coulomb repulsion following spreading of the charge) give the same product distribution as Br atoms born with high recoil energy is particularly interesting in this connection since an average of some 10 electrons²⁰ is emitted by the Br^{80} as a result of the internal conversion and Auger processes.

It has been reported²³ that when solutions of 0.01 mole fraction of CH_3I in H_2O containing 0.2×10^{-4} mole fraction of I_2 are irradiated with neutrons 12% of the I^{128} atoms formed are found in organic combination, independent of scavenger concentration. Because of the low mole fraction of CH_3I and the absence of scavenger effect this has raised the question as to whether failure of bond rupture following the (n,γ) process might be higher than indicated by the reasoning discussed above and related data.⁹⁻¹² On the basis of the Auger radiation theory this result may be ascribed to the production of CH_3 radicals by processes such as $CH_3I + e^- \rightarrow CH_3 + I^-$ or $CH_3I + H \rightarrow CH_3 + HI$, resulting from radiolysis by Auger electrons, followed by reaction of one of the CH_3 radicals with I^{128} to form CH_3I^{128} .

Acknowledgment.—This work was supported in part by the Atomic Energy Commission under contract AT(11-1)-32 and in part by the University Research Committee with funds made available by the Wisconsin Alumni Research Foundation.

(21) V. H. Dibeler and R. M. Reese, *J. Res. Natl. Bur. Std.*, **54**, 127 (1955).

(22) These results are discussed and references given in ref. 2c, pp. 221 and 222.

(23) J. E. Sturm and D. G. Davis, paper no. 106 presented before the Division of Physical Chemistry of the American Chemical Society at the 140th National Meeting, Chicago, Ill., September, 1961.

(20) (a) S. Wexler and T. H. Davies, *J. Chem. Phys.*, **18**, 376 (1950); (b) S. Wexler, *Phys. Rev.*, **93**, 182 (1954); (c) S. Wexler, "Chemical Effects of Nuclear Transformations," International Atomic Energy Agency, Vienna, 1961, Vol. I, p. 115.

EFFECT OF SOLVENT VISCOSITY ON EXCITATION ENERGY TRANSFER BETWEEN UNLIKE MOLECULES

BY W. H. MELHUISE

Department of Chemistry, University of California, Los Angeles, California

Received February 23, 1963

The investigation of excitation energy transfer between 9-methylanthracene and perylene in benzene-dibutyl phthalate mixtures and in lucite (polymethyl methacrylate) showed that the rate constant for energy transfer was strongly dependent on solvent viscosity at constant temperature (298°K.). A mean transfer distance (R_0) of 36 Å. was calculated from the rate constant extrapolated to zero fluidity. This is close to the value predicted by Förster's theory of resonance energy transfer (R_0 theor. = 39 Å.). In lucite, the mean transfer distance was unexpectedly found to be only 28 Å., both at 77 and 298°K.

I. Introduction

The fact that fluorescence quenching is in many cases diffusion controlled has long been known from quenching experiments conducted in solvents of different viscosities. The classic work of Frank and Vavilov¹ on the potassium iodide quenching of rhodamine B in water-glycerol mixtures was followed by the similar, but more refined studies of Stoughton and Rollefson² and La Mer and co-workers.³ The quenching of anthracene in organic solvents was shown to be diffusion-controlled by Bowen and Metcalf,⁴ and the extension of the theory to include medium and weak quenchers was made by Melhuise and Metcalf.⁵ Surprisingly, while self-quenching has for some time been considered to be diffusion-controlled,^{3,6} no self-quenching measurements appear to have been made in a series of solvents of differing viscosities, as was done in the case of fluorescence quenching by an added substance.

It is well known that a chemical reaction becomes diffusion-controlled because reaction in an encounter is so rapid that the rate is determined by the rate of diffusing together of the reacting species. However, in systems where fluorescence quenching occurs by energy transfer over a large distance (this may be the case for the self-quenching of some dyes), solvent viscosity was considered unimportant. Thus in the early experiments of Förster on excitation energy transfer between unlike dye molecules dissolved in water, it was argued⁷ that, since the calculated mean transfer distance (using the dipole-dipole interaction theory of energy transfer and neglecting diffusion) and the measured distance were approximately equal, Brownian motion was not contributing to the transfer rate. This was confirmed experimentally when addition of glycerol to the solvent (water) was found not to affect the rate of energy transfer between acriflavine and rhodamine B. Investigations by Bowen and Brocklehurst⁸ on energy transfer between 1-chloroanthracene and perylene in organic solvents supported Förster's contention; no great change in energy transfer was observed in a liquid solvent (as measured by Bowen and Livingston⁹) and a

frozen glass at 77°K., although these measurements were unfortunately somewhat qualitative. Bowen and Livingston also noted that transfer between 1-chloroanthracene and perylene in benzene and paraffin oil were approximately equal, indicating that diffusion was not playing an important part.

Weinreb¹⁰ has also studied the effect of viscosity on energy transfer between molecules such as naphthalene and anthracene. Although measurements were made by the less satisfactory method of monitoring the acceptor (the method undoubtedly includes the trivial reabsorption-re-emission process), significant changes in energy transfer efficiency were observed when the fluidity of the solvent was changed by varying the temperature. There is some doubt, however, as to the importance of other effects besides that of fluidity, which might also be temperature dependent.

The effect of viscosity on energy transfer between aromatic hydrocarbons has not been extensively investigated in a quantitative manner at constant temperature. In these systems, the absorption-fluorescence overlap is generally less than for dyes (since the extinction coefficients are usually lower) and consequently the mean transfer distance is smaller. Solvent viscosity might therefore be expected to have some effect since the transfer distance and the diffusion distance during the lifetime of the excited state are of the same order of magnitude.

II. Experimental and Results

(a) **Energy Transfer Measurements.**—Excitation energy transfer between 9-methylanthracene and perylene was investigated at 25° in benzene ($\eta = 0.59$ cp.) and di-*n*-butylphthalate ($\eta = 16.5$ cp.) and mixtures of the two solvents. A modified Aminco spectrofluorimeter with a double beam attachment¹¹ was used to excite and observe the fluorescence of the solutions from the same face of the cuvette. A constant mole ratio of 10/1 of 9-methylanthracene to perylene was used and 359 m μ (the absorption maximum of 9-methylanthracene) was chosen for the exciting wave length. Solutions were freed from dissolved air by passing a stream of nitrogen bubbles through the solution until the intensity of fluorescence was constant. The intensity of fluorescence of 9-methylanthracene was measured both at its first (395 m μ) and second (415 m μ) maxima and the energy transfer rate constant computed by the method of Bowen and Livingston⁹ from the decrease in the intensity of the donor fluorescence. This method is free from errors which could be introduced by absorption and re-emission of fluorescence by the acceptor. The equation used was

$$k_t[B] = [C/I(\lambda)] - (1 + k_1[A]) \quad (1)$$

- (1) J. M. Frank and S. I. Vavilov, *Z. Physik*, **69**, 100 (1931).
- (2) R. W. Stoughton and G. K. Rollefson, *J. Am. Chem. Soc.*, **62**, 2264 (1940).
- (3) J. Q. UMBERGER and V. K. La Mer, *ibid.*, **67**, 1099 (1945); B. WILLIAMSON and V. K. La Mer, *ibid.*, **70**, 717 (1948); K. C. Hodges and V. K. La Mer, *ibid.*, **70**, 722 (1948).
- (4) E. J. Bowen and W. S. Metcalf, *Proc. Roy. Soc. (London)*, **A206**, 437 (1951).
- (5) W. H. Melhuise and W. S. Metcalf, *J. Chem. Soc.*, 976 (1954).
- (6) E. J. Bowen, *Trans. Faraday Soc.*, **50**, 97 (1954).
- (7) Th. Förster, *Z. Naturforsch.*, **42**, 321 (1949).
- (8) E. J. Bowen and B. Brocklehurst, *Trans. Faraday Soc.*, **51**, 774 (1955).

- (9) E. J. Bowen and R. Livingston, *J. Am. Chem. Soc.*, **76**, 6300 (1954).
- (10) A. Weinreb, *J. Chem. Phys.*, **35**, 91 (1961).
- (11) W. H. Melhuise and R. H. Murashige, *Rev. Sci. Instr.*, **33**, 1213 (1962).

where

- $I(\lambda)$ = fluorescence intensity of 9-methylanthracene at either maxima (395 or 415 $m\mu$)
 C = a constant = $I(\lambda)$ extrapolated to zero concn. of B
 $[A]$ = molar concn. of 9-methylanthracene
 $[B]$ = molar concn. of perylene
 k_1 = self-quenching constant of 9-methylanthracene (l./mole)
 k_t = transfer rate constant (assumed bimolecular, l./mole)

The k_t values can only be compared if the quantum fluorescence efficiency of 9-methylanthracene is constant in all solvent mixtures. This was found to be true experimentally, with $Q_0 = 0.63$ in all benzene-dibutyl phthalate mixtures. Values of k_t obtained at different fluidities (T/η) are plotted in Fig. 1. At zero fluidity, k_t is estimated to be approximately 350.

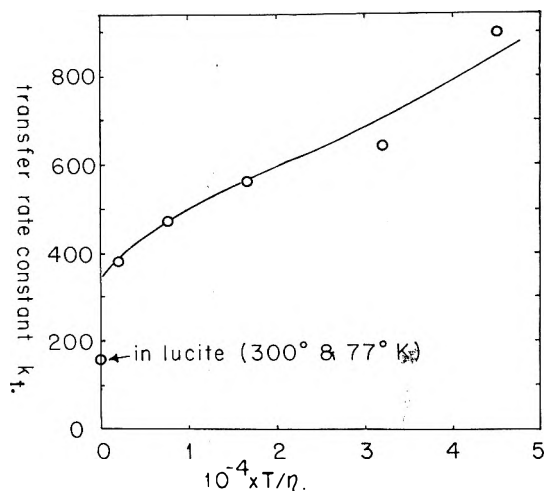


Fig. 1.—Effect of solvent fluidity on energy transfer between 9-methylanthracene and perylene at 25°.

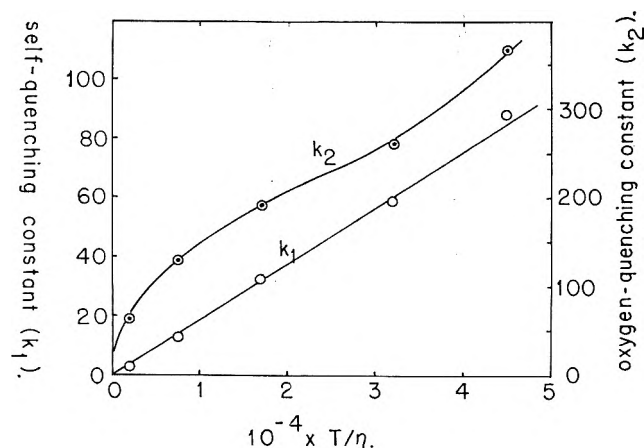


Fig. 2.—Dependence of self-quenching and oxygen-quenching of 9-methylanthracene on solvent fluidity at 25°.

Solid solutions of 9-methylanthracene and perylene in lucite were prepared by polymerizing the monomer (methyl methacrylate) containing a 5/1 mole ratio of 9-methylanthracene to perylene. A small quantity of benzoyl peroxide (0.01%) was added to the monomer before polymerizing at 55° for 48 hr. followed by a further 24 hr. at 80 to 90°. A flat surface was cut and polished on each sample and energy transfer measurements made in the same way as for solutions. Low temperature (77°K.) and room temperature (298°K.) measurements on the plastics were also made in a round quartz dewar which could be filled with liquid nitrogen. In these measurements, the exciting source was a high pressure mercury lamp with suitable filters to isolate the Hg 366 $m\mu$ lines, and liquid filters were used to isolate fluorescence from the samples in the region of 380 to 450 $m\mu$. The fluorimeter used has been described previously.¹²

(b) **Self-Quenching and Oxygen-Quenching of 9-Methylanthracene.**—The self-quenching constant of 9-methylanthracene, k_1 , was determined from the Stern-Volmer law

$$f_0/f = 1 + k_1[A] \quad (2)$$

where

- f_0 = intensity of fluorescence extrapolated to zero A concn.
 f = intensity of fluorescence at the concn. $[A]$
 $[A]$ = 9-methylanthracene concn. (mole/l.)

Measurements were made using the Hg 366 $m\mu$ lines for exciting and a Corning No. 3060 filter in front of the photomultiplier to remove stray exciting light. The oxygen quenching of 10^{-4} M solutions of 9-methylanthracene was also measured and the quenching constant calculated from

$$I_0/I = 1 + k_2[O_2] \quad (3)$$

where

- I_0 = fluorescence intensity in absence of oxygen
 I = fluorescence intensity at an oxygen concn. of $[O_2]$, mole/l.
 k_2 = oxygen-quenching constant

The concentration of dissolved oxygen in the mixed solvents was assumed to be constant at 1.45×10^{-3} M, which is the value for pure benzene. Self-quenching and oxygen-quenching constants as a function of fluidity are plotted in Fig. 2.

Quantum fluorescence efficiencies of 9-methylanthracene in benzene-dibutyl phthalate mixtures and in lucite were measured in the same fluorimeter using a rhodamine B quantum counter and a photomultiplier, as described elsewhere.¹²

(c) **Materials.**—9-Methylanthracene (from the Aldrich Chemical Co.) was purified by chromatography on alumina using a 60/40 mixture of hexane and benzene for elution. Perylene (Aldrich Chemical Co.) was purified by a fractional sublimation technique.¹² Eastman Kodak Co. di-*n*-butyl phthalate was purified by passing down silica gel and alumina columns. Benzene (Baker Analyzed) was used without further purification. Methyl methacrylate (Matheson, Coleman and Bell) was passed down silica gel and alumina columns and fractionally distilled.

III. Discussion

It has often been stated that excitation energy transfer is not limited by the rate at which the excited donor species encounters the unexcited acceptor molecules by diffusion through the solution.^{7-9,13} Unfortunately it is difficult to calculate the rate of encounter formation (pairing of the unlike molecules) involved in energy transfer for two main reasons: (a) the lifetime of the excited state of the donor is usually not known; (b) the models used for calculating the rate of pairing give only an order of magnitude. However, since self-quenching is considered to be a diffusion-controlled process,⁶ the self-quenching constant should give an upper limit to the energy transfer rate constant if energy transfer is also limited by the rate of pair formation. In the case of 9-methylanthracene, it is found that the self-quenching constant changes markedly with the fluidity (Fig. 2) at constant temperature and indicates that self-quenching is probably completely diffusion-controlled. It is interesting to note that self-quenching appears to follow the ideal equation for diffusion-controlled quenching given by Bowen⁶

$$k = k_1/\tau = (8R/3000)(T/\eta) \quad (4)$$

R = the gas constant (erg deg.⁻¹ mole⁻¹)

τ = lifetime of the excited state (sec.), extrapolated to infinite dilution

The slope of the line k_1 vs T/η is theoretically 2.3×10^{-3} with $\tau = 1.1 \times 10^{-8}$ sec.¹⁴; the experimental

(13) Th. Förster, *Discussions Faraday Soc.*, **27**, 7 (1959).

(14) Based on oxygen-quenching data; the oxygen-quenching constant of anthracene in benzene (whose lifetime is about 4×10^{-9} sec.) is 128. The oxygen-quenching constant of 9-methylanthracene in benzene is 360 (Fig. 2) and suggests that the lifetime is about 2.8 times longer than anthracene, that is about 1.1×10^{-8} sec.

value (curve 1, Fig. 2) is 2×10^{-3} . Oxygen-quenching of 9-methylanthracene is much more efficient than self-quenching, a fact which Bowen⁶ has also observed for a number of other substances.

It will be seen from Fig. 2 that the energy transfer rate constant for 9-methylanthracene to perylene transfer is some 10 to 20 times faster than the self-quenching constant of 9-methylanthracene and, moreover, changes considerably with fluidity. This indicates that energy transfer must occur over distances greater than about one solvent diameter (*i.e.*, greater than the encounter distance). The mechanism of energy transfer between 9-methylanthracene and perylene must therefore be envisaged as a diffusional one in which the excited donor molecule can, in its lifetime ($\sim 10^{-8}$ sec.), diffuse approximately 20 to 30 solvent diameters in a fluid solvent ($T/\eta = 4 \times 10^4$) and thus come within the critical distance R_0 of the acceptor molecule and transfer its energy to it. The donor cannot diffuse so far in a viscous solvent and energy transfer is therefore less efficient in solvents of low fluidity. This mechanism would not necessarily hold for very concentrated solutions where the donor and acceptor are always within a distance of R_0 of one another.

Förster's theory of resonance energy transfer¹³ relates the critical transfer distance R_0 (where energy transfer and emission of fluorescence are equally probable) with the fluorescence spectrum and fluorescence efficiency of the donor and the absorption spectrum of the acceptor

$$R_0^6 = A(\kappa^2 Q_{od}/n^4) \int_0^\infty f_d(\bar{\nu}) \epsilon_a(\bar{\nu}) \bar{\nu}^{-4} d\bar{\nu} \quad (5)$$

where

- A = a constant ($= 9.0 \times 10^{-25}$)
- n = refractive index of the solvent
- Q_{od} = quantum fluorescence efficiency of the donor
- $\bar{\nu}$ = wave number (cm.^{-1})
- κ^2 = an orientation factor ($= 2/3$ for freely rotating molecules)
- $\int_0^\infty f_d(\bar{\nu}) d\bar{\nu} = 1$ = normalized fluorescence spectrum of the donor
- $\epsilon_a(\bar{\nu})$ = molar extinction coefficient of the acceptor.

Thus for the solvent benzene

$$R_0 = [1.2 \times 10^{-25} Q_{od} I(\bar{\nu})]^{1/6} \quad (6)$$

where $I(\bar{\nu})$ is the integral in eq. 5.

For 9-methylanthracene and perylene the integral $I(\bar{\nu})$ is about 4.5×10^{-14} and using $Q_{od} = 0.63$ (which was found to be constant in all benzene-dibutyl phthalate mixtures) R_0 is calculated to be 39 Å.

The bimolecular rate constant for energy transfer in l./mole is the reciprocal of the concentration where the sensitizer fluorescence has dropped to $1/2$ of its value in the absence of acceptor; $C(1/2) = 1/k_t$. Förster has shown¹ that for randomly distributed molecules, the intensity of the donor fluorescence drops to $1/4$ of its value in the absence of acceptor at a concentration C_0 (corresponding to a mean molecular distance of R_0). Thus since energy transfer approximately follows the Stern-Volmer law,¹³ it may be shown that $C_0 = 3/k_t$. Hence the transfer rate constant and the mean molecular distance R_0 (the critical distance) are related by

$$k_t = (R_0/5.08)^3 \quad (7)$$

where R_0 is in Ångstroms.

Using $R_0 = 39$ Å. in eq. 7 gives $k_t = 440$, which is somewhat larger than the value obtained by extrapolating the experimental rate constants to zero fluidity (*i.e.*, $k_t = 350$, which corresponds to an R_0 of 36 Å.).

The molecular orientation factor κ^2 has been taken as $2/3$, which is the value for freely rotating molecules. However, Förster¹³ has shown that even for molecules with fixed random orientations, the energy transfer rate constant should only be reduced by 10 to 20%. In this work, the solvent viscosities used are unlikely to affect the rotation of the solute molecules, especially considering the weak solute-solvent forces involved.

The transfer rate constant in lucite ($k_t = 160$ at 77 and 298°K.) is much less than the rate in benzene-dibutyl phthalate mixtures extrapolated to zero fluidity. The lifetime of 9-methylanthracene in lucite is about 20% less than in benzene, as inferred from quantum fluorescence efficiencies, and therefore cannot explain the difference between the two rates. The difference could be due to the solute molecules becoming aligned in the plastic during polymerization in directions which are not favorable to energy transfer. Another possibility is that pairing of the solute molecules by weak van der Waals forces, which might be possible in solution, is less likely in lucite which is polymerized at 55°, and thus the rate would be reduced in the plastic.

SINGLY- AND DOUBLY-CHARGED IONS FROM METHYL AND ETHYL ISOTHIOCYANATES BY ELECTRON IMPACT¹

BY BRICE G. HOBROCK, ROGER C. SHENKEL,² AND ROBERT W. KISER

Department of Chemistry, Kansas State University, Manhattan, Kansas

Received February 25, 1963

Electron impact data are presented for methyl and ethyl isothiocyanates. Partial mass spectra and appearance potentials for some singly- and doubly-charged ions are also given. The heats of formation of NCS and HNCS have been found to be 97 and 18 kcal./mole, respectively, leading to $D(\text{H-NCS}) = 131$ kcal./mole. The proton affinity of isothiocyanic acid is -150 kcal./mole and the ionization potential of the NCS radical is $\leq 10.4 \pm 0.3$ e.v.

Introduction

In a recent communication,³ we reported some of our observations on the species HNCS^+ , formed by rearrangement in the mass spectrum of ethyl isothiocyanate. A detailed study of other ions from this compound has now been completed and is reported herein. Electron impact information has also been determined for methyl isothiocyanate in order to study certain ionic species occurring in its mass spectrum. Appearance potentials are reported for the principal ions from these two compounds; from these data, other derived thermochemical information is obtained.

Two doubly-charged ions appear in significant quantities in the mass spectrum of methyl isothiocyanate. One of these is the doubly-charged parent-molecule ion, $(\text{CH}_3\text{NCS})^{2+}$. The other is the ion $(\text{HCNCS})^{2+}$. Both ions are rather abundant; in fact, they are significantly so in comparison to the commonly encountered relative abundances of approximately 0.01 to 0.1% for doubly-charged ions in many hydrocarbons. Therefore, we wanted to examine further these two particular ions in an attempt to shed what light possible upon the physical properties which one may determine mass spectrometrically and to attempt to understand the structures of these two ions.

Experimental

Methyl isothiocyanate was obtained from K & K Laboratories, Inc., and ethyl isothiocyanate from Eastman Organic Chemicals. Both compounds gave only a single peak upon gas chromatographic analysis. Isopropyl isothiocyanate was prepared from 2-bromopropane and NaSCN in refluxing methanol, with the isomerization accomplished by heating.⁴ The product contained small amounts of methanol, isopropyl alcohol, and water as impurities.

The instrumentation and experimental procedures have been previously described.⁵ The appearance potentials were evaluated from semilogarithmic plots of the ionization efficiency curves and by the method of extrapolated voltage differences.⁶ Upper limits were readily provided by linear extrapolation of the individual ionization efficiency curves. Xenon (ionization potential of 12.13 e.v.) was the energy reference and was introduced simultaneously with the samples.

Results

Partial mass spectra (taken at 70 e.v.) and appearance potentials are presented in Table I. The compositional, but not the structural, nature of each ion is indicated in

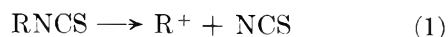
this table. Probable processes for the formation of certain specific ions will be discussed below. Similarly, heats of formation for the ions, consistent with the probable processes, will be indicated. The heat of formation of methyl isothiocyanate has been determined by Sunner⁷ to be 27.1 kcal./mole. By use of this value and Franklin's group method,⁸ the heat of formation of ethyl isothiocyanate is estimated to be 22 kcal./mole. These values are used in the calculations of the heats of formation of the various ions, as discussed below. Heats of formation of other species were taken from the NBS compilation,⁹ unless otherwise noted.

TABLE I
APPEARANCE POTENTIALS OF THE PRINCIPAL IONS FROM METHYL AND ETHYL ISOTHIOCYANATES

<i>m/e</i>	Ionic species	70-e.v. relative abundance	Appearance potential (e.v.)
CH₃NCS			
15	CH ₃ ⁺	10.7	15.3 ± 0.3
35.5	HCNCS ²⁺	8.6	28.0 ± .5
44	CS ⁺	11.8	15.6 ± .4
45	HCS ⁺	28.0	12.9 ± .2
46	NS ⁺ (?)	5.4	12.5 ± .2
58	NCS ⁺	4.3	14.9 ± .5
70	CNCS ⁺	7.5	14.1 ± .3
72	CH ₂ NCS ⁺	48.4	11.9 ± .2
73	CH ₃ NCS ⁺	100.0	9.13 ± .15
C₂H₅NCS			
15	CH ₃ ⁺	8.8	19.6 ± 0.5
26	C ₂ H ₂ ⁺	19.3	18.1 ± .2
27	C ₂ H ₃ ⁺	79.2	15.6 ± .3
29	C ₂ H ₅ ⁺	69.2	12.9 ± .2
44	CS ⁺	11.6	16.1 ± .5
45	CHS ⁺	14.6	15.2 ± .5
58	NCS ⁺	9.7	14.6 ± .4
59	HNCS ⁺	94.7	11.38 ± .15
60	H ₂ NCS ⁺	19.5	12.0 ± .3
70	CNCS ⁺	5.6	16.3 ± .2
71	HCNCS ⁺	4.5	14.0 ± .2
72	H ₂ CNCS ⁺	35.0	12.5 ± .2
87	C ₂ H ₅ NCS ⁺	100.0	9.10 ± .15
89	(C ₂ H ₅ NCS ³⁴) ⁺	5.3	9.10 ± .15

Discussion

An upper limit to the heat of formation of the NCS radical may be set if the process leading to the formation of CH₃⁺ from methyl isothiocyanate is



(7) S. Sunner, *Acta Chem. Scand.*, **9**, 837 (1955).

(8) J. L. Franklin, *Ind. Eng. Chem.*, **41**, 1070 (1949).

(9) F. D. Rossini, D. D. Wagman, W. H. Evans, S. Levine, and I. Jaffe, "Selected Values of Chemical Thermodynamic Properties," National Bureau of Standards Circular 500, U. S. Government Printing Office, Washington, D. C., 1952.

(1) This work was supported in part by the U. S. Atomic Energy Commission under Contract No. AT(11-1)-751 with Kansas State University.

(2) National Science Foundation Undergraduate Research Participant, summer, 1962.

(3) R. C. Shenkel, B. G. Hobrock, and R. W. Kiser, *J. Phys. Chem.*, **66**, 2074 (1962).

(4) H. A. Bruson and J. W. Eastes, *J. Am. Chem. Soc.*, **59**, 2011 (1937).

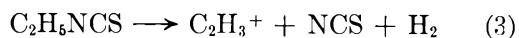
(5) E. J. Gallegos and R. W. Kiser, *ibid.*, **83**, 773 (1961).

(6) F. H. Field and J. L. Franklin, "Electron Impact Phenomena and the Properties of Gaseous Ions," Academic Press, Inc., New York, N. Y., 1957.

for then

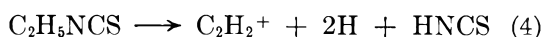
$$\Delta H_f(\text{NCS}) \leq AP(\text{R}^+) - \Delta H_f(\text{R}^+) + \Delta H_f(\text{RNCS}) \quad (2)$$

Using the known heat of formation of CH_3^+ ⁶ and our experimental appearance potential of CH_3^+ from $\text{CH}_3\text{-NCS}$, $\Delta H_f(\text{NCS}) \leq 118$ kcal./mole. Similarly, for the formation of C_2H_5^+ from ethyl isothiocyanate, we calculate $\Delta H_f(\text{NCS}) \leq 96$ kcal./mole. Further, if the process for the formation of C_2H_3^+ from ethyl isothiocyanate is



we find that $\Delta H_f(\text{NCS}) \leq 102$ kcal./mole. The appearance potential of the C_3H_7^+ ion from isopropyl isothiocyanate was measured to be 11.6 ± 0.2 e.v. From eq. 2, and using the known heat of formation of $s\text{-C}_3\text{H}_7^+$,⁶ $\Delta H_f(\text{NCS}) \leq 94$ kcal./mole, taking $\Delta H_f(i\text{-C}_3\text{H}_7\text{NCS}) = 16$ kcal./mole. From these results, we find $\Delta H_f(\text{NCS}) = 97 \pm 6$ kcal./mole by weighting heavily the latter three results.

The heat of formation of HNCS was estimated earlier³ to be about 27 kcal./mole, to within about 5–10 kcal./mole. We now have information to derive an "experimental" value. If the process for the formation of C_2H_2^+ from ethyl isothiocyanate is



then $\Delta H_f(\text{HNCS}) \leq 18$ kcal./mole, a value in fair agreement with the estimated one. Unfortunately, we encountered a minor air leak in our mass spectrometer which prevented us from determining the appearance potential of the C_2H_4^+ ion; such a determination might have allowed us to obtain a check on this value. Therefore, we must accept $\Delta H_f(\text{HNCS}) = 18 \pm 5$ kcal./mole as the "best value" for the present.

From the values of $\Delta H_f(\text{NCS})$ and $\Delta H_f(\text{HNCS})$, it is possible to calculate the H–NCS bond dissociation energy. Thus

$$D(\text{H-NCS}) = \Delta H_f(\text{H}) + \Delta H_f(\text{NCS}) - \Delta H_f(\text{HNCS}) \quad (5)$$

which, upon substitution of the determined and known values, leads to $D(\text{H-NCS}) = 131 \pm 8$ kcal./mole.

HNCS^+ and the ionization potential of HNCS have been discussed previously.³ HNCS^+ is observed in the mass spectrum of ethyl isothiocyanate but does not occur to a significant extent in the mass spectrum of methyl isothiocyanate, as we expected. We have measured the appearance potential of the HNCS^+ ion from isopropyl isothiocyanate to be 13.9 ± 0.3 e.v. If the process is



$\Delta H_f(\text{HNCS}^+) = 255$ kcal./mole. This value is to be compared to the value of 272 kcal./mole derived previously.³ We take as a "best value" $\Delta H_f^+(\text{HNCS}) = 263 \pm 8$ kcal./mole. From $\Delta H_f(\text{HNCS}) = 18$ kcal./mole, we derive the ionization potential of HNCS to be 10.6 e.v., in agreement with the earlier results.³

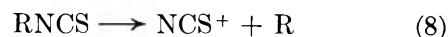
The ion observed at $m/e = 60$ in the mass spectrum of ethyl isothiocyanate has a different appearance potential than the ions of $m/e = 59$ and 58. This indicates that these ions are not the same, differing only

in the sulfur isotope contained in the ion. Rather, they must be different ions. The relative abundances also bear this out. Therefore, we conclude the ion of $m/e = 60$ to be H_2NCS^+ . It is suggested that the H_2NCS^+ arises by the process



which leads to a value of $\Delta H_f(\text{H}_2\text{NCS}^+) = 235$ kcal./mole. Taking this result together with $\Delta H_f(\text{HNCS}^+)$ and $\Delta H_f(\text{H}^+)$, we can derive the proton affinity of isothiocyanic acid to be -150 kcal./mole.

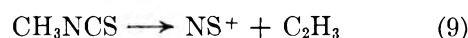
From the appearance potentials of NCS^+ from $\text{CH}_3\text{-NCS}$ and $\text{C}_2\text{H}_5\text{NCS}$, $\Delta H_f(\text{NCS}^+) \leq 338$ kcal./mole, taking the process for the formation of NCS^+ as



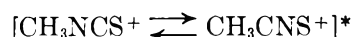
We note that eq. 1 and 8 are complementary reactions, which allows us to determine $I(\text{NCS}) \leq 10.4 \pm 0.3$ e.v.

The ionization potentials of methyl and ethyl isothiocyanates were measured to be 9.13 ± 0.15 and 9.10 ± 0.15 e.v. Watanabe¹⁰ has reported an ionization potential of 9.25 e.v. for methyl isothiocyanate and 9.14 e.v. for ethyl isothiocyanate. In preliminary measurements, we have found the IP of $i\text{-PrNCS}$ to be 9.4 ± 0.3 e.v., a value probably somewhat high. Calculations based on parameters given previously³ lead to $I(i\text{-C}_3\text{H}_7\text{NCS}) = 8.94$ e.v. From our ionization potential measurements and $\Delta H_f(\text{RNCS})$, we find $\Delta H_f(\text{CH}_3\text{-NCS}^+) = 238$, $\Delta H_f(\text{C}_2\text{H}_4\text{NCS}^+) = 232$, and $\Delta H_f(i\text{-C}_3\text{H}_7\text{NCS}^+) = 233$ kcal./mole.

The ion with $m/e = 46$ was found to have an appearance potential of 12.5 e.v. from methyl isothiocyanate. At first one is tempted to believe this ion to be CH_2S^+ . However, the energetics indicate this is not so. An alternative possibility is to consider the ion to be NS^+ . If the process is



then $\Delta H_f(\text{NS}^+) = 251$ kcal./mole. No literature value for $\Delta H_f(\text{NS}^+)$ is available for comparison, but 251 kcal./mole is considered to be reasonable when compared to the values⁶ for $\Delta H_f(\text{CO}^+)$, $\Delta H_f(\text{CS}^+)$, and $\Delta H_f(\text{NO}^+)$. A significant amount of $m/e = 46$ is not observed from ethyl isothiocyanate. It may be that the activated complex from which the unimolecular decomposition occurs in methyl isothiocyanate involves an equilibrium such as



This could then explain the production of the NS^+ ion.

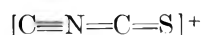
The CH_2NCS^+ ion is abundant in the mass spectra of both methyl and ethyl isothiocyanates. Since the process to form this ion from the methyl isothiocyanate is one involving ionization and the simple abstraction of a hydrogen atom, we calculate $\Delta H_f(\text{CH}_2\text{NCS}^+) = 249$ kcal./mole. Although this same ion is almost certainly formed through the ionization of ethyl isothiocyanate and dissociation of a methyl group, the value of $\Delta H_f(\text{CH}_2\text{NCS}^+) = 278$ kcal./mole is not considered to be as reliable as that found from the study of methyl isothiocyanate.

The formation of CHNCS^+ at $m/e = 71$ from ethyl isothiocyanate is likely accompanied by $\text{CH}_3 + \text{H}$ as

(10) K. Watanabe, T. Nakayama, and J. Mottl, *J. Quant. Spectry. Radiative Transfer.*, **2**, 369 (1962).

neutral fragments. If so, a value of 260 kcal./mole is calculated for $\Delta H_f(\text{CHNCS}^+)$. No literature value is available for comparison. This ion has a very small abundance in the mass spectrum of methyl isothiocyanate.

CNCS^+ appears in surprisingly large amounts in the mass spectra of both molecules at $m/e = 70$. $\Delta H_f(\text{CNCS}^+) = 300$ kcal./mole when calculated from the methyl isothiocyanate case, assuming that H and H_2 are formed. A slightly lower value, 278 kcal./mole, is calculated for neutral fragments $\text{CH}_2 + \text{H}_2 + \text{H}$ from ethyl isothiocyanate; 278 kcal./mole would appear to be the better value. A structure which might be written for this ion would be



which would indicate a linear ion and also possibly explain its apparent stability.

Isoelectronic with the CNCS^+ ion is the doubly-charged $(\text{HCNCS})^{2+}$ ion, observed at $m/e = 35.5$. The very large abundance (8.6%) of this doubly-charged ion suggests a special stability, particularly in view of the fact that the $(\text{HCNCS})^+$ ion at $m/e = 71$ is only about one-half as abundant (4.9%). The

structure of this ion might be written as



so that the charge separation indicated might allow greater stability than is commonly encountered with doubly-charged species. $\Delta H_f(\text{CHNCS}^{2+}) = 673$ kcal./mole is calculated, based upon the formation of H_2 as the neutral fragment and the appearance potential of 28.9 e.v. from methyl isothiocyanate. Although no appearance potential measurements were made on the $m/e = 36.5$ ion, $\text{CH}_3\text{NCS}^{2+}$, it is also relatively abundant (1.2% of the base peak, $m/e = 73$) in methyl isothiocyanate. The presence of these two doubly-charged species would appear to provide further evidence that the NCS groups contained in these two ions, and therefore possibly others as well, retain their structure. The mass spectrum of CH_3SCN , methyl thiocyanate, contains only minute amounts of doubly-charged ions at $m/e = 35.5$ and 36.5. This suggests that if the $\text{CH}_3\text{-NCS}^+$ and CHNCS^+ ions rearranged from the NCS to the SCN structure, large amounts of the doubly-charged ions would not have been observed. Therefore, it is suggested that the structure of the ions containing the NCS group is not altered by rearrangement to SCN.

THE PHOTOOXIDATION OF ACETONE¹

BY GRAHAM S. PEARSON²

Department of Chemistry, University of Rochester, Rochester 20, New York

Received February 28, 1963

The photochemical reaction between acetone and oxygen has been studied at temperatures from 36 to 100° at several oxygen pressures with light of 2537 and 3130 Å. Quantum yields are reported for oxygen disappearance and for methane, ethane, carbon monoxide, carbon dioxide, and methanol formation. A minimum quantum yield is obtained for formaldehyde. At 3130 Å. all quantum yields pass through maxima and oxygen acts as an inhibitor at high oxygen pressures. The effect of a 50-fold variation in intensity and a time dependence study are reported. At 2537 Å. the quantum yields are greater than at 3130 Å. and are independent of oxygen pressure (although the data might possibly be interpreted to involve a slight maximum). The reaction has also been studied with oxygen-18 and isotopic compositions are reported for the oxygenated products. The carbon monoxide comes mainly from methyl group oxidation, whereas the carbon dioxide comes primarily from the carbonyl group. A brief study of the formation of acetone-18 is reported; the quantum yield is higher at 2537 Å. than at 3130 Å. A fairly complete mechanism is suggested and the relative values of several rate constants are estimated.

Introduction

Although the photooxidation of acetone has been studied extensively above 120°,³⁻¹¹ the only data available at room temperature are those of Marcotte and Noyes,³ Cerfontain,⁹ and very recently, Osborne, Pitts,

and Fowler¹² and Kirk and Porter.¹³ It is known that part of the emission of acetone which presumably comes from a triplet state is quenched by oxygen,^{14,15} whereas the singlet emission is unaffected. Any interaction between oxygen and excited acetone molecules must involve the triplet state but not the singlet state. It is also known¹⁶ that an increase in temperature reduces the lifetime of the triplet state appreciably, *i.e.*, a 25° rise reduces the lifetime by one-half. Therefore we may expect at temperatures above 120° the reaction with oxygen to be primarily that of radicals.³ As the temperature is lowered from 120° to room temperature, the lifetime of the triplet state becomes longer and the possibility of triplet state interactions with oxygen be-

(1) This work was supported in part by the Directorate of Chemical Sciences, Air Force Office of Scientific Research, under Contract AF 49(638)-679.

(2) Postdoctoral Fellow, 1960-1961, under a grant from the Shell Fellowship Committee. Rocket Propulsion Establishment, Westcott, Buckinghamshire, England.

(3) F. B. Marcotte and W. A. Noyes, Jr., *Discussions Faraday Soc.*, **10**, 236 (1951).

(4) F. B. Marcotte and W. A. Noyes, Jr., *J. Am. Chem. Soc.*, **74**, 783 (1952).

(5) D. E. Hoare, *Trans. Faraday Soc.*, **49**, 1292 (1953).

(6) R. R. Hentz, *J. Am. Chem. Soc.*, **75**, 5810 (1953).

(7) M. I. Christie, *ibid.*, **76**, 1979 (1954).

(8) J. R. Dunn and K. O. Kutschke, *Can. J. Chem.*, **36**, 421 (1958).

(9) H. Cerfontain, *Academisch Proefschrift*, Amsterdam, 1958.

(10) J. Brown, N. T. Mitchell, and G. R. Martin, *Proc. Chem. Soc.*, **115** (1960).

(11) J. Caldwell and D. E. Hoare, "Abstracts of Photochemistry Meeting," Brussels, June, 1962.

(12) A. D. Osborne, J. N. Pitts, Jr., and S. L. Fowler, *J. Phys. Chem.*, **65**, 1622 (1961).

(13) A. D. Kirk and G. B. Porter, *ibid.*, **66**, 556 (1962).

(14) G. W. Luckey and W. A. Noyes, Jr., *J. Chem. Phys.*, **19**, 227 (1951).

(15) J. Heicklen, *J. Am. Chem. Soc.*, **81**, 3863 (1959).

(16) H. J. Groh, Jr., G. W. Luckey, and W. A. Noyes, Jr., *J. Chem. Phys.*, **21**, 115 (1953); W. E. Kaskan and A. B. F. Duncan, *ibid.*, **18**, 427 (1950).

comes increasingly likely. The present paper provides further data on the acetone-oxygen reaction in the region of 35 to 100° at 2537 Å. and at 3130 Å. An attempt is made to determine the nature of the interaction of oxygen with the triplet state.

Experimental

Spectro Grade Eastman acetone was dried over Drierite, degassed, and distilled in a grease-free vacuum system. The middle third was collected for use. No impurities could be detected in the mass spectrum or vapor phase chromatogram. Oxygen was prepared by heating potassium permanganate (A.R. grade) *in vacuo*.

For 3130 Å. radiation, an Osram HBO 500 lamp was collimated by a quartz lens and filtered through a Corning 9863 filter, a Corning 7740 filter, and 10 mm. of 0.9 M nickel chloride solution. A Hanovia S-100 Alpine burner was used for 2537 Å. and the filter combination consisted of chlorine gas, nickel chloride solution, and a Corning 9863 filter.

A quartz reaction vessel 200 mm. long with windows 23 mm. in diameter was used. Continuous mixing was achieved by a magnetically driven glass stirrer. In experiments at low oxygen pressures, oxygen was added by a "doser" during the course of a run to keep the oxygen pressure approximately constant. Transmitted intensities of the exciting radiation were measured on an R.C.A. 935 phototube connected to a Varian G. 10 graphic recorder. Intensity reductions were effected by wire screens.

A conventional vacuum line was used. Analysis of the reaction products was limited to methane, ethane, carbon monoxide, carbon dioxide, methanol, formaldehyde, and unreacted oxygen. Methane, carbon monoxide, and unreacted oxygen were separated at -196°, measured in a McLeod gage-Toepler pump arrangement,¹⁷ and then either analyzed by heating over cupric oxide at 280° or on a Consolidated 21-620 mass spectrometer previously calibrated for these gases. The filament was of rhenium. The carbon dioxide, ethane, and formaldehyde were distilled from an *n*-pentane mush (-130°), measured, and analyzed mass spectrometrically. The remaining fraction, consisting mainly of unreacted acetone and methanol, was analyzed by gas chromatography with a 3-m. Carbowax 350 on Johns-Manville C22 firebrick column at 60°. Quantum yields were calculated against the CO yield from acetone at 131°, which is unity in the absence of oxygen at both 2537 and 3130 Å.¹⁸

Results

Quantum yields are reported for oxygen disappearance and for methane, ethane, carbon monoxide, carbon dioxide, formaldehyde, and methanol formation. The quantum yield for formaldehyde is a minimum value since some polymerization is to be expected at liquid nitrogen temperatures.⁵

(a) 3130 Å., Oxygen-16.—The quantum yields at 3130 Å. as functions of the oxygen pressure at three temperatures are shown in Table I. In all runs the percentage conversion of acetone was kept well below 1% so that secondary reactions of the products were minimized. All quantum yields show a marked increase as the pressure of oxygen is decreased, the increase being more pronounced at higher temperatures. Methane and ethane are formed only at very low oxygen pressures and then only in small amounts which increase with increasing temperature. During one run of 30 min. duration at 100° with 0.29 mm. of oxygen, illumination of the cell was for 15-sec. periods followed by 52 sec. in the dark to test whether adequate mixing was occurring. The methane quantum yield obtained in this run agrees with values obtained in usual runs.

The effect of a 50-fold variation in light intensity is shown in Table II. At 35° there is little change but at

TABLE I
QUANTUM YIELDS IN ACETONE-OXYGEN MIXTURES
Wave length, 3130 Å.; acetone pressure = 145 mm.; I_a , the quanta absorbed/ml./sec., is 6.67×10^{13}

Oxygen pressure, mm.	$-\Phi_{O_2}$	Φ_{CO}	Φ_{CO_2}	$\Phi_{C_2H_5CO}$	Φ_{HCHO}	Φ_{CH_4}	$\Phi_{C_2H_6}$
$T = 36^\circ$							
2.17	0.122	0.0160	0.104	0.079	0.039	0.0	0.0
1.26	.195	.0209	.108	.076	.031		
0.441	.227	.0297	.124	.080	.025		
.234	.239	.0338	.140	.106	.044		
.114	.277	.0419	.146	.104	.027		
.104	.332	.0518	.165	.131	.045		
.078	.361	.0532	.157	.122	.039		
.0675	.359	.0565	.175	.130	.048	0.0	0.0
.0525	.379	.0627	.206	.142	.042	.0012	.0056
.0408	.393	.0658	.182	.146	.041	.0028	.0139
.0273	.401	.0631	.184	.133	.043	.0030	.0239
.00	..	.03950035	
$T = 70^\circ$							
2.502	0.313	0.0426	0.207	0.075	0.082	0.0	0.0
1.835	.350	.0474		.080			
1.358	.363	.0573	0.240	.097	0.094		
1.148	.438	.0727	.268	.087	.088		
0.553	.481	.0890	.296	.133	.107		
.420	.521	.0994	.320	.146	.108		
.328	.590	.104	.340	.167	.072	0.0	0.0
.114	.932	.197	.465	.255	.092	.007	.020
.083	1.025	.219	.494	.235	.076	.010	.020
.050	1.088	.246	.526	.241	.084	.016	.039
.00	..	.277029	.290
$T = 100^\circ$							
2.309	0.725	0.127	0.413	0.205	0.127	0.0	0.0
1.092	0.912	.169	.500	.272	.137	0	
0.808	0.943	.233	.539	.302	.165	.0003	
.540	1.224	.274	.677	.356	.163	.0027	
.360	1.242	.302	.717	.412	.148	.0018	
.310	1.288	.321	.761	.514	.155	.0031	
.288	1.549	.377				.0054	0.0
.202	1.646	.462	.856		.134	.016	.018
.162	1.693	.525	.842		.115	.0289	.042
.108	1.826	.556	.833	0.603	.145	.0364	.058
.00	..	.737112	.665

TABLE II
VARIATION OF QUANTUM YIELDS WITH INTENSITY IN ACETONE-OXYGEN MIXTURES
Wave length, 3130 Å.; acetone pressure = 145 mm.; O_2 pressure = 1 mm.

Length ^a of run, min.	I_a quanta/ml. sec. $\times 10^{13}$	$-\Phi_{O_2}$	Φ_{CO}	Φ_{CO_2}	Φ_{CH_3OH}
$T = 36^\circ$					
30.0	6.40	0.198	0.024	0.131	0.038
30.0	2.57	.229	.0178	.141	.031
90.0	0.69	.302	.0161	.125	.035
305.0	0.13	.312	.0198	.202	.058
$T = 70^\circ$					
30.0	6.66	0.430	0.0725	0.264	0.096
30.0	2.55	.559	.0524	.294	.123
90.0	0.68	.635	.0477	.284	.091
150.0	0.12	1.279	.0489	.389	.101
$T = 100^\circ$					
30.0	6.73	0.928	0.201	0.508	0.277
30.0	2.45	1.327	.188	.708	.313
60.0	1.16	1.493	.172	.662	.347
90.0	0.70	1.246	.152	.638	.241
105.0	0.39	1.346	.146	.733	.307
60.0	0.14	4.456	.083	.762	.233

^a The results in the first, fifth, and ninth rows were obtained from plots of corresponding yields against oxygen pressure.

higher temperatures the quantum yields of carbon dioxide formation and of oxygen uptake increase with

(17) A. N. Strachan and W. A. Noyes, Jr., *J. Am. Chem. Soc.*, **76**, 3258 (1954).

(18) D. S. Herr and W. A. Noyes, Jr., *ibid.*, **62**, 2052 (1940).

TABLE III
ISOTOPIC COMPOSITIONS OF CARBON MONOXIDE, CARBON DIOXIDE, AND FORMALDEHYDE
Wave length, 3130 Å.; $I_a = 6.67 \times 10^3$ quanta/ml. sec.; length of run = 30.0 min.; acetone pressure = 145 mm.

Oxygen pressure, mm.	$-\Phi_{O_2}$	Φ_{CO}	Percentage		Φ_{CO_2}	Percentage			Φ_{CH_2O}	Percentage		
			CO ¹⁶	CO ¹⁸		CO ¹⁶ O ¹⁶	CO ¹⁶ O ¹⁸	CO ¹⁸ O ¹⁸		CH ₂ O ¹⁶	CH ₂ O ¹⁸	
$T = 36^\circ$												
1.876	0.250	0.055	21.5	78.5	0.135	5.66	76.3	18.10	0.057	14.0	86.0	
0.209	.273	.052	9.8	90.2	.150	6.22	84.7	9.33	.059	14.3	85.7	
.148	.320	.053	9.5	90.5	.161	6.06	84.8	9.10	.059	15.2	84.8	
.0789	.366	.065	17.8	82.2	.173	5.92	84.8	9.36	.067	13.5	86.5	
.0664	.396	.066	10.5	89.5	.193	5.54	84.7	9.83	.059	14.7	85.3	
.0544	.401	.078179	6.68	85.4	8.04	.040	23.0	77.0	
.0410	.427	.064	16.7	83.3	.192	5.80	84.7	9.57	.045	18.1	81.9	
$T = 70^\circ$												
1.962	0.532	0.102	13.5	86.5	0.247	6.40	79.0	14.55	0.075	14.3	85.7	
0.295	.572	.143	9.6	90.4	.321	11.88	82.7	5.42	.067	11.3	88.7	
.237	.641	.154	7.7	92.3	.350	6.05	84.7	9.32	.067	12.2	87.8	
.137	.903	.209	17.3	82.7	.441	4.58	88.1	7.37	.073	11.7	88.3	
.109	.998	.227	20.2	79.8	.475	4.82	87.2	8.04	.086	10.6	89.4	
$T = 100^\circ$												
1.945	1.076	0.248	7.1	92.9	0.500	8.78	76.8	14.4	0.106	24.8	75.2	
0.199	1.752	0.526	21.3	78.7	0.839	4.49	88.5	6.94	0.092	14.2	85.8	

TABLE IV
QUANTUM YIELDS AND ISOTOPIC COMPOSITIONS AT 2537 AND 3130 Å.
Acetone pressure = 145 mm., $I_a = 3.20 \times 10^{12}$ quanta/ml./sec., length of run = 30.0 min.

Oxygen pressure, mm.	$-\Phi_{O_2}$	Φ_{CO}	Percentage		Φ_{CO_2}	Percentage			Φ_{CH_2O}	Percentage		
			CO ¹⁶	CO ¹⁸		CO ¹⁶ O ¹⁶	CO ¹⁶ O ¹⁸	CO ¹⁸ O ¹⁸		CH ₂ O ¹⁶	CH ₂ O ¹⁸	
$T = 36^\circ$												
0.00	..	0.25	100	0	
.176	2.62	.37	39.6	60.4	1.44	8.4	86.3	5.3	0.57	14.6	85.4	
.195	2.61	.41	38.4	61.6	1.83	10.2	80.0	9.8	.80	19.0	81.0	
.210	2.80	.45	37.4	62.6	1.73	13.5	74.8	11.7	.92	19.7	80.3	
.470	2.66	.61	43.4	56.6	1.85	16.8	72.2	11.0	.79	20.7	79.3	
.645	2.63	.46	40.8	59.2	1.39	11.8	82.6	6.6	.72	20.8	79.2	
$T = 100^\circ$												
0.430	5.16	0.82	43.8	56.2	2.25	13.0	75.4	11.6	1.23	15.5	84.5	
3130 Å.; $I_a = 3.3 \times 10^{12}$ quanta/ml./sec.; $T = 36^\circ$												
0.00	..	0.11	100	0	
.075	0.33	.07	0.23	0.087	
.083	.35	.0521082	
.172	.38	.0720055	
.236	.67	.0719047	
.371	.56	.11046	
			37.5 ^a	62.5 ^a	..	23.8 ^a	67.8 ^a	8.4 ^a	..	33.5 ^a	66.5 ^a	

^a Average of preceding five runs.

decreasing intensity whereas the quantum yield of carbon monoxide decreases with decreasing intensity.

A time dependence study was made over the range of 60 to 1800 sec. Plots of amounts against time yielded, within the limits of experimental error which becomes large for short times, straight lines for oxygen uptake and for carbon monoxide, carbon dioxide, and methanol formation. The plot for formaldehyde appears to reach a maximum for long times, indicating that formaldehyde undergoes secondary reactions.

(b) 3130 Å., Oxygen-18.—Several runs were performed with oxygen-18 of percentage composition O₂¹⁸ 97.5; O¹⁸O¹⁷, 0.43; O¹⁸O¹⁶, 1.67; O₂¹⁶, 0.23. After reaction the excess oxygen had the percentage composition O₂¹⁸, 98.0; O¹⁸O¹⁷, 1.57; O₂¹⁶, 0.14. The change in composition was no more than the error in the analysis.

For the runs with oxygen-18 all analyses were by

mass spectrometry and were performed in as short a time as possible after the run was completed so as to minimize errors due to exchange reactions. The methanol was analyzed on the vapor phase chromatograph, the methanol peak collected in a trap immersed in liquid nitrogen, and then analyzed on the mass spectrometer. The isotopic composition of methanol is not listed in Table III but its average value was CH₂O¹⁸H 90%, CH₂O¹⁶H 10%.

The quantum yields agree with the values given in Table I. In this series of runs it was found that at low oxygen pressures, where methane and ethane are formed, hydrogen is also a product with a quantum yield of less than 0.01 at 36° and follows the general trend of approaching zero as the oxygen pressure increases. Isotopic compositions are given in Table III. It can be seen that the carbonyl group in acetone is largely oxidized to carbon dioxide whereas the terminal

TABLE V
ACETONE-18 FORMATION
Acetone pressure = 22.5 mm., length of run = 60 to 260 min.; $T = 36^\circ$

Wave length, Å.	Oxygen pressure, mm.	I_a quanta/ml. sec.	$-\Phi_{O_2}$	Φ_{CO}	Φ_{CO_2}	$CH_3CO^{18}CH_3$	CH_3OH	CO_2^{18}
3130 ^a	1.93	2.68×10^{13}	1.04	0.23	0.41	0.129	0.294	0.039
3130	1.00	4.04×10^{12}	0.62	.18	.34	.078	.155	0.039
2537	1.00	3.30×10^{12}	1.91	.82	.72	.36	.93	.067
3130	0.49	4.04×10^{12}	0.87	.19	.40	.087	.267	.040
2537	0.47	3.30×10^{12}	2.80	.97	.87	.254	1.01	.383

^a Filter of Pyrex glass (Corning 7740) only.

carbon atoms are oxidized to methanol and formaldehyde. It is also evident that most of the carbon monoxide is formed in secondary reactions.

(c) 2537 Å., Oxygen-18.—No fluorescence of acetone is observed at 2537 Å.¹⁵ At 3130 Å. about 90% of the excited acetone molecules are in the triplet state^{15,19} at 25°. Some runs were therefore performed at 2537 Å. to determine whether there was a marked change in the photolysis results from those observed at 3130 Å. The results obtained are given in Table IV.

(d) Acetone-18 Formation.—No acetone-18 could be detected when 145 mm. of acetone were photolyzed under the conditions used. For a brief series of experiments the acetone pressure was reduced to 22.5 mm. Various filter combinations were used and the Osram HBO 500 lamp was used for both 2537 and 3130 Å. At 3130 Å. a Pyrex filter (Corning 7740) alone was used for the highest intensity runs and the usual filter combination for 3130 Å. used for the other runs. Acetone-18 was detected in the products and its quantity estimated by the mass spectrometer either by comparison with the methanol peak, since the methanol was determined by vapor phase chromatography, or by comparison with the acetone-16 peak using the fact that the percentage decomposition of the acetone is less than 1% and thus the acetone left at the end of a run may be regarded as equal to the amount at the beginning of the run to within 1%. The quantum yields for acetone-18 calculated by the two methods agree within 5%. Corrections were made for the amount of acetone-18 formed in the dark reaction and also for the contribution of acetone-16 to the 45⁺ peak on which the calculations were made. Acetone-18 was identified by the ratio of the corrected 60⁺ to 45⁺ peaks being 0.243 compared to 0.246 for the ratio of 58⁺ to 43⁺ for acetone-16. The results obtained are given in Table V. The quantum yield of acetone-18 is greater at 2537 Å. than at 3130 Å. for the same experimental conditions.

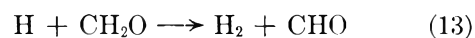
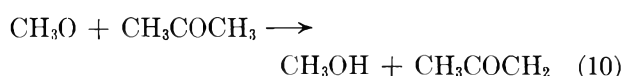
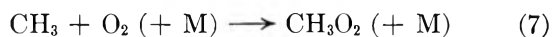
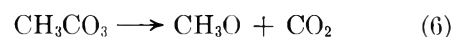
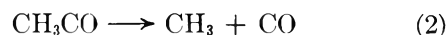
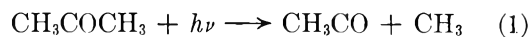
Discussion

Oxygen even at low pressures eliminates the triplet state emission from acetone.^{14,15} The removal of the triplet state will presumably be either by an energy transfer mechanism²⁰ or by direct reaction, as is the case in biacetyl photooxidation.²¹ It has recently been shown that acetone photooxidation with oxygen-18 at room temperature²² results in formation of acetone-18 in relatively high quantum yield. This is not a simple exchange mechanism since $O^{16}O^{18}$ was not found as a product. This finding has been confirmed by Kut-

schke²³ with oxygen-18 labeled acetone and light oxygen.

It is evident that no matter how the reaction starts, *i.e.*, whether by reaction of excited state molecules with oxygen or by reaction of free radicals with oxygen, the secondary reactions will be the same. Consequently the first step in the mechanism is written as (1), which may be followed by (2).

To facilitate the discussion the steps in the reaction will be listed.



Some observations may be made about the mechanism.

(i) At high oxygen pressures, reactions 3, 4, 12, and 13 will not be important and reaction 2 will compete with reaction 5. It is probable that (2) will still make a contribution since there is considerable evidence that acetyl radicals are formed which have retained energy from the primary process. The evidence has been summarized.²⁴ These "hot" acetyl radicals will decompose by (2).

(ii) Formyl Radical.—Dissociation of this radical (12) requires an activation energy of about 15 kcal.^{25,26} Thus it will be unable to compete with its reaction with

(19) J. Hecklen and W. A. Noyes, Jr., *J. Am. Chem. Soc.*, **81**, 3858 (1959).

(20) H. Okabe and W. A. Noyes, Jr., *ibid.*, **79**, 801 (1957).

(21) G. B. Porter, *J. Chem. Phys.*, **32**, 1587 (1960).

(22) R. Srinivasan and W. A. Noyes, Jr., *J. Am. Chem. Soc.*, **82**, 5591 (1960).

(23) K. O. Kutschke, private communication.

(24) W. A. Noyes, Jr., *Radiation Res., Suppl.*, **1**, 164 (1959).

(25) E. C. A. Horner, D. W. G. Style, and D. Summers, *Trans. Faraday Soc.*, **50**, 1201 (1954).

(26) J. G. Calvert, *J. Phys. Chem.*, **61**, 1206 (1957).

oxygen, which is known to be rapid,^{27,28} except at low oxygen pressures. Evidence that reaction with oxygen is by (14) rather than by (14a) has been presented by Horner, Style, and Summers.²⁵



(iii) **Methoxy Radical.**—This will abstract hydrogen both from acetone (10) and from formaldehyde (11). Rate constants are not available for (10) and (11) in the literature. However, values are available for the methyl radical abstractions from acetone²⁹ and from formaldehyde.^{30,31} If the value obtained by Gomer

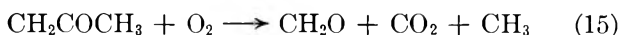


and Kistiakowsky³² for the recombination of methyl radicals is used, it is possible to calculate the rate constants for methyl abstraction at 300°K. This gives the ratio of $k_{11a}/k_3 = 1.2 \times 10^2$ with an energy of activation difference $E_3 - E_{11a} = 3.3$ kcal. mole⁻¹. Methoxy abstraction from alkanes has been shown³³ to parallel the abstraction by methyl radicals but with an activation energy that is lower by about 3 kcal. mole⁻¹. Therefore, it seems reasonable to put $k_{11}/k_{10} = k_{11a}/k_3$ and $E_{10} - E_{11} = 3.3$ kcal. mole⁻¹. Abstraction from formaldehyde may not be neglected if its pressure is even a few tenths of a per cent of the acetone pressure at room temperature. At 100° abstraction from formaldehyde would be unimportant unless its pressure were a few per cent of the acetone pressure.

(iv) **Methylperoxy Radical.**—The formation of this radical by (7) is well substantiated.³⁴ It is also known that there must be a reaction which yields large quantities of methoxy radicals. Reaction 8 has often been used in reaction mechanisms³⁵ and it is retained in this paper for want of definite evidence in favor of the alternative (8a) which leads to ozone formation and which has recently been discussed.³⁶



(v) **Acetonyl Radical.**—The chain reaction must involve the acetonyl radical³⁷ and it has been postulated to react with oxygen to yield formaldehyde, either carbon monoxide, or carbon dioxide, and methyl or methoxy radicals according to (15) and (15a).



Kutschke has shown that the parallel reactions in the azomethane photooxidation, (16) and (17), both occur and that nitrous oxide and nitrogen are formed in a

(27) K. Faltings, W. Groth, and P. Harteck, *Z. physik. Chem.*, **B41**, 15 (1938).

(28) J. F. McKellar and R. G. W. Norrish, *Proc. Roy. Soc. (London)*, **A254**, 147 (1960).

(29) A. F. Trotman-Dickenson and E. W. R. Steacie, *J. Chem. Phys.*, **18**, 1097 (1950).

(30) S. Toby and K. O. Kutschke, *Can. J. Chem.*, **37**, 672 (1959).

(31) A. R. Blake and K. O. Kutschke, *ibid.*, **37**, 1462 (1959).

(32) R. Gomer and G. B. Kistiakowsky, *J. Chem. Phys.*, **19**, 85 (1951).

(33) T. Bercés and A. F. Trotman-Dickenson, *J. Chem. Soc.*, 348 (1961).

(34) D. E. Hoare and A. D. Walsh, *Trans. Faraday Soc.*, **53**, 1102 (1957).

(35) J. H. Raley, L. M. Porter, F. F. Rust, and W. E. Vaughan, *J. Am. Chem. Soc.*, **73**, 15 (1951).

(36) D. F. Dever and J. G. Calvert, *ibid.*, **84**, 1362 (1962).

(37) W. A. Noyes, Jr., "Festschrift Arthur Stoll," Berkhäuser, Basel, 1957, p. 64.

ratio of about 4:1.³⁸ Possibly the ratio of the rate of (15) to that of (15a) would be about the same. Reac-



tion 15a is neglected in this mechanism.

The following facts must be considered.

(1) Quantum yields change slightly with intensity at 36° but at 70 and 100° carbon monoxide quantum yields decrease as the intensity decreases. Carbon monoxide is presumably formed primarily in a radical-radical reaction. The carbon dioxide and oxygen disappearance quantum yields increase as the intensity decreases. The chain ending step is thus assumed to be a radical-radical reaction at 70 and 100°.

(2) At 3130 Å. all quantum yields pass through maxima. This indicates that whereas oxygen is essential to chain propagation it must also act as an inhibitor.

The sums of the carbon, hydrogen, and oxygen contents of the products determined are not in the atomic proportions 3:6:1 after allowing for the oxygen consumed. Products other than those quantitatively determined are formed. These are probably acids¹² and water.^{6,11} An attempt to detect formic acid by infrared analysis of the products of a long run was unsuccessful although a strong absorption band for methanol was observed. This does not exclude formic acid as a product as the sensitivity was not high.

Certain conclusions may be drawn about the mechanism.

(a) **Methane Formation.**—If methane is formed only in reaction 3 one can derive the expressions (if (CHO) is negligible as it would be, if the formaldehyde concentration is low)

$$-\frac{d(\text{O}_2)}{dt} - \frac{d(\text{CO}_2)}{dt} = k_7(\text{CH}_3)(\text{O}_2) \quad (18a)$$

$$\frac{d(\text{CH}_4)}{dt} = k_3(\text{CH}_3)(\text{A}) \quad (18b)$$

$d(\text{CO}_2)/dt$ occurs in (18a) since in the reactions of radicals with oxygen which are of importance in this mechanism, carbon dioxide is formed in all cases other than that of methyl radicals reacting with oxygen. Hence

$$\frac{-\Phi_{\text{O}_2} - \Phi_{\text{CO}_2}}{\Phi_{\text{CH}_4}} = \frac{k_7(\text{O}_2)}{k_3(\text{A})} \quad (18)$$

A plot of the left-hand side of the expression against the oxygen concentration yields straight lines at each of the three temperatures. The following values were obtained for the ratio of k_7/k_3 .

Temp., °C.	k_7/k_3
36	7.25×10^5
70	1.90×10^5
100	5.05×10^4

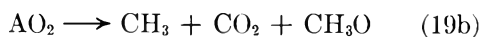
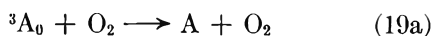
An Arrhenius plot yielded a value for the activation energy difference, $E_3 - E_7 = 9.2$ kcal., in excellent agreement with the value of 9.6 kcal.,³ which was obtained at higher temperatures. Values of k_7 are derived in part (e).

(38) F. Wenger and K. O. Kutschke, *Can. J. Chem.*, **37**, 1546 (1959).

(b) **The Decomposition of the Acetyl Radical.**—If oxygen-18 is used the only source of CO^{16} must be from the decomposition of the acetyl radical (2). Carbon monoxide formed by (2) and (14) must be CO^{18} . If reaction 19c occurs to an appreciable extent the quantum yield of CO^{16} would be of the order of that for methanol.

There is, however, considerable evidence that some acetyl radicals are formed which retain energy from the primary process. The evidence has been summarized.²⁴ The results presented in Table IV suggest that the fraction of "hot" radicals at 36° is about 0.03 at 3130 Å. and 0.17 at 2537 Å. These values are in agreement with those suggested of 0.03 at 3130 Å. and 0.2 at 2537 Å.

(c) **The Triplet State.**—If the triplet state reacts directly with oxygen to give products, the following steps are possible



where A is a normal acetone molecule and ${}^3\text{A}_0$ is an acetone molecule in lower vibrational levels of the triplet state. The following points must be considered.

(i) The initial products from the reaction of triplet acetone molecules with oxygen would probably be the same as those obtained by reaction of radicals from acetone with oxygen. In this respect no evidence concerning the reaction of triplet state acetone molecules would be obtained.

(ii) If reaction 19 occurs the reverse reaction must either be slow or not occur. This has been shown by the oxygen-18 experiments both in this work and in that of Srinivasan and Noyes,²² since there is no increase in the amount of $\text{O}^{16}\text{O}^{18}$ during a run. Recently Kutschke²³ has confirmed this by use of oxygen-18 labeled acetone and light oxygen. Again no increase in $\text{O}^{16}\text{O}^{18}$ was found.

(iii) If much of the reaction of acetone with oxygen at room temperature occurs through the triplet state by (19), (19b), and (19c), $\Phi_{\text{CO}^{16}}$ probably would be about the same as $\Phi_{\text{CH}_3\text{OH}}$ or better $1/2 (\Phi_{\text{CH}_3\text{OH}} + \Phi_{\text{CH}_3\text{O}})$. Since this is not so and since $\Phi_{\text{CO}^{16}}$ agrees closely with the values expected from "hot" acetyl radical decompositions, (19c) is probably unimportant.

(iv) At 2537 Å. acetone does not phosphoresce¹⁵ and it is doubtful if the triplet state is formed. If the reaction proceeds by the triplet state at 3130 Å. and by radical-oxygen reactions at 2537 Å., one might expect differences in behavior at the two wave lengths. Since important differences are not observed evidence for or against the role of the triplet state is not found.

It is concluded that acetone probably is regenerated after reaction of the triplet state molecules with oxygen. The existence of an exchange reaction indicates, however, that this may not be a simple deactivation by collision. This is in contrast to results obtained for the photooxidation of biacetyl at 4358 Å.^{21,39} It is in agreement with the conclusion reached by Kirk and Porter.¹³

(39) N. Padnos, private communication.

(d) **The Formation of $\text{CO}^{16}\text{O}^{16}$ and $\text{CO}^{18}\text{O}^{18}$.**—The formation of $\text{CO}^{18}\text{O}^{18}$ is not difficult to explain if one of the products such as methanol or formaldehyde were oxidized to carbon dioxide. It might be a product of reaction 14a.

The formation of CO_2^{16} is much more interesting. Several possibilities must be considered.

(i) Formation of CO_2^{16} may come from the small fraction of $\text{O}^{16}\text{O}^{18}$ in the oxygen-18. For one run the amount of oxygen used was 1.06×10^{-5} mole. Thus since the oxygen composition is 0.20% O_2^{16} and 1.60% $\text{O}^{16}\text{O}^{18}$ the amount of O^{16} available was 1.91×10^{-7} mole. If one assumes that all of this reacted preferentially with acetyl radicals, the maximum value available for $\text{CO}^{16}\text{O}^{16}$ formation is 1.91×10^{-7} mole. The actual amount of $\text{CO}^{16}\text{O}^{16}$ observed was 3.50×10^{-7} mole. Formation of $\text{CO}^{16}\text{O}^{16}$ is certainly not due mainly to the O^{16} impurity in the oxygen-18.

(ii) Various exchange reactions are possible either between CO_2 and water (probably on the walls) or less probably between carbon monoxide and water, oxygen and water, carbon monoxide and oxygen, or between types of CO_2 . These reactions have been considered theoretically⁴⁰ and their equilibrium constants, K , calculated, but little is known about rates with which equilibrium would be reached. Recently a study has been made of oxygen exchange between carbon monoxide and oxygen.⁴¹ With reaction times from 5 min. to 13 hr., no measurable exchange was found between carbon monoxide and carbon dioxide, carbon dioxide and oxygen, or carbon monoxide and oxygen at temperatures below 395°. Exchange between carbon dioxide and oxygen was found to be important only at temperatures over 800°. In this work, the time between mixing the acetone and oxygen and analyzing the separated products on the mass spectrometer was 1.5 to 2 hr. In one run the carbon dioxide sample was reanalyzed after 24 hr. The first analysis gave $\text{CO}^{16}\text{O}^{16}$, 6.1%; $\text{CO}^{16}\text{O}^{18}$, 84.7%; $\text{CO}^{18}\text{O}^{18}$, 9.2%, whereas the second analysis gave $\text{CO}^{16}\text{O}^{16}$, 6.45%; $\text{CO}^{16}\text{O}^{18}$, 84.4%; and $\text{CO}^{18}\text{O}^{18}$, 9.15%. The change is not more than experimental error. All of these exchange reactions seem to be unimportant.

Tests were also made with the mass spectrometer to ascertain whether exchange reactions during analyses could vitiate results. While exchanges of various types did occur, some with rather annoying pressure dependences, they were insufficient in magnitude to change the principal trends now reported.

(iii) The formation of $\text{CO}^{16}\text{O}^{16}$ may be considered in relation to the observation of Srinivasan and Noyes,²¹ confirmed in this work, that acetone-18 is formed in the photolysis at room temperature. There are three arguments.

(I) If acetone-18 is formed by reaction 19a or by reaction 19 followed by decomposition of the complex, then $\text{O}^{16}\text{O}^{18}$ must be formed. This is not observed.^{22,23}

(II) If (19) occurs irreversibly and is followed by collision with a normal acetone molecule to form a complex, this might decompose to form acetone, an acetylperoxy radical, and a methyl radical. If acetone-18 is formed in this way, the acetylperoxy radical will give $\text{CO}^{16}\text{O}^{16}:\text{CO}^{16}\text{O}^{18}$ in the ratio of 1:2 provided all oxygen

(40) H. C. Urey and L. J. Grieff, *J. Am. Chem. Soc.*, **57**, 321 (1935).

(41) C. A. Bank, E. A. Th. Verdurmen, A. E. de Vries, and F. L. Monterie, *J. Inorg. Nucl. Chem.*, **17**, 295 (1961).

atoms are equivalent in the acetylperoxy radical. It follows that if the quantum yield of acetone-18 is less than 0.5, $\Phi_{\text{CO}_2}^{18}$ must be greater than $\Phi_{\text{CO}_2}^{16}$ (assuming no other source of $\text{CO}^{16}\text{O}^{16}$).

Since the mechanism depends on the triplet state concentration, it is clear that the quantum yields of acetone-18 and of $\text{CO}^{16}\text{O}^{18}$ must decrease with increase in temperature and with decrease in wave length.

(III) A complex may be formed by collision of an acetylperoxy radical with a normal acetone molecule. The formation of the acetylperoxy radical by (5) must be irreversible as no $\text{O}^{16}\text{O}^{18}$ is formed. The same argument as in (II) then follows as to the nature of the carbon dioxide formed. In this case the quantum yields of the products depend on the acetylperoxy radical concentration and the energy of the radical. Consequently, the quantum yields of acetone-18 and $\text{CO}^{16}\text{O}^{16}$ should increase with increase in temperature and decrease in wave length.

(IV) Average values obtained in this work are given to illustrate the trend in the CO_2^{16} quantum yields. At 3130 Å. with $I_a = 6.7 \times 10^{13}$ quanta/ml./sec.: $\Phi_{\text{CO}_2}^{16} = 0.0097$ (36°); = 0.021 (70°); = 0.040 (100°). With $I_a = 3.2 \times 10^{12}$ quanta/ml./sec.: $\text{CO}_2^{16} = 0.047$ at 3130 Å. (36°); = 0.112 at 2537 Å. (36°). Examination of the results in Table V shows that the quantum yield of acetone-18 is greater at 2537 Å. than at 3130 Å. The relation between the acetone-18 and the $\text{CO}^{16}\text{O}^{16}$ quantum yields does not appear to be significant.

The following conclusions about the photochemical exchange of oxygen between acetone-16 and oxygen-18 seem warranted: (a) More than one acetone molecule or an acetone molecule and some fragment from a second acetone molecule must be involved if one is to get exchange without simultaneous formation of $\text{O}^{16}\text{O}^{18}$; (b) Since $\text{CO}^{16}\text{O}^{18}$, $\text{CO}^{16}\text{O}^{16}$, and $\text{CO}^{18}\text{O}^{18}$ are all formed the exchange process is probably very complex and related in some way to the formation of these various carbon dioxide molecules; (c) The data suggest that the reaction of the radical $\text{CH}_3\text{CO}^{16}\text{O}^{18}\text{O}^{18}$ (formed by reaction of the acetyl radical with oxygen-18) with acetone is responsible for the exchange reaction. This is not fully proven and little more can be said at this time.

(e) **Tests of the Mechanism.**—Assumption of the steady state for the methyl radical as in part (a) yields values of k_7/k_3 . Reaction 7 has been shown to be termolecular³⁴ and has the form



Using the published data for methyl radical abstraction from acetone²⁹ and for methyl radical recombination²² it is possible to calculate k_{7a} for each temperature. The following values are obtained where M is acetone, which

Temp., °C.	k_{7a} , ml. ² molecule ⁻² sec. ⁻¹
36	1.06×10^{-31}
70	1.44×10^{-31}
100	1.24×10^{-31}

may be compared with the value obtained at 200° by Hoare and Walsh³⁴ of 1.6×10^{-31} ml.² molecule⁻² sec.⁻¹.

The usual assumption of the steady state for the acetyl radical gives

$$d(\text{CO}^{16})/dt = k_2 I_a / (k_2 + k_5(\text{O}_2)) \quad (20)$$

Actually $I_a(1 - \alpha)$ should replace I_a and a term αI_a should be added to the right-hand side. α would be the fraction of the initially formed acetyl radicals which dissociate because of energy retained from the primary process.¹⁸ At 3130 Å. α is about 0.04 from the present results and hence terms in α are neglected. At 2537 Å. α would be much more important.

A plot of $1/\Phi_{\text{CO}^{16}}$ vs. (O_2) gives a straight line of slope $k_2/k_5 = 1.44 \times 10^{-8}$ mole l.⁻¹ at 36°. This value may be compared with that obtained by Cerfontain⁹ of 1.83×10^{-8} mole l.⁻¹ at 28° from photooxidation of azoethane. Neuman⁴² has obtained a value of $k_2/k_5 = 1.5 \times 10^{-3}$ mole l.⁻¹ at 290°. In view of the uncertainty in the activation energy of (2),²⁶ this value may be compared only roughly with the present value. k_2/k_5 from the present work is in satisfactory agreement with previous work.

Assumption of the steady state for the formyl radical gives

$$(d(\text{CO}^{18})/dt)(d(\text{H}_2)/dt) = k_{12} + k_{14}(\text{O}_2)/k_{12} \quad (21)$$

A plot of $\Phi_{\text{CO}^{18}}/\Phi_{\text{H}_2}$ against oxygen concentration yields a straight line of slope $k_{14}/k_{12} = 3.76 \times 10^5$ l. mole⁻¹, which gives $k_{12}/k_{14} = 2.66 \times 10^{-6}$ mole l.⁻¹ at 36°. The only value available in the literature for k_{12}/k_{14} is that of Marcotte and Noyes, who obtained $k_{12}/k_{14} = 2.66 \times 10^{-6}$ mole l.⁻¹ at 175°. The numerical agreement is purely fortuitous, since the error in the determination of k_{12}/k_{14} is somewhat large. Moreover the activation energy difference $E_{12} - E_{14}$ may be appreciable so that independence of k_{12}/k_{14} with temperature would hardly be expected.

Acknowledgment.—The author is very much indebted to Professor W. Albert Noyes, Jr., for his guidance and encouragement through the course of this work. He also wishes to thank Dr. K. O. Kutschke of the National Research Council, Ottawa, and Dr. D. E. Hoare, Queen's College, University of St. Andrews, Dundee, Scotland, for helpful discussions. Also he is indebted to Mr. Carl Whiteman for carefully going over trends with isotopically labeled carbon monoxide and carbon dioxide in the mass spectrograph.

(42) M. B. Neuman and G. I. Feklisov, *Zh. Fiz. Khim.*, **35**, 521 (1961).

THE THERMAL DECOMPOSITION OF NITRYL PERCHLORATE

BY HERMAN F. CORDES

*Chemistry Division, Research Department, U. S. Naval Ordnance Test Station, China Lake, California**Received March 4, 1963*

The thermal decomposition of solid nitryl perchlorate (NO_2ClO_4) has been studied over a temperature range of 69.99 to 112.3°. The products have been analyzed. The fractional rates of decomposition are independent of sample size. The theory of Mampel gives an excellent fit to the data from 0.5 to 95% decomposition. The rate constants are $k_{\text{initiation}} = 10^{12.6 \pm 0.5} e^{-28.5 \pm 0.8 \text{ kcal./mole}/RT} \text{ sec.}^{-1}$ and $k_{\text{growth}} = 10^{12.5 \pm 0.6} e^{-27.5 \pm 0.9 \text{ kcal./mole}/RT} \text{ sec.}^{-1}$. There is an induction time, $t_{\text{induction}} = 10^{-15.0 \pm 0.9} e^{+30.7 \pm 1.5 \text{ kcal./mole}/RT} \text{ sec.}$

Introduction

Numerous studies have been made on thermal decomposition of ionic solids.¹ Some progress has been made in correlating the observed behavior to chemical reactions in the case of the azides²; however, these systems are complicated by the presence of a secondary solid phase as one of the products. The kinetics of the ammonium perchlorate decomposition have been extensively studied³⁻⁶ and all of the products are gaseous. It was thought that the kinetics of the decomposition of another ionic perchlorate giving only gaseous products would be of considerable interest. Nitryl perchlorate was chosen as the compound for investigation as it was available and decomposed in a reasonable temperature region. This investigation is on the bulk powder. It is hoped that a suitable solvent can be found so that ultimately data can be gathered on single crystals. Considerable care was taken in the gathering of the data so that differential rates could be obtained as these furnish more sensitive criteria in analyzing the data.

Experimental

Nitryl Perchlorate.—This material was obtained from the Callery Chemical Co., Callery, Pa. The material contained less than one-half cation, mole per cent NO^+ as determined by a KMnO_4 titration. The particle size, as seen under a microscope, was about 10 μ or less. This material was transferred in a drybox that did not fume TiCl_4 .

Nitrogen Dioxide.—This material was tank material and was purified by distillation and by bubbling oxygen through the liquid at 0°. Absorption coef. at 436 $m\mu = (2.01 \pm 0.03) \times 10^5$ cc./mole/cm.

Chlorine.—The chlorine was tank material and was purified by distillation and storage over CaO at -78° . Absorption coef. at 330 $m\mu = (6.53 \pm 0.04) \times 10^4$ cc./mole/cm.

Chlorine Dioxide.—The chlorine dioxide was prepared by the method listed in ref. 7. Absorption coefficient at 454 $m\mu = (2.25 \pm 0.37) \times 10^6$ cc./mole/cm.

Apparatus.—The apparatus consisted of a Pyrex vacuum line, the various volumes being calibrated. A pressure transducer was connected to the line. One end of the vacuum line had a standard ball joint to which a Pyrex reaction tube containing the sample could be connected. When the reaction tube was connected to the line, the bottom portion of the tube, with the sample, was immersed in an oil bath. All joints were lubricated with Kel-F stopcock grease. With the exception of the reaction tube and the pressure transducer, all of the system was at room temperature.

Pressures were measured with a Consolidated Engineering Corporation, No. 4-312, 0-25 p.s.i.a. transducer, which was ther-

mostated at $29.6 \pm 0.1^\circ$ and calibrated against an absolute manometer. A stabilized d.c. power source was used for the voltage input to the transducer. The transducer output was partially bucked out with a 0.1- μv . potentiometer; the remaining signal was amplified with a d.c. microvolt amplifier and sent to a recorder. Readings corresponding to $\pm 0.1 \mu\text{v}$. transducer output could be made on the recorder. Noise made these readings uncertain to $\pm 0.2 \mu\text{v}$. The long time stability of the system was $\pm 1 \mu\text{v}$. The transducer had sensitivity of about 60 mm./mv. output. The transducer was electrically calibrated before each run. The response of the transducer was linear to $\pm 0.1\%$ over the region of the measurements. The recorder time could be read to ± 1 sec.

The reaction tube was inserted to a depth of about 5 cm. into an oil bath. The temperature of this bath could be controlled to $\pm 0.02^\circ$. The copper-constantan thermocouple used to measure the temperature was calibrated against the melting point of N.B.S. Calorimetric benzoic acid (temp. taken as 122.38°) and against the $\text{NaBr} \cdot 2\text{H}_2\text{O} = \text{NaBr} + 2\text{H}_2\text{O}$ transition (temp. taken as 50.67°). The correction was linear in mv. output and was $+0.27^\circ$ at 122.38° .

A Beckman DK-2 recording spectrophotometer was used with a 10-cm. cell for all spectral measurements. Corrections for N_2O_4 absorption were made⁸ at 330 $m\mu$, as well as corrections for Cl_2 absorption at 436 $m\mu$.⁹

Products of the Reaction.—For this series of runs, liquid nitrogen was placed around two traps in the system and the system's volume was recalibrated to correct for the apparent increase in volume. The traps were between the reaction tube and the collection volume.

The decompositions were carried out in the same manner as for the rate runs except that the recorder was used as a null instrument.

At the completion of the decomposition, the pressure of non-condensables in the system was measured and a sample of the gas was analyzed on a mass spectrometer. The condensed material was separated into three fractions. The first fraction was volatile at -112° , the second fraction was volatile at -78° , and the third fraction was nonvolatile at -78° .

Fraction Noncondensable at Liquid Nitrogen Temperature.—This fraction was analyzed on a mass spectrometer and was at least 99% O_2 . It contained no N_2 .

Fraction Volatile at -112° .—The total pressure of this fraction was measured in a calibrated volume. The gas was then sparked with a Tesla coil until there was no further increase in pressure. All condensables were frozen out at liquid N_2 temperature and the residual noncondensable pressure was recorded. The noncondensable material was assumed to be O_2 . The noncondensable material was pumped out. The condensables were allowed to vaporize into the calibrated volume and their pressure measured. Samples, at known pressures, were subjected to spectrophotometric analysis.

Results.—The only spectral species observable before sparking were ClO_2 and Cl_2 . Although pure samples of ClO_2 could be analyzed quantitatively on spectrophotometer, mixtures obtained from the decomposition were unstable and did not give consistent results upon expansion. The spectra were only used for qualitative identification. After sparking, Cl_2 and NO_2 were the only spectrally observable species. From the pressure before sparking, the pressure after sparking, the pressure of noncondensables after sparking, and the quantitative amounts of Cl_2 and NO_2 observed in the spectrophotometric cell, the only reasonable original composition derived for this fraction was

(1) W. E. Garner, Ed., "The Chemistry of the Solid State," Butterworth, London, 1955. See particularly chapters 7, 8, and 9.

(2) F. P. Bowden and A. D. Yoffe, "Fast Reactions in Solids," Academic Press, Inc., New York, N. Y., 1958.

(3) A. K. Galway and P. W. M. Jacobs, *J. Chem. Soc.*, 837 (1959).

(4) A. K. Galway and P. W. M. Jacobs, *Proc. Roy. Soc. (London)*, **A254**, 455 (1960).

(5) L. L. Bicumshaw and B. H. Newman, *ibid.*, **A227**, 115 (1954).

(6) L. L. Bicumshaw and B. H. Newman, *ibid.*, **A227**, 228 (1955).

(7) "Handbuch der Preparativen Anorganischen Chemie," Herausgegeben von Georg Brauer, Band I, Ferdinand Enke Verlag, Stuttgart, 1960, p. 274.

(8) T. C. Hall and F. E. Blacet, *J. Chem. Phys.*, **20**, 1745 (1952).

(9) N. S. Bayliss and R. C. Aickin, *Trans. Faraday Soc.*, **33**, 1333 (1937).

Cl₂, ClO₂, NO₃Cl. The chlorine made up about 90% of this fraction although the exact values varied from run to run.

A mass spectrum of a sample before sparking showed no N₂O.

The Fraction Volatile at -78°.—This fraction was treated in the same manner as the -112° volatile fraction. The only reasonable composition was ClO₂ and NO₃Cl with small amounts of Cl₂ present in one sample.

The Fraction Nonvolatile at -78°.—This fraction was found to contain only one absorbing species—NO₂. Upon long standing or upon sparking, the pressure and NO₂ content both increased. A mass spectrometer showed no species but oxides of nitrogen. The NO₂ did not account for all of the pressure. The residual pressure after correction for N₂O₄¹⁰ was assumed to be N₂O₅. Quantitative decomposition of the N₂O₅ was not possible as both long standing and sparking produced some NO, as deduced from a blue deposit at liquid nitrogen temperature.

The results of the analyses are given in Table I. The results are quite variable, as might be expected from a mixture of such species, ClO₂ and N₂O₅ being unstable and NO₂ and ClO₂ reacting to give NO₃Cl.¹¹ With the exception of the N atom balance, the material is all accounted for within experimental error.

TABLE I
MOLES OF PRODUCT PER MOLE OF NITRYL PERCHLORATE AT 106.97°

Product	Run		
	A	B	C
O ₂	1.830	1.739	1.843
NO ₃ Cl	0.148	0.091	0.153
ClO ₂	.148	.169	.115
Cl ₂	.354	.351	.372
NO ₂ ^a	.804	.563	.773
N ₂ O ₅	.000	.149	.013
Σ N atoms	.952	.952	.952
Σ O atoms	6.008	5.960	5.941
Σ Cl atoms	1.004	0.962	1.000

^a Total NO₂ from NO₂ + 2(N₂O₄).

Procedure During a Run.—The reaction tube was evacuated, weighed, and then taken into the drybox where a sample (0.3 to 0.7 g.) of nitryl perchlorate was placed in it. Care was taken not to remove any grease from the joints. The tube was reassembled and the stopcock was closed. The tube was taken out of the box and placed on a vacuum line and continuously evacuated at ~1 μ for 16 hr. The tube was closed, taken off of the line, and weighed to give a rough sample weight. The pressure measuring system was calibrated and the recorder was started. A metal tube with a closed end was inserted in the thermostated bath and the reaction tube was connected to the system with the sample inside the metal tube. This arrangement kept the sample below the bath temperature while the system was being evacuated. When the system had evacuated to ~0.01 mm. or less, the system was sealed. The shield was removed from around the sample and simultaneously the reaction tube was opened to the system. This point was marked on the recorder and was taken as zero time. The pressure was continuously recorded as a function of time on the recorder. Periodically the potentiometer was readjusted to buck out the additional voltage from the transducer; in this way the full sensitivity and full range of the transducer system could be used.

At the completion of the run (~90% decomposition) the reaction tube was closed and removed from the system. The tube was carefully cleaned and weighed. The tube was opened to the air and the remaining sample was decomposed over a flame. The sample tube was evacuated and weighed to give an empty weight. This second weight was taken as the true empty weight and usually did not differ from the first empty weight by more than a few milligrams.

During the decomposition, some sublimation to the region of the bath-air interface occurred. The total amount of sublimation was very small (visually only a thin film).

It is interesting to note that even at 90% decomposition the visible volume of solid in the reaction tube had changed very little from the original size.

(10) F. H. Verhoek and F. Daniels, *J. Am. Chem. Soc.*, **53**, 1250 (1931).

(11) H. Martin, *Angew. Chem.*, **70**, 97 (1958).

The Data

From the final pressure of the gases and the weight loss of the sample, the amount of gas per gram of decomposition was computed. This ratio was assumed to be constant over the whole course of the reaction. No attempt was made to correct for any reactions occurring in the gas phase. No correction was made for the NO₂ ⇌ N₂O₄ equilibrium as a trial test in the worst case gave results for corrected and uncorrected data that differed by less than the experimental error.¹² The fraction decomposed, α, was computed as a function of time. Suitable intervals of time were chosen and Δα/Δt was computed and considered as a derivative.

Plots of α vs. t or dα/dt vs. t did not show any variation with a factor of 10 variation in sample size, although there were apparent minor shifts in the time axis from run to run. When the data were plotted as dα/dt vs. α, the agreement was excellent (Fig. 1).

The α vs. t plots were typical sigmoid curves with inflection points at α ~ 0.2, consequently, the dα/dt vs. α curves were skewed bell shaped curves with a maximum in dα/dt at α ~ 0.2. The latter portions of the dα/dt vs. α plots, past the maximum, showed a linear decrease of dα/dt with increasing α. dα/dt extrapolated to zero at α = 1. In the early portion of the plots α was very nearly proportional to t⁴ with an induction period. During this induction period, a slow, nearly constant evolution of gas was observed. The total gas evolution corresponded to about 0.5% decomposition. In a sample from a new batch of material, this initial gas evolution corresponded to only 1/20% decomposition. The rates for a 5-g. sample agreed within experimental error with the data presented here and agreed with the extrapolation of the present data from 1/2 and 1/20% after correction for the initial gas evolution. The over-all form of the curves suggests a first-order initiation of nuclei followed by three-dimensional growth of these nuclei. The gas evolution early in the run may be due to decomposition of absorbed gases.

One run was periodically interrupted by quenching to room temperature. The system was then evacuated and after 15 to 100 min., the sample was reinserted in the bath and more data were taken. The data when plotted as dα/dt vs. α showed, except for warm-up periods of about 200 sec., complete agreement with uninterrupted runs at the same temperature (Fig. 2). This behavior of the interrupted runs suggests that the nuclei, once formed, are stable, and that the rate is not controlled by a steady state. The total pressure in the system during the interrupted runs was never greater than that corresponding to 5% decomposition. This fact plus the independence of the data on sample size show that the product gases have little or no effect on the decomposition.

Discussion

Mampel¹³ has developed an elegant treatment for the decomposition of uniform spherical particles. The particles are assumed to be randomly initiated on the surface and the nuclei so formed are assumed to grow as

(12) The total moles of gas evolved per mole of reactant lost appear—within the limits of weighing error—to be constant ±10%. The nature of the mixture is such that constancy of composition is not to be expected.

(13) K. L. Mampel, *Z. physik. Chem.*, **A187**, 235 (1940).

sections of spheres into the particles. The radii of the nuclei are assumed to grow linearly with time. A sub-surface at depth z beneath the geometrical surface of a particle is considered and the average fractional decomposition is computed for all such surfaces throughout the mass. An integration over all z is performed to obtain the total fractional decomposition for the whole mass. In terms of dimensionless parameters Mampel's solution is

$$\alpha = 3 \int_0^x (1 - \xi)^2 \left\{ 1 - e^{-\frac{\kappa}{4} \left[\frac{x^3}{3} - x\xi^2 + \frac{2}{3}\xi^3 \right]} \right\} d\xi \quad \text{for } 0 \leq x \leq 1 \quad (1a)$$

$$\alpha = 3 \int_0^{2-x} (1 - \xi)^2 \left\{ 1 - e^{-\frac{\kappa}{4} \left[\frac{x^3}{3} - x\xi^2 + \frac{2}{3}\xi^3 \right]} \right\} d\xi + 3 \int_{2-x}^1 (1 - \xi)^2 \left\{ 1 - e^{-\frac{\kappa}{3} [3x - 4 + 2\xi - \xi^2]} \right\} d\xi \quad \text{for } 1 \leq x \leq 2 \quad (1b)$$

$$\alpha = 1 - \frac{3}{2} \left(\frac{3}{x} \right)^{3/2} e^{-x(x-1)} \times \left[\frac{\sqrt{x}}{3} e^x - \int_0^{\sqrt{x}} \frac{1}{3} e^{n^2} dn \right] \quad \text{for } x \geq 2 \quad (1c)$$

where

α = fractional decomposition

$x = \frac{k_g t}{R}$; $n^2 = \frac{\kappa}{3} (1 - 2\xi + \xi^2)$; $\xi = Z/R$

k_g = growth rate constant

R = radius of a particle

t = the time

$\kappa = \frac{4\pi k_i N_0 R^2}{k_g/R}$; k_i = initiation rate constant

N_0 = density of potential sites on the surface

Equation 1a applies for short time and reduces for very short time to α proportional to t^4 . Equation 1b gives the intermediate portion and spans the inflection point in the α vs. t curve. Equation 1c is the first-order decay portion at long time. As can be seen, both α and its first derivative are continuous at the boundaries of the three equations. For the purpose of analysis of the data, it is more convenient to consider the first derivative. This choice also eliminates a cumulative error introduced in α by the gas evolution during the induction period. Let

$$\frac{1}{4\pi k_i N_0 R^2} \frac{d\alpha}{dt} = F(x, \kappa)$$

Then differentiation and rearrangement of eq. 1a, 1b, and 1c give

$$F(x, \kappa) = \frac{3}{4} \int_0^x (1 - \xi)(x^2 - \xi^2) e^{-\frac{\kappa}{4} \left[\frac{x^3}{3} - x\xi^2 + \frac{2}{3}\xi^3 \right]} d\xi \quad 0 \leq x \leq 1 \quad (2a)$$

$$F(x, \kappa) = \frac{3}{4} \int_0^{2-x} (1 - \xi)(x^2 - \xi^2) e^{-\frac{\kappa}{4} \left[\frac{x^3}{3} - x\xi^2 + \frac{2}{3}\xi^3 \right]} d\xi + 3 \sqrt{\left(\frac{3}{x} \right)^3} e^{-x(x-1)} \int_0^{\sqrt{x}} \frac{1}{3} n^2 e^{n^2} dn \quad 1 \leq x \leq 2 \quad (2b)$$

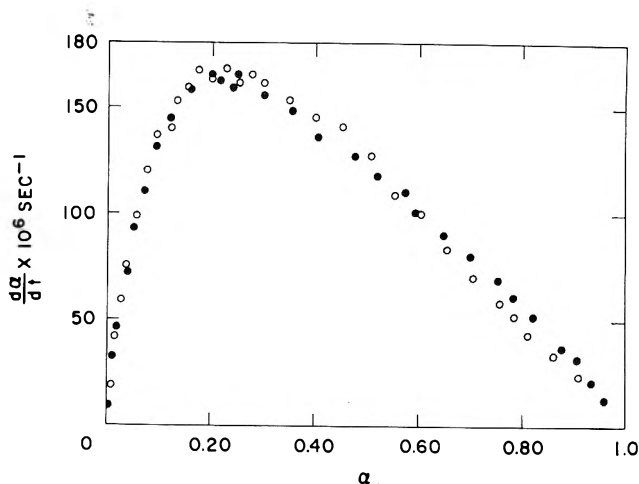


Fig. 1.— $d\alpha/dt$ vs. α at 112.38° showing the agreement between two separate runs (open and closed circles). The points have been selected.

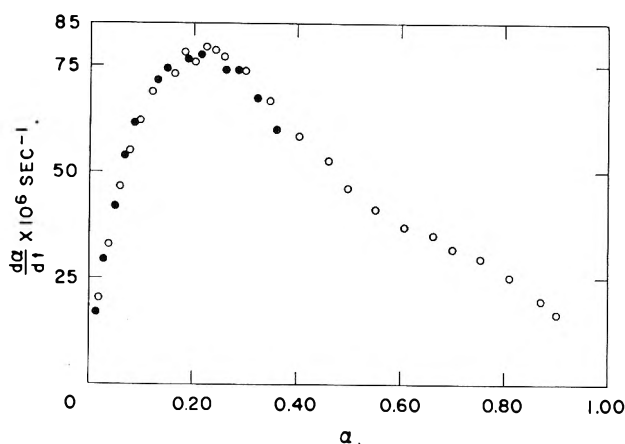


Fig. 2.— $d\alpha/dt$ vs. α at 101.97° showing the effect of interruption upon the data. The open circles are from an uninterrupted run. The closed circles are from an interrupted run. The interruptions occurred after the first point and between every other point thereafter. The points have been selected.

$$F(x, \kappa) = 1 - \alpha; \quad x \geq 2 \quad (2c)$$

Equations 2a and 2b can be expanded in series and evaluated for various x and κ .

These equations were fitted to the nitryl perchlorate decomposition data in the following fashion. The data past the maximum in the rate were plotted as $d\alpha/dt$ vs. α . The straight line obtained (Fig. 3) has a slope from eq. 2c of $-4\pi k_i N_0 R^2$. This line was forced through the point $d\alpha/dt = 0$, $\alpha = 1.0$. Derivations between the high rate portions and this point varied positive or negative from run to run and appear to be due to room temperature fluctuations (causing pressure fluctuations). The parameter $(1/4\pi k_i N_0 R^2)(d\alpha/dt)$ could then be calculated for the data earlier in time than the maximum rate. The parameter was compared with the computed $F(x, \kappa)$. $F(x, \kappa)$ was computed at 0.1 unit intervals in x from $x = 0$ to $x = 2.0$ for a range of κ .

Except near the maximum in $F(x, \kappa)$ this function is not a strong function of κ . The maximum in $F(x, \kappa)$ does, however, serve to define κ , and $(1/4\pi k_i N_0 R^2)(d\alpha/dt)$ and $F(x, \kappa)$ were compared at their maxima to obtain an approximate value of κ . Using this value of κ , $F(x, \kappa)$ was interpolated from the calculated curves at 0.1 unit intervals in x . These values of $F(x, \kappa)$ were marked off on the smoothed curve of $(1/4\pi k_i N_0 R^2)$.

TABLE II
SUMMARY OF RATE CONSTANTS

$T, ^\circ\text{C.}$	$4\pi k_i N_0 R^2$	k_g/R	$t_0, \text{sec.}$	α
112.34	$233 \times 10^{-6} \text{ sec.}^{-1}$	$612 \times 10^{-6} \text{ sec.}^{-1}$	200	0.381
106.97	$155 \times 10^{-6} \text{ sec.}^{-1}$	$491 \times 10^{-6} \text{ sec.}^{-1}$	600	.316
101.97	$104 \times 10^{-6} \text{ sec.}^{-1}$	$293 \times 10^{-6} \text{ sec.}^{-1}$	850	.355
96.97	$66.9 \times 10^{-6} \text{ sec.}^{-1}$	$191 \times 10^{-6} \text{ sec.}^{-1}$	960	.350
79.97	$7.57 \times 10^{-6} \text{ sec.}^{-1}$	$31.7 \times 10^{-6} \text{ sec.}^{-1}$	10^4	.239 ^a
69.99	$2.81 \times 10^{-6} \text{ sec.}^{-1}$	$7.77 \times 10^{-6} \text{ sec.}^{-1}$	3.5×10^4	.362
$\Delta E \text{ act.}$	$28.47 \pm 0.81 \text{ kcal.}$	$27.49 \pm 0.93 \text{ kcal.}$	-30.73 ± 1.48	...
$\log A$	12.57 ± 0.49	12.46 ± 0.56	-15.03 ± 0.88	...
Av.	0.353 ± 0.024

^a Omitted from average. Errors shown are one standard deviation.

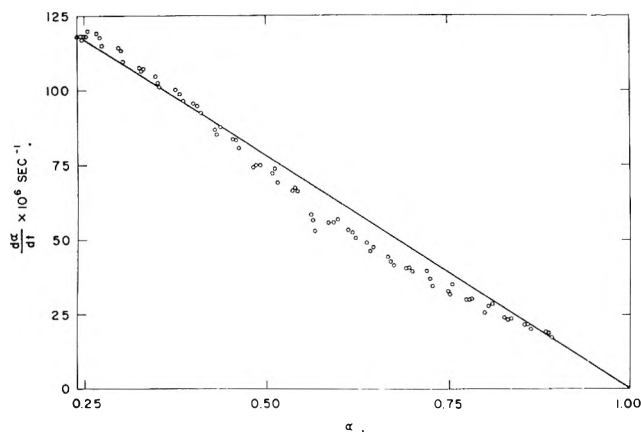


Fig. 3.—The first-order decay portion at 106.97° showing the best guess straight line through the points.

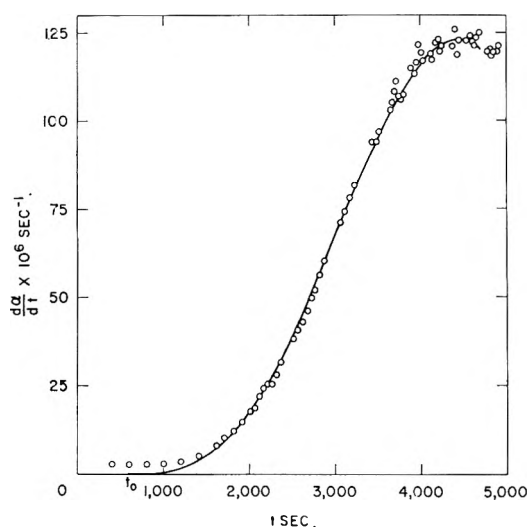


Fig. 4.— $d\alpha/dt$ vs. t for $x < 2.0$ at 106.97°. The solid line is the fit of Mampel's equation to the data.

($d\alpha/dt$) vs. t . The time corresponding to various x was read from this graph and plotted against x . The result was a straight line. The slope of this line gave R/k_g and the intercept gave t_0 , the induction time. From R/k_g and $4\pi k_i N_0 R^2$, α could be calculated and compared with the chosen value at the maximum. The agreement was within $\pm 10\%$. Since the scatter in the data is high near the maximum, this agreement is within experimental error. A plot of $d\alpha/dt$ vs. t and its computed curve are shown in Fig. 4. The agreement is quite good.

Values for k_g/R and $4\pi k_i N_0 R^2$ were obtained in this fashion at all temperatures. Both constants obey the Arrhenius equation as does t_0 . The data, together with their least square Arrhenius parameters, are listed in

Table II. α is also listed and as can be seen is, within experimental error, independent of temperature.

Although the data can be mathematically interpreted in terms of Mampel's theory, there are some physical difficulties which must be considered.

One such difficulty is that the two rate constants appear to be independent of particle size. Several decompositions were made on a slightly impure (NO^+ titer $\sim 1.5\%$) sample of nitryl perchlorate prepared by the reaction of anhydrous perchloric acid with nitryl chloride. This sample of material had visible particle sizes of 10 to 20 times the sizes of the commercial sample. The observed rates (plotted as $d\alpha/dt$ vs. α) were within experimental error of being the same for the two samples. The theory would have predicted the large size sample to have a growth constant smaller by a factor of 0.1 to 0.05 and an initiation rate larger by a factor of 100 to 400. This insensitivity of the rates to visible particle size variation can be explained by assuming that the decomposing unit is a subcrystalline particle smaller than the visible particles and the same for both samples. Nucleation would then have to occur on the interfaces of the subcrystals and desorbing gases and product gases would have to diffuse out by way of the interfaces. A more serious difficulty arises from a consideration of $4\pi R^2 N_0$, the number of potential sites per particle. The definition of α gives

$$4\pi R^2 N_0 = \frac{\alpha k_g / R}{k_i}$$

The growth constant k_g can be related to a "molecular" rate constant, k_u , by

$$k_g = k_u \delta$$

Here δ is of the order of magnitude of an interionic distance.

$$4\pi R^2 N_0 = \frac{\alpha k_u \delta}{R_i R}$$

Now, $4\pi R^2 N_0$ must be larger than unity if the sites are to be permanent fixtures on a particle. This means that

$$\frac{k_u}{k_i} \gg 1 \quad \left(\text{since } \frac{\delta}{R} \ll 1 \right)$$

It seems unlikely that this can be true since k_u and k_i would have the same activation energies. If the sites are not permanent but are in mobile equilibrium with normal sites then $4\pi R^2 N_0$ can be less than unity at any given time. N_0 then should have a temperature

dependence and the equality of the activation energies for $4\pi R^2 N_0 k_i$ and k_g/R would appear to be accidental.

A reasonable interpretation for the data is then the model proposed by Mampel, but with a mobile equilibrium for the active sites. The nuclei grow slowly during an induction period. During this induction period gases are evolved, but are not directly connected with the decomposition. The particle size in Mampel's theory is to be interpreted as a subcrystalline unit.

An additional piece of information can be obtained from the data. This is the average number of nuclei which form per particle during the decomposition. The uncorrected number of nuclei formed per second is

$$\frac{dM}{dt} = N_p \kappa \frac{dx}{dt}$$

Here N_p is the total number of particles. From Mampel's eq. 5a and 5b (ref. 13) the fraction of surface, of the whole mass, which has not decomposed is

$$\begin{aligned} e^{-\kappa x^2/12} & \quad 0 \leq x \leq 2 \\ e^{+4\kappa/3 - \kappa x} & \quad x \geq 2 \end{aligned}$$

The corrected total number of nuclei formed during the decomposition is

$$M = N_p \kappa \left\{ \int_0^2 e^{-\kappa x^2/12} dx + \int_2^\infty e^{4\kappa/3 - \kappa x} dx \right\}$$

The average number of nuclei is then, for $\kappa = 0.35$, found by numerical evaluation to be $M/N_p = 1.45$.

For a nucleus initiated at $t = 0$, the average maximum number of nuclei that could be formed is $1 + \int_0^2 \kappa dx = 1.7$.

This shows that after the initial nucleation of a particle about one-third of the subsequent nuclei are phantom.

Mampel's solution is for the special case of surface initiation of uniform spherical particles, followed by isotropic growth of the nuclei. This rate law is so successful in fitting the present data that these assumptions must be examined further. In the real case, the shapes of the particles are probably nonuniform and nonspherical. Since there is only one maximum and no shoulders in the rate as a function of α there are no large discrete differences in the particle sizes. A narrow and nearly continuous distribution of sizes will lead to a slight broadening of the maximum in the rate, as compared to the result for a single size. The fit of the theory will depend upon how well the true situation can be represented by an average. It will now be shown that the actual geometry of the particles and nuclei is relatively unimportant. Consider a group of uniform particles with initiation constant k_i . The actual rate law for a single particle will depend upon the number of, position of, and the relative times of the nucleations. Replace these rate laws by an average rate law that is the same for all particles after their first initiation. Let α_p be the fraction of a particle decomposed at time $t - t_i$, where t_i is the time of first initiation of the particle. The fraction, α , of the whole mass decomposed at time t will be for first-order initiation

$$\alpha = k_i \int_0^t \alpha_p(t - t_i) e^{-k_i t_i} dt_i$$

This equation can be converted to a differential equation.

$$\frac{d\alpha}{dt} + k_i \alpha = k_i \alpha_p(t)$$

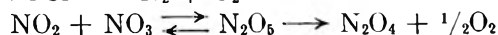
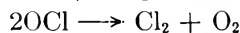
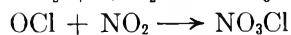
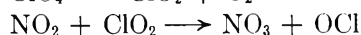
If each individual particle is consumed in a finite time (or if α_p is nearly constant after such time), then the differential equation reduces to the first-order decay law as do Mampel's equations. This first-order decay law is independent of the geometry of the system and the site (surface or interior) of initiation. The rate constant k_i obtained from the first-order portion of the rate law can be used to obtain α_p as a function of time in the earlier portions of the plot. When this is done it is found that, below $\alpha_p = 0.4$ (or $x = 1.3$ in Mampel's equations) $\alpha_p = K(t - t_0)^3$. An induction time is needed here as in the fit to Mampel's equations. This rate law corresponds to three-dimensional growth of the nuclei (not necessarily isotropic growth). The geometry of the particles is unspecified except that long thin rods are excluded. Between $\alpha_p = 0.4$ and $\alpha_p = 1$ this simple t^3 law deviates badly from the data. It is in this range that the effects of geometry and multiple nucleation show up. Models involving either single surface nucleation of spheres or single corner initiation of cubes fit the data much better than the t^3 law and nearly as well as Mampel's equations. Mampel's equations are better because of the consideration of multiple nucleation. As would be expected from the computed average number of initiations, this improvement over single initiation is small.

In short, the geometry used in Mampel's theory should not be taken too seriously for this case. Even the assumption of surface initiation is not important. Mampel's theory is valuable in that it considers both geometrical limiting of nuclear growth and multiple nucleation in tractable mathematical form. The pre-exponential factors for the derived rate constants will depend upon the exact geometrical model which is chosen. For the growth rate constant this variation will be (in terms of some critical size parameter) only about one order of magnitude. The interpretation of the pre-exponential factor for nucleation will also depend upon whether surface or bulk initiation is chosen. The activation energies for the rate constants should be independent of the assumed geometry of the particles and should be reasonable estimates of the activation energies of the real processes. The induction time still remains an empirical entity, although it may be due to slow growth of small nuclei.

The chemistry of the decomposition is mostly speculation. The following rough scheme may be close to the truth.

1. Reactions in the solid
 $\text{ClO}_4^- \longrightarrow \text{ClO}_4 + e^-$ (conduction band)
 $e^- + \text{NO}_2^+ \longrightarrow \text{NO}_2$
2. Desorption
 $\text{ClO}_4(\text{surface}) \longrightarrow \text{ClO}_4(\text{gas})$
 $\text{NO}_2(\text{surface}) \longrightarrow \text{NO}_2(\text{gas})$

3. Gas reactions



The gas phase reactions have all been postulated in other reactions. The important questions concern the reactions in the solid and the nature of the gases coming off of the surface. Since the energies for the solid phase reactions are not known they cannot be compared with the observed activation energies.

THE INTERACTION AND NONINTERACTION OF IONS WITH A NATURAL POLYSACCHARIDE¹

BY J. A. BARRY² AND GEORGE D. HALSEY, JR.

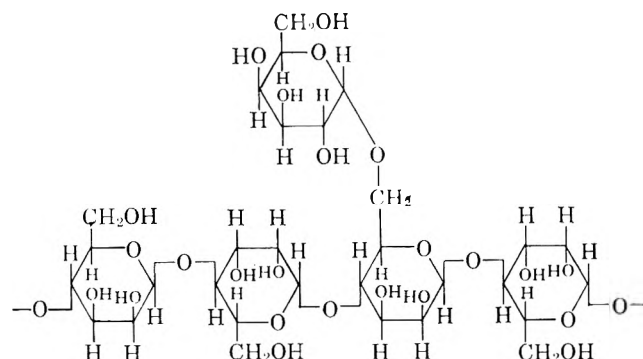
Department of Chemistry, University of Washington, Seattle 5, Washington

Received March 6, 1963

The interaction of a neutral polysaccharide with various ions in aqueous solution has been investigated. No observable binding took place between the polymer and H^+ , Na^+ , K^+ , Ag^+ , Ba^{+2} , $\text{C}_2\text{H}_3\text{O}_2^-$, Cl^- , NO_3^- , SO_4^{2-} , or HSO_4^- . The polysaccharide displayed an affinity only for OH^- , and this affinity has been treated as an adsorption phenomenon. Adsorption isotherms, isosteric heats of adsorption, and integral heats of adsorption were determined for the binding of OH^- to locust bean gum and are discussed herein.

Introduction

The aqueous extract of the locust bean (*Ceratonia siliqua*) is a neutral polysaccharide consisting of a main chain of mannose units with short branches of single galactose units attached through 1,6-glycosidic linkages to the polymannose chain.³



This gum forms very viscous aqueous solutions and dissolves completely only on prolonged heating and agitation. Preliminary studies in this Laboratory of the turbidity of these solutions indicate that the polymer exists as an aggregate in aqueous solution at room temperature with an aggregate molecular weight of 500×10^6 . The present work was undertaken to determine the ability of this polysaccharide to bind small ions in aqueous solution.

Experimental

1. **Polymer Solutions.**—The polysaccharide was extracted from dried locust beans (Cyprus origin)⁴ by agitation of mechanically cracked beans with 80–90° distilled water for approximately 90 min. The resulting hot solution was filtered through several layers of muslin cloth and cooled to room temperature. The polymer was precipitated by addition of 95% ethanol in a 2:1 volume ratio and redissolved in hot distilled water. This solution was diluted to approximately 0.5% by weight and passed through anion and cation exchange columns. The eluent was

concentrated by evaporation and the polymer reprecipitated with 95% ethanol. The gum was washed several times with ethanol and dried at 70° overnight. All solutions were prepared from this purified extract by dissolving the gum in hot ion-exchanged water.

2. **Viscosity measurements** were made with a Cannon-Fenske viscometer No. 100 which was immersed in a water bath thermostated to $\pm 0.005^\circ$. The viscometer was calibrated with a 40% sucrose solution using the values of η and ρ from the International Critical Tables. A second determination of several relative viscosities was made with a calibrated Cannon-Fenske viscometer no. 50 with a flow time for distilled water approximately one-fourth as fast at 20° as the flow time of viscometer no. 100. The polymer solution displayed no viscosity dependence on rate of shear in the viscosity range studied.

3. **Conductivity data** were obtained from resistance measurements of solutions in a standard conductivity cell with 1.3-cm.² platinum electrodes using a Leeds and Northrup "Jones" conductivity bridge equipped with a wide frequency range oscillator. The cell was immersed in an oil bath thermostated to $\pm 0.005^\circ$. The temperatures were measured by means of a calibrated platinum resistance thermometer. Reagent grade KCl and NaCl were purified by double precipitation from concentrated HCl solution and subsequent fusion in a platinum crucible. Baker's reagent grade HCl, H_2SO_4 , Na_2SO_4 , BaCl_2 , AgNO_3 , and NaAc were used without further treatment. NaOH and KOH were prepared from saturated stock solution of the base in ion-exchanged water. The conductivity cell was calibrated with KCl using the data of Jones and Bradshaw.⁵

Results

The conductivities of all electrolytes were measured in aqueous solution and in locust bean gum solution and corrected for solvent in the usual manner. Table I gives the specific conductivities of some pure locust bean gum solutions compared with ion-exchanged water at the same temperature. It can be seen that the conductivity of the polymer solutions is extremely low, indicating an almost complete removal of electrolytes by the ion-exchange purification process.

Stock solutions of each electrolyte were prepared and diluted with water or with polymer solution to ensure an accurate comparison. The conductivities of H_2SO_4 , HCl, NaCl, KCl, Na_2SO_4 , BaCl_2 , NaAc, and AgNO_3 were found to be the same in both solutions within experimental error. This is illustrated in Table II where representative values are given for the specific

(1) This research was supported in part by the United States Air Force through the AFOSR.

(2) Standard Oil Company of California Fellow, 1962–1963.

(3) F. Smith, *J. Am. Chem. Soc.*, **70**, 3249 (1948).

(4) Samples obtained through the courtesy of Tragasol Products, Ltd., Hootan, Wirral, Cheshire, England.

(5) G. Jones and B. C. Bradshaw, *J. Am. Chem. Soc.*, **55**, 1780 (1933).

TABLE I
SPECIFIC CONDUCTIVITY OF LOCUST BEAN GUM SOLUTION

$T, ^\circ\text{C.}$	G./100 ml. LBG	Specific conductivity ^a LBG soln.	Specific conductivity ^a H ₂ O
25.0	0.0502	0.49×10^{-6}	0.32×10^{-6}
20.0	.4554	$.90 \times 10^{-6}$	$.20 \times 10^{-6}$
15.2	.1780	$.50 \times 10^{-6}$	$.11 \times 10^{-6}$
0	.1475	$.41 \times 10^{-6}$	$.20 \times 10^{-6}$

^a Uncorrected for cell constant.

TABLE II
COMPARISON OF SPECIFIC CONDUCTIVITIES OF ELECTROLYTES
IN AQUEOUS SOLUTION AND IN LOCUST BEAN GUM SOLUTION

Elec- trolyte	Nor- mality	Spec. cond. ^a $\times 10^3$	Spec. cond. ^a polymer soln. $\times 10^3$	Molarity		$T,$ $^\circ\text{C.}$
				on a monomer basis	Polymer soln. η_{rel}	
HCl	0.023	0.7093	0.7095	0.010	2.086	25
	.049	1.5421	1.5402	.013	2.605	25
H ₂ SO ₄	.0048	0.2483	0.2474	.010	2.086	25
	.0478	1.8633	1.8634	.010	2.086	25
NaCl	.005	1.5209 ^b	1.5208 ^b	.025		17
	.005	1.6093 ^b	1.6438 ^b	.025	11.892	20
	.005	0.0431	0.0429	.010	2.086	25
	.010	.0847	.0847	.010	2.086	25
KCl	.0005	.00579	.00579	.003	1.213	25
	.005	.05472	.05462	.003	1.213	25
	.002	.841 ^b	.839 ^b	.0088	2.138	20
	.016	3.081 ^b	3.086 ^b	.0088	2.138	20
BaCl ₂	.0031	0.0264	0.0264	.013	2.605	25
	.010	.0776	.0772	.013	2.605	25
Na ₂ SO ₄	.0029	.0264	.0264	.010	2.086	25
	.0058	.0522	.0522	.010	2.086	25
AgNO ₃	.005	.0485	.0487	.008	1.747	25
	.050	.4366	.4376	.008	1.747	25
NaAc	.025	.1376	.1378	.005	1.970	20
	.066	.3444	.3442	.007	2.052	20

^a Uncorrected for cell constant. ^b These measurements made with a different cell.

conductivity of these electrolytes together with the relative viscosity of the polymer solution. Measurements were made over an electrolyte concentration range from 0.0005 to 0.1 *N* and over a polymer concentration range from 0.0022 *M* (moles per liter on a monomer basis) to 0.0277 *M*. The physical limitations of low solubility and high viscosity made it impracticable to exceed a polymer concentration of 0.5% by weight which corresponds to the upper limit of 0.0277 *M*.

The addition of locust bean gum solution to aqueous NaOH or KOH resulted in a decrease in specific conductivity which was directly proportional to the polymer concentration. The reversibility of this phenomenon was checked by determining the decrease in specific conductivity in two ways. (1) Electrolyte solution was diluted with pure water and with polymer solution and the electrical conductivities of the resulting solutions compared. (2) Electrolyte solution was diluted first with polymer solution and subsequently with water. The electrical conductivity of the final polymer-electrolyte mixture was compared to the pure electrolyte solution of the same concentration. The decrease in specific conductivity per mole of monomer was identical for both methods.

Several aqueous solutions of the polysaccharide and NaOH in varying concentrations were allowed to stand

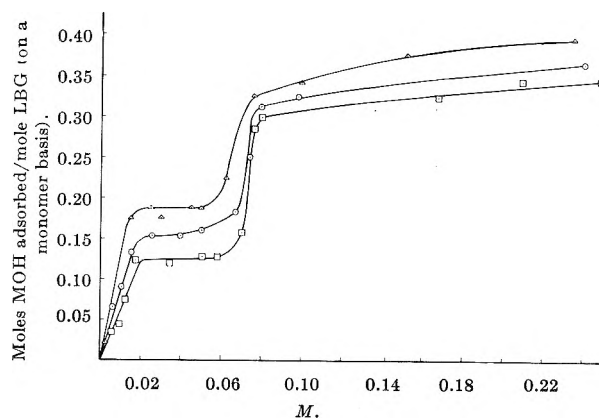


Fig. 1.—Adsorption isotherms for MOH on locust bean gum: \square , 20°; \circ , 15°; \triangle , 0°.

at room temperature for 1 hr. and neutralized with HCl. The relative viscosities for the resultant solutions were identical to those of solutions containing the same concentrations of polymer and NaCl. It can be concluded, therefore, that locust bean gum is not degraded by NaOH at room temperature in the time interval required for conductivity measurements.

The decrease in specific conductivity on addition of a given quantity of the polymer was greater in KOH than in NaOH, but the decrease in electrolyte concentration of the bulk solution corresponding to this conductivity change was independent of the cation present. Since conductivity measurements with electrolytes listed in Table II indicated no interaction between Na⁺ or K⁺ and the polymer, we assume that the decrease in bulk electrolyte concentration is the result of a specific interaction of the polymer with OH⁻.

The limiting equivalent conductance of K⁺ is 1.4 times greater than that of Na⁺. The greater decrease in specific conductivity of KOH solution compared to NaOH solution upon the addition of polysaccharide indicates that the gegenions are also localized on the polymer at the site of the created charge.

The number of moles of base adsorbed per mole of monomer was calculated and is referred to throughout this paper as Γ . Adsorption isotherms at three different temperatures are shown in Fig. 1.

The isosteric and integral heats were calculated using the method of Anderson and Pethica.⁶ At equilibrium

$$\mu_B(C_B, T) = \mu_{ADS}(C_B, T, \Gamma) \quad (1)$$

where the left-hand side of the equation represents the chemical potential of base in the bulk solution and the right-hand side the chemical potential of base adsorbed. Since the gegenions as well as OH⁻ are bound to the polymer, eq. 1 refers to the chemical potential of a neutral adsorbate. We may then write

$$\left(\frac{\partial \mu_B}{\partial C_B}\right)_T dC_B + \left(\frac{\partial \mu_B}{\partial T}\right)_{C_B} dT = \left(\frac{\partial \mu_{ADS}}{\partial C_B}\right)_{T, \Gamma} dC_B + \left(\frac{\partial \mu_{ADS}}{\partial T}\right)_{C_B, \Gamma} dT + \left(\frac{\partial \mu_{ADS}}{\partial \Gamma}\right)_{C_B, T} d\Gamma \quad (2)$$

at constant Γ

$$\left(\frac{\partial C_B}{\partial T}\right)_\Gamma = \frac{\left(\frac{\partial \mu_{ADS}}{\partial T}\right)_{C_B, \Gamma} - \left(\frac{\partial \mu_B}{\partial T}\right)_{C_B}}{\left(\frac{\partial \mu_B}{\partial C_B}\right)_T - \left(\frac{\partial \mu_{ADS}}{\partial C_B}\right)_{T, \Gamma}} \quad (3)$$

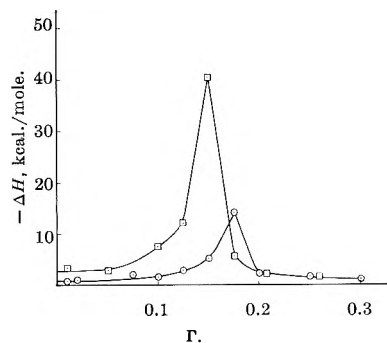


Fig. 2.—Differential heat of adsorption of MOH on locust bean gum: \circ , 0–15°; \square , 15–20°.

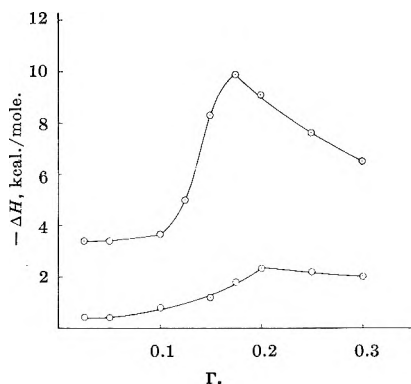


Fig. 3.—Integral heat of adsorption of MOH on locust bean gum: upper curve, 15–20°; lower curve, 0–15°.

The numerator on the right-hand side of eq. 3 is the isosteric heat divided by the temperature, and neglecting $(\partial\mu_{\text{ADS}}/\partial C_{\text{B}})_{T,\Gamma}$ as compared with $(\partial\mu_{\text{B}}/\partial C_{\text{B}})_{T}$, the denominator may be written as RT/C . Thus we have

$$\left(\frac{\partial \ln C_{\text{B}}}{\partial T}\right)_{\Gamma} = -\frac{\Delta\bar{H}}{RT^2} \quad (4)$$

$(\partial \ln C_{\text{B}}/\partial T)_{\Gamma}$ was calculated for the temperature intervals 0–15° and 15–20°, and $\Delta\bar{H}$ was obtained from eq. 4 for these ranges. The results are shown in Fig. 2.

The integral heats of adsorption, ΔH , were obtained by graphical integration of the isosteric heat curves and are shown in Fig. 3 as a function of Γ .

It is probable that the OH^- is bound at localized sites on the mannose and galactose units. The total number of possible positions for hydrogen bond formation on each mannose or galactose unit is eighteen. Obviously these positions are of different energy and are not all sterically available especially when these units are joined in a polymer chain or when one site is already occupied by an OH^- ion. Our adsorption isotherms show a maximum occupancy of approximately 0.4 OH^- per mannose or galactose unit at the lowest temperature investigated.

The increase of total binding with decreasing temperature indicates that lowering the temperature causes additional sites to become available probably due to a decrease in the vibrational and rotational energies of the covalent bonds in the polymer structure at these sites.

The isotherms in Fig. 1 show an inflection point between bulk electrolyte concentrations of 0.05–0.07 N indicating a sharp transition in polymer configuration at this point. This transition leads to an increase in

the sterically available hydrogen-bonding sites and is undoubtedly the result of repulsion between like charges on the macromolecule. Similar phenomena have been observed in other polymer systems^{7,8} and Hill⁹ has shown that it is possible for a polymer to undergo a very large change in length as a consequence of a very small change in ionic strength or in the concentration of an ion bound on the polymer chain. The magnitude of the transition observed in our isotherms appears to be independent of temperature since the difference between the two plateaus for each temperature in Fig. 1 is approximately the same.

The isosteric heat curves shown in Fig. 2 display a sharp increase in the region corresponding to the phase transition followed by a steep drop to within 2 kcal. of the values at $\Gamma = 0$. The approximately constant $\Delta\bar{H}$ at low values of Γ indicates filling of sites of equal energy. As these sites become occupied interaction between adsorbed ions and the subsequent phase change cause a rise in $\Delta\bar{H}$ observed in Fig. 2 between $\Gamma = 0.075$ and 0.15. $\Delta\bar{H}$ is again constant above the point of phase transition indicating that the additional sites which have been made available by a change in polymer configuration are also of approximately equal energy.

A quantitative interpretation of the integral heat curves of Fig. 3 is complicated by the fact that OH^- forms hydrogen bonds in aqueous solution. The experimental molar heat of adsorption is the sum of the breaking of these bonds and the formation of hydrogen bonds with the polymer. It can be seen, however, that there is an increase in the molar heat of adsorption at the point of phase transition which undoubtedly reflects the energy of polymer extension.

Conclusions

It has been demonstrated that increasing the viscosity of an electrolyte solution by the addition of a neutral polymer which does not specifically interact with the electrolyte does not affect the specific conductivity of the solution within the degree of accuracy obtainable with the Jones conductivity bridge. This conclusion agrees with the observations of other workers¹⁰ that ionic mobility is not altered by changes in macroscopic viscosity resulting from polymer molecules.

There is specific interaction between the polysaccharide extracted from the locust bean and OH^- ions. This interaction has been treated as an adsorption phenomenon resulting from hydrogen bond formation at sites on the polymer chain. The fact that no such interaction was noted between the polysaccharide and SO_4^{2-} , HSO_4^- , or $\text{C}_2\text{H}_3\text{O}_2^-$ which are also capable of forming hydrogen bonds is not unusual. Thus, cellulose triacetate adsorbs by hydrogen bond formation phenol and quinol from aqueous solution but not methanol, glucose, ethylene glycol, or mannitol.¹¹ When the solvent is highly polar, hydrogen bond formation is influenced by the relative strength of solvent-solute and adsorbent-solute hydrogen bonds.

(7) J. Riseman and J. G. Kirkwood, *J. Am. Chem. Soc.*, **70**, 2820 (1948).

(8) M. Morales and J. Botts, *Discussions Faraday Soc.*, **13**, 125 (1953).

(9) T. E. Hill, *J. Chem. Phys.*, **20**, 1259 (1952); *Discussions Faraday Soc.*, **13**, 132 (1953).

(10) P. Doty and G. J. Edsall, *Ann. Rev. Phys. Chem.*, **3**, 81 (1952).

(11) C. H. Giles, "Hydrogen Bonding," edited by D. Hadzi, Pergamon Press, New York, N. Y., 1959.

(6) P. J. Anderson and B. A. Pethica, *Trans. Faraday Soc.*, **52**, 1080 (1956).

It is possible that instead of adsorption of OH^- on a hydrogen-bonding site of the polymer, titration of weakly acidic groups, such as alcoholic OH on the polysaccharide, is taking place. In this case charged sites would be created where the protons are removed and the gegenions would be localized at these sites. The adsorption isotherms shown in Fig. 1 are analogous to titration curves, and a change in polymer configuration is seen to take place at $M = 0.07$ providing sites of higher energy for titration with OH^- . These higher energy sites are sterically unavailable at electrolyte concentrations less than $0.07 M$. Similar configuration

changes have been observed in titration curves of serum albumin and ribonuclease.^{12,13}

In either case—whether the phenomenon is treated as adsorption of OH^- and its gegenion or as titration of weakly acidic groups on the polymer and subsequent localization of the gegenion on these charged sites—the polymer can be thought of as a heterogeneous surface providing sites of different energies and undergoing a phase transition as the result of repulsion between like charges on the surface.

(12) C. Tanford, J. D. Hauenstein, and D. G. Rands, *J. Am. Chem. Soc.*, **77**, 6409 (1955).

(13) C. Tanford, S. A. Swanson, and W. S. Shore, *ibid.*, **77**, 6414 (1955).

THE TRIPLET STATE OF FLUORESCEIN IN SULFURIC ACID¹

BY LARS LINDQVIST

Institute of Physical Chemistry, University of Uppsala, Uppsala, Sweden

Received March 18, 1963

Light-induced, reversible changes in absorption of solutions of fluorescein in 0.1 to 10 M deoxygenated sulfuric acid were studied, using the flash photolysis technique. The triplet state of the dye, as well as semioxidized and semireduced dye radicals, were shown to be responsible for the transient absorption changes. The radicals were formed by an electron dismutation reaction between two triplet molecules and also by a corresponding reaction involving one molecule in the triplet state and one in the ground state, the latter reaction occurring only in weakly acidic solution. The reaction scheme is the same as that previously observed in light-excited aqueous dye solutions of pH 0–13.

Introduction

Fluorescein and related dyes are known to be efficient photosensitizers, and their activity in this respect has been shown^{2–4} to be due to the light-induced conversion of the dye to a long-lived, reactive species, which was assumed to represent the dye in the lowest triplet state. The absorption spectrum of the intermediate was recorded in a flash-photolytic study⁴ of fluorescein in aqueous solutions of pH 0 to 13.

Evidence for the possibility of population of a triplet state of the dye had previously been obtained by Lewis and Calvin⁵ in their study of the photomagnetism of fluorescein in boric acid, and the absorption spectrum of the triplet in this solvent had been measured.⁶ The same spectrum has also been obtained⁷ by cross-illuminating fluorescein in an ether–ethanol solution containing 20% hydrochloric acid, cooled by liquid nitrogen. The spectrum of the reactive dye intermediate observed in aqueous solutions⁴ was quite different, however—a result that did not support the assumption that the triplet state of the dye is involved in this case. The discrepancy was considered to be caused possibly by the difference in acidity between the strongly acidic, “glassy” solvents mentioned above and the aqueous solutions studied by flash photolysis. This possibility is investigated in the present study of fluorescein in sulfuric acid. Also, as a complement to the previous study,⁴ the reaction mechanisms and

kinetics of the light-excited dye in this solvent are analyzed and compared to those observed in aqueous solutions.

Experimental

Solutions were prepared from chromatographically pure fluorescein,⁴ triple-distilled water, and concentrated sulfuric acid, reagent grade, which was purified by a fractional vacuum distillation.

The solutions were degassed thoroughly in a vacuum unit described previously.⁴ The amount of solution required for filling a reaction cell (ca. 100 ml.) was cooled with ice and, under agitation, evacuated for 1 min. The solution was then exposed to oxygen-free argon (welding quality) for 1 min. at a pressure slightly below one atmosphere, under continued agitation. This procedure, repeated 6–8 times, proved to be less time-consuming, yet as efficient as the freezing–thawing process used earlier. A correction was applied for the small amount of solvent evaporated during the evacuations.

The flash photolysis apparatus has been described in detail previously.^{4,8} Light flashes for excitation were produced by discharging a capacitor bank of max. 350 μf ., charged to max. 14 kv., across a series-connected pair of 60 cm. long flash lamps. For this study an energy of 6000 j. (100 μf ., 11 kv.) was used, giving a flash duration time of 60 μsec . (1/e-time). The solutions were illuminated in cylindrical, optical silica cells, 20 or 60 cm. long (i.d. 1.6 and 1.0 cm., respectively), provided with annular, cylindrical jackets, through which a filter solution, thermostated at 25°, was circulated. The filter solution consisted of 200 g. of crystalline copper sulfate, 10 g. of ferric alum, and 5 ml. of concentrated sulfuric acid per liter of water, and transmitted light of wave lengths 390–630 $m\mu$. The transient changes in optical density of the flash-exposed solutions were measured as a function of time using a single-beam spectrophotometer essentially comprised of a xenon lamp (Osram XBO 301) or alternatively a zirconium lamp (Sylvania, 100 w), a double monochromator (Zeiss MM 12), a multiplier phototube (EMI 9552, EMI 9554, or DuMont 6911), and an oscilloscope (Tektronix 533). The spectrophotometer recorded only changes in absorption relative to the conditions before flashing, and complementary measurements of the spectra of the solutions before irradiation were

(1) Research sponsored by the U. S. Department of Army, through its European Research Office, under contract No. DA-91-591-EUC-2162 OI-26528-B. (Presented in part at the Symposium on Reversible Photochemical Processes held at Durham, North Carolina, April, 1962.)

(2) G. O. Schenck, *Naturwiss.*, **35**, 28 (1948).

(3) G. Oster and A. H. Adelman, *J. Am. Chem. Soc.*, **78**, 913 (1956).

(4) L. Lindqvist, *Arkiv Kemi*, **16**, 79 (1960).

(5) G. N. Lewis and M. Calvin, *J. Am. Chem. Soc.*, **67**, 1232 (1945).

(6) G. N. Lewis, D. Lipkin, and T. T. Magel, *ibid.*, **63**, 3005 (1941).

(7) V. Zanker and E. Miethke, *Z. Naturforsch.*, **12a**, 385 (1957).

(8) S. Claesson and L. Lindqvist, *Arkiv Kemi*, **11**, 535 (1957).

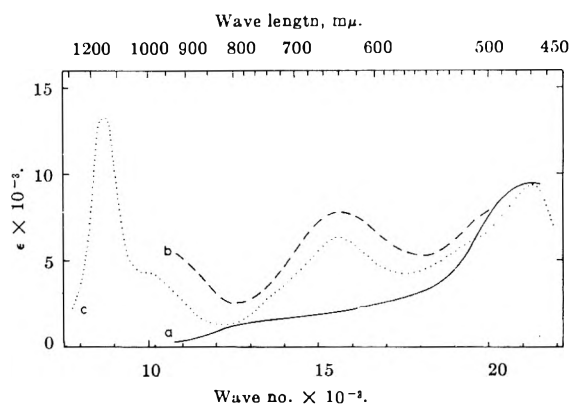


Fig. 1.—(a) Absorption spectrum of $0.5 \mu M$ fluorescein in $0.1 M$ sulfuric acid, as it appears during flashing; (b) same in $9 M$ sulfuric acid; (c) absorption spectrum of the triplet state of fluorescein in ether-ethanol containing 20% hydrochloric acid, at -196° , according to Zanker and Miethke⁷ (ϵ = molar ext. coeff.).

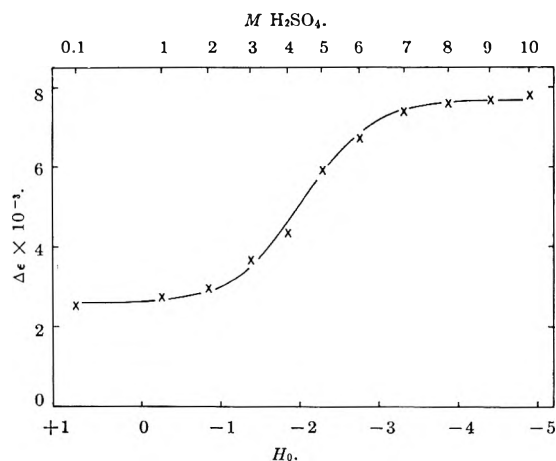


Fig. 2.—Transient increase in molar extinction coefficient ($\Delta\epsilon$) of $0.5 \mu M$ fluorescein in sulfuric acid, observed at $650 m\mu$ during flash exposure, as a function of the acidity function (H_0) and the concentration of the sulfuric acid.

therefore required. A recording spectrophotometer (Bausch and Lomb Spectronic 505) was used for this purpose.

Results and Discussion

Solutions of fluorescein in 0.1 to $10 M$ deaerated, aqueous sulfuric acid were studied. The dye appears in this acid concentration range predominantly as the monocation, which has a pronounced absorption peak at $437 m\mu$ (molar extinction coefficient 5.5×10^4). Dye concentrations were in the range 0.05 to $4 \mu M$, where the dye occurs in the monomeric form, as shown by absorption spectrophotometry.

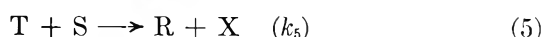
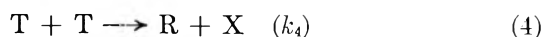
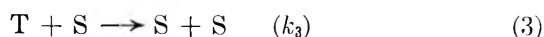
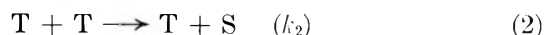
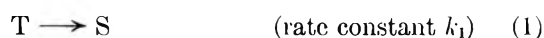
The solutions were exposed to flashes of visible light ($6000 j.$), and light-induced transient changes in absorption measured. During the irradiation the absorption peak at $437 m\mu$ decreased in intensity, and simultaneously a broad, transient absorption band developed in the visible and near-infrared, lasting over a period that was long compared to the flash duration time. The extent of absorption change was not affected when the discharged energy was increased above $6000 j.$, and it was therefore concluded that the solutions were light-saturated during the exposure. This implies that the dye was converted quantitatively to the transient state, and absolute intensity values of the corresponding absorption spectrum were thus obtained.

The structure of the transient absorption spectrum was independent of the dye concentration but varied

with the acidity of the solution. The spectrum observed in dilute ($<2 M$) acid was identical to the previously reported⁴ spectrum of flash-excited fluorescein in $0.025 M$ perchloric acid (spectrum a in Fig. 1) which had been assumed to represent the neutral fluorescein triplet. At increasing acid concentration this spectrum was converted to spectrum b (Fig. 1), with a maximum at $640 m\mu$ that reached its full intensity in $7 M$ sulfuric acid. The similarity of the latter spectrum to that of the fluorescein triplet in acidic, organic "glass"⁷ (spectrum c) strongly suggests that the transient product observed in strongly acidic sulfuric acid solution is the triplet state of the dye, and it is concluded from the protolytic behavior that under these conditions the triplet occurs in a cationic form, whereas in dilute sulfuric acid the neutral triplet appears.

The acid strength of the triplet cation was determined from measurements of the transient increase in absorption at $650 m\mu$ produced by flash irradiation of $0.5 \mu M$ fluorescein in sulfuric acid of varying concentration. The results are shown in Fig. 2, where changes in extinction coefficient are plotted as a function of the Hammett acidity function, H_0 , of the sulfuric acid.⁹ The points at the highest acidities were assumed to represent the extinction coefficient of the pure cationic triplet, and those at the lowest acidities the corresponding value of the neutral triplet. These values were used to calculate the titration curve shown in Fig. 2; the curve was adjusted along the H_0 axis to give a best fit to the experimental points. The good agreement between the shape of the curve and the distribution of the points supports the assumption that an acid-base equilibrium is involved in this case. From the curve a value of $pK_a = -2.1$ is obtained for the triplet cation, which apparently is a considerably stronger acid than the ground state cation ($pK_a = +2.2$). This result is in contrast with the protolytic behavior of the fluorescein monoanion,⁴ the acid strength of which is almost the same in the ground state as in the triplet state.

The triplet decayed after the flash exposure at a rate that varied with the dye concentration as well as with the sulfuric acid concentration. The decay kinetics were studied in detail in $9 M$ sulfuric acid, where the cationic triplet appears. The kinetic analysis was based on the reaction scheme accounting for the triplet decay in aqueous solution⁴



where S, T, X, and R represent the unexcited fluorescein, the triplet, the semioxidized dye, and the semi-reduced dye, respectively.

Assuming complete conversion of the dye to the triplet state during flashing, the relation between the initial rate of decay of the triplet and the over-all dye concentration, C , can be written in the form

$$C[d(1/c_T)/dt]_0 = k_1 + (k_2 + 2k_4)C \quad (1)$$

(9) M. A. Paul and F. A. Long, *Chem. Rev.*, **67**, 1 (1957).

where c_T refers to the concentration of the triplet and the zero subscript to the conditions at the end of the flash exposure (for the present purpose the light intensity was considered negligible 70 μ sec. after initiation of the flash). Values for the time derivative at different concentrations were obtained from measurements of the decay of the transient absorption at the wave length of maximum absorption of the triplet, assuming that no other products were formed that absorb at this wave length. In Fig. 3, which relates to a study of the cationic triplet in 9 M sulfuric acid, values for the left-hand side expression of eq. 1 were calculated from measurements at 650 $m\mu$ and plotted against the over-all dye concentration. The slope and the vertical axis intercept of the straight line obtained give values of the rate constants, which are presented in Table I, together with corresponding values for the neutral and anionic forms of the triplet, obtained previously.⁴

The table gives the rate constants of decay for the neutral triplet in 0.025 M perchloric acid. A brief study of the neutral triplet in 0.1 M sulfuric acid indicated that the values of the rate constants were independent of the acid used, as would be expected if the function of the acid is only to establish the acidity of the solution.

The values of the second-order decay rate constant of the cationic triplet is an indication of a diffusion-controlled reaction. The viscosity of 9 M sulfuric acid is five times higher than that of water, and multiplying the second-order rate constant for the triplet cation with this number gives a value very close to that for the neutral triplet. Due to the high ionic strength of the sulfuric acid, coulombic effects between encountering cations would not be expected to be appreciable.

Reaction 1 includes deactivation of the triplet by phosphorescence or by radiationless transition, as well as quenching by any impurities present in the solution. Table I shows that the neutral triplet, studied in dilute sulfuric acid, has a considerably higher k_1 value than the divalent triplet anion, studied in dilute sodium hydroxide solution, suggesting that the sulfuric acid might possibly contain triplet-quenching impurities not present in the alkaline solution. In order to investigate this possibility solutions of 0.1 μM fluorescein in 0.01 and 1 M sulfuric acid were flash-exposed, and the rate of decay of the neutral triplet, which is formed under these conditions, was measured. In spite of the hundredfold change in sulfuric acid concentration, k_1 was constant to within 100 sec^{-1} . It is concluded from this result that the difference between the k_1 value of the neutral triplet and that of the divalent anion is not due to impurities. (Impurities like ferric

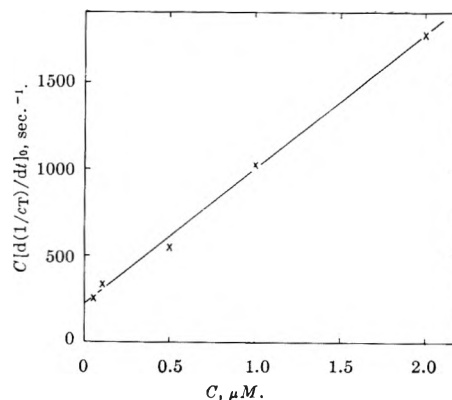


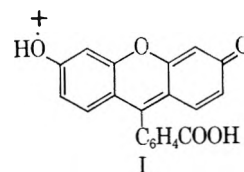
Fig. 3.—Determination of rate constants of decay of the fluorescein triplet cation: the left-hand side expression of eq. 1 as a function of the total fluorescein concentration (C) for a flash-excited solution of the dye in 9 M sulfuric acid.

ions, which would be present in acidic but not in alkaline solutions, might affect the k_1 value, however.)

Reactions 3 and 5 were studied with regard to the triplet cation by exposing fluorescein solutions (1–4 μM) in 9 M sulfuric acid to low-intensity flashes (the light intensity was reduced by means of screens), producing a conversion of 1–5% of the dye to the triplet state. In spite of the excess of unexcited dye present the rate of decay of the triplet was not enhanced, as compared to the rate expected from the occurrence of reactions 1, 2, and 4 alone, and only upper limiting values for the rate constants k_3 and k_5 were obtained, shown in Table I.

The decay of the triplet spectrum after flashing was accompanied by the partial reappearance of the original spectrum of the dye. Additional peaks also developed, however, and these were attributed to semireduced and semioxidized fluorescein formed by the electron transfer reactions 4 and 5. The previous study⁴ gave an absorption peak at 355 $m\mu$ (ext. coeff. 3×10^4) for the semireduced fluorescein radical in aqueous solution of pH 0 to 9. Absorption spectra for two protolytic forms of the semioxidized radical have been obtained from studies of the photooxidation of fluorescein by ferric salts in sulfuric acid.^{4,16} The more acidic form, with a pK_a value of -1.5 , has peaks at 442 $m\mu$ (ext. coeff. 6×10^4) and 770 $m\mu$ (ext. coeff. 4×10^3). This species was assumed to be the radical cation, represented below in one possible electron configuration (I).

The corresponding base, the neutral radical, has a peak at 428 $m\mu$ (ext. coeff. 5×10^4) and a very diffuse band at approximately 800 $m\mu$ (ext. coeff. 1×10^3).



In the present study, peaks were observed at 355, 442, and 770 $m\mu$ in sulfuric acid of high concentration, as would be predicted if one or both of the reactions 4 and 5 did occur. The peak at 355 $m\mu$ appeared even at the highest sulfuric acid concentrations studied, a result that supports the hypothesis⁴ that this peak is due to the neutral semireduced radical, the bridge

(10) L. Lindqvist, to be published.

TABLE I

RATE CONSTANTS OF DECAY OF THE TRIPLET STATE OF FLUORESCEIN

Medium	Triplet species	k_1 , sec. ⁻¹	$(k_2 + 2k_4)$	$(k_3 + k_5)$
			$\times 10^{-9}$, $M^{-1} \text{sec.}^{-1}$	$\times 10^{-9}$, $M^{-1} \text{sec.}^{-1}$
9 M H_2SO_4	Cation	220	0.8	<0.04
0.025 M $HClO_4$	Neutral molecule	600	3.5	2.5
0.1 M H_2SO_4				
0.01 M citrate buffer, pH 5.5	Univalent anion	600	3.5	2.5
0.01 M NaOH	Divalent anion	50	1.7	0.1

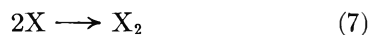
oxygen of which would be expected to accept a proton only in solutions of very high acidities.

The ratio between the rate constants k_2 and k_4 was studied with respect to the cationic triplet, in 9 *M* sulfuric acid, by measuring the concentrations of semi-reduced and semioxidized radicals reached after flashing. The absorption changes at 355 and 770 $m\mu$ were used to calculate these concentrations. It is known from previous work that the extinction coefficient of X at 355 $m\mu$ is small compared to that of R, while the reverse is the case at 770 $m\mu$. (The 442 $m\mu$ peak was not suitable for studying X because of its proximity to the peak of fluorescein at 437 $m\mu$.) From the absorption changes remaining at these wave lengths after the decay of the triplet spectrum, the result

$$k_2/k_4 \approx 1$$

was obtained. This figure is very approximate since the reactions of the radicals were not taken into account.

The disappearance of the radicals constituted the last stage in the reaction sequence following flash excitation. From kinetic evidence the radical reactions



have been proposed⁴ to occur in aqueous solution, both to approximately the same extent. The semireduced radicals left behind due to the consumption of the semioxidized radicals by reaction 7 disappeared very slowly, probably by the reaction with monomeric, semioxidized radicals present in equilibrium with X_2 .

In sulfuric acid the kinetics of the disappearance of the radicals were dependent on the acid concentration. In dilute acid (<2 *M*) the disappearance of the peak of X, measured at 428 $m\mu$, was approximately twice

that of the disappearance of R, measured at 355 $m\mu$. When the peak at 428 $m\mu$ had disappeared, the rate of fading of the peak at 355 $m\mu$ was slowed down considerably. These findings agree with the reaction mechanism described above. On the other hand, in more concentrated sulfuric acid (<4 *M*), where X occurs as the cation, the absorption peaks of X and R, at 442 and 355 $m\mu$, respectively, disappeared at the same rate; that is, there was no evidence for the occurrence of the dimerization reaction 7.

This result is of importance for the understanding of the mechanism of photooxidation of fluorescein, since it has been found¹⁰ that in concentrated sulfuric acid solutions no irreversible photooxidation of the dye by ferric salts takes place, while in dilute acid the dye is photooxidized readily by ferric salts. It is inferred from the above results that one step in the irreversible photooxidation of fluorescein is the dimerization of the semioxidized dye radicals.

At the end of the reaction a slight permanent change in absorption was observed. Below a sulfuric acid concentration of 2 *M* a decrease in absorption at 437 $m\mu$ of ca. 2% per flash was noted. At increasing acid concentration the permanent change decreased and was only ca. 0.2% per flash beyond a molarity of 7 *M*. The photoproduct formed had a spectrum characteristic of that of photooxidized fluorescein.⁴ The change in reversibility occurs at an acidity range where a transition from cationic to neutral triplet fluorescein takes place, as well as a transition from cationic to neutral semioxidized dye, and also a marked change in viscosity. The data did not allow a decision among these possible causes for the change in reversibility.

The general conclusion of the kinetic study is that the triplet decay in sulfuric acid is consistent with the previously⁴ proposed reaction scheme of triplet fluorescein in aqueous solution and thus supports the correctness of this scheme.

ELECTROLYTE-SOLVENT INTERACTION. XI. CONDUCTANCE IN ISODIELECTRIC MIXTURES

BY ALESSANDRO D'APRANO¹ AND RAYMOND M. FUOSS

Contribution No. 1733 from the Sterling Chemistry Laboratory, Yale University, New Haven, Connecticut

Received March 21, 1963

Mixed solvents with dielectric constant equal to 13.2 were made by adding water (22.6 wt. %), methanol (42.4), acetonitrile (29.6), or *p*-nitroaniline (19.9) to dioxane. Tetrabutylammonium picrate showed moderate association ($K_A \approx 400$) in the first three solvents but only slight association in the fourth. Tetrabutylammonium tetraphenylboride is not associated in the acetonitrile mixture and shows at most slight pairing in the nitroaniline mixture. Tetrabutylammonium bromide is highly associated ($K_A = 1200$) in the former, but gives $K_A \approx 0$ in the latter. Solvation of picrate and especially of bromide ions by the highly polar nitroaniline molecules is suggested to account for the observations; the polar constituent of a solvent mixture therefore can influence conductance both by controlling the macroscopic dielectric constant and by specific interaction with ions.

In the preceding paper of this series,² we showed that addition of a highly polar solute such as *p*-nitroaniline to an electrolyte caused a decrease in conductance if at least one of the ions was small. The hypothesis was made that the decrease is due to electrostatic attraction

between the small ion and the dipole, sufficiently strong to stabilize the pair ion-dipole as a kinetic unit. The name "dipole solvate" was proposed, in distinction to chemical solvates such as hydrates, amines, and the like. This hypothesis assigns in general a dual role to the polar component of a polar-non-polar solvent mixture: first, the macroscopic dielectric constant, which controls long range interactions, is determined by the

(1) On leave of absence from the University of Palermo. Grateful acknowledgment is made for a Fulbright Travel Grant and for a DuPont Postdoctoral Fellowship.

(2) A. D'Aprano and R. M. Fuoss, *J. Phys. Chem.*, **67**, 1722 (1963).

polar component; and second, given sufficiently high ion-dipole potential energy at contact, specific short range interaction can occur which (a) decreases mobility and (b) effectively decreases the association constant.

The purpose of this paper is to present further data on systems in which different dipolar co-solutes will be compared with *p*-nitroaniline. Furthermore, a test of the sphere-in-continuum model is presented; by addition of water, methanol, acetonitrile, or *p*-nitroaniline in various amounts to dioxane, solvents whose macroscopic dielectric constants are all equal to about 13.2 are obtained. To a fair first approximation, the continuum model is found to be satisfactory, but for a quantitative description of a given system of mixed solvents, effects specific to the polar component of the mixture must also be considered. The value $D \approx 13$ was chosen as being low enough to cause moderate association, but high enough so that the Fuoss equation

$$\Lambda = \Lambda_0 - Sc^{1/2}\gamma^{1/2} + Ec\gamma \log c\gamma + Jc\gamma - K_{AC}\gamma^2\Lambda \quad (1)$$

can be used to analyze the data. Calculation of Λ_0 and K_A from the data by (1) was done by means of an IBM-709 computer; two programs were used. The first included the J_2 -term³ and the second omitted it. No significant differences were found; we therefore omitted the viscosity term $F\Lambda c$ and the J_2 -term, and used (1).

Experimental

Tetrabutylammonium bromide (m.p. 118–119°), picrate (m.p. 91.6–91.9°), and tetraphenylboride (m.p. 236.6–236.8°) were from laboratory stock. Matheson Coleman *p*-nitroaniline (PNA) was recrystallized first from water (1 g./100 ml.) and then from methanol (1 g./10 ml.); m.p. 146.6–146.8°. Dioxane was purified as described by Lind.⁴ Acetonitrile was distilled from Drierite, and methanol from aluminum amalgam.

Conductances were measured on a modified Shedlovsky bridge⁴ in a cell with constant 0.11772 ± 0.00003 , as determined by cross comparison with a cell calibrated against potassium chloride.⁵ All solutions were made up by weight.

The properties of the solvents are summarized in Table I, where the number in the first column identifies the various mixtures for later reference. The dielectric constants of about 13 were obtained by adding *w* weight per cent of the polar compounds shown in the second column. Some additional properties of PNA solutions in dioxane are the following: 2.99 g. PNA/100 g. solution, $D = 3.53$; 7.14%, $D = 5.60$; 9.18%, $D = 6.72$; 14.73%, $D = 9.79$, $\rho = 1.0660$; 15.59%, $D = 10.35$; 19.66%, $D = 13.05$, $\rho = 1.0792$; 21.85%, $D = 14.33$. For methanol-dioxane mixtures, the following values were found: 49.32 wt. % CH₃OH, $D = 15.41$; 39.26%, 12.13; 30.52%, 9.37. All dielectric constants were measured at 25° and 1 Mc., using the cell and bridge previously described.⁴ Properties of acetonitrile-dioxane mixtures at 25° are summarized in Table II.

The conductance data are summarized in Table III where Λ is equivalent conductance and *c* is concentration (equiv./l.). The heading of each set of data gives the salt used as solute and identifies the solvent by the code number of Table I.

Discussion

The different systems studied can be most conveniently compared by considering plots of Λ' against concentration where Λ' is defined by the equation

$$\Lambda' = \Lambda + Sc^{1/2} - Ec \log c \quad (2)$$

(3) D. S. Berns and R. M. Fuoss, *J. Am. Chem. Soc.*, **82**, 5585 (1960); eq. 2 and 3.

(4) J. E. Lind, Jr., and R. M. Fuoss, *J. Phys. Chem.*, **65**, 999 (1961).

(5) J. E. Lind, Jr., J. J. Zwolenik, and R. M. Fuoss, *J. Am. Chem. Soc.*, **81**, 1557 (1959).

TABLE I

PROPERTIES OF SOLVENTS

No.	<i>w</i>	ρ	<i>D</i>	100 η	10 ⁴ κ_0
1	19.89 PNA	1.0789	13.19	2.102	5.2
2	29.58 CH ₃ CN	0.9418	13.34	0.644	2.9
3	42.35 CH ₃ OH	.9142	13.18	0.643	4.4
4	22.60 H ₂ O	1.0360	13.64	1.794	9.3
5	29.57 CH ₃ CN	0.9421	13.33	0.644	3.4
6	19.72 PNA	1.0786	13.03	2.091	7.5
7	19.72 PNA	1.0786	13.03	2.091	7.5
8	29.57 CH ₃ CN	0.9421	13.33	0.644	3.4

TABLE II

PROPERTIES OF ACETONITRILE-DIOXANE MIXTURES

Wt. % CH ₃ CN	ρ	<i>D</i>	1000 η
24.80	0.9561	11.50	7.09
39.69	.9149	16.81	5.61
61.31	.8611	24.48	4.45
80.47	.8176	30.34	3.85

TABLE III

CONDUCTANCE DATA AT 25°

10 ⁴ <i>c</i>	Λ	10 ⁴ <i>c</i>	Λ
—Bu ₄ NPi in 1—		—Bu ₄ N·BPh ₄ in 5—	
3.568	16.437	3.158	52.84
7.201	15.134	6.299	49.46
10.781	14.283	9.047	47.46
14.658	13.634	11.007	46.33
19.688	13.014	16.001	44.10
—Bu ₄ NPi in 2—		—Bu ₄ N·BPh ₄ in 6—	
2.911	61.76	2.098	14.713
5.024	57.67	3.851	13.872
7.248	54.64	5.658	13.261
10.322	51.58	7.738	12.765
15.423	47.99	10.098	12.254
—Bu ₄ NPi in 3—		—Bu ₄ NBr in 7—	
2.983	54.93	4.180	15.301
5.634	50.12	8.673	14.008
8.019	47.24	12.625	13.277
11.562	44.10	17.896	12.580
15.677	41.50	23.850	12.000
—Bu ₄ NPi in 4—		—Bu ₄ NBr in 8—	
2.777	21.630	4.856	58.64
4.968	19.977	8.166	52.31
7.151	18.855	10.667	49.08
10.358	17.664	13.552	46.28
14.505	16.552	24.570	39.58

When ion pair population is negligible, Λ' is a linear function of concentration at low concentrations

$$\Lambda' = \Lambda_0 + Jc \quad (3)$$

Also for small degrees of association, the Λ' -*c* plots are still linear, because to a satisfactory approximation valid for small values of K_A

$$\Lambda' = \Lambda_0 + (J - K_A\Lambda_0)c + O(c^{3/2}) \quad (4)$$

Consider the picrate systems first (1–4 in Fig. 1). In order to eliminate (to a considerable extent) the influence of viscosity, the conductances were multiplied by solvent viscosity, and to normalize the data to a common origin, Λ_0 was subtracted from the observed conductances in order to construct Fig. 1, where $\eta(\Lambda' - \Lambda_0) = \eta\Delta\Lambda$ is plotted against concentration. The plot is linear for dioxane-PNA as solvent, consistent with the small value of K_A shown in Table IV. But in the mixtures of dioxane with acetonitrile, methanol, and

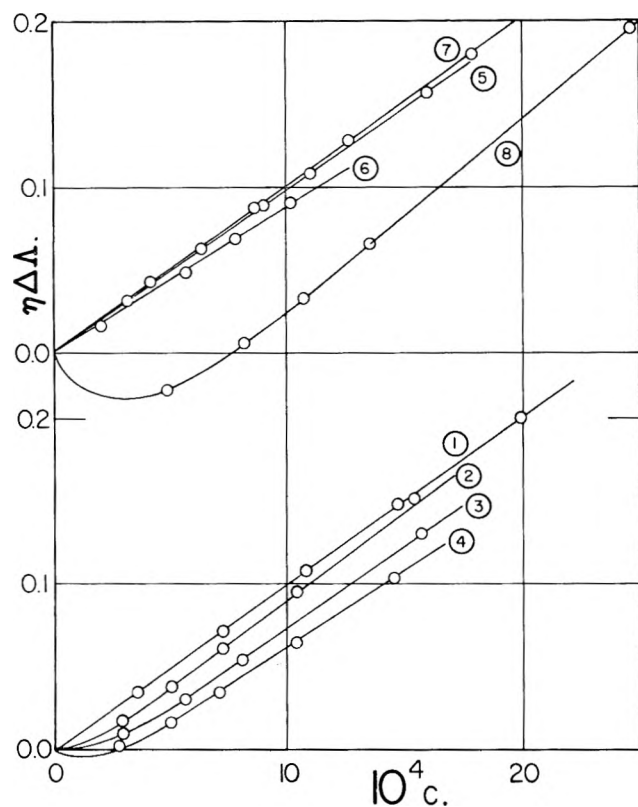


Fig. 1.—Reduced conductance differences, $\eta(\Lambda' - \Lambda_0)$, as a function of concentration. Curves 1-4, $\text{Bu}_4\text{N}^+\text{Pi}^-$; curves 5 and 6, $\text{Bu}_4\text{N}^+\text{BPH}_4$; curves 7 and 8, Bu_4NBr . Solvents identified in Table I.

water, the association constant is nearly an order of magnitude larger. The PNA system clearly is different from the other three. If we postulate an associative equilibrium between picrate ions and PNA dipoles



then the ion-ion pair equilibrium



would be shifted to the left and conductance correspondingly increased. The computer ignores (5); calculation on the basis of (6) alone will therefore give a smaller K_A , because (5) produces more free ions by shifting the pair equilibrium. An alternative hypothesis would be to assume that the PNA molecule stays with the picrate ion in an ion pair and therefore gives a smaller K_A because a_K , the contact distance, is larger. But, considering the high field strengths produced by ionic charges at molecular distances, the first hypothesis (displaced pair equilibrium) seems more plausible;

one would expect the PNA molecule to be squeezed out of an ion pair.

TABLE IV
DERIVED CONSTANTS

No.	Λ_0	$\Lambda_{0\eta}$	S	E	J	K_A
1	19.65 ± 0.05	0.413	128.0	1882	4770	67 ± 17
2	$74.58 \pm .23$.480	447.2	7032	17540	341 ± 25
3	$68.13 \pm .19$.438	431.7	6600	16450	471 ± 24
4	$26.49 \pm .10$.475	155.9	2345	5855	521 ± 34
5	$61.31 \pm .15$.397	403.9	5635	14790	-27 ± 17
6	$17.02 \pm .13$.356	120.9	1650	4520	137 ± 82
7	$18.31 \pm .11$.384	125.3	1800	4500	-66 ± 32
8	$86.13 \pm .64$.554	484.5	8290	18990	1210 ± 54

On the other hand, for isolated ions, the PNA- Pi^- complex appears to be reasonably stable; the Walden product is only 0.413 in PNA-dioxane as solvent, as compared with 0.48 in the acetonitrile and water mixtures. The intermediate value for $\Lambda_{0\eta}$ in the methanol-dioxane mixture might be due to hydrogen bonding between the picrate ion and methanol molecules; experiments with other alcohols are planned. There may be some self-association of methanol in dioxane; note that 42.35% was needed to give a dielectric constant of 13, as compared with only 29.6% acetonitrile. The difference is even more striking on a mole-ratio basis; in the methanol-dioxane mixture, there are 2.02 moles of alcohol per mole of dioxane, but only 0.90 mole of acetonitrile are required to reach the same dielectric constant. For water, 1.43 moles per mole of dioxane give $D \approx 13$, and for PNA, only 0.165 mole is necessary. Comparing systems 2, 3, and 4, it appears that the macroscopic dielectric constant of a mixture determines the association constant to within a factor of about two. Possibly some local unmixing, as suggested by Ramsey⁶ may be involved in the specific second-order differences between various polar solvents.

Tetrabutylammonium tetraphenylboride in acetonitrile-dioxane (5) and in PNA-dioxane (6) shows little association: certainly none in (5) because the computer gives a negative K_A , and a very doubtful $K_A > 0$ in (6). The bromide furnishes the striking example of interaction. In acetonitrile-dioxane, $K_A = 1200$ and the Walden product is 0.55, typical behavior for a salt with one small ion. But in the isodielectric system PNA-dioxane, the properties characteristic of large ions appear: the association constant is zero and the Walden product has dropped to 0.38, practically the same as for the tetraphenylboride. This large qualitative difference between systems 7 and 8 is completely consistent with the hypothesis of dipole solvation of small ions by strong dipoles.

(6) H. K. Bodenseh and J. B. Ramsey, *J. Phys. Chem.*, **67**, 140 (1963).

CONDUCTANCE OF THE ALKALI HALIDES. VII. CESIUM CHLORIDE IN DIOXANE-WATER MIXTURES AT 25°

BY JEAN-CLAUDE JUSTICE¹ AND RAYMOND M. FUOSS

Contribution No. 1734 from the Sterling Chemistry Laboratory of Yale University, New Haven, Connecticut

Received March 20, 1963

The conductance of cesium chloride at 25° was measured in dioxane-water mixtures covering the range of dielectric constant $12.73 \leq D \leq 78.54$. As a function of concentration, the data can be reproduced by the Fuoss three-parameter conductance equation. As in the case of the other alkali halides studied in dioxane-water mixtures, the contact distance a varies with composition of solvent and according to the method of computation. The corrected value for $\Lambda_0(\text{CsCl}, \text{H}_2\text{O}, 25^\circ)$ was found to be 152.81. From this value and data in the literature, $\lambda_0(\text{Cs}^+) = 76.44$, which is about 1% lower than the value 77.16 obtained by Lind³ from cesium iodide conductance and literature data.

We present in this paper conductance data for cesium chloride in a series of dioxane-water mixtures which cover the range $12.73 \leq D \leq 78.54$ in dielectric constant. Symbols are defined in earlier papers of this series.^{2,3}

Experimental

Cesium chloride was used as received (except for drying) from A. D. MacKay, Inc., New York, N. Y. Analysis by the flame photometer showed the presence of the following trace impurities: RbCl, 0.013%; KCl, 0.017%; NaCl, 0.021%; LiCl, 0.059%. Correction to Λ_0 in water for these impurities amounts to -0.258 . The salt samples were dried in a small platinum boat for 24 hr. at 141° and pressure less than 0.1 μ . No loss of weight ($\pm 3 \mu\text{g}$) was observed.

Conductances were measured at $25 \pm 0.003^\circ$, using previously described cells and electrical equipment.^{2,3} All solutions were made up by weight; normality was calculated from molality by the equation $c/m = \rho_0 + km$ where $k = -0.051$. Purification of dioxane has already been described.² The properties of the solvents are given in Table I and the conductance data are summarized in Table II, where $\Delta\Lambda$ is the difference between observed conductance and that calculated from the Fuoss conductance equation with the J_2 -term omitted. Activity coefficients are calculated by the equation

$$-\ln f = \tau/(1 + \tau) \quad (1)$$

In eq. 1

$$\tau = \beta\kappa/2 = \epsilon^2\kappa/2DkT \quad (2)$$

is the dimensionless variable introduced by Fuoss and Onsager.⁴ For the data obtained from aqueous solutions, the equation was of course simplified by setting the association constant K_A equal to zero.

TABLE I
PROPERTIES OF SOLVENTS

No.	w	ρ	D	100η	$10^5\epsilon_0$
1	0.0	0.99707	78.54	0.890	1.46
2	47.5	1.03193	38.60	1.862	0.32
3	64.4	1.03666	23.68	1.980	.109
4	70.5	1.03681	18.73	1.921	.053
5	75.5	1.03626	15.01	1.827	.042
6	78.8	1.03573	12.73	1.756	.035

Discussion

Several modifications of the equation

$$\Lambda = \Lambda_0 - Sc^{1/2}\gamma^{1/2} + Ec\gamma \log c\gamma + Jc\gamma + J_2(c\gamma)^{3/2} - K_{AC}\gamma^2\Lambda \quad (3)$$

were used to analyze the data. For the aqueous sys-

(1) On leave of absence from the University of Paris. Grateful acknowledgment is made for a stipend from the Higgins Fund and for a travel grant from the University of Paris.

(2) J. E. Lind, Jr., and R. M. Fuoss, *J. Phys. Chem.*, **65**, 999 (1961).

(3) J. E. Lind, Jr., and R. M. Fuoss, *ibid.*, **65**, 1414 (1961).

(4) R. M. Fuoss and L. Onsager, *Proc. Nat. Acad. Sci. U. S.*, **47**, 818 (1961).

TABLE II

CONDUCTANCE OF CESIUM CHLORIDE IN DIOXANE-WATER MIXTURES AT 25°

10^5c	Λ	$10^5\Delta\Lambda$	10^5c	Λ	$10^5\Delta\Lambda$
$D = 78.54$			$D = 18.73$		
93.817	144.121	13	23.189	31.403	-13
72.530	145.092	-17	17.928	32.797	29
58.244	145.887	2	13.271	34.325	-3
36.076	147.340	-10	9.109	36.130	-18
19.355	148.854	11	4.763	38.830	8
$D = 38.60$			$D = 15.01$		
45.026	59.191	-1	18.318	23.693	-5
27.453	60.784	5	13.606	25.312	12
18.927	61.795	-5	11.098	26.440	16
8.277	63.542	1	6.879	29.047	-23
$D = 23.68$			$D = 12.73$		
33.919	38.536	4			
28.120	39.403	-3	15.729	17.574	-16
21.232	40.682	15	12.267	18.830	32
14.078	42.371	-13	9.366	23.233	12
7.179	44.726	4	6.395	22.290	-28
			3.172	26.163	9

tem, as already mentioned, K_A was set equal to zero and γ equal to unity. The value $\Lambda_0 = 153.066 \pm 0.016$ was obtained; applying the correction for impurities, the corrected value for $\Lambda_c(\text{CsCl})$ is 152.81. Using $\lambda_0(\text{Cl}^-) = 73.52$ from Lind's value² $\Lambda_0(\text{KCl}) = 149.89$ and Longworth's value⁵ n^- for chloride in potassium chloride, we find $\lambda_0(\text{Cs}^+) = 76.44$, which is about 1% lower than the value 77.16 obtained from Lind's value³ $\Lambda_0(\text{CsI}) = 154.16$ and the value $\lambda_0(\text{I}^-) = 77.00$ derived from Voisin's data⁶ for potassium iodide which give⁷ $\Lambda_0(\text{KI}) = 150.52$, and the value $\lambda_0(\text{K}^+) = 73.52$ from the Lind²-Longworth⁵ data. The discrepancy is greater than the estimated probable errors in the various contributing measurements; further work on cesium is therefore planned.

For the dioxane-water mixtures, four variations of eq. 3 were examined, with the results summarized in Table III. The constants labeled (1) in the table were obtained using eq. 3 as given and computing activities by the Debye-Hückel equation

$$-\ln f = \tau/(1 + \kappa a) \quad (4)$$

Kay's program for the IBM computer⁸ was used to evaluate the constants. The computation was then re-

(5) L. G. Longworth, *J. Am. Chem. Soc.*, **54**, 2741 (1932).

(6) W. E. Voisin, Thesis, Yale University, 1951.

(7) R. M. Fuoss and F. Accascina, "Electrolytic Conductance," Interscience Publishers, Inc., New York, N. Y., 1959, p. 203.

(8) R. L. Kay, *J. Am. Chem. Soc.*, **82**, 2099 (1960).

peated, with J_2 set equal to zero; results are labeled (2) in the table. Omitting J_2 tends to give slightly larger values of Λ_0 as the dielectric constant decreases, but has no significant effect on association constant (the \pm spread for both constants is practically the same for variations 1 and 2). The values of a_J vary with D in both calculations; the spread is about the same, but the pattern of the dependence is different, as shown in the table. As mentioned in several earlier papers of this series, we are now inclined to consider a_J merely a numerical parameter for associated electrolytes, especially when the ions are small. The reason for this

TABLE III
DERIVED CONSTANTS

No.	$\Lambda_0(1)$	$\Lambda_0(2)$	$\Lambda_0(3)$	$\Lambda_0(4)$	
1	153.12	153.07	
2	66.66 \pm 0.02	66.65	66.65	66.64	
3	50.07 \pm .06	50.08	50.10	50.06	
4	45.25 \pm .11	45.27	45.27	45.26	
5	41.59 \pm .14	41.65	41.62	41.63	
6	38.44 \pm .24	38.54	38.38	38.59	
No.	$K_A(1)$	$K_A(2)$	$K_A(3)$	$K_A(4)$	
2	17.1 \pm 1.4	15	16	13	
3	83.2 \pm 4.7	86	95	77	
4	222 \pm 14	230	250	215	
5	818 \pm 27	845	885	810	
6	2106 \pm 76	2165	2175	2130	
No.	$\hat{a}_J(1)$	$\hat{a}_J(2)$	$J(3)$	$J(4)$	
1	4.05	154 \pm 3	
2	6.49 \pm 0.53	5.61	835 \pm 50	685 \pm 40	
3	5.00 \pm .28	5.34	2550 \pm 100	1910 \pm 60	
4	4.61 \pm .31	5.04	4570 \pm 220	3370 \pm 110	
5	5.78 \pm .25	6.43	9500 \pm 270	6600 \pm 120	
6	6.10 \pm .30	6.83	15000 \pm 500	10300 \pm 180	
No.	S	Λ_{07}	E	$10^8 R^-$	$10^8 R^+$
1	95.6	1.360	60.3	1.21	1.20
2	85.4	1.239	254.6	1.30	1.35
3	118.8	0.990	862.6	1.56	1.77
4	146.5	0.868	1594	1.75	2.05
5	181.6	0.759	2875	2.02	2.32
6	211.5	0.676	4380	2.22	2.66

lack of confidence in the physical significance of a_J lies in some recent theoretical considerations⁹ which show that approximating the Boltzmann function by a truncated power series in the derivation of eq. 3 was too drastic for the case of low dielectric constants or small ions (large $b = \epsilon^2/aDkT$). We therefore used a simplified program¹⁰ in which J_2 was omitted, and J

was treated as an empirical constant with no (at present) pre-assigned physical significance. Two other methods of calculating activity coefficients were used; in method 3, eq. 1 was used, and in method 4, the limiting Debye-Hückel equation

$$-\ln f = \tau \quad (5)$$

was used.

The values of K_A by the two variations were practically identical within their arithmetic uncertainty, but the spread in the J -values by method 4 is significantly less than by method 3. This verifies the results obtained in a similar study of data for cesium iodide,³ where the best fit was obtained by using eq. 5, the equation valid for point charges. As remarked earlier, this procedure can be justified on the argument that eq. 5 allows for long range interionic effects (which clearly are independent of the shape or size of the ions), while the short range effects are all subsumed in the K_A term which explicitly and sensitively depends on the contact distance a . We prefer this semi-empirical analysis, which dispenses with a_J values (pending completion of the theoretical re-investigation of the coefficient of the linear term) to calculating a_J 's from the J 's and then making (probably pointless) speculations about their variation with solvent composition. A plot of $\log K_A$ against reciprocal dielectric constant approximates linearity for $D < 30$, just as for the other alkali halides in dioxane-water mixtures, but the slope leads to $\hat{a}_K = 6.2$, which seems unreasonably large. The curve nearly coincides with that for rubidium chloride,¹¹ and like it, becomes concave-down at high dielectric constants.

Finally, we consider briefly the limiting conductances. As seen in Table III, the Walden product steadily decreases as the dielectric constant decreases; part of this is due to ion-dipole interaction,¹²⁻¹⁴ but part is also due to unknown effects which always seem to appear when ordinary small ions and water are put together. A plot of the Stokes radii (R^+ and R^-) against reciprocal dielectric constant is linear for $D < 30$; the linear portions of the curves extrapolate to $R^+ = R^- = 0.80 \text{ \AA.}$, giving $\hat{a}_A = 1.6$ or $\hat{a}_A = 2.4$, depending on whether the Sutherland correction of 3/2 for slipping is applied. The corrected value is, of course, more plausible.

(9) R. M. Fuoss and L. Onsager, *J. Phys. Chem.*, **66**, 1722 (1962); **67**, 621, 628 (1963).

(10) We are grateful to Dr. J. E. Lind, Jr., and Mr. J. F. Skinner, who wrote the program for us.

(11) R. W. Kunze and R. M. Fuoss, *J. Phys. Chem.*, **67**, 914 (1963).

(12) R. M. Fuoss, *Proc. Natl. Acad. Sci., U. S. A.*, **45**, 807 (1959).

(13) R. H. Boyd, *J. Chem. Phys.*, **35**, 1281 (1961).

(14) R. Zwanzig, *ibid.*, **37**, 1603 (1963).

THE ENERGY DEPENDENCE FOR REACTION CROSS SECTIONS OF ION-MOLECULE REACTIONS OF SOME PENTYL AND CYCLOPENTYL HALIDES¹

BY ANDRÉE J. LORQUET AND WILLIAM H. HAMILL

Radiation Laboratory and Department of Chemistry, University of Notre Dame, Notre Dame, Indiana

Received March 27, 1963

Ion-molecule reactions of cyclopentyl chloride, bromide, and iodide, of 3-bromopentane, and of 1-iodopentane have been observed in a mass spectrometer. Primary and secondary ion appearance potentials have been measured. Several of the secondary ion abundance curves exhibit maxima or concealed maxima at electron energies approximating excited state levels of the corresponding primary methyl halide ions. The dependence of reaction cross sections for secondary ions upon repeller field has been correlated with earlier studies.

Introduction

Earlier studies of bimolecular processes in a mass spectrometer have provided evidence in support of the following descriptions.²⁻⁴ The secondary ion current i_s is proportional to the primary ion current i_p , the concentration N of molecules in the ion source, the distance l_e from the electron beam to the exit slit, and the energy-dependent reaction cross section $\sigma(E)$

$$i_s = i_p N l_e \int_0^{l_e} \sigma(E) dl \quad (1a)$$

Since the translational energy E of the ion in the electric field is proportional to l , then

$$i_s/i_p N l_e = Q = E_e^{-1} \int_0^{E_e} \sigma(E) dE \quad (1b)$$

The cross section is assumed to be resolvable into contributions from ion-induced dipole forces $\sigma_L E^{-1/2}$, and knock-on collisions, σ_K .

$$\sigma(E) = P_L(\sigma_L E^{-1/2} - \sigma_K) + P_K \sigma_K \quad (1c)$$

The P 's are the corresponding chemical reaction probabilities. Equations 1b and 1c lead to the relation

$$Q = 2P_L \sigma_L E_e^{-1/2} + \sigma_K (P_K - P_L) \quad (1d)$$

Above a transitional ion energy E_t for which σ_K eclipses $\sigma_L E^{-1/2}$ we have

$$Q = (2P_L \sigma_L E_t^{1/2} - P_L \sigma_K E_t) E_e^{-1} - P_K \sigma_K \quad (2)$$

and above a further limit E_c , which always leads to decomposition of the secondary ion

$$Q = (P_L \sigma_L E_c^{1/2} + P_K \sigma_K E_c) E_e^{-1} \quad (3)$$

Experimental

All substances were purified by gas-liquid chromatography and the purity was established by mass analysis.

Operation of the mass spectrometer (CEC 21-103A, modified) has been described.³ Appearance potentials were determined both by the vanishing current method and also by linear extrapolation since the secondary ion current is frequently very small. The secondary ions were identified by pressure dependence, effect of repeller field, and appearance potential. The electron energy scale was calibrated using xenon. In the high mass range it was necessary to use several mass standards, including $C_3H_5Br_3$, $CHBr_3$, CHI_3 .

Results

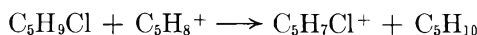
Appearance potentials for both secondary and various possible primary ions appear in Table I. The values for ions at masses 40⁺, 39⁺, 28⁺, 27⁺, 26⁺, and 15⁺ of C_5H_9I are not reliable because of a long exponential

tail; they were not examined more carefully because no secondary ions have similar behavior and high appearance potentials as well.

The proposed ion-molecule reactions appear in Table II. In the case of C_5H_9Cl , two additional secondary ions appeared at m/e 173⁺ and 102⁺. The ion current of the first is quite small, but by analogy with other reactions we postulate



which is the most important reaction type for the other halides. We could not study the second reaction because at mass 102 there is also a primary peak due to $C_5H_7Cl^+$. A possible mechanism for the formation of secondary $C_5H_7Cl^+$ is



There is no similar reaction in the case of C_5H_9Br and C_5H_9I where the peak for $C_5H_8^+$ is small.

The most important secondary ions from cyclopentyl halides which contain only C and H are $C_{10}H_{17}^+$, $C_8H_{13}^+$, $C_7H_{11}^+$, and $C_6H_9^+$. All originate from $C_5H_9^+$ and are of one type, *viz.*, C_nH_{2n-3} .

Several secondary ion current *vs.* electron energy curves showed maxima, or concealed maxima, at energies slightly above onset. The more prominent of these appear in Table III. The displacement of a maximum from the foot of the curve is expressed as ΔE e.v. Excited states of the methyl halide ions are included for comparison.⁵ It should be observed that primary $C_5H_{11}I^+$ also exhibits a small maximum at the foot of the ion abundance curve. These results suggest primary ions in two or more states which produce secondary ions with unequal cross sections. Such effects have been reported previously.⁶

Results for pentyl chloride were well behaved in terms of eq. 1-3, for which the results appear in Table IV. In the other cases anomalous results suggested complications arising from space charge. This possibility was tested by measuring Q for CD_5^+ from CD_4 with added pentyl iodides or xenon at high pressures. Effects were marked at very low repeller field but values of Q for CD_5^+ were normal⁴ from $E_e = 1.2$ to 7 e.v. Consequently, eq. 1 cannot be applied to these reactions, since its energy range coincides with that of space charge effects. Equations 2 and 3 do appear to describe the results for the secondary ions for which results are summarized in Table V.

(1) Supported in part under AEC Contract At(11-1)-38.

(2) N. Boelrijk and W. H. Hamill, *J. Am. Chem. Soc.*, **84**, 730 (1962).

(3) R. F. Pottie, A. J. Lorquet, and W. H. Hamill, *ibid.*, **84**, 529 (1962).

(4) D. A. Kubose and W. H. Hamill, *ibid.*, **85**, 125 (1963).

(5) D. C. Frost and C. A. McDowell, *Proc. Roy. Soc. (London)*, **A241**, 194 (1957).

(6) R. F. Pottie and W. H. Hamill, *J. Phys. Chem.*, **63**, 877 (1959).

TABLE I
 APPEARANCE POTENTIALS OF PRIMARY AND SECONDARY IONS

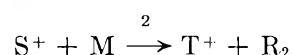
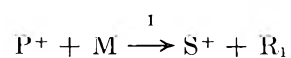
Compound	Primary ion	m/e	Secondary ion	m/e	A.P. (linear extrap.)	A.P. (vanishing current)
Cyclopentyl chloride	$C_5H_9Cl^+$	104 ⁺			10.9	10.5
	$C_5H_9^+$	69 ⁺			12.0	11.6
	$C_6H_9^+$	68 ⁺			11.4	11.0
			$C_7H_{11}^+$	95 ⁺	12.15	11.6
			$C_{10}H_{17}^+$	137 ⁺	12.15	..
			$C_8H_{13}^+$	109 ⁺	12.50	11.6
3-Bromopentane	$C_5H_{11}Br^+$	150 ⁺			10.5	10.2
	$C_6H_{11}Br^+$	152 ⁺			10.5	10.2
	$C_5H_{11}^+$	71 ⁺			10.9	10.5
			$C_{10}H_{22}Br^+$	221 ⁺	10.8	10.25
			$C_{10}H_{22}Br^+$	223 ⁺	10.5	10.25
Cyclopentyl bromide	$C_5H_9Br^+$	148 ⁺			10.4	10.1
	$C_5H_9Br^+$	150 ⁺			10.4	10.1
	$C_6H_9^+$	69 ⁺			11.2	10.9
			$C_{10}H_{18}Br^+$	217 ⁺	10.4	10.1
			$C_{10}H_{18}Br^+$	219 ⁺	10.55	10.1
			$C_{10}H_{17}^+$	137 ⁺	11.2	..
1-Iodopentane	$C_5H_{11}I^+$	198 ⁺			9.3	9.1
	$C_4H_9I^+$	184 ⁺			11.4	11.0
	$C_2H_4I^+$	155 ⁺			15.1	12.6
	CH_2I^+	141 ⁺			20.6	16.1
	HI^+	128 ⁺			10.4	10.3
	I^+	127 ⁺			15.3	13.7
	$C_6H_{11}^+$	71 ⁺			10.1	9.9
			$C_{10}H_{22}I_2^+$	396 ⁺	9.5	9.1
			$C_3H_{10}I_2^+$	324 ⁺	13.4	12.4
			$C_{10}H_{22}I^+$	269 ⁺	9.3	..
			$C_8H_{18}I^+$	241 ⁺	11.0	10.1
Cyclopentyl iodide	$C_5H_9I^+$	196 ⁺			9.2	9.1
	$C_2H_3I^+$	154 ⁺			15.1	..
	$C_6H_9^+$	69 ⁺			10.2	9.8
	$C_6H_8^+$	68 ⁺			10.2(10.7; 11.65) ^a	10.2
	$C_5H_7^+$	67 ⁺			12.5(12.8; 13.85) ^a	11.5
	$C_4H_5^+$	53 ⁺			13.5(14.2; 16.3) ^a	13.3
	$C_3H_6^+$	42 ⁺			13.3	..
	$C_3H_6^+$	41 ⁺			12.8	12.3
	$C_3H_4^+$	40 ⁺			18.0(19.0) ^a	..
	$C_3H_3^+$	39 ⁺			16.2(17.6; 19.0) ^a	..
	$C_2H_4^+$	28 ⁺			17.0	..
	$C_2H_3^+$	27 ⁺			20.4	..
	$C_2H_2^+$	26 ⁺			23.0	..
	CH_3^+	15 ⁺			21.3	..
			$C_{10}H_{18}I_2^+$	392 ⁺	9.3	8.9
			$C_3H_8I_2^+$	322 ⁺	9.1	9.1
			$C_{10}H_{18}I^+$	265 ⁺	9.1	9.0
			$C_{10}H_{17}^+$	137 ⁺	10.4	9.5
			$C_8H_{13}^+$	109 ⁺	12.3	11.4
			$C_7H_{11}^+$	95 ⁺	10.3	9.7
			$C_7H_9^+$	93 ⁺	12.4(15.15) ^a	..
			$C_7H_7^+$	91 ⁺	12.5(13.4) ^a	..
			$C_6H_9^+$	81 ⁺	10.1	9.5

^a These values refer to higher breaks in the ionization efficiency curve.

Curves for Q vs. E_e^{-1} for the following secondary ions were abnormal: 109⁺, 265⁺, 392⁺ from C_6H_9I ; 269⁺, 324⁺, 396⁺ from $C_5H_{11}I$; 217⁺ from C_5H_9Br ; and 221 from $C_6H_{11}Br$. The abnormality was shown not to arise from space charge or focus effects. Thus, ion focus was excellent for 265⁺ at $E_e < 7$ v. and for 396⁺ at $E_e < 10$ v. The phenomenon is much more pronounced at low repeller field. Since Q at constant E_e increased with increasing pressure it appears that a tertiary process is responsible. An example of this behavior is illustrated by the two upper curves of Fig. 1.

Discussion

Let us consider the formation of a tertiary ion T^+ from secondary ion S^+ and also from primary ion P^+



The rate of formation of T^+ at distance l from the electron beam in the direction of the exit slit is

$$dn_T = Nn_S\sigma(l)_2dl \quad (4)$$

where n_S is the number of S^+ , σ is the cross section for reaction, and N is the concentration of molecules.

TABLE II
ION-MOLECULE REACTIONS

	$Q \times 10^{16}$ (cm. ²) at 12 v./cm.
$C_5H_9^+ + C_5H_5Cl \rightarrow C_{10}H_{17}^+ + HCl$	<0.1
$C_5H_9^+ + C_5H_9Cl \rightarrow C_8H_{13}^+ + [C_2H_4 + HCl]$	<0.6
$C_5H_9^+ + C_5H_9Cl \rightarrow C_7H_{11}^+ + [C_2H_6 + HCl]$	<0.8
$C_5H_{11}Br^+ + C_5H_{11}Br \rightarrow (C_5H_{11})_2Br^+ + Br$	27.9
$C_5H_9Br^+ + C_5H_9Br \rightarrow (C_5H_9)_2Br^+ + Br$	50.4
$C_5H_9^+ + C_5H_9Br \rightarrow C_{10}H_{17}^+ + HBr$	0.04
$C_5H_{11}I^+ + C_5H_{11}I \rightarrow (C_5H_{11})_2I^+$	11.9 (6.8) ^a
$C_5H_{11}I^+ + C_5H_{11}I \rightarrow (C_5H_{11})_2I^+ + I$	0.56
$C_5H_{11}^+ + C_5H_{11}I \rightarrow C_8H_{13}I^+ + C_2H_4$..
$C_5H_{11}^+ + C_5H_{11}I \rightarrow C_5H_{10}I_2^+ + C_2H_5$	7.6
$C_5H_9I^+ + C_5H_9I \rightarrow (C_5H_9)_2I^+ + I$	61.4 (40.0) ^a
$C_5H_9I^+ + C_5H_9I \rightarrow (C_5H_9)_2I^+$	0.09
$C_6H_9I^+ + C_5H_9I \rightarrow C_5H_8I_2^+ + C_5H_{10}$.91
$C_5H_9^+ + C_5H_9I \rightarrow C_{10}H_{17}^+ + HI$.14
$C_5H_9^+ + C_5H_9I \rightarrow C_7H_{11}^+ + (C_3H_6 + HI)$.27
$C_5H_9^+ + C_5H_9I \rightarrow C_6H_9^+ + (C_4H_9I)$ (or $C_4H_8 + HI$)	.72
$C_5H_7^+ + C_5H_9I \rightarrow C_7H_7^+ + [C_3H_9I]$	2.5 ^b
$C_5H_7^+ + C_5H_9I \rightarrow C_7H_9^+ + [C_3H_7I]$	1.28
$C_5H_9^+ + C_5H_9I \rightarrow C_8H_{13}^+ + [C_2H_4 + HI]$	2.23
$C_3H_5^+ + M \rightarrow S' \xrightarrow{+M} C_8H_{13}^+ (1.00)$	

^a Values relative to the secondary process corrected for third-order effects. ^b This value is large because of an impurity.

TABLE III

EVIDENCE FOR EXCITED STATES IN PRIMARY AND SECONDARY ION ABUNDANCE CURVES

Reactant	Primary ion	Secondary ion	ΔE , e.v.
CH_3Cl	CH_3Cl^+		0.0, 0.55, 1.60 ^a
C_3H_9Cl	$C_3H_9^+$	$C_7H_{11}^+$	1.5
CH_3Br	CH_3Br^+		0.32, 1.09, 2.41 ^a
C_5H_9Br	$C_5H_9Br^+$	$C_{10}H_{18}Br^+$	1.6, 3
$C_5H_{11}Br$	$C_5H_{11}Br^+$	$C_{10}H_{22}Br^+$	1.5
CH_3I	CH_3I^+		0.58, 1.71, 3.63 ^a
C_5H_9I	$C_5H_9^+$	$C_6H_9^+$	2
C_5H_9I	$C_5H_9^+$	$C_{10}H_{17}^+$	1.9
C_5H_9I	$C_5H_9I^+$	$C_{10}H_{18}I_2^+$	0.9
$C_5H_{11}I$	$C_5H_{11}I^+$		2.2
$C_5H_{11}I$	$C_5H_{11}I^+$	$C_{10}H_{22}I^+$	2
$C_5H_{11}I$	$C_5H_{11}I^+$	$C_{10}H_{22}I_2^+$	1, 1.8

^a From ref. 5.

TABLE IV

VALUES OF E_t AND E_c AND COMPARISON OF OBSERVED WITH PREDICTED PARAMETERS FOR C_5H_9Cl

Primary and secondary ions	E_t , e.v.	E_c , e.v.	$P_L\sigma_L$, $\text{\AA}^2(\text{e.v.})^{1/2}$	$P_L\sigma_K$, \AA^2	$P_K\sigma_K$, \AA^2	Slope 2nd region		Slope 3rd region		σ_L calcd., \AA^2	σ_K calcd., \AA^2	σ_K obsd., \AA^2
						Obsd.	Calcd.	Obsd.	Calcd.	(e.v.) ^{1/2}	\AA^2	\AA^2
$69^+ \rightarrow 95^+$	1.0	...	0.87	1.10	0.52	0.72	0.65	74	70	74
$69^+ \rightarrow 109^+$	0.85	6.5	1.3	1.91	.19	.83	.77	2.0	1.97	74	70	80
$69^+ \rightarrow 137^+$	0.95	...	0.28	0.375	.02	.196	.194	74	70	76

TABLE V

VALUES OF E_t AND E_c OF IONS FORMED ONLY BY SECONDARY PROCESSES

Molecule	Primary and secondary ions	E_t , e.v.	E_c , e.v.
C_5H_9I	$C_5H_9^+ \rightarrow C_5H_8I_2^+$	0.8	1.5
	$C_5H_9^+ \rightarrow C_{10}H_{17}^+$.65	...
	$C_6H_9^+ \rightarrow C_7H_{11}^+$.65	...
	$C_5H_9^+ \rightarrow C_6H_9^+$.65	...
	$C_5H_7^+ \rightarrow C_7H_7^+$	<1.25	4.5
	$C_5H_7^+ \rightarrow C_7H_9^+$	<1.25	3.5

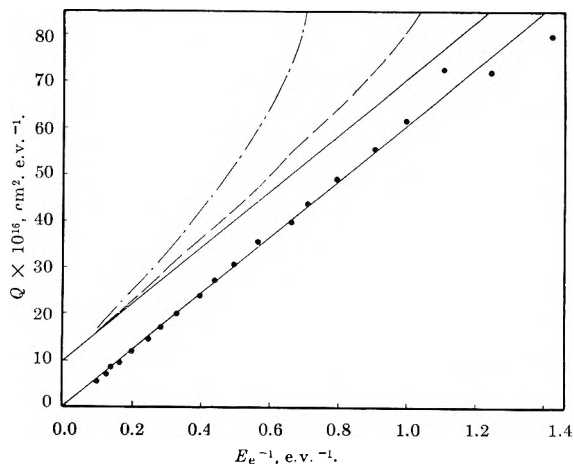


Fig. 1.—The cross section Q for $(C_5H_9)_2I^+$ from C_5H_9I as a function of the primary ion energy E_e at the exit slit. Upper curves describe $(Q_{\text{obsd}} + 10) \times 10^{-16}$ cm.² at molecular concentrations of 1.82 and 8.99×10^{12} moles./cc.; — — and — · —, respectively, referred to their common asymptote. The lowest curve describes $Q_{\text{cor}} = Q_{\text{obsd}} - K_{23}Nl_eE_e^{-2}$ vs. E_e^{-1} according to eq. 9 and 3.

Since n_S is also a function of l as well as the number of primary ions, n_P

$$n_S = Nn_P \int_0^l \sigma(l)_1 dl \quad (5)$$

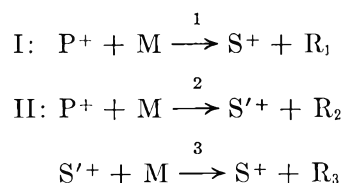
Combining eq. 4 and 5 and integrating over the total distance to the exit slit, l_c , the number of tertiary ions, n_T , is

$$n_T = N^2n_P \int_0^{l_c} \sigma(l)_2 \int_0^l \sigma(l)_1 dl dl \quad (6)$$

In terms of the measured ion current i and energy E

$$i_T = N^2n_P l_c^2 E_e^{-2} \int_0^{E_e} \sigma(E)_2 \int_0^E \sigma(E)_1 dE dE \quad (7)$$

If an ion is produced both by secondary and by tertiary processes, then



The combined observed current at the mass of S^+ is

$$i = Nn_P l_c E_e^{-1} \int_0^{E_e} \sigma(E)_1 dE + N^2n_P l_c^2 E_e^{-2} \int_0^{E_e} \sigma(E)_3 \int_0^E \sigma(E)_2 dE dE \quad (8)$$

For sufficiently large ion energy, E_c , all collisions result in decomposition of the secondary ion. When $E_e \geq E_c$, integration must be carried out for $0 < E < E_c$.

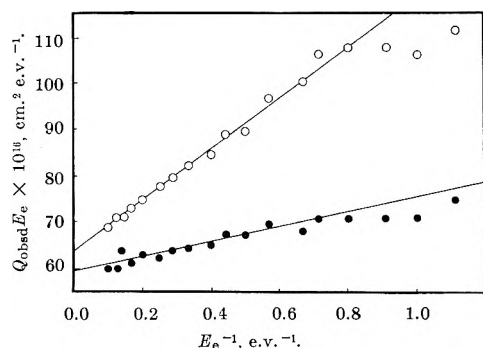


Fig. 2.—The termolecular contribution to $(C_5H_9)_2I^+$ from C_5H_9I for the same runs described in Fig. 1 in terms of QE_e^{-1} vs. E_e^{-1} according to eq. 9.

The resulting definite integrals may be indicated by the constants K_1 and K_{23} . Replacing $i/Nn_p l_e$ by Q gives

$$Q = K_1 E_e^{-1} + K_{23} N l_e E_e^{-2} \quad (9)$$

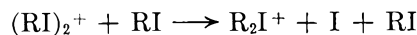
Consequently QE_e vs. E_e^{-1} should be linear and show an intercept independent of pressure and a slope proportional to pressure. Equation 9 evidently can be used to "correct" the observed Q for tertiary ions, leaving the secondary component alone, and then applying eq. 2 and 3.

We illustrate for the case of 396^+ from 198^+ using $C_5H_{11}I$. At $E_e = 1.5$ e.v. and reservoir pressures 281 and 516 μ , $Q(396^+)$ was 9.6 and 11.9×10^{-16} cm.². Plots of Q vs. E_e^{-1} were nonlinear from E_e of 1 to 10 e.v. Plots of QE_e vs. E_e^{-1} in the same interval were linear; intercepts were 21 and 20×10^{-16} cm.² e.v. and slopes were 0.64 and 1.1×10^{-16} cm.² e.v.² at low and high pressures, respectively. The calculated $Q(396^+)$ for secondary ions alone as a function of E_e^{-1} was then well behaved, with an intercept zero as required by eq. 3 for the high energy region and a well defined $E_c = 2.5$ e.v. at both pressures. The ternary contribution may be collision stabilization.

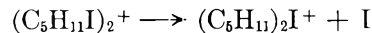
The behavior of $(C_5H_9)_2I^+$ from C_5H_9I is entirely similar. At molecular concentrations $N = 1.82$ and 8.99×10^{12} moles/cc., $Q(265^+)$ was 45 and 67×10^{-16} cm.², respectively, at $E_e = 1.5$ e.v. The nonlinearity of Q vs. E_e^{-1} , and its pressure dependence are shown in Fig. 1. When $Q_{cor} = Q_{obsd} - K_{23} N l_e E_e^{-2}$ from eq. 9 is employed instead, both sets of measurements exhibit a Q vs. E_e^{-1} linear dependence with zero intercept (see Fig. 1) and conform to eq. 3. The procedure for evaluating the contribution of the termolecular process is demonstrated in Fig. 2 for the same runs in plots of QE_e vs. E_e^{-1} according to eq. 9. In four runs, of which only two are shown, pressure ratios were 4.9, 2.7, and 1.4 relative to the lowest while the ratios of the corresponding slopes of QE_e vs. E_e^{-1} were 3.5, 2.5, and 1.5.

In the preceding instance and also in the correspond-

ing formation of $(C_5H_{11})_2I^+$ from $C_5H_{11}I$, the ternary process may be



This mechanism is consistent with the appearance of a small metastable peak at apparent mass 182.7 which can only be understood as evidence for



Depending upon the internal energy of the dimeric ion and its velocity, collision with a molecule may either stabilize or decompose.

Values of E_c for various reactions have been collected in Table VI.

TABLE VI
VALUES OF E_c FOR IONS FORMED BY SECONDARY AND TERTIARY PROCESSES

Molecule	Primary and secondary ions	E_c , e.v.
C_5H_9I	$C_5H_9I^+ \rightarrow C_{10}H_{18}I^+$	1.4
	$C_5H_9I^+ \rightarrow C_{10}H_{18}I_2^+$	2.5
	$C_5H_9^+ \rightarrow C_3H_{13}^+$	2.3
	$C_3H_5^+ + C_3H_{13}^+$	
$C_5H_{11}I$	$C_5H_{11}I^+ \rightarrow C_{10}H_{22}I_2^+$	2.5
	$C_5H_{11}I^+ \rightarrow C_{10}H_{22}I^+$...
	$C_2H_4I^+ \rightarrow C_6H_{10}I_2^+$	2
C_5H_9Br	$C_5H_9Br^+ \rightarrow C_{10}H_{18}Br^+$	3.2
3- $C_5H_{11}Br$	$C_5H_{11}Br^+ \rightarrow C_{10}H_{22}Br^+$...

Unimolecular decomposition of $(C_5H_{11}I)_2^+$ within the source can be detected as an energy-shifted peak for favorable values of accelerating and repeller voltages (V_a and V_r , respectively). It is indicated by a peak situated between 269^+ and 268^+ (the latter attributed to CH_2I_2 impurity). At $V_a = 760$ v. the peak is shifted toward smaller m/e as V_r increases from 5 to 6 v. At $V_a = 350$ v. the peak is detectably shifted by increasing V_r from 1.6 to 1.8 v. and the apparent mass approximates 268 at $V_r = 9$ v. At $V_a = 200$ v. and $V_r = 3$ v. the apparent mass approximates 268. We interpret these results in terms of the preceding unimolecular decomposition. Since this shifted peak appears even at values of E_c well below the observed $E_c = 2.5$ e.v. (Table VI), it may arise entirely from metastable collision complexes. Since the collision complex can form at any primary ion energy between zero and E_e or E_c , the energy loss ΔE to the neutral fragment will be proportional to V_r . The apparent mass m^* is given by

$$m^* = m(1 - \Delta E)/e(V_a + 1/2 V_r)$$

since $E_e \cong 1/2 e V_r$, and we have approximately

$$(m - m^*)/m \propto V_r/V_a$$

which accounts qualitatively for the observations.

COUNTERIONS AND MICELLE SIZE. I. LIGHT SCATTERING BY SOLUTIONS OF DODECYLTRIMETHYLAMMONIUM SALTS¹

BY E. W. ANACKER AND H. M. GHOSE

Chemistry Department, Montana State College, Bozeman, Montana

Received April 1, 1963

Dilute solutions of dodecyltrimethylammonium bromide in 0.500 *m* NaX (X = F, Cl, Br, ClO₃, BrO₃, IO₃, NO₃, CHO₂, SCN) were examined by light scattering. Solutions of the surfactant in 0.500 *m* NaI and NaClO₄ in the concentration range suitable for measurement could not be prepared. Counterion effects on the critical micelle concentration and aggregation number were found to follow only roughly the lyotropic series for anions.

Introduction

It has been observed that when the counterion associated with a given micelle-forming ion is changed, the critical micelle concentration (c.m.c.)^{2,3} and the micelle size^{2,4} also change. The light scattering investigation reported herein was undertaken to augment this information concerning the counterion's role in micelle formation. It encompassed nine univalent anions (F⁻, Cl⁻, Br⁻, ClO₃⁻, BrO₃⁻, IO₃⁻, NO₃⁻, CHO₂⁻, SCN⁻) in combination with the surfactant ion CH₃(CH₂)₁₁N(CH₃)₃⁺. Since the study's inception, the results of other inquiries with a similar objective have been reported.^{5,6}

Experimental

Materials.—Ideally one should prepare a surfactant for each counterion X⁻ of interest. To avoid much of the labor involved in such an undertaking, we examined dilute solutions of dodecyltrimethylammonium bromide (DTAB) in the presence of relatively large amounts of NaX. Except when X⁻ was Br⁻, two different counterions were always present in solution. Our procedure for handling this complication is discussed later.

Dodecyltrimethylammonium bromide was prepared from trimethylamine and 1-bromododecane (b.p. 97.5° at ~1 mm.) by the method of Scott and Tartar.⁷ It was purified through repeated crystallization from ethanol-acetone mixtures. The bromine content was determined gravimetrically: theoretical 25.92%, found 25.92%.

Inorganic salts were of reagent grade and not further purified.

Water used in solution preparation was redistilled from alkaline permanganate.

Methods and Apparatus.—Solutions were prepared by weighing into volumetric flasks both surfactant and solvent (0.500 *m* NaX). Prior to placement in the light scattering photometer, they were filtered under nitrogen pressure through an ultrafine, fritted Pyrex glass funnel directly into the scattering cell.

Refractive index measurements were made in an instrument constructed for previous work.⁸

Scattering measurements were made in a locally constructed 90° photometer. In this instrument incident light is supplied by a G.E. 100-watt AH-4 arc. The light scattered laterally from a 1-in. rectangular cell, 35-ml. capacity, is measured by an RCA 1P21 photomultiplier tube. The output of this tube is fed to a Hewlett-Packard d.c. vacuum tube voltmeter (Model 412A) and finally recorded on a 5-mv. Minneapolis Honeywell recorder. The photometer was calibrated with 0.5% Cornell polystyrene in toluene.⁹⁻¹¹ To make the calibration applicable to aqueous

systems, scattering volume and refractive index correction factors were calculated and applied.

Light of wave length 4358 Å. (as isolated by a Baird interference filter) was used. Temperatures were in the range 31–32°.

Results and Discussion

The concentration gradients of the refractive index, $(dn/dc)_{m_{NaX}}$ and $(dn/dm)_{m_{NaX}}$, required in the determination of micellar aggregation numbers were measured directly for DTAB (Table I) and computed for DTAX (Table II). Refractive index, molarity, and molality are designated by *n*, *c*, and *m*, respectively. In the computational procedure, surfactant solutions were considered to be mixtures of DTAX, NaX, and NaBr. Thus a solution 0.0160 *m* in DTAB and 0.5000 *m* in NaF was regarded as being 0.0160 *m* in DTAF, 0.0160 *m* in NaBr, and 0.4840 *m* in NaF. The measured refractive index difference between a solution and solvent was corrected for differences in NaX and NaBr concentrations. Within experimental error, refractive index *vs.* surfactant concentration plots were linear over the range of interest and gradients could be equated to slopes.

TABLE I

CONCENTRATION GRADIENTS OF THE REFRACTIVE INDEX
4358 Å., 31–32°

X ⁻	dn/dm_{NaX} , ^a kg./mole	$(dn/dm)_{DTAB}^{0.5m NaX}$, kg./mole	$(dn/dc)_{DTAB}^{0.5m NaX}$, l./mole
F ⁻	0.00539	0.0449	0.0456
CHO ₂ ⁻	.00871	.0430	.0442
NO ₃ ⁻	.00960	.0425	.0438
ClO ₃ ⁻	.0100	.0419	.0434
Cl ⁻	.0104 ¹²	.0437	.0447
Br ⁻	.0147	.0432	.0446
BrO ₃ ⁻	.0165	.0414	.0428
SCN ⁻	.0183	.0411	.0426
IO ₃ ⁻	.0260	.0403	.0413

^a Concentration range of 0–0.15 *m*. Gradients for 0.5 *m* solutions in general will be somewhat less. In the case of NaCl, for example, $dn/dm = 0.00994$ in the 0.5 *m* region.

The light scattering data collected are presented in Fig. 1, 2, and 3 as 90° scattering *vs.* surfactant concentration plots. Micellar aggregation numbers and effective charges, *m*'s and *p*'s, were computed according to the considerations of Prins and Hermans¹³ and Mysels and Princen.^{14,15} Because of the presence in most

(12) A. Kruis, *Z. physik. Chem.*, **B34**, 13 (1936).

(13) W. Prins and J. J. Hermans, *Proc. Koninkl. Ned. Akad. Wetenschap.*, **B59**, 162 (1956).

(14) K. J. Mysels and L. H. Princen, *J. Colloid Sci.*, **12**, 594 (1957).

(15) The more recent treatments of Stigter¹⁶ and of Vrij and Overbeek¹⁷ give better values of charge, but it is not yet certain whether this is true of aggregation numbers. At low surfactant and high added electrolyte concentrations, ionic strengths will not change drastically and approximation of constant activity coefficients made in the earlier theories is reasonable. The procedure used here is adequate for the intended purpose.

(1) Presented at the 17th Annual Northwest Regional Meeting of the American Chemical Society in Pullman, Washington, June, 1962.

(2) C. S. Samis and G. S. Hartley, *Trans. Faraday Soc.*, **34**, 1288 (1938).

(3) P. F. Grieger, *Ann. N. Y. Acad. Sci.*, **51**, 827 (1949).

(4) G. S. Hartley and D. F. Runnicles, *Proc. Roy. Soc. (London)*, **A168**, 420 (1938).

(5) I. Cohen and T. Vassiliades, *J. Phys. Chem.*, **65**, 1774 (1961).

(6) K. J. Mysels, Final Report, Project NR 356-254, Office of Naval Research.

(7) A. B. Scott and H. V. Tartar, *J. Am. Chem. Soc.*, **65**, 692 (1943).

(8) E. W. Anacker, *J. Colloid Sci.*, **8**, 402 (1953).

(9) B. A. Brice, M. Halwer, and R. Speiser, *J. Opt. Soc. Am.*, **40**, 768 (1950).

(10) P. Doty and R. F. Steiner, *J. Chem. Phys.*, **18**, 1211 (1950).

(11) C. I. Carr, Jr., and B. H. Zimm, *ibid.*, **18**, 1616 (1950).

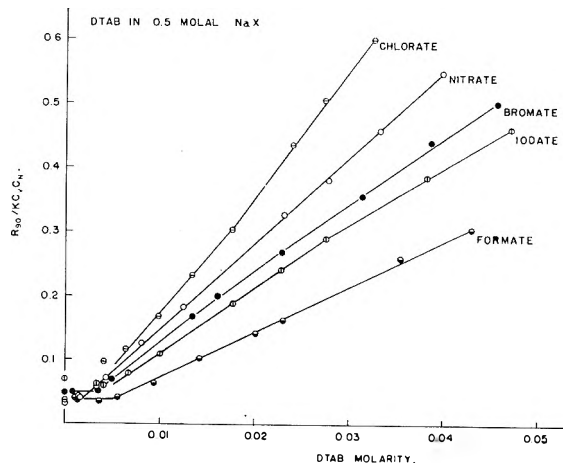


Fig. 1.—Scattering plots for DTAB in 0.5 *m* NaX. R_{90} is the Rayleigh ratio for 90° scattering of unpolarized light. The instrument constant $K = 2.22 \times 10^{-4} \text{ cm}^{-1}$. C_v and C_n are, respectively, volume and refractive index correction factors.¹¹ The product $C_v C_n$ has the following values: 0.663, ClO_3^- ; 0.664, NO_3^- ; 0.667, BrO_3^- ; 0.672, IO_3^- ; 0.663, CHO_2^- .

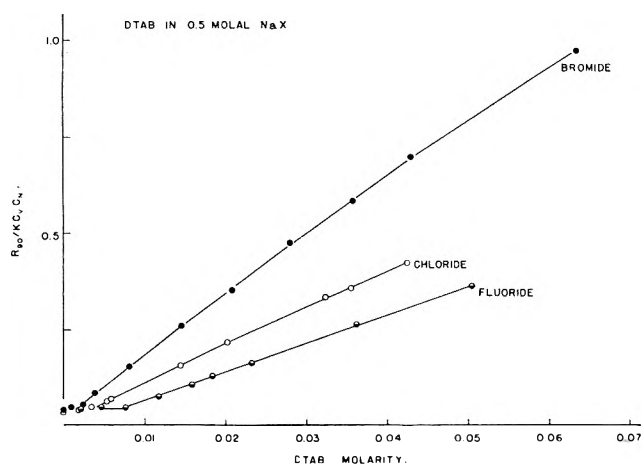


Fig. 2.—Scattering plots for DTAB in 0.5 *m* NaX. The product $C_v C_n$ has the following values: 0.667, Br^- ; 0.664, Cl^- ; 0.662, F^- .

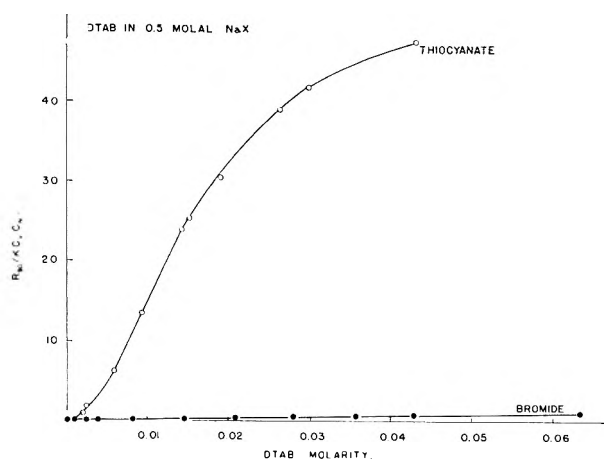


Fig. 3.—Scattering plots for DTAB in 0.5 *m* NaSCN and in 0.5 *m* NaBr. The product $C_v C_n$ equals 0.668 for 0.5 *m* NaSCN.

solutions of two anionic species, computations were carried out for three different micellar models. It was assumed that anions complexed by the micelles are Br^- (model I), X^- (model II), and both Br^- and X^- in proportion to their stoichiometric concentrations (model

III). Of the three models, III is probably the closest to reality and I the farthest. Because at the c.m.c.'s, where scattering data are extrapolated for evaluation, the concentrations of the anions furnished by the sodium salts were 60 to 600 times as large as the concentrations of Br^- furnished by the DATB, models II and III provided the same aggregation numbers within computational limits. The results of these calculations are given in Table III.

TABLE II
COMPUTED CONCENTRATION GRADIENTS OF THE REFRACTIVE INDEX

4358 Å., 31–32°

X^-	$\frac{dn}{d\text{mDTAX}}_{0.5m \text{ NaX, kg./mole}}$	$\frac{dn}{d\text{cDTAX}}_{0.5m \text{ NaX, l./mole}}$
F^-	0.0356	0.0362
CHO_2^-	.0370	.0380
NO_3^-	.0375	.0386
ClO_2^-	.0372	.0386
Cl^-	.0394	.0403
BrO_3^-	.0432	.0446
SCN^-	.0447	.0463
IO_3^-	.0516	.0529

TABLE III

AGGREGATION NUMBERS FOR DTAB IN 0.500 *m* NaX

X^-	C.m.c. (moles/l.)	Model I		Models II, III	
		m^a	p/m^b	m	p/m
IO_3^-	0.0051	62	0.18	38	0.24
CHO_2^-	.0060	34	^e	45	^c
BrO_3^-	.0033	63	0.20	58	0.21
F^-	.0084	38	.26	59	.21
Cl^-	.0038	51	.22	62	.20
NO_3^-	.0008	61	^c	79	^c
Br^-	.0019	84	0.17	84	0.17
ClO_3^-	^e	80 ^f	^d	1.0×10^{1f}	^d
SCN^-	^e	$1.0 \times 10^{4f,g}$	^d	$8.7 \times 10^{3f,g}$	^d
I ⁻				Precipitation	
ClO_4^-				Precipitation	

^a m is the number of dodecyltrimethylammonium ions per micelle, *i.e.*, the aggregation number. ^b p is the effective micellar charge. ^c Linearity of the R_{90} vs. surfactant concentration plot precluded an estimation of p . ^d Upward curvature of the R_{90} vs. surfactant concentration plot prevented an estimation of p . ^e Curvature of the R_{90} vs. surfactant concentration plot at the lowest concentrations precluded an accurate determination of the c.m.c. ^f Value obtained from the linear portion of the R_{90} vs. surfactant concentration plot. ^g Value not corrected for dissymmetry.

Micellar charges could not be estimated in several cases because scattering curves were either linear or concave upward. If one takes the scattering equations^{13,14,18} at face value, the first situation implies that the micelles have zero charge and the second implies that they have a complex charge. Polydispersity is a more realistic possibility.

Solutions of DTAB in 0.500 *m* NaSCN were visibly turbid and probably showed dissymmetry. Since scattering at angles other than 90° is not measurable in our photometer, a dissymmetry correction could not be applied to any of the aggregation numbers for this system. The values given in Table III are probably low.

It was not possible to dissolve enough solid DTAB in either 0.5 *m* NaI or 0.5 *m* NaClO₄ to obtain solutions in the surfactant concentration range required for light scattering work. If an aqueous solution of DTAB

(16) D. Stigter, *J. Phys. Chem.*, **64**, 842 (1960).

(17) A. Vrij and J. Th. G. Overbeek, *J. Colloid Sci.*, **17**, 570 (1962).

(18) E. W. Anacker, *J. Phys. Chem.*, **62**, 41 (1958).

were mixed with either 0.5 *m* NaI or 0.5 *m* NaClO₄, a precipitate formed immediately. The "aggregating powers" of I⁻ and ClO₄⁻ are obviously much greater than those of the other counterions examined.

The order in Table III is such that aggregation numbers increase from top to bottom (models II and III). The effectiveness of a counterion in promoting aggregation seems to correspond roughly to its position in the lyotropic series of anions. According to the quantitative characterization of Bruins,¹⁹ the lyotropic series for anions is: F⁻, IO₃⁻, BrO₃⁻, Cl⁻, ClO₃⁻, Br⁻, NO₃⁻, ClO₄⁻, I⁻, SCN⁻. The formate ion does not appear in Bruin's list. As is well known, the lyotropic series denotes the relative order of influence exerted by ions on various phenomena. Exceptions often occur and the order for any one phenomenon may change with concentration.

If the order in Table III had been based on decreasing c.m.c., the tabulation of counterions would have read: F⁻, CHO₂⁻, IO₃⁻, Cl⁻, BrO₃⁻, Br⁻, NO₃⁻. This order differs from the one based on increasing aggregation numbers, but it is still in fair agreement with the lyotropic series listing of Bruins. Critical micelle concentrations were obtained by a least squares procedure similar to one described previously.⁸ In this work, a point was weighted by the corresponding micellar concentration. Marked curvature at the lowest surfactant concentrations in the scattering plots precluded anything but the roughest estimations of c.m.c.'s for the runs involving NaClO₃ and NaSCN.

Although the number of different counterions examined in each case was small, the results of other investigations^{2-6,20} involving ionic surfactants—anionic as well as cationic—are consistent with the observation that counterion effects follow lyotropic series. Several studies²¹⁻²³ have revealed that nonionic surfactants are not immune to ion effects. Thus, there is a decrease in c.m.c. and an accompanying increase in aggregation number of nonylphenol +50 ethylene oxide as the lyotropic number of either cation or anion of the added electrolyte is decreased.²²

There is no simple explanation of lyotropic series. Correlations between the position of an ion in a series and its heat of hydration,²⁴ size,²⁵ and standard free energy of formation²⁶ have been made. Because of instances of inapplicability,²⁷ or because of exceptions,^{28,29} none of these properties alone can serve as the basis of a general theory. Undoubtedly, the interplay of a number of factors is responsible for lyotropic effects.

In the case of surfactants in aqueous media, the ex-

tent of a counterion's interaction with water is probably an important factor in determining its relative aggregating power. If no hydration occurred and size were the only consideration, one would expect that the smaller the counterion, the stronger its attachment to the micelle and the greater its aggregating power. Thus, if hydration were not involved, dodecyltrimethylammonium micelles should increase in size as the counterion changes in the order: I⁻, Br⁻, Cl⁻, F⁻. The opposite was found to be true. It seems significant that the heats of hydration increase in the order: I⁻, Br⁻, Cl⁻, F⁻.³² Aggregation numbers increase as the counterion changes from IO₃⁻ to BrO₃⁻ to ClO₃⁻ in DTAX. Although the order of this sequence might be explained solely on the basis of counterion size, hydration is not ruled out as a contributing factor. According to Rice,³³ IO₃⁻ probably becomes I(OH)₆⁻ in solution, whereas BrO₃⁻ and ClO₃⁻ take on no more than one molecule of H₂O. Hence, both counterion size and degree of hydration change in directions consistent with the observed trend in aggregation number.

Other investigators have suggested that ion effects in surfactant solutions are influenced by hydration. In discussing the effect of altering counterions upon the formations of micelles by lauryl sulfates, Mysels⁶ stated that the observed changes indicated that hydrated ions are less closely attached to the aggregates than unhydrated ones and therefore contribute less to their formation. Schick, *et al.*,²² attributed the decrease in c.m.c. and increase in aggregation number of nonylphenol +50 ethylene oxide on decreasing the lyotropic number of either cations or anions of the added electrolytes to reduced ion hydration. This explanation of Schick, *et al.*, cannot be wholly correct since a decrease in the lyotropic number of an anion is generally regarded as being accompanied by an increase in hydration—not a decrease.

If one assumes a monotonic variation of the heat of hydration with lyotropic number,³⁴ then one upon noticing the differences existing between the order in Table III and the lyotropic series for anions can justifiably suspect that other factors besides hydration are important in determining an ion's aggregating power. The nature of the micelle-forming species must be one of them. As has already been stated, Schick, *et al.*, found that in the case of nonylphenol +50 ethylene oxide a decrease in the lyotropic number of the anion of the added electrolyte caused an increase in the aggregation number. With DTAX micelles, we found the opposite behavior—a decrease in the lyotropic number of the anion generally brought about a decrease in the aggregation number.

Mysels⁶ sees in nonelectrostatic interactions between hydrophobic surfaces of aggregates and ions yet another factor to be considered in a full explanation of the counterion's role in micelle formation. Probably there are more.

Acknowledgments.—Sincere appreciation is expressed to the Research Corporation of New York for financial

(19) E. M. Bruins, *Proc. Acad. Amsterdam*, **35**, 107 (1932).
 (20) E. W. Anacker, Thesis, Cornell University, 1949.
 (21) L. Hsiao, H. N. Dunning, and P. B. Lorenz, *J. Phys. Chem.*, **60**, 657 (1956).
 (22) M. J. Schick, S. M. Atlas, and F. R. Eirich, *ibid.*, **66**, 1326 (1962).
 (23) P. Becher, *J. Colloid Sci.*, **17**, 325 (1962).
 (24) A. Voet, *Trans. Faraday Soc.*, **32**, 1301 (1936).
 (25) W. Pauli and E. Valko, "Kolloidchemie der Eiweisskörper," 2nd Ed., Theodor Steinkopff, Leipzig, 1933, p. 120.
 (26) L. H. N. Cooper, *Nature*, **139**, 284 (1937).
 (27) Lyotropic effects occur in the absence of water.^{30,31}
 (28) For the halide ions, lyotropic numbers increase with size. For the chlorate, bromate, and iodate ions, lyotropic numbers decrease with size.
 (29) A comparison of the tabulations of Cooper²⁶ and Bruins¹⁹ reveals a number of reversals in order.
 (30) A. Voet, *Chem. Rev.*, **20**, 169 (1937).
 (31) J. W. McBain, "Colloid Science," D. C. Heath and Co., Boston, Mass., 1950, p. 132.

(32) R. M. Noyes, *J. Am. Chem. Soc.*, **84**, 513 (1962).
 (33) O. K. Rice, "Electronic Structure and Chemical Binding," McGraw-Hill Book Co., New York, N. Y., 1940, p. 440.
 (34) Although Voet³⁰ assumed a linear relationship, the type of dependence has in no way been established. Data are available for the hydration of only four univalent anions.³²

assistance. This research was supported in part by a grant from The Petroleum Research Fund administered

by the American Chemical Society. Grateful acknowledgment is hereby made to the donors of said fund.

ELECTROPHORESIS OF GLUTAMATE-TARTRATE MIXTURES IN ACETATE BUFFERS¹

BY LAWRENCE B. FRIEDMAN² AND JAMES C. NICHOL

Department of Chemistry, University of Minnesota, Duluth 12, Minnesota

Received April 3, 1963

In this paper, results of a moving boundary study on glutamate-tartrate mixtures in acetate buffers are presented. In contrast to previous experiments with an aspartate-glutamate-acetate system, it is found that the limiting value of the apparent refractometric per cent of tartrate, at zero ratio of the sum of glutamate and tartrate constituent concentrations to the concentration of buffer, is pH dependent in the pH range 4.4 to about 7.6. The limiting apparent refractometric per cent of tartrate, calculated for the descending case, ranges from 46.1 at pH 4.4 to 48.3 at pH 7.6. The limiting true refractometric per cent of tartrate, calculated from the known compositions of the original solutions and the molar refractions of the species therein, varies from 51.81 at pH 4.4 to 52.18 at pH 7.6.

Previously, Nichol, Dismukes, and Alberty³ have studied the moving boundary behavior of equimolar aspartate-glutamate mixtures in acetate buffers. In particular, they have observed that for the pH range 4.4 to about 7.6, the apparent refractometric per cent of aspartate, in the limit of zero ratio of total aspartate and glutamate to buffer, has the same value, 47.6, regardless of the pH of the solution. This value differs slightly from the true values obtained from the known compositions of the original solutions and the molar refractions of the species present therein. The true values vary from 48.58 at pH 4.4 to 47.75 at pH 7.6.

If the coincidence of limiting values were characteristic of weak electrolyte systems in general, it would suggest a regularity in behavior which might provide a clue to the development of extrapolation functions in series form, analogous to those available for strong electrolytes.⁴ At the very least, it would solve the problem of predicting the limiting values for such mixtures of weak electrolytes as could be converted entirely to mixtures of strong electrolytes by a pH adjustment (to about 7.6 in the above case), since the strong electrolyte equations are quite easy to manipulate. Obviously, it would be unwise to draw a conclusion regarding the coincidence of limiting values in general from a single set of experiments, particularly since the deviation of apparent from true limiting values for the system concerned is so slight in the strong electrolyte case. This last fact suggests that the combination of equivalent refractions and mobilities for the aspartate-glutamate system might be such as to minimize variations in the apparent limiting values with pH. Therefore it was considered worthwhile to devise a new system, experimentally realizable, in which true and apparent limiting refractometric fractions of the protein-analogous components would differ appreciably. Although molar refraction, mobility, and dissociation

constant values could have been "invented" to create a hypothetical system with the desired properties, it was felt that the calculations would be much more convincing if backed up by experimental data. Otherwise, the objection could be raised that the invented values might represent an unrealizable experiment. This paper describes experiments and calculations with a system involving tartrate and glutamate constituents in acetate buffer and demonstrates that the limiting value of the apparent refractometric fraction can vary with pH. In this system there is a greater range of mobilities and molar refractions for the protein-analogous constituents than in the acetate-aspartate-glutamate case. Furthermore, the present system is more complex than those previously studied because of the presence of divalent ions (tartrate) in the pH range to be covered.

Theory

The descending and ascending moving boundary systems are illustrated in Fig. 1. In order to predict the apparent refractometric fractions of tartrate and glutamate, the compositions of all phases present, along with values for the mobilities of all ions, the apparent dissociation constants of all weak acids, and the molar refractions of all acids and salts, are required. Since it was found necessary to derive special equations for the calculation of the compositions, they are discussed here. Derivations were carried out for the descending system only because the question of the pH dependence of the apparent analysis was clearly answered using the descending equations, and the additional time and effort required for the ascending calculations did not seem justified. The determination of the dissociation constants, molar refractions, and mobilities is described in the Experimental section.

Compositions of the End Phases.—The composition of the δ solution (buffer) in terms of NaA and HA (see Fig. 1 for symbols) is obtained readily from a knowledge of the number of moles of HR and NaOH used to make up the solution. If the α phase is made up of A moles of HA, B moles of HG, C moles of H₂T, and D moles of NaOH per liter, the concentrations will be given by

$$C_{HA} = A - a, C_{NaA} = C_A = a, C_{HG} = B - b, \\ C_{NaG} = C_G = b, C_{HT} = C - c, C_{NaHT} =$$

(1) (a) This work was supported by P.H.S. Research Grant No. A-2240 from the Division of Arthritis and Metabolic Diseases, Public Health Service, and by Grant No. G16272 from the National Science Foundation. (b) Presented at the 142nd National Meeting of the American Chemical Society, Atlantic City, N. J., September, 1962.

(2) Gibbs Chemical Laboratory, Harvard University, Cambridge, Massachusetts. National Science Foundation Undergraduate Research Participant, 1960-1961.

(3) J. C. Nichol, E. B. Dismukes, and R. A. Alberty, *J. Am. Chem. Soc.*, **80**, 2610 (1958).

(4) J. C. Nichol and L. J. Gosting, *ibid.*, **80**, 2801 (1958).

$$C_{HT} = c - c^1, C_{Na_2T} = C_T = c^1, \text{ and } D = a + b + c + c^1 \quad (1)$$

where a , b , c , and c^1 are the quantities of HA, HG, H₂T, and HT⁻, in moles per liter, reacting with NaOH. For a given solution, the equilibrium relationships, in terms of the apparent dissociation constants, K , may be written

$$\begin{aligned} K_{HA} \frac{(A - a)}{a} &= K_{HG} \frac{(B - b)}{b} = \\ &= \frac{K_{H_2T}(C - c)}{c} = \frac{K_{HT}(C - c^1)}{c^1} \quad (2) \end{aligned}$$

where K_{H_2T} and K_{HT} are the first and second dissociation constants for tartaric acid. If it is assumed that the ratios of the apparent dissociation constants are invariant for all the mixtures involved, the above equations can be combined, and a , c , and c^1 eliminated, to yield the relationship

$$Lb^5 + Mb^4 + Nb^3 + Pb^2 + Qb + R = 0 \quad (3)$$

which will be valid for all experiments with this system. Here, the constants L , M , N , P , Q , and R are simple combinations of the ratios of the equilibrium constants and the known total concentrations. Equation 3 may be solved by Newton's method, and the remaining desired concentrations determined with the aid of the relationships used to eliminate a , c , and c^1 in the course of the derivation of eq. 3.

Composition of the Intermediate Phases.—To obtain the composition of the descending β -phase use is made of (a) the known α -phase composition and the relative ion mobilities, r , (b) the electroneutrality condition in the β -phase, (c) the four moving boundary equations involving concentration changes of the sodium ion and acetate, glutamate, and tartrate constituents across the α, β -boundary, and (d) the mass action relationship

$$C_{HG}^\beta = \frac{K_{HA}}{K_{HG}} \frac{C_G^\beta}{C_A^\beta} C_{HA}^\beta \quad (4)$$

Three equations in C_A^β , C_{HA}^β , and C_G^β are obtained. From these C_{HA}^β can be eliminated and an equation of the form

$$U\psi^4 + V\psi^3 + W\psi^2 + X\psi + Y = 0 \quad (5)$$

derived, where $\psi = C_G^\beta/C_A^\beta$. Equation 5 may be solved by Newton's method, and all the required concentrations obtained readily with the aid of the relationships used to eliminate them in the course of the derivation of eq. 5.

The composition of the γ -phase may now be calculated from the statement of conservation of the weak acid

$$C_{HA}^\gamma = C_{HA}^\beta + C_{HG}^\beta \quad (6)$$

and from the Kohlrausch regulating function for monovalent weak acids⁵

$$\begin{aligned} C_A^\gamma \left(\frac{1}{r_A} - \frac{1}{r_{Na}} \right) &= C_A^\beta \left(\frac{1}{r_A} - \frac{1}{r_{Na}} \right) + \frac{C_{HA}^\beta}{r_A} + \\ C_G^\beta \left(\frac{1}{r_G} - \frac{1}{r_{Na}} \right) &+ \frac{C_{HG}^\beta}{r_G} - \frac{C_{HA}^\gamma}{r_A} \quad (7) \end{aligned}$$

(5) E. B. Dismukes and R. A. Alberty, *J. Am. Chem. Soc.*, **76**, 191 (1954).

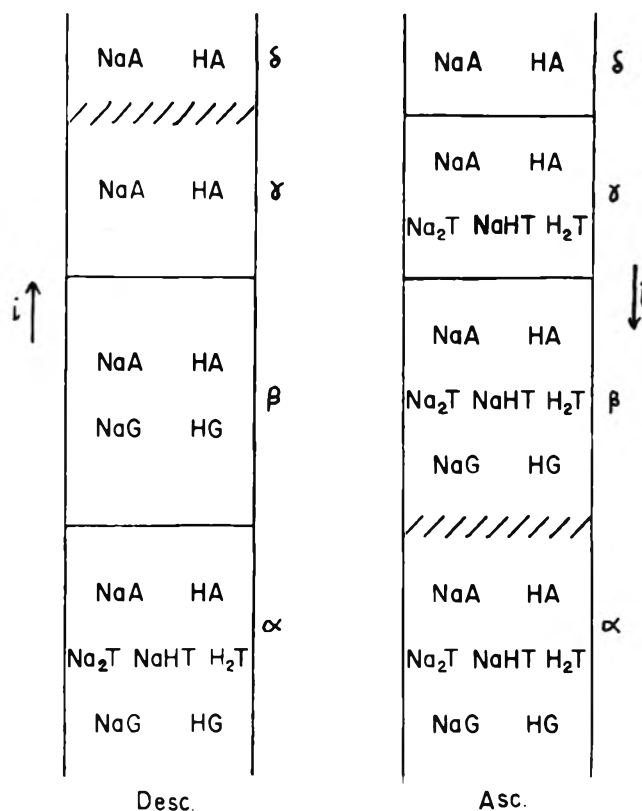


Fig. 1.—Diagram representing the electrophoresis of tartrate and glutamate constituents, T and G, in sodium acetate-acetic acid buffer, NaA-HA. The arrow indicates the direction of positive current, and // // // // represents the boundary near the initial boundary position.

Apparent Refractometric Fractions of Tartrate and Glutamate.—The value for tartrate, $F_{T(desc)}$, is calculated from

$$F_{T(desc)} = \frac{\sum C_j^\alpha k_j - \sum C_j^\beta k_j}{\sum C_j^\alpha k_j - \sum C_j^\gamma k_j} \quad (8)$$

where k_j = molar refraction of substance j , and j may be a weak acid or its sodium salt. Obviously, $F_{G(desc)} = 1 - F_{T(desc)}$.

Experimental

Moving boundary experiments were performed in a Spinco Model H electrophoresis apparatus at 1.00°. An 11-ml. quartz Tiselius cell with reference paths was used, and schlieren and interference fringe photographs were taken simultaneously using Kodak metallographic plates. Fringe displacements and mobilities were determined using a Gaertner Model M2001P comparator as described previously.³ Conductances were measured at 0° using a Jones conductance bridge and a cell of the Jones and Bollinger type.

A number of moving boundary systems were tested experimentally and the acetate-tartrate-glutamate system was found to be most satisfactory with respect to the formation of stable moving boundaries.

Apparent ionization constants for acetic and glutamic acids were available from previous work.³ The constants for tartaric acid, determined at 1.00° and 0.1 ionic strength by Schwarzenbach's method,⁶ were found to be $K_{H_2T} = 8.0 \times 10^{-4}$ and $K_{HT} = 6.3 \times 10^{-5}$.

Of the molar refractions required, those of acetic acid, sodium acetate, glutamic acid, and sodium glutamate had been determined previously.⁵ The values for disodium tartrate and for tartaric acid were determined from interference fringe measurements on the pure solutions (see ref. 5 for the method of calculation used for tartaric acid), and were found to be $k_{Na_2T} = 0.03523$ and $k_{HT} = 0.01948$ l. mole⁻¹, respectively. To determine the

(6) G. Schwarzenbach, A. Willi, and R. O. Bach, *Helv. Chim. Acta*, **30**, 1317 (1947).

TABLE I
 APPARENT REFRACTOMETRIC ANALYSIS OF EQUIMOLAR MIXTURES OF TARTARIC AND GLUTAMIC ACIDS

Expt.	C_A/C_B	δ -Soln.		α -Soln.			Refractometric % tartrate			
		C_{NaOH}	C_{HA}	C_{NaOH}	C_{HA}	$C_{HG} + C_{HT}$	(Exptl.)	(Theor.)	(Exptl.)	(Theor.)
1	0.2	0.1000	0.1000	0.1300	0.1000	0.0200	46.8	46.29	53.4	52.65
2	.4	.1000	.1000	.1600	.1000	.0400	46.4	44.76	56.5	55.91
3	.6	.1000	.1000	.1900	.1000	.0600	..	43.53	58.5	58.54
4	.2	.1000	.2000	.1000	.2000	.0200	44.2	44.20	52.3	...
5	.4	.1000	.2000	.1000	.2000	.0400	41.4	40.83	56.7	...
6	.6	.1000	.2000	.1000	.2000	.0600	37.5	36.70	59.6	...
7	.2	.1000	.3000	.1000	.3000	.0200	43.7	43.45	50.7	...
8	.4	.1000	.3000	.1000	.3000	.0400	41.2	40.70	53.4	...
9	.6	.1000	.3000	.1000	.3000	.0600	38.5	37.80	55.2	...

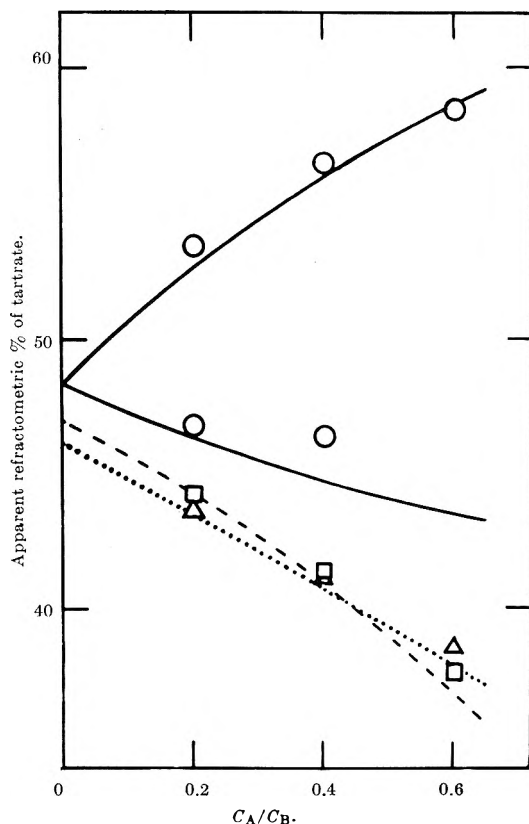


Fig. 2.—Plot of apparent refractometric per cent of tartrate vs. C_A/C_B , the ratio of the sum of tartrate and glutamate constituent concentrations to the concentration of buffer salt. The curves represent predicted values and the symbols represent experimental points. The top curve is ascending, the others descending; —, \circ , the acetic acid/acetate ratio in the buffer is zero; ---, \square , the ratio is 1:1;, Δ , the ratio is 2:1.

molar refraction of sodium hydrogen tartrate, fringe displacements, Δn , were determined for partly neutralized solutions of tartaric acid, and the equation

$$\Delta n = k_{Na_2T}C_{Na_2T} + k_{NaHT}C_{NaHT} + k_{H_2T}C_{H_2T} \quad (9)$$

was solved for the unknown, k_{NaHT} , which was found to be $0.02699 \text{ l. mole}^{-1}$. The concentrations C_T , C_{HT} , and C_{H_2T} were calculated with the aid of the dissociation constants as described above for the solutions used in the moving boundary experiments.

Relative mobilities for sodium, glutamate, and acetate ions were available from previous work.⁴ The relative mobility for divalent tartrate ion, determined using the moving boundary system $Na_2T(\alpha) \leftarrow NaA(\beta) : NaA(\gamma)$ with $Na_2T(\alpha)$ at 0.1 ionic strength, was found to be -22.3 , on the basis of the value of 22.2 assigned to sodium ion. To obtain the relative mobility of hydrogen tartrate ion, experiments were run on the system Na_2T , $NaHT(\alpha) \leftarrow NaA(\beta) : NaA(\gamma)$, with the α -solution at 0.1 ionic strength. The constituent mobility of tartrate, \bar{r}_T^α , was then determined from $\bar{r}_T^\alpha = \nu^{\alpha\beta}\sigma^\alpha$, where $\nu^{\alpha\beta}$ is the boundary displacement in ml. coulomb⁻¹ and σ^α is the relative conductance. Finally, r_{HT} was calculated to be -11.0 using the defining relationship for the constituent mobility of tartrate

$$\bar{r}_T^\alpha = \frac{r_T C_T^\alpha + r_{HT} C_{HT}^\alpha}{C_T^\alpha + C_{HT}^\alpha + C_{H_2T}^\alpha} \quad (10)$$

in which all quantities are known except r_{HT} .

Results

In Table I are presented the compositions of the end solutions and the corresponding observed and predicted values of the apparent refractometric per cent of aspartate for a series of nine moving boundary experiments. To facilitate comparison with Fig. 2, the values of C_A/C_B , the ratio of the sum of tartrate and glutamate constituent concentrations to the concentration of buffer salt, are listed in the second column of Table I. Experiments 1–3 represent the strong electrolyte case, and the theoretical values therefore have been calculated using the equations of Dole.⁷ The slow descending boundary in experiment 3 convected, and therefore no refractometric per cent analysis is given. It is possible that the rather poor agreement between the experimental and theoretical values of experiment 2 is caused by an incipient instability. Experiments 4–9 involve weak electrolyte systems of steadily decreasing pH for the α -solutions. Since equations were derived only for the descending system, no theoretical ascending values are listed.

In order to give a clearer picture of the variation in analysis with concentration and pH, the apparent refractometric per cent of tartrate is plotted against C_A/C_B in Fig. 2. The ascending experimental values for experiments 4–9 are omitted to avoid cluttering the figure (see Table I). If they are plotted, it will be observed that reasonable extrapolations of the two curves can be made to the corresponding limiting descending values. However, no definite conclusion can be drawn in the absence of calculations at low C_A/C_B values. The limiting value at $C_A/C_B = 0$ for the strong electrolyte case (solid lines) was obtained using the extrapolation functions derived by Nichol and Gosting.⁴ The weak electrolyte curves (dashed and dotted lines) were simply extended graphically to $C_A/C_B = 0$ from the theoretical values calculated using the closed form equations discussed above in the theory section. Theoretical points were calculated down to C_A/C_B ratios of 0.02, so that precise extrapolations were possible. In Table II these apparent limiting refractometric per cents of aspartate are compared with the true values, calculated from the known molar refractions and concentrations of the various constituents in the original solution.

(7) V. P. Dole, *J. Am. Chem. Soc.*, **67**, 1119 (1945).

TABLE II
LIMITING VALUES OF THE REFRACTOMETRIC PER CENT OF
TARTRATE

Acetic acid/acetate ion ratio in buffer	-----Refractometric %-----	
	Apparent	True
0	48.3	52.18
1	47.0	52.05
2	46.1	51.81

Discussion

The most significant conclusion to be drawn is that the limiting apparent values, calculated and experimental, are pH dependent. Therefore it appears that the coincidence observed for the aspartate-glutamate-acetate system is simply a result of the particular combination of mobilities and molar refractions for this system. It is also important to note that the calculated limiting apparent values, as well as those obtained by extrapolation of the experimental points of Fig. 2, are distinctly different from the true ones, which cluster around 52% (Table II). An appreciable error in the analysis of the protein-analogous components would be made by using the experimental data to extrapolate to zero "protein" concentration, especially at low pH.

The agreement between the experimental and calculated apparent refractometric fractions is good, particularly for the weak electrolyte experiments (4-9),

considering the numerous assumptions made in the course of the derivations, and provides a satisfactory test of weak electrolyte moving boundary theory for a more complex system than those previously studied.³ In this regard, the assumption of constant relative mobilities might seem open to question for ions of increasing charge and complexity. Indeed, tartrate mobilities calculated from some of the boundary velocities in the present research are several per cent lower than would be expected if the relative mobilities were to remain constant. To determine the effect of relative mobility changes on the theoretical predictions, calculations were carried out for the strong electrolyte case using a value for the relative mobility of tartrate about 8% below the one given in the Experimental section. The concentrations of new phases and the refractometric per cent of tartrate were not greatly affected, deviations of from 0 to 1%, and of about 2%, respectively, from the original values being obtained.

Finally, it is of interest that the crossing over of the theoretical curves in Fig. 2 at a C_A/C_B ratio of about 0.4 is confirmed by the positions of the experimental points.

Acknowledgment.—The authors are indebted to Mr. Robert Fulton for assistance with the numerical computations.

NOTES

PURE QUADRUPOLE RESONANCE OF CHLORINE (Cl^{35}) IN POTASSIUM TETRACHLOROPLATINATE (II)

By E. P. MARRAM, E. J. McNIFF,

Arthur D. Little, Inc., Cambridge 40, Massachusetts

AND J. L. RAGLE

Northrop Space Laboratories, Hawthorne, California

Received February 7, 1963

Pure quadrupole resonance studies of halogens in potassium hexahaloplatinates(IV) and tetrahaloplatinates(II) have been reported by Nakamura and co-workers.^{1,2} Attempts by these workers to obtain the Cl^{35} resonance in potassium tetrachloroplatinate(II) were not successful, presumably due to inadequate spectrometer sensitivity.² Since we had previously observed the Cl^{35} resonance in polycrystalline specimens of this compound, we report the results here to complete the data of Nakamura.

Table I gives quadrupole coupling constants for Cl^{35} , calculated on the assumption that the asymmetry parameter is zero. Spectra were obtained with a conventional Zeeman-modulated superregenerative spectrometer using lock-in detection.

The corresponding covalent character $(1 - i)$ calculated from Townes and Dailey's relation³

$$eQq = (1 - i)(1 - s^2)(eQq)_{atm}$$

(1) D. Nakamura, Y. Kurita, K. Ito, and M. Kubo, *J. Am. Chem. Soc.*, **82**, 5783 (1960).

(2) K. Ito, D. Nakamura, Y. Kurita, and M. Kubo, *ibid.*, **83**, 4526 (1961).

(3) C. H. Townes and B. P. Dailey, *J. Chem. Phys.*, **17**, 782 (1949).

TABLE I
QUADRUPOLE COUPLING CONSTANTS OF Cl^{35} IN POTASSIUM
TETRACHLOROPLATINATE(II)

Temp., °C.	eQq , Mc./sec.
-196 (liquid N_2)	36.26
-79 (CO_2 + toluene)	36.14
0	35.85

is 0.39. Here $(eQq)_{atm}$ denotes the atomic quadrupole coupling constant, i is the amount of ionic character in a Pt-Cl bond, and s^2 is the amount of s-hybridization in the orbital used by the chlorine in bonding with the platinum. Following Dailey and Townes,⁴ s^2 is assumed to be 15%. The net charge ρ on the platinum ion is calculated to be

$$\rho = 2 - 4(1 - i) = 0.44$$

These values are consistent with those calculated by Nakamura and co-workers for the other haloplatinate.²

(4) B. P. Dailey and C. H. Townes, *ibid.*, **23**, 118 (1955).

LIMITING CONDUCTANCE OF THE RUBIDIUM ION

By ROBERT W. KUNZE, RAYMOND M. FUOSS, AND
BENTON B. OWEN

Contribution No. 1750 from the Sterling Chemistry Laboratory,
Yale University, New Haven, Connecticut

Received February 14, 1963

The purpose of this note is to present a corrected value of the limiting conductance of the rubidium ion in water at 25°. In 1952, the value of 77.81 was re-

ported.^{1,2} More recently, the value of 77.25 was reported,³ based on $\Lambda_0(\text{RbBr}) = 155.42$ obtained from Λ - c data by extrapolation by means of the Fuoss-Onsager equation (unassociated equation, J_2 -term retained) and Owen's value¹ of 78.17 for the bromide ion. Kunze⁴ found for rubidium chloride $\Lambda_0 = 153.57$. Using Lind's value⁵ $\Lambda_0(\text{KCl}) = 149.89$ and Longworth's transference number⁶ $n_0(\text{K}^+) = 0.4906$ in potassium chloride, we have $\lambda_0(\text{Cl}^-) = 76.35$. Kunze's value of $\lambda_0(\text{Rb}^+)$ is therefore 77.22, which is in excellent agreement with Lind's.

The discrepancy between the more recent values and that of Voisinet is beyond the probable experimental error of the determinations, and called for explanation. Fortunately a sample of the rubidium chloride used by Voisinet was still available in this Laboratory. It was analyzed for alkali metals by the Beckmann flame photometer, using standards prepared by adding known impurities to Kunze's rubidium chloride. Voisinet's rubidium chloride was found to contain 1.25% potassium chloride, 0.15% cesium chloride, 0.07% sodium chloride, and 0.02% lithium chloride. These lead to a correction $\Delta\Lambda_0 = -1.14$. Extrapolation of Voisinet's data by the Fuoss-Onsager equation (unassociated program, J_2 -term retained) gave $\Lambda_0 = 154.53$, whence $\Lambda_0(\text{corr.}) = 153.39$. Using $\lambda_0(\text{Cl}^-) = 76.35$, the corrected value from Voisinet's data is $\lambda_0(\text{Rb}^+) = 77.04$. The unweighted average of Lind's, Kunze's, and Voisinet's Λ - c data for rubidium chloride, all extrapolated by the same method to zero concentration, and all corrected for their known alkali impurities is 77.17. We therefore recommend the value $\lambda_0(\text{Rb}^+) = 77.20 \pm 0.05$.

- (1) B. B. Owen, *J. chim. phys.*, **49**, C-72 (1952).
- (2) W. E. Voisinet, Dissertation, Yale University, 1951.
- (3) J. E. Lind, Jr., and R. M. Fuoss, *J. Phys. Chem.*, **66**, 1727 (1962).
- (4) R. W. Kunze and R. M. Fuoss, *ibid.*, **67**, 914 (1963).
- (5) J. E. Lind, Jr., and R. M. Fuoss, *ibid.*, **65**, 999 (1961).
- (6) L. G. Longworth, *J. Am. Chem. Soc.*, **54**, 2741 (1932).

REFLECTION CORRECTIONS FOR LIGHT-SCATTERING MEASUREMENTS FOR VARIOUS CELLS WITH THE BRICE-TYPE PHOTOMETER

BY Y. TOMIMATSU AND K. J. PALMER

Western Regional Research Laboratory,¹
Albany 10, California

Received February 12, 1968

Absolute calibration of the Brice-type light-scattering photometer² involves, among other factors, consideration of suitable corrections for reflection effects.^{2,3} Calibration is generally carried out at $\theta = -90^\circ$ using square or semioctagonal cells. In subsequent measurements in cells of different shapes or at angles other than -90° , the reflection effects may not be the same, thus scattering measurements made under these conditions must be corrected so that application of the instrumental constant established during calibration will give proper turbidity values.

Putzeys and Minet⁴ have shown that for measurements of -90° intensity of non-absorbing solutions in

square cells, the reflection effects are self-compensating. Sheffer and Hyde⁵ and Oth, *et al.*,⁶ have pointed out that for angular or dissymmetry (Z) measurements on asymmetric systems, one must take into consideration the reverse asymmetry of light scattered by the fraction of the primary beam reflected at the exit window. Their treatment, as summarized by Stacey,⁷ is not strictly correct in that attenuation of scattered light by reflection at the air-glass interface in the direction of measurement is neglected.³ In the case of Z measurements in the semioctagonal cells, the effect of (back reflection of scattered light from the $+45$ and $+135^\circ$ directions is assumed to be negligible due to the geometry of the cell; but in the case of angular measurements in cylindrical cells,⁸ the effect of the frosted 0 to $+180^\circ$ inside face of the cell on reflection from the air-glass interface is not known.

In this note we present expressions for Rayleigh's ratio R_θ , for the various cells, in terms of the calibration factor for -90° scattering from square cells, which permit facile evaluation of the reflection effects for the various cells. We also present measurements of reflection effects which indicate that, for semioctagonal cells, the assumption of no effective back reflection from the $+45$ and $+135^\circ$ directions is valid and that the frosted inside 0 to $+180^\circ$ surface of the cylindrical cell has essentially no effect on reflection of scattered light from the air-glass interface. The latter observation leads to a correction which is twice as large (see eq. 13 below) as reported previously.³

We are concerned primarily with the evaluation of reflection effects on the intensity of scattered light measured in different types of cells. For transmitted intensity the reflection effects will remain the same, even for cylindrical cells, since flat entrance and exit windows are used. The following relationships are for the Brice-type photometer for non-absorbing scattering systems. For scattering from an asymmetric system contained in a clear-glass container, the reflection effects to be considered are (neglecting reflections at the glass-solution interfaces): 1, reflection of the primary beam at the entrance window; 2, reflection of the transmitted primary beam at the exit window with the attendant reverse asymmetry of the scattered light due to this reflected beam; 3, reflection of light scattered in the $180 + \theta$ direction; 4, reflection of scattered light at the air-glass interface in the direction of measurement, θ . Consideration of only the above reflection effects with unpolarized incident light gives (per unit irradiated volume)

$$I_\theta = \left(\frac{1 + \cos^2 \theta}{\sin \theta} \right) \left[\frac{(1-f)I_0 R_\theta}{r^2} + \frac{f(1-f)I_0 R_{180+\theta}}{r^2} + \frac{f(1-f)I_0 R_{180+\theta}}{r^2} \right] (1-f) = \frac{I_0}{r^2} \left(\frac{1 + \cos^2 \theta}{\sin \theta} \right) (1-f)^2 (R_\theta + 2fR_{180+\theta}) \quad (1)$$

where I_θ is the measured scattered intensity at angle θ , f is the fraction of light reflected at an air-glass interface, r is the distance to the detector cathode, and R

- (1) A laboratory of the Western Utilization Research and Development Division, Agricultural Research Service, U. S. Department of Agriculture.
- (2) B. A. Brice, M. Halwer, and R. Speiser, *J. Opt. Soc. Am.*, **40**, 768 (1950).
- (3) Y. Tomimatsu and K. J. Palmer, *J. Polymer Sci.*, **54**, S21 (1961).
- (4) P. Putzeys and J. Minet, *Ann. Soc. Scient. Bruxelles*, **69**, 29 (1955).

- (5) H. Sheffer and J. C. Hyde, *Can. J. Chem.*, **30**, 817 (1952).
- (6) A. Oth, J. Oth, and V. Desereux, *J. Polymer Sci.*, **10**, 551 (1953).
- (7) K. A. Stacey, "Light-Scattering in Physical Chemistry," Academic Press, New York, N. Y., 1956, p. 85.
- (8) L. P. Witnauer and H. J. Scherr, *Rev. Sci. Instr.*, **23**, 99 (1952).

is the fraction of the incident light scattered in the direction indicated by the subscript, *i.e.*, Rayleigh's ratio. The three terms in the brackets correspond to items 1 to 3 listed above, and the $(1 - f)$ term corresponds to item 4.

Upon introducing refractive effects² and the volume viewed by the phototube, $V = W_s L h$, for clear-glass square cells, we obtain for $\theta = -90^\circ$, since $R_{-90} = R_{+90}$

$$I_{-90} = \frac{W_s L h I_0 R_{-90}}{r^2 [1 - (b/r)(n-1)/n]^2 n^2} \quad (2)$$

where b is one-half the width of the square cell and n is the refractive index of the solution.

For transmitted intensity, I_g , in the substitution method,² we have

$$I_g = \frac{I_0 (W_s L) T (1.039) D T_c}{\pi r^2 [1 - (b/r)(n-1)/n]^2} \quad (3)$$

where T is the diffuse transmittance of the solid opal; D is a correction factor, which, when applied to T , makes the solid opal equivalent to a perfect reflecting diffusor; T_c is the transmittance of the filled compensating cell; and 1.039 is a factor which corrects for back reflection³ from the solid opal. Dividing eq. 2 by 3 gives

$$R_{-90} = \frac{T D n^2 (1.039) T_c I_{-90}}{\pi h I_g} \quad (4)$$

and introducing T_s , the transmittance of the filled scattering cell, in the denominator and its numerical equivalent 0.914 in the numerator gives

$$R_{-90} = \frac{n^2 T D}{\pi h (1.049)} \frac{T_c I_{-90}}{T_s I_g} \quad (5)$$

which is the same as the expression for τ in ref. 3 upon substituting $R_{-90} = 3\tau/16\pi$. Thus, we have shown that the general expression for I_θ (eq. 1) when combined with eq. 3 reduces to give the expected expression for τ for $\theta = -90^\circ$ in clear glass square cells. For the working standard method, eq. 5 becomes

$$R_{-90} = \frac{n^2 T D}{\pi h (1.049)} \frac{R_w}{R_c} a \frac{I_{-90}}{I_w} = K \frac{I_{-90}}{I_w} \quad (6)$$

where a is the working standard constant and R_w/R_c is the residual refraction correction. Equations 5 and 6 are left in terms of R_{-90} for convenience in treating angular measurements in terms of R_θ . It is evident that K in eq. 6 is related to K_B , the constant for the equivalent expression for τ , by

$$K = \frac{3K_B}{16\pi} \quad (7)$$

It is further evident that both K and K_B are devoid of any reflection effects in the scattering measurement, since they are self-compensating for the square-cell case, and we may write

$$R_\theta = \frac{K}{(1-f)^2} \frac{\sin \theta}{1 + \cos^2 \theta} \frac{I_\theta}{I_w} - 2f R_{180+\theta} \quad (8)$$

as the general expression for Rayleigh's ratio in terms of the instrumental constant K when all first-order re-

flexion effects are taken into consideration. This K will apply as long as the same geometry is used in the measurements.

Semioctagonal Cells.—For -90° scattering, eq. 6 holds. For dissymmetry measurements, appropriate substitutions into eq. 8, noting the absence of effective reflection of scattered light at the $+45$ and $+135^\circ$ air-glass interface, give

$$Z = \frac{R_{-45}}{R_{-135}} = \frac{(I_{-45}/I_w) - f(I_{-135}/I_w)}{(I_{-135}/I_w) - f(I_{-45}/I_w)} \quad (9)$$

Cylindrical Cells.—For cylindrical cells, eq. 8 holds only if the same geometry is used. Since smaller slits are used with the cylindrical cells, at $\theta = -90^\circ$, eq. 8 becomes

$$R_{-90} = K' \frac{I_{-90}}{I_w} \quad (10)$$

where K' now differs from K . However, an arbitrary calibration is made such that

$$(L_{-90}/I_w)_{\text{sq. cell}} = k (L_{-90}/I_w)_{\text{cy1. cell}} \quad (11)$$

so that $K' = kK$ and

$$R_{-90} = kK (L_{-90}/I_w)_{\text{cy1. cell}} \quad (12)$$

For angular measurements eq. 8 becomes

$$R_\theta = kK \frac{\sin \theta}{1 + \cos^2 \theta} \frac{1}{(1-f)^2 (1-4f^2)} \times \left[\frac{I_\theta}{I_w} - 2f \frac{I_{180+\theta}}{I_w} \right] \quad (13)$$

For dissymmetry measurements in cylindrical cells

$$Z = \frac{R_{-45}}{R_{-135}} = \frac{(I_{-45}/I_w) - 2f(I_{-135}/I_w)}{(I_{-135}/I_w) - 2f(I_{-45}/I_w)} \quad (14)$$

In the above treatment we have neglected second-order effects. Furthermore, in the case of cylindrical cells we have assumed perpendicular incidence of all pertinent light rays. In practice the arbitrary calibration factor k should partially compensate for any deviation from this assumption. All indicated scattering ratios are net scattering ratios, *i.e.*, with solvent scattering subtracted.

Experimental

Reflection effects were evaluated as follows: Preliminary tests indicated that black Mylar film, when placed inside the scattering cell against the surface of interest with the dull surface facing the center of the cell, was the most effective in eliminating the reflection from the air-glass interface. The film could be shaped to fit the curved 0 to 180° surface of the cylindrical cell and, after overnight soaking in water, the film showed no tendency to contaminate a water solution in the short time required to make the measurements. Painting the outside surface with dull black paint gave poor reproducibility and incomplete absorption of light due to reflection at the glass-paint interface. Painting the inside surface also gave poor reproducibility. Fluorescein (1 mg./l.) in 0.1 *M* sodium acetate was used; all measurements were made at $\lambda = 436 \text{ m}\mu$.

Results summarized in Table I show that, for square cells, the expected decrease in -90° intensity occurs when the reflection from the $+90^\circ$ face is removed. For the cylindrical cell a similar decrease is observed at all three angles measured, indicating that the frosted inside 0 to 180° surface has no effect on reflection of scattered light at the air-glass interface. This can be confirmed qualitatively by observing the transmitted beam through the frosted surface of an empty and a filled cell. In the

former case the transmitted beam is effectively diffused but, with water present, the beam remains collimated, though somewhat fuzzy. In the case of the semioctagonal cell, the expected decrease is observed for -90° . The $(I_{-90}/I_w)/(I_0/I_w)(\sin \theta)$ ratios without Mylar film confirm the fact that for geometrical reasons there is no effective reflection of light scattered in the $+45$ and $+135^\circ$ directions in this cell.

TABLE I

REFLECTION EFFECTS FOR VARIOUS SCATTERING CELLS^a

Cell	θ	Ratio ^b
Square, 30 × 30 mm., clear glass	-90°	1.043
Cylindrical, 26 mm. i.d., flat entrance and exit windows, inside 0 to 180° surface frosted	-90°	1.045
	-45°	1.038
	-135°	1.047
Semioctagonal, 40 × 40 mm., clear glass	-90°	1.046
	-45°	1.043 ^c
	-135°	1.048 ^c

^a Black Mylar film, dull surface facing center of cell, placed inside of cell covering $+90^\circ$ face for square and semioctagonal cell and 0 to 180° surface for cylindrical cell. ^b Ratio of scattering ratios without and with Mylar film in place. ^c $(I_{-90}/I_w)/(I_0/I_w)(\sin \theta)$ without Mylar film.

The results summarized in Table I provide experimental verification for the assumptions made in deriving the equations presented to account for reflection effects in square, semioctagonal, and cylindrical cells.

ELECTROLYTE-SOLVENT INTERACTION.

X. DIPOLE SOLVATION

BY ALESSANDRO D'APRANO¹ AND RAYMOND M. FUOSS

Contribution No. 1731 from the Sterling Chemistry Laboratory, Yale University, New Haven, Connecticut

Received February 23, 1963

Solvents of high dielectric constant obviously are composed of polar molecules. When an electrolyte is dissolved in such a solvent, the solvent dipoles in the immediate vicinity of the ions must be oriented by the ionic fields. A choice between two extremes may be made in the model used to describe the system: (1) treat the solvent as a continuum and consider volume polarization or (2) treat solvent molecules which are nearest neighbors to ions as individuals and use the continuum for more distant solvent. We present herewith experiments which show that the second model is more realistic, in that it accounts for a variety of experimental detail which cannot easily be explained on the basis of a continuum.

Consider acetonitrile ($D = 36.0$) as solvent; the molecules are fairly small and have a dipole moment² of 3.51. If we locate the dipole as a point dipole at the nitrogen atom, and estimate distances using Hirschfelder models, the potential energy of an acetonitrile molecule in contact with a bromide ion is 1.5–2.0 times kT . This is almost enough energy to stabilize an aggregate $\text{Br}^- \cdot \text{CH}_3\text{CN}$; let us make the working hypothesis that, due to electrostatic attraction, one acetonitrile molecule on a time average stays with the bromide ion ("solvates" it). Experiments on the two-component system Bu_4NBr in acetonitrile cannot test this hypothesis. But suppose we now add a much stronger dipole, such as *p*-nitroaniline (PNA) whose moment³ is 6.32. We would expect that the PNA would displace

(1) On leave of absence from the University of Palermo. Grateful acknowledgment is made for a Fulbright Travel Grant and for a DuPont Postdoctoral Research Fellowship.

(2) G. L. Lewis and C. P. Smyth, *J. Chem. Phys.*, **7**, 1085 (1939).

(3) C. G. LeFèvre and R. J. W. LeFèvre, *J. Chem. Soc.*, 1130 (1936).

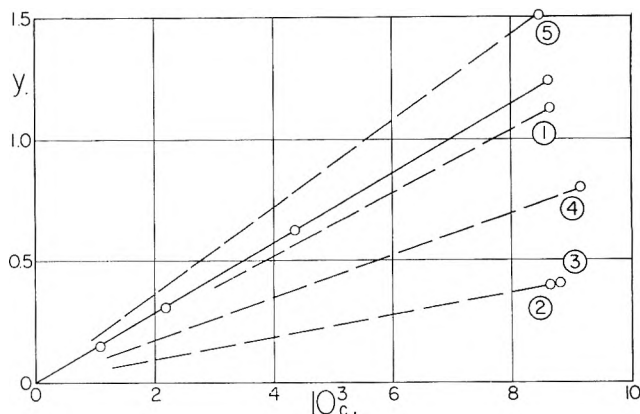


Fig. 1.—Percentage decrease in conductance produced by *p*-nitroaniline. Solid curve, Bu_4NBr at $c = 9.70 \times 10^{-4}$, variable PNA. Numbered points described in text.

the acetonitrile molecules which by hypothesis are solvating the bromide ions, and therefore slow the latter down, because PNA is much more bulky than MeCN. The prediction was therefore made that addition of PNA to a dilute solution of Bu_4NBr in MeCN would decrease the conductance, to an extent proportional to its own concentration. The data of Table I verify the prediction; here c' is the concentration of PNA (moles/l.),

TABLE I
EFFECT OF PNA ON CONDUCTANCE OF Bu_4NBr IN MeCN
 $c(\text{Bu}_4\text{NBr}) = 0.9704 \times 10^{-3}$

$10^3 c'$	Λ_p	$-\Delta\Lambda/\Delta c'$
0.0	150.29	202
1.091	150.07	208
2.208	149.83	216
4.351	149.35	215
8.617	148.44	

Λ_p is $1000\kappa(\text{obsd.})/c$, and $\Delta\Lambda/\Delta c'$ is the chord slope from the origin to the corresponding data point. The total effect (1.25%) is far too large to ascribe to any changes in bulk properties of the solvent caused by addition of PNA: the dielectric constant of a solution of PNA at $c' = 8.813 \times 10^{-3}$ was 35.95 ± 0.05 vs. $D_0 = 36.00$ and the viscosity was 3.448×10^{-3} vs. 3.449×10^{-3} . The specific conductance of this solution was 1.53×10^{-7} ($\kappa_0 = 1.3 \times 10^{-8}$) which was a magnitude smaller than 1% of the specific conductance (1.4584×10^{-4}) of the Bu_4NBr solution. A small correction was made for the density changes; at $c' = 0$ (Table I), $\rho = 0.77695$, and at $c' = 8.617 \times 10^{-3}$, $\rho = 0.77768$.

Further experiments were then made, with the results shown in Fig. 1, where $100(\Lambda - \Lambda_p)/\Lambda$ is plotted against c' . Assume that a displacement occurs



where the corresponding mass action equation is

$$[\text{PNA} \cdot \text{Br}^-]/[\text{MeCN} \cdot \text{Br}^-][\text{PNA}] = K \quad (2)$$

(due to the enormous excess of solvent, its concentration has been absorbed in the constant K). Abbreviate by setting $[\text{PNA} \cdot \text{Br}^-] = x$; then $[\text{MeCN} \cdot \text{Br}^-] = (c - x)$, where c is the stoichiometric concentration of

Bu₄NBr. The equivalent conductances Λ_p of Table I were computed as $10^3\kappa/c$, where κ is the observed specific conductance at a given value of c' , with c fixed at 0.9704×10^{-3} . Letting λ_1, λ_2 , and λ_3 represent the conductances of the ions Bu₄N⁺, MeCN·Br', and PNA·Br', respectively

$$\Lambda_p = \lambda_1 + (1 - x/c)\lambda_2 + x\lambda_3/c \quad (3)$$

$$= \Lambda - (x/c)(\lambda_2 - \lambda_3) \quad (4)$$

$$= \Lambda - \Delta\lambda K[\text{PNA}] \quad (5)$$

where $\Delta\lambda$ is the difference in conductance of bromide ion solvated by acetonitrile and by PNA, and (2) has been substituted in (4) to get (5). Then y , the ordinate in Fig. 1, is given by

$$y = 100K(\Delta\lambda/\Lambda)[\text{PNA}] \quad (6)$$

i.e., linearity in PNA as observed. Point 1 of Fig. 1 corresponds to $c = 1.156 \times 10^{-4}$ Bu₄NBr; at $c' = 8.63 \times 10^{-3}$, $\Lambda = 156.56$. The value of y is a little smaller than at $c = 9.70 \times 10^{-4}$; over half of this difference is due to the larger Λ at the lower concentration of salt. As eq. 6 predicts, y is primarily determined by the concentration of PNA, independent of salt concentration, because the ratio x/c appears in (2) and (4).

If the model is correct, larger ions should show a smaller effect. Point 2 shows the effect of PNA at $c' = 8.65 \times 10^{-3}$ on Bu₄N·BPh₄ at $c = 1.018 \times 10^{-3}$. The total effect is only 0.4%; if we split it equally between the two ions (which are nearly the same size), then the effect on bromide ion is 1.0%, or five times as great. Point 3 corresponds to tetrabutylammonium picrate, $c = 10.13 \times 10^{-4}$ and $c' = 8.82 \times 10^{-3}$; again, with both ions large, the decrease in conductance is small.

On the other hand, if we go to the bromide of a smaller cation, the total effect should increase. Point 4 for PNA at $c' = 9.15 \times 10^{-3}$ and Me₄NBr at $c = 9.87 \times 10^{-4}$ at first glance appears to contradict the whole argument. But in acetonitrile, with $D = 36$, salts with both ions small show some association to pairs: for example,⁴ for Me₄N·NO₃ in acetonitrile, the association constant K_A is 23. At $c = 10^{-3}$, if we assume about the same association constant for Me₄NBr, the conductance would have about 2.5% ion pairs. Addition of PNA, by association with bromide ions, would by mass action increase the dissociation of ion pairs, increasing the conductance and opposing the solvation effect; the net effect would therefore be a smaller decrease in conductance. The final experiment, shown as point 5, was therefore made. It corresponds to $c' = 8.47 \times 10^{-3}$ and Me₄NBr at $c = 1.163 \times 10^{-4}$, about a tenth the concentration of point 4 and where association effects are nearly negligible. Now the effect for Me₄NBr at a given PNA concentration is greater than for Bu₄NBr, as it should be. We therefore believe that our experiments demonstrate that ions and dipoles can associate under the influence of electrostatic forces. Incidentally, these experiments also confirm the triple ion hypothesis⁵ according to which an ion pair, acting as a dipole, can associate with a single ion under the action of mutual Coulomb forces.

A simple calculation shows that the order of magnitude of the observed change in conductance is reason-

able. Consider a solution containing N_1 large cations, Z_1 small anions, Z_2 dipoles stronger than solvent (*e.g.*, PNA in the above example), and Z_3 anion-dipole complexes in a total volume V . Add δZ more dipoles; consider them as point dipoles whose potential energy is zero unless they strike a target volume v which represents the volume of an anion plus dipole; in v , let the potential energy be pkT where p is a pure number. Then

$$-\delta Z_1 = \delta Z_3 = Z_1 v e^p \delta Z \quad (7)$$

and

$$\delta Z_2 = (V - Z_1 v) \delta Z \approx V \delta Z \quad (8)$$

by use of Boltzmann's methods.⁶ Dividing (7) by (8) and integrating

$$Z_1 = N_1 \exp(-Z_2 v e^p / V) \quad (9)$$

The exponent is small compared to unity; hence approximately

$$Z_3 = N_1 v e^p Z_2 / V \quad (10)$$

and converting to moles/l. (L is Avogadro's number) and using our earlier symbols for concentrations of the various species

$$x/c[\text{PNA}] = Lve^p/1000 \quad (11)$$

or

$$K = Lve^p/1000 = 2.52 \times 10^{-3} \bar{r}^3 e^p \quad (12)$$

if we represent the volume v as a sphere of radius \bar{r} (in Ångström units). From the slope of the $y - c'$ line of Fig. 1, $(K \Delta\lambda/\Lambda) = 1.4$. Suppose we estimate $\Delta\lambda/\Lambda$ as $1/2$ and \bar{r} as 4. This leads to $p \approx 3$, *i.e.*, an energy of association of about $3kT$ between a bromide ion and a molecule of *p*-nitroaniline.

(6) R. M. Fuoss and F. Accascina, "Electrolytic Conductance," Interscience Publishers, Inc., 1959, Chapters 16 and 18.

THE IONIZATION CONSTANTS OF *o*-NITROPHENOL AND 4-NITRO-*m*-CRESOL FROM 5 TO 60°

BY R. A. ROBINSON AND ADAM PEIPERL

*Solution Chemistry Section, National Bureau of Standards,
Washington, D. C.*

Received February 18, 1963

There is some evidence¹ that, for a series of substituted anilinium ions, the enthalpy change on ionization is a linear function of the change in free energy on ionization. It would follow that, if two acids of like structure have similar *pK* values, their enthalpy changes on ionization should also be similar.

The ionization constant of *p*-nitrophenol has already been measured² over a temperature range; in order to test this postulate, similar measurements have now been made with *o*-nitrophenol and 4-nitro-*m*-cresol in aqueous solution.

o-Nitrophenol (Eastman) was recrystallized once from methanol (m.p. 45.0°); 4-nitro-*m*-cresol (Calbiochem) was recrystallized twice from water (m.p.

(1) A. I. Biggs, *J. Chem. Soc.*, 2572 (1961).

(2) G. F. Allen, R. A. Robinson, and V. E. Bower, *J. Phys. Chem.*, **66**, 171 (1962).

(4) D. S. Berns and R. M. Fuoss, *J. Am. Chem. Soc.*, **83**, 1321 (1961).

(5) R. M. Fuoss and C. A. Kraus, *ibid.*, **55**, 2387 (1933).

129.5°). Measurements were made with a Cary spectrophotometer.

o-Nitrophenol, in alkaline solution at 25°, has maximum absorption at 414 m μ , ϵ_2 4,630; this is slightly temperature dependent, for at 5° the maximum occurs at 412 m μ and ϵ_2 4,570. At 60°, it occurs at 420 m μ with ϵ_2 4,600. The acid solution has maximum absorption at 350 m μ with ϵ_1 3,150 at 5°, 3,090 at 25°, and 2,950 at 60°. The corresponding data for the cresol are: in alkaline solution, 5°, 393 m μ , ϵ_2 16,400; 25°, 396 m μ , ϵ_2 16,700; 60°, 401 m μ , ϵ_2 16,800; in acid solution, 5°, 315 m μ , ϵ_1 7,760; 25°, 315 m μ ; ϵ_1 7,560; 60°, 315 m μ , ϵ_1 7,180.

For p*K* measurements the solutions were buffered with equimolar mixtures of KH₂PO₄ and Na₂HPO₄, ($-\log a_{\text{H}\gamma\text{Cl}}$) values of which have recently been recomputed.³ Measurements were made at a number of wave lengths and in buffer solutions of different total ionic strength (*I*). Some typical results are given for 25° in Table I. The p*K* values have been corrected, as described previously,⁴ for the effect of the phenol on the $-\log(a_{\text{H}\gamma\text{Cl}})$ value of the buffer.

TABLE I^a

IONIZATION CONSTANTS AT 25°

o-Nitrophenol, $2 \times 10^{-4} M$; 1 cm. cells; 410 m μ , $D_1 = 0.087$, $D_2 = 0.913$; 417 m μ , $D_1 = 0.054$, $D_2 = 0.927$

<i>I</i>	$-\log(a_{\text{H}\gamma\text{Cl}})$	410 m μ			417 m μ			p <i>K</i> (cor.)
		<i>D</i>	α	p <i>K</i>	<i>D</i>	α	p <i>K</i>	
0.10	6.974	0.382	0.357	7.229	0.364	0.355	7.233	7.228
.06	7.013	.398	.377	7.232	.380	.373	7.238	7.230
.04	7.040	.408	.389	7.237	.392	.387	7.239	7.231
.02	7.080	.429	.407	7.244	.407	.404	7.248	7.232
Mean								7.230

4-Nitro-*m*-cresol, $5.5 \times 10^{-5} M$; 1 cm. cells; 390 m μ , $D_1 = 0.037$, $D_2 = 0.891$; 400 m μ , $D_1 = 0.015$, $D_2 = 0.909$

<i>I</i>	$-\log(a_{\text{H}\gamma\text{Cl}})$	390 m μ			400 m μ			p <i>K</i> (cor.)
		<i>D</i>	α	p <i>K</i>	<i>D</i>	α	p <i>K</i>	
0.10	6.974	0.265	0.267	7.413	0.254	0.267	7.413	7.412
.06	7.013	.281	.288	7.411	.271	.286	7.410	7.410
.04	7.040	.295	.302	7.404	.285	.302	7.405	7.403
.02	7.080	.308	.317	7.413	.300	.319	7.410	7.409
.01	7.111	.320	.331	7.416	.312	.332	7.414	7.409
Mean								7.409

^a *I* is the total ionic strength of the equimolar phosphate buffer; $\alpha = (D - D_1)/(D_2 - D_1)$ is the degree of dissociation of the phenol. D_1 = optical density of acid solution (phenol completely in the undissociated form); D_2 = optical density in alkaline solution (phenol completely dissociated); *D* = optical density in phosphate buffer.

The data at other temperatures are summarized in Table II where, for brevity, we record only the degree of dissociation (α) in the phosphate buffer, with *I* = 0.1, and the average, corrected p*K*.

Our value for *o*-nitrophenol at 25°, p*K* 7.230, is in good agreement with p*K* 7.234 found by Judson and Kilpatrick⁵ and p*K* 7.229 by Dippy, Hughes, and Laxton.⁶ It is higher, however, than the figure, 7.210, given by Biggs.⁷

The results from 5 to 60° can be represented by the equation⁸

$$pK = A_1/T - A_2 + A_3T$$

where *T* (= °C. + 273.15) is the temperature in de-

TABLE II

IONIZATION CONSTANTS FROM 5 TO 60°

		<i>o</i> -Nitrophenol					
		5°	10°	15°	20°	25°	30°
α		0.269	0.288	0.311	0.331	0.356	0.379
p <i>K</i> (cor.)		7.499	7.424	7.353	7.293	7.230	7.180
		35°	40°	45°	50°	55°	60°
α		0.398	0.421	0.443	0.471	0.490	0.509
p <i>K</i> (cor.)		7.135	7.085	7.043	6.993	6.966	6.931
		4-Nitro- <i>m</i> -cresol					
		5°	10°	15°	20°	25°	30°
α		0.194	0.210	0.232	0.247	0.267	0.289
p <i>K</i> (cor.)		7.671	7.596	7.525	7.466	7.409	7.354
		35°	40°	45°	50°	55°	60°
α		0.308	0.328	0.349	0.370	0.392	0.415
p <i>K</i> (cor.)		7.303	7.257	7.215	7.176	7.133	7.099

grees Kelvin. For *o*-nitrophenol we find $A_1 = 2223.12$, $A_2 = 4.3092$, $A_3 = 0.013709$; for 4-nitro-*m*-cresol $A_1 = 2075.02$, $A_2 = 3.1531$, $A_3 = 0.012082$. We have calculated the free energy, enthalpy, and entropy changes at 25° and compared them with the corresponding changes for *p*-nitrophenol, as follows

	p <i>K</i> , 25°	ΔG° , kj. mole ⁻¹	ΔH° , kj. mole ⁻¹	ΔS° , j. deg. ⁻¹ mole ⁻¹
<i>p</i> -Nitrophenol	7.156	40.85	19.73	-71
<i>o</i> -Nitrophenol	7.230	41.29	19.23	-74
4-Nitro- <i>m</i> -cresol	7.409	42.29	19.16	-78

Thus, three substituted phenols with similar ionization constants have similar enthalpy and entropy changes on ionization.

CONDUCTANCE IN DIMETHYLSULFOLANE

BY JEHUDAH ELIASSAF,¹ RAYMOND M. FUOSS, AND
JOHN E. LIND, JR.

Contribution No. 1735 from the Sterling Chemistry Laboratory of
Yale University, New Haven, Connecticut

Received April 4, 1963

Burwell and Langford² reported that the equivalent conductances of tetraphenylarsonium chloride and of trimethylphenylammonium iodide in sulfolane (tetramethylene sulfone) are "independent of concentration to within 1%" at low concentrations, and that contact distances (\hat{a}) of the order of hundreds of Ångstrom units would be needed to fit the data at higher concentrations. There seems to be no *a priori* reason to expect such peculiar behavior in these systems; we therefore reconsidered the sulfolane data and also made some exploratory measurements in 2,4-dimethylsulfolane, which has a lower dielectric constant. Our conclusion is that the conductance is normal in both solvents; the theoretical slope in sulfolane, however, is so small that, over a narrow concentration range, the theoretical tangent appears to be horizontal. Hence points near the tangent seem to be independent of concentration.

Sulfolane has a dielectric constant of 44 at 30° and a viscosity of 0.0987 poise. The limiting slope becomes $S = 0.54\Lambda_0 + 7.3$. For limiting conductances of the order of 10, *S* is about 13. If one considers an unas-

(1) Grateful acknowledgment is made for a postdoctoral fellowship from a research grant made to Yale University by the California Research Corporation.

(2) R. L. Burwell, Jr., and C. H. Langford, *J. Am. Chem. Soc.*, **81**, 3799 (1959).

(3) R. G. Bates and R. Gary, *J. Res. Natl. Bur. Std.*, **65A**, 495 (1961).

(4) R. A. Robinson and A. K. Kiang, *Trans. Faraday Soc.*, **51**, 1398 (1955).

(5) C. M. Judson and M. Kilpatrick, *J. Am. Chem. Soc.*, **71**, 3110 (1949).

(6) J. F. J. Dippy, S. R. C. Hughes, and J. W. Laxton, *J. Chem. Soc.*, 2995 (1956).

(7) A. I. Biggs, *Trans. Faraday Soc.*, **52**, 35 (1956).

(8) H. S. Harned and R. A. Robinson, *ibid.*, **36**, 973 (1940).

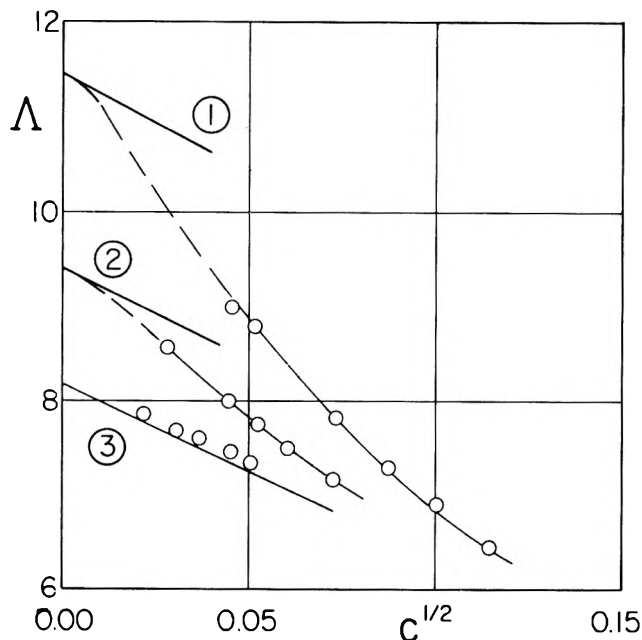


Fig. 1.—Phoreograms in dimethylsulfolane: 1, KCNS; 2, Me_3PhNI ; 3, Ph_4AsI .

sociated electrolyte in sulfolane over the concentration range 0.0010–0.0036 (that shown for Ph_4AsCl in ref. 2, excluding the lowest point), the conductance should change by about 0.37 Λ unit. If Burwell and Langford's point at the lowest concentration is disregarded, a line of theoretical slope will fit their other data within several per cent; their Λ scale is so compressed that the theoretical tangent becomes almost horizontal.

Experimental

2,4-Dimethylsulfolane was distilled at 100° and about 1 mm. from sodium hydroxide, using nitrogen to sweep air out of the system³; the solvent conductance was $2\text{--}4 \times 10^{-8}$. The viscosity at 25° is 0.0904. The dielectric constant is 29.5 and the density⁴ is 1.1314. Tetraphenylarsonium iodide was prepared as described by Lyon and Mann⁵ and recrystallized twice from water. Trimethylphenylammonium iodide (Eastman) and potassium thiocyanate were recrystallized from ethanol. Conductances were measured at 25.00°, in a cell with constant equal to 0.1245. Electrical equipment and techniques have already been described.⁶ Typical conductance data are summarized in Table I. The accuracy is only about 1%.

TABLE I

CONDUCTANCE IN DIMETHYLSULFOLANE					
KCNS		PhNMe ₃ I		Ph ₄ AsI	
10 ² c	Λ	10 ² c	Λ	10 ² c	Λ
13.02	6.44	5.22	7.17	2.55	7.35
10.01	6.90	3.66	7.51	2.03	7.46
7.70	7.29	2.73	7.76	1.323	7.61
5.39	7.83	1.93	8.02	0.941	7.70
2.65	8.80	0.82	8.56	.480	7.85
0.00	11.47	0.00	9.40	.000	8.22

The phoreograms are shown in Fig. 1. The conductance curve for tetraphenylarsonium iodide (curve 3) lies above the limiting tangent, similar to the curves for the alkali halides in water. The positive deviations from the Onsager tangent can be described by the Fuoss-Onsager equation

$$\Lambda = \Lambda_0 - Sc^{1/2} + Ec \log c + Jc \quad (1)$$

using a contact distance δ of 5–6 Å. Trimethylphenylammonium

(3) We are grateful to Professor Burwell for suggesting this method of purification.

(4) E. Hirsch and R. M. Fuoss, *J. Am. Chem. Soc.*, **77**, 6115 (1955).

(5) D. R. Lyon and F. G. Mann, *J. Chem. Soc.*, 666 (1942).

(6) J. E. Lind, Jr., and R. M. Fuoss, *J. Phys. Chem.*, **65**, 999 (1961).

iodide (curve 2) has a larger limiting conductance, because the cation is smaller, and, for the same reason, shows a moderate amount of association ($K_A \approx 40$). As shown in Fig. 1, the curve now approaches the limiting tangent from below. In the case of potassium thiocyanate (curve 1) both ions are small; the expected consequences appear. The limiting conductance is large, and the phoreogram drops rapidly away from the limiting tangent as concentration increases, showing considerably more association ($K_A \approx 80$) than the quaternary salt.

THE ADSORPTION OF METHANE AND NITROGEN ON SILICA GEL, SYNTHETIC ZEOLITE, AND CHARCOAL

By A. J. KIDNAY AND M. J. HIZA

Cryogenic Engineering Laboratory, National Bureau of Standards, Boulder, Colorado

Received December 29, 1962

Nitrogen adsorption has been studied extensively at liquid nitrogen temperatures in conjunction with surface area measurements, but very little work appears to have been done on methane in this temperature region. The available methane data are limited to adsorption measurements on sodium chloride,¹ sodium bromide,² and graphite³ and heat capacity measurements on rutile.^{4–6}

In earlier work,⁷ isotherms of methane on silica gel were determined at 76 and 88.5°K. These isotherms exhibited unusual behavior in that, when the amount of methane adsorbed is plotted against the relative pressure (p/p_0), the higher temperature isotherm exhibits the greater capacity over the entire pressure region studied.

The work reported here was undertaken to obtain more information regarding the temperature dependence of methane adsorption and the adsorption isotherms of methane and nitrogen on commercial adsorbents.

Experimental

The adsorption apparatus used in this work was of a standard volumetric design and consisted of a calibrated gas buret, constant volume manometer, adsorption bulb, and vacuum system. For pressures greater than 10 mm., mercury was used as the manometric fluid; for lower pressures, a low vapor pressure oil (specific gravity 0.9827) was used. All pressure readings were made with a cathetometer, to a precision of 0.02 mm. of fluid. Liquid nitrogen was the refrigerating bath for all of the runs. The bath pressure could be held above or below normal atmospheric pressure, thus allowing the temperature to be controlled from 70 to 82°K. A two junction copper-constantan thermocouple, calibrated with a platinum resistance thermometer, was used for the temperature measurements.

The three adsorbents used were silica gel,^{8a} synthetic zeolite,^{8b} and coconut shell charcoal.^{8c}

(1) S. Ross and H. Clark, *J. Am. Chem. Soc.*, **76**, 4291 (1954).

(2) B. B. Fisher and W. G. McMillan, *J. Chem. Phys.*, **28**, 549 (1958).

(3) L. Bonnetain, X. Duval, and M. Letort, *Compt. rend.*, **234**, 1363 (1958).

(4) K. S. Dennis, E. L. Pace, and C. S. Baughman, *J. Am. Chem. Soc.*, **75**, 3269 (1953).

(5) E. L. Pace, E. L. Heric, and K. S. Dennis, *J. Chem. Phys.*, **21**, 1225 (1953).

(6) E. L. Pace, D. J. Sasmor, and E. L. Heric, *J. Am. Chem. Soc.*, **74**, 4413 (1952).

(7) M. J. Hiza and A. J. Kidnay, "The Adsorption of Methane on Silica Gel at Low Temperatures," *Advances in Cryogenic Engineering*, Vol. 6, Plenum Press, Inc., New York, N. Y., 1961.

(8) (a) Davison Chemical Co., "High Capacity" grade, 6–10 mesh; (b) Linde Molecular Sieves 5A, 1/16-in. pellets; (c) Barnebey-Cheney Co., Type IG-1, 8–10 mesh.

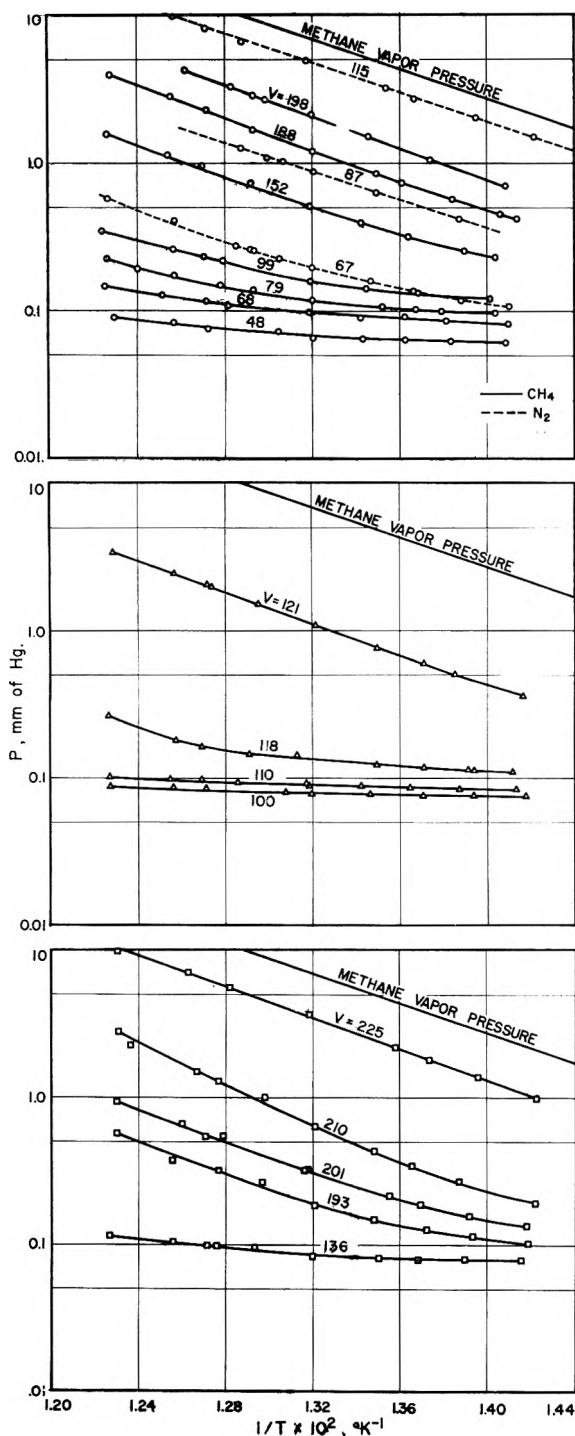


Fig. 1.—The isosteres of methane and nitrogen on silica gel, O; synthetic zeolite, Δ ; and charcoal, \square .

Results and Discussion

The adsorption isosteres for nitrogen on silica gel and methane on all three adsorbents are shown in Fig. 1.⁹ The vapor pressure curve for methane has been included for comparison purposes. There are two features worthy of note about the methane isosteres in the low pressure region; they have a very small slope and most of them exhibit a marked curvature.

Surface Area—The monolayer volume was evaluated for both the nitrogen and methane isotherms with the Brunauer-Emmett-Teller equation

(9) Due to lack of space, the adsorption isotherms discussed in this note are not presented graphically; however, the tabular values for both the isotherms and isosteres can be obtained from the National Bureau of Standards, Cryogenic Data Center, Boulder, Colorado.

$$\frac{p}{v(p_0 - p)} = \frac{c'' - 1}{v_m c''} \left(\frac{p}{p_0} \right) + \frac{1}{v_m c''} \quad (1)$$

Since the "knee" of the isotherms occurs at relatively low pressures for all of the adsorbents, the values of v_m were obtained for relative pressures (p/p_0) less than 0.2.

The surface area can be evaluated from the monolayer volumes if one can obtain a value for the area occupied by an adsorbed molecule. The best value for the area occupied by a nitrogen molecule appears to be 15.8 \AA^2 .¹⁰ Livingston¹¹ gives a section area ratio (CH_4/N_2) of 1.04, which gives a molecular area for CH_4 of 16.4 \AA^2 . The v_m (76°K.) and surface area values for the three adsorbents are presented in Table I. Considering that there is some uncertainty regarding the area value of the methane molecule, the agreement between the two sets of surface areas is excellent.

Since the molecular structure of the zeolite is supposedly quite uniform, it is interesting to compare nitrogen v_m values for this adsorbent. Lederman¹² gives an average v_m of 113.4 cc. (STP)/g., which is 4.7% lower than this report.

Heat and Entropy Changes during Adsorption.—The Clapeyron equation for an adsorption process can be written in the form

$$\left[\frac{d \ln p}{d \left(\frac{1}{T} \right)} \right]_v = \frac{\Delta H_{\text{iso}}}{R} \quad (2)$$

assuming that the volume of the adsorbed phase is negligible in comparison with the gas phase and that the gas behaves ideally.

TABLE I

Adsorbent	v_m , cc. (STP)/g.	Surface area, $\text{m}^2/\text{g}.$
Nitrogen		
Silica gel	157	665
Zeolite	119	506
Charcoal	213	904
Methane		
Silica gel	158	697
Zeolite	117	514
Charcoal	213	941

Thus the slope of the adsorption isostere, when plotted as $\ln p$ against $1/T$, is directly proportional to the isosteric heat of adsorption. Referring again to Fig. 1, it is evident that for methane on all three adsorbents, the initial heat of adsorption is considerably less than the heat of condensation, and furthermore, at low coverages, the isosteric heat of adsorption is changing fairly rapidly with temperature. Systems having heats of adsorption less than heats of condensation below one monolayer coverage are rare, although not unknown. The most widely studied systems exhibiting this phenomenon are water vapor on charcoal,¹³ mercury vapor on charcoal,¹⁴ and iodine on silica gel.¹⁵

(10) A. S. Joy, *Vacuum*, **3**, 254 (1953).

(11) H. K. Livingston, *J. Colloid Sci.*, **4**, 447 (1949).

(12) P. B. Lederman, "Adsorption of Nitrogen-Methane on Linde Molecular Sieves Type 5A," Ph.D. Dissertation, University of Michigan, 1961.

(13) A. S. Coolidge, *J. Am. Chem. Soc.*, **49**, 708 (1927).

(14) A. S. Coolidge, *ibid.*, **49**, 1949 (1927).

(15) W. A. Patrick and W. E. Land, *J. Phys. Chem.*, **38**, 1201 (1934).

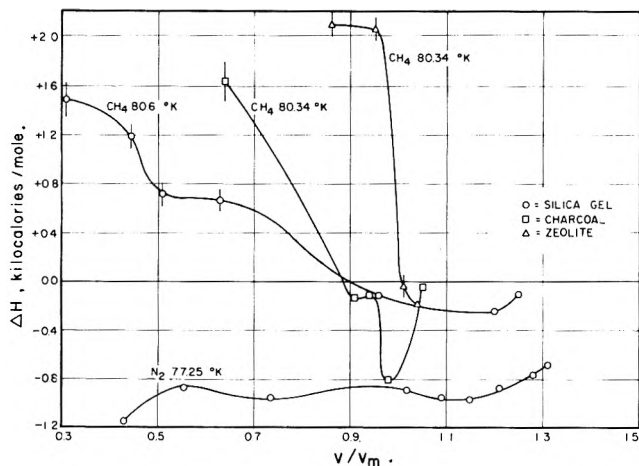


Fig. 2.— ΔH for the process (condensed phase) \rightarrow (adsorbed phase).

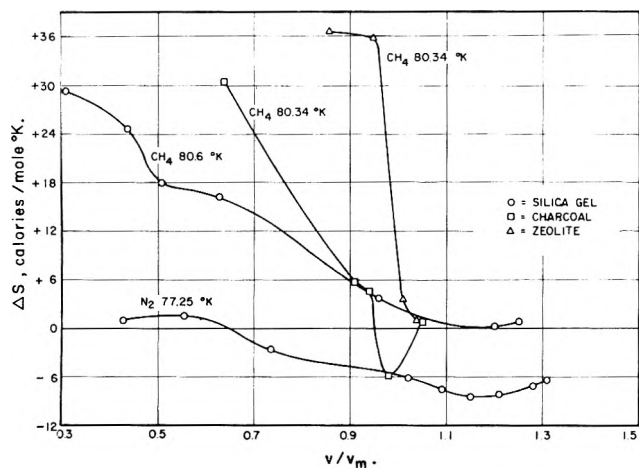


Fig. 3.— ΔS for the process (condensed phase) \rightarrow (adsorbed phase).

Several systems^{16,17} have been studied in which the heat of condensation is greater than the heat of adsorption at coverages greater than one monolayer.

Heat and entropy changes for adsorption data are best presented by considering the process

(condensed phase) \rightarrow (adsorbed phase)

and calculating the thermodynamic relations for this reaction. The ΔH for the process is the difference between the isosteric heat of adsorption and the heat of condensation, and is given by the equation

$$\frac{\ln [(p/p_0)_{T_2}/(p/p_0)_{T_1}]_v}{\left[\frac{1}{T_2} - \frac{1}{T_1} \right]} = \frac{\Delta H}{R} \quad (3)$$

For nitrogen, the ΔH values were calculated from the isosteres at coverages below one monolayer and from the isotherms at 75.77 and 78.73°K. for coverages above one monolayer.

The free energy and entropy changes are calculated from the relationships

$$\Delta F = RT \ln (p/p_0) \quad (4)$$

$$\Delta S = \frac{\Delta H - \Delta F}{T} \quad (5)$$

The ΔH and ΔS relationships for the three adsorbents are shown in Fig. 2 and 3. The vertical lines in Fig. 2 are an estimate of the error in the ΔH values.

Concluding Remarks

Although the shapes of the adsorption isotherms for methane and nitrogen on silica gel are similar, the ΔH values differ greatly. Nitrogen adsorbed on silica gel follows the general trend of adsorption data, in that the heat of adsorption is greater than the heat of condensation at all coverages; methane, on the other hand, exhibits the reverse trend.

Examination of eq. 3 shows that whenever the higher temperature isotherm lies above the lower temperature one when plotted on a relative pressure basis $[(p/p_0)_{T_2} > (p/p_0)_{T_1}]$, the heat of adsorption is less than the heat of condensation. Thus the general trend of the earlier isotherm data⁷ for methane on silica gel agrees with the data of this report, even though the absolute values of the isotherms differ somewhat, due to differences in samples and activation techniques.

Nomenclature

- "c" = a constant
 - F = free energy
 - ΔF = $F_a - F_c$
 - H = enthalpy
 - ΔH = $H_a - H_c$
 - ΔH_{iso} = $H_a - H_g$
 - p = measured pressure, mm.
 - p_0 = normal vapor pressure, mm.
 - R = gas constant
 - S = entropy
 - ΔS = $S_a - S_c$
 - T = absolute temperature
 - v = volume of gas adsorbed at pressure p
 - v_m = volume of gas required to form a monolayer
- Subscripts
- a = adsorbed phase
 - c = condensed phase
 - g = gas phase
- Superscripts
- denotes partial molar quantity

THE EFFECT OF PRESSURE ON THE QUENCHING OF FLUORESCENCE

BY A. H. EWALD

C.S.I.R.O. Division of Physical Chemistry, High Pressure Laboratory, Sydney, N.S.W., Australia

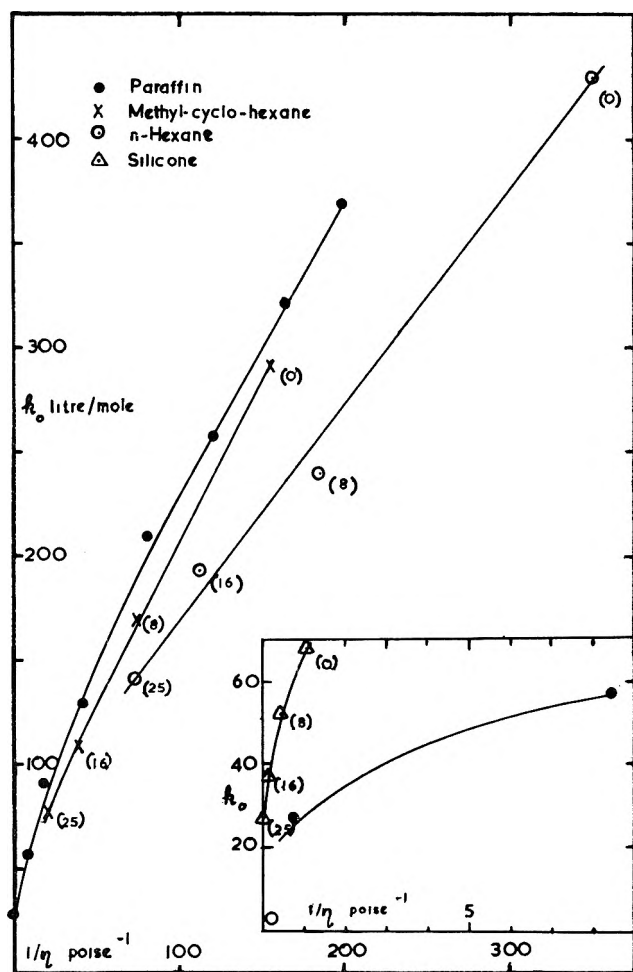
Received January 7, 1963

The effect of pressure on the quenching of fluorescence was measured in order to study the effect of hydrostatic pressure on very fast reactions in the liquid phase. It follows from kinetic considerations that the rate of a reaction becomes viscosity dependent when the time required by the reacting molecules to diffuse together becomes comparable with the time required to form the transition state.¹ This condition will occur in ordinary solvents only for reactions with very low activation energies but has been shown to arise in extremely viscous media also for reactions with the higher activation energies common in ionic reactions. The reaction between an excited molecule and a strong quenching agent has a very low activation energy and although it is very fast its rate can be studied by observing relative fluorescence intensities. The quenching of the fluorescence of anthracene by carbon tetrabromide

(1) S. D. Hamann, *Trans. Faraday Soc.*, **54**, 507 (1958).

(16) J. deD. Lopez-Gonzalez, F. G. Carpenter, and V. R. Deitz, *J. Phys. Chem.*, **65**, 1112 (1961).

(17) C. F. Prenzlow and G. D. Halsey, Jr., *ibid.*, **61**, 1158 (1957).



this study are reported the temperature dependence of various proton transfer rates in aqueous solutions of dimethylammonium (DMA) and trimethylammonium (TMA) chlorides. The rates and mechanisms for these reactions at room temperature were given by Loewenstein and Meiboom.³ The experimental procedure employed follows closely that given in ref. 2 and the same notation of the rate constants will be used. The only substantial modification is the use of the modified Carr-Purcell spin echo technique⁴ to measure the broadening of the water line. This permitted a more accurate determination of k_7 , namely, the reaction involving the ammonium, amine, and water species.

Experimental Procedure

The n.m.r. spectrometer and its operation at various sample temperatures were described elsewhere.⁵ Frequency calibration was obtained by the side-band technique. Solutions were prepared from C.P. materials. The concentration of the ammonium was determined by the Volhard method and the concentration of the hydrogen ions by potentiometric titration against standardized base.

The acid dissociation constants, K_A , defined in concentration terms, were determined by the differential potentiometric method.⁶ A Metrohm Type E184C pH meter equipped with a combined (glass-calomel) type H electrode was used to measure the e.m.f. of the solutions. The dissociation constants are represented by

$$\log K_A = \frac{A}{T} + \frac{\Delta C_p}{R} \log T + B$$

in Table I.⁷ The values of A and B are in fair agreement with the results given by Everett and Wynne-Jones⁸ for the low concentration of these salts.

TABLE I

Concn. (M)	A	B	Temp. range, °C.	No. of measurements
	(CH ₃) ₂ NH ₂ Cl ($\Delta C_p = 23.1^8$)			
0.51	-1010.8 ± 69.7	-36.40 ± 0.23	26-60	18
1.03	-946.7 ± 59.1	-36.36 ± 0.19	24-60	20
2.00	-814.2 ± 88.3	-37.08 ± 0.28	19-65	27
	(CH ₃) ₃ NHCl ($\Delta C_p = 43.8^8$)			
0.48	+994.3 ± 65.0	-67.03 ± 0.24	25-60	20
0.97	+949.7 ± 38.0	-67.97 ± 0.14	25-60	20

Interpretation and Results

Trimethylammonium Chloride.—The TMA concentration was $0.96 \pm 0.03 M$ in all measurements, assuming thus implicitly that the results are independent of the TMA concentration.² The specific rate, $R \equiv 1/\tau$, obtained from the line shapes of the methyl resonance was plotted semilogarithmically as a function of the reciprocal of the absolute temperature, T . Inter- and extrapolated values of R for constant values of $1/T$ were then plotted as a function of the reciprocal of the hydrogen ion concentration. The slopes of the lines thus obtained give values for the rate constants ($k_6 + k_7$) and the intercepts give the values of k_4 .

(2) T. M. Connor and A. Loewenstein, *J. Am. Chem. Soc.*, **83**, 560 (1961), and ref. 4-8 therein.

(3) A. Loewenstein and S. Meiboom, *J. Chem. Phys.*, **27**, 1067 (1957).

(4) S. Meiboom and D. Gill, *Rev. Sci. Instr.*, **29**, 688 (1958).

(5) A. Loewenstein and A. Szöke, *J. Am. Chem. Soc.*, **84**, 1151 (1962).

(6) A. L. Bacarella, E. Grunwald, H. P. Marshall, and E. L. Purlee, *J. Org. Chem.*, **20**, 747 (1955).

(7) All errors throughout this paper are given as standard errors. J. Topping, "Errors of Observation and Their Treatment," The Institute of Physics, London, 1956, p. 107.

(8) D. H. Everett and W. F. K. Wynne-Jones, *Proc. Roy. Soc. (London)*, **A177**, 499 (1941).

The activation energies, E , for ($k_6 + k_7$) and for k_4 were obtained from Arrhenius plots, using the least squares method to draw the straight line. Values of K_A used in the calculations were taken from Table I. The E values obtained for ($k_6 + k_7$) and for k_4 were 4.4 ± 0.5 and 7.3 ± 0.2 kcal./mole, respectively.

Further check on the reliability of the results was obtained by recalculating the experimental R values from the values of k_4 and ($k_6 + k_7$) obtained in the manner described above. The purpose of this calculation was to check whether the R vs. $1/T$ plots deviate significantly from the almost linear shape used and to check to what extent such a deviation would affect the R vs. $1/[H^+]$ plots. It was found that the calculated values of R agree well with the experimentally measured values and only a slight correction to the R vs. $1/T$ line shape was applied. The results thus obtained from 19 measurements in the temperature range 19-48° are

$$E \text{ for } k_6 + k_7 = 4.4 \pm 1.7 \text{ kcal./mole, } A = 6.6 \times 10^{11}$$

$$E \text{ for } k_4 = 7.3 \pm 0.2 \text{ kcal./mole, } A = 9.1 \times 10^5$$

where A denotes the pre-exponential factor in the Arrhenius equation.

The value of k_7 at various temperatures was determined from a separate series of (13) measurements of the broadening of the water line over the temperature range of 19 to 50°. T_1 values for pure water were substituted⁵ for the "natural" T_2 values. A correction taking into account the contribution to the water line broadening from the direct exchange with water (k_4) was applied, taking values of k_4 from the methyl broadening measurements. The result obtained was: E for $k_7 = 6.6 \pm 1.2$ kcal./mole, $A = 2.9 \times 10^{13}$.

The values of ($k_6 + k_7$) and of k_7 at 25° are 4.20 and 4.11×10^8 sec.⁻¹ mole⁻¹, respectively. This indicates that over the whole temperature range studied practically only reaction 7 is occurring, *i.e.*, all proton transfers involve solvent (water) molecules. This conclusion agrees well with other results,^{2,3} the rates are however slightly lower than previously reported.^{2,3}

Dimethylammonium Chloride.—As in the case of methylammonium² there is one major difficulty in obtaining the E values: the magnitude of k_4 is smaller than its value in ammonium or TMA and the accuracy of the measurements is insufficient to permit the estimation of its contribution at various temperatures. Furthermore, since in DMA the activation energies are lower than in TMA, the absolute accuracy of the measurements must be higher. Two procedures were applied to overcome these difficulties in an attempt to obtain fairly reliable results. (a) The contribution of k_4 may be totally neglected (as was assumed in the case of methylammonium²) and the values of ($k_6 + k_7$) calculated directly from the observed R values. The result thus obtained was: E for $k_6 + k_7 = 1.8 \pm 0.5$ kcal./mole, $A = 2.5 \times 10^{10}$, and ($k_6 + k_7$) at 25° equal to 1.25×10^9 sec.⁻¹ mole⁻¹. (b) Plots of R vs. $1/T$ and of R vs. $1/[H^+]$ (at $1/T$ constant) were drawn as for TMA. Straight lines were passed through the points, using the least squares method, with slopes giving ($k_6 + k_7$) for various $1/T$ values. Since the temperature dependence is small no information could be obtained from the intercepts (k_4). Also, since the abscissa of the plot is $1/[H^+]$ which varies over 1-2 orders

of magnitude, the least squares method had to be modified to give a minimum in the *relative* error (*i.e.*, $(Y_i - Y/Y_i)^2 = \text{min}$). The result thus obtained is

$$E \text{ for } k_6 + k_7 = 3.5 \pm 0.2 \text{ kcal./mole, } A = 7.6 \times 10^{11}, \\ \text{and } k_6 + k_7 = 9.55 \times 10^8 \text{ sec.}^{-1} \text{ mole}^{-1} \text{ at } 25^\circ$$

The concentration of DMA was $2.06 \pm 0.2 M$ and a total of 23 measurements were taken in the temperature range of 19–67°.

The temperature dependence of k_7 was evaluated separately by measuring the water line broadening as for TMA. No correction that takes into account the contribution of k_4 to the broadening was applied, but it can be assumed safely to be small. The result for 11 measurements in the temperature range of 24 to 48° is $E = 2.6 \pm 1.2 \text{ kcal./mole, } A = 7.9 \times 10^{10}$, with k_7 at 25° equal to $10.07 \times 10^8 \text{ sec.}^{-1} \text{ mole}^{-1}$. The ratio k_7 to $(k_6 + k_7)$ is near unity over all temperature ranges meaning that the reaction involving the water molecules is predominant.²

Acknowledgment.—The author thanks Dr. A. Szöke and Mr. S. Stampfer for their kind assistance.

THE HEAT OF FORMATION OF URANIUM DICARBIDE^{1,2}

BY ELMER J. HUBER, JR., EARL L. HEAD, AND CHARLES E. HOLLEY, JR.

University of California, Los Alamos Scientific Laboratory, Los Alamos, New Mexico

Received February 1, 1963

The carbides of the actinide elements are becoming of increasing technical importance in the development of nuclear reactors. Their thermodynamic properties, therefore, are of practical as well as theoretical interest. Several bibliographies and reviews on the uranium carbides have recently appeared,^{3–9} but few experimental determinations of the thermodynamic properties of these carbides have been made.

This paper describes an indirect experimental determination of the heat of formation of uranium dicarbide, UC_{1.90}, from measurements of its heat of combustion in oxygen. From these measurements, ΔH was calculated for the reaction



and, since the heats of formation of U₃O₈ and CO₂ are known, the heat of formation of UC_{1.9} could be determined.

Experimental

Materials.—Two separate samples of UC_{1.9}, designated I and II, were used.¹⁰ Sample I was finely powdered; sample II was in

- (1) Work done under the auspices of the Atomic Energy Commission.
- (2) Presented in part at the Symposium on Thermodynamics of Nuclear Materials, International Atomic Energy Agency, Vienna, Austria, May 21–25, 1962.
- (3) M. Comstock, U. S. Atomic Energy Commission Report, TID-3906 (1960).
- (4) M. Bloomfield, North American Aviation, Inc., Report, NAA-SR-Memo-6512 (1961).
- (5) J. L. Kane, U. S. Atomic Energy Commission Report, MND-2081 (1959).
- (6) R. W. Nichols, *Nucl. Eng.*, **3**, 327 (1958).
- (7) A. Strasser, *ibid.*, **5**, 353 (1960).
- (8) F. A. Rough and W. Chubb, Battelle Mem. Inst. Report, BMI-1441 (1960).
- (9) M. H. Rand and O. Kubaschewski, U. K. Atomic Energy Research Establishment Report, AERE-R 3487 (1960).

chunks. Chemical analyses for U, C, H, O, and N and spectrochemical analysis for metallic impurities were made. The Si, Fe, and Pb were assumed to be in their elemental state, and the N was assumed to be combined as UN. The results are listed in Table I, and the lattice constants are also included.

A metallographic analysis of sample II showed traces (<1%) of a gray phase (graphite flakes?) present at the grain boundaries and distributed as "spots" throughout a part of the sample.

TABLE I

ANALYSES OF URANIUM CARBIDE SAMPLES I AND II (Wt. %)

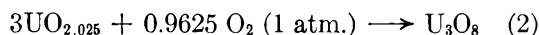
	I	II
UC _{1.90}	99.62 (UC _{1.86})	99.85 (UC _{1.90})
C (free)	0.15	0.14
H ₂ O	.056	
UN	.099	
Fe	.06	0.01
Pb	.01	
Si		0.01
a ₀	3.5257 ± 0.0010 Å.	3.5249 ± 0.0004 Å.
c ₀	5.9990 ± 0.0030 Å.	5.9968 ± 0.0008 Å.

The calorimeter and the general procedure, which involved the determination of the amount of heat evolved from the combustion of weighed amounts of UC_{1.9} and UC_{1.9}-UO₂ mixtures in a bomb calorimeter at a known initial pressure of oxygen, have been described.¹¹ The energy equivalent of the calorimeter was 2386.5 ± 0.8 cal./deg. as determined by the combustion of standard benzoic acid.

Eight combustions were made with sample I, UC_{1.9}, and four with sample II, UC_{1.9}, on sintered U₃O₈ disks. Four additional runs were made with sample II, UC_{1.9}-UO₂ mixtures in a platinum dish, since in previous experiments,^{12,13} it was shown that it was necessary, when burning U metal and UC, to use such a "combustion moderator" to ensure that the combustion product was stoichiometric U₃O₈.

Ignition was by means of a 0.010-in. diameter uranium fuse wire which was ignited electrically.

The uranium dioxide had the formula UO_{2.025}. Its heat of combustion was measured separately. For the reaction



a value of 74.31 ± 0.04 kcal. was found.

Each combustion product was analyzed by heating to constant weight at 750° in oxygen and noting any change in weight. Any water and carbon dioxide given off was collected and weighed. The amount of CO₂ found and the change in weight of the oxide provide two pieces of information from which to determine the three unknowns: amount of unburned carbide, amount of adsorbed CO₂, and the formula of the uranium oxide. Fortunately, for the combustion of the UC_{1.9}-UO₂ mixtures the amount of CO₂ found was 1 mg. or less, and the weight change was insignificant. It was therefore possible to conclude in this case that within the uncertainties of the analyses, including the blanks, the oxide was U₃O₈, the CO₂ was adsorbed, and combustion was complete. For the combustions without UO₂, it was assumed that all the CO₂ came from unburned carbide. The formula found for the oxide was U₃O₈ within the uncertainties involved. However, the procedure is not really satisfactory. (See Appendix for further discussion.)

Listed in Table II are the results of the runs.

The average initial temperature of the runs was 25.02°, and the initial oxygen pressure was 25 atm.

Calculations.—The calculations were carried out in the manner previously described,¹³ using the following values for heats of formation: PbO, -52.1 kcal.; Fe₃O₄, -267.1 kcal.; SiO₂, -217 kcal.; CO₂, -94.05 kcal.; U₃O₈, -852.7 kcal.; UN, -68.5 kcal.; NO₂, +8.1 kcal. The 1961 atomic weights were used.¹⁴

- (10) They were prepared by W. G. Witteman of this Laboratory, who also measured the lattice constants.
- (11) C. E. Holley, Jr., and E. J. Huber, Jr., *J. Am. Chem. Soc.*, **73**, 5577 (1951).
- (12) E. J. Huber, Jr., C. E. Holley, Jr., and E. H. Meierkord, *ibid.*, **74**, 3406 (1952).
- (13) J. D. Farr, *et al.*, *J. Phys. Chem.*, **63**, 1455 (1959).
- (14) A. E. Cameron and E. Wichers, *J. Am. Chem. Soc.*, **84**, 4175 (1962).

TABLE II
THE HEAT OF COMBUSTION OF UC_{1.9}

Mass UC _{1.9} g.	Mass UO ₂ g.	Mass U mg.	Energy equiv., cal./deg.	ΔT, °K.	Firing energy, cal.	Energy from UC ₂ , cal./g.	Dev.
Sample I							
1.5131		78.52	2393.6	1.1090	1.3	1693.6	16.4
1.6617		76.27	2394.3	1.2178	1.3	1708.9	1.1
1.6669		75.55	2394.2	1.2298	1.1	1718.1	8.1
1.7288		75.29	2394.2	1.2644	1.1	1703.7	6.3
1.4756		76.34	2394.2	1.0877	1.1	1707.8	2.2
1.6498		80.15	2394.3	1.2006	1.2	1693.3	16.7
1.4774		76.03	2394.3	1.1062	0.9	1732.2	22.2
1.7381		75.45	2394.3	1.2781	1.4	1722.3	12.3
						Av. 1710.0	10.7
						2 × standard dev.	9.6
Sample II							
1.5592		122.12	2394.6	1.1754	1.7	1729.0	8.8
1.5060		113.32	2394.6	1.1313	1.7	1719.7	0.5
1.5542		108.10	2394.6	1.1618	1.8	1721.1	0.9
1.3714		117.48	2394.5	1.0356	1.8	1711.0	9.2
						Av. 1720.2	4.9
						2 × standard dev.	7.4
Sample II with UO ₂							
0.7366	17.2995	61.10	2391.6	1.2118	1.3	1700.4	0.0
.8354	16.2635	57.36	2391.6	1.2395	0.9	1697.2	3.2
.8209 ₅	15.1206	56.68	2391.6	1.1865	0.9	1700.0	0.4
.8405	17.4308	52.18	2391.7	1.2873	1.0	1703.9	3.5
						Av. 1700.4	1.8
						2 × standard dev.	2.7

The calculated values of the heats of formation for the three series of runs were: for sample I, $\Delta H_f = -19.7 \pm 2.0$; for sample II, -18.6 ± 1.95 ; and for sample II burned with UO₂, -21.1 ± 1.4 kcal./mole. The uncertainties attached to these values include the uncertainties in the calorimetric measurements and in the energy equivalent of the calorimeter, both expressed as twice the standard deviation, combined with the uncertainties in the amounts of impurities and the uncertainties in the heats of formation of the corresponding oxides. Because sample II was of higher purity than sample I, and because the combustions with UO₂ were 100% complete and the oxide formed was more probably U₃O₈ than in the combustion without UO₂, the value $\Delta H_f = -21.1 \pm 1.4$ kcal./mole is taken for the heat of formation of UC_{1.90}. This value is the same, within the uncertainties involved, as the value obtained for the heat of formation of UC.¹³ Estimated values in the literature are those of N.B.S. Circular 500,¹⁵ -42 kcal./mole; Kubaschewski and Evans,¹⁶ -38.8 kcal./mole; Krikorian,¹⁷ -27 ± 8 kcal./mole; and Rand and Kubaschewski,⁹ -30 kcal./mole.

Acknowledgments—The authors acknowledge the valuable assistance of C. G. Hoffman, metallographic analysis; and G. C. Heasley, G. B. Nelson, and Helen D. Cowan, chemical analysis.

Appendix

The difficulty of preparing stoichiometric U₃O₈ is well known. For much the same reasons, the determination of the formula of a uranium oxide is difficult unless the uranium content is accurately known. The following experiment shows that within an uncertainty of a few units in the third decimal place, the oxidation

(15) "Selected Values of Chemical Thermodynamic Properties," N.B.S. Circular 500, 1952, p. 362.

(16) O. Kubaschewski and E. L. Evans, "Metallurgical Thermochemistry," 2nd Ed., Pergamon Press, London, 1956, p. 278.

(17) O. H. Krikorian, "High Temperature Studies. Part II. Thermodynamic Properties of the Carbides," University of California Radiation Laboratory Report, UCRL-2888, April, 1955.

of UO₂ in oxygen under such conditions that it ignites, followed by cooling in oxygen, leads to U₃O₈.

A piece of uranium metal sheet (99.98% U, 0.01% C, 0.01% other metals) weighing 7.3747 g. was oxidized slowly in oxygen as the temperature was raised to 1000° and then lowered to give an oxide weighing 8.7061 g. and having the formula UO_{2.689}. This was then reduced at 1000° with CO to give an oxide weighing 8.3667 g. and having the formula UO_{2.004}. Finally, this was burned in oxygen so that it ignited and glowed, and then cooled in oxygen, giving an oxide weighing 8.6961 g. and having the formula UO_{2.669}.

In a similar experiment, the combustion product from a calorimetric experiment on a UC_{1.9}-UO₂ mixture weighing about 17 g. was heated in oxygen at 750° with no resultant change in weight. It was then reduced with CO and reoxidized with oxygen. The final weight was 2 mg. less than the starting weight. Therefore, it was concluded that the combustion product was very close to UO_{2.667} or U₃O₈.

THE HEAT OF FORMATION OF SCANDIUM OXIDE¹

By ELMER J. HUBER, JR., GEORGE C. FITZGIBBON,
EARL L. HEAD, AND CHARLES E. HOLLEY, JR.

University of California, Los Alamos Scientific Laboratory,
Los Alamos, New Mexico

Received March 11, 1963

The heats of formation of the oxides of the metals of groups IA and IIA increase with decreasing atomic number. This tendency also appears in group IIIA for La₂O₃ and Y₂O₃. The heat of formation of Sc₂O₃ is of considerable interest because, if its heat of formation should be larger than that of Y₂O₃, it would be the oxide with the highest heat of formation per oxygen atom.

The authors reported a preliminary value for the heat of formation of Sc₂O₃ as $\Delta H_{298^\circ} = -456.23 \pm 0.55$ kcal./mole.² This value was based on experiments in which scandium metal was burned on impure scandium oxide disks, and the scandium oxide combustion product did not have the right lattice size. These experiments have now been supplemented by combustion on purified scandium oxide disks, and experiments have been done on the heat of solution of scandium metal and scandium oxide.

Experimental

Scandium Metal.—Scandium oxide obtained from the Laboratoire des Terres Rares, Paris, France, was purified by the thiocyanate method of Fischer and Bock.³ Metal was prepared from this purified oxide by the Ames Laboratory, A.E.C., through the courtesy of Dr. F. H. Spedding. It was found by analysis to contain the following per cent impurities: C, 0.062; H, 0.0085; O, 0.0375; N, 0.0075; Ta, 0.009; Mg, 0.01; Al, 0.05; and Y, 0.05. No other metallic impurities were detected. The total impurities amount to about 0.24%.

An X-ray pattern revealed hexagonal Sc only with no impurities. A metallographic examination showed unidentified impurities at the grain boundaries.

If it is assumed that the C, H, O, and N are combined with scandium as the carbide, hydride, oxide, and nitride, the scandium is 99.51 mole % metal (atomic weight of Sc = 44.96).

Combustion of Scandium.—The method, which involves the

(1) Work done under the auspices of the Atomic Energy Commission.

(2) E. J. Huber, Jr., and C. E. Holley, Jr., "Experimental Thermochemistry," Vol. 2, H. A. Skinner, Ed., Interscience Publishers, Inc., New York, N. Y., 1962, Chapter 5, p. 89.

(3) W. Fischer and R. Bock, *Z. anorg. allgem. Chem.*, **249**, 146 (1942).

determination of the heat evolved from the combustion of a weighed sample of the metal in a bomb calorimeter at a known initial pressure of oxygen, has been described.⁴ The same units and conventions are used here.

The scandium was burned on sintered disks of Sc_2O_3 in oxygen at 25 atm. pressure. The metal did not gain weight when exposed to this pressure for 1 hr. Ignition was by means of a magnesium fuse wire. Completeness of combustion was determined by dissolving the combustion products in hydrochloric acid solution, measuring the amount of gas formed, and analyzing the gas for hydrogen with a mass spectrograph. The average initial temperature for the runs was 24.9°.

The results are listed in Table I. The first 10 runs were done on impure Sc_2O_3 disks which contained a few per cent of ThO_2 . The completeness of combustion varied between 99.03 and 100.00%. The last three runs were done on purified Sc_2O_3 disks. For these three runs, the completeness of combustion was 97.4, 94.0, and 93.5%, respectively. No satisfactory explanation for this difference is readily available.

The scandium oxide from the first 10 runs had a lattice constant of about 9.948 Å., which is high. This is believed to be due to ThO_2 from the impure disk dissolving in the molten Sc_2O_3 from the combustion. From the last three runs the lattice constant was 9.8450 ± 0.0003 Å.

The average value of 5056.1 ± 4.6 cal./g. for the heat of combustion must be corrected for the impurities present.

TABLE I
THE HEAT OF COMBUSTION OF SCANDIUM

Mass of Sc burned, g.	Wt. of Mg, mg.	Wt. of Sc_2O_3 , g.	Energy equiv., cal./deg. ^a	ΔT , °K.	Energy from firing, cal.	Sc, cal./g.	Dev. from mean, cal./g.
0.4460	6.05	24.7	2397.0	0.9602	5.9	5067.1	11.0
.5937	6.05	16.8	2394.8	1.2720	9.7	5054.5	1.6
.5414	8.03	17.0	2394.9	1.1636	6.0	5059.5	3.4
.5808	6.01	16.9	2394.8	1.2473	4.7	5073.8	17.7
.5419	6.53	16.8	2394.8	1.1631	5.2	5059.3	3.2
.4881	5.93	16.8	2394.8	1.0453	6.1	5044.4	11.7
.5096	6.93	17.1	2394.9	1.0951	6.8	5053.0	3.1
.5649	7.02	16.9	2394.8	1.2123	6.7	5054.2	1.9
.5223	6.02	16.3	2394.7	1.1195	7.0	5051.4	4.7
.5113	5.94	16.8	2394.8	1.0981	6.5	5061.4	5.3
.5150	6.50	15.1	2394.3	1.1032	4.9	5044.9	11.2
.5199	6.67	17.4	2395.0	1.1147	5.3	5048.8	7.3
.5448	6.82	18.0	2395.1	1.1687	4.2	5056.9	0.8
					Av.	5056.1	6.4
					2 × standard dev.		4.6

^a The specific heat of Sc_2O_3 is estimated at 0.066 cal./g./deg.

Correction for Impurities.—The calculated percentage composition of the scandium by weight is Sc metal, 99.37; ScH_2 , 0.19; Sc_2O_3 , 0.11; ScN , 0.03; ScC_2 , 0.18; Ta, 0.01; Mg, 0.01; Al, 0.05; Y, 0.05. The heat of combustion of Sc metal corrected for impurities is 5062.1 ± 5.6 cal./g., or 0.12% larger than the uncorrected value.⁵ This value would be decreased by 0.06% if the combustion products, CO_2 , H_2O , and NO_2 , were assumed to react with the Sc_2O_3 to form $\text{Sc}_2(\text{CO}_3)_3$, $\text{Sc}(\text{OH})_3$, and $\text{Sc}(\text{NO}_3)_3$. This is not believed to occur because of the rather unreactive nature of fired Sc_2O_3 .

The uncertainty attached to this corrected value includes the uncertainty in the energy equivalent of the calorimeter, which is 0.04%, the uncertainty in the calorimetric measurements, 4.6 cal./g. or 0.09%, and the uncertainty in the correction for the impurities,

(4) E. J. Huber, Jr., C. O. Matthews, and C. E. Holley, Jr., *J. Am. Chem. Soc.*, **77**, 6493 (1955).

(5) The heat of formation of ScH_2 is taken as -52 kcal./mole. That of ScN is estimated at -75 kcal./mole, and of ScC_2 at -30 kcal./mole. The heats of combustion of Mg, Al, Y, and Ta are taken as 5900, 7400, 2560, and 1350 cal./g., respectively. The heats of formation of $\text{H}_2\text{O}(\text{g})$ and NO_2 are taken as -58 and $+8$ kcal./mole.

which is estimated at 0.06%. The combined uncertainty is 0.12% or 5.6 cal./g., which does not include the possibility that the CO_2 , H_2O , and NO_2 may react with the Sc_2O_3 . The value for the heat of combustion of 2 moles of Sc is 455.18 ± 0.50 kcal. under bomb conditions.

Heat of Solution of Scandium.—The heat of solution of scandium metal was measured in a solution of HCl which contained a small amount of Na_2SiF_6 . The latter compound was used as a solution aid for Sc_2O_3 and was present in the Sc metal experiments so that the final solution would be the same in both cases.

The solution calorimeter has been described.⁶ The same metal was used as for the combustion experiments. The solvent was saturated with hydrogen before the start of the experiment, and the atmosphere above the solution was hydrogen. The metal was contained in a small Pyrex glass ampoule which was broken to start the reaction. The results of five experiments are shown in Table II.

TABLE II
THE HEAT OF SOLUTION OF SCANDIUM METAL
Solvent: 4.020 M HCl plus 200 mg. of Na_2SiF_6

Mass of Sc dissolved, g.	Mass of solvent, g.	Energy equiv., cal./arbitrary unit	Temp. rise, arbitrary units	Energy from Sc, cal./g.	Dev., cal./g.
0.12962	383.88	15.257	28.335	3335.1	0
.13012	385.35	15.278	28.395	3333.9	1.2
.13048	386.42	15.258	28.515	3334.4	0.7
.13027	385.80	15.290	28.395	3333.2	1.9
.13078	387.31	15.335	28.475	3338.9	3.8
			Av.	3335.1	1.5
			Cor. for H_2O evap.	15.6	
			Heat of soln. of Sc metal	3350.7	
			2 × stand. dev.		2.0

The average value for the five experiments is 3350.7 ± 2.0 cal./g. for the heat of solution of this scandium metal in this solvent. When corrected for the presence of impurities, this becomes 3359.2 ± 5.7 cal./g. or 151.02 ± 0.26 kcal./mole, where the uncertainty includes an estimated uncertainty of 0.16% in the correction for the impurities.⁷

The Heat of Solution of Scandium Oxide.—Scandium oxide as ordinarily prepared by ignition of the oxalate to 1000–1100° is only slowly soluble in HCl solutions, even in the presence of fluorosilicate ion. If, however, the oxide is prepared by ignition at only 600°, it will dissolve rapidly enough in the presence of fluorosilicate ion to be used in the experiments. Prepared in this manner it is about 99.2% Sc_2O_3 , with the impurities probably being oxalate fragments plus some excess carbon.⁸

The heat of solution of this scandium oxide was measured in the same solvent as for the scandium metal including the saturation of the solvent with hydrogen and the presence of a hydrogen atmosphere above it. An amount of Sc_2O_3 was used so that the concentration

(6) G. C. Fitzgibbon, E. J. Huber, Jr., and C. E. Holley, Jr., "A New Solution Calorimeter," Los Alamos Scientific Laboratory, L A Report, in preparation.

(7) H. Bommer and E. Hohmann, *Z. anorg. allgem. Chem.*, **248**, 357 (1941), give 149.0 ± 0.7 kcal./mole for the heat of solution of scandium metal in dilute hydrochloric acid solution.

(8) E. L. Head and C. E. Holley, Jr., to be published.

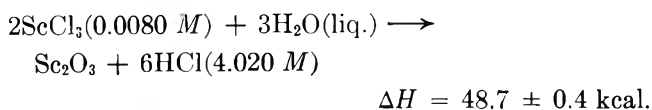
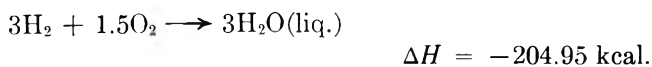
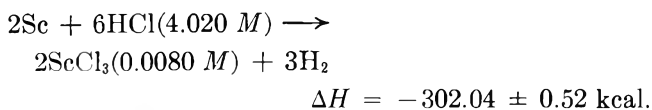
of scandium in the final solution would be the same as in the final solution from the metal. The results of five runs are shown in Table III. The final average value is 348.6 ± 3.0 cal./g., or 48.7 ± 0.4 kcal./mole. This value is not correct because of the impurities in the Sc_2O_3 ; however, the state of the impurities is not known and a correction for them is not possible. The value given should be regarded as a lower limit on the heat evolved because the impurities probably would have a smaller heat of solution than the oxide.

TABLE III
THE HEAT OF SOLUTION OF SCANDIUM OXIDE
Solvent: 4.020 M HCl plus 200 mg. of Na_2SiF_6

Mass of Sc_2O_3 dissolved, g.	Mass of solvent, g.	Energy equiv., cal./arbitrary unit	Temp. rise, arbitrary units	Energy from Sc_2O_3 , cal./g.	Deviation, cal./g.
0.19576	377.99	15.003	4.515	346.0	2.6
.20006	386.29	15.345	4.587	351.9	3.3
.19966	385.52	15.270	4.540	347.2	1.4
.19918	384.59	15.270	4.597	352.5	3.9
.19997	386.12	15.250	4.531	345.4	3.2
			Av.	348.6	2.9
			$2 \times$ stand. dev.		3.0

The Heat of Formation of Sc_2O_3 .—Using methods already described,⁴ the heat of formation of cubic Sc_2O_3 is calculated from the combustion results to be $\Delta H^0_{f2980} = -456.16 \pm 0.50$ kcal./mole.

From the heat of solution measurements the heat of formation of Sc_2O_3 may be calculated as



Because the heat of solution of the Sc_2O_3 is a minimum value, this calculated heat of formation is a maximum value. The difference between the two values, 2 kcal., may be attributed in part, at least, to the impurity of the Sc_2O_3 used in the heat of solution experiments, and the combustion value should be more nearly correct.

This value of -456.16 ± 0.50 kcal./mole is to be compared with $\Delta H^0_{f298} = -447.28 \pm 0.23$ kcal./mole reported by Mah.⁹ In her work the combustion was carried out on Alundum instead of on Sc_2O_3 . Because of this discrepancy, Mrs. Mah did some experiments on scandium metal supplied by us. She obtained 5065.0 cal./g.¹⁰ when the combustion was carried out on a scandium oxide liner. This value falls within our range of values. She obtained 4964.3 cal./g. when the combustion was carried out on an Alundum disk, checking her previously published value of 4964.2 cal./g. These

(9) A. D. Mah, U. S. Bur. Mines Report Invest. 5965 (1962).

(10) A. D. Mah, private communication.

results indicate that the discrepancy was caused by the Alundum.

This new value for the heat of formation of scandium oxide is the same as the value for yttrium oxide, -455.45 ± 0.54 kcal./mole,¹¹ within the experimental uncertainties involved.

Acknowledgments.—The authors acknowledge the valuable assistance of D. Pavone, F. H. Ellinger, O. R. Simi, and R. M. Douglass in the analytical work.

(11) E. J. Huber, Jr., E. L. Head, and C. E. Holley, Jr., *J. Phys. Chem.*, **61**, 497 (1957).

FURTHER REMARKS ON THE "RATE-QUOTIENT LAW"¹

BY O. K. RICE

Department of Chemistry, University of North Carolina,
Chapel Hill, North Carolina

Received February 4, 1963

In a recent publication, Pritchard² considers the effect upon the rate of dissociation of a diatomic molecule arising from a "bottleneck" with respect to quantum jumps up the vibrational ladder. He believes the possible presence of a bottleneck could vitiate the argument which this author gave,³ indicating the equality between the equilibrium constant for association of atoms and dissociation of diatomic molecules and the quotient of the rate constants (to which the author will refer as the "rate-quotient law"), even under conditions such that equilibrium quotas were not maintained in some of the excited vibrational levels. One of the essential bases of this author's argument was the assumption that activation and deactivation were rapid processes compared to reaction, which meant that the vibrational relaxation of the diatomic molecule was supposed rapid compared with the rate of reaction. The author quoted data⁴ which indicated that under ordinary circumstances this condition is fulfilled. Recently, Camac and Vaughan⁵ have investigated the dissociation of O_2 up to 8000° , where the time for attainment of equilibrium between vibration and translation is of the same order of magnitude as the time required for dissociation. In this case, they find it impossible to analyze the data so as to determine a rate constant for dissociation, as is to be expected, but the normal situation is that relaxation is fast compared to reaction.

The data for relaxation in shock waves are, however, presumably sensitive only to relaxation of some of the lower vibrational levels, and a bottleneck is something which might hinder the relaxation of the higher vibrational levels. Pritchard's argument, therefore, requires some further consideration.

Pritchard's bottleneck arises not from any decrease in the rate of transition as the vibrational energy level increases, because the probability of such transitions is assumed to increase as the vibrational quantum number goes up. Actually, it arises from the decrease in population due to the Boltzmann factor, which, coupled with the increase in the rate of the quantum jumps, might conceivably mean that a minimum transition rate

(1) Work supported by the National Science Foundation.

(2) H. O. Pritchard, *J. Phys. Chem.*, **66**, 2111 (1962).

(3) O. K. Rice, *ibid.*, **65**, 1972 (1961).

(4) E. F. Smiley and E. H. Winkler, *J. Chem. Phys.*, **22**, 2018 (1954).

(5) M. Camac and A. Vaughan, *ibid.*, **34**, 460 (1961).

occurs at some energy level below the dissociation, or would, were equilibrium established at each energy level. It does not appear that the actual rate expressions he suggests would result in such a minimum, but it is certainly conceivable. However, this cannot be properly described as a bottleneck (Pritchard actually does not use this word, but he does compare the process to that occurring in an hour glass), since it does not depend on an intrinsically slow rate. Since the intrinsic transition rates are supposed to be faster for high vibrational levels than for low ones, there cannot be any hindrance to the vibrational relaxation, and this author's argument for the rate-quotient law will go through as before. The hypothesis of rapidity of activation or deactivation of a molecule in an excited state will, indeed, be strengthened if Pritchard's assumptions concerning the rates of vibrational transitions are correct.

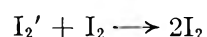
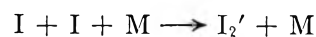
It is quite true that the trend in the rate of vibrational transitions suggested by Pritchard would have an effect on the rate of reaction and on its temperature coefficient, though if we judge by the table given in his article⁶ on the recombination of H atoms in the presence of He the effect should not be drastic. The problem which we are discussing here is a different one, however, since it does not involve the effect on either the dissociation or the association but the relation between the two.

In his article, Pritchard² gives a figure which correctly shows the course of the behavior of a system of dissociating diatomic molecules, there being an induction period in which the upper levels reach their steady states, and after this the rate changes very slowly as the concentration of molecules decreases and the concentration of atoms reaches its equilibrium value. It should only be emphasized that the induction period will normally be very short. However, in discussing the association he states that the rate (essentially of production of molecules in energy levels near the ground state) will be "modified by a parameter which depends on the extent to which the populations of the lower levels are disturbed." It would seem that this accounts for a large part of the difference in our views. If the vibrational relaxation is fast, molecules will appear in the ground state essentially as soon as they are deactivated to a point where redissociation is unlikely; competition between the latter process and redissociation is rate-determining, and intermediate levels have no effect.

It may be worth while to consider the possible effects of a real bottleneck, in which the intrinsic rate of transition over a range of vibrational levels is actually very small. In such a case the rate-determining step in either direction will be passage through the bottleneck. Once an associating pair has passed through the bottleneck it will be quickly deactivated. The energy levels above the bottleneck will usually be expected quickly to come to a steady state, and the probability that a molecule in one of them will redissociate will be high. On the other hand, a dissociating molecule, once having passed through the bottleneck, will dissociate relatively quickly, so again a steady state will be reached. The fate of a molecule passing through the barrier in either direction will depend only on collisions

with the third body and will be independent of the number of reacting molecules or atoms present (except as one of them may, itself, be the third body). The conditions for application of the arguments presented in an earlier paper³ thus are fulfilled, provided the rate of reaction is considered to be the rate of passage past the bottleneck.

However, there is a conceivable exception to the situation described in the preceding paragraph. If the bottleneck occurs over a range of levels whose energy is sufficiently low, it might be that under some circumstances, the equilibrium number of molecules above the bottleneck would be comparable to the number of dissociated atoms. In this case it would not be possible to set up a steady condition for molecules in these levels. If one had some scheme for measuring disappearance of atoms, it would be found that they would at first disappear as though they were forming a quasi-molecule all of whose energy levels were above those of the bottleneck. This would not be simply related to the rate of dissociation, which would be governed by passage through the bottleneck. On the other hand, if one measured the rate of association as the rate of appearance of molecules in their lower energy states, as is, effectively, the common practice in flash photolysis, one would at first observe an increasing rate, over a long induction period. Some deviations from simple third-order kinetics have, indeed, been observed in the recombination of I atoms.⁷ A decrease in the rate constant was observed as a run proceeded; this was attributed to a heating effect, and under other conditions did not occur.⁸ Also at very low ratios, $(I_2)/(M)$, of the concentration of I_2 to the inert gas M the apparent (initial) rate constant was observed to decrease. It was suggested⁷ that some of the recombination went through a mechanism



where I_2' represents some excited state; at very low $(I_2)/(M)$ ratios the second reaction might be slower than the first and, in a sense, rate-determining, especially if (I_2') comes essentially to an equilibrium value due to the first reaction and its reverse occurring relatively rapidly. This would resemble a bottleneck, but in view of the specific role of I_2 in deactivating I_2' it would seem likely that the latter would be I_2 in another attractive potential-energy curve.

Measurements of the rate of dissociation of I_2 in a shock wave, in the presence of various third bodies at temperatures between 1000 and 2000°K., show an apparent activation energy some 4–9 kcal. less than the dissociation energy.⁹ This suggests the possibility of a bottleneck and hence a rate-determining process at the energy levels which are this far from dissociation. At 1000°K., however, no quasi-molecule with energy of dissociation as small as 9 kcal. would be stable with respect to the atoms, so the conditions would not be such as to cause violation of the rate-quotient law. It seems, however, unlikely that such a bottleneck is the

(7) M. I. Christie, A. J. Harrison, R. G. W. Norrish, and G. Porter, *Proc. Roy. Soc. (London)*, **A231**, 446 (1955).

(8) G. Porter and J. A. Smith, *ibid.*, **A261**, 28 (1961).

(9) D. Britton, N. Davidson, W. Gehman, and G. Schott, *J. Chem. Phys.*, **25**, 804 (1956).

(6) H. O. Pritchard, *J. Phys. Chem.*, **65**, 504 (1961).

true explanation of the temperature coefficients in the shock waves, since temperature coefficients are not directly related to average energy of the dissociating molecules when equilibrium is not established between energy levels.

THE REACTIONS OF ENERGETIC CARBON ATOMS IN METHANE; OXYGEN AND PHASE DEPENDENCE; RADIATION DAMAGE EFFECTS¹

By G. STÖCKLIN, H. STANGL, D. R. CHRISTMAN,
J. B. CUMMING, AND A. P. WOLF²

Chemistry Department, Brookhaven National Laboratory,
Upton, L. I., New York

Received February 12, 1963

The reactions of energetic carbon-11 species impinging on a gaseous system comprised of 2% oxygen and 98% methane have been described by MacKay and Wolfgang.³ The oxygen was added to "minimize radiation induced reduction of unsaturated hydrocarbon products and to act as a scavenger for carbon atoms."³ Results for oxygen-free methane were not reported since a consistently high CO yield was obtained by these authors in runs where oxygen had not been purposely added.⁴ A similar result while not apparent in the case of higher homologous hydrocarbons studied by the same authors^{5,6} was experienced in a study of the C¹¹ + H₂ system.⁵ They suggested that C¹¹O might have arisen either from trace-impurity oxygen in the hydrogen or from oxidation of the C¹¹ at the wall of the vessel.

In order to gain more information on the methane system we have continued the study of methane, varying a variety of chemical and physical parameters. We have used the nuclear reactions C¹²(n,2n)C¹¹ and C¹²(p,pn)C¹¹ to produce the carbon-11.

Experimental

Purification of Methane.—Traces of CO₂ were removed from the methane (Phillips Research Grade) by passing the methane through Ascarite. The gas was then transferred to a 500-cc. stainless steel oven containing calcium turnings (previously degassed at room temperature; 24 hr. pumping at 10⁻⁵ mm.; temperature raised to 350°; baked at 350° for 3 days while pumping). The oven, containing CH₄, was closed to the line and kept at 350° for 15 min. This procedure reduced the oxygen content from 100–200 p.p.m. (O₂ content of our Phillips methane sample) to below 10 p.p.m. (limit of assay method) of O₂. The N₂, normally at 200 p.p.m., was reduced to 50 p.p.m.

Miscellaneous Compounds.—The acetylene and ethylene used were Matheson, C.P. grade. Each gas was purified by multiple crystallization. The oxygen (Matheson, C.P. grade) was used without further purification.

Irradiation Techniques.—The experimental irradiation technique for the C¹²(n,2n)C¹¹ reaction was essentially that described by Suryanarayana and Wolf.⁷ The induced specific activities ranged from 3000–6000 d.p.m./cc. methane at NTP. The tank material was quartz.

The Brookhaven Cosmotron was used for the C¹²(p,pn)C¹¹ reaction. Proton energies of 2–3 g.e.v. were used at intensities of 10¹⁰–10¹¹ protons per pulse (12/min.) in an external beam.

(1) Work performed under the auspices of the U. S. Atomic Energy Commission.

(2) Requests for reprints should be directed to this author.

(3) C. MacKay and R. Wolfgang, *J. Am. Chem. Soc.*, **83**, 2399 (1961).

(4) Dr. Colin MacKay, private communication.

(5) C. MacKay, M. Pandow, P. Polak, and R. Wolfgang, "Chemical Effects of Nuclear Transformation," IAEA, Vienna, 1961, Vol. II.

(6) C. MacKay and R. Wolfgang, *Radiochim. Acta*, **1**, 42 (1962).

(7) B. Suryanarayana and A. P. Wolf, *J. Phys. Chem.*, **62**, 1369 (1958).

The irradiation cylinder was 2S aluminum, 200 mm. l. × 40 mm. i.d. The cylinder was lined up with the beam by taking a picture of the beam (Polaroid film) at both ends of the tank using one pulse to expose the film. Details of the shadow cast by the tank in the developed film allowed simple correction of alignment. The total activity induced in the gas was compared with that induced in polyethylene foils⁸ held at both ends of the tank during the run, appropriate corrections for C¹¹ loss from the foil being made first. In all cases, using methane, we found 95+ % of the activity produced (using the foil as the absolute monitor) to be in the gas phase. The specific activities were 2000–4000 d.p.m./cc. methane at NTP.

The total activity cannot be assayed directly when using the n,2n reaction. However, in all cases studied, the activity produced was proportional to the integrated value for the deuterons impinging on the LiH target. The fact that nearly all the carbon-11 activity produced by the p,pn reaction is found in the gas, coupled with the fact that product distributions were identical at the same doses for the two nuclear reactions, leads us to suggest that 95–100% of the activity is also recovered in the gas phase when using the n,2n reaction.

Dosimetry.—Dose measurements were made using conventional ferrous sulfate dosimetry. The carbon-11 activity per accompanying dose in d.p.m./mg. of C per e.v./molecule is ~6 × 10⁶ for the n,2n reaction and ~5 × 10⁷ for the p,pn reaction. The methane received 10⁻⁴ to 10⁻³ e.v./molecule in most runs. (See also Table I.)

TABLE I
DOSE DEPENDENCE IN METHANE (n,2n)
YIELDS IN PER CENT OF TOTAL CARBON-11 IN GAS PHASE

	4.8 × 10 ⁻⁴ e.v./ molecule	8.3 × 10 ⁻⁴ e.v./ molecule
CO ^a ^a
CH ₄	13.9 ± 2.2	6.9 = 0.5
C ₂ H ₂	17.7 ± 1.4	14.0 = .7
C ₂ H ₄	12.4 ± 1.1	6.6 = .6
C ₂ H ₆	23.9 ± 2.0	29.4 = .6
C ₃ H ₈	11.2 ± 2.3	20.2 ± .6
Allene	3.0 ± 1.0
Higher boiling	17.9	22.9

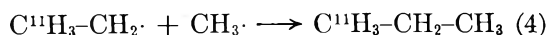
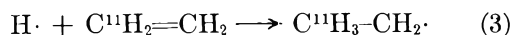
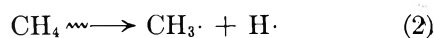
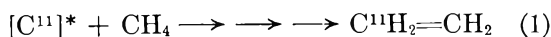
^a Below detectable limit of ~0.2%.

Activity Assay and Compound Identification.—The compounds produced were identified and the activities measured by a combination of g.l.c. and gas phase effluent counting.⁹ The columns were attached to a single manifold allowing rapid switch-over during successive runs.

The specific activity of the irradiated gas was determined by by-passing the columns and sending an aliquot directly through our effluent window counter. In some instances static internal proportional counting of an aliquot from the tank was carried out.

The Effect of Dose and Scavenger.—Concomitant radiolysis of the methane during carbon-11 production clearly affects product distribution (Table I). A factor of two in absorbed dose produces an increase in ethane-C¹¹ yield and an even greater increase in propane-C¹¹ yield. The yields of methane, ethylene, and acetylene are seen to decrease. Several mechanisms are probably operative.

The most probable mechanism for propane formation in our view is outlined by eq. 1–4.



(8) J. B. Cumming, A. M. Poskanzer, and J. Hudis, *Phys. Rev. Letters*, **6**, 484 (1961).

(9) Cf. F. Cacace, *Nucleonics*, **19**, 5, 45 (1961), for a review of this technique. The specific techniques used will be found in G. Stöcklin, F. Cacace, and A. P. Wolf, *Z. Anal. Chem.*, **194**, 406 (1963).

In this mechanism the ethylene-C¹¹ scavenges a radiolytically produced hydrogen atom, the resultant radical then reacting with a radiolytically produced methyl radical. An alternative to this mechanism involving reaction of ethylene-C¹¹ with a methyl radical and then a reaction with a hydrogen atom cannot be distinguished from the mechanism given by eq. 1-4 under our conditions. A third mechanism, which might account for the major portion of the propane-C¹¹, involving the scavenging of methyl-C¹¹ radicals by radiolytically produced ethylene is ruled out by the data in column 4, Table II. The addition of scavenger ethylene¹⁰ would be expected to lead to an unchanged yield of propane-C¹¹ or perhaps to enhance it slightly (efficient scavenging of C¹¹H₃·) if this mechanism were operative. The appreciable drop observed in the propane-C¹¹ yield is inconsistent with the consequence of mechanism three but in support of mechanism one (and its alternative).

The mechanism of ethane-C¹¹ formation can also be understood in terms of the reactions of the accompanying radiolytically and recoil produced species.

TABLE II

SCAVENGER AND PHASE DEPENDENCE OF PRODUCT DISTRIBUTION IN THE CARBON-11 RECOIL PRODUCTS IN METHANE [C¹²(n,2n)C¹¹]

	Yields in % of total carbon-11 in gas phase ^a				Solid CH ₄ glass at -196°
	0.00% O ₂	0.12% O ₂ ^b	2.0% C ₂ H ₂	1.2% C ₂ H ₄	
CO ^c	20.4 ± 3.1 ^d	.. ^e ^c	.. ^e
CH ₄	13.9 ± 2.2 ^d	<0.15	1.9 ^c	4.5
C ₂ H ₂	17.7 ± 1.4	32.3 ± 2.3	32.8	25.2 ± 0.1 ^d	28.1
C ₂ H ₄	12.4 ± 1.1	30.5 ± 0.3	29.5	23.5 ± 0.6	27.2
C ₂ H ₆	23.9 ± 2.0	<0.5	6.0	3.4 ± 0.1	11.3
C ₃ H ₈	11.1 ± 2.3 ^c	.. ^e	1.7 ± 0.2	4.5
Allene	3.0 ± 1.0	<1.0	.. ^e ^c	.. ^e
Higher boiling	17.9	15.9 ^e	29.8	46.2 ^f	24.4

^a Approximate absorbed dose for these runs = 4 to 5 × 10⁻⁴ e.v./molecule. Irradiation time = 40 min. Additive concentrations are in volume % with total pressure equal to 1 atm. at 25°. Solid methane was flash evaporated. ^b Oxygen concentration at which we observe the maximum C₂¹¹H₂ and C₂¹¹H₄ yields. ^c Below detectable limit of ~0.2%. ^d A.D. of replicate runs. ^e The average yield of all higher boiling products of all other methane-oxygen mixtures studied (given in Fig. 1) is 18.4 ± 1.7. At all oxygen concentrations above 2% we observed a 2% yield of CH₃OH also. ^f The yield of cyclopropane is 2.8 ± 0.7 and the yield of propene is 1.5 ± 0.3. Isobutane, *n*-butane, butene-1, isobutylene, and propyne are all present but each in yields less than 1%. We were unfortunately unable to analyze for C₃-hydrocarbons. One might expect a fair yield of these compounds.

The ethane-C¹¹ yield is reduced from 23.9 to 3.4% for 1.2% of added ethylene and to 6% for 2.0% of added acetylene. With added oxygen the yield drops from 23.9% to less than 0.5%. The ethylene-C¹¹ yield rises from 12.4% in the unscavenged system to a maximum of 30.5% when 0.12% oxygen is present. The yield of acetylene-C¹¹ also rises under the same conditions.

Oxygen is a good alkyl radical trap and hydrogen atom trap. It can also react with such things as triplet "radicals" but its efficiency is probably not as great in this case.¹¹ The scavenger action of ethylene and acetylene is well known.

Based on these observations it is reasonable to as-

(10) In the high conversion radiolysis of methane using ethylene-C¹⁴ as a scavenger, F. Schmidt-Bleek, M. Koyama, and F. S. Rowland, University of Kansas (private communication) find the main products to be C₂¹⁴H₂ and C₂¹⁴H₄. Their system is also very sensitive to oxygen.

(11) D. W. Setser, D. W. Placzek, R. J. Cvetanović, and B. S. Rabinovitch, *Can. J. Chem.*, **40**, 2179 (1962).

sume that reduction by hydrogen atoms is probably occurring in the unscavenged system.

At least part of the ethane-C¹¹ observed may be formed by methylene-C¹¹ insertion reactions (*cf.* reference 12). When using ethylene scavenger the methylene insertion products, ethane-C¹¹ (C¹¹H₂: + CH₄) and cyclopropane¹² (C¹¹H₂: + CH₂=CH₂) account for 6.2% of the carbon-11 produced. Added acetylene allows a 6% yield of ethane-C¹¹ to be formed. The presumed cyclopropene-C¹¹ (C¹¹H₂: + CH≡CH), if formed at all, would not be detected under our conditions. The ethane-C¹¹ yield from the C-11 insertion reaction in methane containing oxygen might be less than what would be expected because of the known but inefficient¹¹ reaction of oxygen with such species.

Ethane-C¹¹ cannot arise from methyl radical recombination (C¹¹H₃· + CH₃·) since the addition of ethylene scavenger to the system before irradiation reduces the propane-C¹¹ yield rather than enhancing it.

In addition, consideration of rate constants for known hydrogen abstraction reactions and for radical recombination reactions, the dose rate in our system, and the *G*-values for radical production in methane indicates that hydrogen abstraction is several orders of magnitude less frequent than radical recombination. An abstraction reaction leading to ethane-C¹¹ (CH₃-CH₂· + RH → C¹¹H₃-CH₃ + R·) is therefore unlikely.

The data are therefore at least in qualitative agreement with the hypothesis that ethane-C¹¹ formation in unscavenged methane is caused primarily by hydrogen atom reduction of ethylene-C¹¹ and by methylene-C¹¹ insertion reactions.

In the case of the reaction of energetic carbon in the methane system, no significant oxidation of the carbon-11 occurs at the walls since the absence of gaseous oxygen in the methane eliminates the appearance of CO. Further it is unlikely that the wall is acting as a third body since (1) the gas pressure is 1 atm., and (2) the geometry of our reaction vessels and their materials of construction are quite different in different experiments; yet no effect is observed in product distribution at comparable absorbed doses.

The addition of oxygen (data plotted in Fig. 1) essentially eliminates methane-C¹¹, ethane-C¹¹, and propane-C¹¹ (*cf.* columns 1 and 2, Table II). Oxygen can react as a scavenger for hydrogen atoms, as suggested by MacKay and Wolfgang, but it is also reacting as a general radical scavenger. Furthermore in view of the marked dependence of product distribution on varying oxygen concentration it seems reasonable to assume that the oxygen may also be reacting with non-thermal and excited species.

The effect of oxygen can be summarized as follows: (1) the elimination of the radiolytically produced species which transform part of the "primary" recoil products (*e.g.*, stabilized C₂H₂ and C₂H₄) to other

(12) The ratio of propene-C¹¹ to cyclopropane-C¹¹ is ≈ 0.53. This ratio is comparable to what was found for the butenes/methylcyclopropane ratio when propylene and methylene (from ketene) were allowed to react at ~1 atm. total pressure [J. N. Butler and G. B. Kistiakowsky, *J. Am. Chem. Soc.*, **82**, 759 (1962)]. Nothing more than a qualitative comparison with the work of Butler and Kistiakowsky (energy of CH₂·, energy of the adduct, ratios, etc.) is possible here because of the error limits of our ratios.

(13) The systems ethane-oxygen and propane-oxygen (paper in preparation) do not show this rise at any oxygen concentration we were able to achieve. It is possible that a self-protective effect (*e.g.*, such as radiolytically induced olefin formation, *i.e.*, *in situ* scavenger production) may be operating here.

compounds thereby causing an initial rise¹³ in the yield of acetylene-C¹¹ and ethylene-C¹¹, and (2) the reaction of oxygen with energetic carbon atoms and with some of the precursors of the observed products resulting in a continual decrease of acetylene, ethylene, and other products as the oxygen concentration is increased. This effect reflects the competition of oxygen with the substrate for the precursors involved (*cf.* curves in Fig. 1).

The effect of added acetylene (column 3, Table II) is self-protective in nature, the yield of acetylene and ethylene going up as in the case of added oxygen. Apparently acetylene is not as reactive as ethylene in interfering with some of the other reactions.

The Effect of Phase.—If one considers the yield of acetylene and ethylene to be indicative of the amount of radiation damage the system receives during carbon-11 formation, in the sense that the yields of these products at relatively low oxygen concentrations (where the curves, Fig. 1, are at their maximum) are those to be expected when no radiation is present (*i.e.*, when only energetic carbon atoms are introduced), then it can be suggested that there is little dose effect in the solid. However, it also can be seen (column 5, Table II) that sizable yields of products eliminated in the gas phase by oxygen do appear in the solid, *e.g.*, methane, ethane, and propane ($\Sigma = 20.3\%$). Consequently it is unlikely that the ethane formed in the solid phase irradiation is produced by the reduction of ethylene (*i.e.*, C₂¹¹H₄ = 30% in CH₄+O₂ gas; C₂¹¹H₄ = 28% in CH₄ glass). In the gas phase in the absence of O₂ it is probable that at least some of the ethane is formed in this way. In the solid phase a large fraction of the ethane is probably formed by methylene-C¹¹ insertion into methane.¹⁴

The pronounced phase effect leading to decreased ethylene and acetylene yields observed in ethane and propane (*cf.* reference given in footnote 14) is not apparent here. This may be a reflection of the relative inability of methane, because of its limited number of degrees of freedom, to de-excite the energetic intermediates which lead to acetylene and ethylene. Their formation is thus relatively unhindered, sufficient energy being available in the complex for the requisite bond rupture and rearrangement processes.

The Effect of the Type of Nuclear Reaction.—In all cases, in duplicate systems, the product distributions resulting from inducing the C¹²(p,pn)C¹¹ reaction were the same within experimental error as those resulting from the C¹²(n,2n)C¹¹ reaction. We therefore felt it superfluous to include product data from the C¹²(p,pn)C¹¹ runs. Nevertheless the use of these two nuclear processes allowed us to cross check the effect of such parameters as varying radiation intensity and type of radiation, the effect of irradiation vessel materials, and such other parameters as might be thought to have an effect on the results. In addition it provides another case where the initial recoil energy of the reactive fragment has no bearing on the product

(14) The yields of the presumed methylene insertion products (*e.g.*, C¹¹H₂: + CH₄ → C¹¹H₃-CH₃) in condensed phases is curiously constant in three systems, being 11.3% in methane, 11.5% in ethane, and 12.1% in propane. (Ethane and propane reactions are discussed by G. Stöckli and A. P. Wolf, *J. Am. Chem. Soc.*, **85**, 229 (1963)). This would suggest that the formation of C¹¹H₂: is independent of the compound being irradiated in a homologous series of this sort, a fixed fraction being formed and then reacting in a statistical way with the substrate.

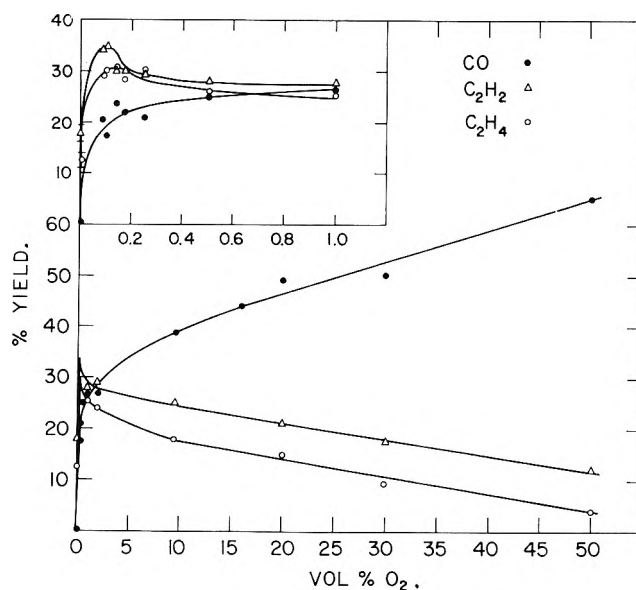


Fig. 1.—Oxygen dependence of acetylene-C¹¹ and ethylene-C¹¹.

distribution observed. The maximum recoil energy for the C¹²(n,2n)C¹¹ process is 1.1 Mev., whereas the mean recoil energy¹⁵ for the C¹²(p,pn)C¹¹ process is ~1.8 Mev.

Acknowledgment.—The authors wish to acknowledge the helpful discussions with Dr. H. A. Schwarz of this Laboratory relative to free radical reactions and the radiation chemistry of the system.

(15) S. Singh and J. M. Alexander, University of California Lawrence Radiation Laboratory Report, UCRL-9911, October 24, 1961.

DIELECTRIC PROPERTIES OF THE HYDRATE OF TRICHLOROFLUOROMETHANE

BY WALLACE S. BREY, JR., AND JOHN W. LEGG

Department of Chemistry, University of Florida, Gainesville Florida

Received February 26, 1963

Many non-polar molecules of relatively small size, as well as some quaternary nitrogen compounds, form clathrate compounds with water, in which these molecules are present in cavities in a continuous lattice of the host water.¹⁻⁴ The water structure is somewhat like ice, in that each oxygen has two covalent bonds to hydrogen atoms and two hydrogen bonds to hydrogens on other oxygens, but the ice arrangement is distorted in a way to accommodate more readily the enclathrated molecules. It has been suggested⁵ that structures of this type may be of significance in relation to the interaction of side chains of proteins with water.

It appeared of interest to determine how the physical properties of clathrates of water compare with those of ice itself, and accordingly the dielectric properties of the hydrate of trichlorofluoromethane (Freon 11) have been investigated. The real and imaginary parts of the complex dielectric constant have been measured over the frequency range from 500 c./sec. to 300 kilocycles, and over the temperature range of -50 to +2°.

(1) T. A. Wittstruck, W. S. Brey, A. M. Buswell, and W. H. Rodebush, *J. Chem. Eng. Data*, **6**, 343 (1961).

(2) M. von Stackelberg and W. Jahns, *Z. Elektrochem.*, **58**, 25 (1954).

(3) W. F. Claussen, *J. Chem. Phys.*, **19**, 1425 (1951).

(4) M. Bonamico, G. A. Jeffrey, and R. K. McMullan, *ibid.*, **37**, 2219 (1962).

(5) I. M. Klotz, *Science*, **128**, 815 (1958).

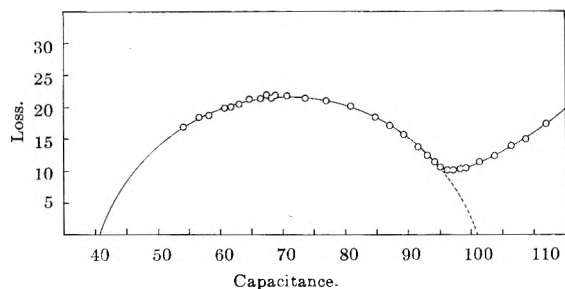


Fig. 1.—Cole-Cole plot for the hydrate of trichlorofluoromethane at 2°. Numerical values are those of the capacitance and loss as measured for the partially filled cell; these are proportional, respectively, to the real and imaginary parts of the dielectric constant.

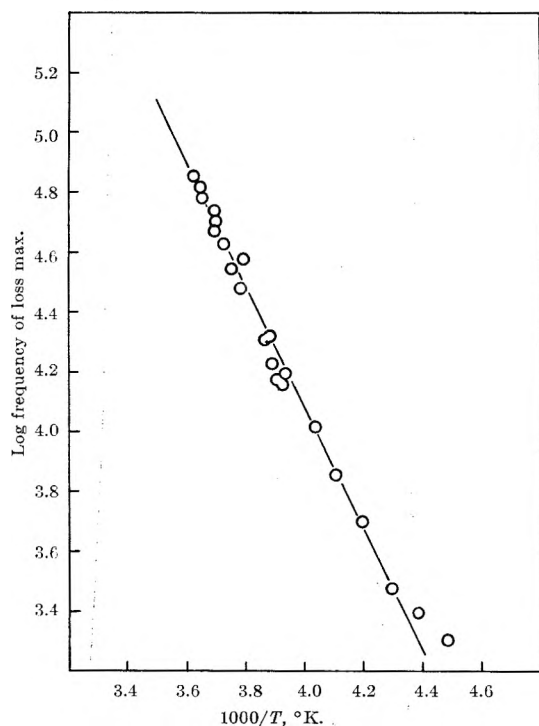


Fig. 2.—Arrhenius plot of the logarithm of the frequency at which the maximum loss is found for the Freon hydrate.

Experimental

A General Radio Type 716-C impedance bridge with 716-P4 guard circuit, 1302-A or 1330-A oscillator, and Tektronix oscilloscope were used for the electrical measurements. The substitution method was employed, with a General Radio precision variable capacitor to obtain the initial balance. Samples were contained in a Balsbaugh Type 350M three-terminal cell constructed of monel and Teflon. This cell was placed inside a glass vessel, which was partially filled with silicone oil to facilitate heat transfer. Dry nitrogen, introduced through a tube at the bottom of the vessel, served to stir the oil and to maintain a positive pressure of dry gas against entrance of moist air. For temperatures above -20° , the vessel was placed in a thermostatically-controlled water-ethylene glycol bath maintained within a range of $\pm 0.1^{\circ}$. For temperatures below this, the vessel was placed in a dewar flask containing acetone, to which Dry Ice was added manually to maintain the temperature within $\pm 0.2^{\circ}$.

The trichlorofluoromethane was obtained from the Matheson Company and redistilled before use. Water with a specific conductance of less than 3×10^{-6} ohm $^{-1}$, stored in Pyrex and protected from atmospheric CO_2 , was used to prepare the hydrate. In order to ensure uniform packing of the hydrate between the electrodes, it was pre-formed in another vessel, the resulting crystals pulverized with a glass rod, and the powder packed between the cell electrodes with a suitably shaped plunger. The mixture from which the hydrate was precipitated contained a slight excess of liquid Freon which evaporated after the hydrate was formed.

Results and Discussion

Cole-Cole plots were made of the loss against the capacitance, as measured for the partially-filled cell, at each temperature. These quantities are proportional to the imaginary and real parts of the dielectric constant of the hydrate. An example, showing results at 2° , is given in Fig. 1. These plots indicate a wide distribution of relaxation times since the centers are well below the axis in each case. This is in strong contrast to the behavior of ice, which shows strictly a single relaxation time, both in previously reported results⁶ and in comparison experiments in the same cell in which measurements on the hydrate were made.

In Fig. 2 there is plotted the logarithm of the frequency at which the loss is a maximum against the reciprocal of the absolute temperature. The data are for a sample aged at 2° until the loss had stabilized in time. The activation energy for relaxation of the polarization is calculated to be 9.2 kcal./mole and the frequency factor to be 1.3×10^{-13} sec. $^{-1}$. The activation energy is slightly lower than that reported for ice, and the frequency factor is appreciably larger.⁶

For all the samples there is found an appreciable low-frequency conductivity, as represented by the high-capacitance end of the curve in Fig. 1. This cannot be the result of ionic charge carriers, since no appreciable concentration of ions is present. It may be the result of surface polarization, since this is a heterogeneous system. However, the principal loss region cannot be attributed to the effects of polarization. The changes occurring on aging the hydrate constitute evidence for this statement. Initial curves showed loss maxima in the vicinity of 25 kilocycles at 2° , but this frequency shifted to higher values as the samples aged. Aging was also accompanied by change in crystal form to larger, needle-like crystals, and it would be expected that increased perfection of the crystals would shift the loss maximum to lower rather than higher frequencies.

The aging effects, in themselves, seem quite significant. Grinding of the aged crystals, or mere exposure of them to the atmosphere for a period of time, shifted the loss maximum back to lower frequencies. This change might result from either condensation of moisture or loss of Freon. In either case, the surface of the crystal would become more ice-like. It is likely, therefore, that the aging process consists in a change toward the true clathrate crystal lattice, perhaps involving the diffusion of molecules from trapped droplets of liquid Freon to vacant positions. In this process, the ice content of the crystals is reduced, while exposure to the atmosphere reconstitutes the surface layer of ice. The loss maximum as measured during the aging process is then the average of a low value for ice and a larger value for clathrate. Further support for this conclusion is given by the large distribution of relaxation times obtained in the Cole-Cole plots, both during and after aging, and by the fact that X-ray patterns of the clathrate seem invariably to show the presence of a small amount of ice. Since the aging and "regeneration" were followed at $+2^{\circ}$, this conclusion would imply that the clathrate structure can stabilize a surface layer of ice at temperatures above the normal melting point.

(6) R. P. Auty and R. H. Cole, *J. Chem. Phys.*, **20**, 1309 (1952).

Acknowledgment.—The authors acknowledge with gratitude the generous support of the National Institutes of Health for this research.

THE THERMODYNAMIC PROPERTIES OF THE SYSTEM: HYDROCHLORIC ACID, LITHIUM CHLORIDE, AND WATER FROM 15 TO 35°

BY HERBERT S. HARNED

Contribution No. 1732 from the Department of Chemistry of Yale University, New Haven, Connecticut

Received March 27, 1963

In two earlier communications, the thermodynamics of the systems hydrochloric acid, sodium chloride¹ and hydrochloric acid, potassium chloride² in aqueous solution over considerable temperature ranges were discussed. In this contribution, a similar study of hydrochloric acid–lithium chloride mixtures is presented.

The activity coefficients of the two electrolytes may be represented by the linear equations

$$\log \gamma_1 = \log \gamma_{1(0)} - \alpha_{12(0)} m_2 \quad (1)$$

$$\log \gamma_2 = \log \gamma_{2(0)} - \alpha_{21(0)} m_1 \quad (2)$$

when the system is at constant total molality, temperature, and pressure. The activity coefficients of the acid and salt in the mixtures are represented by γ_1 and γ_2 , and their molalities by m_1 and m_2 , respectively. The activity coefficients of the acid and salt in water at a molality, $m = m_1 + m_2$, are represented by $\gamma_{1(0)}$ and $\gamma_{2(0)}$. The parameters, $\alpha_{12(0)}$ and $\alpha_{21(0)}$, are constant at a given temperature and pressure at constant total molality.

Since the magnitudes of $\alpha_{12(0)}$ and $\alpha_{21(0)}$ for this system are small, being one-fifth to one-tenth of those for the systems containing sodium and potassium chlorides, quadratic terms in eq. 1 and 2 would be extremely difficult to detect and are not required to express the known properties of this system.

Values of $\alpha_{12(0)}$ were computed from the electromotive force data of Harned and Copson.³ These results were smoothed graphically and are recorded in Table I at total constant molalities of 0.5, 1, 1.5, 2, 3, and 4 and at 5° intervals from 15 to 25°. We note that these values are in close agreement with those previously determined.^{4,5}

Calculation of the Parameter, $\alpha_{21(0)}$, in Eq. 2 and the Excess Heat of Dilution.—If the parameter, $\alpha_{12(0)}$, is known for a system which is represented by eq. 1 and 2, then $\alpha_{21(0)}$ may be computed by means of the equation

$$\alpha_{21(0)} = \alpha_{12(0)} + \frac{2}{2.303m} (\phi_{2(0)} - \phi_{1(0)}) \quad (3)$$

where $\phi_{1(0)}$ and $\phi_{2(0)}$ are the osmotic coefficients of the acid and salt in water at a concentration, m .⁶ By this equation and the osmotic coefficients given by Robinson and Stokes⁷ and the values of $\alpha_{12(0)}$ in Table I, we find

(1) H. S. Harned, *J. Phys. Chem.*, **63**, 1299 (1959).

(2) H. S. Harned, *ibid.*, **64**, 112 (1960).

(3) H. S. Harned and H. R. Copson, *J. Am. Chem. Soc.*, **55**, 2206 (1933).

(4) H. S. Harned, *ibid.*, **57**, 1865 (1935).

(5) H. S. Harned and B. B. Owen, "The Physical Chemistry of Electrolytic Solutions," 3rd Ed., Reinhold Publ. Corp., New York, N. Y., 1958, p. 608.

(6) Ref. 5, p. 603, eq. (14-5-7).

(7) R. A. Robinson and R. H. Stokes, "Electrolyte Solutions," Butterworths Science Publications, London, 1955, p. 468.

TABLE I

DATA FOR THE CALCULATION OF HYDROCHLORIC ACID IN LITHIUM CHLORIDE SOLUTIONS

$t, ^\circ\text{C.}$	$\log \gamma_{1(0)}$	$\alpha_{12(0)}$	$\log \gamma_{1(0)}$	$\alpha_{12(0)}$
	$m_1 + m_2 = 0.5$		$m_1 + m_2 = 1$	
15	$\bar{1}.8841$	0.0065	$\bar{1}.9153$	0.0062
20	$\bar{1}.8817$.0061	$\bar{1}.9118$.0058
25	$\bar{1}.8792$.0056	$\bar{1}.9079$.0054
30	$\bar{1}.8766$.0050	$\bar{1}.9041$.0049
35	$\bar{1}.8737$.0046	$\bar{1}.8999$.0043
	$m_1 + m_2 = 1.5$		$m_1 + m_2 = 2$	
15	$\bar{1}.9616$	0.0059	0.0166	0.0056
20	$\bar{1}.9574$.0054	.0103	.0051
25	$\bar{1}.9524$.0049	.0039	.0046
30	$\bar{1}.9469$.0044	$\bar{1}.9969$.0041
35	$\bar{1}.9415$.0040	$\bar{1}.9894$.0037
	$m_1 + m_2 = 3$		$m_1 + m_2 = 4$	
15	0.1377	0.0050	0.2700	0.0044
20	.1287	.0045	.2582	.0039
25	.1192	.0040	.2460	.0033
3000350029
3500310024

that $\alpha_{21(0)}$ at 25° equals -0.014 at total concentrations from 0.5 to 3 molal.

The excess heat of mixing, ΔH_M^E , may be calculated by the equation⁸

$$\Delta H_M^E = 2.303RT^2 m_1 m_2 \frac{(\alpha_{12(0)} + \alpha_{21(0)})}{dT} \quad (4)$$

Since the osmotic coefficient of lithium chloride is known at 25° only, $\alpha_{21(0)}$ cannot at present be evaluated at other temperatures by eq. 3. However, it is reasonable to assume that the ratio, $\alpha_{21(0)}/\alpha_{12(0)}$, is constant over a short range of temperature. This ratio is constant for the hydrochloric acid–potassium chloride system from 0 to 40° and varies only 10% for the hydrochloric acid–sodium chloride system from 0 to 50°. For the system under discussion, this ratio equals -2.6 and this value leads to the results at one molal total concentration given in Table II.

TABLE II

VALUES OF THE PARAMETERS OF EQ. 1 AND 2 FROM 15 TO 35° FOR THE HYDROCHLORIC ACID, LITHIUM CHLORIDE SYSTEM AT 1 *m* TOTAL CONCENTRATION

$t, ^\circ\text{C.}$	$\alpha_{12(0)}$	$\alpha_{21(0)}$	$\alpha_{12(0)} + \alpha_{21(0)}$
15	0.0062	-0.0161	-0.0099
20	.0058	$-.0151$	$-.0093$
25	.0054	$-.0140$	$-.0086$
30	.0049	$-.0127$	$-.0078$
35	.0043	$-.0112$	$-.0069$

These results yield a temperature coefficient of $(\alpha_{12(0)} + \alpha_{21(0)})$ of 0.00015 at 25°. Consequently, the heat of mixing at equimolar solutions is

$$\Delta H_M^E = 2.303 \times 2 \times (298.16)^2 (0.5)^2 \times 0.00015 \sim 15 \text{ cal. per mole of solute at } 25^\circ$$

Young, Wu, and Krawetz's⁹ calorimetric determination of this quantity is approximately 13 cal.

Acknowledgment.—This contribution was supported in part by the Atomic Energy Commission under Contract AT(30-1)1375.

(8) H. A. C. McKay, *Discussions Faraday Soc.*, **24**, 76 (1957).

(9) T. F. Young, Y. C. Wu, and A. A. Krawetz, *ibid.*, **24**, 37 (1957).

LONG-RANGE SPIN COUPLINGS INVOLVING METHOXY GROUPS IN AROMATIC COMPOUNDS

BY STURE FORSÉN

Research Group for Nuclear Magnetic Resonance,
Division of Physical Chemistry, The Royal Institute of Technology,
Stockholm 70, Sweden

Received March 18, 1963

In view of the recent interest in long-range coupling of proton spins in unsaturated compounds¹ we wish to report some observations on spin couplings *via* five bonds in methoxy derivatives of *o*-hydroxyacetophenone and salicylaldehyde. Observations of spin couplings between methoxy groups bonded to aromatic rings and the ring hydrogens seem not to have been previously reported. In the proton magnetic resonance (p.m.r.) spectrum of 2-hydroxy-6-methoxyacetophenone, however, the signal of the methoxy group can be resolved into a doublet with a splitting of 0.31 ± 0.03 c.p.s. From the spectrum of the aromatic hydrogens it is evident that the splitting is due to spin coupling of the OCH₃ protons with the proton in the 5-position.

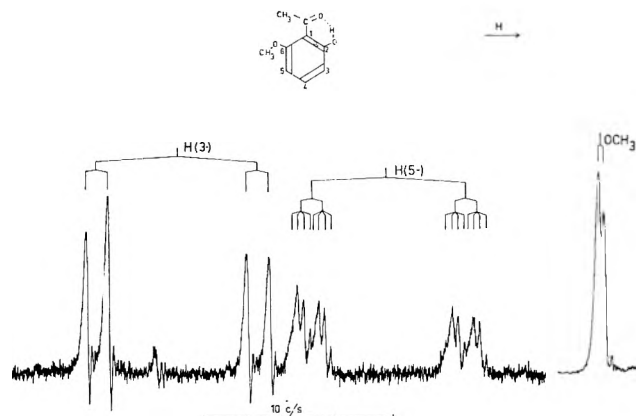


Fig. 1.—Part of the p.m.r. spectrum of 2-hydroxy-6-methoxyacetophenone (ca. 10% in CCl₄) showing the signals from the methoxy group and the ring hydrogens in 3- and 5-position.

The p.m.r. spectrum of the methoxy group and of the hydrogens in the 3- and 5-positions in 2-hydroxy-6-methoxyacetophenone is shown in Fig. 1. The assignment of the signals in the aromatic region is based upon comparison with the p.m.r. spectrum of 2-hydroxy-6-methoxybenzaldehyde (in this compound the aldehydic proton is stereospecifically spin coupled to the ring proton in the 3-position, $J_{\text{CHO-H}(3)} \approx 0.57$ c.p.s.^{1,2}) and with the p.m.r. spectra of a number of other methoxy derivatives of *o*-hydroxyacetophenone and salicylaldehyde.

The observed splitting shown in Fig. 1 of the methoxy signal and the signal of the hydrogen in the 5-position equals the spin coupling constant, $J_{\text{OCH}_3\text{-H}(6)}$.

(1) For a recent discussion of long-range couplings between proton spins see paper by C. N. Banwell and N. Sheppard, presented at the General Discussion on High Resolution n.m.r. arranged by the Faraday Society, Oxford, September, 1962. The paper will appear in *Discussions Faraday Soc.*, 1963.

(2) S. Forsén and B. Åkermark, to be published.

to within a few per cent, since the proton in the 5-position is not strongly coupled to the other ring protons.

A p.m.r. study of other methoxy derivatives of acetophenone and benzaldehyde has given unequivocal evidence for spin coupling of the ring protons with the methoxy group only in 2-hydroxy-6-methoxyacetophenone and in the 3-methoxy derivatives of 2-hydroxyacetophenone and 2-hydroxybenzaldehyde. In all these cases the ring hydrogen *ortho* to the methoxy group was involved in the spin coupling. In 2-hydroxy-6-methoxybenzaldehyde the splitting of the signals from the ring hydrogen and the methoxy group is markedly less than in the corresponding acetophenone derivative and the spin coupling constant is estimated to be about 0.15 c.p.s. In the 3-methoxy derivatives of 2-hydroxyacetophenone and 2-hydroxybenzaldehyde the ring proton in the 4-position was found to be coupled not only to the OCH₃ group but also to the phenolic OH group²; the OH coupling could be suppressed by the addition of a small amount of triethylamine to the solution. The spin coupling constant between the proton in the 4-position and the methoxy group is estimated to be about 0.20–0.25 c.p.s. in both compounds.

In the compounds mentioned above where the methoxy groups have been observed to be coupled to the neighboring ring proton, one would expect the rotation of the OCH₃ group around the oxygen–aromatic carbon axis to be somewhat restricted due to interaction with the neighboring ring substituent. The restriction should be particularly effective in 2-hydroxy-6-methoxyacetophenone, where the acetyl group is “locked” in one rotational configuration by the intramolecular hydrogen bond to the OH group in the 2-position. A possible interpretation of the present results on spin coupling of methoxyl groups with ring hydrogens is that the value of the spin coupling constant between the methoxy group and the ring proton is dependent on the orientation of the O–CH₃ axis with respect to the plane of the aromatic ring. The effective value of the spin coupling constant in the absence of restriction in the rotation of the OCH₃ group could then be so small as to render an experimental observation difficult. On the other hand when the rotation of the OCH₃ group is restricted due to interaction with a neighboring substituent the effective value of the spin coupling constant may in favorable cases be so large as to permit observation on the p.m.r. spectra.

This interpretation provides however no explanation as to why the aromatic methoxyl groups are spin coupled to the *ortho* ring hydrogens whereas phenolic hydroxyl groups are coupled to the *meta* hydrogens.

Acknowledgments.—The p.m.r. spectra discussed in this work were obtained on a Varian A-60 p.m.r. spectrometer, the cost of which was defrayed by a grant from Knut and Alice Wallenbergs Stiftelse. The work was sponsored by a grant from the Swedish Technical Research Council. Thanks are due to Drs. E. Forslind and R. Hoffman for pleasant discussions.

COMMUNICATIONS TO THE EDITOR

STRUCTURAL RIGIDITY AND INTERNAL B-N COÖRDINATION INFLUENCES ON THE HYDROLYSIS RESISTANCE OF BORATE ESTERS

Sir:

Increased hydrolytic stability of borate esters can be achieved in molecules possessing nitrogen atoms stereo-electronically positioned to form partial dative bonding with the boron atom.¹⁻⁴ The B¹¹ n.m.r. chemical shifts of a number of bicyclic azaboroxanes indicate that stereochemical constraint plays a major role, in addition to the amount of B-N interaction, in stabilizing a borate ester toward hydrolysis.

These B¹¹ n.m.r. spectra were obtained using a Varian high resolution n.m.r. spectrometer operating at 12.83 Mc. The chemical shifts were solvent insensitive and are reported relative to BF₃·Et₂O.⁵

The B¹¹ chemical shift value may be considered to be roughly proportional to the electron shielding around a boron nucleus when closely related molecular species are involved. Higher chemical shift values indicate greater electronic shielding around the boron and, in the case of azaboroxanes, increased B-N bonding. From Fig. 1, it is apparent that the B¹¹ chemical shift of the bicycloborate esters is primarily determined by ring size. For a [3,3,3]-bicycloborate ester, the chemical shift value δ occurs around -14; for a [3,3,4]-bicycloborate ester, $\delta = -10$; a [3,4,4]-bicycloborate ester, $\delta -4$; a [4,4,4]-bicycloborate ester, $\delta -1$ to -2 . If the amount of B-N bonding is the most important factor in accounting for the hydrolytic stability of the bicycloborate esters, then it is expected that there should be a consistent relationship between the B¹¹ chemical shift and rate of hydrolysis. From Fig. 1, it is apparent that there is a direct relationship between B¹¹ chemical shift and rate of hydrolysis in the four simplest structural species I, III, V, and VIII; however, the more structurally complicated molecules reveal no such simple relationship.

Qualitatively, it is possible to explain the hydrolysis rates on the basis of stereochemical constraint of the molecule. Compound IX was found to be far more resistant to hydrolysis than VIII which differs only by methyl groups attached to the ring system. This relationship has previously been explained as resulting from the relief of methyl-methyl interactions to produce a shortened B-N distance.⁴ However, a shortened B-N distance would be expected to give rise to a significantly higher B¹¹ chemical shift value which is not observed. A more acceptable explanation involves molecular rigidity due to steric influences during proton attack.

(1) The synthesis and chemical properties of the bicyclic azaboroxanes discussed in this paper were carried out by R. Swidler, U. S. Patent 3,067,609, to be published. However, the general synthetic procedure⁴ as well as the method of determining hydrolysis rate half-times² has already been reported.

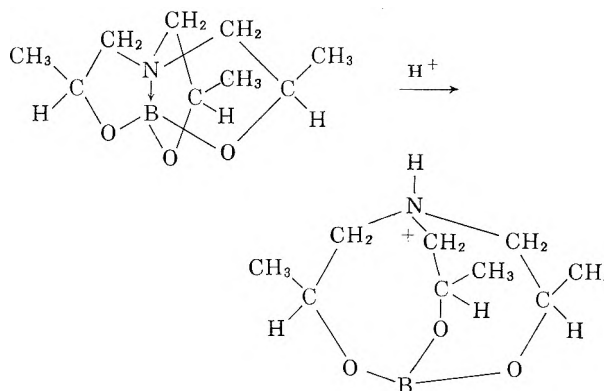
(2) M. F. Lappert, *Chem. Rev.*, **56**, 959 (1956).

(3) H. C. Brown and E. A. Fletcher, *J. Am. Chem. Soc.*, **73**, 2808 (1951).

(4) H. Steinberg and D. L. Hunter, *ibid.*, **82**, 853 (1960).

(5) T. P. Onak, H. Landesman, R. E. Williams, and I. Shapiro, *J. Phys. Chem.*, **63**, 1533 (1959).

The subsequent or nearly simultaneous attack of a water molecule on the boron atom may also influence the rate of hydrolysis.



In proceeding through such a transition state, the methyl groups would be forced either into interference with adjacent rings and/or into methyl group-hydrogen eclipsing on adjacent carbons. VIII, having no methyl groups, will be involved only in hydrogen-ring or hydrogen-hydrogen interactions.

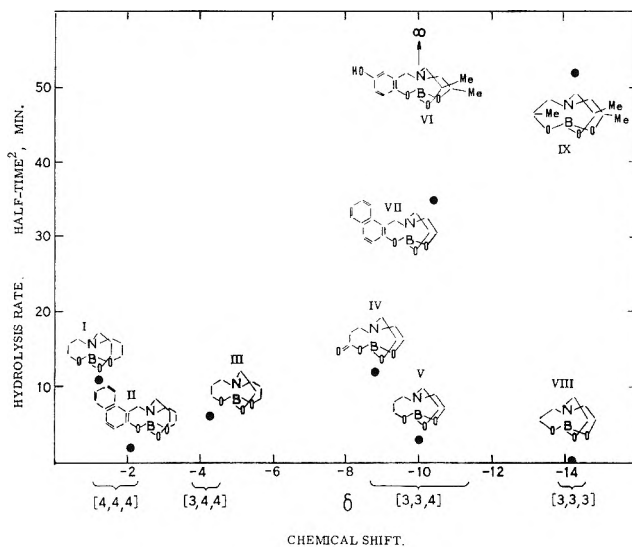


Figure 1.

Molecular models reveal VII [3,3,4] to be exceptionally rigid when compared to II [4,4,4]. In aqueous acid, the hydrolysis half-time for VII was 30-40 min.; in contrast only 2 min. was required for II. Structural rigidity as a major factor in borate ester hydrolytic stability is readily apparent in this case; had the amount of B-N bonding as revealed by the B¹¹ chemical shift been the dominant factor II would have been more stable than VII.

(6) Space-General Corporation, El Monte, California.

OLIN MATHIESON CHEMICAL CORPORATION THOMAS P. ONAK
PASADENA, CALIFORNIA ROBERT E. WILLIAMS⁶

STANFORD RESEARCH INSTITUTE RONALD SWIDLER
SOUTH PASADENA, CALIFORNIA

RECEIVED MARCH 7, 1963

FORMATION AND INFRARED CHARACTERIZATION OF BOROXINE

Sir:

In the infrared spectra of the products formed in the explosive oxidation of pentaborane in this Laboratory, two absorption peaks were observed at approximately 915 and 935 cm^{-1} which were not present in any known boron hydrides or in $\text{H}_2\text{B}_2\text{O}_3$. This latter compound was first synthesized by Hammond, Bauer, and Wiberley^{1,2} and later characterized by Ditter and Shapiro.³

The conditions for producing the unidentified compound in maximum yield were developed by treating pentaborane and oxygen in mixtures with ratios varying from $6\text{B}_5\text{H}_9$ to 10O_2 through 6O_2 to $1\text{B}_5\text{H}_9$. The total pressure of the mixtures was approximately 30 mm. In the pentaborane-rich mixtures no explosion occurred upon heating. Boric acid was slowly formed as a product. At a ratio of 1 to 1 and at higher oxygen-rich ratios, explosions resulted at approximately 50° with the formation of the new intermediate. The maximum concentration of new intermediate was formed when the oxygen to pentaborane ratio was 3 to 1. Infrared absorption spectra were taken over the time interval shown in Fig. 1 after transfer from the explosion vessel to an evacuated infrared gas cell. Mass spectra were taken of samples removed directly from the explosion vessel. As shown in Fig. 1, the new intermediate was found to decompose at room temperature within 1 hr. to B_2H_6 and B_2O_3 with B_2O_3 being the ultimate product. The mass spectrum was the same as that of boroxine, the new compound recently reported by Sholette and Porter⁴ (after correcting for the isotopic abundances of boron, since they reported the mass spectrum for a ^{10}B -enriched sample).

The infrared spectrum agrees well with the planar structure proposed for boroxine by these authors. There is a single B-H stretching vibration, no OH bands, and a strong B-O band. The infrared spectrum is very similar to that of $\text{H}_2\text{B}_2\text{O}_3$,^{2,3} but since both molecules belong to the D_{3h} point group this result is not unexpected.

(1) W. H. Bauer and S. E. Wiberley, Abstracts of Papers of 133rd National Meeting, American Chemical Society, San Francisco, Calif., April, 1953, p. 13L.

(2) W. H. Bauer and S. E. Wiberley, "Explosive Oxidation of Boranes," Advances in Chemistry Series, No. 32, American Chemical Society, Washington, D. C., 1961.

(3) J. F. Ditter and I. Shapiro, *J. Am. Chem. Soc.*, **81**, 1022 (1959).

(4) W. P. Sholette and R. F. Porter, *J. Phys. Chem.*, **67**, 177 (1963).

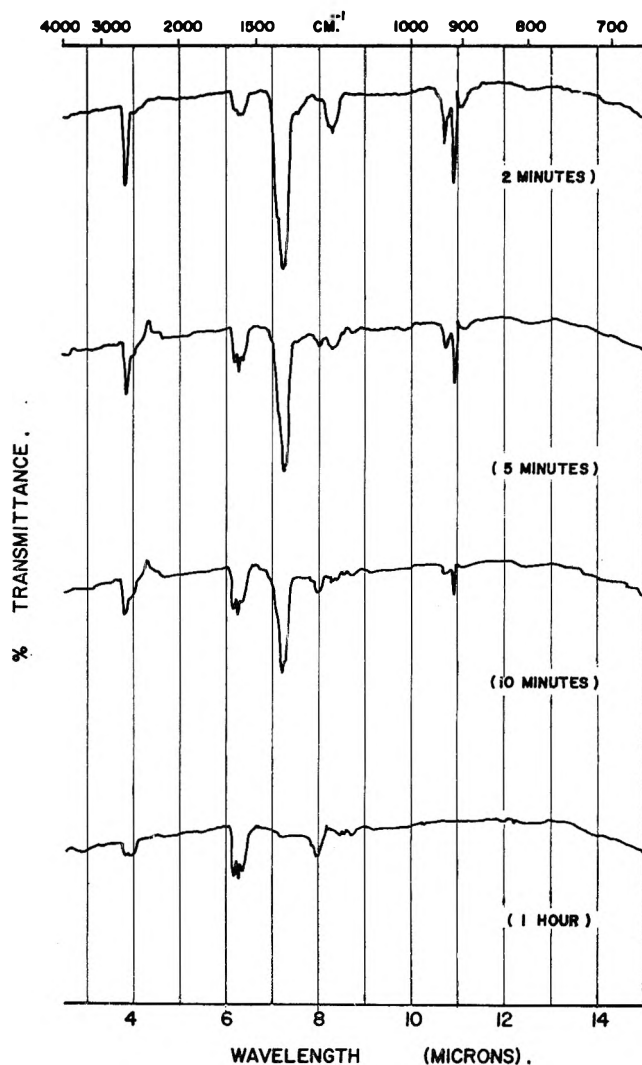


Fig. 1.—Infrared spectra of boroxine formed in the explosive oxidation of pentaborane showing its subsequent decomposition to diborane. The time intervals shown are the times the spectra were taken after the explosion of a 3 to 1 oxygen-pentaborane mixture.

Acknowledgment.—This research was supported by the Air Force Office of Scientific Research under grant Number AF-AFOSR-429-63.

DEPARTMENT OF CHEMISTRY
RENSSELAER POLYTECHNIC INSTITUTE
TROY, NEW YORK

GEORGE H. LEE, II
WALTER H. BAUER
STEPHEN E. WIBERLEY

RECEIVED MAY 17, 1963